E.O. Paton Electric Welding Institute of the National Academy of Sciences of Ukraine

International Scientific-Technical and Production Journal

The Paton WELDING JOURNAL

June–July / 2014
Nos. 6–7

Published since 2000

English translation of the monthly «Avtomaticheskaya Svarka» (Automatic Welding) journal published in Russian since 1948

Founders
E.O. Paton Electric Welding Institute of the NAS of Ukraine,
International Association «Welding»

Publisher
International Association «Welding»

Translators
A.A. Fomin, O.S. Kurochko,
I.N. Kutianova
Editor
N.A. Dmitrieva
Electron galley
D.I. Sereda, T.Yu. Snegiryova

Address
E.O. Paton Electric Welding Institute,
International Association «Welding»
11, Bozhenko Str., 03680, Kyiv, Ukraine
Tel.: (38044) 200 60 16, 200 82 77
Fax: (38044) 200 82 77, 200 81 45
E-mail: journal@paton.kiev.ua
www.patonpublishinghouse.com

State Registration Certificate
KV 4790 of 09.01.2001
ISSN 0957-798X

Subscriptions
$348, 12 issues per year,
air postage and packaging included.
Back issues available.

CONTENTS

PROCESSES OF ARC WELDING. METALLURGY. MARKETS

CONSUMABLES FOR MECHANIZED METHODS OF WELDING

CONSUMABLES FOR MANUAL ARC WELDING

TECHNOLOGIES, EQUIPMENT AND CONTROL IN CONSUMABLES PRODUCTION

ENSURING INTEGRITY OF WELDED STRUCTURES AND CONSTRUCTIONS AT THEIR LONG-TERM SERVICE WITH APPLICATION OF RENOVATION TECHNOLOGIES

O.I. STEKLOV[1], **A.A. ANTONOV**[1] and **S.P. SEVOSTIANOV**[2]
[1]I.M. Gubkin Russian State University of Oil and Gas
65 Leninsky Ave., 119991, Moscow, RF. E-mail: svarka@gubkin.ru
[2]Company «Gazprom VNIIGAZ»
PO 130, 115583, Moscow, RF. E-mail: VNIIgaz@vniigaz.gazprom.ru

Main pipelines in the Russian Federation have been in operation for a long time. Rate of failures in them because of initiation of various corrosion and stress-corrosion defects has increased. Application of welding repair technologies allows considerably lowering the risk of pipeline integrity violation. However, application of welding technologies in repair of pipelines in long-term service requires allowing for additional factors, which are not encountered in work performance on new pipelines. This and additional weldability studies, as well as certain requirements to welding consumables and allowing for stressed state resulting from application of renovation welding technologies, are described in this paper. 9 Ref., 8 Figures.

Keywords: *main pipeline, repair technologies, weldability, corrosion, stress corrosion cracking, requirements to welding consumables, residual stresses, ultrasonic impact treatment*

Most of welded structures and constructions, making up half of the country's metal reserves and built in the pre-restructuring period, are at the stage of ageing and failure rate increase because of damage accumulation, which is due to degradation processes in metals, fatigue, creep and corrosion.

Average age of oil-and-gas pipelines is more than 30 years and more than 70 % of tank fleet have exhausted their specified service life. Bridges, overpasses and other facilities are in a complicated state. A considerable part of housing and communal facilities require renovation. Therefore, one of the important problems of welding fabrication, alongside implementation of new projects, is maintaining the integrity of welded structures after long-term service using renovation welding and related technologies in order to prevent technogeneous and ecological catastrophies. Solution of this problem is considered in the case of main oil-and-gas pipelines.

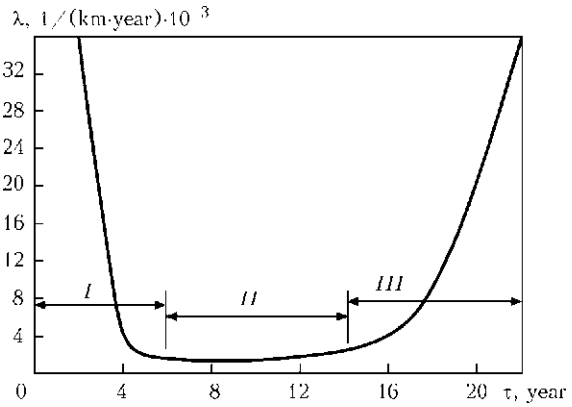

Figure 1. Dependence of specific failure rate index on service life of main oil pipelines (for *I*–*III* see the text)

A characteristic regularity of failure rate in the case of analysis of technical condition of the entire system of main oil pipelines, conducted in 1990s [1], is shown in Figure 1. Specific failure rate index λ (1/1000 km·year), depending on operation life τ of the main pipelines, is characterized by three periods:

I — debugging, period of early failures at decreasing rate, when defficiencies of design, construction and welding-assembly operations are revealed;

II — normal operation with failures, predominantly of random nature;

III — increase of failure rate, in connection with degradation processes in the metal, protective coatings and corrosion.

Such a situation is characteristic also for main gas pipelines, as well as other facilities of oil-and-gas complex [2]. In connection with the above-mentioned problems, an extremely urgent issue now is that of monitoring and assessment of the predicted life of constructions to determine the admissible terms of service, repair and renovation, prediction and assessment of technogeneous and economic risk. The basis of monitoring is technical diagnostics «by the state».

Specialized monitoring systems are developed for various objects, allowing for the structure features and service conditions.

For gas-and-oil pipeline systems a complex three-level monitoring system is promising [3], which includes:

- geotechnical diagnostics based on aerospace monitoring data;
- in-pipe diagnostics;
- ground-based instrumental diagnostics, primarily, of potentially hazardous pipeline sections, detected by the data of in-pipe and geotechnical diagnostics.

Such a comprehensive approach to evaluation of gas pipeline technical state allowed improving the effectiveness of planning diagnostic and repair operations, as well as reliability of the entire gas transportation system and somewhat lowering accident rate [4].

Owing to improvement of methods of pipeline condition diagnostics and evaluation using in-pipe flaw detection, a large number of defects of corrosion and corrosion-mechanical origin are detected on pipeline outer surface.

The most critical kind of defects are stress corrosion cracks, i.e. stress corrosion cracking (SCC) defects or their clusters (in the form of «crack field»), which have a predominantly longitudinal orientation and are located both in base metal and in the zone of shop longitudinal welds. This kind of defects are responsible for up to 70 % of emergency failures of main gas pipelines.

Currently available normative documents specify the dimensions of admissible defects, determining their rejection level. SC cracks, the depth of which goes beyond negative tolerance for pipe wall thickness, were qualified as inadmissible defects, which must be removed (cutting-out pipe defective section). Calculation of safe pressure can be an alternative, at which the defective pipeline can fulfill its function without failure, but with productivity loss during product pumping. It should be noted that in such a situation the operators face several problems.

The first is to establish the actual technical state before assigning the overhauling status to the object, with complete or partial replacement of defective elements, sections, pipes, etc. At this stage either the project or most of the kinds of resources for repair operations performance are still absent. This stage is characterized by that the object still cannot be taken out of service for overhauling, but operative data about its technical state have already been obtained. This period, as a rule, is associated with completion of in-pipe examination of the pipeline and obtaining first preliminary (express), and then also final report on pipe defectiveness state.

Second problem in development of the above situation in the object in service consists in that when obtaining information about the defects preventing normal (without pressure lowering) pipeline operation, repair operations on defective section replacement cannot be performed because of impossibility of bringing heavy construction machinery to the site. In terms of location this is mainly true for pipelines in marsh, flood-plain and water barrier crossing areas. Timewise, it coincides with spring–summer period and autumn, up to marsh freezing and establishing of winter passageways along the route. Thus, starting from seasonal thawing of marshes through the entire summer period of operation up to autumn–winter freezing of marshes and creating ice crossings the operators are limited as to promptness of removing defects, preventing pipeline normal service.

The first problem can be partially solved by eliminating defects before pipeline taking out of service for overhauling, through involving service resources and performance of emergency-reconditioning repair. Now the second problem is associated with an unsurmountable obstacle — conditions, under which such inadmissible defects as SC cracks cannot be eliminated by widely accepted technologies. The more so, since in the majority of normative documents such defects are unrepairable, and are eliminated by the only method of cutting-out the defective section and mounting, welding-in of a new pipe.

Special repair technologies play a particular role under these conditions for the operators. These technologies, without cutting-out the defective section and, hence, without involving a large complex of heavy construction machinery, allow performance of repair, restoring pipeline operability. Figure 2 gives the classification of these technologies. Such technologies include application of reinforcing elements (sleeves) (Figure 3) and repair welding (building-up) of all kinds of defects, including such hazardous defects as SCC [5].

Application of technology of defect repair by welding (building-up) after obtaining information about inadmissible hazardous defect, preventing normal operation, will allow operators ensuring its elimination by repair operations, also in difficult-of-access marshy areas. Another advantage provided by such technologies is the ability to restore the pipe without its replacement.

Application of repair welding (building-up) technologies for structures after long-term serv-

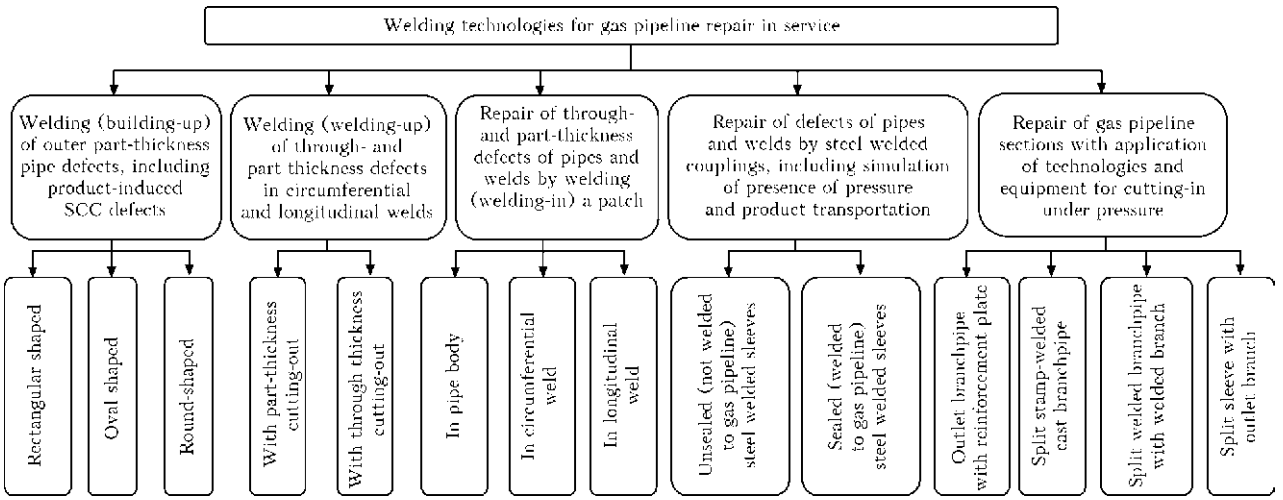

Figure 2. Welding technologies for gas pipeline in-service repair

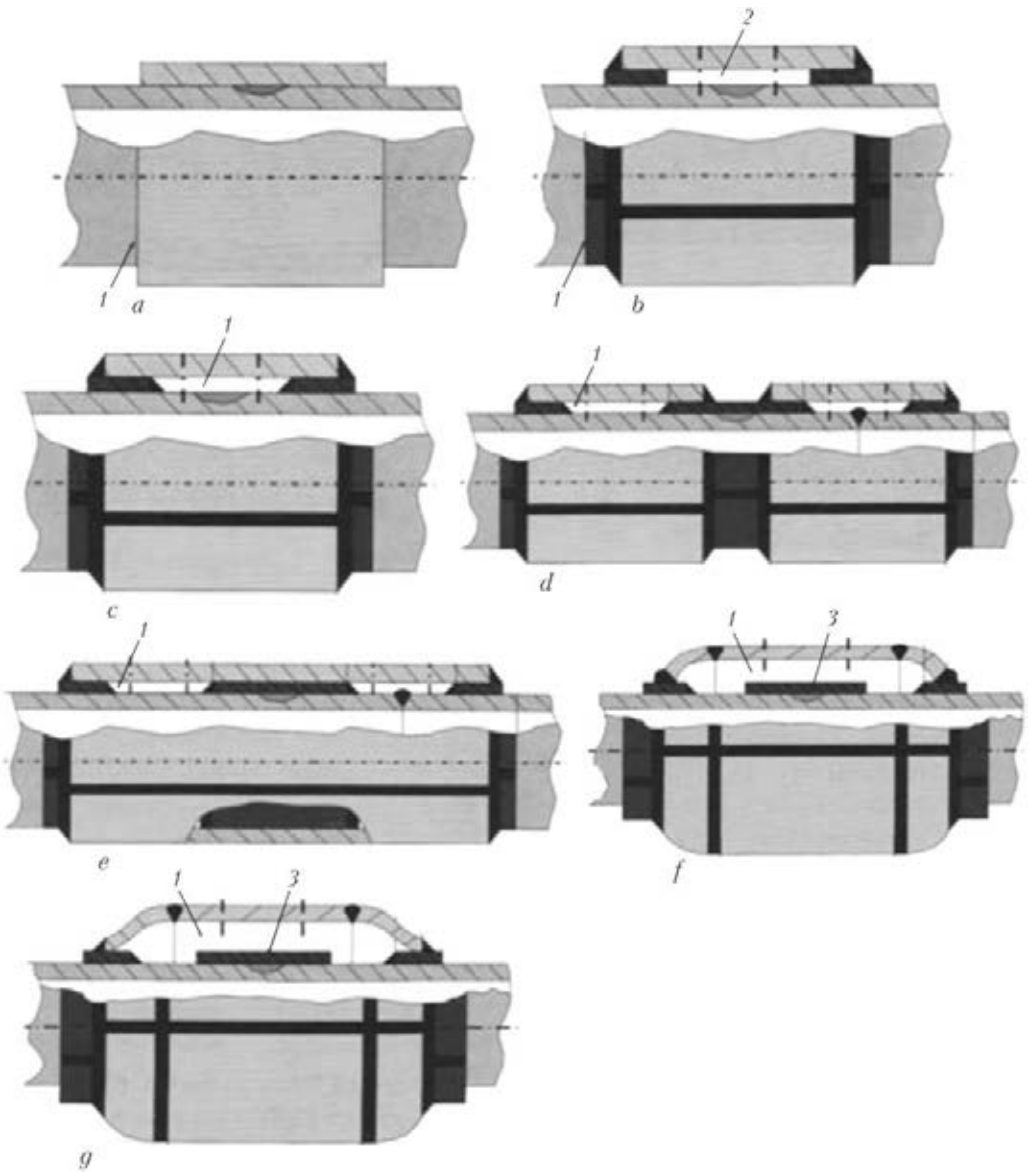

Figure 3. Schematics of repair by welded sleeves of defects in pipes and welds of sections of main gas pipeline linear part: *a*, *b* — unsealed reinforcing sleeves; *c*–*g* — sealed reinforcing sleeves and sleeve assemblies; *1* — sealant; *2* — composite; *3* — temporary sleeve

ice raises a number of key issues: evaluation of material weldability after long-term service; substantiated selection of welding (filler) consumables; optimization of technological process of welding (building-up); substantiation of application of additional postweld related technologies.

Summing up, the following can be noted.

In long-term service of equipment, an essential lowering of weldability of metal being repaired is possible, in connection with degradation processes in the metal as a result of strain ageing, saturation with active reagents from natural and technogeneous media, that requires analysis allowing for the conditions and term of service. Particularly important is evaluation of material weldability under service conditions at the impact of hydrogen-evolving and hydrogen-producing media and for structures operating at elevated temperatures under creep conditions. Unfortunately, no systemic studies on this problem have been performed so far.

Selection of filler materials, allowing for the impact of active media, should ensure the specified strength characteristics of the deposited metal and its «cathodicity» relative to base metal.

Proceeding from design strength of the object and allowing for good weldability, it is rational to ensure strength characteristics from the condition of σ_t^w, $\sigma_y^w \le \sigma_t^m$, σ_y^m (where «w» and «m» indices are the welded joint and base metal, respectively).

To ensure resistance to electrochemical corrosion, the following condition should be fulfilled: $\varphi^w \ge \varphi^m$ (where φ^w, φ^m are the electrode potentials of welded (built-up) and base metal, respectively).

Technology of repair-reconditioning operations is determined, allowing for the above principles, in particular without hydrocarbons bleeding [6].

We will single out only the first group — welding (building-up) of outer part-through defects of pipes, including product-induced SCC defects, from the general classification of welding technologies in gas pipeline repair (see Figure 2). Criteria for application of this kind of repair are as follows:

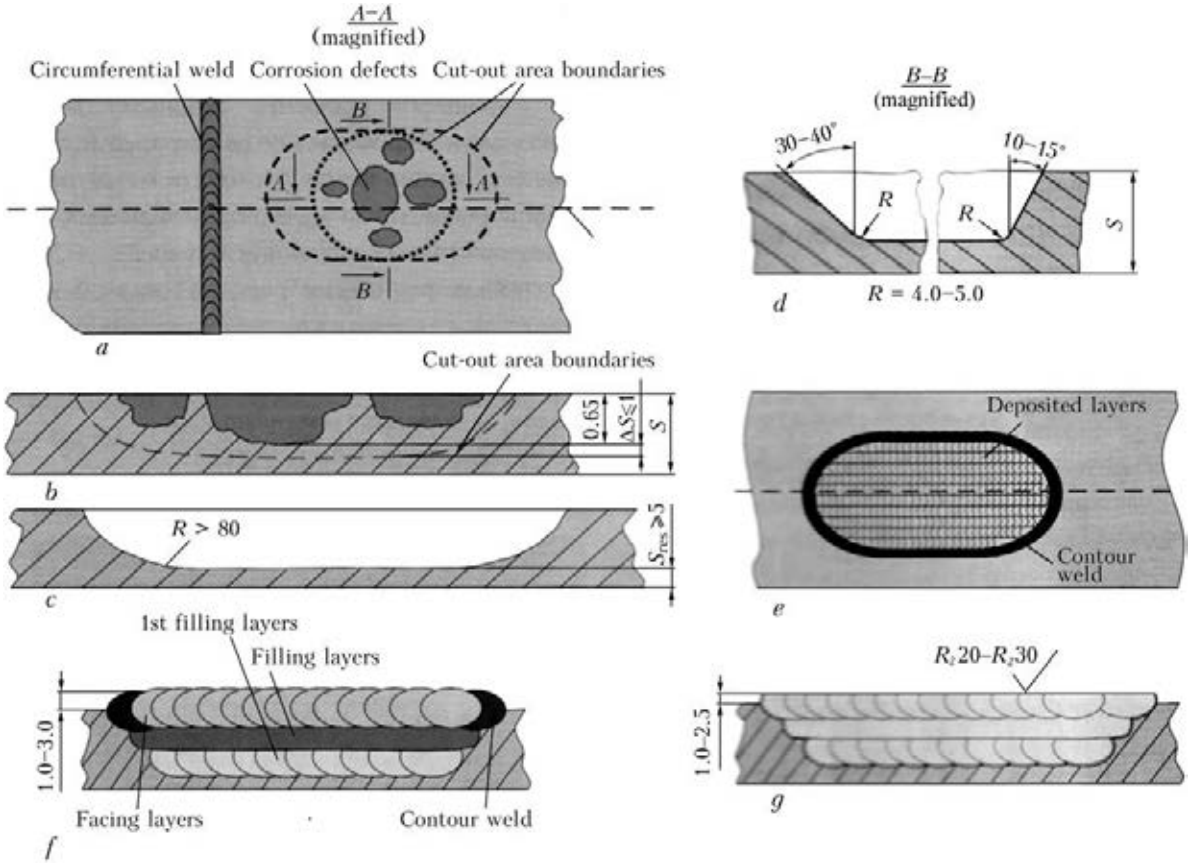

Figure 4. Sequence of technological operations of repair by welding (building-up) of part-thickness outer defects in pipe metal: *a* — appearance of pipe with defective section; *b* — transverse section of pipe along *A–A* line with defective area, respectively; *c* — transverse section of pipe along *A–A* line after mechanical cutting-out of defective layer; *d* — transverse section of pipe along *B–B* line after mechanical cutting-out of defective layer; *e* — pipe appearance after repair; *f* — transverse section of pipe along *A–A* line after repair; *g* — transverse section of pipe along *B–B* line after mechanical scraping of facing layer

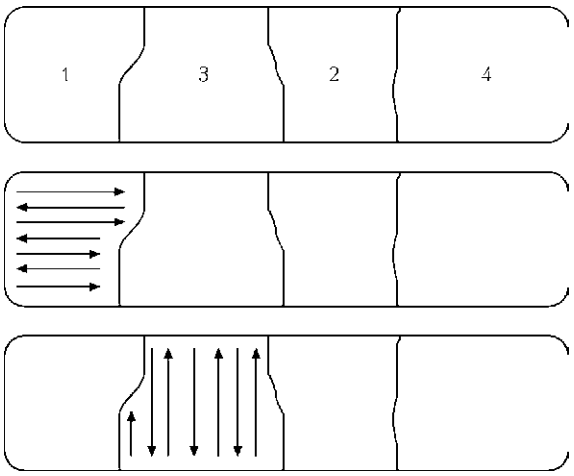

Figure 5. Dividing extended repair section into separate zones 1–4, and sequence of filling them with deposited metal using welding technologies

• ensuring temperature-plastic stability of molten and heated metal in the zone of heat source impact (arc, plasma), proceeding from the conditions of «not burning through» and preservation of strength in the localized heat zone;

• admissible deformability of pipe body in welding (building-up) zone under the impact of inherent stress-strain state in thermodeformational welding cycle, proceeding from the condition of strength of a pipeline with geometry defects;

• admissible level of inherent residual welding stresses in building-up zone.

For gas pipeline admissible value of residual welding stresses in building-up zone is determined from the condition of prevention of SCC, arising at total working σ_{work} and residual σ_{res} stresses exceeding threshold (critical) $\sigma_{th}\sigma_{work} + \sigma_{res} \le \sigma_{th}$. Hence,

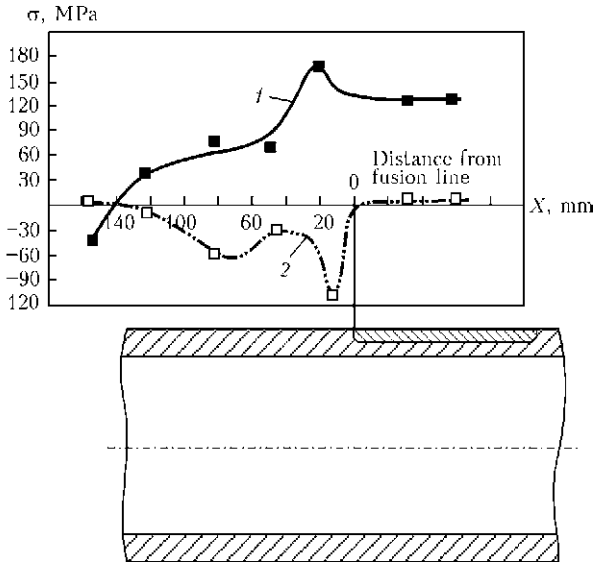

Figure 6. Characteristic diagram of residual stress distribution in the axial direction after repair building-up: *1* — longitudinal; *2* — circumferential stress

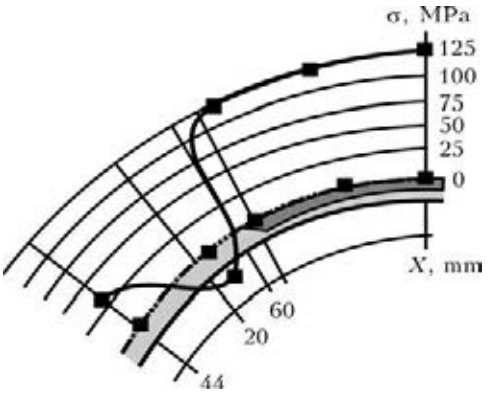

Figure 7. Characteristic diagram of residual stress distribution in the circumferential direction after repair by building-up: solid curves — longitudinal stresses; hatched — circumferential

$$\sigma_{res} \le \sigma_{th} - \sigma_{work}.$$

Allowing for safety factor $\sigma_{work} \approx 0.5\sigma_y$, and σ_{th} value is equal to approximately $0.76\sigma_y$ based on generalization of failure rate statistics [7]. Admissible value of $\sigma_{res} \le (0.2–0.3)\sigma_y$.

An important condition of this technology is welding with a controllable thermal cycle, with heat input and current, minimum admissible in terms of process stability:

$$q/V \to \min, \quad I_w \to \min.$$

For example, in practice for manual arc welding with 2.6–3.2 mm consumable electrodes it corresponds to I_w = 90–120 A. Schematics of repair technologies are given in Figure 4.

In welding-up of extended defects, in order to reduce pipe body deformation, caused by thermodeformational cycle of welding, building-up zone should be divided into smaller sections with reverse-successive direction of welding (building-up) (Figure 5).

A procedure and portable equipment have been developed in order to determine the level and distribution of σ_{res} in building-up zone. The procedure is based on application of nondestructive methods of express-diagnostics of stress-strain state (for instance, equipment based on Barkhausen noise method) at the first stage, allowing detection of the areas of examined section with maximum values of residual stresses. More

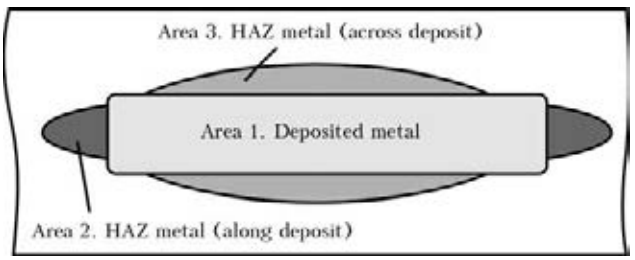

Figure 8. Characteristic field of residual stresses after pipe deposition

precise determination of residual stress value in the detected areas is performed using the method of drilling a blind hole with recording of displacement by speckle-interferometer, in keeping with GOST R 52891–2007. Integrated application of several methods, fundamentally different by their operating principles, allows increasing final result validity. Investigations revealed that residual stress fields after repair building-up have a characteristic pattern of distribution in the axial and circumferential directions, independent on building-up technology [8] (Figures 6 and 7).

Thus, after any repair building-up, a field of residual stresses, shown in Figure 8, develops in the main pipe.

In order to fulfill the specified conditions, recommendations on the technology of postweld treatment of building-up zone have been developed. A fundamental point is localized lowering of residual welding stresses in the zone of their maximum values. Classical thermal methods of lowering the level of residual stresses are not always applicable, that is related both to complexity of organizing heating only in the local deposit area, and to ineffectiveness of such a method in terms of cost.

In recommendations on postweld treatment, a considerable place is taken up by technologies of local impact on individual zones in the deposit area, having peak values of tensile residual stresses. Lowering of such peak values involves general redistribution of residual stress field, because of their mutual balance. A promising approach is lowering peak values, ensuring total favourable redistribution of residual stresses, by the method of ultrasonic peening treatment [9].

Conclusions

1. Application of special welding technologies allows extension of active service life of main pipelines.

2. When preparing for application of welding technologies in main pipelines after long-term service, it is necessary to perform additional weldability studies.

3. When selecting welding consumables, attention should be given to ensuring the specified strength characteristics and cathodicity relative to base metal.

4. Admissible residual stresses after performance of repair building-up should not exceed 20–30 % of yield point.

5. Residual stress fields, developing after repair building-up performance, have a common characteristic shape, irrespective of deposition sequence or direction of beads. The highest value of tensile stresses develops in the base metal near building-up zone along pipe axis.

6. Application of local methods of postweld impact on residual stress fields allows lowering stress-strain state level in the impact zone, in the built-up section and in base metal regions adjacent to building-up zone.

1. Chernyaev, V.D., Chernyaev, K.V., Berezin, V.L. et al. (1997) *System reliability of main transport of hydrocarbons*. Ed. by V.D. Chernyaev. Moscow: Nedra.
2. Varlamov, V.L., Kanajkin, V.A., Matvienko, A.F. et al. (2012) *Monitoring of defects and prediction of state of Russian main gas pipelines*. Ekaterinburg: UNPTs.
3. Steklov, O.I. (2006) Complex technical diagnostics of main gas-and-oil pipelines. *Territoriya Neft i Gaz*, **4**, 20–23; **5**, 12–17; **6**, 48–55.
4. Varlamov, D.P., Dedeshko, V.N., Kanajkin, V.A. et al. (2012) Improvement of reliability of main gas pipelines by using repeated in-pipe flaw detection. *The Paton Welding J.*, **3**, 20–25.
5. Vyshemirsky, E.M., Shipilov, A.V., Bespalov, B.I. et al. (2006) New welding and repair technologies in construction and repair of gas pipelines. *Nauka i Tekhnika v Gaz. Promyshlennosti*, **2**, 27–34.
6. Steklov, O.I., Shafikov, R.R., Sevostianov, S.P. (2009) Theoretical-experimental substantiation of possibility of main pipeline repair using welding technologies without interrupting of gas pumping. *Svarochn. Proizvodstvo*, **7**, 12–17.
7. Steklov, O.I., Varlamov, V.P. (2012) Assessment of threshold stress level of corrosion cracking in system of main pipelines. *Truboprovod. Transport (Teoriya i Praktika)*, **3**, 4–9.
8. Antonov, A.A., Steklov, O.I., Antonov, A.A. (Jr) et al. (2010) Investigation of technological residual stresses in welded joints of main pipelines. *Zagot. Proizvodstvo v Mashinostroenii*, **3**, 13–19.
9. Antonov, A.A., Letunovsky, A.P. (2012) Reduction of residual welded stresses by ultrasonic peening method. *Truboprovod. Transport (Teoriya i Praktika)*, **2**, 21–26.

INVESTIGATION OF CRACKING SUSCEPTIBILITY OF AUSTENITIC MATERIAL USING PVR-TEST PROCEDURE

K.A. YUSHCHENKO, V.S. SAVCHENKO, N.O. CHERVYAKOV, A.V. ZVYAGINTSEVA, G.G. MONKO and **V.A. PESTOV**
E.O. Paton Electric Welding Institute, NASU
11 Bozhenko Str., 03680, Kiev, Ukraine. E-mail: office@paton.kiev.ua

Comparative investigation of hot cracking sensitivity of commercial welding wires has been performed. It is shown that an all-purpose method of weldability evaluation can be the machine method with controllable forced deformation during TIG welding (PVR-test method), which allows separating the conditions of initiation of solidification cracks and ductility dip cracks in the weld and HAZ metal, and provides comprehensive information about quantitative characteristics of cracking sensitivity. 6 Ref., 9 Figures.

Keywords: *weldability, hot cracks, crack resistance evaluation, high-alloyed steels, nickel alloys*

Austenitic high-alloyed steels and their welded joints are rather sensitive to hot cracking. Their sensitivity is abruptly increased in fusion welding of stably austenitic steels and nickel alloys, which preserve face-centered cubic lattice in the entire temperature range. Considering the complexity of thermodeformational processes, taking place in fusion welding of the above materials and diversity of the kinds of initiating cracks, evaluation of material sensitivity to cracking and their classification are an urgent problem. Valuable information about hot cracking sensitivity can only be obtained in the case, when practically all the crack types are studied in one sample during one experiment.

In this case external influence during sample realization is the same for all the zones of the studied sample, however, having different formation mechanisms, different kinds of cracks develop non-simultaneously, thus determining the priorities at evaluation of crack resistance of the joint as a whole.

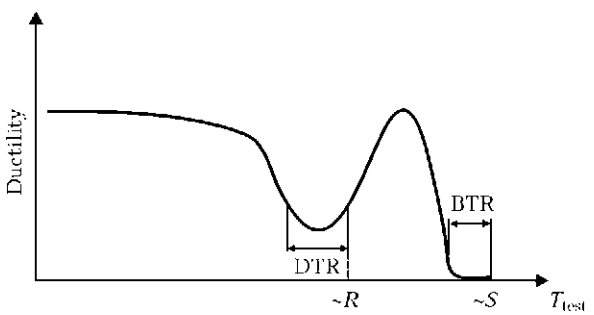

Figure 1. Hot cracking in welded joints of high-alloyed steels and alloys: R — recrystallization [2]

According to international standard ISO 17641-1:2004 hot cracks are violations of material integrity, formed at high temperature along grain boundaries (dendrite boundaries), when deformation or strain rate exceed a certain level. In their turn, cracks are subdivided into solidification, liquation and ductility dip cracks [1]. Causes for cracking are numerous, but usually they initiate, when local ductility is insufficient to counteract the developing welding deformations. Exact mechanism of hot crack initiation has not yet been clarified.

Temperature interval of solidification crack initiation (BTR) depends on the range of the metal solid-liquid state at weld solidification. Lower boundary of this range is determined by the value of solidus temperature T_S when solidification is over. Temperature range of ductility dip (DTR) is determined by approximate ratio of $(0.6–0.8)T_S$ (Figure 1). In this temperature

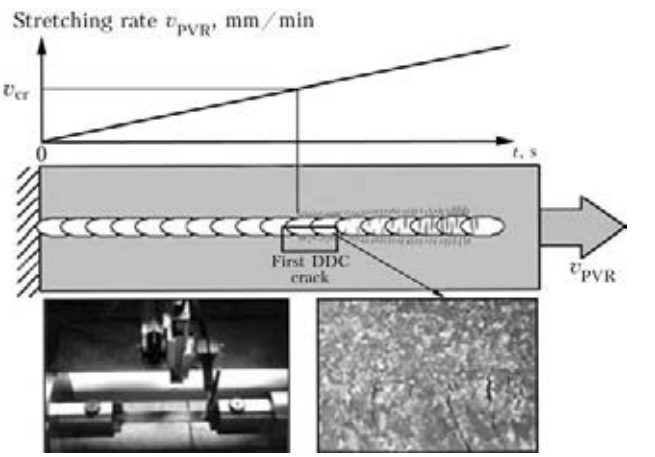

Figure 2. Testing schematic at application of PVR-test method [6]

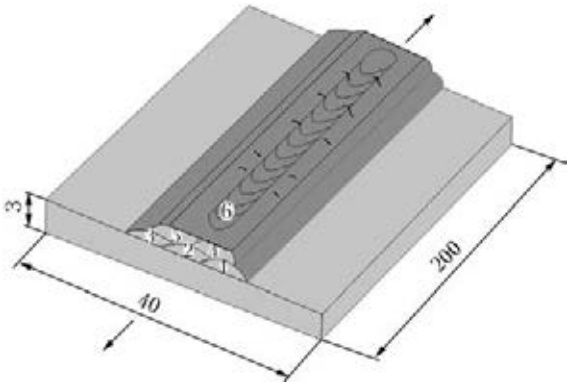

Figure 3. Schematic of conducting an experiment on evaluation of crack resistance of metal of welds with stably austenitic structure: 1–5 — sequence of weld performance when making a sample by TIG welding with filler wire; 6 — control weld with simultaneous forced deformation (TIG without filler); arrows — direction of forced deformation

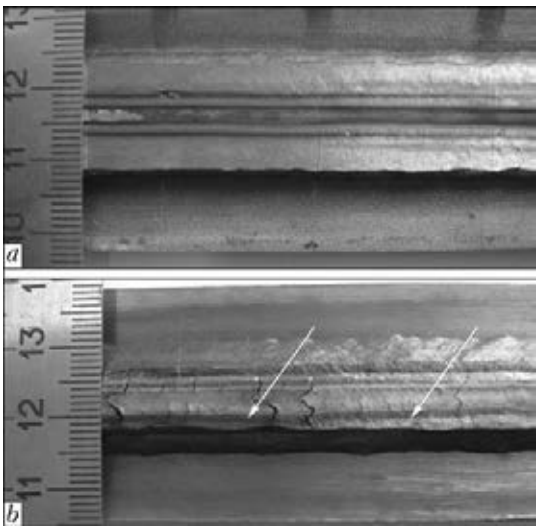

Figure 4. General view of sample surface after testing by PVR-procedure: *a* — welding wire Sv-06Kh18N10; *b* — EP-690; arrows show hot cracks

range cracks initiate and propagate along the boundaries of high-angle austenitic grains.

There exist numerous procedures for determination of hot cracking sensitivity [3, 4]. According to standard ISO 17641-1:2004, testing for hot cracking sensitivity is subdivided into two main groups: testing with natural rigidity and testing with external load application. PVR-test belongs to the second testing group, alongside MVT-test and hot tensile testing.

According to ISO 17641-3:2005, this method is applicable for evaluation of weldability of structural materials during performance of single- and multipass welding of austenitic corrosion-resistant steels, nickel-base alloys and nickel-copper alloys. It, however, can be also applied for other materials, such as aluminium alloys and high-strength steels [5].

This evaluation method is realized by performance of nonconsumable-electrode welding without filler along the plate central axis with simultaneous longitudinal deformation of the sample, changing in time.

Critical strain rate v_{cr}, at which first cracks appear, was selected as the criterion of cracking sensitivity (Figure 2). During welding performance cracks can initiate simultaneously both in the weld metal, and in the HAZ metal [6]. These cracks, as a rule, appear at different v_{cr}. This allows quantitative characterization of sensitivity to a certain crack type. More accurate information about the moment of cracking initiation can be derived by studying weld surface with application of optical methods of magnification.

The objective of his work was investigation of hot cracking sensitivity of commercial welding wires by PVR-test method.

Sv-06Kh18N10 wire is used for welding of structures from general purpose high-alloyed steels, and it provides a certain amount of δ-ferrite in welds, which counteracts hot crack initiation.

EP-690 wire is recommended for welding structures from austenitic steels with stably austenitic structure. δ-ferrite, which in some cases is an undesirable component because of met-

Table 1. Chemical composition of studied welding wires, wt.%

Wire grade	C	Si	Mn	Cr	Ni	Mo	N	S	P
Sv-06Kh18N10 (GOST 2646–70)	0.05	0.7	1.5	19.1	10.1	–	–	< 0.02	< 0.02
EP-690	≥ 0.03	0.5	9.8	18.2	14.1	2.5	0.06	< 0.02	< 0.02

Table 2. Chemical composition of high-chromium nickel-base welding consumables, wt.%

Material grade	C	Mn	Ni	Cr	Fe	Nb	Mo	Ti	S	P	Al	Si
Inconel 690	0.025	0.24	Base	29.72	10.3	–	–	0.28	0.002	0.005	0.87	0.32
Inconel 52	0.026	0.31	Same	28.80	8.5	0.03	0.03	0.51	0.001	0.004	0.72	0.12
Inconel 52MSS	0.024	0.29	»	30.30	7.2	2.52	3.51	0.25	0.0008	0.0006	0.22	0.15

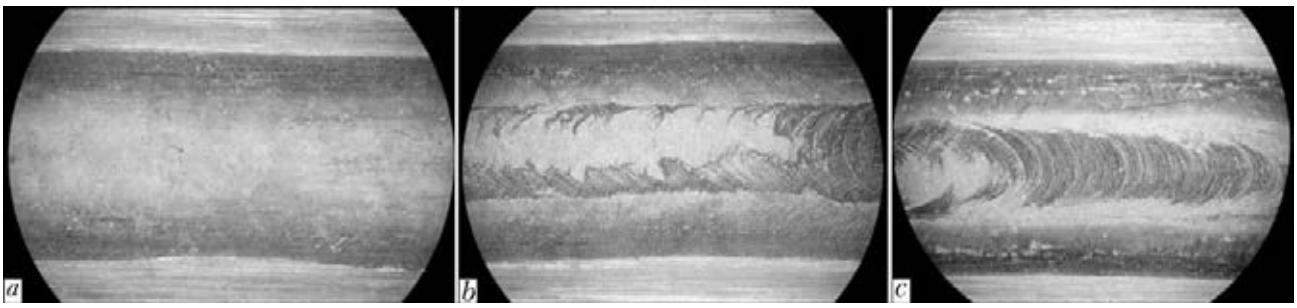

Figure 5. Fragments of surface of welds (×50) made by Sv-06Kh18N10 wire at testing with application of PVR-method at forced strain rate: *a* — 2; *b* — 8; *c* — 12 mm/h; arrows show ductility dip cracks

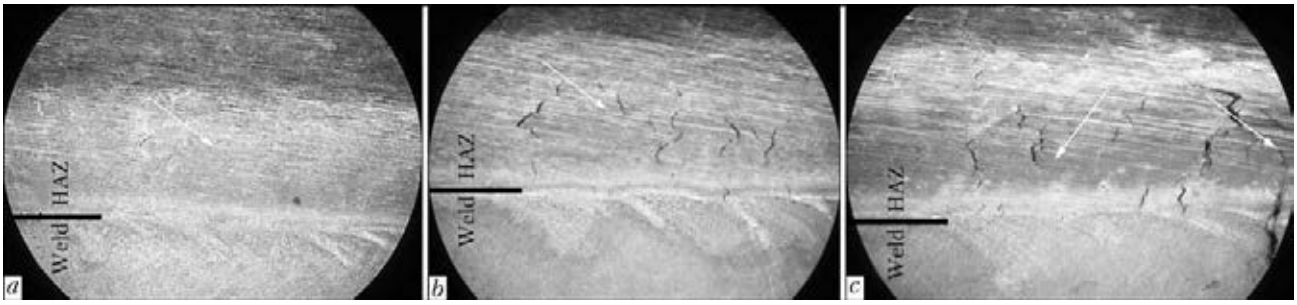

Figure 6. Fragments of surface of welds (×50) made with EP-690 wire at testing with application of PVR-method at forced strain rate: *a* — 2; *b* — 8; *c* — 12 mm/min; arrows show ductility dip cracks

al embrittlement in service, is absent in the weld composition. In this case, sufficient crack resistance in welding should be achieved by further alloying of welds by such elements as manganese, molybdenum and nitrogen.

Composition of welding wires is given in Table 1.

Also studied were high-chromium nickel-base filler materials of the type of Inconel 690 alloy, which are widely used in manufacture of components of nuclear power plants (Table 2). Kinetics of the influence of molybdenum and niobium, additionally alloying Inconel 52MSS wire, on hot cracking sensitivity was studied.

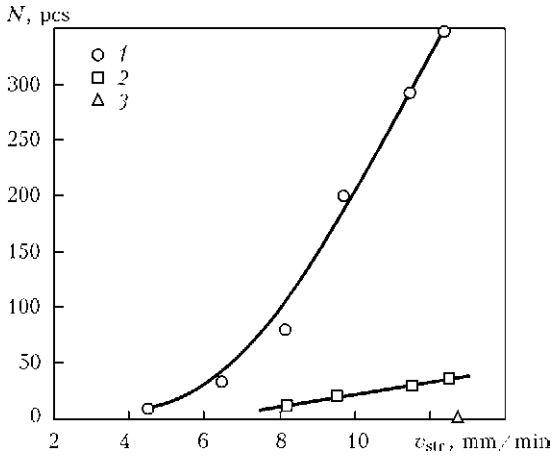

Figure 7. Dependence of number of hot cracks in the metal of welds studied using PVR-test method, which have stably austenitic structure: *1*, *2* — ductility dip cracks and solidification cracks, respectively (EP-690 wire); *3* — no cracks (Sv-06Kh18N10)

Samples were made using stably austenitic high-alloyed Kh20N16AG6 steel, on which beads were deposited by welding wires Sv-06Kh18N10 and EP-690, as well as nickel alloy Inconel 690, on which multilayered beads were deposited by Inconel 52 and Inconel 52MSS wires.

Schematic of bead deposition to produce samples at forced loading, according to PVR-test procedure, is given in Figure 3.

Control weld was made by TIG welding without filler in the following mode: I_w = 60 A; U_a = = 9.5 V; v_w = 7.2 m/h.

Welding with simultaneous deformation of the sample was performed in FP100/1 rupture machine with rigid loading system. During testing loading at sample deformation is recorded, as well as the extent and speed of sample grip displacement.

Analysis of the surface of welds, made with Sv-06Kh18N10 wire, showed complete absence of hot cracks in the metal of the control weld and HAZ, when making the control weld (Figures 4, *a* and 5). Thus, a conclusion can be made that chromium-nickel high-alloyed welds, made with Sv-06Kh18N10 wire, are not susceptible either to solidification cracks, or to ductility dip cracks.

Investigation of the surface of welds made with EP-690 wire showed that hot cracks initiate in the metal of welds and HAZ of the control weld, particularly at high values of strain rate (Figure 6), crack number increasing with increase of strain rate (Figure 7). Considering that

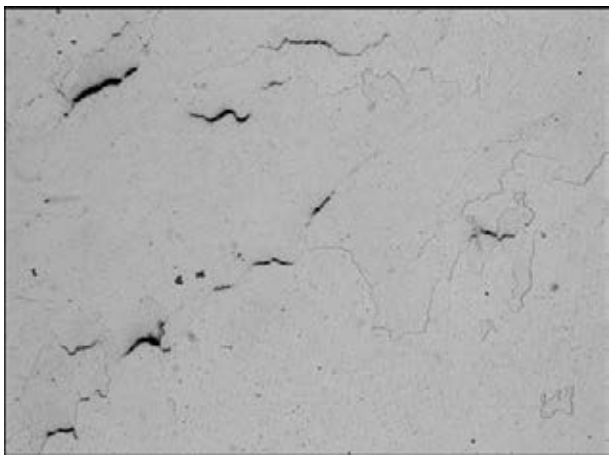

Figure 8. Microstructure (×100) of weld with ductility dip cracks

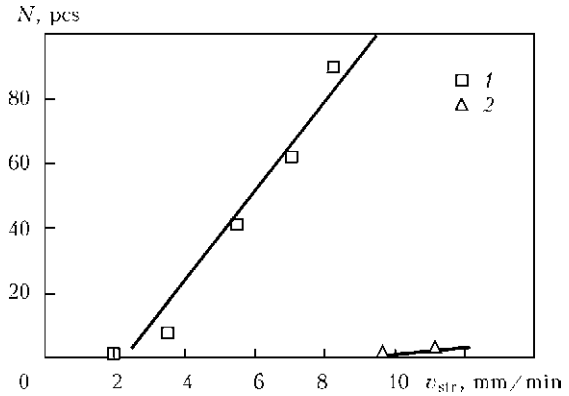

Figure 9. Number of ductility dip cracks in metal of welds, studied using PVR-test method, made with welding wire Inconel 52 (*1*) and Inconel 52MSS (*2*)

cracking susceptibility is proportional to the number of cracks, which initiated in welding by PVR-test procedure, it can be assumed that the studied welded joints should be the most sensitive to initiation of ductility dip cracks (Figure 8).

Data generalization by the results of testing welds made with high-chromium consumables (Figure 9) shows that welds, made with Inconel 52 welding wire with stably austenitic structure, are sensitive to formation of ductility dip cracks, initiating in HAZ, particularly, when making multipass welds. On the other hand, additional alloying of welds by niobium and molybdenum (Inconel 52MSS wire) leads to an abrupt reduction of the number of cracks. Thus, additional alloying of stably austenitic welds by molybdenum and niobium is an effective method of improvement of nickel alloy weldability.

Conclusions

1. Machine method with adjustable forced deformation during TIG welding (PVR-test) can be a versatile method of weldability evaluation. This method allows separating the conditions of development of solidification and ductility dip cracks, as well as obtaining exhaustive information on quantitative characteristics of cracking sensitivity.

2. The main type of cracks in welding of abovementioned materials by modern welding wires with reduced quantity of impurity elements are not solidification cracks, but ductility dip cracks.

3. It is confirmed that presence of δ-ferrite is a cardinal method of hot cracking prevention. In the case, when such a method cannot be used because of service conditions of welded joints, it is rational to additionally alloy the welds by elements which change thermodeformational conditions in welding, and thus prevent cracking.

4. Welds with Ni–Cr–Fe basic alloying system are susceptible to ductility dip cracking. On the other hand, additional alloying of welds by niobium and molybdenum leads to considerable reduction of the number of ductility dip cracks in multipass welding.

1. *ISO 17641-1:2004*: Destructive tests on welds in metallic materials. Hot cracking tests for weldments. Arc welding processes. Pt 1: General.
2. Hemsworth, W., Boniszewski, T., Eaton, N.F. (1969) Classification and definition of high temperature welding cracks in alloys. *Metal Constr. and British Welding J.*, 1(**25**), 5–16.
3. Lippold, J.C., Kotecki, D.J. (2005) *Welding metallurgy and weldability of stainless steels*. Jonh Wiley&Sons.
4. Derlomenko, V.V., Yushchenko, K.A., Savchenko, V.S. et al. (2010) Technological strength and analysis of causes of weldability deterioration and cracking. *The Paton Welding J.*, **9**, 20–23.
5. *ISO/TR 17641-3:2005*: Destructive tests on welds in metallic materials. Hot cracking tests for weldments. Arc welding processes. Pt 3: Externally loaded tests.
6. Herold, H., Streitenberger, M., Pchennikov, A. (2000) Modelling of the PVR-test to examine the origin of different hot cracking types. *IIW Doc. IX-H-474–00*.

Received 11.04.2014

APPLICATION OF SHIELDING GASES IN WELDING PRODUCTION (REVIEW)

B.E. PATON, S.T. RIMSKY and **V.I. GALINICH**
E.O. Paton Electric Welding Institute, NASU
11 Bozhenko Str., 03680, Kiev, Ukraine. E-mail: office@paton.kiev.ua

Main welding-technological properties of pure shielding gases and gas mixtures in consumable and non-consumable welding of different materials were analyzed. It is outlined that knowledge of properties of shielding gas components allows their efficient selection from point of view of welding process optimizing, increase of quality indices and service properties of welded parts, improvement of conditions of work and rise of its efficiency as well as providing of environmental safety of the works. A conclusion is made based on given data that arc method will remain one of the leading technological processes of material joining in the near and far future. 34 Ref., 3 Tables, 3 Figures.

Keywords: *arc welding, consumable and non-consumable electrodes, pure gases, compositions of gas mixtures, welding methods, fields of application, materials to be welded*

Developments of active gas-shielded arc welding methods using consumable and non-consumable electrodes have been stated at the E.O. Paton Electric Welding Institute in the thirties of the last century and are still continued. Development and wide industrial application of active gas-shielded arc welding intensified when the method of consumable-electrode CO_2 welding [1] was for the first time proposed and developed in the USSR. Before this, pore formation in the welds was the main obstacle for application of CO_2 as a shielding atmosphere. The reason of porosity was boiling of weld pool metal due to emission of carbon monoxide as a result of its insufficient deoxidation. Application of welding wires with increased content of silicon such as Sv-08GS and Sv-08G2S type eliminated this disadvantage [2] and provided the possibility of wide application of carbon dioxide in welding production.

Further works, carried at the E.O. Paton Electric Welding Institute, allowed determining the conditions providing for the possibility of effective influence on nature of change of physical processes in discharge gap. As a result, new method of consumable-electrode shielded-gas pulsed arc welding (PAW) using program control of formation of each droplet of the consumable electrode, and, as a consequence, size and shape of the weld in all spatial positions [3, 4] was developed. Pulsed rise of arc current significantly affects nature of arc discharge and improve its stability, that allows consequently reducing low margin of the welding current which supports arcing. For example, welding of aluminum in argon using 1.6 mm diameter wire provides for stable PAW process at around 30 A current instead of 110–120 A. The low current margin of welding of stainless steel in argon using 2.0 mm diameter wire makes 130 A instead of 250–280 A in stationary arc welding. At that, a fine drop transfer of electrode metal is observed in all cases, that not only allow welding in all spatial positions, but also simplifing equipment for mechanized welding of different materials, reducing metal loss due to burn-off and sputtering, providing high mechanical properties of the weld metal and improving its formation [3, 5].

Developments of the E.O. Paton Electric Welding Institute in field of arc methods of welding attract specific attention of the scientists and experts from other countries and, in particular, form the basis for development of efficient compositions of shielding gas media and technology of production of critical designation structures.

Evolution of fusion welding as one of the most important technological processes in industry and building is tightly related with development of the procedures of molten metal shielding from air. Application of mixtures of argon with oxidizing gases CO_2 and O_2 was developed, based on new prospects of application of method of active gas-shielded welding of steel. The widest distribution received Ar + CO_2, Ar + CO_2 + O_2 and Ar + O_2 mixtures. Composition of Ar-based gas mixtures can include 0.5–8 % O_2 and 3–25 % CO_2 [6] depending on class of steels to be welded.

Application of the oxidizing Ar-based gas mixtures in consumable-electrode welding allowed eliminating or reducing to minimum many well-known disadvantages typical for welding in pure CO_2, in particular, providing significant decrease

of sputtering and spitting of electrode metal, improving weld formation, reducing specific consumption of wire per unit of weld length [7], rising weld metal mechanical properties and its resistance to nucleation and propagation of brittle fractures [8].

Developed at the E.O. Paton Electric Welding Institute automatic and semi-automatic machines for gas-shielded welding of high-volume parts are successfully used in many countries [3–5]. Thus, production of welding equipment showed on average 3–4 times increase and significant rise of quality of the parts.

Industrial application of consumable-electrode gas-shielded arc welding uniformly expands, and there are many reasons to believe that the same situation will take place in future. Analysis of reference data [7, 9–13] showed that the gas-shielded arc welding dominates among other methods of fusion welding. Besides, a tendency is preserved for change of manual stick electrode welding to mechanized methods. From this point of view, the perspective branches, which master new types of metal-intensive products and expect investments related with that, are automotive industry, aircraft industry, high-speed railway transport, and, to lesser degree, shipbuilding. The main factors, influencing volumes of application and range of used shielding gases, are change in variety of materials to be welded, high quality requirements to welded joints and structures, increase of efficiency of welding operations and acceptable indices of welding processes from point of view of hygiene and environment.

Typical structure of prime cost of welding works in consumable-electrode gas-shielded welding consists of expenses for shielding gas (5 %) and wire (15 %) plus labor expenses 80 % [14, 15]. Therefore, application of more expensive shielding gas (for example, Ar-based mixture of gases instead of CO_2) can be fully justified, since increase of labor productivity provided as a result of such change (i.e. reduction of expenses for welders' salary) compensates rise of cost of shielding gas.

Process of welding in Ar-based gas mixtures, together with technological and environment advantages, is characterized by improved hygiene and environment indices in comparison with CO_2 welding, since less amount of dust and toxic gases is emitted into the welder's breathing zone and air of workroom [16, 17]. It is possible to reduce intensity of general and local ventilation, i.e. set capacities of ventilation installations and, respectively, expenses for electric power and servicing, due to decrease of the level of harmful emissions in welding and, consequently, sickness rate of the workers. Somewhat increased specific level of ozone emissions during welding in argon mixtures is not an obstacle for application of this process, since keeping of optimum modes of welding and application of simple protective means provide for a concentration of ozone in the welder's breathing zone below the level of maximum concentration limit [18].

Application of argon mixtures with oxidizing gases O_2 and CO_2 as shielding gases allows eliminating number of technological disadvantages, typical for process of welding in pure argon and carbon dioxide, thus, expanding area of application of mechanized consumable-electrode welding. Experience, accumulated at the E.O. Paton Electric Welding Institute and abroad, shows that such shielding mixtures are Ar + O_2, Ar + + CO_2 and Ar + O_2 + CO_2, which are mainly used in welding of steels. Table 1 gives the methods of welding and compositions of shielding gases, used for welding of different materials.

Pure gases and their mixtures, indicted in this Table, have series of important welding-technological properties.

Carbon dioxide a long time was mainly used in the East European counties and developing countries due to its relatively low cost and availability. However, CO_2 welding using commercial silicon-manganese wires has significant disadvantages such as increased level of sputtering and spitting of electrode metal, narrow and deep penetration of base metal with high bead, sometimes unsatisfactory mechanical properties of weld metal and, in particular, its impact toughness at negative temperatures. They became a reason of stable tendency to replace CO_2 with Ar-based mixtures in these countries at recent time at the branches, where great attention is paid to weld metal and welded joint quality indices. Among industrialized countries, only Japan preserves high volumes of application of CO_2 welding (around 70 % of total scope of welding works, made by mechanized gas-shielded welding) [19]. Japan is the country with limited energy resources, therefore, it is obvious that the main direction of works on reduction of disadvantages of CO_2 welding in Japan lies in improvement of power sources or application of new solid and flux-cored welding wires [19] because of increased energy consumption of argon production in comparison with CO_2.

It should be noted that process of CO_2 welding is very sensitive to the changes in mode parameters. Small diameter wire (0.8–1.4 mm) or low

Table 1. Pure shielding gases and gas mixtures for welding of different materials

Composition, vol.%						Welding method	Field of application*	Material to be welded
Ar	He	CO_2	O_2	H_2	N_2			
Pure gases								
100	–	–	–	–	–	TIG	●	Copper, aluminum, titanium, molybdenum and other non-ferrous, active and refractory metals and their alloys, corrosion-resistant low- and high-alloy chromium-nickel steels
				–	–	MIG	▼	Non-ferrous metals and chromium-nickel steels
–	100	–	–	–	–	TIG	❍	Copper, aluminum and other non-ferrous metals and alloys
–	–	100	–	–	–	MAG	●	Carbon and low-alloy steels
				–	–		▼	Stainless steels
–	–	–	–	–	100	MAG	▼	Copper and copper alloys
Two-component mixtures								
70	30	–	–	–	–	TIG	▼	Aluminum and other non-ferrous metals, low- and high-alloy chromium-nickel steels
98–96	–	–	2–4	–	–	MAG	▼	Low- and high-alloy steels
90–92	–	–	8–10	–	–	MAG	❍	Carbon and low-alloy steels
97–98	–	2–3	–	–	–	MAG	●	Alloy and high-alloy steels
75–90	–	10–25	–	–	–			Carbon and low-alloy steels
90–95	–	–	–	5–10	–	MIG	▼	High-alloy chromium-nickel steels
85–90	–	–	–	–	10–15	MIG	▼	Copper and copper alloys
Three-component mixtures								
50–69	30–45	–	1–5	–	–	MAG	▼	High-alloy chromium-nickel steels
55–67	30–40	3–5	–	–	–	MAG	▼	Increased-strength high-alloy chromium-nickel steels
70–87	–	10–25	3–5	–	–	MAG	●	Carbon and low-alloy steels
65	25	–	–	10	–	MAG	▼	Corrosion-resistant high-alloy chromium-nickel steels
60	30	–	–	–	10	MIG	▼	Copper and copper alloys
Four-component mixtures								
76	20	3	–	1	–	MAG	❍	Corrosion-resistant high-alloy chromium-nickel steels
65	26.5	8	0.5	–	–	MAG TIME	▼	Increased-strength low-alloy fine grain manganese steels and chromium-nickel steels

*● — wide application; ▼ — limited; ❍ — rare.

currents (with short circuiting) and high currents (using immersed arc) are preferable for CO_2 welding in order to receive satisfactory weld formation and reduce metal loss for sputtering. The average modes, showing maximum sputtering, should be eliminated. For example, unfavorable modes for 2.0 mm diameter wire lie in the range of 280 A $\leq I_w \leq$ 400 A and 28 V $\leq U_a \leq$ 32 V. Unfortunately, such recommendations are difficult to fulfill on practice, since average currents and wires of 1.0–1.2 mm diameter are, in particular, necessary for providing of high efficiency and optimum heat input in welding of metals of average thicknesses.

Argon is the most widely used component of the shielding gas mixtures, mainly, in TIG welding of non-ferrous, active and refractory metals (Cu, Al, Ni, Mo and others) and their alloys as well as alloy and high-alloy steels. Argon MIG welding of carbon and low-alloy steels does not find noticeable application due to unsatisfactory transfer of electrode metal through arc and formation of undercuts during its wandering over metal surface. At that, the welds are susceptible to nitrogen, hydrogen and carbon oxide induced pore formation. Low potential of argon ionization (15.75 eV) provides for stable arcing at low voltage, facilitate its excitation and rise stability. Arc plasma in argon has high-energy internal core and outer zone with low level of emitted energy that results in undesirable formation of finger-type penetration (Figure 1, *d*) [20].

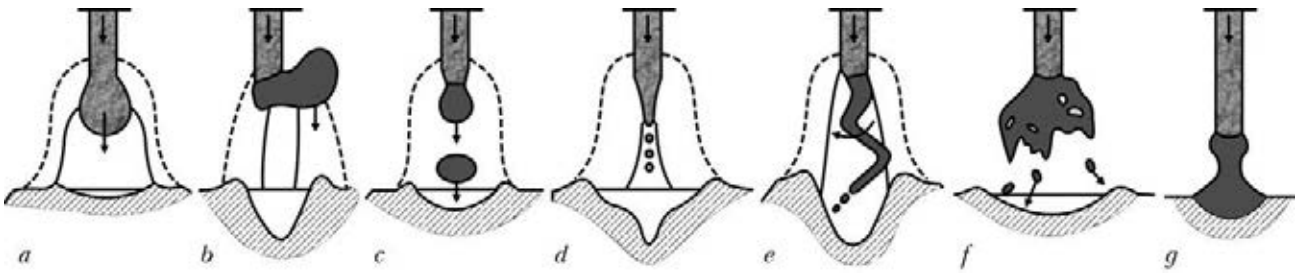

Figure 1. Effect of type of metal transfer on shape of penetration according to IIW classification [20]: *a* — drop; *b* — globular; *c* — fine drop; *d* — spray; *e* — spray-rotation; *f* — with drop explosion; *g* — short circuiting

Helium, among gases used in welding, takes the second place in density (0.178 kg/m^2) after hydrogen (0.083 kg/m^2). In comparison with argon (1.784 kg/m^2) helium has higher thermal conductivity, that provides for uniform energy distribution on arc column section allowing producing deep and wide parabolic shape of penetration and small weld reinforcement with smooth transfer to base metal. High potential of helium ionization (24.58 eV) requires keeping of increased arc voltage in comparison with welding in argon at the same arc length and welding current. Therefore, helium is used as a rule in mixtures with argon for welding of aluminum and other materials in the cases when high energy concentration in the weld zone is necessary.

World market of helium was small and stable for the long time. However, novel developments of the technology of gas-shielded welding revealed new prospects for expanding its application. This is explained by usage of high-production processes of welding of different materials in He-containing gas mixtures, for example, Ar + + He, Ar + He + CO_2 [9–12, 21–23], as well as metal electrode transferred-arc welding in ionized shielding gases with high energy density (TIME process) [24, 25]. Usage of such processes, providing for application of the shielding gas of increased price, is, in particular, relevant for countries with high level of labor remuneration at industry, since increase of price of the shielding gas is compensated by reduction of share of expenses in a general prime cost of welding works due to obvious increase of welder's work productivity.

Oxygen, as one of the components of gas mixtures, is used in small quantities (from fractions of percent to several percent) for activation of metallurgical processes in welding of steel as well as can be present in form of additive in amount of 3–5 vol.% used as one of the mixture components of so-called raw argon (i.e. purged from nitrogen additives and other gases to sufficient level in air separation machine in process of production, but not cleaned of oxygen).

Ar + CO_2 mixtures. Addition of oxygen can improve process of welding and remove some disadvantages related with application of pure argon. Addition of 3–5 % O_2 to argon and usage of welding wire, alloyed with silicon and manganese, allow increasing resistance to pore formation in the welds on killed, semikilled and rimmed steel. Presence of oxygen in argon virtually does not change arc shape, however significantly improves stability of arcing and provide positive effect on nature of electrode metal transfer and promote rise of number of drops transferred per unit of time due to reduction of its surface tension.

Fine drop (spray) metal transfer is achieved at lower value of welding current with virtually no sputtering in comparison with application of pure argon.

Content of oxygen in Ar + O_2 mixture can vary from 0.5–5.0 %. Optimum content of oxygen in mixture for welding of carbon and low-alloy steels makes 3–5 %. This mixture provides for good weld appearance and high level of weld metal mechanical properties, in particular, impact toughness at negative temperatures. More than 5 % content of oxygen rapidly rises loss of alloying elements, and technological characteristics of welding process show no changes. At the same time, Ar + O_2 mixture as well as pure CO_2 are not used in nonconsumable-electrode welding due to electrode breakdown and contamination of weld metal by tungsten oxides.

Ar + O_2 mixtures, containing minimum amount of oxygen (1–2 %), have limited application in welding of ferrite steels and are mainly used for welding of austenite steels. Firstly, it can be explained by the fact that they are produced by mixing of expensive pure gases and, secondly, that the mixtures with low content of oxygen have the same disadvantages in welding as pure argon (narrow penetration of the base metal in weld root, low weld pore formation resistance, wandering of the arc across welded edges, resulting in undercuts and lacks of fusion, intensive heat and light irradiation of the arc, emission of ozone of more than the allowable concentration in the welder's breathing zone). All these disadvantages can be specifically well

observed in welding with spray transfer and sufficiently long arc, therefore, application of argon-oxygen mixture with small additions of oxygen can not be technically and economically approved for welding of carbon and low-alloy steels.

Ar + CO_2 mixtures. Efforts made in discovering a shielding medium, which could combine advantages of argon, carbon dioxide and argon-oxygen mixture, promoted application of mixtures of these gases.

Shape of the arc and nature of electrode metal transfer during welding in Ar + CO_2 mixtures significantly depend on mixture composition. The same mode of welding in mixtures with different content of CO_2 provides different electrode metal transfer, namely, nonshort-circuit drop metal transfer (Figure 1, *a*) or transfer with short-circuiting of arc gap (Figure 1, *g*), fine drop transfer (Figure 1, *c*) and spray transfer (Figure 1, *d*). The shape of base metal penetration changes and finger-type penetration escapes (see Figure 1, *d*) in 20 % CO_2 content and more at currents above the critical value. If the mixture includes more than 35–40 % CO_2, the process in many aspects will be similar to welding in pure CO_2, however level of sputtering, at that, is lower.

Improvement of weld formation in use of Ar + + 20–25 % CO_2 mixtures is observed for wide range of modes. Reinforcement height is significantly lower than in CO_2 welding, the bead has smooth transfer to the base metal, and range of the currents, at which spray (fine drop) transfer takes place, promotes formation of fine-rippled surface as in submerged arc welds (Figure 2). Favorable weld shape, small height of reinforcement and decreased level of loss of electrode metal for sputtering provide for obvious reduction of consumption of electrode wire per unit of weld length.

The recommendations on optimum composition of Ar + CO_2 mixtures from the foreign companies, manufacturing gas mixtures, are controversial. Obviously, it is mainly caused by aggressive competition at sales market and patent matters as well as differences in chemical composition of used steels and welding wires. Ar + 10–15 % CO_2 mixture is widely advertised in Europe [9, 11, 12]. However, accumulated experience showed that Ar + 20 % CO_2 mixture should be considered the optimum one. It has better combination of technological and metallurgical properties and its application can help to eliminate finger-type penetration, resulting in lacks of fusions and pores typical for argon, as well as narrow and deep penetration, dangerous from point of view of crack formation in the welds, characteristic for carbon dioxide.

Structural steel joints, welded in shielding Ar-based gas mixtures using standard wires, traditionally used for CO_2 welding (Sv-08G2S and Sv-08GS on GOST 2246–70), differ by high indices of mechanical properties (Table 2) [7]. The values of impact toughness of weld metal at negative temperatures as well as indices of resistance of weld metal, produced in Ar + CO_2 mixture, to nucleation and propagation of brittle fracture [8] should be particularly noted. Improvement of mechanical and service properties of the welds and joints, produced in Ar-based mixtures, take place as a result of reduction of oxygen content in the welds, formation of favorable microstructure of the metal with domination of acicular ferrite and satisfactory formation of the welds. The indices of cold and crack resistance of welds at the level of values of joints, welded at increased specific heat input using argon mixtures, can not be received during CO_2 welding under similar conditions (Figure 3) [7, 26, 27]. In general, our data and results published by other researchers [17, 28], indicate that the indices of mechanical properties of weld metal, produced in Ar-based gas mixtures, correspond with the requirements made to the joints and structures operating under conditions of negative temperatures, dynamic loads and other unfavorable factors.

The disadvantage of Ar + CO_2 mixture is its high price in comparison with pure CO_2 and Ar + + O_2 mixture. It is promoted by the fact that the mixture is produced from pure gases and in contrast to argon-oxygen mixture it can not be produced directly by air separation using air-separation units. Application as an initial component of «raw argon», containing up to 5 % O_2, is technically and technologically acceptable method for cheapening of argon mixtures with CO_2.

Ar + O_2 + CO_2 mixtures have found wide distribution in Germany and Great Britain [9,

Figure 2. Appearance of fillet weld made in Ar + 20 % CO_2 mixture using Sv-08G2S wire of 1.2 mm diameter at I_w = = 260 A and U_a = 28 V

11, 12, 14]. «Coxogen» mixture (Ar + 5 % O_2 + + 15 % CO_2) has lower oxidizing power and better technological properties than pure CO_2. Welding of carbon and low-alloy steels using Mn- and Si-deoxidized wire provides such advantages as lower sputtering of electrode metal, better weld appearance, lower susceptibility of welds to formation of pores and hot cracks in comparison with CO_2 welding. The mechanical properties of weld metal and welded joint are the same as during welding in Ar + 20–25 % CO_2 mixture and impact toughness of the welds, made in this mixture, is higher.

Since consumable-electrode gas-shielded welding process dominates in Europe, the main attention is paid to the problem of selection of shielding gas composition. The criteria for its optimizing include level of sputtering, weld spatters and slag on the surface of base metal, and formation of the weld (shape of penetration and appearance). Welding of carbon and low-alloy steels using low-oxidizing Ar-based mixtures with small content of oxidizing gases (1–4 % O_2 and up to 10 % CO_2) are proposed [28] based on approaches mentioned above. It should also be considered that all the disadvantages of pure argon, indicated above, appear during welding of these steels in low-oxidizing Ar-based mixtures.

Low-oxidizing Ar-based mixtures cannot be considered as general purpose shielding gases for welding of carbon and low-alloy steels in terms of Ukrainian industry, since the most widespread in our country wires Sv-08G2S and Sv-08GS have higher level of alloying in comparison with wires of similar designation (SG-1, SG-2, SG-3, DIN 8559) applied in Europe. Besides, European welding production uses small diameter wires and milder welding modes in comparison with that used in Ukraine. The accumulated experience showed that it is good to limit the range of shielding gases of domestic welding production by one or two compositions of universal designation.

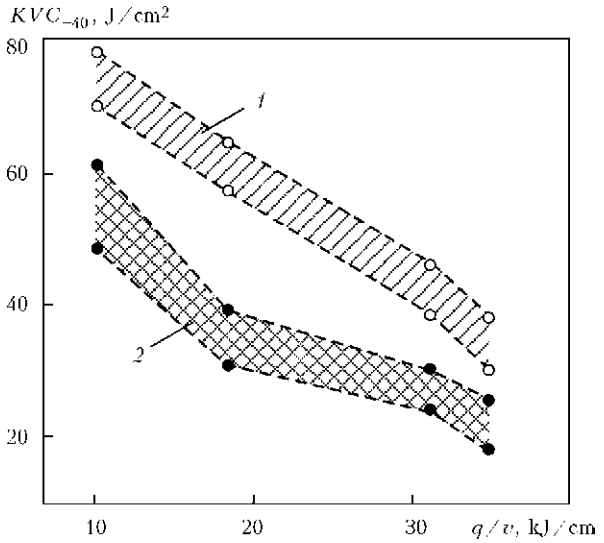

Figure 3. Effect of welding heat input on impact toughness of weld metal made on 09G2S steel using Sv-08G2S wire in Ar + 20 % CO_2 mixture (*1*) and pure argon (*2*)

Ar + 20–25 % CO_2 and Ar + 3–5 % O_2 + 20–25 % CO_2 belong to such wide spread mixtures. They have optimum combination of welding characteristics, reasonable price and allow solving most of technological tasks during mechanized welding of general purpose steels even when the welders violate indicated mode parameters.

Welding in argon mixtures in contrast to CO_2 welding provides for the possibility of application of pulsed-arc process [29, 30] with controlled fine drop transfer and frequency of drop detachment corresponding to frequency of application of current pulses. The fine drop transfer takes place at lower average value of the welding current in comparison with conditions without pulse application (Table 3). Using of PAW allows utilizing the wire of the same diameter for many variants of technology, whereas welding without pulses usually provides for application of different diameter wire depending on thickness of metal to be welded, its thermal-physical characteristics, spatial position of the weld and other indices.

Table 2. Mechanical properties of joints from low-alloy structural steels produced in Ar + 20 % CO_2 mixture using Sv-08G2S wire at different modes of welding [7]

Base metal (thickness, mm)	Wire diameter, mm	I_w, A	U_a, V	σ_y, MPa	σ_t, MPa	δ_5, %	ψ, %	KCV, J/cm², at T, °C		
								+20	–20	–40
09G2S (12)	2.0	400–420	30–32	390	550	26	63	145	67	47
15S2AF (16)	1.6	340–360	28–30	556	678	26	60	105	51	46
10KhSND (20)	2.0	380–410	28–30	540	650	28	62	145	66	44
09G2 (20)	1.6	360–390	28–29	486	592	29	69	153	81	57

Notes. 1. Mechanized welding was carried out using direct current of reversed polarity. 2. Consumption of shielding gas was 18–22 l/min. 3. Indicted are average values on results of testing of 3–5 specimens.

Table 3. Critical welding current of transition to spray metal transfer during welding in Ar + 20 % CO_2 mixture using Sv-08G2S wire

Wire diameter, mm	I_w, A		
	Reversed polarity	Straight polarity	PAW
1.0	240	–	160
1.2	260	350	180
1.4	280	380	210
1.6	340	420	240
2.0	400	460	–

Transfer to new economy relationships and structures together their development in Ukrainian industry will expand fields of application of mechanized consumable electrode welding in Ar-based oxidizing mixtures instead of pure CO_2. However, data on application of gas mixtures in welding of steels are unmatched, and they are difficult to use in practical activity. Therefore, summary of data necessary for application of the most widespread mixture of Ar + CO_2 in mechanized welding of steels are given in the recommendation tables [31].

The largest technical-economical effect of steel welding in Ar-based shielding mixtures is provided in the following branches:

- production of metal structures, which should have no weld spatters according to work conditions;
- production of metal structures of critical designation, being operated at negative temperatures and alternating dynamic loads;
- multipass welding of fillet and butt joints of heavy-plate metal;
- increased rate welding of small section welds;
- welding of parts using robots and automatic machines on automated assembly lines.

Ar + He + CO_2 mixtures, with argon as the main component, are used in stationary and pulsed arc welding, and mixtures having predominate content of helium (60–80 %) are applied in short-circuiting arc welding. Foreign publications [21–23, 32] consider different compositions of gas mixtures with helium (vol.%: (69–55)Ar + (40–30) He + (3–5) CO_2)), providing good technological indices, in particular, rise of efficiency in thick metal welding, deep and wide penetration of base metal, improvement of formation and appearance of the welds. The main peculiarity of welding in Ar + He + CO_2 mixtures is high process efficiency at modes with spray-rotation metal transfer (see Figure 1, *e*). Such a transfer takes place in using of 1.0–1.2 mm diameter wire, mechanism of its feeding of up to 50 m/min rate and power source with good dynamic characteristics [22, 33].

Ar + He + CO_2 + O_2 mixtures require special technology, power sources and mechanisms of wire feed. Thus, TIME-process [24, 25, 33] uses the gas mixture (vol.%: 65 Ar + 26.5 He + + 8 CO_2 + 0.5 O_2) providing high speed of wire melting (up to 25 kg/h) with 50 m/min feed rate at welding current around 600 A. There are also high-productive methods such as Rapid Arc and Rapid Melt [10, 11, 32] which are carried out in shielding mixtures with helium (vol.%: (60–65) Ar + (25–30) He + 10 CO_2). Their application provides for exceeding of classical limit of wire feed 20 m/min and support different types of electrode metal transfer, including spray-rotation (see Figure 1, *e*).

Rigid limitation on composition of the shielding medium, provided by technological recommendations of TIME-process developers [23, 33], have no grounds since similar indices of efficiency and quality can be received using cheaper and simpler in production Ar-based mixtures without helium, for example, Ar + CO_2 + O_2, and by thorough selection and correction of the mode parameters [11, 14, 34].

Many gas-shielded arc welding methods are known at present time, using which the same works can be fulfilled. However, technical-economical results obtained at that will vary depending on production conditions and structure peculiarities. Each of the welding methods has specific technological capabilities and can be used for certain type of welding works, therefore, selection of optimum composition of shielding gas and method of welding requires complete understanding of peculiarities and capabilities of each of the methods and their consideration based on specific production conditions. Significant influence at that can have mechanization and automation of the welding processes, in particular, taking into account a wide range of existing at present time types of manipulators and pozitioners as well as robots and computer-controlled regulation systems.

1. Lyubavsky, K.V., Novozhilov, N.M. (1953) Consumable-electrode shielded-gas welding. *Avtogen. Delo*, **1**, 4–8.
2. Novozhilov, N.M., Sokolova, A.M. (1958) Development of electrode wires for CO_2 welding of low-carbon and low-alloy steels. *Svarochn. Proizvodstvo*, **7**, 10–14.
3. Paton, B.E., Potapievsky, A.G., Podola, N.V. (1964) Consumable electrode pulsed arc welding with program control of process. *Avtomatich. Svarka*, **1**, 1–6.
4. Paton, B.E., Voropaj, N.M., Buchinsky, V.N. et al. (1977) Control of arc welding process by programming of electrode wire feed rate. *Ibid.*, **1**, 1–5, 15.

5. Paton, B.E., Lebedev, A.V. (1988) Control of melting and electrode metal transfer in CO_2 welding. *Ibid.*, **11**, 1–5.
6. Paton, B.E., Kirsanov, A.V., Podgaetsky, V.V. et al. *Shielding gas mixture*. USSR author's cert. 448106. Int. Cl. B 23 K 35/38. Prior. 26.06.72. Publ. 30.10.74.
7. Svetsinsky, V.G., Rimsky, S.T., Galinich, V.I. (1994) Welding of steels in shielding argon-based gas mixtures on in industry of Ukraine. *Avtomatich. Svarka*, **4**, 41–44.
8. Svetsinsky, V.G., Rimsky, S.T., Kirian, V.I. (1992) Evaluation of fracture toughness of welds made in shielding gases and by submerged-arc process. *Ibid.*, **8**, 16–19.
9. Lucas, W. (1992) Choosing a shielding gas. Pt 2. *Weld. and Metal Fabr.*, **6**, 269–276.
10. Dilthey, U., Reisgen, U., Stenke, V. et al. Schutzgase zum MAGM-Hochleistungsschweissen. *Schweissen und Schneiden*, 47(**2**), 118–123.
11. Dixon, K. (1999) Shielding gas selection for GMAW of steels. *Weld. and Metal Fabr.*, **5**, 8–13.
12. Salter, G.R., Dye, S.A. (1971) Selecting gas mixtures for MIG welding. *Metal Constr. and British Welding J.*, 3(**6**), 230–233.
13. Cresswell, R.A. (1972) Gases and gas mixtures in MIG and TIG welding. *Weld. and Metal Fabr.*, 40(**4**), 114–119.
14. Ameye, M. (2011) Einfluss der verschiedenen Schutzgase im Zusammenwirken mit Schweissverfahren und Werkstoffen. *Der Praktiker*, **7**, 271–273.
15. Kajdalov, A.A., Gavrik, A.N. (2011) Efficiency of application of shielding gas mixtures in arc welding of steels. *Svarshchik*, **4**, 28–31.
16. Press, H., Florian, W. Formation of toxic substances in gas welding. Pt 2: Amount of toxic substances formed in the gas shielded welding processes MAG, MIG and GTA. *IIW Doc. VIII-880–80*.
17. Haas, B., Pomaska, H.U. (1980) Influence of process specific welding parameters on fume generation in solid wire GMA (MAG) welding. In: *Proc. of IIW Col. on Welding and Health* (Estoril, Portugal, 8 July, 1980), 8.
18. Levchenko, O.G. (1986) Influence of shielding gas composition and welding parameters on total emission of welding aerosol. *Avtomatich. Svarka*, **1**, 73–74.
19. Kosiishi, F. (2007) Advanced welding consumables. *J. JWS*, 76(**1**), 61–64.
20. Stenbacka, N., Persson, K.-A. (1989) Shielding gases for gas metal arc welding. *Welding J.*, **11**, 41–47.
21. Lyttle, K., Stapon, G. (2005) Simplifying shielding gas selection. *Practical Welding Today*, **1**, 22–25.
22. Ernst, M. (1999) Lichtbogen stabil gehalten. *Produktion*, **8**, 23.
23. Urmston, S. (1996) Quality — all things to all welders. *Weld. and Metal Fabr.*, 64(**4**), 150–152.
24. Church, J.G. *Welding system*. Pat. 4.463.143 USA. Publ. July 1984.
25. Lahnsteiner, P. (1991) T.I.M.E. — Process ein neues MAG-Schweissverfahren. *Schweisstechnik*, **12**, 182–186.
26. Rimsky, S.T. (2011) Control of properties of the weld metal by regulating the level of oxidation of the weld pool in gas-shielded welding. *The Paton Welding J.*, **12**, 16–19.
27. Roshchupkin, N.P., Bliznets, N.A., Svetsinsky, V.G. et al. (1984) Experience of industrial application of shielding argon-based gas mixtures by All-Union plants «Soyuzstalkonstruktsiya». *Avtomatich. Svarka*, **3**, 51–53.
28. (2001) SAGOS 3: Schutzgas fuer zwei Werkstoffgruppen. *Stahlmarkt*, 51(**11**), 66.
29. Pfeiffer, G. (1989) Zuend- und Spritzeruntersuchungen beim MAG-Impulsschweissen. *ZIS-Mitteilungen*, 31(**6**), 545–549.
30. Rimsky, S.T., Svetsinsky, V.G., Shejko, P.P. et al. (1993) Consumable electrode pulsed arc welding of low-alloy steels in argon mixture with CO_2. *Avtomatich. Svarka*, **2**, 38–41.
31. Rimsky, S.T. (2006) *Manual on technology of shielded-gas mechanized welding*. Kiev: Ekotekhnologiya.
32. (2005) Das Schutzgas machts. *Blech. Rohre Profile*, 52(**8/9**), 28–30.
33. Church, J.G., Imaizumi, H. Welding characteristics of a new welding TIME-process. *IIW Doc. XII-1199*.
34. Oeteren, K.-A. (1992) «Neues Schutzgas» metal-aktivgasgeschweisst — ein wirtschaftliher Vorteil? *Der Praktiker*, **2**, 90–94.

Received 11.04.2014

EFFECT OF STRUCTURAL FACTORS ON MECHANICAL PROPERTIES AND CRACK RESISTANCE OF WELDED JOINTS OF METALS, ALLOYS AND COMPOSITE MATERIALS

L.I. MARKASHOVA, V.D. POZNYAKOV, E.N. BERDNIKOVA, A.A. GAJVORONSKY and **T.A. ALEKSEENKO**
E.O. Paton Electric Welding Institute, NASU
11 Bozhenko Str., 03680, Kiev, Ukraine. E-mail: office@paton.kiev.ua

Investigated are structure and phase composition of weld metals as well as HAZ of welded joints (of carbon, low-alloy structural and cold-resistant steel, nickel and aluminum alloy and others) in fusion welding and reconstruction repair surfacing using different welding consumables (electrodes, fluxes and wires). Analytical estimations of role of forming structural parameters in change of complex of mechanical properties, as well as nature of distribution and localizing of deformations, level of local internal stresses, intensity and extension of stress concentrators, being potential sources of crack formation generated in welding, were carried out based on experimental data, received on different structural levels (from grain to dislocation ones). The results of carried investigations were used for correction of technological processes of welding that allowed providing high complex of mechanical properties and crack resistance of welded joints. 12 Ref., 7 Figures.

Keywords: *arc welding, structural steels, welded joints, structural factors, mechanical properties, crack resistance*

Metal structures and mechanisms of different type used in present time should correspond the main requirements for safety under service conditions. It in particular concerns welded joints of these metals. At that, the most critical criteria characterizing, as a rule, joint safety are yield strength, low brittle transition temperature, crack resistance and good weldability of used metals and alloys. It is a well-known fact that structure and phase composition of these materials play significant, and sometimes vital, role in providing of necessary properties of all types of materials. Therefore, the first «startup» problem is examinations for detection of the most complete scope of structural factors, forming under different conditions of technological treatment (grain, subgrain, dislocation structures and phase composition etc.). And the second problem, being a guiding line for the production engineers in development of optimum technological modes, is investigation of technology ↔ structure ↔ properties relationship, including the structures providing for the maximum necessary service requirements.

This work considers structural factors, which determine properties of the joints, produced by fusion welding [1–9], from such materials as high-strength low-alloy, austenite stainless steels as well as aluminum alloys etc. The factors of following types are the subject of examination, namely non-metallic inclusions (NMI); reinforcement (strengthening) phases; phase composition, depending on alloying (pearlite, ferrite, bainite, martensite and others), and considering structural parameters, such as size of grain and subgrain, dislocation density etc.

The next processes are also considered by analysis of technology ↔ structure ↔ properties relationship. They are peculiarities of deformation localizing and its distribution; structural conditions of formation of local and internal stresses, their changes under thermal-deformation conditions of welding and further internal loading; nature and mechanisms of local internal stress relaxation as well as role of structure and phase composition of metal in processes of realizing of different mechanisms of relaxation of these stresses (due to plastic mechanisms or crack formation). Some examples of such experimental and analytical approaches to estimations are presented in this work.

Effect of NMI on weld properties (strength, impact toughness, cold resistance), formation of

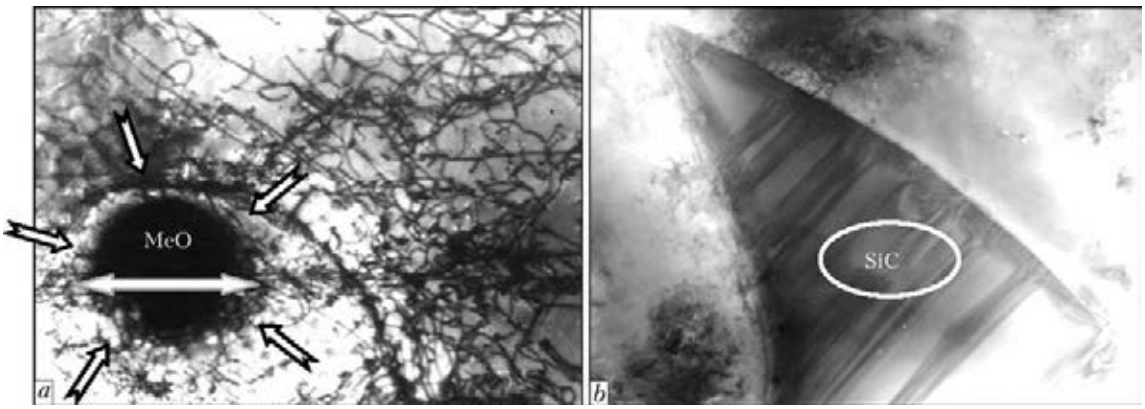

Figure 1. Nature of dislocation configurations ($\tau_{l.in}$ concentrators) in zone of NMI distribution in welded joints, namely oxide phases (*a* — ×10,000), and rise of local stresses along Al/SiC interface and in internal volumes of SiC-phases (*b* — ×20,000)

lamellar cracks etc. were investigated on the welded joints of series of steels. They are the joints of carbon, low-alloy structural and cold-resistant steels [4] produced in gas-shielded submerged arc welding using different coated electrodes (rutile and ilmenite type) [5], submerged arc welding with zirconium [6] and joints with stable austenite welds depending on flux type (basic, acid) [7].

It was shown that formation of specific dislocation configurations of different density and, respectively, various on intensity internal stress fields takes place in weld metal depending on NMI size and their distribution. The fields with high dislocation density are observed in the case of formation of fine-disperse NMI in zone of their accumulation, but at dense distribution in the weld metal. This means formation of the zones with high level of the local internal stresses $\tau_{l.in}$ in area of disperse NMI accumulation. NMI chains distributions are in particular unfavorable (even of disperse size d_p ~ 0.2–0.4 μm) and promote formation of directed dislocation accumulations — $\tau_{l.in}$ concentrators comparable with values of theoretical strength $\tau_{l.in} \sim \tau_{theor}$. At the same time, NMI of larger size (d_p ~ 1.5–1.7 μm), at uniform distribution in grain internal volumes (Figure 1, *a*), do not promote formation of any significant on value local internal stresses in the weld metal and, respectively, have no essential effect on crack resistance of the welded joint metal.

The results of carried investigations and analytical estimations allowed determining the reasonable levels of sufficient weld metal deoxidation, providing not only general reduction of NMI volume fraction, but also more optimum their distribution, and grounding of choice of welding wire compositions [5] as well as application of basic type fluxes for optimizing of welding of carbon, low-alloy structural and stainless steels by stable austenite welds [7].

Investigations on different structural levels showed that *reinforcing and carbide phases* can, depending on their size, be a reason and source of joint fracture with their strengthening effect in welded joint metal. Thus, the maximum strength characteristics of the joints in case of welding of aluminum alloys, reinforced by silicon carbide particles SiC [8], are provided at SiC particle size of around 0.6–0.8 μm. Increase of size approximately to 2 μm resulted in rise of elastic $\tau_{l.in}$ stresses along aluminum matrix/SiC interface, that is verified by change of contrast in this area (Figure 1, *b*) during transmission electron microscope examination. Rising of size of reinforcing phases (welding of aluminum alloys [8]) and carbides (welding of nickel alloys [1]) provokes an avalanche-like increase of dislocation density in the phase internal volumes, along the interfaces and intergranular boundaries, and, as a result, rise of internal stresses and crack formation (Figure 2).

Effect of structure and phase composition of metal. Effect of specific structure-phase constituents on general change of strength characteristics, impact toughness as well as crack resistance of the welded joints was determined based on example of welding of high-strength steels during experimental investigations and further analytical estimations. These steels characterize by wide variety of phase constituents in the joint structure (ferrite F, upper bainite B_u, lower bainite B_l and martensite M). Differential contribution of the various typical structures in change of strength properties and fracture toughness was evaluated based on well-known dependencies of Hall–Petch, Orowan, Krafft etc., whereas, the crack resistance (depending on structures) was evaluated (in accordance with dependencies of Stroh, Conrad) on nature of formation of dislocations in these structures immediately after welding as well as on dynamics of

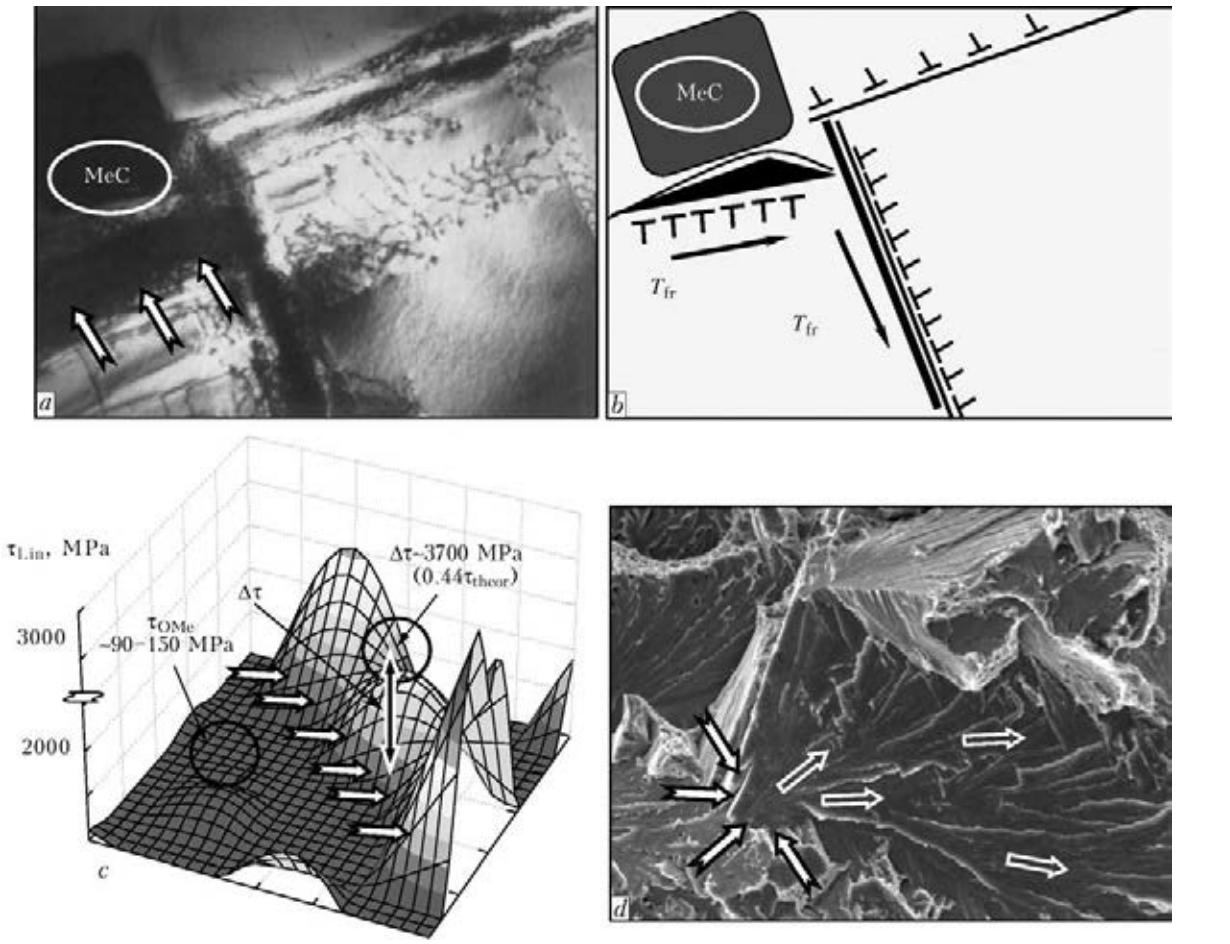

Figure 2. Carbide phases of coarse size as $\tau_{l.in}$ concentrators at intergranular boundaries: *a* — carbide phases at intergranular boundary (×15,000); *b* — schematic representation of crack nucleation in this zone; *c* — $\tau_{l.in}$ rise and their gradients Δτ along intergranular boundary; *d* — nature of brittle transcrystalline fracture in direction opposite to stress concentrator (×1010)

dislocations at further external loading (static, dynamic, cyclic etc.) [9–12]. Capability of the metal structure constituents to relaxation of increasing local internal stresses by plastic relaxation mechanism or brittle fractures was evaluated depending on distribution of the forming dislocation configurations (and, respectively, intensity of local internal stresses) and their extension.

Thus, problem of increase of strength and crack resistance of the wheels and, respectively, reduction of wear level is still relevant in reconstruction repair of surfaces of railway wheels after long term operation, regardless different technological developments. It, in many respects, depends on welding technology and chemical composition of the deposited metal, i.e. on welding wires providing production of the welds with ferrite-pearlite (F-P) and bainite-martensite (B-M) structures.

The investigations were carried out on specimens of solid-rolled railway wheels (from wheel steel 2 of composition, wt.%: 0.55–0.65 C; 0.5–0.9 Mn; 0.22–0.45 Si; ≤0.1 V; not more than 0.03 P and 0.035 S acc. to GOST 10791–89) after reconstruction repair. Mechanized CO_2 welding using Sv-08G2S (F-P weld) and PP-AN180MN (B-M weld) grade wires was used. The results of examination of structure and phase components (F, P etc.), their volume fraction, grain size as well as changes of microhardness of fusion line (FL), HAZ and base metal of railway wheel after reconstruction repair provided the next data.

Application of PP-AN180MN wire from point of view of indices of strength, ductility and crack resistance promoted the optimum structure, which is provided by absence of rapid gradients on size of the structural constituent, uniform phase composition (at transfer from weld metal to wheel steel) and noticeable refinement of structure of the deposited metal (in comparison with F-P weld).

Detailed transmission examinations of weld and HAZ metal, depending on composition of deposited metal, showed the peculiarities of thin structure change (substructure, dislocation density etc.) (Figure 3). The most obvious structural changes in using of Sv-08G2S wire take place at

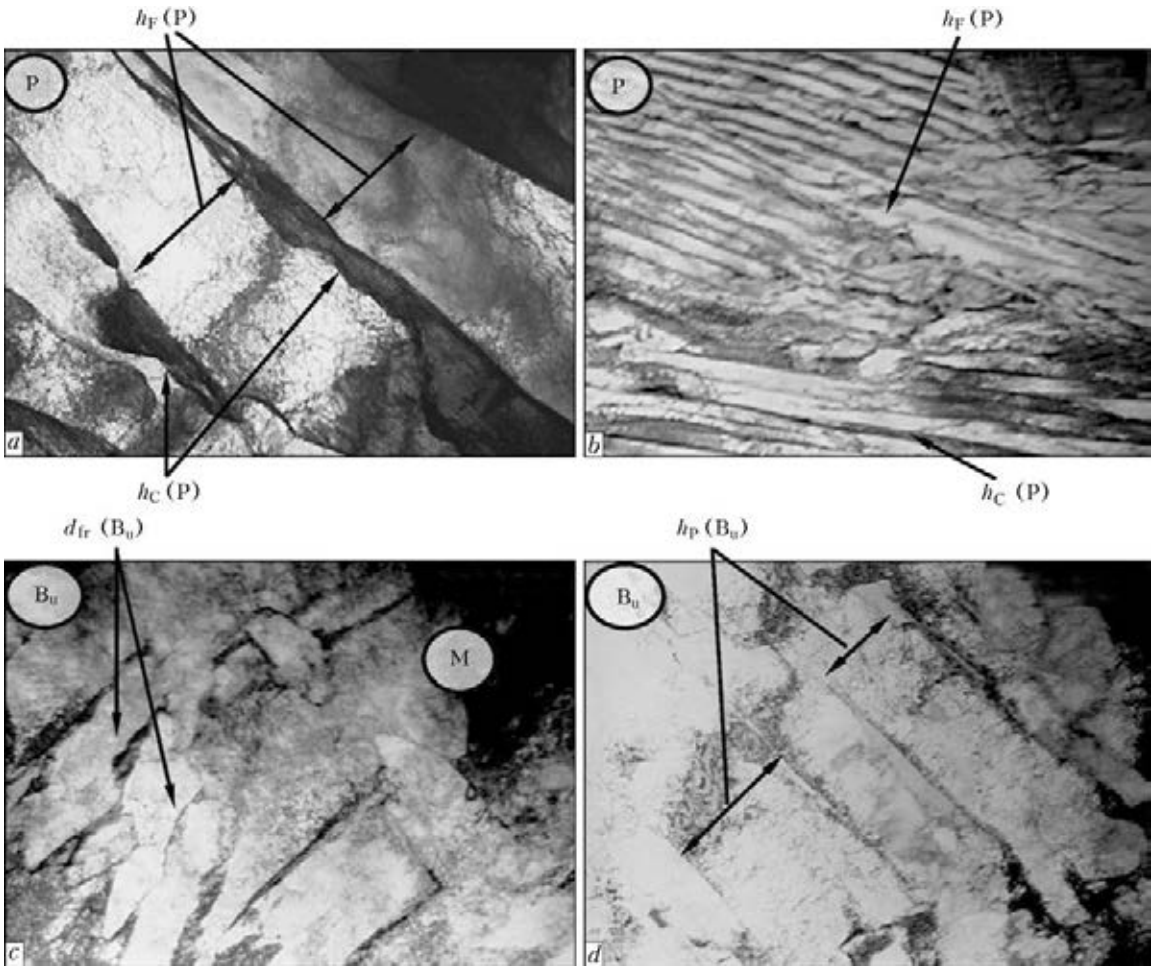

Figure 3. Fine structure of different zones of wheel steel 2 joints in welding using Sv-08G2S (*a*, *b*) and PP-AN180MN (*c*, *d*) wires: weld metal at distance δ ~ 4000 (*a*, *c* — ×20,000) and ~ 500 μm (*b* — ×30,000) from FL; *d* — HAZ area of coarse grain (×30,000)

transfer from weld metal (i.e. deposited metal) to HAZ (to wheel steel) due to rapid refinement of width of ferrite laths (h_F) and cementite plates (h_C) of pearlite structure and increase of dislocation density. This possibly will result in significant strengthening in the fusion zone (from weld side) as well as promote formation of the local stress concentrators being the reason of crack formation (Figure 3, *a*, *b*).

Weld metal (Figure 3, *c*) with B-M structure consisting of B_u, B_l, M and ferrite fringes (F_f) is characterized by formation of the disperse fragmented bainite structure with fragment sizes B_l(d_{fr}) of around 0.15–0.50 μm at uniform distribution of the dislocation density approximately $5\cdot(10^{10}–10^{11})$ cm^{-2}. The width of laths of bainite and martensite structures makes $h_{B_u} \approx$ ≈ 0.5–1.2, $h_{B_l} \approx$ 0.4–0.7 and $h_M \approx$ 1.0–1.5 μm, respectively. The parameters of thin metal structure of area I of HAZ virtually do not change (Figure 3, *d*) at transfer into wheel steel, and uniform distribution of the dislocation density is also observed that, obviously, should promote the optimum combination of strength properties, ductility and absence of the local stress concentrators, i.e. crack formation sources.

Experimental database, obtained as a result of examinations at all structural levels (from macro to micro) allowed carrying out the analytical estimations of the most significant mechanical and service characteristics of the welded joints of wheel steel 2 depending on wire composition. It was shown that total (general) strengthening of weld metal ($\Sigma\sigma_y$ ~ 480 MPa) in the joints welded by Sv-08G2S wire (Figure 4, *a*) was mainly caused by effect of cementite plates ($\Delta\sigma_{d.s}$ ~ 190–230 MPa) of pearlite constituent, and $\Sigma\sigma_y$ rapidly (1.5 times) increases to ~ 800 MPa in approaching to HAZ in local zone of transfer from weld to FL (at depth of about 500 μm from FL) due to rise of contribution of substructure ($\Delta\sigma_s$ to ~ 300 MPa) and dislocation ($\Delta\sigma_d$ to ~ 60 MPa) strengthening.

Smooth change of the general level of strengthening $\Sigma\sigma_y$ from ~ 827–885 (weld metal) to ~ 857 MPa (HAZ area I) takes place in the welded joints, produced with PP-AN180MN wire (Figure 4, *b*) in area of transfer from weld to

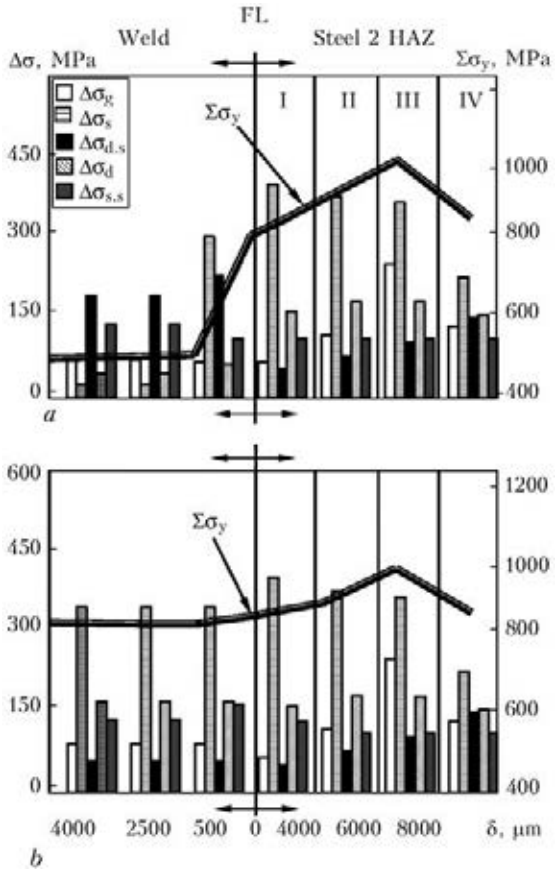

Figure 4. Differential contribution of various structural constituents Δσ in integral value of strengthening $\Sigma\sigma_y$ of metal of wheel steel 2 joints in welding using Sv-08G2S (*a*) and PP-AN180MN (*b*) wires: I–IV — overheating, normalizing, incomplete recrystallization and recrystallization areas of HAZ

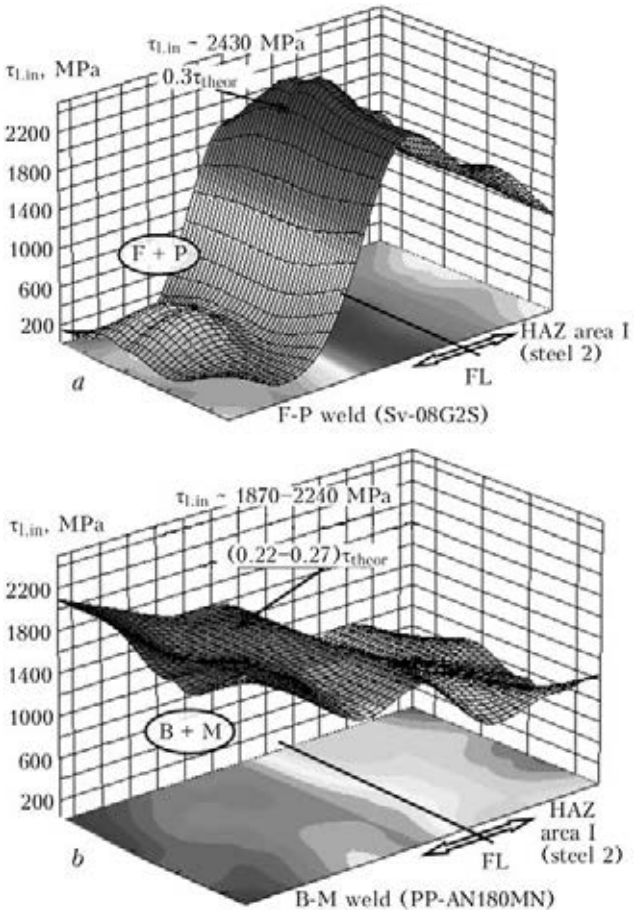

Figure 5. Level of local internal stresses forming in different zones of wheel steel 2 joints, depending on composition of deposited metal: *a* — Sv-08G2S; *b* — PP-AN180MN wire

HAZ. The largest contribution in the integral strengthening is made by substructure ($\Delta\sigma_s$ ~ ~ 345 MPa), carbide phase particles ($\Delta\sigma_{d.s}$ ~ ~ 75 MPa) and rise of general dislocation density ($\Delta\sigma_d$ ~ 140–200 MPa) due to B_l and M constituents. Thus, comparison of the strengthening effect of all forming structures in the investigated F-P and B-M welds allowed determining the most significant on effect structural factors, which are the B_l structures in given case.

The following was shown by the results of calculation estimations of fracture toughness K_{1C} for F-P and B-M welds as well as analysis of K_{1C} and σ_y relationship. It is determined that K_{1C} value is somewhat higher (on average by 20 %) in welding using PP-AN180MN wire (B-M welds) that is caused by grain size refinement, formation of substructure and uniform dislocation distribution. High strength level is also observed that indicates good combination of strength and ductile characteristics of the welded joint. Low K_{1C} index is typical for F-P weld that is related with formation of the coarse grain pearlite constituent, gradient on grain structure size.

Calculation estimations of $\tau_{l.in}$, in comparison of these values with theoretical strength of the material, are given in Figure 5 and show the following. The lower general level of local internal stresses distributed in weld is formed in the joints, produced by Sv-08G2S wire (Figure 5, *a*). $\tau_{l.in}$ value approximately corresponds to 200–400 MPa that makes ~ $0.04\tau_{theor}$. Rapid (by order) increase of the dislocation density from ~ $(4–6)\cdot10^9$ cm^{-2} to ~ $(5–8)\cdot10^{10}$ m^{-2} in approximation to HAZ (at ~ 500 μm depth from FL) and transfer to wheel steel (HAZ area I) results in formation of gradients ($\tau_{l.in}$ ~ 2000 MPa) of the internal stresses (relatively to weld metal). The maximum values of inner stresses structurally initiated by local dislocation accumulations, define $\tau_{l.in}$ of 2240–2430 MPa order, that make $(0.3–0.4)\tau_{theor}$.

Using of PP-AN180MN wire (Figure 5, *b*) provides higher $\tau_{l.in}$ values in the weld metal of 1870–2240 MPa order that makes around $0.25\tau_{theor}$. It is shown that $\tau_{l.in}$ distribution in B-M weld has gradientless nature and uniformly reduce (to 900–1000 MPa) at transfer in HAZ metal of wheel steel 2. Thus, B-M structure,

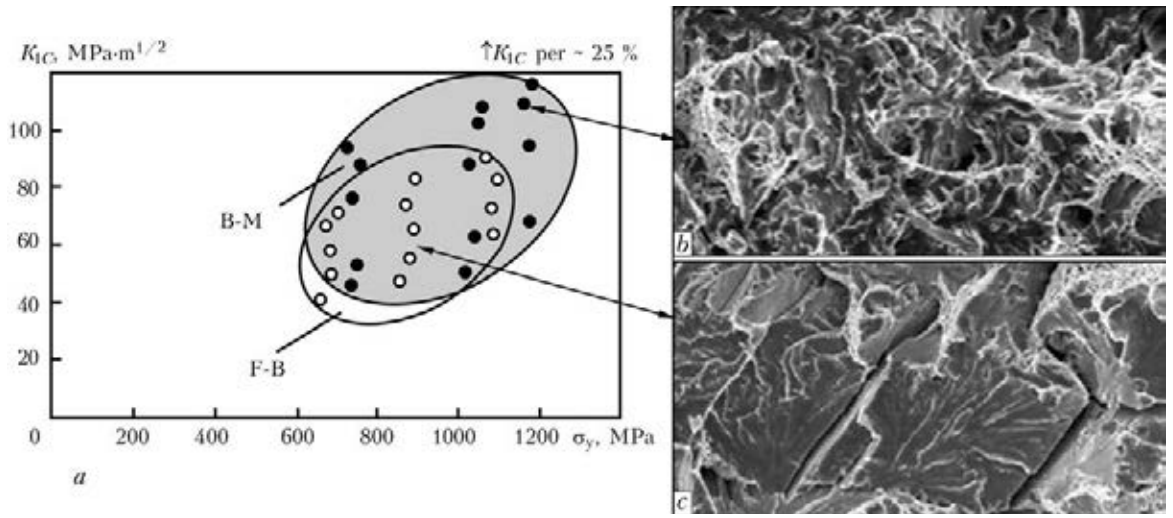

Figure 6. Comparison σ_y and K_{1C} values of welded joints of steel 17Kh2M (*a*), and nature of their fracture depending on type of welding wire (×600); *b* — F-B; *c* — B-M weld

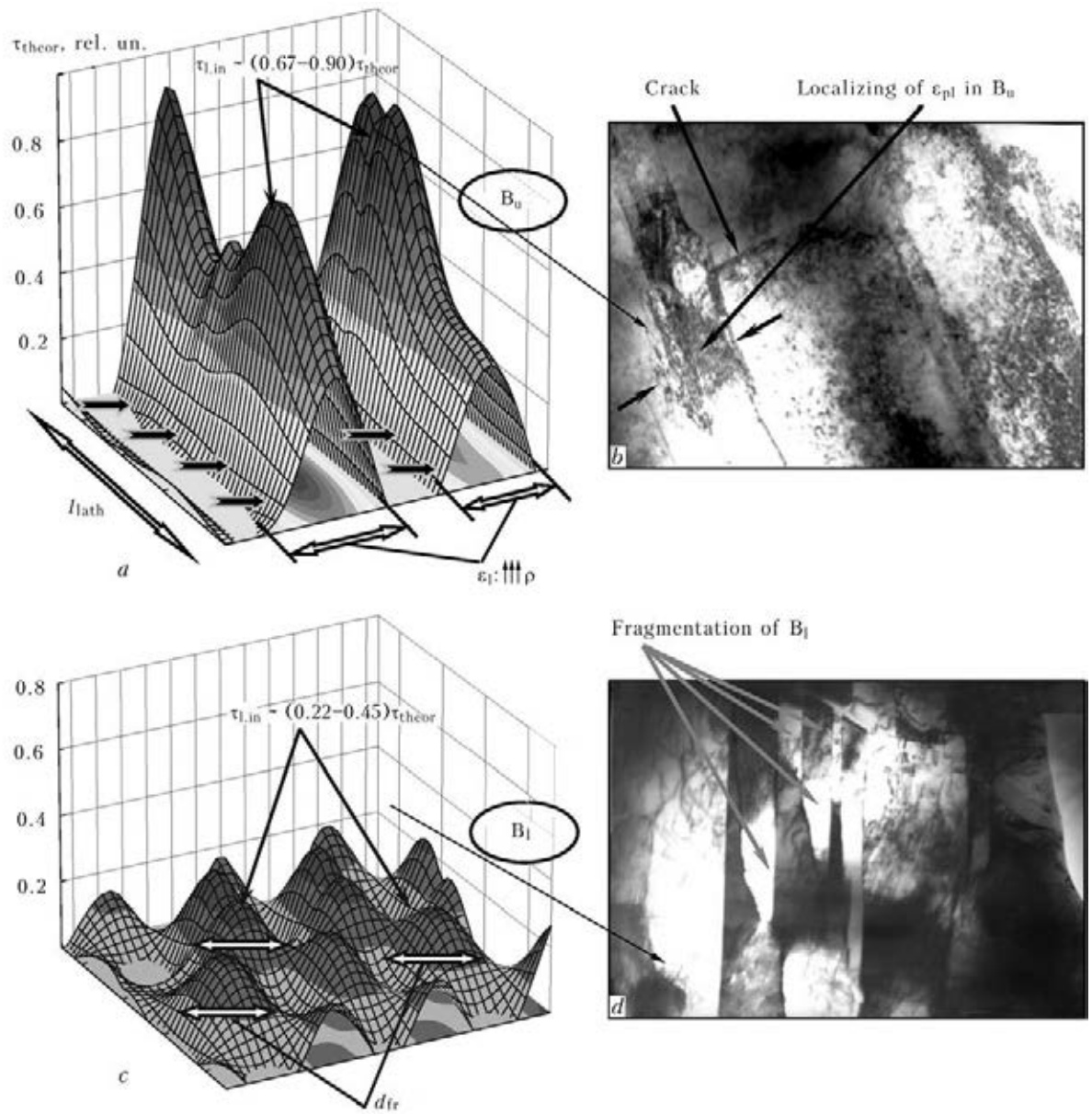

Figure 7. Estimation of $\tau_{l.in}$ values in comparison with τ_{theor} values, and corresponding structure (×30000) of upper (*a*, *b*) and lower (*b*, *d*) bainite

forming from weld metal side as well as wheel steel side (HAZ area I) is characterized by the most uniform distribution of local internal stresses, absence of their gradients and do not provoke crack formation.

Thus, the most optimum on service characteristics (strength, ductility, crack resistance) is application of PP-AN180MN wire in formation of B-M type structure. It was demonstrated by the investigations of structural parameters of joint metal, being formed in reconstruction repair of railway wheels using wires of different chemical composition (Sv-08G2S and PP-AN180MN) as well as analytical estimation (on the basis of structural examinations) of changes of mechanical properties.

Analytical approach to estimation of the relationship of mechanical properties and crack resistance was also used in investigation of welded joints of high-strength steel 17Kh2M using different wire types Sv-08G2S (F-B weld) and Sv-10KhN2GSMFTYu (B-M weld) (Figure 6).

The results of carried estimations of $\tau_{l.in}$ values as well as relationship of these values with theoretical strength of the material, which are given on diagrams of Figure 7 for different variants of weld metal chemical composition (F-B and M-B type), show the following. The highest $\tau_{l.in}$ values in structure of upper bainite are typical for the F-B weld metal (Figure 7, *a*, *b*). And the lowest values, notably at comparatively uniform their distribution in the welded metal, are observed in the case of joint with M-B weld. The latter, obviously, is promoted (as verified by structural examinations) by formation of fine grain M and B_l structures (Figure 7, *c*, *d*). It can be observed that nature of the structures, formed in using of different on chemical composition of welding wires, significantly effect distribution as well as level of the local internal stresses of welded joint metal.

1. Yushchenko, K.A., Belchuk, M.V., Markashova, L.I. et al. (1989) Fine structure of welded joint HAZ of high-temperature nickel alloy of Hastelloy type. *Avtomatich. Svarka*, **2**, 19–22.
2. Savchenko, V.S., Markashova, L.I., Yushchenko, K.A. (1994) Influence of composition and fine structure of welds on processes of thermoplastic strain and formation of underbead cracks in welding of austenitic steels. *Ibid*., **4**, 6–10.
3. Pokhodnya, I.K., Vasiliev, A.D., Orlov, L.N. et al. (1981) To problem of structural and chemical heterogeneity of one-pass weld metal. *Ibid*., **12**, 1–6.
4. Zalevsky, A.V., Parfesso, G.I., Markashova, L.I. et al. (1982) About metallurgical role of zirconium dioxide in welding fluxes. *Ibid*., **4**, 54–56.
5. Pokhodnya, I.K., Kolyada, G.E., Yavdoshchin, I.R. et al. (1982) Influence of oxidation level on peculiarities of structure and mechanical properties of weld metal produced by rutile and ilmenite electrodes. *Ibid*., **2**, 10–14.
6. Markashova, L.I., Zalevsky, A.V. (1985) On mechanism of submicroscopic oxide inclusions. In: *Weldability and technology of welding of structural steels and cast irons*. Kiev: PWI, 112–114.
7. Solokha, A.M., Markashova, L.I., Yushchenko, K.A. et al. (1984) Causes of reduction of low-temperature impact toughness of stably austenitic welds. *Avtomatich. Svarka*, **8**, 24–26.
8. Markashova, L.I., Ryabov, V.R., Statsenko, V.V. et al. (1995) Examination of structure of dispersion-hardened composite material (Al–4 % C). *Ibid*., **6**, 21–26.
9. Markashova, L.I., Grigorenko, G.M., Arsenyuk, V.V. et al. (2004) Structural approach to evaluation of mechanical properties in HAZ of joints from steels and alloys. In: *Proc. of Int. Conf. on Mathematical Modelling and Information Technologies in Welding and Related Processes* (13–17 Sept. 2004, Katsiveli, Crimea, Ukraine). Kiev: PWI, 174–179.
10. Markashova, L.I., Grigorenko, G.M., Poznyakov, V.D. et al. (2008) Structural factors determining the strength, plasticity properties and fracture of welded joints. In: *Proc. of Int. Conf. on Mathematical Modelling and Information Technologies in Welding and Related Processes* (27–30 May 2008, Katsiveli, Crimea, Ukraine). Kiev: PWI, 87–94.
11. Markashova, L.I., Grigorenko, G.M., Poznyakov, V.D. et al. (2009) Structural criterion of evaluation of strength, ductility and crack resistance of metals, alloys, composite materials and their welded joints. In: *Proc. of 4th Int. Conf. on Mechanics of Fracture of Materials and Strength of Structures*. Lviv: PMI, 447–451.
12. Markashova, L.I., Poznyakov, V.D., Gajvoronsky, A.A. et al. (2011) Evaluation of strength and crack resistance of railway wheel metal after long-term service. *Fiz.-Khimich. Mekhanika Materialiv*, **6**, 73–79.

Received 28.03.2014

PECULIARITIES OF DEGRADATION OF METAL OF WELDED JOINTS OF STEAM PIPELINES OF HEAT POWER PLANTS

V.V. DMITRIK and **S.N. BARTASH**
National Technical University «Kharkov Polytechnic Institute»
21 Frunze Str., 61002, Kharkov, Ukraine. E-mail: svarka126@ukr.net

The peculiarities of degradation of structure and damageability of metal of welded joints of the steam pipelines of heat power plants of long-term operation period (more than 250,000 h) under the conditions of creep and low-cyclic fatigue are given. It is shown that welded joints of steels 15Kh1M1F and 12Kh1MF are damaged mostly along the areas of fusion, overheating and partial recrystallization of metal in the near-weld zone and also in the places of joining pipe elements of different thicknesses. 13 Ref., 1 Table.

Keywords: *welded joints of steam pipelines, degradation, structure, creep cracks, fatigue cracks, carbides*

The revealing of peculiarities of degradation of structure of metal of welded joints of steam pipelines of heat power plants of long-term operation period (more than 250,000 h) under the conditions of creep and low-cyclic fatigue is challenging as the effect of initial stage of their damageability. The damageability of steam pipelines mostly occurs simultaneously by the mechanism of creep micropores formation and mechanism of fatigue microcracks formation [1–4]. Welded joints of steam pipelines, characterized by a considerably increased structural, chemical and mechanical heterogeneity, are respectively damaged more intensively (except of bends) than the base metal. The service life of welded joints of steam pipelines amounts approximately to 0.6–0.8 of the base metal life [2, 5–9, 11–12].

The damageability of welded joints of steam pipelines (Table) is provided by technological, design and service factors. During service life of welded joints of more than 250,000 h, the peculiarities of damageability, revealed by metallographic methods, are strictly different from the similar peculiarities of damageability of welded joints, life duration of which amounts to 60,000–200,000 h. [2, 10]. The metal structure of HAZ of welded joints of steam pipelines as well as that of weld and base metal is transformed at different intensiveness into ferrite-carbide mixtures, which are differed by grain size of α-phase; level of grains polygonization; rate of carbide reactions $M_3C \rightarrow M_7C_3 \rightarrow M_{23}C_6$; rate of coagulation of carbides of the group I; level of segregation of chromium and molybdenum in near-boundary zones of grains of α-phase; presence of places, where boundaries of grains of α-phase detach from coagulating carbides; local liquidation of grain boundaries of α-phase, which can be considered as an initial stage of primary recrystallizaiton [7, 9–10].

The change in metal structure of long-term operated steam pipelines is predetermined by physical and chemical processes, the intensiveness of which in metal of welded joints of steam pipelines is stronger than in their base metal [9–10, 13]. The presence of difference in gradients of chemical potentials of chromium and molybdenum across the section of crystals of α-phase causes their diffusion movement to the near-boundary zones of crystals, thus leading to segregation phenomena. The conditions for occurrence of carbide reactions $M_3C \rightarrow M_7C_3 \rightarrow M_{23}C_6$ are created. The release of carbon from M_3C and M_7C_3 results in formation of new carbides of the group II of Mo_2C and VC. In carbides the amount of molybdenum reaches to 50 %.

It was revealed that VC carbides almost do not coagulate at the service life of welded joints (steels 15Kh1M1F and 12Kh1MF) up to 300,000 h. It is rational to specify the capability of Mo_2C carbide to coagulation. The decrease in chromium and molybdenum in the nodes of the crystal of α-phase decreases the retardation effect of dislocations, which results in polygonization of grains of α-phase (formation of subgrain structure).

At the local clustering of dislocations near the grain boundaries of α-phase they can partially penetrate through the boundary and break up in other grain in the form of vacancies, interstitial atoms, and also can cut off the elongated carbides $M_{23}C_6$. The energy of grains boundaries grows to the level facilitating the formation of dislocations in the neighboring grains.

Types of damageability of welded joints of steam pipelines at their long operation (more than 250,000 h)

Damageability zone. Types of cracks. Direction of crack propagation	Metallographic peculiarities of damageability	Causes of damageability
Creep cracks		
Zones of fusion, overheating and partial recrystallization of HAZ metal, weld metal (WM) and rarely base metal (BM). The cracks are propagating from the outer surface of welded joints perpendicularly to the axis of steam pipeline element. Transverse cracks are formed in welded T-joints with a thinned wall of connecting pipe.	Along the boundaries of the contact of 3 or 2 coarse grains of α-phase, at the places of contact of grains with coagulating carbides $M_{23}C_6$. Along the grain boundaries of α-phase, where new products of austenite decay in the form of granular pearlite (area of partial HAZ recrystallization) are located.	1. Design, caused by high concentration of local stresses, in the zones of contact of steam pipeline elements of different thicknesses. Presence of undercuts. 2. Technological, caused by presence of original rejected structure or structure close to the rejected one, which is predetermined by an increased welding heat and heat treatment performed with violation of requirements of standard documentation; discrepancy of chemical composition as to requirements of standard documentation. 3. Service, caused by service conditions: difference of real condition of steam pipelines from the design one; increase in number of starts–stops of power units; increased rate of heating up during the process starting; conditions of manoeuvrable operation mode of power units.
Corrosion-fatigue cracks		
Zones of contact of pipe elements of different thicknesses, areas of fusion, overheating and partial recrystallization of HAZ metal, WM and BM (rarely). The cracks are developing from the inner surface of welded joints. Shape of cracks — thread-like, with branches, in the form of blunt crack filled with corrosion products, and sharp cracks with side branches.	Cracks formation occurs along the boundaries and in body of grains, with domination of one or another type, which depends on service conditions.	Initiation and growth of cracks cause mutual effect of cyclic thermal stresses and corrosion environment on metal and are also activated by degradation of structure.

The presence of structural, chemical and mechanical heterogeneities results in higher level of degradation of metal of welded joints than of base metal. To improve the reliability of operation of welded joints of steam pipelines and to increase their service life it is rational to delay the physical and chemical processes, which occur in their metal at the long operation under the conditions of creep and low-cyclic fatigue, that can be possible by applying steels of new generation.

1. Antikajn, P.A. (2001) *Metals and strength design of boilers and pipelines*. Moscow: Energoservis.
2. Khromchenko, F.A. (1992) *Service life of welded joints of steam pipelines*. Moscow: Mashinostroenie.
3. Dmitrik, V.V. (2013) *Welded joints of steam pipelines*. Kharkov: Majdan.
4. Dmitrik, V.V., Tsaryuk, A.K., Bugaets, A.A. et al. (2006) Evaluation of remaining life of welded joints of pipelines for thermal power plants. *The Paton Welding J.*, **2**, 6–10.
5. Dmitrik, V.V. (2004) To creep of welded joints from low-alloy Cr–Mo–V heat-resistant pearlitic steels. *Vost.-Evrop. Zhurnal Pered. Tekhnologij*, **6**, 88–92.
6. *RD 135-34. 1-003-01 (RTM-1s)*: Welding, heat treatment and control of pipe systems of boilers and pipelines in mounting and repair of power equipment. Moscow: NPO OBT.
7. Anokhov, A.E., Alekseeva, I.A. (1982) Accumulation of damages in welded joints of steam pipelines from 12Kh1MF steel during creep process. *Svarochn. Proizvodstvo*, **9**, 34–35.
8. Khromchenko, F.A. (2001) *Reliability of welded joints of pipes, boilers and steam pipelines*. Moscow: Energoizdat.
9. Berezina, T.G., Borodina, E.R., Ashikhmina, L.A. et al. (1974) Fine structure of heat affected zone in welding of 15Kh1M1F steel. *Avtomatich. Svarka*, **12**, 19–22.
10. Khromchenko, F.A., Kalugin, R.I., Lappa, V.A. et al. (1999) Peculiarities of structural changes in welded joints of 15Kh1M1F steel during creep. *Svarochn. Proizvodstvo*, **10**, 12–15.
11. *MU34-70-161–87*: Technical recommendations on metallographic analysis in evaluation of quality and investigation of damage causes of steam pipeline welded joints of 12Kh1MF and 15Kh1M1F steels for heat power plants. Moscow: F.E. Dzerzhinsky VTI.
12. *RD 34.17.421–92*: Type instruction on control and service life prolongation of metal of boiler base elements, turbines and pipelines of heat power plants. Moscow: ORGRES Service of best practice.
13. Dmitrik, V.V., Shelepov, I.G. (2005) To evaluation of remaining life of welded joints of heat power plant pipelines on structural factors. *Energetika i Elektrifikatsiya*, **9**, 41–43.

Received 20.05.2014

INTERACTION OF HYDROGEN WITH DEFORMED METAL

A.P. PALTSEVICH, V.S. SINYUK and **A.V. IGNATENKO**
E.O. Paton Electric Welding Institute, NASU
11 Bozhenko Str., 03680, Kiev, Ukraine. E-mail: office@paton.kiev.ua

This work investigates the peculiarities of formation of residual hydrogen as a result of plastic strain of metal, containing diffusible hydrogen. Characteristic of this process is increase of content of hydrogen trapped by dislocations, $[H]_{def}$. It is testified by appearance of a peak in thermodesorption spectrum with maximum rate of removal at 150–170 °C as well as rise of $[H]_{def}$ at increase of plastic strain level. Also, it was experimentally showed that $[H]_{def}$ reduces after long period of storage of deformed specimens at room temperature. This confirms reversible nature of dislocations as hydrogen traps. A value of hydrogen diffusion coefficient in the plastically deformed weld metal is determined by interaction of hydrogen with dislocations and being 3 orders lower than for the undeformed metal. The experiments showed that rise of metal strength provides for reduction of value of plastic strain, at which fracture takes place, under effect of diffusible hydrogen. At that, content of $[H]_{def}$ in the moment of fracture also significantly decreases with increase of metal strength. 12 Ref., 3 Tables, 5 Figures.

Keywords: *diffusible hydrogen, residual hydrogen, deformation-trapped hydrogen, plastic strain, hydrogen thermodesorption analysis*

Behavior of hydrogen in metals is considered as a rule from point of view of its solubility, diffusion and interaction with structure defects [1, 2]. One of the irregularities of crystalline structure of metal of welds and steels is the dislocations, representing itself linear defects of crystalline structure [3, 4]. Annealed crystals contain from 10^4 to 10^6 dislocations per 1 cm^2. Plastic strain of crystalline materials is carried out by nucleation and movement of the dislocations, at that their density rises to 10^{10}–10^{12} cm^{-2} [5]. Fixing and redistribution of the interstitial atoms (hydrogen, carbon and nitrogen), among which hydrogen has the lowest bonding energy and the highest diffusion coefficient [3, 6–8], take place in iron and steels under effect of the stress dislocation fields. Therefore, hydrogen is fixed first on the «fresh» dislocations [8] formed as a result of plastic strain.

Absorption of hydrogen by weld pool metal takes place in arc welding of steels. Prevention of cold crack formation [9] is a relevant problem for high-strength steels. A mechanism of crack formation in many respects is related to interaction of hydrogen with dislocation structure of weld metal and near-weld zone, caused by thermo-deformation welding cycle. At the same time, level of experimental data, indicating typical peculiarities of the interaction of hydrogen with dislocations in steels and welds, is not enough, regardless the presence of theoretical backgrounds of interaction of hydrogen with dislocation and its role in formation of the cold cracks. Therefore, present work is dedicated to investigation of the interaction of hydrogen with plastically deformed weld metal.

VSt3sp (killed) steel as well as weld metal, produced by single-pass welding using low-hydrogen electrodes UONI-13/55 and pilot electrodes IP (Table 1), were used as material for investigations.

Determination of effect of the cold plastic strain on behavior of hydrogen in metal of single-pass weld was carried out by means of comparison of its condition in relation to residual hydrogen after removal of $[H]_{dif}$ in deformed and undeformed specimens. Deforming of the speci-

Table 1. Chemical composition of investigated materials, wt.%

Material	C	Si	Mn	S	P	Cr	Ni	Ti	Mo	V	Al
Steel VSt3sp	0.12	0.139	0.37	0.022	0.012	0.12	0.10	–	–	–	–
Weld metal (UONI-13/55)*	0.062	0.274	0.96	0.008	0.0019	–	–	0.024	–	–	–
Weld metal (IP)*	0.04	0.270	0.98	0.007	0.015	0.88	2.36	0.005	0.45	0.18	0.007

*Chemical composition was determined by spectral analysis on multilayer deposit.

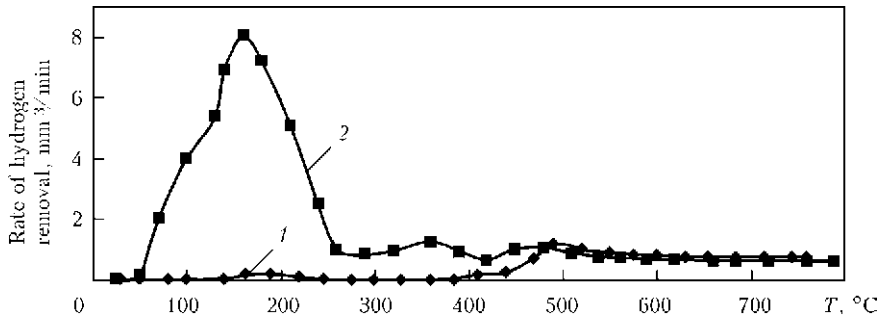

Figure 1. Thermodesorption of residual hydrogen from deformed and undeformed weld metal: *1* — specimen without deformation; *2* — specimen with 6 % deformation

mens in clamps with water-cooled jaws was carried out using bending in mandrel for 2–5 min after cooling in water. The specimens represent themselves a weld bead deposited on workpiece of 10 × 15 × 45 mm size. A value of plastic strain in central part of the weld was set by mandrel curvature radius. Specimens of 15 × 4 × 1 mm size were cut out from upper part of the deposited metal after holding during 5 days at room temperature. Measurement of content of the residual hydrogen was carried out with the help of thermodesorption analysis (TDA) [10]. It was improved for measurement of content of fractions of hydrogen in metal, emitted in process of heating to 900 °C with regulated speed, which made 5 °C/min during analysis.

Figure 1 represents the results of TDA of undeformed weld metal and 6 % bending deformed weld metal, which were deposited using IP electrodes (see Table 1). Given data show that the residual hydrogen, which starts to remove at reaching of temperature around 500 °C, is present in TDA spectrum of the both specimens. Presence of $[H]_{def}$ peak with maximum temperature of 150–170 °C is typical for the deformed specimen. The reason of its appearance is connection of hydrogen with dislocation structure of the deformed metal, from which it is removed by heating. The same peak of hydrogen was received in work [11] in TDA of pure iron after thermal saturation, cold plastic strain and removal of diffusible hydrogen.

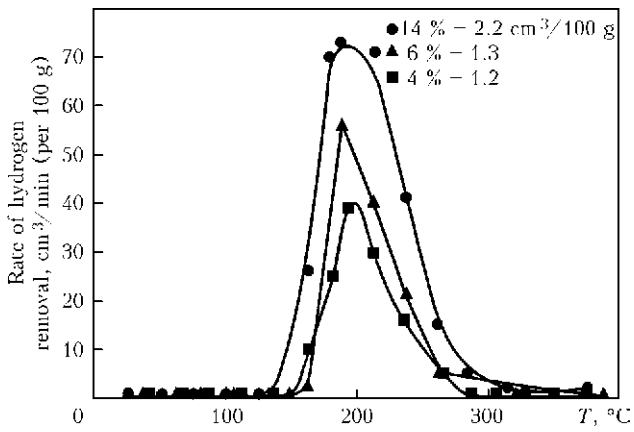

Figure 2. Effect of level of plastic strain on $[H]_{def}$ content

Figure 2 shows effect of the level of plastic strain of single-pass weld metal, produced by UONI-13/55 electrodes, on redistribution of hydrogen. It can be seen on presented data that reduction of the level of plastic strain decreases hydrogen concentration in the deformed metal $[H]_{def}$.

Dislocations are referred to the reversible hydrogen traps due to low bonding energy [3, 6, 7]. In this case desorption of the diffusible hydrogen from specimen should promote transfer of hydrogen, kept by the dislocations, into crystalline lattice and, thus, reduction of $[H]_{def}$ concentration. For verification of reduction of $[H]_{def}$ concentration a series of welded specimens, produced by UONI-13/55 electrodes, was deformed by 6 % and kept in laboratory at T = 16–25 °C. Specimens for performance of TDA and determination of $[H]_{def}$ concentration were cut out from the welded joints within time intervals, indicated in Figure 3. Reduction of hydrogen concentration from 1.4 to 0.2 $cm^3/100$ g is observed in the deformed welds after long period of time. The peculiarity of such decrease is shifting of the maximum of $[H]_{def}$ removal peak from 120 to 170 °C. Thus, removal of hydrogen from dislocation structure of the deformed metal takes place at room temperature.

Investigations of effect of plastic strain on hydrogen diffusion at room temperature were carried out using cylinder specimens, received by sampling of metal from the weld pool into quartz tube during welding by 5 mm diameter UONI-13/55 electrodes. Initial specimen of 4.8 mm diameter and 15 mm length was deformed by flatting (deformation around 30 %) and turned to cylinder shape. The experiments were performed with the help of chamber allowing collection of emitted hydrogen from the specimen approximately during 16 h for one measurement cycle. This permitted to increase measurement sensitivity. Figure 4 shows the kinetics of removal of hydrogen at room temperature for the deformed and undeformed metal.

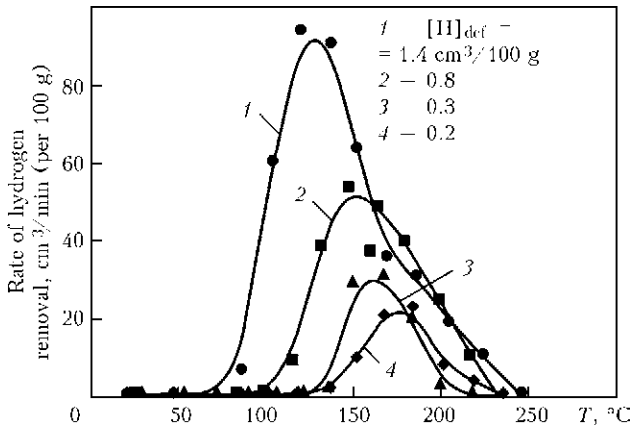

Figure 3. Thermodesorption of hydrogen from welded specimens: *1* — after 5; *2* — 64; *3* — 95; *4* — 124 days

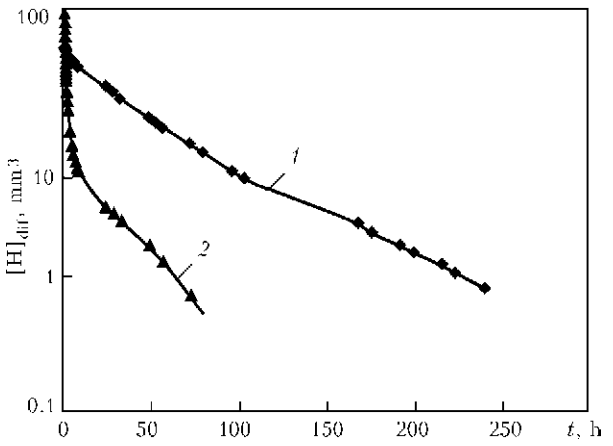

Figure 4. Kinetics of hydrogen removal from deformed (*1*) and undeformed (*2*) specimens

TDA of the specimens after end of the stage of measurement of hydrogen removal kinetics showed presence of $[H]_{def}$ in the deformed specimen in the amount of 0.6 ml/100 g with maximum removal rate at T = 150 °C, and absent of $[H]_{def}$ in the undeformed specimen. Virtually all hydrogen in plastically deformed metal is trapped with the dislocation structure. In order that the hydrogen atom can escape from the metal, it firstly should break the energy barrier and detach from the dislocation holding it. Therefore, value of diffusion coefficient in the deformed metal is determined by interaction of hydrogen with dislocations and makes $3.2 \cdot 10^{-8}$ cm^2/s. Value of effective diffusion coefficient for the undeformed metal in the beginning of degassing makes 10^{-5} cm^2/s, and this value gradually decreases to $3 \cdot 10^{-8}$ cm^2/s after removal of 90 % of diffusible hydrogen.

Effect of hydrogen on fracture of steel VSt3sp and weld metal, produced by relemting of pilot electrode IP in copper water-cooled mould, was determined by uniaxial tensile tests of preliminary hydrogen-charged specimens using servohydraulic machine INSTRON-1251 at deformation rate 10^{-3} s^{-1}. Hydrogen saturation of the specimens was electrolytic in 5 % solution of sulfuric acid with 0.05 % addition of sodium thiosulfate at current density of 10 mA/cm^2 during 4 h. Table 2 shows the results of mechanical tests. $[H]_{dif}$ was removed from the fractured specimens at room temperature during 5 days after mechanical tests, and then TDA was carried out (Figure 5). It can be seen based on given data that fracture of metal of high-strength weld, containing hydrogen, takes place at significantly lower value of the plastic strain than that of steel VSt3sp. At that, content of $[H]_{def}$ at the moment of fracture for high-strength weld metal is noticeably lower than for steel VSt3sp. Fracture of VSt3sp steel specimen provokes formation of hydrogen trapped by plastic strain and its content makes $[H]_{def}$ = 1.2 cm^3/100 g. At that, 0.65 cm^3/100 g of hydrogen is contained in the dislocations (peak at 150 °C) and 0.55 cm^3/100 g is present in molecular form in the microvoids (peak at 250 °C) [12].

Structure and properties of the plastically deformed steels are recovered by heating at (0.4–0.5)T_{melt} (recrystallization annealing). Heat treatment to indicated temperatures effects the dislocation structure [8] and can influence its interaction with the dissolved hydrogen. In this connection the investigations were carried out on effect of treatment temperature of the deformed weld metal on its interaction with dissolved hydrogen.

Single-run welds on steel VSt3sp, deposited by UONI-13/55 electrodes, which were stored after welding at T = 20–25 °C during one month, and then bending deformed by approximately 16 %, were used as metal specimens. Specimens of 15 × 5 × 1 mm size were cut out from weld metal upper layer. They were heat treated at 20–950 °C temperature range in argon media and then electrolytic hydrogenation was carried out

Table 2. Mechanical properties of materials studied

Material	$\sigma_{0.2}$, MPa	σ_t, MPa	δ, %	ψ, %	$[H]_{dif}$, cm^3/100 g	$[H]_{def}$, cm^3/100 g
Steel VSt3sp	270	420	33.4	54	0	0
	250	420	15.6	15	8.5	1.2
Weld metal (IP)	670	930	15.3	55	0	0
	720	830	0.7	1	8.0	0.15

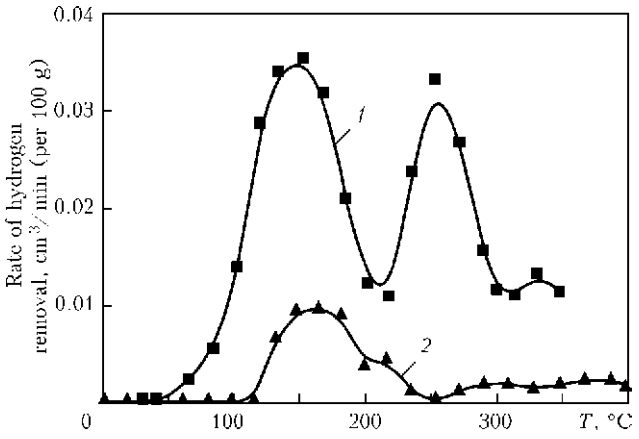

Figure 5. Spectrum of thermodesorption of residual hydrogen from specimens after fracture: *1* — steel VSt3sp, $[H]_{def}$ = 1.2 cm^3/100 g; *2* — IP weld metal, $[H]_{def}$ = = 0.15 cm^3/100 g

Table 3. Effect of heat treatment of deformed weld metal (UONI-13/55) on electrolytic hydrogen saturation

Number of experiment	Condition of specimen	Heat treatment*, °C	$[H]_{dif}$, ml/100 g	$[H]_{dis}$, ml/100 g
1	Deformation-free	Without HT	2.2–3.0	0
2	16 % deformed	20	7.4–7.7	0.2
3	Same	950	4.2	0
4	»	850	2.3	0
5	»	700	4.3	0
6	»	550	8.4	0
7	»	400	7.0	0.2

*Duration of heat treatment 0.5 h.

based on procedure mentioned above. Content of $[H]_{dif}$ at T = 20–25 °C was measured using chromatographic method after hydrogenation. TDA of $[H]_{res}$ was carried out after $[H]_{dif}$ desorption ending. Table 3 gives the experiment results. It can be seen from presented data that heat treatment of the specimens at $T > A_3$ (950 °C) and below A_1 including 550 °C, removes the dislocation structure, capable to interact with the dissolved hydrogen due to reduction of the dislocation density, and, probably, formation of Cottrell clouds by nitrogen and carbon atoms, having stronger bonding energy than hydrogen. Capability of the dislocation structure to interact with hydrogen in the process of electrolytic saturation is still preserved in treatment at 400 °C and below. Thus, the heat treatment temperature, which provides change of effect of the dislocation structure on hydrogen absorption, agrees with the temperature of crystallization treatment of the deformed steel.

Conclusions

Interaction of the dissolved hydrogen with the dislocation structure, forming as a result of plastic strain of steels and welds, was determined in experimental way. Typical temperature of removal of the hydrogen fraction, bonded with dislocation fracture, is 100–200 °C with maximum rate of removal at 150–170 °C.

Content of dislocation-trapped hydrogen in the metal is unsteady and reduce in dwell time at room temperature, that indicates reversible nature of dislocations as hydrogen traps.

Removal of hydrogen from crystalline lattice and dislocations is general process, characterizing by variable value of diffusion coefficient. The diffusion coefficient, which is determined by trapping of hydrogen with dislocation, is 3 orders lower than the coefficient of hydrogen diffusion in the crystalline lattice.

Value of plastic strain, which provides for fracture, reduces under effect of diffusible hydrogen with the increase of metal strength. At that, content of hydrogen trapped by dislocations at the moment of fracture also significantly reduces with rise of metal strength.

1. Geld, P.V., Ryabov, R.A. (1974) *Hydrogen in metals and alloys*. Moscow: Metallurgiya.
2. Geld, P.V., Ryabov, R.A., Kodes, E.S. (1979) *Hydrogen and imperfections of metal structure*. Moscow: Metallurgiya.
3. Novikov, I.I. (1975) *Defects of crystalline structure of metals*. Moscow: Metallurgiya.
4. Ivanova, V.S., Gorodienko, L.K., Geminov, V.N. et al. (1965) *Role of dislocations in strengthening and fracture of metals*. Ed. by V.S. Ivanova. Moscow: Nauka.
5. Gulyaev, A.P. (1978) *Metals science*. 5th ed. Moscow: Metallurgiya.
6. Kolachev, B.A. (1985) *Hydrogen brittleness of metals*. Moscow: Metallurgiya.
7. Maroeff, I., Olson, D.L., Eberhart, M. et al. (2002) Hydrogen trapping in ferritic steel weld metal. *Int. Materials Rev.*, 47(**4**), 191–223.
8. Cotterill, P. (1963) *Hydrogen embrittlement of metals. Successes of physics of metals*. Vol. 9. Moscow: Metallurgizdat.
9. Pokhodnya, I.K., Yavdoshchin, I.R., Paltsevich, A.P. et al. (2004) *Metallurgy of arc welding. Interaction of metals with gases*. Kiev: Naukova Dumka.
10. Paltsevich, A.P. (1999) Chromatographic method for determination of hydrogen content in components of electrode coatings. *Avtomatich. Svarka*, **6**, 45–48.
11. Choo, W.Y., Jai Yong Lee (1982) Thermal analysis of trapped hydrogen in pure iron. *Metallurg. Transact. A*, **13**, 135–140.
12. Moreton, G., Coe, F.R., Boniszewski, T. (1971) Hydrogen movement in weld metal. Pt 1. *Metal Construction and British Welding J.*, 3(**5**), 185–187.

Received 25.04.2014

EFFECT OF SCANDIUM-CONTAINING WIRE ON STRUCTURE AND PROPERTIES OF JOINTS OF ALUMINUM-LITHIUM ALLOYS PRODUCED BY ARGON-ARC WELDING

L.I. MARKASHOVA, O.S. KUSHNARYOVA and **I.I. ALEKSEENKO**
E.O. Paton Electric Welding Institute, NASU
11 Bozhenko Str., 03680, Kiev, Ukraine. E-mail: office@paton.kiev.ua

Relevance of application of complex experimental-analytical approach for estimation of the most important mechanical properties is shown by the example of welded joints of complexly alloyed aluminum-lithium alloy 1460 of Al–Cu–Li system, produced by argon-arc welding using filler wires Sv-1201 and Sv-1201 + + 0.5 % Sc. The estimation of service properties (strength, ductility, crack resistance) of the welded joints was carried out considering specific contribution of structural factors (chemical composition, grain, subgrain and dislocation structure as well as size and volume fraction of forming phase precipitates). Effect of each of specific structural-phase parameters on mechanical properties of the welded joints, their change under influence of postweld heat treatment and external loads as well as role of structural-phase condition for concentration and mechanism of relaxation of the internal stresses at metal alloying with scandium were determined. 12 Ref., 5 Figures.

Keywords: *aluminum alloys, welded metal, scandium, heat treatment, structural-phase condition, phase precipitates, substructure, dislocation density, service properties, crack resistance*

Approach to optimizing and correction of structure ↔ property relationship with technology of welding and postweld heat treatment (PWHT), which should provide sufficient level of welded joint service properties [1], is highly relevant considering rising necessity in materials for manufacture of structures, operating under complex service conditions, that to significant extent refers to airspace equipment. Superlight Al–Li alloys can be referred to such materials with special properties. They have sufficient level of specific strength, ductility and crack resistance under complex service conditions as well as manufacturability at cryogenic temperatures [2, 3].

In this case it should be noted that some important properties of the complexly alloyed Al–Li alloys (strength characteristics, fracture toughness, crack resistance, resistance to external loads, including dynamic ones) rapidly change in process of manufacture of the structures and at their operation, that is mainly related with special structural-phase transformations in process of different technological operations as well as under effect of welding conditions [3]. Changes of the mechanical properties of similar types of alloys are also representative from this point of view. They are caused by heat treatment and related not only with effect of chemical composition and main structural factors, but also with changing of their phase composition [4].

Estimation of effect of the different special structure-phase constituents on change of the most important for service conditions mechanical properties, namely strength indeces and ductility of the welded joints, is relevant considering complexity of the structure-phase condition of these materials and, in particular, processes of phase formation under various conditions of thermodeformation influence. It is also interesting to study an effect of structural and phase characteristics of the welded joints on process of accumulation of the internal stresses and possibility of their plastic relaxation, that indicates crack resistance of material being deformed, in particular, under complex aerodynamic conditions.

Solving of such problems, first of all, require the most complete experimental database, reflecting real structure-phase composition of examined material, which is formed using technological modes of argon-arc welding, changes of this state under conditions of PWHT and external loads.

The basic experimental information about structure-phase condition of the weld metal of aluminum alloy 1460 welded joints (Al–3 % Cu–2 % Li–0.08 % Sc), produced using filler wires Sv-1201 (Al–6.5 % Cu–0.25 % Zr–0.3 % Mn) with scandium (0.5 %) and without it, was received during the following stages of examina-

Figure 1. Microstructure (×30,000) of weld metal of Al–Lu alloy 1460 welded joints produced using filler wire Sv-1201 (*a*, *c*, *e*) and Sv-1201 + 0.5 % Sc (*b*, *d*, *f*): *a*, *b* — after welding; *c*, *d* — after annealing; *e* — near-boundary PFZ; *f* — density of distribution of phases and dislocations in near-boundary PFZ

tion: 1 — immediately after argon-arc welding; 2 — PWHT (aging at T = 150 °C during 22 h and annealing at T = 350 °C for 1 h); 3 — external dynamic loading of produced welded joints. Complex methodological approach, including optical, analytical scanning microscopy (Philips SEM 515, Holland) as well as microdiffraction transmission electron microscopy (JEOL JEM-200CX, Japan) with accelerating voltage 200 kV, was used for the examination at different structural levels.

The examination of structure-phase changes in weld metal of the joints after welding and PWHT depending on scandium alloying found [5–7] that application of Sv-1201 wire without scandium immediately after welding forms grain structure, differing by special structure-phase condition inside the grains (Guinier–Preston zones, Al_3Li, Al_3Zr) and intergrain boundary (IGB). More exactly it is caused by presence in IGB of the eutectics, which are complex on phase composition, solid, elongated and consist mainly from Al–Li and Al–Cu phases, as well as formation of special near-boundary zones free from precipitates (PFZ), which as a rule provokes decrease of mechanical properties of the welded joints (Figure 1, *a*, *d*).

The following peculiarities of structural changes are observed after welding using of Sc-containing wire Sv-1201.

First of all, size of the weld crystalline particles are almost 3 times lower than in use of filler without scandium (Figure 1, *b*). PWHT (350 °C, 1 h) results in refining of the substructure (blocks, subgrains). This promotes the more active redistribution of the chemical elements, that

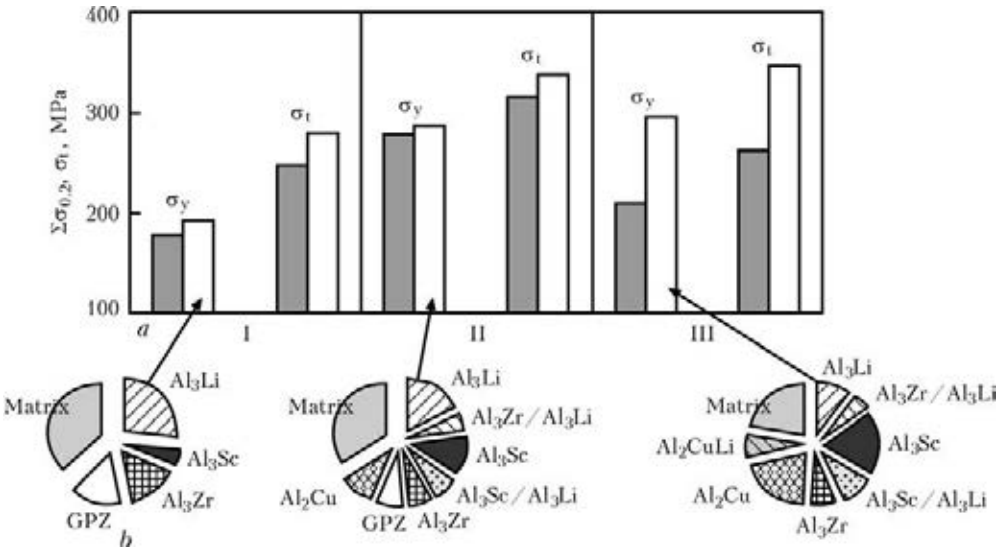

Figure 2. Histogram of differential contribution of separate structural parameters in integral change of yield strength and tensile strength of welded joint of alloy 1460, produced using filler wire Sv-1201 (dark columns) and Sv-1201 + + 0.5 % Sc (white) (*a*), and sector diagrams of volume fractions of phases in use of Sv-1201 + 0.5 % Sc (*b*): I — after welding; II — aging (150 °C, 22 h); III — annealing (350 °C, 1 h)

is caused by processes of solid solution decomposition and further formation of new phases (Figure 1, *c*). Additional scandium alloying also provides for rise of the general dislocation density and activation of the processes of their redistribution (Figure 1, *d*).

Secondly, heat treatment at scandium alloying promotes change of IGB structure, namely density of the grain boundary eutectics becomes somewhat weaker (loose) and volume fraction of lithium phases along IGB significantly reduces. The Sc-containing phase precipitates forming during heat treatment fill up IGB area and make them significantly narrower, that, in turn, promotes for leveling of negative effect of this zone, clearly observed in the case of scandium absence (Figure 1, *f*). As for the grain boundary eutectic developments, then eutectic in the weld metal with additional scandium alloying «breaks up» during heat treatment and decomposes on separate individual phase developments (Figure 1, *d*).

Experimental results, received at different structural levels from marco- (grain) to micro- (dislocation) allowed carrying out the analytical estimation for determination of differential ($\Delta\sigma$) contribution of the different structure-phase parameters in change of integral ($\Sigma\sigma_y$) values of the mechanical characteristics and, first of all, strength as well as ductility and crack resistance. At that, the estimation of total value of increment of yield strength $\Sigma\sigma_y$ for the weld metal without scandium and with scandium was carried out on analytical dependencies of Hall–Petch, Orowan etc. [8–10] considering resistance of metal lattice to movement of free dislocations (lattice friction stress $\Delta\sigma_0$), chemical composition (solid solution strengthening $\Delta\sigma_{s.s}$), grain ($\Delta\sigma_g$) and subgrain ($\Delta\sigma_s$) strengthening as well as real dislocation density (dislocation strengthening $\Delta\sigma_d$) and phase precipitates (dispersion strengthening $\Delta\sigma_{d.s}$).

The estimation showed that integral value of the weld metal strength and actual contribution of different structural factors change depending on technological modes (welding, heat treatment) as well as alloying. Increase of strength characteristics ($\Sigma\sigma_y$) approximately by 16 MPa (8 %) immediately after welding, by 8 MPa (3 %) after aging (150 °C, 22 h) and by 86 MPa (29 %) after annealing (350 °C, 1 h) is observed in Sc-containing weld in comparison with weld without scandium. In the latter case, the phase developments have the maximum effect in strengthening (around 31 %) and dislocation density has the lowest one (almost to 7 %). Figure 2, *a* provides for the information on contribution of other structural factors in strengthening for the examined weld compositions at indicated modes. It should be noted that Al_2Co (20 %) and Al_3Sc (20 %) precipitates (Figure 2, *b*) have significant contribution in the level of dispersion strengthening of the weld metal. They are the main strengthening phases. Contribution of the phases of other type in dispersion strengthening is not so significant and makes 5–10 %. Given estimation of changes of the yield strength, carried out with consideration of structures being really formed in the weld metal, allows also estimating the ultimate weld strength (σ_t) using dependence [10]

$$\frac{\sigma_y}{\sigma_t} = \left(\frac{\sigma_y}{\aleph}\right)^2 (1 + m) \sqrt{1 + \frac{2}{1 + m}\left(\frac{\aleph}{\sigma_t}\right)^2},$$

where $m = 0.3$; $\aleph$ is the coefficient of deformation strengthening.

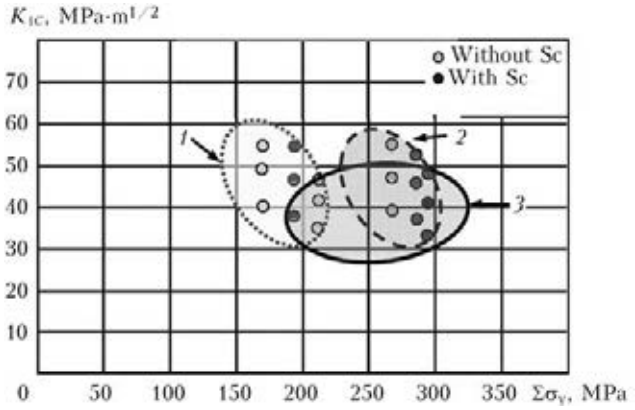

Figure 3. Diagram of change of calculation strength and fracture toughness for weld metal of alloy 1460 welded joint after welding (*1*), aging (150 °C, 22 h) (*2*) and annealing (350 °C, 1 h) (*3*)

Effect of the structural factors on change of parameters of weld metal fracture toughness (K_{1C}) (Figure 3) was also determined. K_{1C} values were determined on Krafft dependence [11] $K_{1C} = (2E\sigma_y\delta_c)^{1/2}$ (where E is the Young's modulus; σ_y is the calculation strengthening; δ_c is the critical crack opening, received on data of fractographic analysis of fractures considering size of facets (or pits on fracture surface)).

It was determined that scandium alloying provides for reduction of K_{1C} parameter on average by 5 % and makes 35–43 MPa·m$^{1/2}$ (Figure 3) together with rise of yield strength of the weld metal immediately after welding. The same situation takes place after aging, namely, on average 6 % reduction of K_{1C} to 32–41 MPa·m$^{1/2}$. Annealing has lager effect on change of K_{1C} parameter of the weld metal without scandium, i.e. 25 % reduction of strength is observed in comparison with K_{1C} after welding. Scandium alloying promotes virtually no change in fracture toughness, and provokes more strength increase, that indicates the optimum combination of resource characteristics of such welded joints (see Figures 2 and 3).

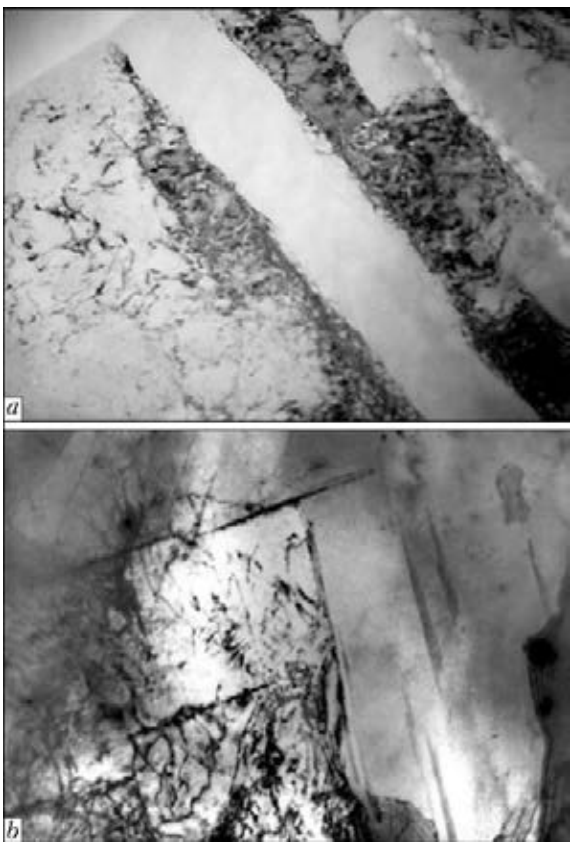

Figure 4. Fine structure (×37,000) of annealed (350 °C, 1 h) weld metal of alloy 1460 welded joint under conditions of dynamic loading: *a* — weld without scandium; *b* — Sc-containing weld

Examination of the weld metal fine structure after annealing (350 °C, 1 h), which particularly demonstrates a role of scandium and further dynamic loading, shows non-uniform distribution of the dislocations with clear deformation localizing in the examined zone without scandium, and the deformed metal receives respectively unstable structural condition. The latter is observed in an avalanche-like barrier-free metal flow, that is indicated by strong slip systems and shear bands (Figure 4, *a*). At that, significant non-uniformity is observed in the distribution of dislocation density along the shear bands, where $\rho \sim 1\cdot10^8$–$2\cdot10^9$ cm^{-2} inside the shear bands, and $\rho \sim 8\cdot10^{10}$–$2\cdot10^{11}$ cm^{-2} directly along the band boundary, that results in formation of steep gradients of the local internal stresses ($\Delta\tau_{l.in}$).

Estimation of $\tau_{l.in}$ considering dislocation density [12] determined that the shear boundaries represent themselves the elongated local stress concentrators, where $\tau_{l.in}$ = 600–1500 MPa ($G/(0.45–0.18)$, where G is the shear modulus). In turn, values of $\tau_{l.in}$ in internal volumes of the shear bands rapidly decrease up to 5–15 MPa (approximately 2 orders) (Figure 5, *a*). As a result, steep ($\Delta\tau_{l.in}$ = 590–1480 MPa) elongated gradient of the local internal stresses, being the reason of crack formation and, consequently, reduction of the properties, is developed in the weld metal without scandium under conditions of dynamic loading

Structure of another nature is observed in the weld metal in the case of scandium alloying under similar conditions of dynamic loading. It is characterized by more uniform dislocation distribution without significant gradients as well as general refinement (fragmentation) (see Figure 4, *b*). At that, phase precipitates of special type with Sc-containing constituents (Figure 5, *b*) provide for stable blocking of the appearing strong slip systems. These phases promote structure fragmentation and, respectively, more uni-

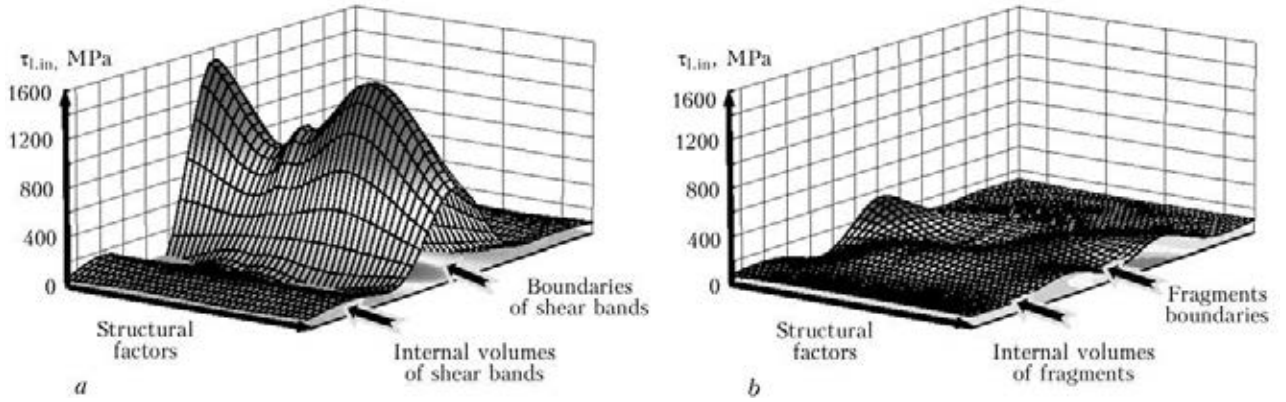

Figure 5. Distribution of local internal stresses in weld metal, produced using filler wire Sv-1201 (*a*) and Sv-1201 + + 0.5 % Sc (*b*), after heat treatment (350 °C, 1 h) and external dynamic loading

form distribution of internal stresses in the weld metal. Formation of the structures of similar type rises possibility of plastic relaxation of the increasing internal stresses due to connection of additional rotation mechanisms to the dislocation ones, that is supported by tough nature of the welded joint fracture.

Conclusions

1. Scandium alloying of weld metal in comparison with its condition without scandium for all studied modes of welding and heat treatment results in the dispersion of phases, grain and subgrain structure, rise of dislocation density and their uniform distribution, activation of processes of phase formation in the internal grain volumes and reduction of volume fraction of grain boundary eutectics.

2. Analytical estimations of differential contribution of the various structural-phase parameters in the change of strength properties (σ_y, σ_t), ductility (K_{1C}) and crack resistance of the examined welded joints showed that scandium alloying promoted for rise of general value of yield strength $\Sigma\sigma_y$ of the welded joints, in particular, after annealing. Phase developments make the largest contribution in strengthening ($\Delta\sigma$), and dislocation density has the lowest one.

3. Scandium alloying promotes the more uniform distribution of rising local internal stresses, fragmentation of strong shear bands, forming in the weld under conditions of dynamic loading, that improves the welded joint crack resistance and, respectively, increase of relaxation possibility of the weld due to connection of additional rotation mechanisms of plastic relaxation to the dislocation ones.

1. Markashova, L.I., Grigorenko, G.M., Arsenyuk, V.V. et al. (2002) Criterion for evaluation of mechanical properties of dissimilar material joints. In: *Proc. of Int. Conf. on Mathematical Modelling and Information Technologies in Welding and Related Processes* (16–20 Sept. 2002, Katsiveli, Crimea, Ukraine). Kiev: PWI, 107–113.
2. Fridlyander, I.N., Chuistov, K.V., Berezina, A.L. et al. (1992) *Aluminium-lithium alloys. Structure and properties*. Kiev: Naukova Dumka.
3. Davydov, V.G., Elagin, V.I., Zakharov, V.V. (2001) Studies of VILS in field of increase in quality and manufacturability of aluminium alloy semi-products. *Tekhnologiya Lyog. Splavov*, **5/6**, 6–16.
4. Zakharov, V.V. (2003) Some problems in application of aluminium-lithium alloys. *Metallovedenie i Termich. Obrab. Metallov*, **2**, 8–14.
5. Markashova, L.I., Grigorenko, G.M., Ishchenko, A.Ya. et al. (2006) Effect of scandium additions on fine structure of weld metal in aluminium alloy 1460 welded joints. *The Paton Welding J.*, **2**, 20–25.
6. Markashova, L.I., Grigorenko, G.M., Lozovskaya, A.V. et al. (2006) Effect of scandium additions on structure-phase state of weld metal in aluminium alloy joints after heat treatment. *Ibid.*, **6**, 7–11.
7. Markashova, L.I., Kushnaryova, O.S. (2012) Welded joints of complexly alloyed aluminium-lithium alloys, structure and operational properties. In: *Transact. on Building, Materials Science, Machine-Building*. Issue 64. Dnepropetrovsk: PGASA, 75–80.
8. Konrad, G. (1973) Model of deformation strengthening for explication of grain size effect on metal flow stress. In: *Extrafine grain in metals*. Ed. by L.K. Gordienko. Moscow: Metallurgiya, 206–219.
9. Kelly, A., Nickolson, R. (1966) *Dispersion hardening*. Moscow: Metallurgiya.
10. Goldshtejn, M.I., Litvinov, V.S., Bronfin, B.M. (1986) *Physics of metals of high-strength alloys*. Moscow: Metallurgiya.
11. Romaniv, O.N. (1979) *Fracture toughness of structural steels*. Moscow: Metallurgiya.
12. Koneva, N.A., Lychagin, D.V., Teplyakova, L.A. et al. (1986) *Theoretical and experimental examination of disclinations*. Leningrad: LFTI, 116–126.

Received 28.03.2014

UNDERWATER WELDING AND CUTTING IN CIS COUNTRIES

V.Ya. KONONENKO
E.O. Paton Electric Welding Institute, NASU
11 Bozhenko Str., 03680, Kiev, Ukraine. E-mail: office@paton.kiev.ua

At the present time there are two main types of welding works under water: hyperbaric dry welding and wet welding. Both methods are successfully applied at the territory of CIS countries for repair and construction of metal structures under water. Hyperbaric dry welding is the most demanded in cases of repair works at underwater gas pipelines passages across water barriers, because it provides high predicted level of mechanical properties of welded joints. Wet welding is demanded at construction and repair of hydrotechnical objects such as berths, basements of extracting platforms and also at lifting and emergency repair of ships and vessels. For its fulfillment the covered electrodes and mechanized welding process using self-shielding flux-cored wires are used. The mechanical properties of welded joints, which are provided by these technologies, are at the level of mechanical properties of joints produced in welding in air using electrodes of the type E42 and E46. However during realization of these technologies there is a possibility of defect formation caused by a sharp cooling of weld metal and human factor during work of a diver-welder under water. At the present time to perform underwater cutting the most challenging are the technologies of underwater electric-oxygen cutting and cutting using exothermal electrodes, which are produced both at the territory of CIS countries as well as beyond their borders. These technologies provide comparatively low level of productivity and necessity of additional mechanical treatment of the cutting zone in case of the further producing of welded joints. Using dry and wet welding at the territory of CIS countries a great volume of works was performed connected with repair of underwater pipelines, berth erections, lifting and repair of ships and vessels. The most significant work at the recent time was performed in construction of off-shore ice-resistant stationary platform «Prirazlomnaya». 9 Ref., 3 Tables.

Keywords: *dry underwater welding, wet welding, covered electrodes, flux-cored wires, mechanical properties of joints, performed works*

At the present time there are two main types of performance of welding works under water [1]:

- hyperbaric dry welding, which is performed inside the dry inhabited chamber, mounted around the welded elements under pressure, the value of which depends on the depth [2];
- wet welding, which is performed under the conditions of direct contact with water under pressure, the value of which depends on the depth of performance of welding works.

Hyperbaric dry welding was applied for the first time by the company «Taylor Diving and Salvage» (USA) in 1967 [2]. The main purpose of this welding method consists in prevention of contact between arc burning zone and metal being welded with water, that offers essential advantages to produce the full-strength welded joint independently of outer conditions and depth. It should be noted that use of this technology as applied to the repair of tubular elements of stationary basements, hulls of ships, berths and other hydrotechnical objects with the developed surface is connected with great material costs. Dry welding also represents a significant inconvenience in inhabited chambers during repair of underwater pipeline passages across small water barriers. In this case it is impossible to use specialized deep-seated ships with the necessary equipment and hoisting mechanisms.

However, considering the high predictable level of quality of joints, produced using dry welding, recently the colleagues of the company «Podvodservis Ltd.» in Russia successively performed a whole number of works on repair of gas pipelines passages across small water barriers using specialized Zakharov caisson (SZC) [3, 4]. SZC is designed for its mounting to the defective area of the repaired pipeline of diameter from 325 to 1420 mm at the depths up to 60 m. SZC represents a diving bell, made in the form of a metallic box opened from the bottom, the side surfaces of which are manufactured with the possibility of its mounting on the pipeline outer surface. The air-tightness of arrangement on the surface of main pipeline is provided by a rubber sealer positioned around the perimeter of box sides adjacent to the outer surface. The welding of pipe defect is performed in gas environment by a diver-welder with diving equipment, working inside the SCZ. The supply of air for breath-

ing of a diver and discharge of exhaled air out of the caisson are performed through the special hose-cable without violations of required composition of gas mixture inside the caisson. Using this equipment the repair works of underwater gas pipeline at the passage across the Lena river at 10 m depth by the OJSC «Sakhatransneftegaz», gas pipeline (branching to Zarechie) of 530 mm diameter, across the Ob river at 8 m depth by the «Tyumentransgaz Ltd.» and also reserve line of 1220 mm diameter of the underwater passage of gas pipeline Yamburg–Yelets 2 were performed.

With the purpose of the further implementation of technology of welding in the specialized caisson under water, in particular, to provide a possibility not only to reweld certain defects of a pipe body, but also to create technology of repair of a pipeline using method of «coil cut-in», the designers of «Podvodservis» together with «Gazprom Transgaz Yugorsk Ltd.» developed, tested and commissioned the repair complex with a fit-on frame [4]. The design of caisson allows embracing all the surface of pipeline of 1220 m diameter and provides a possibility of simultaneous work of two divers-welders. The complex of technical facilities includes the equipment (welding and auxiliary) for cutting, alignment and welding of pipe body, the specialized caisson, designed for sealed positioning on the pipeline and also the fit-on frame, providing alignment of pipe areas during cutting. The complex has equipment for heat treatment and next ultrasonic flaw detection of welds. The work of the repair complex is based on the principle of dry hyperbaric welding in inert gases.

Welding inside the caisson at atmospheric pressure. This technological process is performed under dry conditions at atmospheric pressure. A chamber is put on the pipe, being repaired, and hermetically joined to it. The welder is working inside the chamber and after the performance of repair works it remains on the object. This technological process did not find a wide application in the world practice. The works in this working chamber are restricted by the depth of a basin, which amounts usually to 10–12 m, however, on the Volga river in Russia the repair works at the depth of 30 m were performed using this technology.

Besides the repair of pipelines the dry welding at atmospheric pressure is applied for repair of berth erections. For this purpose the specialized caisson is manufactured, being opened from the side and top part. Sealing along the side surface is performed in places of chamber adjacent to the berth structure being repaired. As a rule, the length of a caisson is 5–6 m, the height is 3–4 m. The caisson is moved during repair of berth structure. After its drying for repair the standard welding consumables, used for welding in air, are applied. Such caissons are used in Lithuania and Latvia. It is quite profitable to perform repair works as far as there is no need in lowering of a diver under water in welding of main number of defects. The repair of these metal structures at depth of more than 3 m is performed using covered electrodes designed for wet welding by the diving equipment.

Wet welding. In wet welding the welder and object, being welded, are located in the water environment. The process is performed without any additional fixtures and devices. Due to that, the welder has more freedom in movements, which makes the wet welding very efficient and economic method of welding under water, first of all, in restoration of metal structures with the developed surface at the depth of up to 20 m [3].

To perform such works the electrodes of foreign production are most often applied in CIS countries, however, in Ukraine and Russia the electrodes for wet underwater welding are also designed and produced under laboratory and industrial conditions. Mechanical properties of the joints, which are provided using these electrodes, are given in Table 1. It should be noted that the field of application of wet method of welding with covered electrodes is restricted due to low mechanical properties of joints, insufficient efficiency of the process and high requirements to the skill of diver-welder.

To increase the probability of producing joints with the predicted level of quality it is necessary to decrease the probability of cold cracks formation, which is achieved due to control of thermal cycle of welding [3]. It can be realized due to technological measures by adjustment of welding condition parameters, facilitating the decrease in cooling rate of welded joint and probability of formation of tempered structures and, as a result, of underbead cracks. It is possible to decrease the cooling rate of welded joint also by deposition of heat insulating layer on its surface.

The experience in manufacture and service of metal structures of pipe steels of increased strength shows that during selection of electrode consumables for its welding in the air it is necessary to try producing the weld metal with higher ductile properties, even if its strength is somewhat lower than the strength of base metal [3]. Ductile weld with the strength lower than that of base metal is a soft interlayer, which

Table 1. Mechanical properties of joints produced using wet welding under water

Grade of electrode	Tensile strength σ_t, MPa	Yield strength σ_y, MPa	Elongation δ_5, %	Impact toughness KCV_{-20}, J/cm^2	α_{bend}, deg, acc. to class B of AWS D3.6M
Covered electrodes					
EPS-52	390–420	Not standardized	6–20	N/D	Not standardized
EPS-AN1	≥ 420	Same	≥ 14	Same	Same
E38-LKI-1P	410	»	≤ 8	»	»
Self-shielding flux-cored wires					
PPS-AN1	400–430	300–320	14–16	≥ 10	180
PPS-AN2	400–440	300–340	13–18	≥ 25	180
PPS-AN5	420–460	320–360	13–17	≥ 25	180
PPS-EK1	400–460	300–360	14–18	≥ 25	180

during tension begins to deform earlier than yield strength of base metal is achieved, that results in contact strengthening of weld metal. A great number of works under water was performed using electrode consumables, providing a considerably lower level of weld metal strength than that of base metal. Some of these works were performed during welding of pipe steels, the carbon equivalent (C_{eq}) of which amounted to 0.38–0.40 %, and σ_t = 440–500 MPa (Table 2). The same as in welding in the air the use of electrode consumables providing weld metal with the lower level of strength than that of base metal (σ_t = 410–430 MPa) allowed solving the problem of repair underwater welding. The weld metal of the lower strength began to deform plastically under the influence of working loads, which caused its contact strengthening. Here, the total level of strength of welded joints was sufficient to provide the reliable operation of underwater passages of gas pipelines.

The technology of mechanized wet underwater welding using self-shielding flux-cored wires, developed at the E.O. Paton Electric Welding Institute [5], is widely applied in the CIS countries since 1969. Technological process is universal and allows obtaining sufficiently high predicted level of mechanical properties of the joints in case of welding of low carbon and a number of low-alloy hull steels at all the spatial positions using flux-cored wires of ferrite class, if a user has certain skills (Table 3). Using this technology the efficiency of the process is considerably increased, which is 3–6 times higher as compared to welding using covered electrodes. This aspect is extremely important during the work of a diver under water. To the disadvantages of the method of mechanized wet welding using self-shielding flux-cored wire, the same as in welding using covered electrode, the sharp cooling of metal of welded joint in water and its significant saturation with hydrogen and oxygen can be referred [3]. It can lead to cold cracks formation in welded joints produced on some low-alloy pipe steels of increased strength with $C_{eq} \geq 0.39$ % using electrode consumables of ferrite class. Using this technological process a number of works on repair of underwater pipeline passages across the water basins [3, 6] and other hydrotechnical objects was performed in the former USSR.

The most significant recent work using the technology of mechanized wet welding was performed in 2004–2005 during construction of the off-shore ice-resistant stationary platform (OIRSP) «Prirazlomnaya» [7–9] at the FSUE «PO Sevmashpredpriyatie». The lower part of the OIRSP is the caisson, representing a welded structure of cold-resistant steels of the sizes 126 × × 126 × 24.3 m and mass of about 70,000 t and providing storage of 700,000 barrels of oil. It is not possible to assembly such a structure on the beds of the plant «Sevmashpredpriyatie». To join the sections (superblocks) the known technology of stage-by-stage afloat assembly was applied using a dry caisson. It consists in the fact that on the stocks in manufacture of each section of 126 × × 31.5 × 24.2 m a half of dry caisson is mounted in its lower part, which is removed later. At the territory of CIS this technology was not used till recently. The joining of two halves of a dry caisson was performed under water at the depth of 8 m using the technology of mechanized wet welding with self-shielding flux-cored wire. The work is characterized by welding in overhead (126 m per section) and vertical (16 m per section) positions. Under supervision of the Russian Maritime Register of Shipping, not taking into account the interruptions for fitting-out of elements of the platform, 1800 m of one-pass weld was made in overhead and vertical positions at the depth of 8 m during 55 working days, taking into account the preparatory-final time. To per-

Table 2. Basic works performed at restoration of underwater pipeline passages across water barriers

Location of work performance	Type of damage	Technology of repair
The Dnieper river, 10 m depth. Water conduit, ∅1020 × 12 mm, steel 09G2 (1969)	Two cracks: 1 — $L \approx 1.5$ m with opening in the upper part of a pipe up to 30 mm, 2 — $L \approx 250$ mm along the weld	Technological backings and additional inserts are introduced inside the repaired area of pipe. They were joined with pipe by multilayer butt welds
The Beysug river, 5 mm depth. Oil pipeline, ∅1020 mm, steel 14KhGS (1970)	Crack along the site butt, due to lack of penetration in weld root	Mechanical grooving with fixation of crack ends by drilling. Groove is filled by multilayer butt weld
The Volga river, 12 m depth (Volgograd city region). Two pipes of water conduit, ∅1020 × 12, steel VSt3sp. The repair was performed within 2 months (1971)	9 areas with cracks of $L \leq 2500$ mm and ruptures of $L \leq 1500$ mm with opening of up to 200 mm	After mechanical grooving the inserts were introduced to windows and then joined to pipe by multipass butt welds of $L \approx 38$ m. Most of welds were located in vertical and overhead positions
The Kazanka river, 6 m depth (Kazan). Water conduit, ∅820 mm, steel VSt3sp (1972)	Partial rupture of pipe, which occurred as a result of violation of laying out technology	After mechanical grooving a patch was mounted to the formed window and then joined to pipe by multilayer butt weld
The Dnieper river, 6 m depth (Kherson city region). Water conduit, ∅720 mm, steel VSt3sp (1973)	Rupture along the site weld in 1/2 diameter	Mounting of two half-couplings with special inner grooving at the defective area. Half-couplings were joined to pipe by fillet multipass welds
The Moskva river, 8 m depth. Gas pipeline passage, ∅720 mm, steel 09G2 (1974)	Under the effect of dynamic loads a crack in HAZ metal of site butt was formed	After mechanical grooving and fixation of ends of crack by drilling, the formed groove was filled by multipass butt weld
The Ukhta river, 10 m depth. Gas pipeline passage, ∅820 mm, steel 14KhGS (1975)	Crack as a result of lack of penetration in root of site butt	Same
The Ob river, 6 m depth (region of Peregrebnoye village). Gas pipeline passage ∅1020 mm, steel 09G2 (1976)	Crack formed during service due to lack of penetration in site butt	»
The Donuzlav lake (Crimea). Depth of 4 m at zero visibility. Gas pipeline passage, ∅720 mm, steel 09G2 (1977)	Cleavages formed as a result of corrosion damage	Mechanic grooving of defective areas. Welding by 1.4 mm diameter wire, as the thickness of metal in the welding zone did not exceed 4 mm
The Daugava river, 18 m depth (region of Riga). Water conduit of ∅720 mm, steel 09G2 (1978)	Complete rupture of pipe	Defective area of pipe was removed by electro-oxygen cutting. An insert of 0.5 mm length with a gap, not exceeding 10 mm, was mounted after mechanical treatment inside the pipe. The insert was joined to pipe using fillet multipass welds
The Ob river, 7 m depth. Passage of oil pipeline Aleksandrovskoye–Anzhero–Sudzhensk by pipe of ∅1020 × × 18 mm, steel 18G2SAF (1980–1981)	Lack of penetration in root of two site butts. Cracks in laying out of siphon	Defective areas of pipe with cracks were removed. After mechanical treatment of formed edges the patches with backing elements were mounted to the pipe using a screw-jack. Due to high carbon equivalent of steel the repair was made using a combined method. The first 3 passes were produced by wet method using special self-shielding flux-cored wire. The further filling of groove was performed using manual welding with covered electrodes in the caisson with preliminary heating of pipe
The Volga river, 5 m depth (Kazan region). Two joining couplings at the city water intake of ∅1420 mm. The work was performed within 30 days (1982)	Gaps between the pipe and joining half-couplings around perimeter of pipe reaching 160 mm	At the distance of 3 m from the repaired couplings the operation hatches were cut out, through which a diver entered inside the pipe and semi automatic machine was delivered. Pipes to half-couplings were joined using multipass fillet welds of 8–20 mm leg. The total length of welds was 28 m. To liquidate large gaps, the covering elements were applied
The Ob river, 12 m depth (region of Nefteyugansk town). Passage of the product conduit by pipe of ∅820 mm, steel 17G1S (1982)	Fracture of site butt at 1/3 of length	The defective area was removed using electro-oxygen cutting. After mechanical treatment the insert with backing elements was mounted into the formed cavity and joined to pipe around perimeter by multipass butt weld

Table 2 (cont.)

Location of work performance	Type of damage	Technology of repair
The Dnieper river, 12 m depth (region of Kremenchug city). Passage of gas pipeline Yelets–Kremenchug–Krivoj Rog. Pipe of ∅1420 × 18.7 mm, steel of type X70 (1987)	Cleavage in site butt	After mechanical grooving with 90° angle of edges opening for the depth of 16 mm the produced groove was filled by multipass butt weld. Flux-cored wire was used providing austenite structure of weld metal
The Kama river, 12 m depth (region of Perm city). Passage of gas pipeline by the pipe of steel 17G1S (1990)	Crack of site butt of 100 mm length	Same

form the works the semi-automatic machines A1660 and PSP-3 [3] for underwater welding and flux-cored wire PPS-EK1 [7–9] were used.

Two repairs of underwater gas pipeline passages (see Table 2) were performed using flux-cored wires providing austenite structure of weld metal, and under the full-scale conditions (Chernomorskoe town) at the depth of 10 m the pipe specimen was rewelded by position welding using the same wire, which withstood the test pressure of 20 MPa [3].

Currently a great volume of works using the technology of mechanized wet welding is performed in Russia at repair of berth erections. The semi-automatic machines for underwater welding A1450 and A1660, produced in the 1980s, and flux-cored wire PPS-EK1 are used. Thus, only the company «Baltijsky Proekt» uses about 900 kg of wire per year to produce mechanized underwater welding, which is quite comparable with that amount of flux-cored wire produced at the PWI for Navy of USSR and for civil purposes.

To realize the technology of mechanized wet welding and also welding using covered electrodes the sets of equipment were designed as well as technological documentation and methods of training for divers-welders were worked out.

Cutting of metal under water. Cutting of metal structures under water is a quite significant element of technological process in performance of underwater technical works. The technology of cutting under water using exothermal electrodes, produced by the leading word manufacturers, is the most challenging today [3]. Unfortunately, it should be noted that such technologies as cutting under water using flux-cored wire and explosion cutting, developed at the PWI, nowadays are practically not demanded. The electrodes for exothermal underwater cutting, designed at the PWI, the production of which was organized in Russia, do not enter the market at the present time.

Some number of electrodes of the grade ANR-T8 and other of 8 mm diameter for electro-oxygen underwater cutting, manufactured under the

Table 3. Characteristic examples of restoration of berth erections and oil extracting platforms

Region	Technology of works performance
Repair of berth erections	
Port Dudinka. Violation of integrity of a sheet-pile wall. Locks between the sheets and piles were separated (1982–1987)	Repair was made in winter after interruption of navigation. Using fillet welds of 6–10 mm leg the doubling sheets of 6–8 mm thickness were welded on. Depth of works fulfillment was from 1 up to 14 m. More than 5 km of berth wall was repaired
Klaypeda port. Sheet-pile berth wall (1982–1983)	Technology was the same. Depth was 2–12 m, length of fillet welds with 6–8 mm leg was 287 m
St.-Petersburg sea port. AP BASU «Baltijskie Buksiry» (1996)	Technology was the same. Depth of 2–12 m, total length of fillet welds with 8–10 mm leg was 360 m
Repair of stationary oil extracting platforms	
Deep water platform 12 at the 26 Baku Commissars sea oil deposit at the Caspian Sea (1991)	Restoration of load-carrying capacity of tubular element of vertical support of 820 × 10 mm of steel 17GS. The support was completely cramped at the depth of 4 m. The defective area was removed. New area of vertical support was joined to platform by butt welds
Reconstruction of underwater part of support unit of multipurpose underwater station LAM-22 (2000)	Arrangement of underwater structures with the anodes PAKM-75. Within 12 days 115 anodes were assembled and welded at the depth of 20 m. The total length of welds, made at all spatial positions, was 55.2 m. The performance of works was supervised by the representative of Lloyd, Germany

laboratory conditions, reaches the consumer. The quality of these electrodes is sufficiently high, which is confirmed by their regular use at the territory of Russia and Ukraine.

Tendencies of progress. In our opinion, the technology of welding in a dry chamber, containing both welder and also welding unit, will be also further used for assembly and repair of critical hydrotechnical constructions, such as high-pressure pipelines and separate elements of stationary platforms under water and also in case of low transparency of water.

We assume the increase in volumes of repair works using new covered electrodes with improved welding and technological properties. At negligible volumes of welding works the application of electrodes is preferable in case of obtaining the strength values adequate to the mechanized method.

The mentioned consumables allow making the conclusion about high efficiency of technology of mechanized wet welding using self-shielding flux-cored wires. The quality of works depends greatly on the level of specialist training. Technological solutions developed and tested in practice allow quick and efficient repair of ship hulls and other hydrotechnical objects at minimum labor costs.

Conclusions

1. Technology of mechanized wet welding under water using self-shielding flux-cored wire was successfully applied for repair of underwater pipeline passages across the water barriers at the end of the last century.

2. At the present time the repair of underwater pipeline passages using technology of welding under hyperbaric conditions is the most challenging, taking into account a considerable level of wear both from the position of corrosion damage as well as from the position of long effect of dynamic loads.

3. The application of welding technology inside the caisson at atmospheric pressure for repair of underwater pipeline passages is little promising.

4. For underwater cutting the electrodes for exothermal cutting are the most challenging.

1. Paton, B.E., Savich, I.M. (1987) To the 100th anniversary of underwater welding. *Avtomatich. Svarka*, **12**, 1–2.
2. Evans, N.H. (1974) Welding in offshore constructions. *Metal Constr. and British Welding J.*, **5**, 153–157.
3. Kononenko, V.Ya. (2011) *Underwater welding and cutting*. Kiev: Ukraina.
4. Kononenko, V.Ya. (2010) Application of method of dry underwater welding in repair of underwater passages of gas and oil pipelines in Russia. *The Paton Welding J.*, **5**, 42–46.
5. Savich, I.M. (1969) Flux-cored wire underwater welding. *Avtomatich. Svarka*, **10**, 70.
6. Kononenko, V.Ya. (2004) *Technology of underwater welding and cutting*. Kiev: Ekotekhnologiya.
7. Kononenko, V.Ya. (2005) Technology of wet mechanized welding in construction of IRSSP «Prirazlomnaya». *The Paton Welding J.*, **9**, 33–35.
8. Kononenko, V.Ya. (2006) *Technologies of underwater wet welding and cutting*. Kiev, PWI.
9. Kononenko, V.Ya. (2005) Application of the technology of mechanized underwater welding in construction of OIRSP «Prirazlomnaya». *The Paton Welding J.*, **12**, 47.

Received 22.04.2014

MARKET OF WELDING CONSUMABLES IN UKRAINE

A.A. MAZUR, S.V. PUSTOVOJT, V.S. PETRUK and **N.S. BROVCHENKO**
E.O. Paton Electric Welding Institute, NASU
11 Bozhenko Str., 03680, Kiev, Ukraine. E-mail: office@paton.kiev.ua

The systemized economic and statistic information about the state and development of Ukrainian market of welding consumables is presented. The quantitative and cost values of volumes of production, consumption and export–import of welding consumables are given. 5 Tables, 13 Figures.

Keywords: *welding, welding production, equipment, welding consumables, economy, statistics, market*

Welding as a method for producing permanent joints of metals and non-metals is a key technology in production of more than a half of GDP in the industrialized countries. It specifies the serious tasks before welding production of any country, which are to be solved considering high nowadays requirements.

Welding production in Ukraine (Table 1) includes a highly-developed research component, production of modern welding equipment and consumables as well as structures and other welding products and the system of training of engineering and working staff. All this allows demonstrating Ukraine as a country with a high level of development of welding production.

The regional structure of welding production of Ukraine is presented in Table 2. The greatest number of enterprises is focused in the Donetsk-Pridneprovsky region, producing 57 % of welding structures manufactured in Ukraine. About 45 % of engineers and technicians and 44 % of workers are engaged in their production. There are also 23.5 % of higher establishments of the III–IV and 53 % of the I–II levels of accreditation functioning in the region, which educate engineering-technical staff for welding production.

Table 1. Welding production in Ukraine

Characteristics	Number
Enterprises–producers of welded structures (having 5 and more welders), un.	~2,000*
Enterprises–manufacturers of welding equipment, un.	39
Enterprises–manufacturers of welding consumables, un.:	
in total	64
certified (UkrSEPRO)	33
System of staff training, un.:	
higher educational establishments	17
secondary schools	17
colleges	487
Staff, pers.:	
workers of welding specialties	~80,000*
engineers and technicians	>5,000*

*Evaluative data.

The domestic school of welding technologies as to its merits occupies one of the leading places in the world. Such achievements of Ukrainian welders as automatic welding of armor bodies of the legendary tank T-34, unique welded structures of the civil period, such as main oil-and-gas pipelines, the E.O. Paton all-welded bridge in Kiev, electroslag welding of metal of almost unlimited thickness, welding in aerospace engineering, in space and under water are wildely known.

The events of the recent years had a negative influence on the economy of Ukraine and its production potential, but a high research level still allows the Ukrainian school of welders to keep the position of one of the world leaders. The evidence of this is the Ukrainian technologies and equipment for flash-butt welding of rails of unlimited length, that is particularly important in construction of modern high-speed railroads, and the recent developments in welding of live tissues widely used in all the continents. As to the opinion of academician S. Glaziev, the author of theory of technological structures, these both projects meet the requirements of the VI technological structure, i.e. they are the technologies of the future.

It is clear that study of state and dynamics of development of the world and national welding production including economic and statistical analysis of the market of welding consumables has already been for more than 50 years as one of the scientific priorities of the Institute. Rich information banks were accumulated, necessary

Table 2. Regional structure of welding production in Ukraine, %

Region	Enterprises	Welded structures	Engineers and technicians	Workers	Higher educational establishments of the III–IV a.l.	Higher educational establishments of the I–II a.l.
Central[1]	22.4	14.1	11.4	16.8	23.5	17.6
Donetsk-Pridneprovsky[2]	34.4	57.0	44.9	43.5	23.5	64.7
Eastern[3]	12.5	9.7	24.0	14.7	5.9	11.8
Southern[4]	10.6	8.0	8.3	9.5	17.7	5.9
Western[5]	20.1	11.2	11.4	15.5	29.4	0

Notes. 1 — Kiev, Regions of Kiev, Chernigov, Cherkassy, Kirovograd, Zhitomir; 2 — Regions of Donetsk, Dnepropetrovsk, Lugansk, Zaporozhie; 3 — Regions of Kharkov, Sumy, Poltava; 4 — Regions of Nikolaev, Odessa, Kherson, Crimea Republic; 5 — Regions of Vinnitsa, Volyn, Trans Carpathian, Ivano-Frankovsk, Lvov, Rovny, Ternopol, Khmelnitsk, Chernovtsy.

staff was trained, methods of investigations were mastered, on the basis of which three principles are laid:

- the first one: the investigation of phenomena both in statics as well as in dynamics during a quite long period;
- the second one: to provide the objectivity the evaluation should be given in combination with the corresponding values of world and leading countries;
- the third one: during investigation of state of the investigated phenomenon the preference should be first of all given to real values, as far as the cost values can distort the real situation. Except of all the rest the use of real values provides a possibility to avoid the influence of varying exchange rates during international comparison of the values.

As an example of the higher objectiveness of real values as compared to the cost ones, the dynamics of GDP of Ukraine in the cost figures and that of welding production in real values (Figure 1) can be given. According to the data of the State Statistics Committee in general almost all the values of welding production, determined in natural values, turned to be much lower than the values of GDP, calculated in the cost figures. It was caused by the fact that the volumes of machine building and metal treatment, in the first turn, the production of metal-consuming types of products, dropped sharply (Table 3).

The main structural material, which is widely applied in production of welded structures, is steel. Annually in Ukraine about 30 mln t of steel rolled metal is produced, the considerable part of which is exported to many countries of the world, and the visible consumption inside the country in the last years amounts to almost 6 mln t, of which 2/3 part falls to manufacture of welded structures (Figure 2). The analysis of the given data shows that the welded structures in Ukraine amount from 2/3 to 3/4 part of rolled metal consumption, that corresponds to the similar world values.

The values in Figure 3 evidence that the welded structures are the leading type of metal

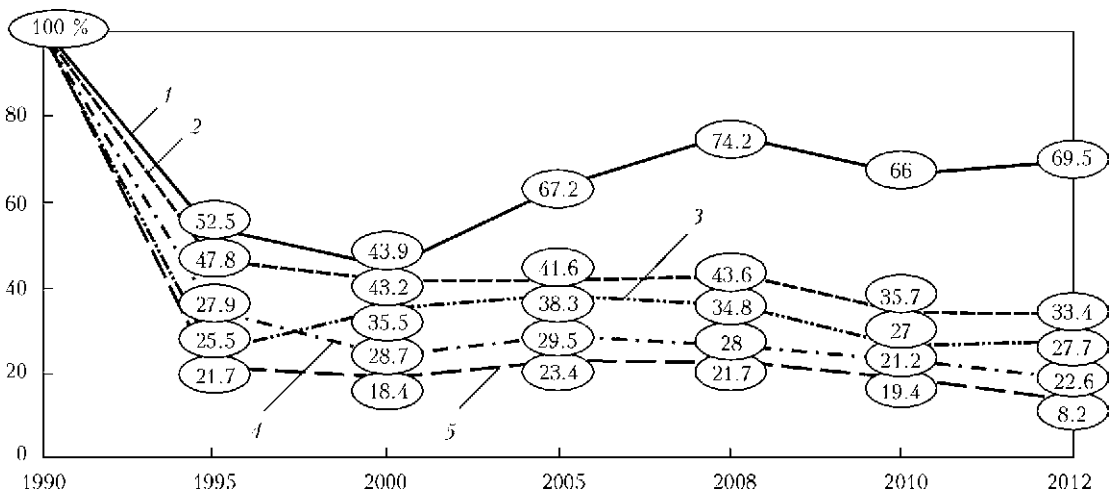

Figure 1. Main indices of Ukrainian economy and welding production, %: *1* — GDP; *2* — products of machine building; *3* — consumption of rolled metal; *4* — production of welded structures; *5* — consumption of welding consumables

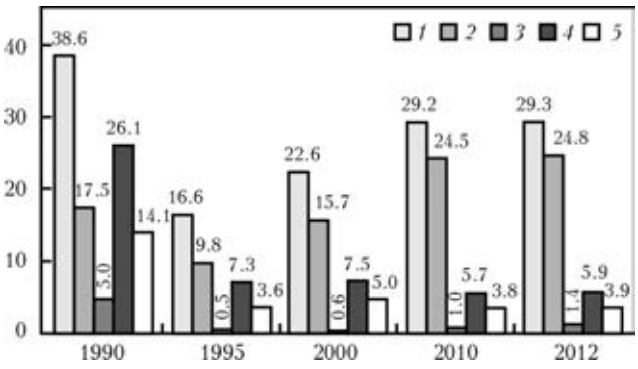

Figure 2. Production of welded structures in Ukraine, mln t: *1* — production of rolled metal; *2* — import of rolled metal; *3* — production of welded structures; *4* — export of rolled metal; *5* — visible consumption of rolled metal

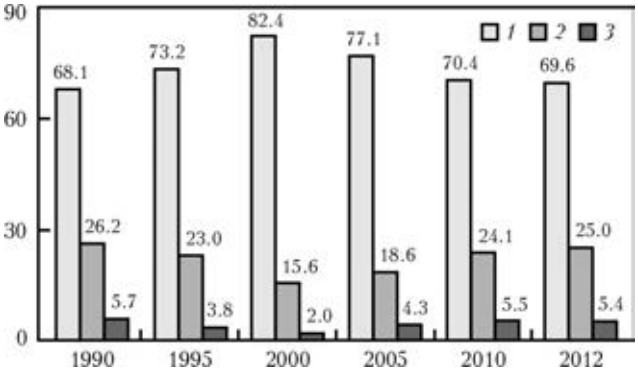

Figure 3. Structure of production of metal billets in Ukraine, %: *1* — welded structures; *2* — castings; *3* — forging and stamping pieces

billets produced in the country, leaving castings, forgings and stamping pieces far behind.

One of the main components of welding production is welding consumables. Figure 4 presents the dynamics of production of welding consumables in Ukraine, their export and import, allowing establishing the annual volumes of domestic consumption, i.e. volumes of domestic market.

Figure 5 shows seven main Ukrainian manufacturers of welding consumables, the share of which was 96.1 % of annual output in 2012, whereas the share of smaller manufacturers was

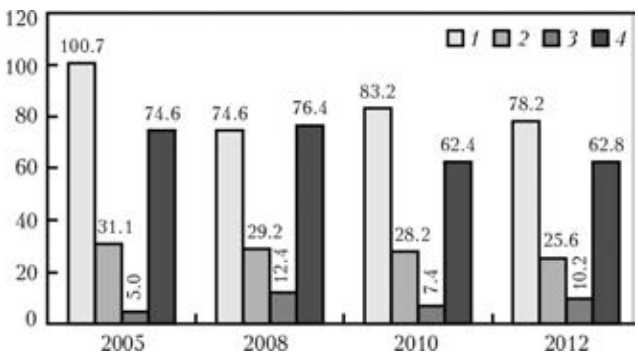

Figure 4. Ukrainian market of welding consumables, thou t: *1* — volume of production; *2* — export; *3* — import; *4* — visible consumption

Table 3. Output of metal-consuming types of industrial products in Ukraine

Products	1990	2012	Decrease in volume of production, times
Ferrous rolled metals, mln t:			
output	38.6	18.4	2.1
consumption	26.1	5.9	4.4
Pipes, mln t	6.5	2.2	3
Bridge cranes, pcs	1389	117	12
Tractors, thou pcs	106	5.28	20
Combine-harvesters, pcs	1500	50	30
Metal cutting machine-tools, thou pcs	37	0.11	342
Forging-press equipment, thou pcs	10.9	0.05	214
Excavators, thou pcs	11.2	0.08	143
Passenger cars, thou pcs	156	69.7	2.2
Buses and lorries, thou pcs	40.3	6.5	6.2
Freight cars, thou pcs	80	47.6	1.7

3.9 %. Yet very recently their volume at the market amounted to more than 9 %, which evidences about the continuing process of concentration of welding consumables production.

The capacities of Ukrainian enterprises on production of welding consumables satisfied the needs of many machine building plants of the former USSR, but after its collapse the volumes of production decreased considerably. 1/4–1/3 of the production volume falls to export. The visible use of welding consumables inside the country at the recent years amounts to 63,000 t.

In the structure of production of welding consumables (Figure 6) almost a half belongs to the production of electrodes (as compared to 1990 their volume increased nearly by 20 %), about 30 % falls to welding fluxes. As compared to

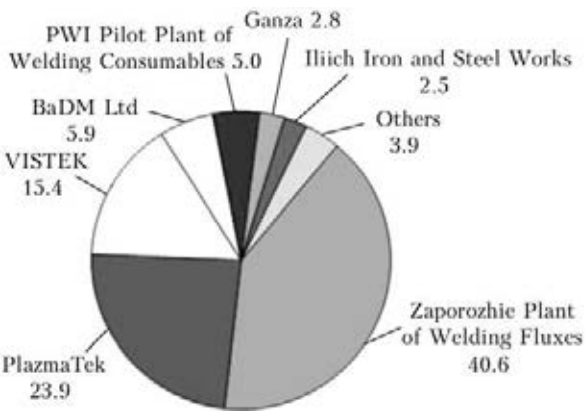

Figure 5. Share in output of welding consumables by the main Ukrainian producers, %

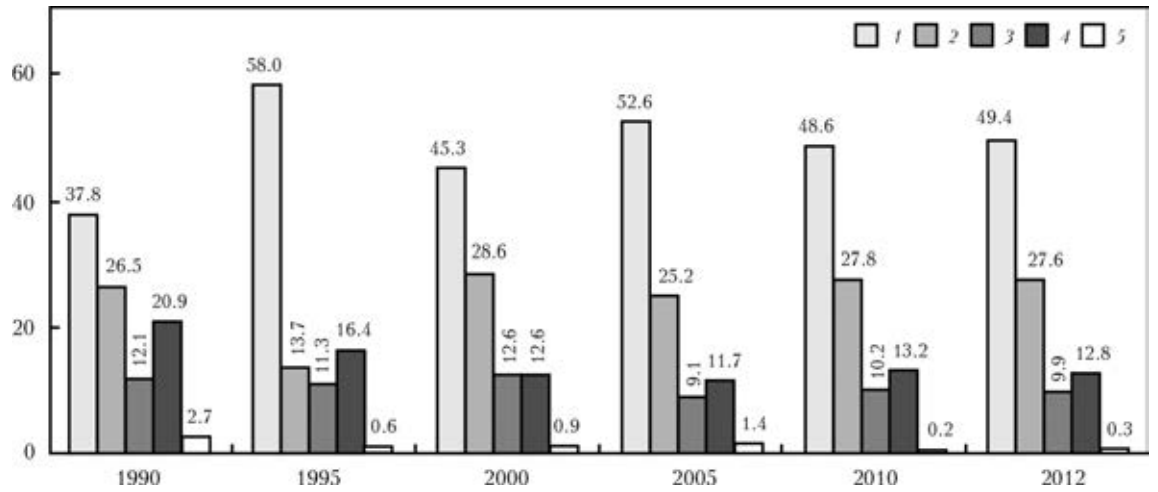

Figure 6. Structure of output of welding consumables, %: *1* — electrodes; *2* — standard wire; *3* — flux-cored wire; *4* — flux; *5* — alloyed wire

1990 the production of alloyed and flux-cored wire was decreased.

The presence of data on the structure and volume of consumption of welding consumables allows determining the volume of application of each of the main methods of arc welding (as to the deposited metal) during the last 47 years (Figure 7).

In Ukraine in the 1960–1980 the level of mechanization of arc welding was comparable with that of the leading countries. Thus, in 1965 the volume of manual welding in Ukraine amounted to 63 % and was constantly decreasing to 44.9 % till 1985 (Table 4). However stagnation of the USSR economy in the second half of the 1980s, different shocks and reformations negatively influenced the whole economy of Ukraine and, in particular, its welding production (see Figure 7). In the 1990–1995 the volume of manual welding sharply jumped to the level of 30 years old values (to 65.1 %) and further was slowly decreasing to 48.9 % (in 2012), being inferior to the similar value of leading countries. At the same time in the period of the 1965–1990 the volume of welding in CO_2 grew from 9.5 to 37.2 %, and then again sharp decrease to 23 % (in 2000) and slow rise to 33 % (in 2012) are observed. Automatic submerged arc welding was all the time at a sufficiently high level — 20 ± ± 3 % in the 1970–1980 due to its application in ship building and production of building structures and pipes. Then in the 1990–1995 the recession to 7.5 % is observed, and in the next years the stabilization at the level of 15.5 ± 1 % took place due to production of pipes of large diameter for main pipelines. Quite unsatisfactory situation

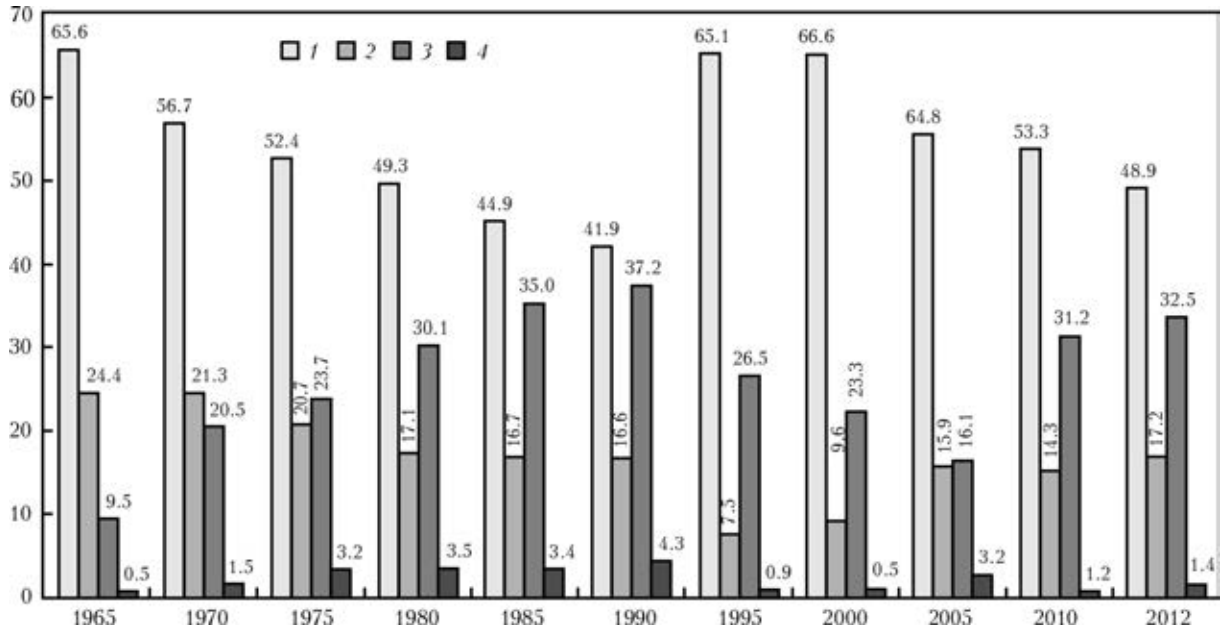

Figure 7. Technological structure of arc welding methods in Ukraine, % (as to deposited metal): *1* — manual welding; *2* — submerged arc welding; *3* — welding in shielding gas; *4* — welding using flux-cored wire

Table 4. Structure of arc welding methods, % (as to deposited metal)

Country	Welding method	1965	1975	1985	1995	2000	2005	2012
West Europe	MAW	74	58	34	18	15	12	8.9
	CO_2		31	56	70	71	75	63.9
	FCW		2	3	6	6.5	6.5	19.1
	ASAW		9	7	6	7.5	6.5	8.1
USA	MAW	71	53	42	25	19.5	15	10.3
	CO_2		25	38	54	54	58.5	61.4
	FCW		13	13	19	19	19.5	22.1
	ASAW		9	7	7	7.5	7	6.2
Japan	MAW	85	67	44	22	14	12	7.3
	CO_2		20	39	52	54	54.5	49.5
	FCW		1	11	25	25	27	35.9
	ASAW		9	10	7	7	6.5	7.3
Ukraine	MAW	63	52.4	44.9	65.1	66.6	64.8	48.9
	CO_2	9.5	23.7	35	26.5	23.3	16.1	32.5
	FCW	0.5	3.2	3.4	0.9	0.5	3.2	1.4
	ASAW	27	20.7	16.7	7.5	9.6	15.9	17.2

Note. MAW — manual arc welding; FCW — flux-cored wire welding; ASAW — automatic submerged arc welding.

can be observed with the flux-cored wire, i.e. increase in values almost from 0 to 4.3 % in 1990 and the next drop to the level of 1.2–1.4 %.

The reduction in consumption of welding consumables decreased the anthropogenic impact of welding on the environment. The cooperation of the E.O. Paton Electric Welding Institute with the Kiev Institute of Labor Medicine and Odessa Centre of Protection of Breathing Organs of Welders allows creating the necessary research base for economic evaluation of problems of hygiene and ecology in welding production. The results of these investigations, carried out for evaluation of anthropogenic impact of welding production on environment, presented in Table 5, from which it follows that emission of harmful substances to the atmosphere during welding amounts to hundred fractions of a percent from the amount of general emissions, and has no danger for the environment. Nevertheless, the specifics of welding processes, especially manual and semi-automatic ones, where welder stands directly in the zone of arcing, requires taking of necessary measures not only to protect their breathing organs, but also to make the environment in the welding shops healthier.

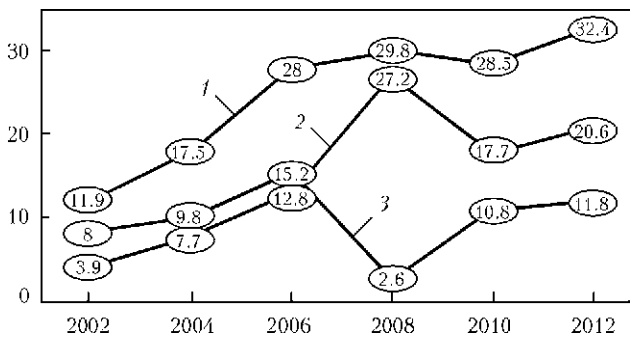

Figure 8. Foreign trade balance of Ukraine on welding consumables, mln USD: *1* — export; *2* — import; *3* — balance

The production of welding consumables in Ukraine is oriented to the consumption not only in different branches of domestic industry, but also to delivery to the foreign markets. The volume of export at the Ukrainian market amounts almost to 30 % of the volume of their production (see Figure 4), whereas import does not exceed 12,400 t. Such correlation of export–import provides in general the positive foreign trade balance on welding consumables (Figure 8).

However, in the recent years the Ukrainian producers of welding consumables feel severe competition in struggle for a user on the side of importers, which became especially acute after

Table 5. Anthropogenic impact of welding production on the environment

Year	Emissions of harmful substances to the atmosphere, thou t				
	Total	Including			
		Automobile transport	Stationary sources	Welding production	
				In total	% from total emissions
1990	15500	6100	9400	6.90	0.044
1995	7500	1800	5700	1.92	0.026
2000	5900	1900	4000	1.17	0.021
2005	6600	2200	4400	1.84	0.028
2010	6678	2547	4131	1.27	0.019
2012	6821	2486	4335	1.28	0.019

entering of Ukraine to the WTO and opening of the domestic market. The dynamics of growth of import of welding consumables in Ukraine from 2002 to 2012 (from 3.9 to 27 mln USD) exceeds the dynamics of export growth of that period (from 11.9 to 29.8 mln USD). It resulted in decrease of the positive foreign trade balance down to 2.6 mln USD. The financial crisis of 2008 weakened the positions of importers (due to the growth of dollar exchange rate), that resulted in decrease of volumes of import of welding consumables. However, by 2010 in connection with overcoming crisis phenomena in the economy the tendency to growth of import in foreign trade balance of Ukraine on welding consumables was renewed.

The structure of export and import of welding consumables is presented in Figure 9. The domestic producers export mainly alloyed wire, electrodes and fluxes, and in the structure of import the main volume falls to welding fluxes and electrodes for manual arc welding.

In accordance with data of the governmental statistics the main trade partners of Ukraine in 2013 were countries of Europe, Asia, and Russia

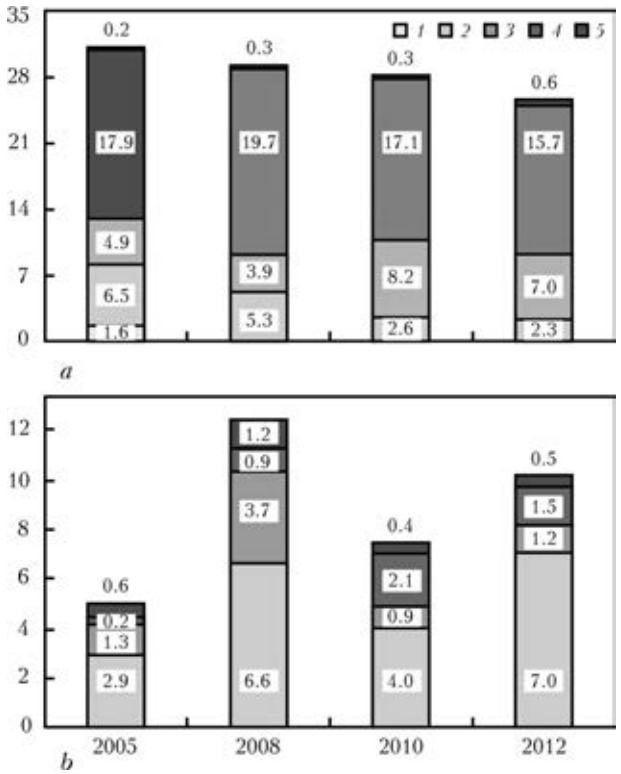

Figure 9. Structure of export (*a*) and import (*b*) of welding consumables, %: *1* — standard wire; *2* — flux; *3* — alloyed wire; *4* — flux-cored wire; *5* — electrodes

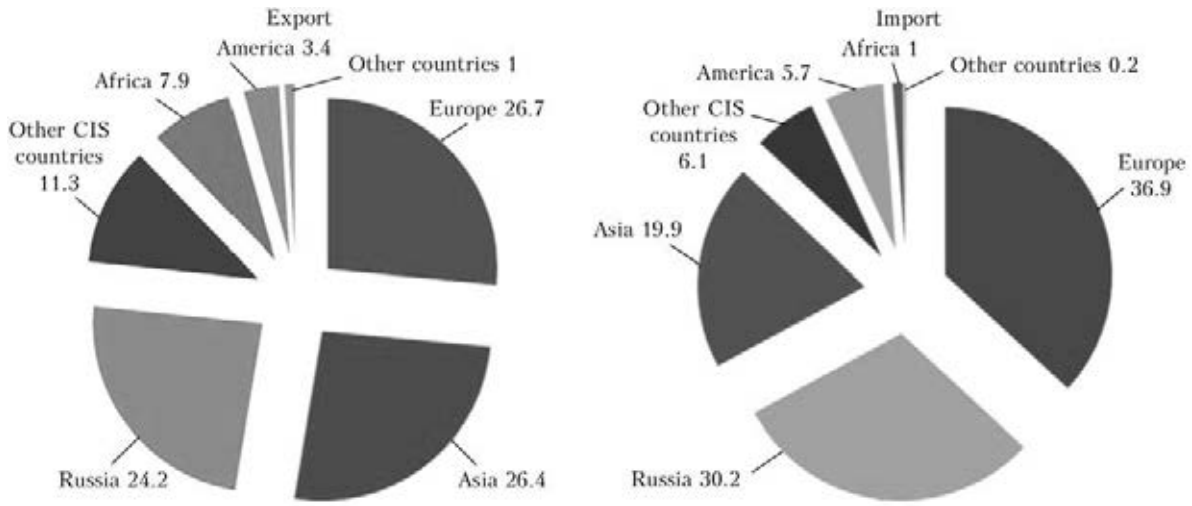

Figure 10. Foreign trade activity in Ukraine, %

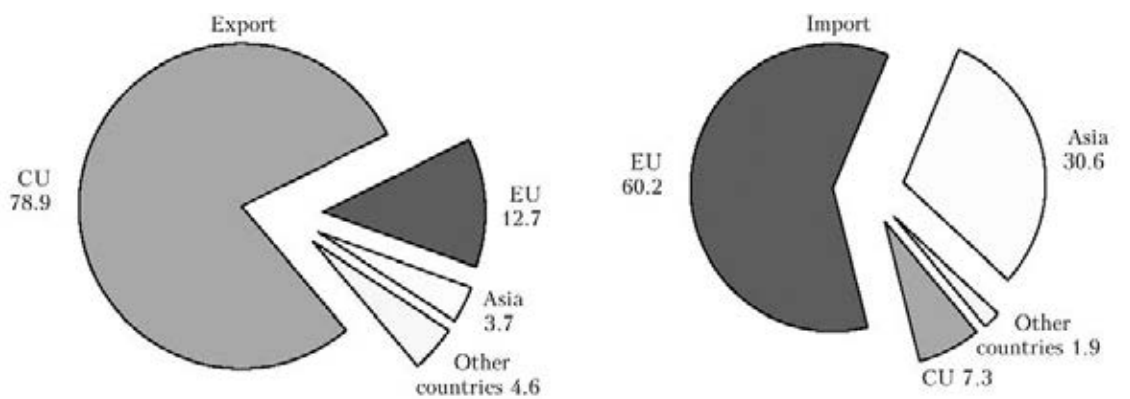

Figure 11. Geography of export–import of welding consumables in 2012, %

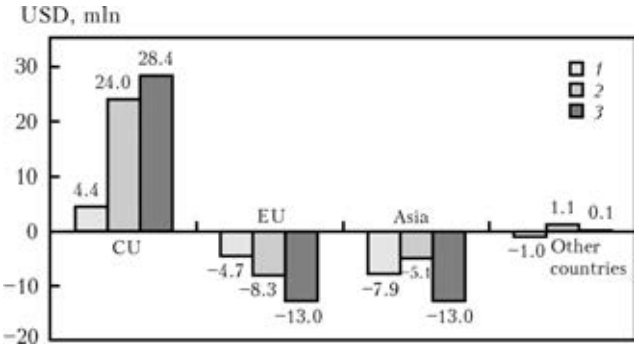

Figure 12. Foreign trade balance of Ukraine on groups of goods and regions in 2012: *1* — welding equipment; *2* — welding consumables; *3* — in total

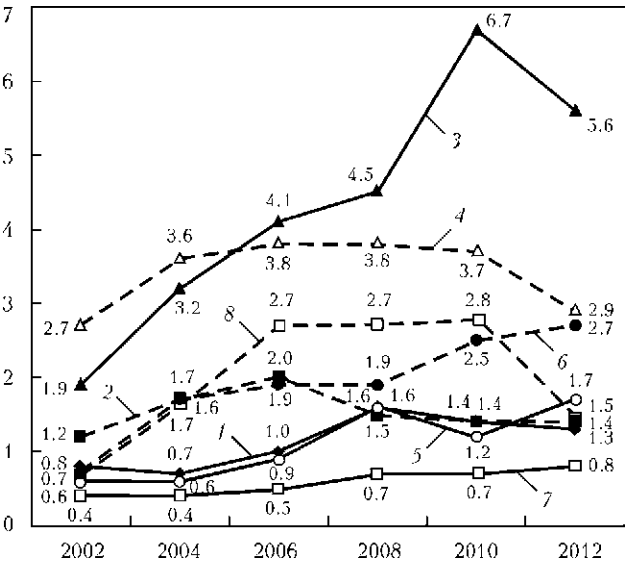

Figure 13. Average cost of welding consumables, thou USD/t: *1*, *2* — export and import of alloyed wire; *3*, *4* — export and import of flux-cored wire; *5*, *6* — export and import of covered electrodes; *7*, *8* — export and import of flux

(Figure 10). Almost 35.5 % of export of Ukrainian products and 36.3 % of import falls to Russia and other CIS countries. Export and import to Europe and Asia amount, respectively, to 26.7 and 26.4, and to 36.9 and 19.9 %.

The foreign trade activity at the market of welding consumables differs greatly from the foreign economic activity of Ukraine in general (Figure 11). Thus, according to the results of 2012, 75 % of volume of export of welding consumables falls to the countries of the Customs Union (CU) (mainly Russia, Belarus and Kazakhstan) and only 12.7 % to the countries of the European Union. In import of welding consumables the different situation is observed: 60.2 % of volume belongs to deliveries from the EU countries and 7.3 % — CU countries. Also in the structure of import the volume of deliveries from the Asian countries is high, i.e. 30 % (mainly from China), which during the last years had a tendency to annual growth. The foreign trade balance on the groups of goods of welding technologies is given in Figure 12. The dynamics of average cost of welding consumables in export–import is shown in Figure 13.

Conclusions

Welding remains the leading technological process in Ukrainian industry, and the national market of welding consumables is developing dynamically. The development and modernization of welding production requires the presence of corresponding economic, statistic and marketing information allowing taking the grounded decisions at determination of directions of research works and developments, and also working out the strategy at the macro- and microlevel. The distinct dependence between consumption of steel metal products and demand on the specific types of welding technologies allow using the forecasts of development of markets of metal consumption as the base for prediction of welding production.

The article is written according to the results of analysis of the market of welding technologies in Ukraine, performed by the Department of Economic Investigations of the PWI, according to the statistic data of the State Statistics Committee and the Custom Service of Ukraine, economic-statistic review «SVESTA-2010», materials, published in the journal «Avtomaticheskaya Svarka», «The Japan Welding News for the World», by the corporations ESAB, Lincoln Electric, etc.

Received 19.05.2014

PHYSICAL-METALLURGICAL AND WELDING-TECHNOLOGICAL PROPERTIES OF GAS-SHIELDED FLUX-CORED WIRES FOR WELDING OF STRUCTURAL STEELS

V.N. SHLEPAKOV
E.O. Paton Electric Welding Institute, NASU
11 Bozhenko Str., 03680, Kiev, Ukraine. E-mail: office@paton.kiev.ua

Peculiarities of process of gas-shielded arc welding using flux-cored wire are considered. Given are the data on metallurgical characteristics and classification of the gas-shielded flux-cored wires with different core types as well as examples of their successful application in industry. 6 Ref., 1 Table, 2 Figures.

Keywords: *arc welding, low-carbon and low-alloy steels, flux-cored wire, shielding gas, stability of melting and transfer of metal, type of flux core, content of gases in weld metal, technical-economic aspects of application*

Long-term application of solid flux-cored wires in mechanized and automatic gas-shielded welding was mainly caused by their availability and small price. Eventually, understanding of technological and economic advantages of application of the flux-cored wires was verified by the results of analysis of expenses for welding performance and quality of welded joints. This allows the flux-cored wire taking the leading position in performance of welding operations in different branches of industry and building in countries with high level of economic development [1]. Gas-arc welding using the flux-cored wire allows responsing the demands of manufacturers of welding structures, since it differs by versatile, good operation characteristics and high efficiency, that provides for significant reduction of economic expenses.

Today a variety of types of the flux-cored wires are classified on international standards ISO in accordance with class of steel, for which they are designed. Standard ISO 17632 [2] is used for the most widespread classes of normal strength structural steels, and ISO 18276 [3] is applied for high strength ones. Shielding gases for performance of gas-arc welding are classified on standard ISO 14175 [4]. The classification in accordance with indicated standards is further used.

The specialists in area of fusion arc welding know well that change of solid wire to flux-cored one does not require variation of basic technology or application of another equipment. Current welding equipment provide for a wide range of regulation of statistical and dynamic characteristics of power sources with the help of microprocessor technology, that allows setting of the optimum welding parameters for each wire type. Feed mechanisms of the semi-automatic machines are as a rule equipped with two pairs of rolls for reduction of wire pressure, prevention of its deformation or break of geometry, that deteriorate wire feeding through the hoses.

Metallurgical characteristics of gas-shielded flux-cored wires. Established classification of the flux-cored wires on type of flux core, which is included into international standards, divide them on three main types, namely rutile, basic and metallic.

Rutile type (on title of mineral — rutile) includes the wires with basis of a slag system composed of titanium oxides in combination with other oxides (for example, silicates and alumosilicates), formed in melting of low-basicity slags. Change of composition and application of fluxing agents reveal wide capabilities for regulation of technological properties of these wires. They are divided on rutile ones with slowly setting and rapidly setting slag according to the welding technological properties, that determines a possibility of their application for welding of joints in different spatial positions.

Among the basic type are the wires with slag basis core. They include the systems of carbonate-fluoride-oxide type with high portion of oxides of alkaline-earth metals. This due to high basicity of forming slag melt allows providing high refining capability of the slag and reducing level of oxidation of the molten metal. Possibilities of regulation of technological properties of these wires are narrower in comparison with rutile ones due to more globular metal transfer, that, how-

ever, can be compensated by application of pulse process of welding.

Wires with metallic core are the wires containing powders of iron, ferroalloys and other metallic powders with insignificant additives of mineral substances, rising arcing stability and improving welding technological properties of the wire. Quantity of the mineral additives makes generally from 0.5 to 1.5 % of wire weight. Welding-technological properties of the flux-cored wires with metallic core are close to the properties of solid ones, but they provide for higher arcing stability and efficiency of melting, insignificant loss of electrode metal and favorable weld formation.

Effect of metallurgical characteristics of the flux-cored wires of indicated types can be evaluated on generalized data of typical content of gases and non-metallic inclusions in the weld metal. The Table shows the data on content of gases and non-metallic inclusions in the weld metal, produced by flux-cored wires with different type of core in Ar + 18 vol.% CO_2 mixture (M21 on ISO 14175 [4]).

Peculiarity of the seamless flux-cored wires is low content of diffusible hydrogen in the deposited metal due to their heat treatment in process of manufacture and tightness of the structure. Content of oxygen in the weld metal depends on composition of non-metallic part of the core (slag system type) and refining properties of the slag. The complex systems of microalloying and melt treatment, allowing reducing metal pollution with the non-metallic inclusions, are used in recent time for reduction of the level of oxygen content and oxide inclusions in the wires with metallic core, where slag volume is insignificant.

Assortment of the flux-cored wires for CO_2 welding or welding in Ar + CO_2 mixture includes the wires for welding of structural steel having yield strength of 360–500 [2] and 550–890 MPa [3]. The manufacturers produce the flux-cored wires of 1–2 mm diameter, that allows welding of structures from metal of 2–50 mm thickness and more depending on class of steel being welded.

Peculiarities of gas-arc welding using flux-cored wire. There are three main types of electrode metal transfer in the weld pool during gas-arc welding, namely, short-circuit, drop and spray. Mode of the metal transfer can have mixed nature in some ranges of parameters. Using of current pulse power supplies with programmable control significantly expands the possibilities of regulation of electrode metal transfer, in particular, pulse-spray transfer with controlled surface tension of molten metal. The main methods of control of characteristics of regulated transfer are based on a force balance, determining droplet detachment from electrode wire [5].

Surface tension of the molten metal (pinch effect caused by effect of electromagnetic forces at the end part of electrode) has the main role in transition from drop form to spray one. Composition of the shielding gas has also significant effect. Application of gas mixtures (two- or three-component) allows optimizing chemical activity, ionization potential and thermal conductivity of gas-shielded media [6]. Replacement of carbon dioxide by argon-based mixtures significantly improves the characteristics of metal transfer, i.e. reduce drop size, thus promoting transition from drop to spray-drop transfer. Fundamentally, the spray transfer is also drop, but in form of very fine drops. It is possible to regulate the transfer by means of changing of mode parameters (welding current, wire stickout and arc voltage) for the wires of specific diameters considering received technological characteristics of the welded joint. Change of the core composition allows regulating the arcing characteristics, in particular, the indices of welding process stability using elements and compounds with small ionizing potential and low values of electron work function in the core composition. This results in increase of concentration of positive ions in arc periphery area. In turn, presence of slag melt on the surface of electrode metal provides for the possibility of surface tension control.

Generalized results of analysis of content of gases and non-metallic inclusions in metal deposited with flux-cored wires of different type in shielding gas M21 [4]

Flux-cored wire	[N], wt.%	[O], wt.%	$[H]_{dif}$, $cm^3/100$ g	NMI, vol.%*
Rutile type	0.005–0.008	0.057–0.065	6–15	0.38–0.48
Basic type	0.009–0.011	0.035–0.045	3–5	0.31–0.34
With metallic core	0.004–0.010	0.078–0.083	5–10	0.53–0.61
Seamless	0.009–0.010	0.045–0.057	4–5	0.33–0.44

*On data of metallographic investigations of microsections without etching.

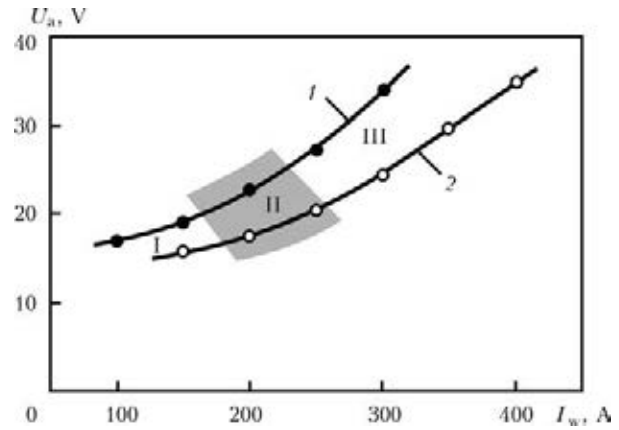

Figure 1. Range of parameters of welding in mixture of gases M21 [4] using flux-cored wires with metallic core type of 1.2 (*1*) and 1.6 (*2*) mm diameter: I — area of drop transfer; II — mixed; III — spray transfer; shaded — area of transition of drop to spray transfer

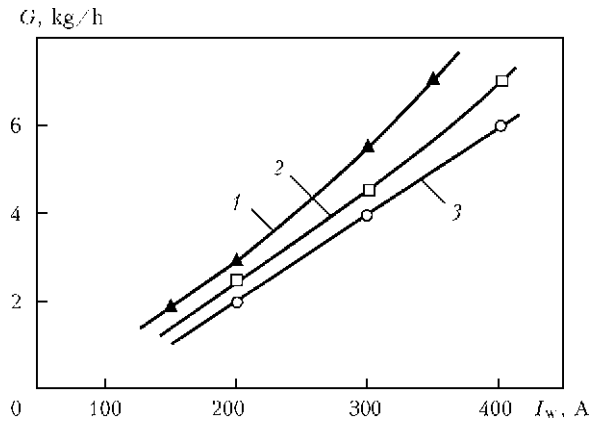

Figure 2. Efficiency of deposition in CO_2 using flux-cored wire of 1.2 mm diameter with metallic core (*1*), rutile (*2*) and solid (*3*) ones in range of applied welding currents

Figure 1 shows an example of dependence of type of metal transfer on diameter of flux-cored wire and mode parameters. Figure 2 illustrates efficiency of deposition using flux-cored wires with different core types in comparison with solid wire in the range of applied currents. Regular nature of melting and transfer of metal provides for high stability of welding parameters in the process of production of welded joints, that is in particular important in automatic and robotic welding.

Technical-economic aspects of application. Gas-shielded flux-cored wire welding has high potential in significant rise of efficiency and quick adjustment to performance of various welded joints of different designation structural steels due to application of more concentrated energy, high current density and possibility of regulation of indices of metal melting and transfer. The current flux-cored wires are successfully used in semi-automatic, automatic and robotic welding of the structures of wide assortment using serial sets of equipment. They have virtually no difference from solid wires on feed indices, safety of electric contact and arc regulation. A single difference is a recommendation to use rollers with female profile in feed mechanisms, in particular, during welding using wires of more than 1.6 mm diameter in order to prevent wire surface deformation and increased wear of contact tips. A procedure of production of welds using flux-cored wire is the same as in using of solid wire, but the welds in flux-cored wire welding have smoother shape of penetration and their geometry is less dependent on welding parameters. It is also necessary to consider that the flux-cored wire provides for higher rate of performance of weld of specified size at smaller energy consumption, minimum spattering independent on form of electrode metal transfer and lager stability of welding parameters. Obviously that indicated advantages of the flux-cored wire compensate increase of expenses on welding consumables.

Reduction of heat input in the base metal during gas-shielded flux-cored wire welding makes its more optimum for joining of steels sensitive to overheating. This is in particular important for the joints of increased and high-strength steels, overheating of HAZ in which is inacceptable. Control of rate of energy input allows solving this problem. If high rate of welding is necessary, then application of automatic or robotic units is recommended. The flux-cored wires with metallic core have the largest efficiency of melting. At that, several passes can be made without removal of slag traces and bevel angle of butt joints can be significantly reduced up to 40° and less.

Large variety of types of the welded joints, size and shapes of metal structures does not allow selecting recommended type of flux-cored wire without reference to specific object. Task of the enterprises, dealing with metal structure manufacture, is to find the optimum solution providing necessary level of welding quality and efficiency. Application of the gas-shielded flux-cored wire welding is one of the ways for solving the tasks of rise of production efficiency, and experience of its application verifies the possibility of improvement of quality of welded structures in many branches of industry and building.

Manufacture of the structures of heavy transport equipment, mining machines, road-building equipment and lifting devices is one of the first areas of successful application of the flux-cored wire with basic type core. Application of robotic welding using flux-cored wire with metallic core expanded in recent years. Welding by flux-cored wires with rutile type core has found wide usage

in manufacture of building metal structures, and then in shipbuilding due to high welding-technological indices. Application of semi-automatic process was specifically successful in manufacture of ship panels, where necessity of welding in different spatial positions is combined with requirements to weld shape, penetration and spattering. Similar tasks are now solving in construction of drilling platforms due to application of the gas-shielded flux-cored wires of all types depending on class of steel to be welded, thickness of metal and spatial positions of the welds. Usage of the gas-shielded flux-cored wire is mastered in recent time during production of power installations and construction of main pipelines, where steels of increased and high strength in combination with high indices of ductility and toughness are used. The tendency is also outlined in using of the flux-cored wires in vertical automatic welding of large thickness metal with forced weld formation.

1. Tsusumi, S., Ooyama, S. Investigation on current usage and future trends of welding materials. *IIW Doc. XII-1759-03–2003*.
2. *Standard EN ISO 17632:2008*: Welding consumables. Tubular cored electrodes for gas-shielded and non-gas-shielded metal arc welding of non-alloy and fine grain steels. Classification. 34 p.
3. *Standard EN ISO 18276:2006*: Welding consumables. Tubular cored electrodes for gas-shielded and non-gas-shielded metal arc welding of high-strength steels. Classification. 34 p.
4. *Standard EN ISO 14175:2008*: Welding consumables. Gases and gas mixtures for fusion welding and allied processes. 16 p.
5. Adonyi, Y., Nadzam, J. (2005) Gas metal arc welding. In: *New developments in advanced welding*. Cambridge: Woodhead Publ., 1–20.
6. Zavodny, Y. (2001) Welding with right shielding gas. *Welding J.*, **12**, 49–50.

Received 07.05.2014

APPLICATION OF FLUX-CORED WIRES FOR WELDING IN INDUSTRY

R. ROSERT
ITW Welding GmbH
67317, Altleiningen, Germany. E-mail: reinhard.rosert@gmx.de

Mechanized and automated processes of flux-cored wire arc welding and surfacing are ever wider applied in many countries in manufacture and repair of various products and structures in many industries and productions. Some advantages of flux-cored wire MAG process are considered, compared to solid wire MMA and MAG processes. One of effective applications of flux-cored wires, in particular, is main pipeline construction. Types of welding systems developed in a number of countries for making position butt joints of pipelines are given. 3 Tables, 12 Figures.

Keywords: *mechanized arc welding, flux-cored wire, application advantages, welding (surfacing) efficiency, automated welding systems, mechanical properties*

Welding belongs to the most widely spread processes applied in industry for fabrication of metal structures. This accounts for development of numerous welding processes and filler materials. The main objectives of these developments are development of welding consumables for welding various steel types, and development of new and high-efficient welding processes.

Tendencies in development of welding processes are evolving towards mechanization and automation. The graph (Figure 1) shows how individual welding processes are distributed by various regions of the world. In the USA, Japan and EU mainly mechanized and automated welding processes are used. Application of stick electrodes is relatively small.

In China and many Asian countries more than 50 % of all welding consumables are stick electrodes. Level of mechanization is lower, respectively thus lowering welding process efficiency. Application of manual arc welding with stick electrodes in these countries is preferable, as the cost of welding equipment and auxiliary materials is relatively low.

An alternative to application of stick welding electrodes are flux-cored wires. Flux-cored wire is an endless electrode in the form of wire, filled with the following components for diverse applications: slag- and gas-forming, arcing stabilizers, alloying powders, ferromaterials and microalloying elements.

There exist two main kinds of flux-cored wire: seamless (Figure 2, *a*) and rolled (Figure 2, *b*).

Depending on purpose, basic and rutile flux-cored wires are used, both slag-containing and metal-powder ones. Figure 3 shows flux-cored wire classification by various criteria. Application of flux-cored wires offers the following advantages:

- performance of high-quality welds by less skilled welders;
- shorter time to train welders in technique in different spatial positions;
- reducing the risk of lack-of-penetration at torch deviation from the correct trajectory, as the weld column is very wide;
- minimizing sensitivity of penetration and weld quality to unforeseen change of welding mode settings;
- lowering defect repair costs.

At present flux-cored wires are becoming ever wider accepted in different productions such as shipbuilding, bridge, pipe and turbine construction, drilling platforms, car industry, steel structures, vessel and apparatus building, chemical engineering, rail vehicles, casting and metallur-

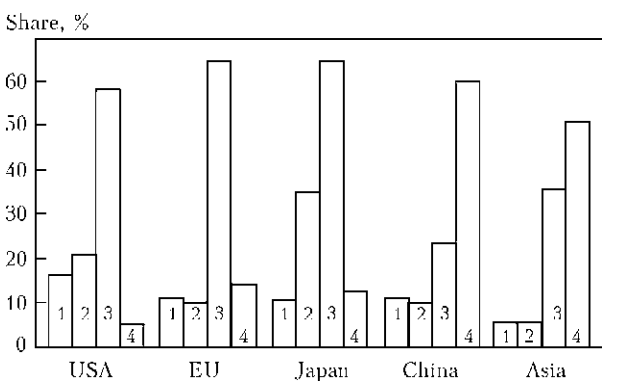

Figure 1. Structure of welding process application in world fabrication, as it was in 2010: 1 — submerged-arc; 2 — gas-shielded flux-cored wire; 3 — gas-shielded solid wire; 4 — stick electrode welding

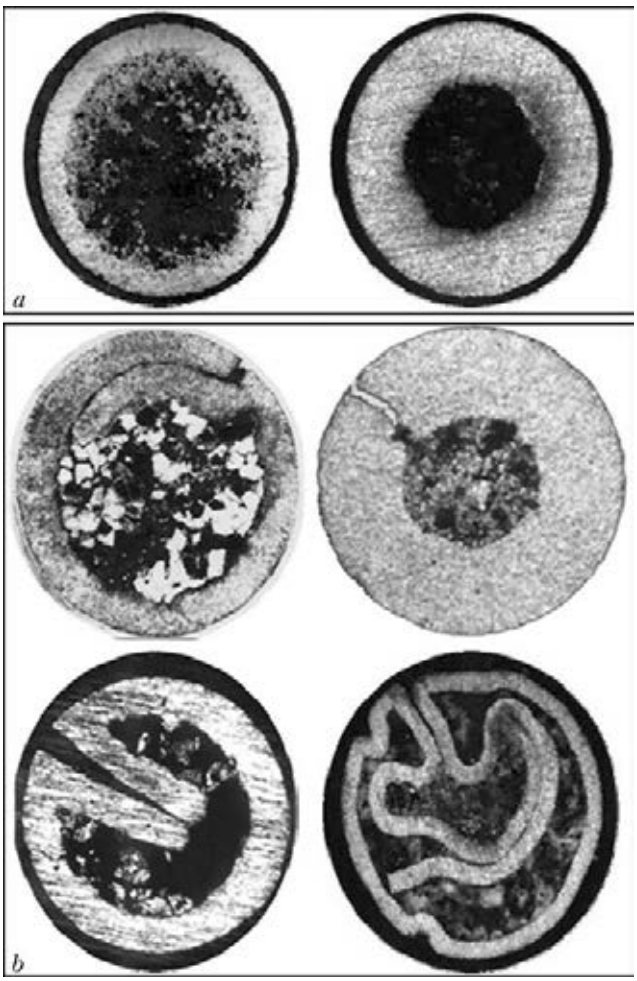

Figure 2. Seamless (*a*) and rolled (*b*) flux-cored wires

gical industry, mobile cranes, machines for road construction and repair.

Efficiency of flux-cored wire welding is directly related to welding current and reaches high values (Figure 4).

In industry mostly rutile flux-cored wires with rapidly-solidified slag are used, which allow out-of-position welding by high currents. Deposited metal composition provides the required me-

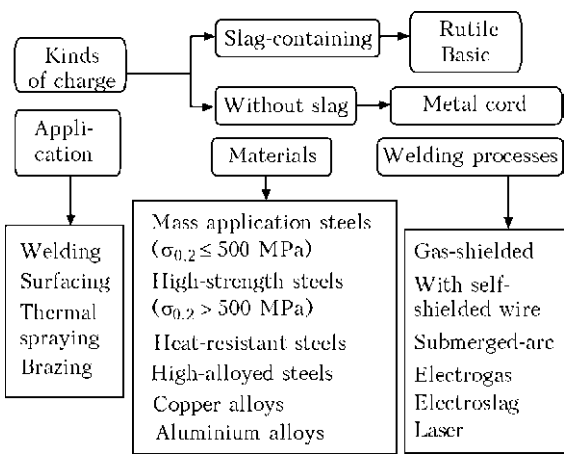

Figure 3. Flux-cored wire classification

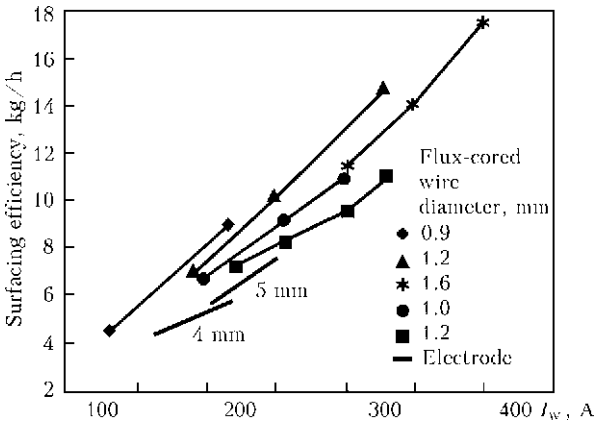

Figure 4. Efficiency of surfacing by various filler materials depending on welding current (downhand welding position)

chanical properties and high impact toughness (up to −60 °C).

Cost-saving potential in welding operations is limited to selection of efficient welding process, mechanization (increasing effective arcing time), downtime reduction (removing slag and spatter).

The greatest time-saving, compared to solid wire or electrode welding, is realized in out-of-position welding (inconvenient conditions).

Flux-cored wires are applied with success in welding position butt joints (construction of large-diameter pipelines). For instance, «Northern Gateway» for natural gas supply to Germany was mainly made with such wires.

Application of pipelines for water or gas has a certain history:

- first pipeline systems for water supply (stone or wooden);
- 1911 — first attempt to weld a pipeline;
- 1922 — first application of arc welding of pipelines;

Table 1. Comparison of advantages of application of flux-cored and solid wires

Criteria	Flux-cored wire	Solid wire
Total edge penetration	+	–
Edge wetting; welding reliability	+	–
Risk of lacks-of-penetration	+	–
Smooth transitions without undercuts	+	–
Cracking susceptibility	+	–
Spattering	+	–
Process stability	+	–
Pore formation/internal defects	+	–
Efficiency in cramped spaces	+	–
Possibility of supplying special types	+	–
Microalloying at low temperatures	+	–
Price	+	–
Production costs	–	+

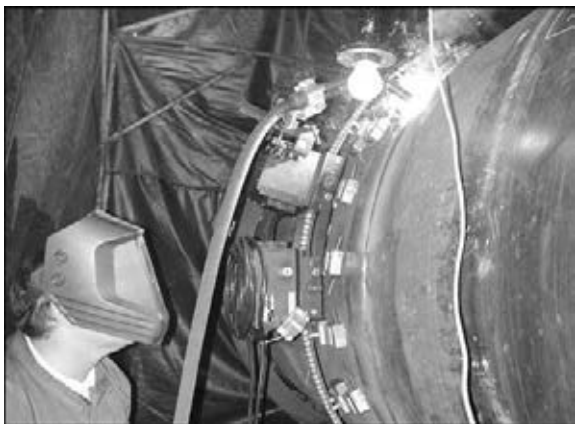

Figure 5. CRC Evans system for position butt welding (USA)

Figure 7. BUGO system for position butt welding (USA)

• 1927 — first attempt of welding using electrode with rutile type coating;

• 1969 — application of gas-shielded mechanized welding;

• 1980 — application of automatic analog welding systems;

• 1993 — application of technology of unsupported root welding;

• 2000 — application of automatic digital welding systems.

At present manual arc and automatic welding processes are used. Comparing them reveals the following advantages of automatic welding:

• better quality of welded joints in terms of ensuring required mechanical properties;

• saving on required numbers of staff (welders, operators) and equipment;

• faster operator training in automatic welding process;

• welding consumable saving;

• total saving in pipeline construction (downtime reduction).

About 25,000 km of various pipelines are built in the world every year. Considering that average pipe length is between 12 to 15 m, more than 1.6 mln pipes are required for the above pipeline length. Two variants of automatic welding are mainly used: self-shielded flux-cored wire and gas-shielded flux-cored wire welding.

A range of flux-cored wires has been developed for gas-shielded welding of large-diameter pipes, allowing for the requirements on mechanical properties of applied pipe steels. Respective power sources and welding apparatuses were developed in parallel. Such a system includes the following components: two welding heads with a drive; power source and generator; flexible guide; controller and diverse spare parts.

Appropriate power source can be applied for the following welding processes: TIG; MMA with basic and rutile electrodes; MIG/MAG with solid and flux-cored wire; welding with flux-cored wire for the root pass. Welding head operation is monitored using digital processing. Various welding programs are saved for welding, depending on pipe thickness and material. Welder selects a program, for instance, for root welding. Correction of welding parameters (within certain ranges during welding) can be performed from the control panel. General technological procedure is described below.

Weld root is welded first. This is done with solid welding wire of 1.14 mm diameter. Welding speed is 15–20 cm/min. Weld root height is 4 mm. Beginning from the second layer, welding

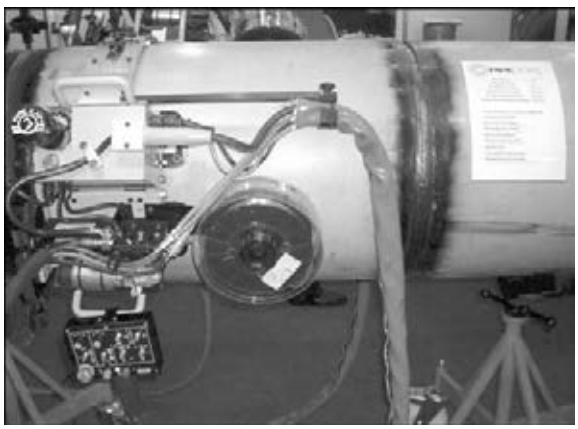

Figure 6. GULKO system for position butt welding (Canada)

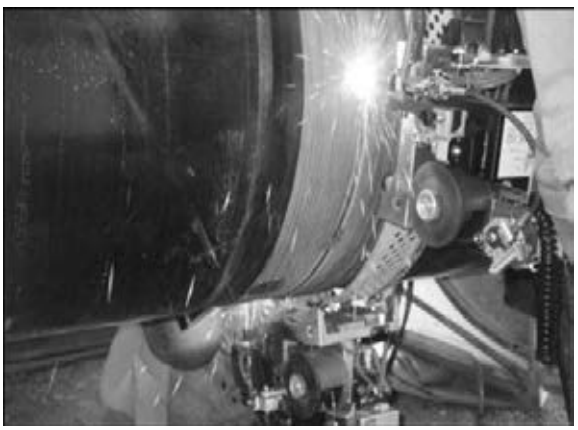

Figure 8. PWT system for position butt welding (Italy)

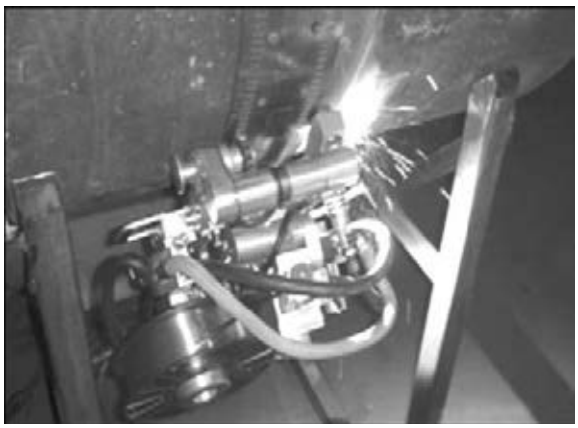

Figure 9. ITS system for position butt welding (Russia)

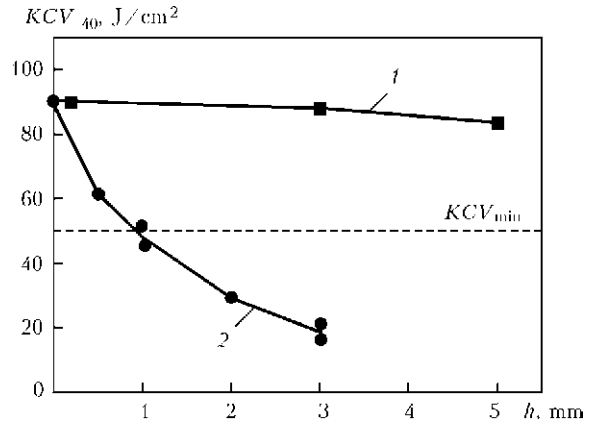

Figure 10. Dependence of impact toughness of lower-lying weld layers welded by solid (*1*) and flux-cored (*2*) wires on weld root layer height

is performed with rutile flux-cored wire. Welding parameters mainly depend on the type of shielding gas, pipe diameter and wall thickness and edge preparation.

Two welding heads are usually used from both sides of the pipe. The second welding head starts welding only after the first welding head has operated for 3 h. This ensures continuous two-sided process for welding all the layers. Shielding gas selection should be given attention in welding. For most of the systems shielding gases of the following composition are used: 75–82 % Ar, 25–18 % CO_2.

Photos of pipe welding heads from different manufacturers are given in Figures 5–9. Systems differ by wire feed mechanisms, mechanism of heads fastening to the pipe, etc. Spools of 200–300 mm diameter of 5 to 16 kg weight are used. The operator should mainly follow the welding process, and some corrections can be made.

Metal-powder wires began to be used for root welding. This is related to the fact that solid wire of 560 MPa grade has performed well at impact toughness testing up to –20 °C.

Impact toughness testing at –40 °C and lower temperatures showed unreliable and unstable results that is due to insufficient alloying and absence of margin of viscoelastic properties of weld metal in the root zone at critical low temperatures.

Geometrical features of the groove (gap and root face) determine the root weld height. When even 1 mm of the height of weld root layer, made with solid wire, is included into the section of the sample for *KCV* impact toughness testing, an abrupt lowering of impact toughness values of the entire sample takes place. This leads to lowering of reliability of automatic welding process.

Figure 10 shows dependence of impact toughness of lower layers of the weld, made by MIG/MAG technology, on weld root layer height h in the impact testing sample*.

Analysis of Figure 10 leads to the conclusion that at not more than 3 mm height of weld root layer inside the groove and application of solid wire, weld metal impact toughness will always drop abruptly. To avoid it, it is necessary to mechanically saw out the extra height of weld root layer that is negative for the efficiency of automatic welding. When metal-powder wire is used, impact toughness of metal from weld lower layers is independent of root layer height. No mechanical removal of «extra» metal of the root layer is required here. Table 2 gives the recommended parameters for pipe welding. Figure 11

Table 2. Parameters of position welding of pipes by metal-powder wire

Weld layer	Welding direction	Wire feed rate, cm/min	Current kind, polarity	Current, A	Arc voltage, V	Wire extension, mm	Welding speed, cm/min
Root	Downhill	60–150	= (+)	90–130	14–17	5–16	18–23
Hot pass	Same	620–660	Same	230–250	23–25	7–12	40–45
Filling pass	Uphill	530–600	»	200–220	22–23.5	10–15	30–35
Facing pass	Same	520–600	»	190–220	22–23.5	10–15	30–35

*Karasyov, M.B. (2012) New technologies, equipment and materials of CJSC «NPF ITC» In: Proc. of Int. Sci.-Technol. Seminar on Technologies of Resistance Arc and Specialized Welding Processes in Modern Industry (St.-Peterburg, May 16–18, 2012), 126–141.

Table 3. Impact toughness of weld metal in joints made with rutile flux-cored wire

Notch position	Test temperature, °C	Sample section, mm	Fracture energy KV, J	Impact toughness KCV, J/cm^2	Averaged impact toughness KCV, J/cm^2
Weld metal from below	−40	8.04×10	85.8	106.7	113.7
		8.06×10.01	88.2	109.3	
		8.06×10.01	100.8	124.9	
	−20	8.05×10	114.0	141.6	139.3
		8.02×10	114.6	142.9	
		8.04×10.01	107.4	133.4	
Weld metal from above	−40	8.05×10.01	88.8	110.2	102.7
		8.03×10	91.8	114.3	
		8.04×10.01	67.2	83.5	
	−20	8.05×10	105.6	131.2	138.1
		8.04×10.02	118.2	146.7	
		8.05×10	109.8	136.4	

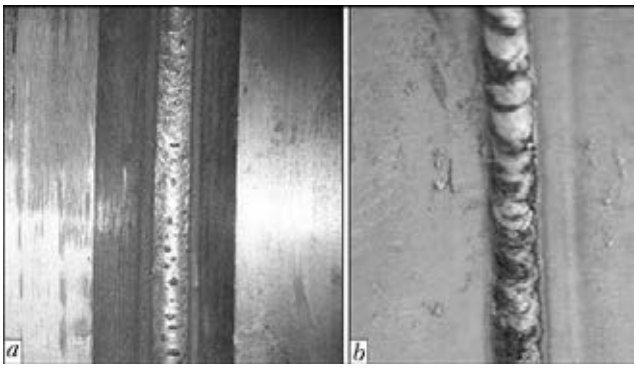

Figure 11. Appearance in welding with metal-powder wire of weld root (*a*) and reverse side (*b*)

shows, as an example, appearance of weld root on a pipe produced by metal-powder wire welding.

Table 3 gives the values of impact toughness of welded metal produced by welding, here filling and facing layers were made with rutile flux-cored wire, and the root layer was made with solid wire. Figure 12 shows macrosection of such a joint.

Thus, the given data are indicative of the advantages of flux-cored wire application, compared to solid wires and electrodes, in pipeline construction. Application of flux-cored wires provides high cost-effectiveness, compared to technology of electrode welding, and good mechanical indices.

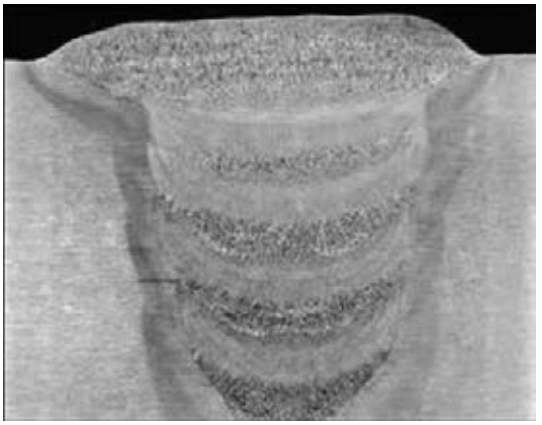

Figure 12. Macrosection (×3.5) of welded joint made with rutile flux-cored wire

Good prospects for flux-cored wire application are confirmed by examples given in this paper.

Received 30.04.2014

ROLE OF WELDING FLUX IN FORMATION OF WELD METAL DURING ARC WELDING OF HIGH-STRENGTH LOW-ALLOY STEELS

V.V. GOLOVKO, S.N. STEPANYUK and **D.Yu. ERMOLENKO**
E.O. Paton Electric Welding Institute, NASU
11 Bozhenko Str., 03680, Kiev, Ukraine. E-mail: office@paton.kiev.ua

Analysis of research results in area of welding metallurgy of high-strength low-alloy (HSLA) steels showed a change of role of welding flux in providing of weld metal quality indices. It is concluded that current welding fluxes should actively participate in processes of weld pool refining, regulation of metallurgical processes of formation of non-metallic inclusions (NMI), having certain composition, morphology and nature of distribution in solid solution, in order to provide necessary structural composition of weld metal and complex of its mechanical properties in welding of HSLA steels. Existing industrial experience allowed the authors determining that agglomerated fluxes have significant advantage in producing the welds with predicted complex of NMI. These fluxes are characterized by high technological flexibility due to regulation of their oxidizing ability, possibility to effect formation of NMI of certain composition and morphology in the welds. Welded joints, produced using these type fluxes, receive the complex of mechanical properties at the level of base metal values. 13 Ref., 7 Figures.

Keywords: *high-strength low-alloy steel, welding, welding flux, non-metallic inclusions, microstructure, mechanical properties*

Today steels are still the most widespread structural material in building, machine building and power engineering, regardless the numerous predictions of rapid growth in application of polymeric materials. It may be assumed that this situation will last in the future decades. Welding takes a strong leading position among the methods of joining of steel parts, and arc welding remains the main technology in this field. Analysis of consumption of welding consumables for arc methods of welding during the last decade showed that submerged-arc welding covers 7–10 % of total volume of arc methods, and there are no reasons of significant change of such situation.

Submerged-arc welding, appeared in the 1930s of XX century, went through a stage of intensive development, in course of which deep fundamental investigations of metallurgical, electric and physical-chemical processes were carried out. They formed a basis for wide implementation of automatic welding in different branches of industry to the middle of the 1970s. The investigations carried during these years in combination with accumulation of practical experience of application of fluxes and improvement of technology for production of quality steels promoted a change in determination of flux role in process of weld formation. If the flux has a role of passive protection of weld pool from ambient atmosphere and working personnel from arc influence at initial stage of development, then in recent years the flux became an active participant of metallurgical processes taking place in zone of arcing and liquid pool.

Requirements to operation of welded structures determine the necessity of ensuring of service properties of the welded joints at the level of current high-strength steels, therefore the flux in combination with electrode wire should provide alloying, microalloying, modifying and refining of the weld metal. At that, high welding technological properties of the flux should be provided in order to receive quality welds in wide range of modes and welding technologies.

Rolled sheets of low-alloy steels, used at present time for manufacture of welded structures, differ by combination of high indices of strength, ductility and toughness due to formation of fine grain (up to 1 μm) ferrite-bainite or bainite-martensite microstructure. Welded joints of such steels should have the complex of mechanical properties at the level of base metal values. The welding fluxes in this case take the leading role in producing of necessary microstructure of weld metal and mechanical properties of welded joint.

Number of works is dedicated to investigation of conditions of microstructure formation in HSLA steel weld metal. It was determined as a result of their performance that non-metallic inclusions (NMI) [1–4] are one of the factors, hav-

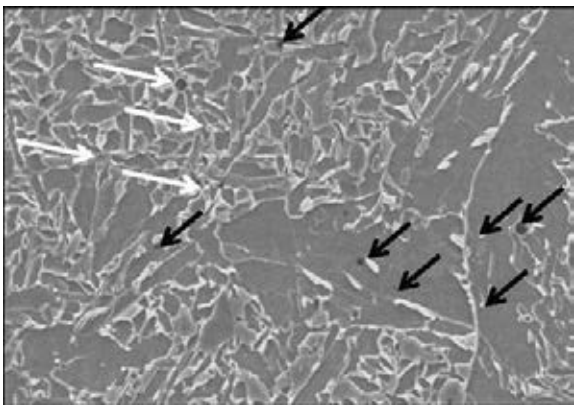

Figure 1. Microstructure (×1000) of HSLA steel weld metal (SEM JSM-35): light arrows — ferrite-forming NMI in process of re-solidification; dark — other NMI

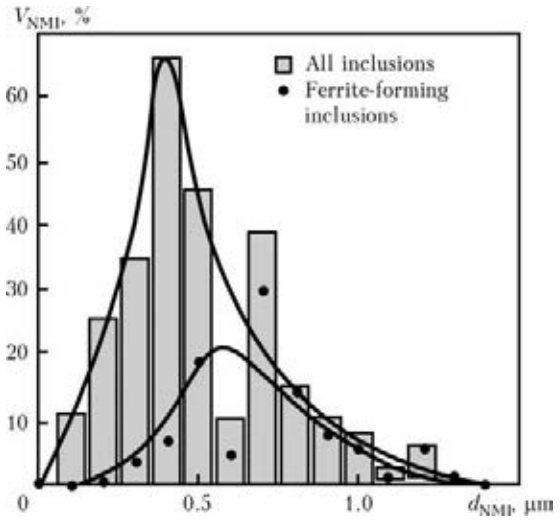

Figure 2. Block diagram of size distribution of all inclusions and inclusions, being the centers of nucleation acicular ferrite in HSLA steel weld metal [9]

ing defining effect on structure. Current fluxes should protect weld pool from ambient atmosphere as well as set required level of oxygen potential of slag phase [5] and together with low-alloy wire promote formation of NMI of predicted amount, composition and size [6]. The weld metal, produced in submerged-arc welding of current HSLA steels, contains 0.02–0.04 % of oxygen and less than 0.01 % of sulfur. Using known expression $V_{NMI} = 5.5$ [% O + % S], it can be determined that 0.15–0.30 vol.% of NMI corresponds to given content of oxygen and sulfur. However, only around 30 % of them (Figures 1 and 2) actively effect nucleation of ferrite phase [7, 8].

The most efficient in this relation are inclusions of 0.3–1.0 μm size, having specific morphology [9]. Nuclei of NMI formation in the weld metal are refractory oxides (for example Al_2O_3), which are present in form of crystals in weld pool liquid metal. When titanium oxide precipitates on the surface of refractory inclusion, then zones with reduced content of alloying elements, having high mobility in γ-phase, can be formed in adjacent areas of solid solution. The inclusions of given type are the most efficient centers of nucleation of bainite microstructure [9, 10].

Deoxidizing elements such as aluminum, silicon, titanium and manganese are used in metallurgy for refining of iron-based alloys. Technology of manufacture of agglomerated fluxes allows regulating the value of their oxygen potential in wide limits [11]. Regulation of oxygen content in the weld metal, due to change of oxidizing ability of slag phase, in combination with introduction of active deoxidizers in the flux composition provides for the possibility of application of agglomerated fluxes not only for reduction of NMI volume fraction in the weld, but also formation of the inclusions of specific size and composition (Figures 3 and 4).

Using of such type fluxes in arc welding significantly expands the field of application of methods of predictable effect on formation of NMI of specific composition and morphology in the weld metal [12]. Welded joints in this case receive the complex of mechanical properties at the level of values of HSLA steels [13]. Reduction of oxygen content in titanium-alloyed welds decreases NMI average size as well as rise precipitation of titanium compounds on the surface of refractory inclusions of Al_2O_3 type. Analysis of chemical composition of NMI of such morphology and surrounding them metallic matrix, carried out using microprobe for X-ray spectrum analysis, showed that the inclusions containing thin film of titanium compound on their surface have higher concentration of manganese in external layer and reduced content of manganese in zones of solid solution adjacent to the inclusion

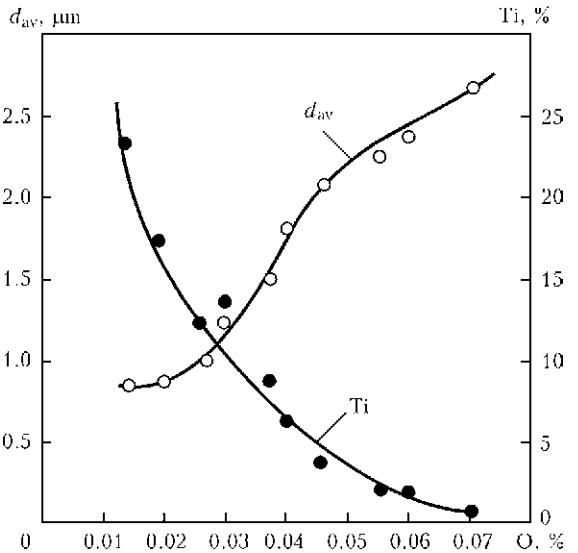

Figure 3. Effect of oxygen content in weld metal on average size of NMI and content of titanium in them

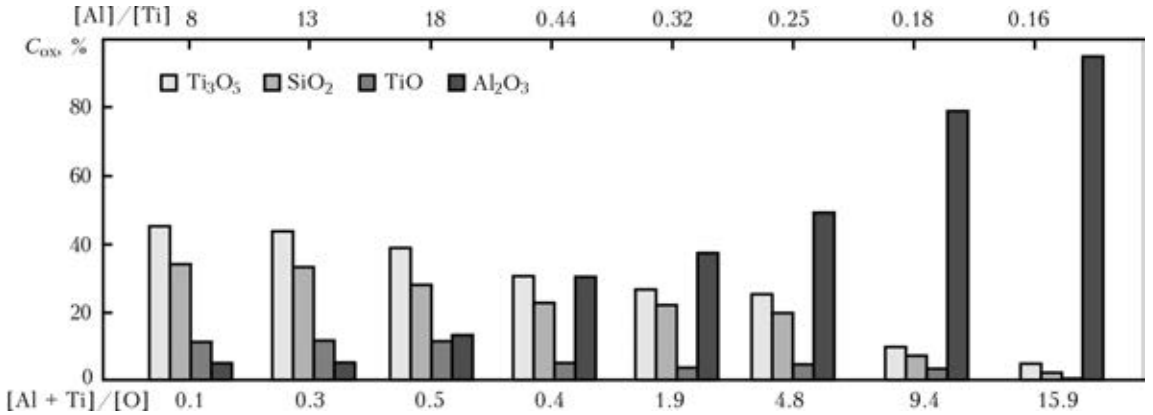

Figure 4. Change of NMI content in weld metal depending on oxidizer/deoxidizer relationship in weld pool

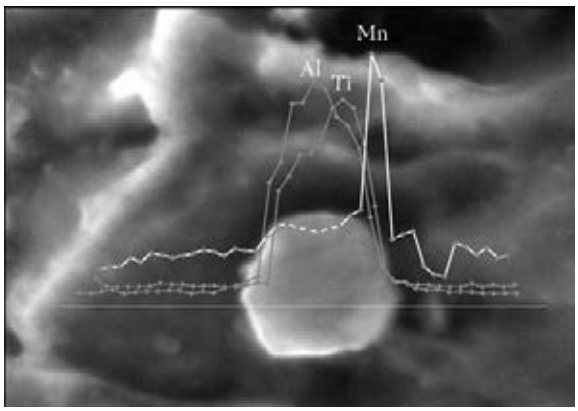

Figure 5. Distribution of elements in NMI and adjacent zones of solid solution

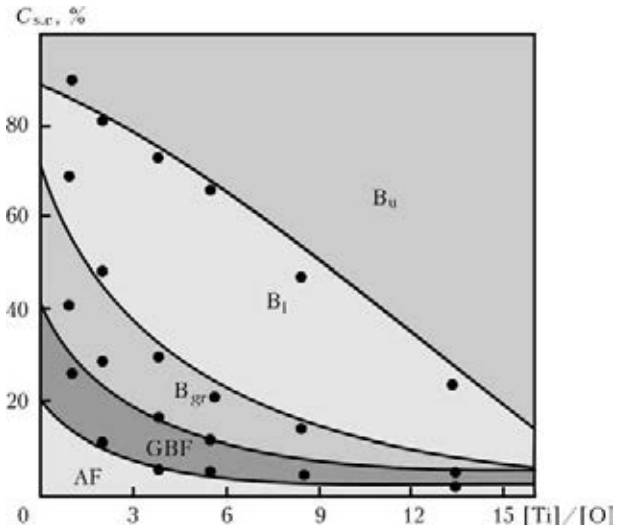

Figure 6. Effect of titanium/oxygen relationship in NMI on content of structural constituents and resistance to weld metal fracture

(Figure 5). Inclusion of such morphology promotes for formation of ferrite phase of increased toughness in the process of $\gamma \rightarrow \alpha$ transformation (Figure 6).

Complex of mechanical properties of the weld is determined by combination of its structure constituents. Rise of portion of microstructural fractions of increased hardness results in growth of indices of metal strength (Figure 7, *a*) and high content of microstructures, forming in $\gamma \rightarrow \alpha$ transformation low temperature zone, characterize by brittle fracture resistance at low climate temperatures (Figure 7, *b*). Optimum combination of indices of strength, toughness and duc-

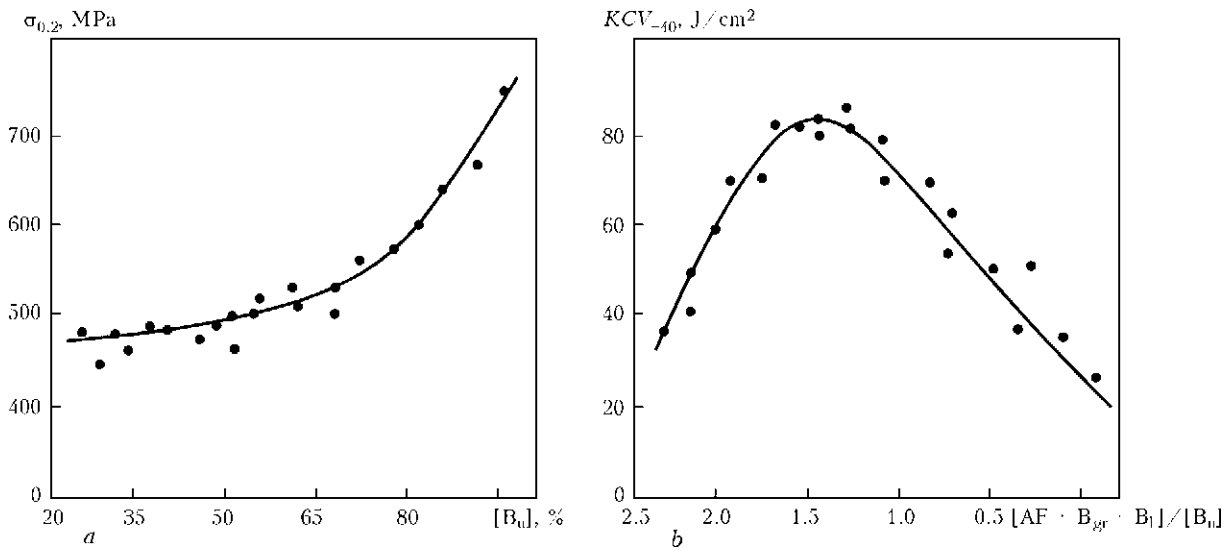

Figure 7. Effect of relationship of structural constituents on yield strength (*a*) and impact toughness (*b*) of weld metal

tility is determined by complex of given structural constituents for each separate case.

As shown by data in Figures 6 and 7, increase of content of such tough constituents as acicular and grain-boundary ferrite, granular and lower bainite up to 60 % provides for growth of impact toughness of weld metal, and at that yield strength does not exceed 500–550 MPa level, typical for welds with ferrite structure. Growth of portion of upper bainite in weld microstructure promotes for rise of indices of strength, but reduces impact toughness at low temperatures.

Conclusion

Research investigations and significant practical experience in area of welding of HSLA steels resulted in obvious change of role of welding flux in providing of weld metal quality. Current welding fluxes should actively participate in weld pool refining, regulation of metallurgical processes of formation of NMI, having specific composition, morphology and nature of distribution in solid solution, in order to provide necessary structural composition of the weld metal and complex of its mechanical properties in welding of HSLA steels. The industrial experience showed that agglomerated fluxes, characterizing by high technological flexibility due to their oxidizing ability, have significant advantage in this relation. Welded joints, produced using these type fluxes, possess the complex of mechanical properties at the level of values of HSLA steels.

1. Zhang, L., Thomas, B.G. (2003) State-of-the-art in evaluation and control of steel cleanliness: Review. *ISIJ Int.*, 43(**3**), 271–291.
2. Shin, S.Y., Oh, K., Lee, S. et al. (2011) Correlation study of microstructure, hardness and Charpy impact properties in heat affected zones of three API X80 line pipe steels containing complex oxides. *Metal Materials Int.*, 17(**1**), 29–40.
3. Zinngrebe, E., Van Hoek, C., Visser, H. et al. (2012) Inclusion population evolution in Ti-alloyed Al-killed steel during secondary steelmaking process. *ISIJ Int.*, 52(**1**), 52–61.
4. Wegrzyn, T. (2011) Proposal of welding methods in terms of the amount of oxygen. *Ibid.*, 47(**1**), 57–61.
5. Golovko, V.V. (2006) Influence of oxygen potential of welding fluxes on solid solution alloying in weld metal. *The Paton Welding J.*, **10**, 7–10.
6. Golovko, V.V., Pokhodnya, I.K. (2013) Effect of non-metallic inclusions on formation of structure of the weld metal in high-strength low-alloy steels. *Ibid.*, **6**, 2–10.
7. Lee, T.K., Kim, H.J., Kang, B.Y. et al. (2000) Effect of inclusion size on the nucleation of acicular ferrite in welds. *ISIJ Int.*, **40**, 1260–1268.
8. Grong, O., Kolbeinsen, L., Eijk, C. et al. (2006) Microstructure control of steels through dispersoid metallurgy using novel grain refining alloys. *Ibid.*, 46(**6**), 824–831.
9. Sarma, D.S., Karasev, A.V., Jonsson, P.G. (2009) On the role of non-metallic inclusions in the nucleation of acicular ferrite in steels. *Ibid.*, 49(**7**), 1063–1074.
10. Seo, J.S., Kim, H.J., Lee, C. (2013) Effect of Ti addition on weld microstructure and inclusion characteristics of bainitic GMA welds. *Ibid.*, 53(**5**), 880–886.
11. Golovko, V.V., Podgaetsky, V.V., Bondarenko, T.P. (1993) Oxidability of slag melts of system MgO–Al_2O_3–SiO_2–CaF_2. *Avtomatich. Svarka*, **9**, 28–30.
12. Golovko, V.V., Kostin, V.A., Zhukov, V.V. et al. (2010) Influence of alloying with manganese and titanium on peculiarities of austenite decomposition in low-alloy weld metal. *Vestnik Chernig. GTU*, **45**, 125–133.
13. Golovko, V.V. (2012) Agglomerated fluxes in local welding production (Review). *The Paton Welding J.*, **2**, 33–35.

Received 23.04.2014

TUNGSTEN CARBIDE BASED CLADDING MATERIALS

A.P. ZHUDRA
E.O. Paton Electric Welding Institute, NASU
11 Bozhenko Str., 03680, Kiev, Ukraine. E-mail: office@paton.kiev.ua

The paper presents materials for cladding by composite alloys based on tungsten carbides. Brief description of the technology of producing special cladding hard alloys of type, macrocrystalline tungsten carbide, fused tungsten carbide WC + W_2C with crushed, surface-melted and spherical granules is given. Process schematic and unit for thermocentrifugal sputtering of refractory compound ingots with application of plasma arc as the heat source is described. Comparative data are given on hardness, chemical and stoichiometric compositions of tungsten carbide granules produced by different technologies. Macrostructures of composite layers, produced by the method of plasma-powder cladding, are shown. Schematic and macrostructure of a layer produced by the method of induction furnace impregnation is given. Commercial grades of powders of fused tungsten carbides in spherical granules and main grades of strip relit are presented. 22 Ref., 3 Tables, 8 Figures.

Keywords: *tungsten carbides, relit, composite alloys, cladding, spherical granules, oxy-acetylene cladding, plasma cladding, thermocentrifugal sputtering, strip relit*

High wear-resistance of deposited composite alloys with metallic matrix, strengthened by tungsten carbides, led to their wide acceptance for equipment protection from various kinds of intensive wear. This is related first of all to unique properties of reinforcing phase of such alloys, namely tungsten carbides. The most widely accepted by industry is tungsten monocarbide WC with 6.13 % C stoichiometry. It features high hardness of *HV* 2200, compressive strength of 5–7 GPa and modulus of elasticity of 700 GPa, while preserving its mechanical properties in a broad temperature range, is resistant to friction corrosion and is capable of forming a strong bond with metals [1, 2]. Tungsten carbide is much harder and performs much better under the conditions of wear and corrosion and high impact loads than martensite, ferric and chromium carbides. It is widely used in production of a number of steel grades, and in cladding in manufacture of flux-cored wires, strips and electrodes.

Moreover, WC monocarbide is the main component of sintered hard alloys of VK type, produced by powder metallurgy. Sulzer Metko WOKA, H.C. Starck, C&M Technologie, DURUM VERSCHLEISS–SCHUTZ (Germany), REED TOOL, KENNMETAL (USA), Beijing Advanced Materials, BAM (China), Volgoburmash (Russia) and many other companies manufacture special metal-ceramic particles of VK-6 type of an oval shape (Figure 1, *a*) for drill tool strengthening [3, 4]. The process of manufacturing such materials consists in long-time mixing of fine carbide particles with cobalt or nickel binder, preliminary low-temperature sintering under pressure, and then final sintering at the temperature of 1350–1600 °C in vacuum or hydrogen atmosphere. Here shrinkage and compaction at sintering practically eliminate porosity [5].

Tungsten carbide is sometimes mixed with other hard carbides to improve their properties. For instance, titanium carbide and tantalum or niobium carbides are sometimes used for improvement of chemical and thermal stability, as well as for preservation of high-temperature hardness.

Volume fraction and size of carbide particles can change, depending on requirements, and over the recent years a tendency of application of nanocrystalline carbide particles has been observed, which are effective for improvement of alloy wear resistance.

Many companies recommend crushed scrap of metal-ceramic alloys of VK or VN type for strengthening components for mining and metallurgical industry [3, 6]. Owing to their relatively high strength, such materials are particularly important in those cases, when application of particles of 1.5 mm and greater size is required.

Over the recent years, DURUM VERSCHLEISS–SCHUTZ, Sulzer Metco WOKA, BAM and other companies have been widely advertising the so-called macrocrystalline tungsten carbide. This is granulated powder (Figure 1, *b*) with predominantly up to 200 μm granule size, containing 6.13 % of total carbon, 0.03 % of free carbon and up to 0.15 % of impurities, mainly, iron [3, 4].

Macrocrystalline tungsten carbide is used predominantly for plasma-powder cladding in com-

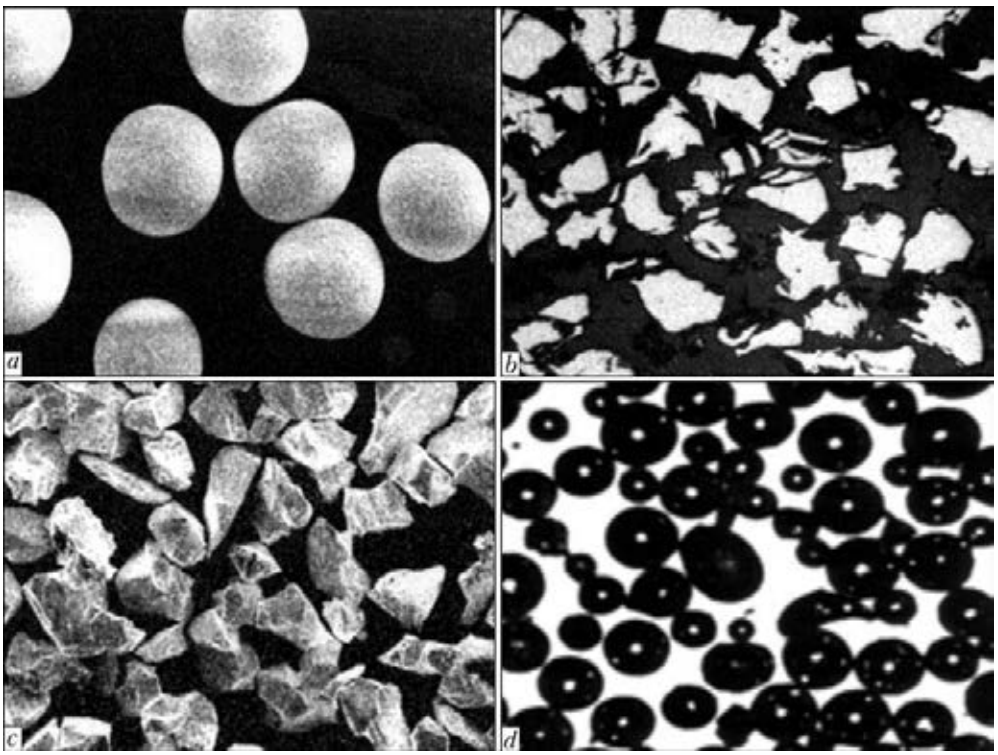

Figure 1. Cladding consumables from tungsten carbides produced by different methods: *a* — VK-6 alloy granules; *b* — macrocrystalline WC; *c* — crushed fused WC + W_2C; *d* — surface-melted WC + W_2C

bination with nickel-based matrix alloy. Its application is the most promising under abrasive conditions with small angles of incidence and low surface stresses. All the above-mentioned materials have become accepted to varying degrees in different industries.

Nowadays, however, fused tungsten carbide — relit (Figure 1, *c*) is the most widely accepted material as the reinforcing phase to produce highly wear-resistant composite layers. This is eutectic alloy of tungsten mono- and semicarbide WC + W_2C with 2735 °C melting temperature and microhardness from *HV* 1000 up to *HV* 2400, depending on manufacturer [1, 7].

Mostly cast tungsten carbide is used in the form of grit produced as a result of crushing of ingots, melted in Tamman resistance heating furnaces at 3100 °C. After sieving by fractions, the produced powder is used for plasma-powder induction or furnace cladding. For oxy-acetylene cladding so-called tubular-grain relit was used for a long time, and over the recent years strip relit has been used.

Alongside the high hardness and strength, fused tungsten carbide also has several disadvantages, related to the technology of producing it. A considerable part of grains features non-uniform composition, has characteristic casting defects, cracks and non-equiaxiality. In the long run this is negative for performance of deposited composite layers. In this connection, a continuous search for the ways to improve this material is going on worldwide.

Considering intense development of plasma-powder cladding processes over the recent decade, an important factor is spherical shape of powder particles, which ensures maximum looseness and stable operation of metering devices, respectively. At some time, US and Canadian specialists [8–11] developed an induction-plasma technology of producing spherical particles of fused tungsten carbide. It consists in surface melting of earlier prepared crushed grains during their passage through induction plasma column. As a result, particles of a spherical shape with preserved chemical composition are produced (Figure 1, *d*). To avoid losses due to particle overheating and their subsequent evaporation, thorough optimization of melting and spheroidization processes is required that involves development of expensive computer programs. Other disadvantages of this technology include higher power cost, need for preliminary crushing of ingots, large amount of wastes (non-spherical particles) of up to 30 % and size limitation predominantly to 200 μm that significantly narrows the area of its application.

PWI developed and has successfully implemented on production scale technology of thermocentrifugal sputtering of ingots of fused tungsten carbide, which allows producing powder with spherical particles of 50 up to 1000 μm size

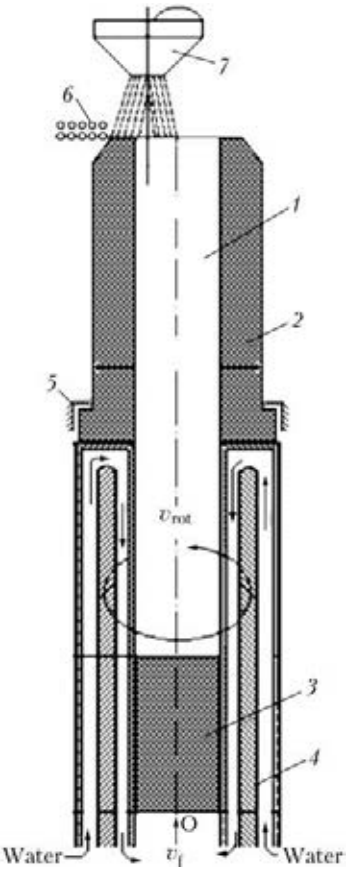

Figure 2. Schematic of thermocentrifugal sputtering of refractory compounds using plasma arc as the heat source: *1* — sputtered rod; *2* — graphite bushing; *3* — graphite pusher; *4* — water-cooled shaft; *5* — component of graphite bushing connection with the shaft; *6* — liquid metal drop; *7* — direct-action plasmatron

[12, 13]. Schematic of the process of thermocentrifugal sputtering is shown in Figure 2. With this method, the edge of quickly rotating blank is surface-melted in a vacuum chamber filled with inert gas, and the formed melt under the impact of centrifugal forces comes off the ingot periphery and is spheroidized in flight. Owing to repeated remelting, alloy composition is homogenized, content of

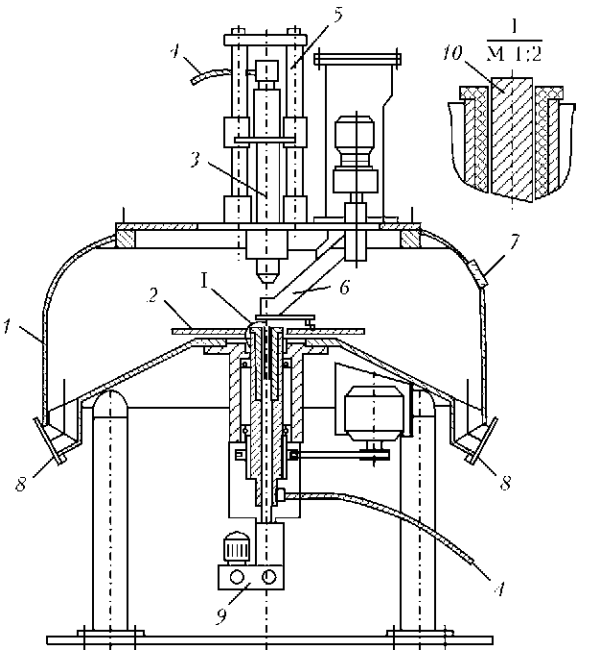

Figure 3. Schematic of unit for ingot sputtering: *1* — chamber case; *2* — spindle component; *3* — plasmatron; *4* — current contact jaw; *5* — plasmatron adjustment mechanism; *6* — rod loading mechanism; *7* — viewing window; *8* — finished product collectors; *9* — rod feed mechanism; *10* — sputtered rod

free carbon and foreign matter is reduced. Figure 3 shows the schematic of the unit to produce spherical granules of tungsten carbide by the method of thermocentrifugal sputtering [12].

Produced granules have perfect spherical shape, stable stoichiometric composition, fine globular structure and, as a result, hardness higher than *HV* 3000 and high strength. The technology ensures producing specified grain-size composition of powder particles in a narrow range of dimensions and presence of wastes (non-spherical component) in the range of 5–8 %. Appearance and macrostructure of spherical granules of tungsten carbide are shown in Figure 4.

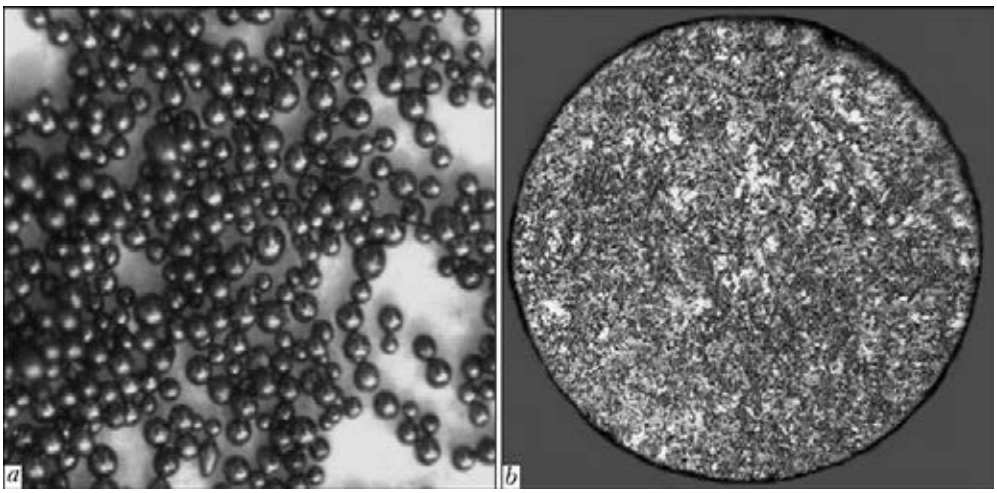

Figure 4. Appearance (*a*) and macrostructure (*b*) of spherical granules of tungsten carbide

Table 1. Composition and properties of tungsten carbide with spherical and crushed granules

Chemical composition (wt.%) and characteristics	Spherical	Crushed
Tungsten	94.5–95.5	94.3 (min)
Total carbon	3.8	0.1–3.8
Free carbon	0.02–0.05	0.1 (max)
Iron	0.1–0.3	0.5 (max)
Impurities (Cr, V, Nb, etc.)	0.5–0.8	1.2 (max)
Hardness *HV*	2800–3100	2000–2200
Microstructure	High-quality, acicular, globular	Acicular
Yield, 50 g/s	7.2–8.0	10.5–12.0
Density, g/cm^3	10.0–10.8	7.6–8.4
Wettability	Excellent	Excellent

Table 2. Phase composition and hardness of tungsten carbide produced by different technologies

Kind of particles	C, %	Phase	Phase content, wt.%	*HV*
Crushed	3.9	WC	36.20	1800–2300
		W_2C	63.80	
Macrocrystalline	6.0	WC	95.42	1900–2150
		W_2C	4.08	
Spherical (surface melting)	3.9	WC	31.12	1900–2800
		W_2C	57.20	
Spherical (sputtering)	4.0	WC	22.66	2600–3300
		W_2C	77.34	

Table 1 gives the composition and properties of fused tungsten carbide with spherical and crushed granules.

Investigations revealed that unique hardness and increased strength characteristics of spherical tungsten carbide granules are largely dependent on stoichiometric composition of WC + W_2C eutectic alloy. Maintaining it in the range of 78–82 % W_2C–18–22 % WC in combination with fine-grained macrostructure, which forms as a result of high solidification rates, ensures granule microhardness above *HV* 3000.

Table 2 gives the data on phase composition and hardness of tungsten carbide granules, produced by different technologies, which are indicative of the advantages of material manufactured by thermocentrifugal sputtering [14].

Moreover, spherical granules are much less susceptible to the process of dissolution in steel matrix at deposition of composite layers. This is an extremely important aspect, as at penetration of tungsten carbides into a liquid matrix melt tungsten and carbon diffusion takes place with subsequent formation of complex ferric-tungsten carbides, which lead to essential embrittlement of the matrix [15–17].

As was noted earlier, in addition to high hardness and strength, tungsten carbide powder in

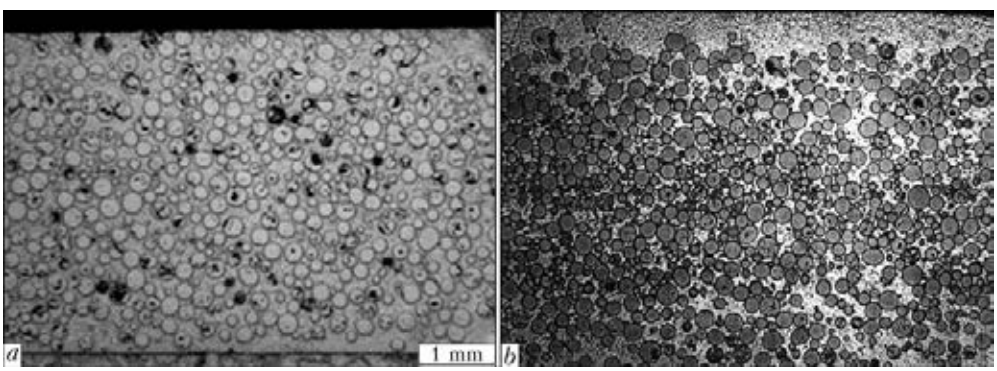

Figure 5. Macrostructure of composite layer deposited by plasma-powder method: *a* — C–Fe–V–Cr matrix + 50 % WC + W_2C; *b* — Ni–Cr–Si–B matrix + 50 % WC + W_2C

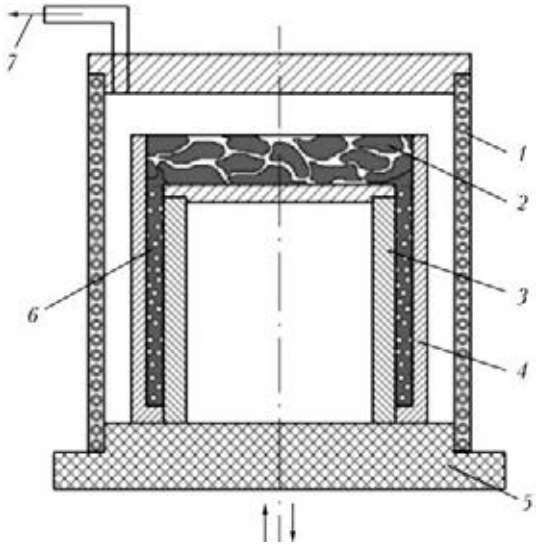

Figure 6. Schematic of induction furnace cladding (impregnation method): *1* — inductor; *2* — material for binding composite alloy (German silver); *3* — part for cladding; *4* — technological shell; *5* — furnace hearth; *6* — deposited composite alloy; *7* — pumping down system

spherical granules also has high flowability that predetermined its broad application in plasma-powder and laser cladding [18, 19]. These processes ensure feeding of matrix and reinforcing powder into the weld pool so as to minimize the thermal impact on tungsten carbide particles and, thus, prevent their dissolution. Reinforcing phase concentration in the deposited layer higher than 50 % is achieved here.

Figure 5 shows macrostructures of composite alloys on nickel and iron base reinforced by spherical granules of tungsten carbide.

In addition to traditional cladding methods, it is widely applied in powder metallurgy, when manufacturing composite layers by the method of impregnation of pre-compacted granules of tungsten carbide powder by matrix melt. Figure 6 shows a schematic of induction furnace cladding by impregnation method. Composite alloys produced by such a technology, feature unique wear resistance owing to a high concentration of reinforcing phase in the alloy. This process has become widely accepted in manufacture of slide bearings of submersible drive oil pump units and other components of drilling equipment. Figure 7 shows the appearance of a bushing and macrostructure of the deposited layer, produced by impregnation in induction vacuum furnace.

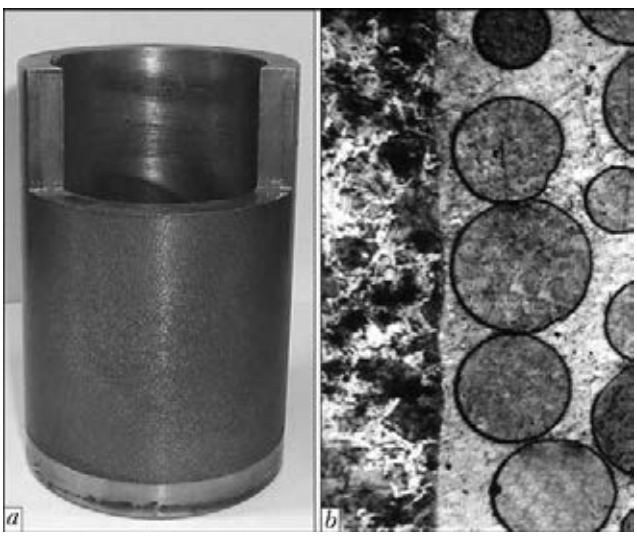

Figure 7. Appearance of bushing (*a*), and macrostructure of deposited layer produced by impregnation in induction vacuum furnace (*b*)

Commercial production of tungsten carbide in spherical granules by thermocentrifugal sputtering method was organized in Ukraine at the end of the previous century. Unique equipment was developed, technology of sputtering and screening of the produced material by particle size and removal of non-spherical component was developed. Volume of annual manufacture of the material is within 25–30 t. It is successfully exported to leading companies of European countries, USA and Russia. Particle-size distribution of cast tungsten carbides is within 0.04–2.50 mm and it has the designation of PKVS (i.e. fused spherical tungsten carbide) [20].

A large fraction of fused tungsten carbides, both with crushed and with spherical granules, is used in cladding of drilling tools. Strip relit has become widely accepted for these purposes

Table 3. Main strip relit grades

Grade	Size of particles of main relit fraction, mm	Dimensions, mm		Marking (colour)
		B = 0.5	H = 0.3	
LZ-4-6 LS-4-6	0.28–0.45	6	3	White
LZ-6-7 LS-6-7	0.45–0.63	7	3	Yellow
LS-8-7	0.63–0.80	7	3	Orange
LZ-11-7 LS-11-7	0.63–1.10	7	3	Green
LSZ-6/4-7	0.45–0.63-S 0.28–0.45-Z	7	3	Red
LSZ-8/4-7	0.63–0.80-S 0.28–0.45-Z	7	3	Brown
LSZ-8/6-7	0.63–1.10-S 0.45–0.63-Z	7	3	Blue
LSZ-11/4-7	0.63–0.80-S 0.28–0.45-Z	7	3	Light blue
LSZ-11/6-7	0.63–0.80-S 0.45–0.63-Z	7	–	Violet

Note. Overlap of not less than 1 mm; length of 670 ± 5 mm; S — spherical; Z — granular (crushed) tungsten carbide.

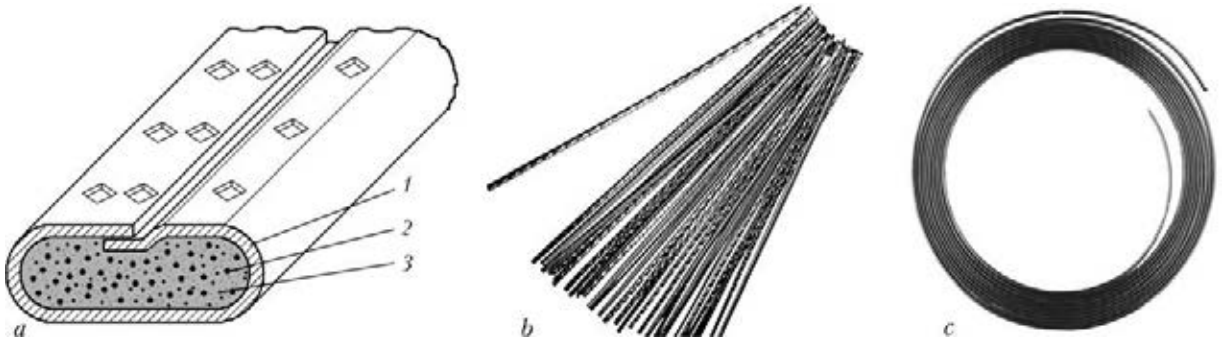

Figure 8. Section (*1* — shell; *2* — WC + W_2C; *3* — charge) (*a*), and appearance of strip relit in rods (*b*) and bundle (*c*)

in Ukraine and CIS countries. This material is a strip, inside which relit granules with a complex of de-oxidizing alloying and fluxing components are packed [16, 21]. Depending on requirements to deposited layer, the composition of this material can include crushed or spherical tungsten carbide grains or their mixture. The material is manufactured in the form of rods for gas cladding or continuous strip electrode in case of its application as filler material in mechanized plasma cladding. Appearance of strip relit in the form of rods or in a bundle is shown in Figure 8, and Table 3 gives commercial grades of strip relit rods [22].

Cones and blades of drill bits, connecting elements of drill strings, calibrators and a number of other types of drilling tools are clad by strip relit. Moreover, it has become applied in strengthening components of crushing equipment, road-construction machinery and various kinds of screws. In metallurgical industry strip relit is used for cladding valves, cones and bowls of blast furnaces, thus ensuring the maximum interrepair cycle.

Note that unique properties of fused tungsten carbides are by far not exhausted. Work on its improvement by alloy doping with elements of transition metal group already at the initial research stage allowed producing granules with hardness exceeding *HV* 3000. Results of this work will be presented in subsequent publications.

1. Samsonov, G.V., Vitryanyuk, V.N., Chaplygin, F.I. (1974) *Tungsten carbides*. Kiev: Naukova Dumka.
2. Pierson, H.O. (1996) *Handbook of refractory carbides and nitrides*. New Jersey: Noyes Publ.
3. *WOKA carbide materials for wear protective. Welding and PTA applications*: Bull.
4. (2013) *Durum Verschleiss–Schutz GmbH Products and services*: Bull.
5. Tretiakov, V.I. (1976) *Principles of metals science and technology of production of sintered hard alloys*. Moscow: Metallurgiya.
6. (2000) *Vautid Hardfacing Materials. Vautid–Verschleiss–Technik*: H. Wohl GmbH Bull.
7. Meerson, G.A., Zelikman, A.N. (1973) *Metallurgy of rare metals*. Moscow: Metallurgiya.
8. Nicolas, M.D., Maher, I.B. (1997) Ceramic and metallic powder spheroidization using induction plasma technology. In: *Proc. of United Thermal Spray Conf*. (15–19 Sept. 1997, Indianapolis, USA).
9. Bourdin, E., Fauchais, P., Boulos, M. (1983) Induction plasma technology. *Int. J. Heat and Mass Transfer*, 26(**4**), 567–582.
10. Pawlovski, L. (1995) *The science and engineering of thermal spray coatings*. Chichester: John Wiley & Sons.
11. Muns, R. (1995) *Particulate systems*. Montreal: McGill University.
12. Zhudra, A.P., Bely, A.I., Dzykovich, V.I. et al. *Unit for centrifugal spraying of rods from refractory metals*. USSR author's cert. 1381840. Fil. 10.07.86. Publ. 15.11.87.
13. Yushchenko, K.A., Zhudra, A.P., Bely, A.I. et al. *Method of producing of granulated refractory materials*. Pat. 20516A Ukraine. Int. Cl. B22F 9/10. Fil. 14.10.94. Publ. 15.07.97.
14. Dzykovich, V.I., Zhudra, A.P., Bely, A.I. (2010) Properties of tungsten carbide powders produced by different technologies. *The Paton Welding J*., **4**, 22–24.
15. Howards, A. (1951) Some characteristics of composite tungsten carbide weld deposits. *Welding J*., **2**, 144–162.
16. Frumin, E.I., Zhudra, A.P., Pashchenko, M.A. (1979) Physical-chemical processes in surfacing with strip relit. *Svarochn. Proizvodstvo*, **8**, 11–13.
17. Zhudra, A.P., Makhnenko, V.I., Pashchenko, M.A. (1975) Peculiarities of automatic arc surfacing of composite alloys. *Avtomatich. Svarka*, **8**, 16–19.
18. Happer, D., Gill, M., Wid Hart, K. et al. (2002) Plasma transferred arc overlays reduce operating costs in oil and processing. *In: Proc. of Int. Spray Cent. TISC* (Essen, Germany, May 2002), 278–293.
19. Som, A.I. (2004) Plasma-powder surfacing of composite alloys based on cast tungsten carbides. *The Paton Welding J*., **10**, 43–47.
20. *TU U 24.1-19482355-001:2010*: Tungsten carbides. Spherical fused of PKVS grade. Introd. 16.02.2011.
21. Frumin, E.I., Zhudra, A.P., Pashchenko, M.A. (1977) Strip relit for surfacing of drill bits. *Svarochn. Proizvodstvo*, **2**, 16–18.
22. *TU U28.7-194823555-002:2014*: Strip relit of grades LZ-4; LZ-6; LZ-11; LS-4; LS-6; LS-8; LS-11; LSZ-6/4; LSZ-8/6; LSZ-11/6.

Received 24.04.2014

FLUX-CORED STRIPS FOR WEAR-RESISTANT SURFACING

A.P. VORONCHUK
E.O. Paton Electric Welding Institute, NASU
11 Bozhenko Str., 03680, Kiev, Ukraine. E-mail: office@paton.kiev.ua

Advantages of flux-cored strip application as electrode material for wear-resistant surfacing are considered. The list of batch-produced flux-cored strips, their typesizes and form of delivery is given. Examples of techniques of strip application for surfacing cones and cups of blast furnace charging equipment, pans of coneless charging devices, beaters of coal-pulverizing mills, cutters for hot cutting of metal, and production of wear-resistant bimetal sheets are presented. Kinds of new specialized equipment for surfacing with flux-cored strips are shown, namely A1812M apparatus for surfacing cones and cups of blast furnace charging equipment, AD 380.03 unit for plate surfacing, UD298M unit for surfacing cutters for hot cutting of metal. All the equipment is fitted with control systems based on microcontrollers. Enterprises, where new developments have been introduced, are listed. 8 Ref., 1 Table, 6 Figures.

Keywords: *flux-cored wire, compositions, surfacing, equipment, technology, surfacing efficiency, application*

Hardfacing is an effective method of increasing wear resistance and serviceability of parts of machines exposed to intensive abrasive wear. A large range of parts are surfaced during manufacture, and reconditioning surfacing is also used.

Alloys of the type of high-chromium cast irons with a high degree of alloying of up to 40 % and higher became widely accepted for strengthening various parts, operating under the conditions of intensive abrasive and gas-abrasive wear. For these purposes leading European companies such as Castolin (Sweden), Buller (Switzerland), Durum (Germany), Welding Alloys (Great Britain) and others offer flux-cored wires made by rolling in specialized mills. Manufacturing flux-cored wires with filling coefficient above 40 % by drawing method, which is widely used in Ukraine and other CIS countries, is very difficult. Therefore, this problem could be much simpler solved by development of similar compositions of flux-cored wire strips. This surfacing material readily allows achieving filling coefficients up to 60–70 %, and its manufacturing technology excludes the drawing process.

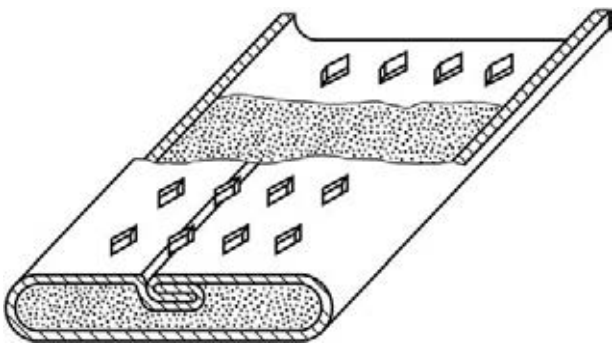

Figure 1. Design of single-lock flux-cored strip with tight lock joint

At present flux-cored strip is a well-known surfacing material, which is widely applied for manufacture and strengthening of a wide range of parts in metallurgical, power, mining, road-construction and other industries. Unlike flux-cored wire the main advantage of flux-cored strips is high deposition rate.

At present annual production volume of flux-cored strips in CIS countries is equal to about 600 t and has a stable growth tendency.

Flux-cored strip, the design of which is shown in Figure 1, has become the most widely accepted in industry [1, 2]. Currently available equipment allows manufacturing two typesizes of material of 16.5 × 4 and 10 × 3 mm section. Flux-cored strip is supplied in bundles of 80–160 kg weight with row-by-row laying. Bundle inner diameter is 400–460 mm, outer diameter is up to 850 mm and width is 115–130 mm. Reliable sealing of flux-cored strip lock joint, its supply in bundles of large weight ensure continuous high-efficient surfacing that is particularly important at strengthening of large-sized parts with large working surfaces.

Surfacing with flux-cored strips is performed both by an open arc and by submerged arc. The process of submerged-arc surfacing by flux-cored strip practically does not differ from submerged-arc welding by other electrode materials.

Flux-cored strip typesize, surfacing modes and its schematics are selected depending on typesize

Flux-cored strips for surfacing

Flux-cored strip grade	Deposited metal composition, wt.%											Hardness *HRC*	Purpose
	C	Cr	Mn	Si	Ni	Nb	Mo	V	W	B	Ti		
PL-AN-101	3.0	25	2.0	3.0	2.0	–	–	–	–	–	–	50–56	Surfacing of parts, exposed to abrasive wear in service (bulldozer and gripper jaws, excavator bucket teeth, coke crusher rolls, plough disks, protective surfaces of cones, cups, etc.)
PL-AN-171	1.2	25	2.2	1.0	–	–	–	–	–	3.5	–	54–59	
PL-AN-180	4.5	30	–	–	–	–	1.0	–	–	–	–	58–62	
PL-AN-181	4.5	30	3.0	–	–	–	–	–	–	–	–	58–60	
PL-AN-111	5.0	38	1.0	2.5	38.0	–	–	–	–	0.3	–	50–58	Surfacing of parts, exposed to intensive abrasive and gas-abrasive kinds of wear at normal and elevated temperatures (cones and cups of blast furnace charging equipment, chutes, hoppers, etc.)
PL-AN-179	5.0	22	–	–	–	7.0	6.0	1.0	2.0	–	–	58–62	
PL-AN-185	5.0	22	–	–	–	7.0	–	–	–	–	–	56–60	
PL-AN-186	4.5	30	–	–	–	–	–	–	–	0.7	–	57–62	
PL-AN-132-1	0.1	4	1.5	1.0	–	–	2.0	–	2.5	–	–	18–28	Surfacing of parts exposed to contact loads at elevated temperature (roller conveyor rollers, rolls, etc.)
PL-AN-132-2	0.15	4	1.5	1.0	–	–	2.0	–	2.5	–	–	28–34	
PL-AN-132-3	0.2	4	1.5	1.0	–	–	2.0	–	2.5	–	–	35–45	
PL-AN-187	0.2	11	10.0	–	–	–	–	–	–	–	0.8	18–26	Surfacing of parts exposed to high contact loads in service (crane wheels, guides, etc.)
PL-AN-115	0.1	–	1.5	0.8	–	–	–	–	–	–	0.5	18–26	Surfacing of large-sized steel parts to restore their geometrical dimensions (cones and cups of blast furnace charging equipment, agglomachine trucks, etc.)
PL-AN-189	0.35	3	0.8	0.6	–	–	–	0.3	9.0	–	–	44–50	Surfacing of rolls for hot rolling of metal
PL-AN-190	0.4	3	0.8	0.6	–	–	–	0.3	9.0	–	–	44–50	
PL-AN-191	0.25	5	0.7	1.0	–	–	1.2	0.4	–	–	–	46–52	
PL-AN-183	0.4	2	1.6	1.6	5.5	0.6	1.8	0.5	–	–	–	47–54	Surfacing of blades for hot cutting of metal
PL-AN-150	0.12	16	2.0	5.0	9.0	–	–	–	–	–	–	27–34	Submerged-arc surfacing of fittings operating at up to 545 °C ambient temperature
PL-AN-151	0.12	16	4.0	5.0	8.0	1.0	6.0	–	–	–	–	38–50	

of the part being strengthened. Surfacing can be performed in one, two and more layers; by isolated beads and in wide layers, with oscillation range from 50 up to 400 mm. Surfacing currents here can be varied from 300 up to 1200 A, arc voltage — from 25 up to 38 V, electrode displacement rate — from 5 up to 100 m/h. Twin and multiarc surfacing is applied to increase the efficiency, that is provided by specially developed equipment. Wear-resistant layer of 2 to 8 mm thickness can be deposited in one pass by one arc, and surfacing efficiency reaches 25–30 kg of deposited metal per hour.

Flux-cored strip consumption when recalculated per 1 kg of deposited metal is equal to 1.1–1.2 kg in the presence of volatile components in the powder filler and 1.20–1.35 kg in the presence of mineral components [2].

For surfacing with flux-cored strips, batch-produced welding equipment is additionally fitted with special nozzles and feed rollers, providing reliable electrode material feed. AD 231 unit is most often used.

The Table gives flux-cored strip grades, which have been mastered and are batch-produced by industry.

Flux-cored strip advantages are the most fully realized in surfacing of batch-produced parts. In this case, original technologies with application of specialized equipment are used for strengthening.

A traditional example of application of flux-cored strip for strengthening parts for metallurgical production is surfacing of blast furnace charging equipment. Unique units U-50, U-75 and U-125 have been developed for these pur-

Figure 2. A1812M unit

poses [2–4]. Starting from 2002, the units are fitted with new upgraded surfacing apparatus A1812M (Figure 2), and control system of SU 320 type [5]. The apparatus ensures surfacing by two tandem or parallel arcs, as well as transverse oscillations of the electrode with 50 to 500 mm amplitude. Unit design also envisages surfacing performance around a circle and open-arc and submerged-arc welding of large-sized parts with flux-cored and solid-drawn wires. Unit control system is based on a microcontroller, and units are fitted with asynchronous AC motors with frequency converters.

Mechanized surfacing of cones and cups with self-shielded flux-cored wires is 4 times more efficient than the process of flux-cored wire surfacing.

New apparatuses and control systems have been introduced with success in OJSCs «Mittal Steel Krivoy Rog», Ukraine), «Azovmash» (Mariupol, Ukraine) and ZSMK (Novokuznetsk, RF).

One of the examples of comprehensive solution of strengthening problems is surfacing of 5 to 20 mm plates [6, 7]. Specialized surfacing unit AD 380.03 is used for these purposes [8]. It consists of a carriage with two surfacing heads, moving along a guide, and two tables for fastening 3000 × 1500 mm steel plates. The carriage can move with working and travel speed. The unit is fitted with two power sources with a flat external characteristic.

Figure 3. General view of AD 380.03 unit

Figure 4. Bimetal sheets after surfacing

Self-shielded flux-cored strip ensuring deposited metal of the 4.5Cr, 30Cr, 1Mo composition (wt.%) is used as electrode material. Deposited layer hardness is *HRC* 60.

Flux-cored strip of 10 × 3 mm cross-section is used for surfacing 5 to 7 mm sheets, and strip of 16.5 × 4.0 mm cross-section is applied for 8 mm and thicker plates.

The unit is controlled by electric circuit based on a microcontroller, which allows sheet surfacing to be performed by two programs.

The unit allows surfacing to be performed in the automatic mode by the developed program on two tables alternatively with the efficiency of 1 sheet of 3000 × 1500 mm size per work shift at twin-arc surfacing.

The unit for sheet surfacing and the strengthened sheet are shown in Figures 3 and 4. Another example of wide application of flux-cored strip for wear-resistant surfacing is the process of

Figure 5. U-877 unit

strengthening of coal-crushing mill beaters [2, 3]. Beater surfacing is performed in specialized units U-877 (Figure 5), consisting of surfacing system, rotating table and five water-cooled iron moulds mounted on it, into which beaters to be surfaced are placed. Beater surfacing is performed in the automatic mode with electrode oscillations across the entire width of the part being surfaced. One unit allows surfacing 100–120 beaters per shift.

Surfacing of low-carbon steel cast billets is performed with PL-AN-101 flux-cored strip, which allows producing a deposited layer of the following composition, wt.%: 3C, 25Cr, 3Si, 2Ni, 2Mn. 1.6–1.8 kg of wear-resistant alloy is deposited on one beater. Application of this technology and electrode material in the form of flux-cored strip allowed extending service life of strengthened parts 2 times, compared to earlier applied all-cast beaters from Hadfield steel.

Positive results were obtained also, when strengthening parts of coneless charging equipment of blast furnaces using flux-cored strip. We developed the technology of surfacing fast-wearing parts of the pan and other elements of the structure of charging equipment of «Paul-Wurth» company (Luxembourg).

Technology and UD298M unit (Figure 6) were developed for flux-cored strip open-arc surfacing of cutters for hot cutting of metal, which allows strengthening cutter working edges in the automatic mode [2]. Here, efficiency of surfacing process increases rapidly. Flux-cored strip PL-AN-183 was developed as surfacing material. Its application markedly, by 1.5 to 2 times, increases the resistance of strengthened parts compared to those surfaced with flux-cored wire PP-Np-35V9Kh3SF. Here, the efficiency of surfacing process rose 2 to 3 times.

Flux-cored strips became widely accepted also at strengthening of a wide range of components for mining equipment. This electrode material is also used for strengthening bulldozer blades, cone crusher lining, grinding fan blades and many other components exposed to intensive abrasive wear and other kinds of wear in service.

Figure 6. UD298M unit

1. Danilchenko, B.V., Shimanovsky, V.P., Kopylets, I.P. et al. *Flux-cored strip electrode*. USSR author's cert. 1152159. Int. Cl. B 23 K 35/40. Publ. 22.12.1984.
2. Zhudra, A.P., Voronchuk, A.P. (2012) Cladding flux-cored strips (Review). *The Paton Welding J.*, **1**, 34–38.
3. Shimanovsky, V.P., Voronchuk, A.P., Zvezdin, S.M. (1990) Consumables and equipment for hard-facing of blast furnace cones and cups. In: *Equipment and consumables for surfacing*: Transact. Kiev: PWI, 71–73.
4. Danilchenko, B.V., Shimanovsky, V.P., Voronchuk, A.P. et al. (1989) Hard-facing of rapidly wearing parts with self-shielded flux-cored strips. *Avtomatich. Svarka*, **5**, 38–41.
5. Zhudra, A.P., Voronchuk, A.P., Fomakin, A.A. et al. (2009) New equipment for hard-facing of charging device bells and cups. *The Paton Welding J.*, **9**, 44–46.
6. Zhudra, A.P., Voronchuk, A.P. (2010) Wear-resistant flux-cored strip hard-facing. *Svarshchik*, **6**, 6–10.
7. Zhudra, A.P., Voronchuk, A.P., Kochura, V.O. et al. (2012) Technology, equipment and consumables for production of sheet lining elements. *Svarochn. Proizvodstvo*, **11**, 40–43.
8. Zhudra, A.P., Voronchuk, A.P., Veliky, S.I. (2009) Equipment and consumables for hard-facing of lining plate elements. *The Paton Welding J.*, **6**, 44–46.

Received 02.04.2014

INVESTIGATION OF INFLUENCE OF MICROALLOYING WITH TITANIUM AND BORON OF WELD METAL ON ITS MECHANICAL PROPERTIES IN UNDERWATER WELDING

S.Yu. MAKSIMOV, V.V. MACHULYAK, A.V. SHEREMETA and **E.I. GONCHARENKO**
E.O. Paton Electric Welding Institute, NASU
11 Bozhenko Str., 03680, Kiev, Ukraine. E-mail: office@paton.kiev.ua

One of the negative consequences of effect of extreme conditions of underwater welding is a low level of properties of welded joints, in the first turn, of ductility. Traditionally, this task is solved by optimization of microstructure of weld metal due to rational alloying. The purpose of this work was to establish the influence of microalloying of weld metal with titanium and boron on its mechanical properties in underwater welding using flux-cored wire. The structure of metal formed as a result of microalloying was investigated, and values of mechanical properties of deposited metal were determined. Optimal proportions of microalloying were established, at which high values of elongation of weld metal are provided. It is shown that its mechanical properties meet the requirements of A class of Specification on underwater welding ANSI/AWS D3.6. 5 Ref., 2 Tables, 7 Figures.

Keywords: *underwater welding, flux-cored wire, weld metal, microalloying, structure, mechanical properties*

Extreme conditions of underwater welding negatively influence the properties of welded joints. Traditionally, to improve mechanical properties of weld metal the purposeful alloying is used, thus optimizing its microstructure. Microstructure, which shows the optimum values of combination of strength and ductility of welded joints of low-carbon structural steels, is considered to be acicular ferrite (AF).

Figure 1 presents the schematic diagram of transformations at continuous cooling for wet underwater welding using electrode consumables, providing weld metal of ferrite type. The main structural components in weld metal are grain-boundary ferrite and ferrite with the second phase, which are characterized by low ductile properties. According to the results of investigation of microstructure of welds, performed under water using electrodes of the type E6013 under the conditions of Mexican Gulf, it was recommended to increase the content both of oxygen and also manganese in metal to increase the volume of AF (Figure 2).

As an alternative to adding of manganese the authors of work [2] used additions of titanium and boron to the charge of flux-cored wire having obtained more than 90 % of AC in weld metal during welding in air, here the content of boron and titanium was in the limits of 0.004–0.008

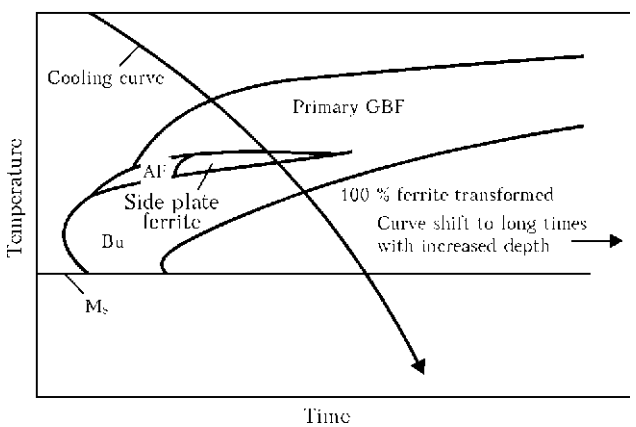

Figure 1. Schematic thermokinetic diagram for underwater welding [1]

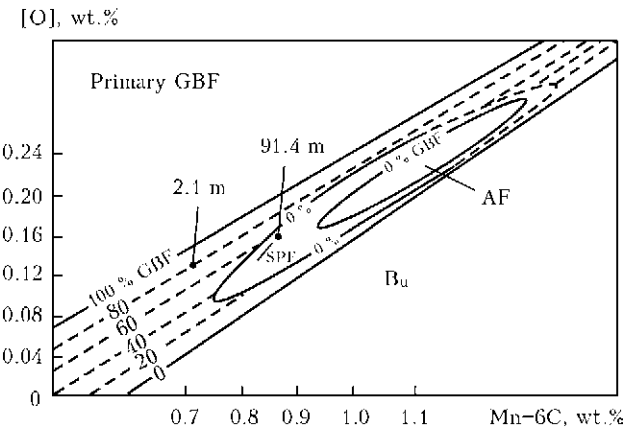

Figure 2. Predicted formation of structural components in wet underwater welding [1] at different depth

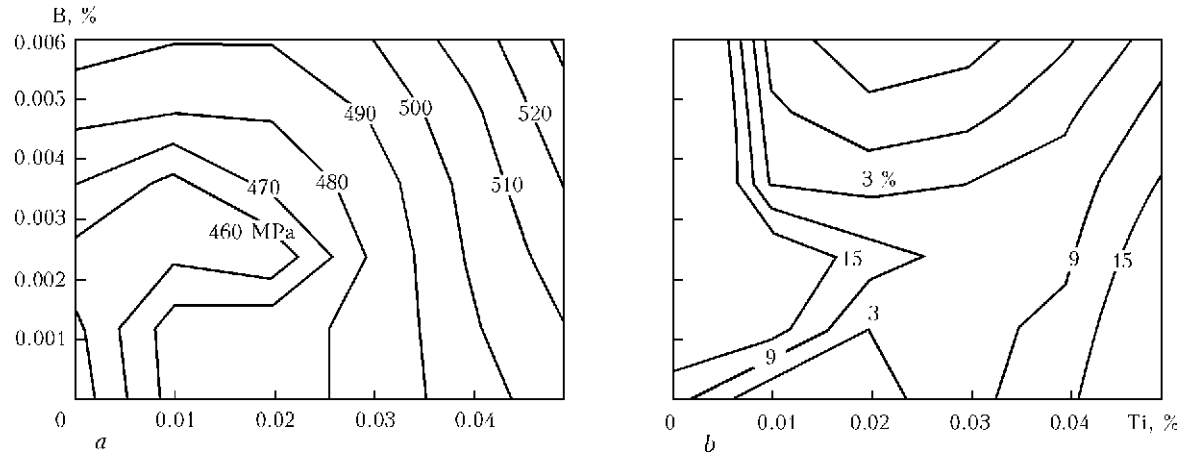

Figure 3. Influence of content of titanium and boron in weld metal on tensile strength (*a*) and elongation (*b*)

and 0.04–0.08 %, respectively. Titanium was added to form the inclusions, which serve as nuclei to AF formation. Besides, titanium as a potential deoxidizer protects alloying elements including boron from burning out. Boron facilitates also the formation of inclusions, which are mainly accumulated along the boundaries of austenite grains and hinder the formation of hypoeutectoid phases, for example, grain-boundary ferrite. Under the conditions of manual wet underwater welding the maximum attainable amount of AF (about 60 %) is formed at the lower level of alloying, such as 0.03 % Ti and 0.0015 % B [3]. The authors of work [3] explain this by the fact that necessity in titanium and boron for optimization of AF content is decreased as a result of increase in crystallization rate during welding in water environment. Close results were obtained also during use of flux-cored wire, in particular, two regions with maximum amount of AF at the level of 56–57 % were revealed. Moreover, the content of titanium and boron in weld metal for the first region amounts to 0.023–0.027 and to 0.0002 %, and for the second one — 0.030–0.032 and 0.0016–0.0023 %, respectively [4].

The aim of this work was to determine the efficiency of influence of microalloying with titanium and boron on mechanical properties of weld metal in underwater welding using flux-cored wire.

To conduct the investigations, a batch of flux-cored wires of the type PPS-AN1 of 1.6 mm diameter with additions of titanium and boron to the charge due to decrease of amount of iron powder was manufactured. Titanium and boron were added as FeTi and FeB in the amount of 10, 20 and 2, 4 %, respectively, both separately as well as together. To obtain specimens of deposited metal, the multipass welding of butt joints of steel St3 of 14 mm thickness was performed in laboratory pool at the depth of 1 m under the conditions: U_a = 30–32 V; I_w = 160–180 A, the polarity is reverse.

Of each butt joint the sections and specimens for mechanical tests in accordance to the requirements of A class of Specifications on underwater welding ANSI/AWS D3.6 [5] were manufactured. Chemical composition of weld metal is given in Table 1, the results of mechanical tests — in Table 2.

Table 1. Chemical composition of weld metal made by Ti- and B-containing flux-cored wire under water

Number of sample	Elements, wt.%						
	C	Si	Mn	S	P	Ti	B
1	0.026	0.013	0.20	0.016	0.018	–	–
2	0.013	0.004	0.17	0.022	0.015	0.003	0.002
3	0.015	0.004	0.20	0.022	0.019	< 0.002	0.002
4	0.017	0.005	0.23	0.021	0.014	0.005	< 0.002
5	0.031	0.106	0.47	0.021	0.021	0.032	< 0.002
6	0.039	0.017	0.37	0.023	0.021	0.007	0.0033
7	0.038	0.114	0.58	0.030	0.018	0.0053	0.005
8	0.024	0.020	0.28	0.024	0.023	0.006	0.002
9	0.044	0.080	0.62	0.027	0.018	0.049	0.006

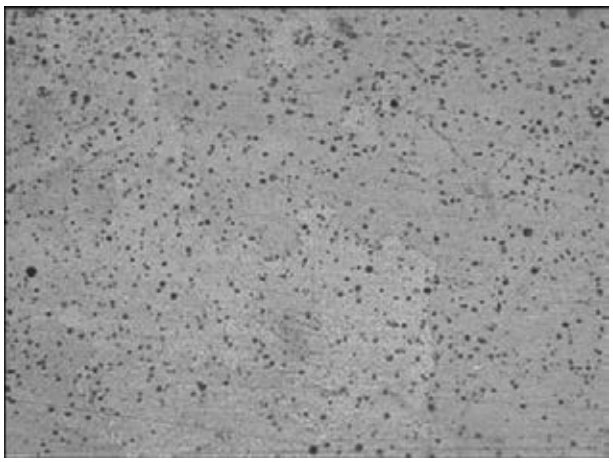

Figure 4. Microstructure (×500) of weld metal without alloying

Table 2. Results of mechanical tests of welds

Number of specimen	σ_y, MPa	σ_t, MPa	δ, %	ψ, %	α_{bend}, deg
1	333.0	440.0	11.3	22.0	50
2	381.6	459.6	12.3	22.0	90
3	374.6	458.6	17.7	35.8	180
4	393.2	469.8	10.7	18.7	69
5	447.5	485.6	7.0	16.0	61
6	342.5	466.3	7.0	16.0	31
7	450.9	485.6	3.7	15.4	135
8	392.1	468.6	16.0	28.2	81
9	494.1	532.4	6.3	12.9	50

As is seen from the given data, alloying with titanium and boron in all cases leads to negligible increase in strength properties of weld metal. Regarding ductility, their influence bears ambiguous nature. For the convenience of the analysis of the obtained results using the specialized package of programs (Origin 7, Statistica 6) polynominal interpolation of experimental data was performed, and distribution of values of elongation and tensile strength depending on boron and titanium content in weld metal was obtained (Figure 3). It was established that the compositions, providing the highest ductile properties, are in the limits of 0.0015–0.0025 % B and to 0.01 % Ti.

Metallographic investigations were carried out using microscopes Polyvar and Neophot-32. The hardness was measured in the durometer M-400 (LECO). Digital image of the structure was obtained using digital camera Olympus.

The structure of weld metal produced with the wire PPS-AN1 (specimen 1) represents ferrite matrix and fine carbides, precipitated both in the body of crystallites, as well as along their boundaries (Figure 4). Microhardness of metal of the last pass amounts to $HV1$ = 1880–2130 MPa. During adding of boron the amount of carbides is decreased, which results in decrease of microhardness down to $HV1$ = 1760–1810 MPa in the specimen 2 and $HV1$ = = 1870 MPa in the specimen 3. The structure of

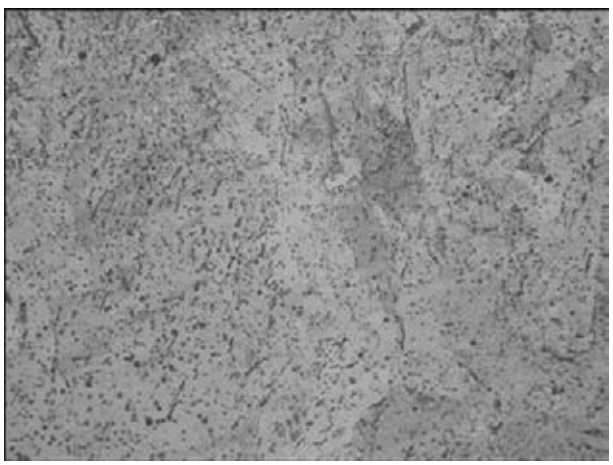

Figure 5. Microstructure (×500) of weld metal alloyed with boron

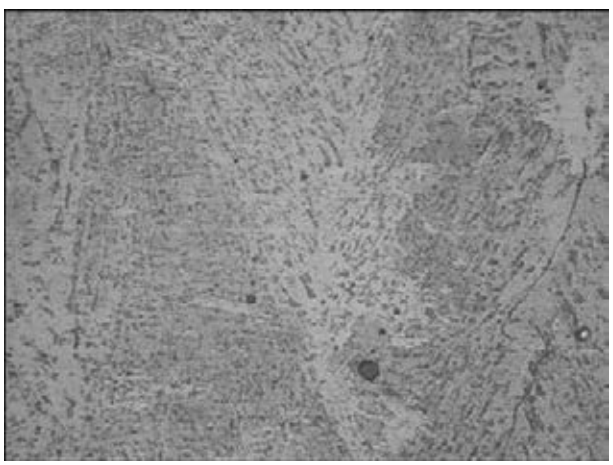

Figure 6. Microstructure (×500) of weld metal alloyed with titanium

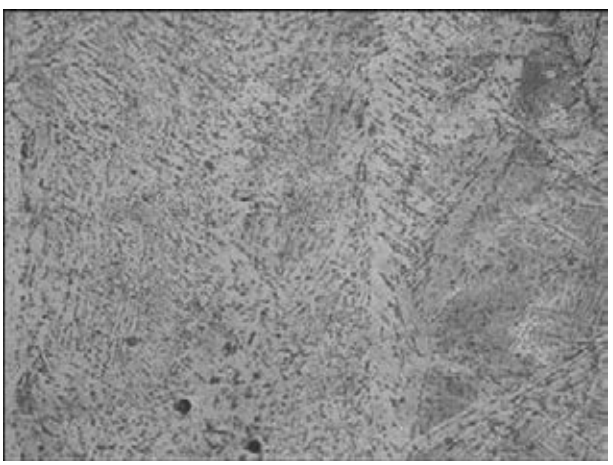

Figure 7. Microstructure (×500) of weld metal alloyed with titanium and boron

weld metal represents ferrite-carbide mixture (Figure 5).

In the welds alloyed with titanium (specimen 4), the structure is composed of ferrite of different modifications: with ordered and non-ordered second phase, polygonal ferrite and small amount of AF areas and bainite (Figure 6). The hardness of metal increases to $HV1$ = 2430–2850 MPa. At increase of titanium content (specimen 5) the size of polygonal ferrite precipitates was increased, AF was not detected. The hardness of weld metal was somewhat decreased — to $HV1$ = = 2300–2450 MPa.

Combined adding of titanium and boron does not lead to such noticeable changes in structure of weld metal as in separate alloying. Depending on the ratio of content of alloying elements the ratio of amount of ferrite with the ordered and non-ordered second phase is changed (Figure 7), and at maximum level of alloying (specimen 9) the areas of bainite with increased hardness ($HV1$ = 2970 MPa) are revealed.

The analysis of results of metallographic investigations shows that the areas with the best ductile properties and maximum amount of AF do not coincide. The highest ductility is observed in welds with ferrite-carbide structure. The appearance of structure components of AF type and upper bainite results in decrease of elongation and increase of strength. To explain the mechanism of influence of microalloying of weld metal with titanium and boron on its properties the additional more profound investigations are required.

As to optimization of content of titanium and boron in weld metal, then several batches of flux-cored wires, providing alloying in above-set limits, were manufactured and tested for this purpose. The following mean values of mechanical properties were obtained: σ_t = 469 MPa, $\sigma_{0.2}$ = = 378.2 MPa, δ = 20.8 %, α_{bend} = 180°. Thus, rational alloying with titanium and boron provides increase in elongation of weld metal by 1.8 times at negligible increase in tensile strength. By its mechanical properties the weld metal meets the requirements of class A of Specifications on underwater welding ANSI/AWS D3.6.

Conclusion

1. Microalloying with titanium and boron of metal of welds, performed under water using flux-cored wire, allows efficient controlling of their ductile properties.

2. The limits for titanium and boron content (0.005–0.010 and 0.0015–0.0025 %, respectively) were established, at which the elongation of welds metal of low-alloyed steels of strength class K40 is 1.8 times increased at negligible increase in tensile strength.

3. The region with the best ductile properties does not coincide with the region of maximum amount of AF. To specify the mechanism of influence of microalloying of weld metal with titanium and boron on its properties in the conditions of underwater welding, the more comprehensive investigations are required.

1. Ibarra, S., Grabbs, C., Olson, D.L. (1988) Fundamental approaches to underwater welding metallurgy. *J. of Metals*, **12**, 8–10.
2. Oh, D.W., Olson, D.L. (1990) The influence of boron and titanium on low carbon steel weld metal. *Welding J.*, **4**, 151–158.
3. Sanchez-Osio, A., Liu, S., Olson, D.L. et al. (1993) Underwater wet welding consumables for offshore applications. In: *Proc. of 12th Int. Conf. on Offshore Mechanics and Arctic Engineering*, Vol. 3, Pt A, 119–128.
4. Maksimov, S.Yu., Krazhanovsky, D.V. (2006) Content of acicular ferrite in weld metal in wet welding. *The Paton Welding J.*, **1**, 45–47.
5. *ANSI/AWS. D3.6*: Specification for underwater welding.

Received 28.03.2014

EFFECTIVENESS OF APPLICATION OF NEW CONSUMABLES IN WELDING AND SURFACING OF COPPER AND ITS ALLOYS (Review)

V.M. ILYUSHENKO, V.A. ANOSHIN, T.B. MAJDANCHUK and **E.P. LUKIANCHENKO**
E.O. Paton Electric Welding Institute, NASU
11 Bozhenko Str., 03680, Kiev, Ukraine. E-mail: office@paton.kiev.ua

Results of investigations on development of high-efficient electrode and filler materials for welding and surfacing of copper and alloys on its base are considered. It is shown that increased requirements to quality of welded joints and deposited metal can be satisfied, primarily due to development of reliable welding consumables: electrode and filler wires, fluxes (fused and activating flux-pastes), as well as special coated electrodes. Arc welding and surfacing processes improved on their base provide the required level of thermophysical properties of welded joints, high strength and tightness of welds, reliable service durability in friction assemblies and corrosion media, etc. Effectiveness of new welding consumables is confirmed by their practical application in manufacture of welded crucible moulds of electrometallurgical furnaces, welding busbars, electrode holders, enlargement of hot-rolled coils for their further rolling, making various bimetal items by surfacing, etc. 10 Ref., 5 Tables.

Keywords: *arc welding and surfacing, copper and its alloys, electrode and filler wires, fluxes, coated electrodes, welded joints, thermophysical properties, quality*

Owing to unique combination of physico-chemical properties: electric and heat conductivity, corrosion resistance, high level of mechanical and antifriction properties, heat and cavitation resistance, adaptability to fabrication, copper and alloys on its base are widely used in various industries. There is, probably, not a single industry, where copper and its low- and complex-alloys (bronzes, brasses) are not used. Therefore, a highly urgent task is development and continuous improvement of technologies of welding and surfacing these metals and, primarily, development of high-efficient welding and surfacing materials.

Systematic studies in this area began at PWI as far back as in the 1950–1960s of the previous century (V.V. Podgaetsky, D.M. Rabkin, Yu.M. Korenyuk, etc.). The most effective were studies, made in the 1970–1980s, when a group and then Laboratory of Welding and Surfacing of Copper and Its Alloys was set up within the new Department of Physico-Metallurgical Processes of Welding Refractory and Reactive Non-Ferrous Metals (Department Head was Prof. S.M. Gurevich) [1].

This review provides generalization of the results of investigations on development of reliable welding consumables and manufacturing technologies, allowing for increased requirements to quality of welded joints and deposited metal: ensuring the required level of electric conductivity, high strength and tightness (including vacuum) of welds, ensuring operating reliability in friction assemblies and corrosion environments, etc.

The most significant of them are developments in the field of arc welding and surfacing processes.

Welding and surfacing wires. Solid and flux-cored wires are used as electrode materials for mechanized processes of welding and surfacing of copper and its alloys.

In keeping with GOST 16130–90, industry manufactures a number of wires for welding copper and its low-alloyed structural alloys of chromium copper type: M1; M1r; MSr1; MN-ZhKT5-1-0.2-0.2; BrKh0.7; BrKMts3-1; BrOTs4-3. For bronze welding and surfacing, in view of the difficulty of drawing doped alloys, the wire range is narrow: BrKMts3-1; BrAMts9-2; BrAZhMts10-3-1.5; BrOTs4-3; BrOF6.5-0.15. Wires from some high-strength aluminium bronzes (BrAZhNMts, BrMtsAZhN type) are made by special specifications.

It is characteristic that the above wires for welding copper, while having satisfactory welding-technological properties in submerged-arc welding, in MIG/MAG process, as well as ensuring composite welds, as a rule do not meet the requirements on thermophysical properties of welded joints. Heat and electric conductivity do not exceed 20–30 % of those for welded copper (except for welds, made by submerged arc with copper wire). However, in submerged-arc welding with increase of welded copper thickness

Table 1. Composition of new welding wires, wt.%

Alloy grade	Li	B	Mg	Cr	Si	Al	Total impurities, not more than
ML0.2	0.1–0.3	–	–	–	–	–	0.03
MBMg	–	0.1–0.3	0.1–0.3	–	–	–	0.03
MLBMg	0.05–0.2	0.05–0.3	0.05–0.2	–	–	–	0.03
MLAKB	0.05–0.2	0.05–0.3	–	–	0.1–0.25	0.1–0.25	0.03
MLKhMg	0.1–0.25	–	0.1–0.4	0.15–0.4	–	–	0.03

(>15–20 mm) copper welding wire does not ensure the required tightness of welds or required ductility of welded joints. Better results in this case are achieved at application of special welding wire BrKhT0.6-0.5, developed at PWI. Simultaneous alloying of welds with chromium and titanium improves the metal mechanical properties, particularly at high temperatures, and increases metal resistance to porosity. The same principle of additional alloying of weld metal with chromium and titanium was the basis for development of special filler flux-cored wire PP-BrKhT12-2, designed for plasma-arc welding of copper and chromium copper. This flux-cored filler wire is used with success in manufacture of welded moulds of crucibles of electrometallurgical furnaces in OJSC «Sibelektroterm» (Novosibirsk, RF) [2, 3].

Wires from MNZhKT and BrKMts alloys are used for welding copper in shielding gas atmosphere. As was already noted, thermophysical properties of welds are quite low here. OK Autrod 19.12 wire recommended by ESAB company for these purpose, by our data does not ensure the required electric conductivity of joints, either. Owing to joint investigations of PWI and «Giprotsvetmetobrabotka» (now Company «Institute of Procesing of Non-Ferrous Metals», Moscow), compositions of effective welding consumables for welding copper and its low alloys have been developed (Table 1) [4–6].

Wires from ML0.2 and MBMg alloys, recommended as filler materials for nonconsumable electrode welding, provide tight, well-formed welds with high electric conductivity (more than 90 % of that of copper) and have mechanical properties on the level of those of base metal. Filler wire from ML0.2 alloy is applied with success for argon-arc welding of buses from oxygen-containing copper, and wire from MBMg alloy — for enlargement of hot-rolled copper coils by argon-arc welding for their further rolling and rolled stock application without cutting out welds at the user's facility. Wires from MLBMg, MLAKB and MLKhMg alloys were developed as all-purpose ones, and can be applied for welding copper and its low alloys both by consumable and nonconsumable electrodes, providing increased energy efficiency of the arc, high quality and electric conductivity of welded joints. Alongside application of inert gases (argon, helium and their mixtures) wire from MLBMg alloy guarantees high quality of welds and also welding in nitrogen atmosphere. Manufacture of new welding wires has been mastered in Moscow Experimental Plant of Quality Alloys.

In view of certain complexity of manufacturing these wires (melting in vacuum furnaces, rod pressing, rolling, annealing of billets and drawing), a more accessible filler material for TIG process is flux-cored wire of PP-AN-M1 grade, developed by PWI [3]. Doping flux-cored wire composition with effective deoxidizers ensures the required quality and thermophysical properties of welded joints in helium-arc welding of thick-walled elements of various electrical engineering products (motors, busbars, etc.).

An important objective of welding fabrication also is expansion of application of surfacing technologies with the objective of both restoring the worn parts, and manufacturing bimetal products. Pursuing investigations in the field of surfacing with antifriction copper alloys (aluminium and tin bronzes), PWI developed a number of grades of bronze flux-cored wires (Table 2), which, as a rule, provide a comparatively simple solution of the problem of ensuring the required composition of deposited metal [7, 8].

Developed wires and technologies of mechanized surfacing have been introduced with success in manufacture of bimetal bushings, thrust bearings and other components of friction assembles of heavy-duty mechanisms (ore mining and processing equipment, critical fittings, bearing bushings of electric motors, etc.) [1].

Coated electrodes. Comparatively small volumes of welded products from copper and its alloys can be manufactured by coated-electrode manual welding. Known electrodes of «Komsomolets-100» grade, mainly applied for this pur-

Table 2. Composition and properties of metal deposited with flux-cored wires, wt.%

Wire grade	Cu	Al	Fe*	Mn	Ni	Sn	Zn	Pb	P
PP-BrANMts	Base	7.5–10	2–4	1–2	1–2	–	–	–	
PP-BrMtsAN	Same	7.5–9		9–11	1–2	–	–	–	–
PP-BrOF	»	–	≤1	–	–	9–10	–	–	0.4–0.8
PP-BrOTs	»	–		–	–	9–10	1.5–3	–	–
PP-BrOTsS	»	–		–	–	5–6.5	5–6.5	2–4	–
PP-BrOS	»	–		–	–	7.5–9	–	18–21	–

*Iron content in steel surfacing.

Table 3. Properties of the metal of welds and welded joints made with coated electrodes

Electrode grade	Mechanical properties			ΣCr, Si, Al, Mn, Fe in weld metal, wt.%	Weld electrical conductivity, % of that for copper	Deposition rate*, g/min
	Weld metal	Welded joint				
	σ_t, MPa	δ, %	α, deg			
ANTs-1	210–240	20–25	130–180	≤1.1	40–70	110–150
ANTs/OZM-2	180–220	25–35	160–180	≤0.8	50–80	85–125
ANTs-3M	230–260	30–33	180	≤1.4	40–60	110–150
«Komsomolets-100»	250	10	–	≤6.0	20–25	40–50

*Data on deposition rate are given for 3 mm electrodes.

Table 4. Composition of metal deposited with bronze electrodes, wt.%

Electrode grade	Cu	Al	Mn	Fe	Si	Sn	P	Ni
ANBA-1	Base	7.0–8.0	1.5–2.0	≤3.0	≤0.5	–	–	–
ANBO-1	Same	–	0.5–1.0	≤2.0	–	5.0–7.0	0.15–0.25	0.3–0.8
ANBO-2	»	–	0.5–1.0	≤2.0	–	8.5–10.5	0.5–0.8	–

pose, were developed as far back as in the 1950s of the previous century and have essential drawbacks: over-alloyed weld metal, in particular by manganese and iron (up to 5–6 %), which abruptly lowers its heat and electric conductivity; low weld quality; high preheating and concurrent heating of items being welded. To eliminate these drawbacks PWI developed high-efficient electrodes of ANTs grade (ANTs-1, ANTs/OZM-2, ANTs-3M) (Table 3) [4]. An advantage of the new electrodes is the ability to perform copper welding without preheating or concurrent heating (for δ = 10–15 mm) or with low preheating (up to 200–400 °C) for thicker metal. This is achieved through application of forced welding modes and concentrated heat input, ensured at melting of thick-coated electrode. Efficiency of welding with new electrodes is 2–3 times higher compared to «Komsomolets-100». Electric and heat conductivity of welded joints is equal to 70–80 % of that for copper. Welding and repair of products with application of high-efficient electrodes of ANTs-3 grade has been mastered with success by a number of metallurgical plants of CIS countries in manufacture of crucibles, repair of moulds, bottom plates and electrode holders of various metallurgical furnaces and other products.

Considering that Ukraine has no manufacture of electrodes for welding and surfacing of bronzes (aluminium and tin), PWI performed a package of research on development of such electrodes of grades ANBA-1 for welding Al-bronzes, and ANBO-1, ANBO-2 — for welding Sn-bronzes (Table 4) [8, 9]. Standard wire of BrAMts9-2 grade was used as rods for electrodes of ANBA-1 grade, and for electrodes of ANBO-1 grade — copper wire M1T, for ANBO-2 grade — bronze wire BrOF6.5-0.4.

Developed electrodes for bronze welding and surfacing have good welding-technological properties, and by a number of indices (slag separability, resistance to pore formation) they are superior to foreign analogs. Test batches of developed electrodes are made at the PWI Science and Technology Complex.

Table 5. Activating fluxes for TIG welding of copper and its alloys

Flux grade	Flux system	Remark
AN-M15A	MgF_2–B	Welding of copper commercial grades
AN-M17A	MgF_2–Na_3AlF_6–B(P)	Welding of bronzes
AN-M19A	AlF_3–MgF_2	Microplasma welding of thin copper
AN-M21A	AlF_3–CaF_2–MgF_2	Nitrogen-arc welding of copper strips for subsequent rolling
AN-M23A	AlF_3–CaF_2–MgF_2–B	Welding of copper-nickel alloys
AN-M25A	Cu_2O–Sn	Welding of brasses

Fused welding fluxes and flux-pastes. The possibility of application for these purposes of a number of fused flux grades designed for steel welding was shown already in the first works on automatic submerged-arc welding of copper and its alloys. With increase of welded copper thickness (above 20 mm), however, standard fused fluxes, even with exact following of all technological recommendations (flux drying, scraping and degreasing of edges being welded, respective preparation of electrode wire, etc.) do not ensure the required weld tightness.

As shown by investigations, the most effective measure to prevent weld porosity in copper welding turned out to be application of low-silicon manganese flux manufactured by air-stream granulation with higher oxidation degree [3]. New flux of AN-M13 grade ensures producing vacuum-tight welds in manufacture of crucible moulds for VAM and ESM furnaces.

Owing to development of low-melting AN-M10 flux based on fluoride compounds of alkali-earth metals, electroslag welding of thick copper was performed with success for the first time in the word practice for fabrication of crucible bands of continuous casting machines and rolling rods from non-ferrous metals, as well as current conduits from thick-walled compact sections [2].

To improve weld quality and effectiveness of arc heat application, and, therefore, also efficiency of TIG welding of copper and its alloys, special flux-pastes based on halogenides of alkali and alkali-earth metals have been developed (Table 5).

Ability of making a metallurgical impact on weld pool with minimum weld alloying, which results in welded joints being close to base metal as to their thermophysical properties, should be regarded as one of the advantages of ATIG-process of copper welding. Application of flux-pastes enables considerable enhancement of technological capabilities of TIG welding: widening the range of thicknesses welded in one pass, and increasing welding speed [2, 10].

Thus, developed welding consumables and improved technological processes of welding and surfacing of copper and alloys on its base allowed an essential improvement of welded and surfaced product quality, reaching required level of service properties of welded joints and deposited metal, as well as ensuring further mastering of mechanized processes of welding and surfacing of these materials.

1. (2013) *Welding and surfacing of copper and alloys on its base*. Kiev: IAW.
2. Ilyushenko, V.M., Anoshin, V.A. (1994) Advanced methods of welding of copper and its low alloys (Review). *Avtomatich. Svarka*, **5/6**, 38–40.
3. Ilyushenko, V.M., Anoshin, V.A. (1998) Experience of application of consumables for welding and surfacing of copper and its alloys. In: *Proc. of 1st Int. Conf. on «State-of-the-art and Prospects of Development of Welding Consumables in CIS Countries»* (Moscow, 1998), 138–140.
4. Anoshin, V.A., Kostenko, Yu.I., Nikolaev, A.K. et al. (1982) New electrode materials for arc welding of copper. In: *Advanced methods of welding and surfacing of heavy non-ferrous metals and alloys*. Kiev: PWI, 13–22.
5. Ilyushenko, V.M., Anoshin, V.A., Kostenko, Yu.I. et al. (1985) Development of low-alloy wires for shielded-gas welding of copper. In: *Current problems of welding of non-ferrous metals*. Kiev: Naukova Dumka, 340–344.
6. Nikolaev, A.K., Kostin, S.A. (2012) *Copper and heat-resistant alloys*: Encycl. terminol. vocabulary. Moscow: DPK Press.
7. Ilyushenko, V.M., Anoshin, V.A., Bondarenko, A.N. et al. (2010) Development of flux-cored wires for welding and surfacing of aluminium bronze. In: *Proc. of 5th Int. Conf. on Welding Consumables. Technologies. Production. Quality. Competitiveness* (Kiev, 2010), 40–42.
8. Ilyushenko, V.M., Anoshin, V.A., Bondarenko, A.N. et al. (2013) Development of electrode materials for welding and surfacing of complexly alloyed bronzes. In: *Abstr. of Int. Conf. on Welding and Related Technologies — Present and Future* (Kiev, PWI), 72–73.
9. Korchemny, V.V., Skorina, N.V., Anoshin, V.A. (2007) Development of electrodes for welding and deposition of aluminium bronzes. *The Paton Welding J.*, **8**, 31–33.
10. Ilyushenko, V.M., Lukianchenko, E.P. (1998) Development of fluxes-pastes for surfacing of copper and some its alloys. In: *Proc. of 1st Int. Conf. on «State-of-the-art and Prospects of Development of Welding Consumables in CIS Countries»* (Moscow, 1998), 146–148.

Received 15.04.2014

EVALUATION OF SUITABILITY OF WELDING WIRE OF Sv-10GN1MA TYPE PRODUCED BY ESAB FOR MANUFACTURING NPP EQUIPMENT

I.M. LIVSHITS
«Izhora Welding Consumables» Ltd.
1 Lenin Ave., Kolpino, St.-Petersburg, RF. E-mail: iosif.Livshits@omzglobal.com

In order to extend the service life of commissioned NPP reactors, more stringent requirements are made of welded joints of equipment from 10GN2MFA steel, in particular, as regards limitation of impurities in weld metal. Evaluation of wire of Sv-10GN1MA type produced by ESAB was made to determine its suitability for manufacture of above-mentioned equipment. Comprehensive evaluation of deposited metal chemical composition, weld metal mechanical properties after respective heat treatment, radiographic testing of joints, determination of critical brittleness temperature allowed recommending the wire for application in nuclear engineering. 4 Tables.

Keywords: *arc welding, power equipment, life extension, requirements to welded joints, welding wire, testing, recommendations*

In keeping with the currently valid normative documents, welding wire of 10GN1MA grade supplied to TU 14-1-1549–76 specification should be applied for welding structures of nuclear power plants from steel of 10GN2MFA grade. This wire was manufactured by Russian companies «Serp i Molot» (Moscow) (this enterprise is not working now), «Elektrostal» (Elektrostal, Moscow region), and «Izhstal» (Izhevsk).

In view of the need to extend the service life of newly commissioned NPP reactors up to 60 years, higher requirements began to be made of steel welded joints, in terms of the content of impurities, not only such as sulphur, phosphorus, but also a number of others, in particular, cobalt, copper, arsenic, tin, antimony, vanadium, niobium, etc.

To ensure meeting these requirements, OJSC NPO TsNIITMASH developed special specifications for Sv-10GN1MA wire, allowing for all the limitations on composition.

For a number of reasons Russian enterprises are unable to ensure manufacturing of Sv-10GN1MA wire, in view of considerable tightening of requirements to impurity content, as the price for such a wire would rise several times. Therefore, its application was becoming not cost-effective.

ESAB Company, which is manufacturing wire of Sv-10GN1MA type, in one of its enterprises, allowing for all limitations and at a quite acceptable price, became involved, by its own initiative, in finding a solution of this problem.

Normative documentation requirements on wire composition and actual chemical composition of manufactured wire are given in Table 1.

In keeping with the normative documentation, currently in force in RF, application of foreign-made welding consumables for manufacture of NPP equipment is only possible after obtaining the appropriate resolution. Mechanism of obtaining such a resolution requires performance of a number of procedures, including testing of welded joint (determination of deposited metal composition and weld metal mechanical properties).

With this purpose «Izhora Welding Consumables» (IWC) conducted respective testing. The following materials were used for testing:

- Sv-10GN1MA welding wire of 4.0 mm diameter, melt 382418, manufactured by ESAB;
- FTs-16 fused flux manufactured by IWC.

Plates from VSt3sp (killed) steel of 700 × × 150 × 30 mm size with preliminary surfacing of edges by PT-30 electrodes, simulating 10GN2MFA steel, were used as base material.

The following scope of testing was conducted:

1. Determination of deposited metal composition. In order to determine deposited metal composition, controlled combination of welding consumables was used to perform 8-layer deposition on a plate from VSt3sp steel. Composition was determined by X-ray fluorescence method in ARL-1600 instrument. Results of determination of deposited metal composition are given in Table 1.

Table 1. Composition of 10GN1MA wire, wt.%

Source	C	Si	Mn	Cr	Ni	Mo	V	S	P
TU 14-1-1549–76	0.08–0.12	0.15–0.35	1.1–1.5	≤0.3	1.6–1.8	0.60–0.75	–	≤0.02	≤0.02
TU 2730.09.033–2012	0.08–0.12	0.15–0.30	1.1–1.5	Same	1.5–1.8	0.60–0.75	≤0.02	≤0.01	≤0.01
TU 2730.09.045–2013	0.08–0.12	0.15–0.30	1.1–1.5	»	1.5–1.8	0.60–0.75	≤0.02	≤0.01	≤0.01
Melt 382418	0.102	0.24	1.27	0.12	1.65	0.65	≤0.009	≤0.0015	≤0.007

Table 1 (cont.)

Source	N	Nb	Ti	Cu	As	Sb	Co	Sn	Al
TU 14-1-1549–76	–	–	–	–	–	–	–	–	–
TU 2730.09.033–2012	≤0.01	≤0.02	≤0.05	≤0.06	≤0.02	≤0.005	≤0.02	≤0.005	≤0.05
TU 2730.09.045–2013	≤0.01	≤0.02	≤0.02	≤0.06	≤0.02	≤0.005	≤0.02	≤0.005	≤0.02
Melt 382418	≤0.007	≤0.005	≤0.001	≤0.04	≤0.003	≤0.002	≤0.011	≤0.005	≤0.013

Table 2. Results of static tensile testing of weld metal

Sample marking	T_{test}, °C	Tensile strength, MPa	Conventional yield strength, MPa	Relative elongation, %	Reduction in area, %
175P-1	20	610 600	495 490	26 24.5	71 71
	350	560 570	430 425	18.5 21.5	64 65
175P-2	20	600 600	475 480	28 28	70 73
	350	550 550	400 410	26 23	66 66
PN AE G-7-010–89 requirements (not less than)	20	539	343	16	55
	350	490	294	14	50

2. Determination of mechanical properties of weld metal after heat treatment for the following modes:

• tempering at the temperature of 650 + 10 °C with soaking for 9–10 h (175P-1 marking);

• tempering at 620 + 10 °C with soaking for 5–6 h + tempering at 650 + 10 °C with soaking for 36–38 h (175P-2 marking).

Produced welded joints were subjected to visual examination, measurement and radiographic testing. Examination results were positive. In order to determine mechanical properties of weld metal, the following samples were made:

• type II to GOST 6996–66 for static tensile testing at 20 and 350 °C;

• type IX to GOST 6996–66 for impact bend testing and for confirmation of critical brittleness temperature.

Results of determination of weld metal mechanical properties at static tensile testing are given in Table 2, and those for confirmation of critical brittleness temperature are given in Table 3.

In keeping with the requirements of normative documentation two values of critical brittleness temperature (T_{cr}), depending on structure operating conditions of +15 and –10 °C, have been specified for combination of welding wire Sv-10GN1MA + flux FTs-16. Critical temperature confirmation is performed by a special procedure, when impact toughness is determined at con-

Table 3. Results of testing for confirmation of weld metal brittleness temperature

Sample marking	T_{test}, °C	Impact toughness KCV, J/cm^2	Ductile component, %
175P-1 (T_{cr} ≤ 15 °C)	+15	167–219	94–95
	+45	176–225	100
175P-1 (T_{cr} ≤ 10 °C)	–10	125–156	62–81
	+20	174–210	94–97
175P-1 (T_{cr} ≤ 15 °C)	+15	147–183	76–92
	+45	166–228	88–100
175P-1 (T_{cr} ≤ 10 °C)	–10	100–168	56–76
	+20	135–181	78–90

Table 4. Results of impact bend testing of weld metal

Sample marking	T_{test}, °C	Impact toughness KCV, J/cm^2	Ductile component, %
175P-1 ($T_{cr} \le -40$ °C)	10	157–181	77–91
	0	123–168	70–94
	–20	127–140	72–81
	–30	95–111	55–59
	–40	68–96	44–48
175P-2 ($T_{cr} \le -40$ °C)	10	142–196	74–83
	0	117–152	62–77
	–20	84–125	52–63
	–30	77–113	47–59
	–40	43–87	34–48

firmed temperature (+15 and –10 °C) and at temperature by 30° higher than the confirmed one, i.e. at +45 and +20 °C. Depending on the obtained results and values of weld metal yield point, critical brittleness temperature is confirmed or not confirmed.

In addition to confirmation procedure, there is the procedure of T_{cr} determination, when in order to determine the temperature, at which transition from ductile to brittle fracture takes place, impact toughness testing of weld metal in a broad temperature range from +50 to –100 °C is performed.

Obtained testing results confirmed complete correspondence to normative documentation requirements on deposited metal composition and weld metal mechanical properties (Table 4).

Test results provided confirmation of $T_{cr} \le -40$ °C. To determine critical brittleness temperature, testing should be performed at lower temperature. However, testing was interrupted because of insufficient number of samples.

Thus, welding wire Sv-10GN1MA supplied by ESAB Company fully meets the requirements of national standards applied in nuclear engineering, and can be approved for welding of NPP equipment.

Received 15.04.2014

FLUX FOR ELECTRIC ARC SURFACING PROVIDING HIGH-TEMPERATURE REMOVAL OF SLAG COATING

N.M. STRELENKO[1], **L.A. ZHDANOV**[1] and **I.A. GONCHAROV**[2]
[1]NTUU «Kiev Polytechnic Institute»
37 Pobeda Ave., 03056, Kiev, Ukraine. E-mail:strelenkon@gmail.com
[2]E.O. Paton Electric Welding Institute, NASU
11 Bozhenko Str., 03680, Kiev, Ukraine. E-mail: office@paton.kiev.ua

It was shown as a result of analysis of mechanisms of slag crust removal from the weld metal surface that the spinels at slag–metal interface and their intergrowth have the main influence on this process. It was found on the basis of analysis of structure of spinels and slag melt that to prevent the formation of spinels at the interface and intergrowth of metal and slag, it is necessary to provide the presence in the slag melt of a structural element with configuration of a linked structure, differed from tetra- and octahedral structures, and not capable to formation of spinels. It was established that prevention of formation of spinels in providing necessary welding-technological properties of flux of SiO_2–Al_2O_3–MgO–CaF_2 system can be attained at adding of zirconium oxide in the amount of 3.5–5.5 % into flux composition. The flux has been developed, which provides a spontaneous removal of slag coating at high temperatures. 13 Ref., 6 Figures.

Keywords: *submerged arc surfacing, high-temperature removal of slag coating, metal–slag interface, complex compounds of oxides, spinels, zirconium oxide, slag systems*

The process of submerged arc surfacing is one of the widely spread methods of restoration of parts of metallurgical, mining, machine-building equipment, agricultural machines and automobile transport. Using surfacing it is possible to deposit a layer of almost any thickness, different chemical composition and physical-mechanical properties by applying optimum combination of wire–flux filler materials. In restoration of parts the general-purpose fluxes AN-348A, OSTs-45, AN-60, AN-47 and specialized fluxes AN-20, AN-28, AN-26, AN-44 found the widest application. The submerged arc surfacing is used in restoration of parts, having flat and cylindrical surfaces, including also surfaces of intricate configuration, with a sufficient wear usually (up to 3–5 mm). In this case the surfacing is usually made with a partial or complete overlapping of the deposited layer.

Coming from specifics of used materials, the technology of surfacing should be realized in a multi-pass, continuous condition, and with preheating in some cases. This stipulates the strict requirements for removal of slag coating from the deposited bead surface within the range of elevated temperatures. The fluxes, produced by industry now, do not meet this requirement.

Therefore, the aim of the present work was the evaluation of factors and detailed study of mechanism, defining and providing the process of high-temperature removal of slag, formation of slag system, and optimization of the flux composition.

Removal of slag coating from the weld metal surface can be provided by [1–3]:

- increase in difference of coefficients of thermal expansion (CTE), which generate shearing forces during welded joint cooling;
- decrease in oxidizing ability of slag in molten state at its crystallization;
- delay of processes chemisorption at the slag–metal interface by increasing the surface and interfacial tension, which retards the process of intergrowth of metal and slag.

The oxidizing ability of slag in crystallization and processes of chemisorption cause the formation of chemical compounds of spinel type, which can strongly retain the slag coating on the weld metal surface. Even in case of a significant difference in coefficients of linear expansion at spontaneous removal of slag crust the thin glassy layers of solid flux, strongly bound with metal, remain on the metal. Their removal requires additional forces because they will interfere the further technological operations.

Effect of CTE on high-temperature removal of slag is not adequate in general case. In work [4] the thermogram of dilatometry of welding slags in the process of heating and cooling is presented. The processing of data for flux AN-348A, carried out by us, showed that during heating of slag crust after 870 °C temperature the decrease in value of CTE is observed, which even becomes negative. This is, probably, due to break of chemical bonds in structural constituents of a chain silicate, which is accompanied by their decomposition for simpler mineral compounds. As

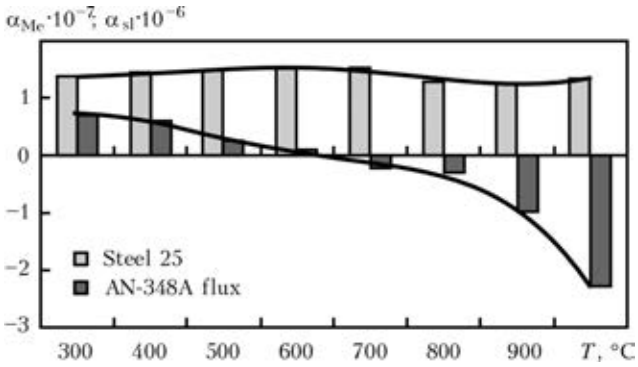

Figure 1. CTE change in cooling of slag (α_{sl}) [5] and metal (α_{Me}) [6]

a result, the structure of material is ordered and simplified with a system transition into the more stable state, which is typical of formation of a pyroxene structure. It is clear that the main interest is the change of CTE during the slag cooling. Data in Figure 1 show that unlike the metal, where CTE has the same sign of expansion value with increase in temperature at some maximum in the range of 500–700 °C, CTE for fluxes is characterized by the change in sign. During cooling the slag is elongated and, as result, in the range of 600–700 °C the values of CTE are in the region of zero. After that the CTE of slag begins to increase and reaches its maximum after 200 °C . The given data show that it is the high-temperature region, where the maximum difference in CTE is observed, and with decrease in temperature the difference in CTE of metal and slag is decreased. At the same time the removal of slag crust for flux AN-348A is observed only after the slag cooling. It should be noted that values CTE for metal and slag are differed almost by one order. The given data allow us to conclude that the difference in CTE of metal and slag does have a determinative influence on the processes of slag coating removal in the range of high temperatures.

Figure 2. Surface of weld metal and slag crust in arc surfacing under flux DFK-2: *a* — macrospinels at the weld metal surface (×2); *b* — macro- and microimaging of slag crust (×1500)

Other factors, influencing the process of slag removal, include also its oxidizing ability at slag–metal interface in the conditions, when slag is in solid or solid-molten state and forms the weld. In this case the intensive processes of chemisorption at slag–metal boundary with formation of complex compounds, retaining the slag on the metal surface, can proceed. Problems, connected with the formation of spinels, initiator of which is the weld metal, and final building of lattice of oxidized surface, have been studied comprehensively enough [2–4]. Data on effect of complexing elements in the flux composition and its oxidizing ability on the processes of formation of spinels are insufficient in literature.

To study this problem, we have manufactured special «short fluxes» on the base of slag system TiO_2–MgO–MnO–SiO_2–Al_2O_3 with increased content of oxides of titanium and magnesium: 40 and 30 % TiO_2, 17 and 32 % MgO. Fluxes DFK-2 and DFK-3 are high-titanium, «short» and have ultra-narrow interval of crystallization. Melting temperature of flux DFK-2 is 1380 °C at viscosity of 0.45 Pa·s, and in DFK-3 flux the temperature interval of crystallization at viscosity of 0.9–0.5 Pa·s is 1400–1500 °C. Selection of high-titanium fluxes for clarification of problem about effect of flux composition on complexing at slag–metal boundary was predetermined by the fact that titanium itself is the element, on the base of which the spinels can be built, and change in concentration of magnesium oxide should regulate the flux oxidizing ability.

Results of investigation of surface of weld metal and slag crust show the presence of macroformations on the weld metal surface, the prints of which are available on slag crust (Figure 2). Local chemical analysis of slag crust showed that these formations are macrospinels, which are formed on the base of titanium microspinels (53–69 %) and manganese (20–23 %) [7].

Taking into account the high crystallization capability of titanium-containing slags, the presence of macrospinels on the surface of weld metal for flux with increased content of titanium oxide (flux DFK-2), their association with the process of formation of microspinels on the slag surface, and also changed character of slag bonding with metal at increase of magnesium oxide in flux composition (flux DFK-3; Figure 3), it can be assumed that adding into the flux composition of elements, which reduce the oxidizing ability of slag surface during its crystallization and after the slag solidification, should decrease abruptly the possibility of formation of spinel-like formations at slag–metal interface and prevent the in-

tergrowth of slag coating with the oxidized surface of weld metal.

Spinels are characterized by common structure formulae: $Me^{2+}[Me^{3+}]O_4$ and $Me^{3+}[Me^{2+}Me^{3+}]O_4$, where Me^{2+} is the Mg^{2+}, Zn^{2+}, Mn^{2+}, Fe^{2+}, Ni^{2+}, Co^{2+}; Me^{3+} is the Al^{3+}, Mn^{3+}, Fe^{3+}, V^{3+}, Cr^{3+}, Ti^{4+}; [ ] are the ions in octahedral voids. Spinels are crystallized in cubic system, forming mainly the octahedral crystals. In elementary cell of spinel structure 32 oxygen anions form the most dense cubic packing with 64 tetrahedral voids (8 is occupied by cations) and 32 octahedral voids (16 is occupied by cations).

Slag melts in accordance with polymeric theory of constitution of slags [8, 9] represent the dense packed ion melts, where oxygen ions are observed in two types of voids, namely tetrahedral and octahedral. Tetrahedral voids are occupied by cations Si^{4+}, Ti^{4+} and partially by Al^{3+}, Fe^{3+}. These elements are located in quaternary coordination by oxygen and are the complexing agents. Octahedral voids are occupied by cations Ca^{2+}, Mg^{2+}, Fe^{2+} and partially by Al^{3+}, Fe^{3+}, Ti^{3+}, Ti^{4+}, Ti^{6+}.These elements are located in six-dimensional coordination and do not form complexes. It is evident that the presence of cations of a common sign in slag and metal leads to the appearance of spinels.

To prevent the formation of spinels between metal and slag and eliminate their intergrowth, it is necessary to have the element in slag melt, which does not form spinels, has an increased affinity to oxygen at temperatures typical of the process of crystallization of slag melt, forms strong chemical compounds, and the configuration of linked structure in complexes is differed from tetra- and octahedral ones. One of these elements is zirconium oxide, which at the condition of realization of maximum coordination number by oxygen (eight), forms the high-temperature cubic modification [10]. This modification is retained in interaction with cations, having the degree of oxidation, which differs from cation Zr^{4+}, i.e. from all the spinel-forming elements.

Change in phase composition of zirconium dioxide is started from temperature of 900 °C, at which the decrease in fraction of monoclinic phase is observed, at 1050 °C the phase monoclinic-tetragonal transition is occurred, and already at 1100 °C the phase composition is completely defined by meta-stable tetragonal ZrO_2. From 2300 °C up to melting point of 2715 °C it is transferred into non-stable cubic modification. Oxides CaO and MgO provide stabilizing properties to modification ZrO_2, which partially loss this property in the presence of Al_2O_3 [11]. Adding of zirconium oxide into slag melt changes not only its oxidizing ability, but also the physical properties. Here, on the one hand, it is necessary to prevent the formation of refractory slags, that

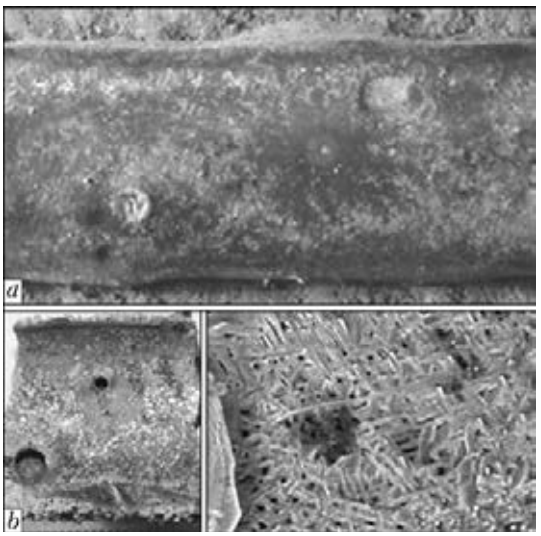

Figure 3. Surface of weld metal and slag crust in arc surfacing under flux DFK-3: *a* — traces of intergrowth of weld metal and slag surfaces (×2); *b* — macro- and microimaging of slag crust (×1500)

is connected with the possibility of zirconium oxide to be built-in into silicate, polymeric matrix and, by distributing uniformly in it, to modify it (size of ZrO_2 crystallites is 7–19 nm) [12], and, on the other hand, it is necessary to provide the reduction in oxidizing potential at the slag–metal interface.

To realize the offered mechanism of control of spinel formation and to develop the flux for electric arc surfacing, which will provide the high-temperature removal of slag coating, we have selected the traditional system SiO_2–Al_2O_3–MgO–CaF_2, for which the following concentrations of components were established: 20, 28, 18 and 14 % with additions of 4 % TiO_2 and MnO. Seven experimental agglomerated fluxes with changeable content of ZrO_2 from 0 to 15 % were manufactured, which were marked as DFZr; DFZr-1.5; DFZr-2.5; DFZr-3.5; DFZr-5.5; DFZr-10 and DFZr-15. Ratio of concentrations of components in fluxes was corrected by main components.

Using fluxes of series DFZr, the multilayer surfacing was performed on specimens of steel VSt3sp (killed) by 4 mm diameter wire Sv-08G1NMA. When it was possible, the surfacing was made in a continuous mode with record of temperature of slag removal by infrared, no-contact thermometer of Fione 506ip type. Slag removal was evaluated by 5-point scale using differential method [13].

As a result, spontaneous removal of slag coating for fluxes DFZr-3.5 and DFZr-5.5 in the fifth layer at 600–700 °C was established. Using fluxes DFZr, DFZr-10 and DFZr-15, the continuous process of surfacing was not successful. To apply flux DFZr, the large mechanical force is required to remove the slag crust, fluxes DFZr-10 and DFZr-15 did not provide the quality formation

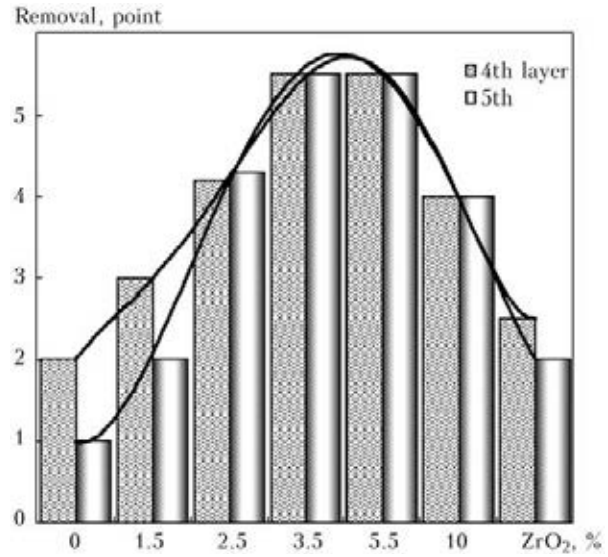

Figure 4. Relationship of removal of slag coating of series DFZr fluxes in the fourth and fifth layers

of weld metal and, as a consequence, slag was sticking, and additional mechanical actions were required. Generalized results on slag crust removal are presented in Figure 4. Temperature relationships of viscosity of welding fluxes of series DFZr obtained by a rotary method (Figure 5) allow explaining the deterioration of weld formation at increase of zirconium oxide in flux composition by significant increase in slag refractoriness. For fluxes, containing 2.5–5.5 % Zr, polytherms of viscosity are in the one range of values. The rate of viscosity growth for these fluxes is somewhat higher than for flux DFZr, that has a positive effect on their forming capacities. It is worthy to note that fluxes DFZr-2.Zr and DFZr-3.5 have viscosity of 0.13 and 0.16 Pa·s at 1460 °C, and DFZr-5.5 — 0.06 Pa·s. This proves the non-adequate effect of zirconium oxide of structure formations in slag melt.

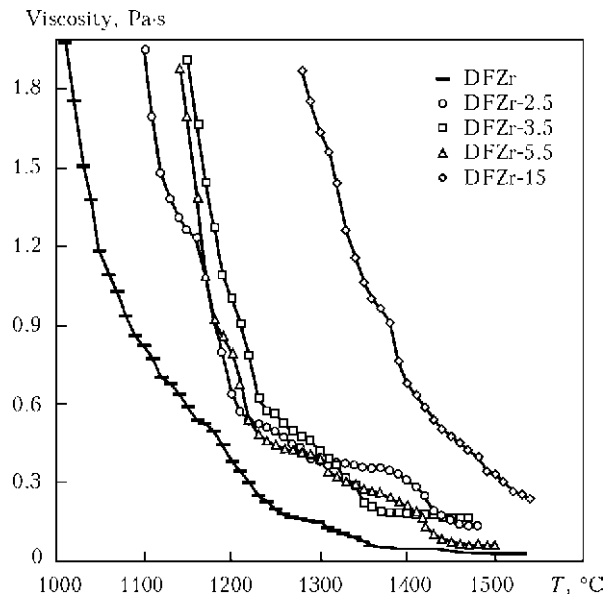

Figure 5. Viscosity of series DFZr fluxes versus temperature

Local chemical analysis of slag crust showed that its base (points 3 and 4; Figure 6, *a*) are the polymers of composition, wt.%: 24–27 SiO_2, 17–19 TiO_2, 20–25 CaO, 9–11 Al_2O_3 with addition of 11–13 MnO and 3–4 MgO. The observed formations (points 1 and 2; Figure 6, *a*) are spinels on base of iron oxide, wt.%: 67–69 FeO with 6–14 MnO, 4–8 TiO_2, 4–12 CaO, 1–7 MgO, 8–31 Al_2O_3, 5–7 SiO_2. The given composition of local formations and base of slag crust show that spinels are formed between the slag and metal. Moreover, the slag crust base is non-uniform (see Figure 6, *a*), and the surface layer is enriched with TiO_2, CaO and MnO, that proves also about the processes of slag and metal intergrowth. It is these factors that are the cause of a poor removal (see Figure 4).

Addition of ZrO_2 to the flux changes the slag crust structure (Figure 6, *b*, *c*). At 3.5 % ZrO_2 content the clearly expressed separate formations of white color are observed on the slag surface,

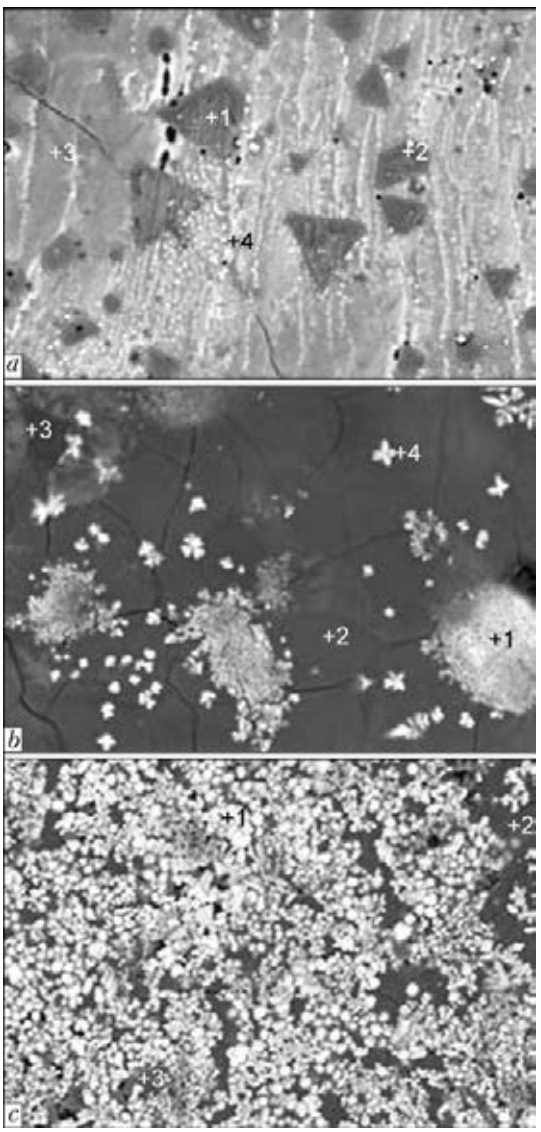

Figure 6. SEM-microstructure (×1550) of slag crust surface: *a* — flux DFZr; *b* — DFZr-3.5; *c* — DFZr-15

which are the compounds on zirconium oxide base (chemical composition in points 1 and 4 is, wt.%: 57–67 ZrO_2, 6–10 SiO_2, 8–13 CaO, 5 TiO_2, 5–7 MnO, 3–4 Al_2O_3) (see Figure 6, *b*). The slag crust base (points 2 and 3) represents a monolithic, smooth structure with microcracks (wt.%: 19–21 SiO_2, 7–12 TiO_2, 25–49 CaO, 4–10 Al_2O_3, 13–30 MnO, 4–8 ZrO_2). Coming from composition of formations, available on the slag crust surface, and appearance on microimaging of base of slag surface, it is seen that spinels and intergrowth of slag crust with weld metal is not observed. As a result, spontaneous removal of crust, including that at elevated temperatures, is provided (see Figure 4). The presence of zirconium oxide in the composition of flux base proves the partial built-in of zirconium cation Zr^{4+} into polymeric lattice of silicon anions, resulting in transfer of viscosity polytherm into the region of the higher temperatures.

Structure of surface of slag with increased content of zirconium oxide (DFZr-15) consists completely of formations of zirconium compound, which are arranged on the slag surface adjacent to weld metal. Composition of zirconium compounds is close to earlier described structures, wt.%: 62–72 ZrO_2, 6–10 SiO_2, 7–11 CaO, 3 TiO_2, 6–7 MnO, 3–4 Al_2O_3 (point 1; see Figure 6, *c*). Composition of base (points 2 and 3) is also close to base of flux DFZr3.5, wt.%: 20–23 SiO_2, 9–10 TiO_2, 19–24 CaO, 10–11 Al_2O_3, 7–8 MnO, 13–26 ZrO_2. The increased content of zirconium oxide in slag base, i.e. its building-in into polymeric ion frame, leads to increase in melting temperature of flux, the slag becomes more refractory, that influences negatively on its forming capabilities in welding. Weld surface becomes non-uniform, influencing negatively on the processes of slag removal.

As a result, experimental fluxes DFZr-3.5 and DFZr-5.5 can be recommended as a basic composition of flux for surfacing works providing the high-temperature removal of the slag coating. Technical Specifications were worked out and registered for this flux (TS U 24.6-05416923-101:2011, welding flux of ANK-73 grade).

Conclusions

1. On the basis of analysis of literature data the possible causes and mechanism of high-temperature removal of slag crust from the weld metal surface were defined. It was shown that during the process of slag cooling the difference in CTE is observed in high-temperature region proper, and at the temperature decrease the difference in CTE of metal and slag is decreased.

2. It was found that spontaneous removal of slag coating in the region of high temperatures can be provided only by prevention of spinel formations at slag–metal interface and absence of slag intergrowth with weld metal surface.

3. It was shown on the basis of analysis of structure of spinels and slag melt, from the point of view of polymeric theory of slag constitution, that to prevent the formation of spinels at the interface, development of processes of metal and slag intergrowth, it is necessary to provide the presence of structure element in slag melt, having an increased affinity to oxygen not capable to formation of spinels, and configuration of linked structure of which was different from tetra- and octahedral ones.

4. It is shown that it rational to add the zirconium oxide into composition of fluxes for providing the high-temperature removal of slag crust. The study of microstructure and local chemical analysis of slag crusts of fluxes of SiO_2–Al_2O_3–MgO–CaF_2 system with different concentration of ZrO_2 showed that its adding into flux composition in the amount of 3.5–5.5 % prevents the formation of spinels and intergrowth of slag crust with weld metal. Flux has been offered for electric arc surfacing, guaranteeing the high-temperature (up to 600 °C) removal of the slag coating.

1. Zhdanov, L.A., Strelenko, N.M., Zvorykin, K.O. et al. (2010) Physical-chemical peculiarities of slag crust removal from weld metal surface and procedural base of evaluation methods. *Tekhnolog. Sistemy*, **1**, 109–115.
2. Pokhodnya, I.K., Yavdoshchin, I.R., Karmanov, V.I. et al. (1974) Mechanism of adhesion of slag crust with weld surface. *Avtomatich. Svarka*, **5**, 5–9.
3. Moravetsky, S.I. (2011) Detachability of slag crust in arc welding (Review). Pt 1: Mechanism of chemical adhesion of slag crust to weld metal. *The Paton Welding J.*, **1**, 28–31.
4. Moravetsky, S.I. (2011) Detachability of slag crust in arc welding (Review). Pt 2: Character of the effect of main factors on detachability of slag crust. *Ibid.*, **2**, 20–23.
5. Ignatov, M.N., Ignatova, A.M., Naumov, S.V. et al. (2012) Study of relationship between thermal expansion coefficients of weld metal and welding slags and temperature in range of 100–1000 °C. *Obrabotka Metallov*, 56(**3**), 116–119.
6. Zubchenko, A.S., Koloskov, M.M., Kashirsky, Yu.V. et al. (2003) *Handbook of steel and alloy grades*. Moscow: Mashinostroenie.
7. Strelenko, N.M., Zhdanov, L.A. (2012) Specifics of formation of spinels on slag–metal interface in submerged-arc welding. *Visnyk Donbas. Mashynobud. Akademii*, 28(**3**), 260–263.
8. Novikov, V.K. (1987) Development of polymer model of silicate melts. *Rasplavy*, 6(**1**), 21–23.
9. Novikov, V.K., Nevidimov, V.N. (2006) *Polymer nature of melted slags*. Ekaterinburg: GOU VPO UG-TU-UPI.
10. Orgel, L. (1965) *Introduction to chemistry of transition metals*. Moscow: Mir.
11. Pashkeev, I.Yu. (2005) Interaction of ZrO_2 in melts of system Al_2O_3–ZrO_2 with additions of oxides of lanthanum subgroup. *Vestnik YuUGU*, **3**, 92–95.
12. Poddenezhny, E.N., Bojko, A.A. (2003) Classification of methods for manufacturing of ultradispersed oxide powders (Review). *Vestnik P.O. Sukhoj GGTU*, **1**, 21–28.
13. *RD 03-613–03*: Sequence of welding consumables application in production, mounting, repair and reconstruction of technical devices for dangerous manufacturing entity. Technological schedule of certification of welding consumables. Moscow: PIO OBTB.

Received 29.04.2014

NEW CAPABILITIES OF THE OLDEST ENTERPRISE ON PRODUCTION OF WELDING FLUXES

A.V. ZALEVSKY[1], **V.I. GALINICH**[1], **I.A. GONCHAROV**[1], **N.Ya. OSIPOV**[2], **V.I. NETYAGA**[2] and **O.P. KIRICHENKO**[2]
[1]E.O. Paton Electric Welding Institute, NASU
11 Bozhenko Str., 03680, Kiev, Ukraine. E-mail: office@paton.kiev.ua
[2]Company «Zaporozhstekloflyus»
2 Diagonalnaya Str., 69035, Zaporozhie, Ukraine. E-mail:contact@steklo.zp.ua

At Company «Zaporozhstekloflyus» the technology of two-stage melting of flux (duplex-process) was mastered, where firstly the charge is melted in separate melting unit, and then the melt is finally melted in another unit. This allowed decreasing the content of harmful impurities in melt: oxides of iron and sulphur by 2–3 times, phosphorus — by 4–6 times, and, thus, improving the flux quality. In addition, raw base for production of fused fluxes was widened that is extremely important under conditions of deterioration of raw material quality. Due to the double refining of melt of fluxes the duplex-process solved in principle the problem of utilization of slag crust, formed in submerged-arc welding. Production of fused semi-products designed for application in charge of welding consumables (covered electrodes, flux-cored wires and agglomerated fluxes) was mastered. 5 Ref., 1 Table, 1 Figure.

Keywords: *welding fluxes, duplex-process, melt refining, slag base, special fused products, sodium silicate*

Submerged-arc welding is the leading technological process in manufacture of large-size welded metal structures. Among four components of this process, such as welding equipment, base metal, welding wire and flux, a high quality of the latter and its welding-technological capabilities provide a user with required technical and economical characteristics of welding, and remain a decisive factor for a manufacturer of fluxes in sale of the own products.

However, the traditional technologies of manufacture of welding fused fluxes, i.e. melting in open gas or electric arc furnaces can already scarcely deal with this problem. The reasons are not only in deterioration of quality of traditional raw materials and growth of requirements to the quality of welded metal structures, but also in the technologies themselves, as each transition in flux melting from one grade to another or change in quality of charge consumables determine the efficiency of flux melting furnaces, influences the life of lining, predetermine the volume of consumption of power carriers, and result, as a rule, in additional production costs.

In the last years the requirements to restriction of content of harmful impurities in steels of critical welded structures were rapidly increased [1, 2]. To provide the required characteristics of quality of welded joints, it is necessary to restrict the content of these impurities in fluxes. Thermodynamic analysis of pyrometallurgical processes, running in flux melting furnaces, showed complications of simultaneous decrease in sulphur and phosphorus in the melt [3].

Appearance of two-stage flux melting (duplex-process) [4], at which the charge is melted at the separate melting unit and then at the second one its refining is performed, allows not only decreasing the content of oxides of iron, sulphur and phosphorus in the melt and thus improving the quality of flux, but also extending the source of raw materials for production of fused fluxes, which is extremely important under the conditions of deterioration of quality of raw materials. Besides, due to double refining of melt of fluxes the duplex process almost solved the problem of utilization of slag crust, formed during submerged-arc welding, which thus allowed decreasing the negative effect on the environment. Thus, since the moment of implementation of this technology (2000) within the frames of innovation project of the PWI Technopark, at the «Zaporozhstekloflyus» 32,279 t of slag of production of silicomanganese and 31,328 t of slag crust of flux AN-60 was utilized as well as agglomerated fluxes used in production of large-diameter pipes at Hartsyzsk Pipe Plant.

Separation of flux melting into two stages provides certain economic advantages: the main consumptions of heat are spent to decomposition and melting of charge consumables at relatively low temperatures, therefore for this purpose it is eco-

nomically rational to use cheaper power carriers (coal dust, coke gas) instead of electric power. The latter is used only to increase the temperature of a melt for its deoxidation, removal of phosphorus and iron oxides and formation of the required pumice-like grain structure during the following granulation.

From the metallurgical point of view the principal change in the processes of melt refining occurs, i.e. the process of desulphuration occurs separately from the dephosphorization process. Such double refining allows conducting more profound purification of melt from harmful impurities: sulphur and iron oxides by 2–3 times and phosphorus by 4–6 times. The results of investigations of refining process of melt of flux AN-348A applying the traditional technology (in open gas furnace) and duplex-process are given in the Figure.

Such wide technological capabilities of duplex-process allowed extending the nomenclature of products of «Zaporozhstekloflyus», as well as starting the production of pumice-like and agglomerated fluxes and also mastering the production of consumables as raw materials for manufacture of the latter. Thus, the production of agglomerated fluxes at the mentioned enterprise is performed almost on the own source of raw materials. For example, for manufacture of flux ANKS-28 a slag base of charge was melted, which contained traditional raw materials: slag of silicomanganese, fluorspar, dolomite, crust of used flux, etc. On the base of this flux the technology of surfacing of roller tracks of MP-350 mixers was developed, which at the necessary quality of tracks (absence of cracks, hardness of deposited layer in the limits of *HRC* 36–38) does not require heat treatment of deposited metal, increases efficiency of deposition twice, decreases labor-intensiveness of deposition and consumption of electric power by 30–40 %.

At the present time at «Zaporozhstekloflyus» the industrial production of new products, such as special fused products designed for use in charge at production of agglomerated fluxes, flux-cored wires and other welding consumables was mastered:

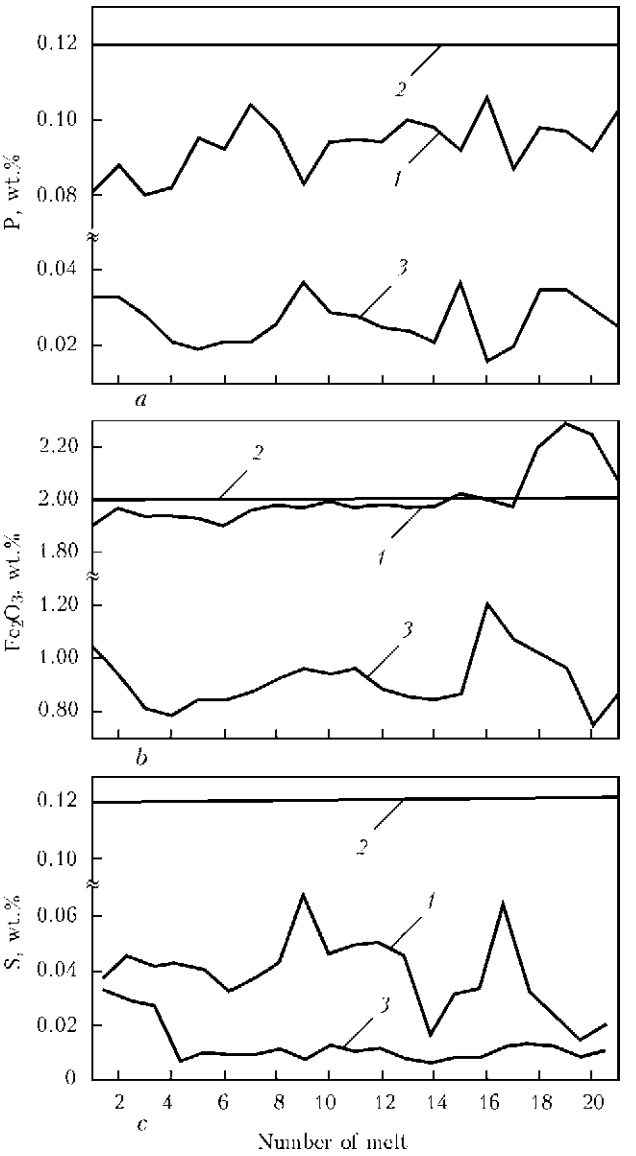

Statistic data on change or content of phosphorus (*a*), iron oxides (*b*) and sulphur (*c*) in melt during melting of flux AN-348A using traditional technology in open gas furnace (*1*) and duplex-process (*3*); *2* — norm acc. to GOST 9087

• grade MS represents a refined manganese slag (basicity index according to Bonishevsky is less than 1.0);

• CS — the slag of neutral type with refined properties (basicity index according to Bonishevsky is 1.1);

• AR — the slag of aluminate-rutile type with good welding and technological properties (basicity index according to Bonishevsky is 0.6).

Chemical composition of fused products, wt.% (maximum values of sulphur — 0.03 %, carbon — 0.1 %)

Type	MnO, %	SiO_2, %	CaO, %	Al_2O_3, %	Fe_2O_3, %	MgO, %	CaF_2, %	TiO_2, %	P, %
MS	34–41	34–41	7–12	2–8	1.5 (max)	0.5–3.0	3–7	1 (max)	0.06 (max)
CS	6–8	34–38	19–23	12–15	1.5 (max)	11–15	6–10	4–7	0.07 (max)
AR	8–12	16–18	6–10	30–34	2.2 (max)	7 (max)	4–8	16–19	0.06 (max)

The compositions of fused products are given in the Table.

The enterprise has a potential to manufacture fused slag base for agglomerated fluxes of aluminate-basic type, for example, similar to fluxes UV-309 P or OP-132. The Plant, being the largest manufacturer of sodium silicate (glass block) in CIS countries and Europe, is establishing the modern production of liquid glass for the needs of different branches of domestic economy: production of welding consumables, detergents, construction.

Duplex-process has also a positive influence on welding and technological properties of traditional grades of fluxes. Thus, the standard flux of the grade AN-348A with the bulk density of 0.9–1.1 g/cm^3 (AN-348AP grade of flux), manufactured using method of duplex refining, was tested at the Company «Word Building Systems Ukraine» in welding [5] of:

- butt welds in manufacture of girths of main girders of steel 09G2SD of 32 mm thickness with X-edge preparation using wire of the grade Sv-08GA of 4 mm diameter for the bridge at the speedway Kiev–Odessa;
- in welding of girth welds of double T-girders of thin-sheet steel 09G2S using wire Sv-08G2S of 1.2 mm diameter;
- in manufacture of girders of steel St3 of 12 mm thickness at the Lincoln automatic production line «Conrak» at simultaneous welding, using wires Sv-08GA of 1.6 mm diameter, of two butts in flat position using two arcs into the one pool for each butt. Earlier for this purpose the ceramic flux Lincoln 780 was applied. In all variants of welding the pores, cracks, undercuts and roughness at the surface of welds were absent. Here pumice-like flux AN-348AP provided a self-removal of slag crust at the second and next passes, uniform formation of weld metal with smooth transition to the base metal and fine-rippled surface of silver color, monotonous along the whole length of a butt, which rendered the best marketable state of a product as compared to the earlier applied glass-like fluxes AN-348A and AN-348AM. Especially the tests of modernized flux AN-348AP of fine granulation at automatic production line «Conrak» should be noted, where it surpassed the agglomerated flux Lincoln 780 by all the characteristics. The flux AN-348AP according to TU U 05416923.049–99 is successfully applied at this enterprise since 2004.

Alongside with the famous grades of fluxes AN-348A, AN-60, AN-47, OSTs-45, manufactured according to GOST 9087, TU U 05416923.049–99 and Russian standard GOSTR 52222, and used in welding of low-alloyed and carbon steels, «Zaporozhstekloflyus» produces also fluxes of grades AN-20S, AN-20P, AN-20SP, AN-26 for welding and surfacing of stainless steels.

To perform speed welding of large-diameter pipes of low-alloyed steels of conventional and increased strength, as well as bridge structures, sheet panels of tanks, the production of pumice-like flux of the grade AN-47DP was developed and mastered. Its industrial tests showed that it is the only flux, which provides normal formation of inner weld in welding of spirally-welded pipes.

At the present time «Zaporozhstekloflyus» performs modernization of flux-melting workshop for production of high-quality fused fluxes with a wide range of consumer properties following the new technology.

The industrial line on production of agglomerated fluxes of productivity of up to 5000 t per year was created, which provides organizing the production of domestic agglomerated fluxes in Ukraine. Application of agglomerated fluxes of fused products in industry instead of expensive imported charge components will provide a high quality of fluxes and their compatibility not only at the Ukrainian but also at the world market.

1. Morozov, Yu.D., Matrosov, M.Yu., Nastich, S.Yu. et al. (2008) High strength pipe steels of new generation with ferritic-bainitic structure. *Metallurg*, **8**, 39–42.
2. Pogozhev, A.V., Tskitishvili, E.O., Matrosov, Yu.I. et al. (2013) Experience of application of accelerated cooling in manufacturing of steel plate 70 for pipes of gas pipeline «Middle Asia–China». *Ibid*., **3**, 66–70.
3. Zhdanov, L.A., Duchenko, A.N., Goncharov, I.A. et al. (2012) Thermodynamic analysis of slag melts in manufacture of fused welding fluxes. *The Paton Welding J*., **11**, 23–27.
4. Mednikov, Yu.A., Plyasunov, V.A., Zhuchaev, V.A. et al. (1997) Mastering of new technology of welding flux melting. *Stal*, **9**, 42–43.
5. Duda, N.I., Galinich, V.I., Zalevsky, A.V. (2004) Experience of application of fused pumice-like flux of AN-34AP grade. *Svarshchik*, **4**, 24–25.

Received 24.04.2014

FLUX-CORED WIRES FOR SURFACING OF STEEL HOT MILL ROLLS

I.A. KONDRATIEV and **I.A. RYABTSEV**
E.O. Paton Electric Welding Institute, NASU
11 Bozhenko Str., 03680, Kiev, Ukraine. E-mail: office@paton.kiev.ua

The flux-cored wires and technologies of arc surfacing of steel hot mill rolls were developed. The results of investigations and practical experience allows recommending the developed flux-cored wires for surfacing of steel rolls of the following mills: for roughing (blooming and slab) — PP-Np-25Kh5MSGF; for continuous billet — PP-AN147, PP-Np-35V9Kh3GSF; for heavy-section and rail-beam — PP-Np-25Kh5MSGF; for medium- and light-section — PP-Np-25Kh5MSGF, PP-AN147, PP-AN204; for wire — PP-Np-35V9Kh3GSF, PP-AN132; for sheet — PP-AN132, PP-Np-25Kh5MSGF; for pipe ones — PP-AN147, PP-Np-35V9Kh3GSF. 3 Ref., 1 Table, 1 Figure.

Keywords: *arc surfacing, flux-cored wires, mill rolls, hot hardness, heat resistance, wear resistance*

Nowadays the surfacing of mill rolls for their restoration and increase in life is applied almost at all the metallurgical enterprises in Ukraine. Using modern methods of mechanized surfacing a roll can be created with a very ductile and strong core, which is well resistant to mechanical loads and also has a wear- and heat-resistant surface. Surfacing allows significantly increasing of life of rolls, decreasing their consumption, increasing yield of efficient rolled metal due to improvement of accuracy of rolling, decreasing expenses for processing and cost of rolled metal [1].

The efficiency of application of surfacing of mill rolls depends significantly on right selection of composition of deposited metal. Therefore, it is necessary to perform a thorough analysis of conditions of rolls operation, character and intensity of their wear. At different metallurgical enterprises the rolls of mills even of the same type are worn out to different extent and should be surfaced using different consumables.

For wear-resistant surfacing of steel hot rolls of different mills most often, though not always reasonably, the flux-cored wire of grade PP-Np-35V9Kh3GSF is applied. The deposited metal of Cr–W type of steel possesses a high resistance to abrasion at higher temperatures but its thermal life is comparatively low, and the rolls, deposited using this wire, often come out of order due to formation of fire net and spallings. Therefore, to deposit the rolls using this wire, to which the requirements of maximum cleanness of surface of body or grooves of a roll are specified, is not rational.

The experience in development of steels for dies of hot deformation of metals, conditions of work of which are largely close to those for work of hot mill rolls, indicates the challenge in use of Cr–W–Mo (partial replacement of tungsten with molybdenum) and Cr–Mo steels for these purposes. As to heat resistance, these steels are almost not inferior to Cr–W ones and, as to resistance to thermal fatigue, are significantly superior to them. It is connected with the fact that molybdenum facilitates formation of fine-grain

Properties of deposited metal of different alloying systems

Grade of flux-cored wire	Heat resistance, number of cycles	Wear of specimen ΔM, g	Heat resistance T_d, °C	Impact toughness a_n, J/cm^2	Hardness *HRC*
PP-Np-35V9Kh3GSF	70	0.12	680	7	51
PP-Np-25Kh5MSGF	200	0.35	650	42	46
PP-AN147	190	0.15	650	35	47
PP-AN132	130	0.13	670	13	50
PP-AN204	170	0.21	650	23	29–50*

*After ageing at 480 °C for 3 h.

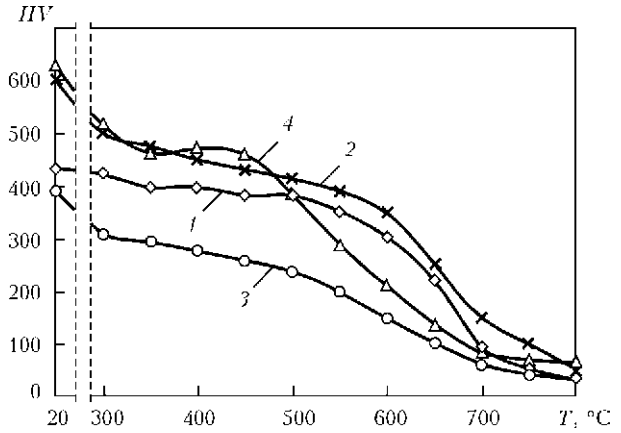

Hot hardness of deposited metal: *1* — surfacing with wire PP-Np-25Kh5MSGF; *2* — PP-Np-35V9Kh3GSF; *3* — steel 150KhNM hardened and tempered for hardness *HRC* 50; *4* — PP-AN204

structure, hinders precipitation of carbide particles along the grain boundaries and, thus, increases the ductility of steel.

For surfacing of layer of Cr–Mo steel the flux-cored wire of grades PP-Np-25Kh5MSGF and PP-AN147, and for Cr–W–Mo steel PP-AN132 one were developed. The properties of metal deposited by these wires are presented in the Table.

The heat resistance was determined by a number of heating–cooling cycles until the appearance of crack net became visible by a naked eye. The wear resistance was evaluated by the loss of mass ΔM of deposited specimen caused by friction wear of metal against the metal at 600 °C for 1 h of tests. The heat resistance of deposited metal T_d was characterized by the temperature of two-hour tempering, after which the hardness amounted to *HRC* 40.

Tungsten-free metal, deposited using wires PP-Np-25Kh5MSGF and PP-AN147, has the highest resistance to thermal fatigue and the best combination of values of heat and wear resistance belongs to the metal, deposited using wire PP-AN147.

During surfacing of rolls with complicated grooves the mechanical treatment of deposited layer encounters great difficulties due to relatively high hardness. For such rolls the application of surfacing materials of the type of maraging or dispersion-hardening steels and, in the first turn, sparcely alloyed and tool maraging steels is challenging. A high strength of steels of the mentioned group is a total result of realization of mainly two hardening processes: formation of interstitial solid solution and shear (martensite) mechanism of γ–α transformation. After surfacing such steels have hardness of *HRC* 28–30 and are sufficiently easily treated mechanically. After tempering the hardness is increased to *HRC* 48–55, and the deposited metal acquires high service properties. Besides, it enables carrying out of surfacing without preliminary and concurrent preheating.

To deposit a layer of maraging steel of alloying Fe–Ni–Mn–Si–Mo system the flux-cored wire PP-AN204 was developed [2, 3]. The main properties of metal deposited using this wire are presented in the Table. Besides, hot hardness of deposited metal as compared to the deposited metal of the type of known tool steels was investigated (Figure).

Heating of specimens was performed in the special inductor in vacuum, measurements of hardness were carried out at 1 kg loading and 60 s holding. It is seen from the given data that hot hardness of maraging deposited metal is at the same level as hot hardness of Cr–Mo and Cr–W die steels, deposited with the corresponding flux-cored wires.

According to the results of laboratory investigations and pilot-industrial verifications, performed in the recent years, the compositions of deposited metal and, respectively, compositions of charge of flux-cored wires for surfacing of hot mill rolls were specified. The results of investigations and practical experience allow recommending any of the developed flux-cored wires for surfacing of steel rolls of the following mills: for roughing (blooming, slab) — PP-Np-25Kh5MSGF; for continuous billet — PP-AN147, PP-Np-35V9Kh3GSF; for heavy-section and rail-beam — PP-Np-25Kh5MSGF; for medium- and light-section — PP-Np-25Kh5MSGF, PP-AN147, PP-AN204; for wire — PP-Np-35V9Kh3GSF, PP-AN132; for sheet — PP-AN132, PP-Np-25Kh5MSGF; and for pipe ones — PP-AN147 and PP-Np-35V9Kh3GSF. However, it should be noted that the final selection of wire grade for surfacing of definite rolls is required, basing on the full-scale tests.

1. Ryabtsev, I.A., Kondratiev, I.A. (1999) *Mechanized electric arc surfacing of metallurgical equipment parts*. Kiev: Ekotekhnologiya.
2. Kondratiev, I.A. (1994) Self-shielded flux-cored wire for surfacing of maraging steel layer. *Avtomatich. Svarka*, **1**, 49–51.
3. Kondratiev, I.A., Ryabtsev, I.A., Chernyak, Ya.P. (2006) Flux-cored wire for surfacing of maraging steel layer. *Ibid*., **4**, 50–53.

Received 09.04.2014

DISCRETE FILLER MATERIALS FOR SURFACING IN CURRENT-CONDUCTING MOULD

Yu.M. KUSKOV
E.O. Paton Electric Welding Institute, NASU
11 Bozhenko Str., 03680, Kiev, Ukraine. E-mail: office@paton.kiev.ua

Discrete filler is the most promising filler material for electroslag surfacing in current-conducting mould. Particles of different dispersity can be used as such filler, namely shot, tablets, chips, powders, shorts, granules, etc. At correct selection of particle size and mass velocity of their feeding into the slag pool, a modified fine-grained structure of deposited metal with improved mechanical and other service properties can be formed. This is confirmed by positive results of surfacing the forming rolls of different mills, in particular mill 2000. The most wide-spread surfacing consumable is filler in the form of steel and cast iron shot. Shot can be mainly produced by three technological methods: mechanical fragmentation of liquid metal jet, dispersion by centrifugal forces, and dispersion by energy carrier flows. The latter method is the most wide-spread, in particular, at application of air as dispersing agent. During dispersion and further formation and cooling of pellets they are saturated with oxygen, nitrogen and hydrogen. Oxygen saturation depends on shot material, its dimensions and production method. In order to apply shot of a wider granulometric composition, fine shot as well as coarse (after fragmentation) shot can be formed into tablets by powder metallurgy. The process of their melting in the slag is similar to melting of regular-sized 0.8–2.5 mm shot. Chips of alloyed steels and alloys are a special kind of discrete filler. The main requirement to such filler is limitation of its dimensions and shape and absence of lubricoolant in it, contributing to a change of deposited metal composition, particularly by carbon. Other fillers, in particular, in the form of wastes from various productions (slurry wastes, wastes generated at ingot dressing, tool treatment, etc.) do not provide stable quality of deposited metal, but can be applied in development of resources-saving surfacing technologies. 4 Ref., 3 Tables, 9 Figures.

Keywords: *electroslas surfacing, current-conducting mould, shot, chips, tablets, granules*

Developed at PWI design of current-conducting mould [1] in electroslag surfacing (ESS) allows application of electrodes and filler materials (billets of various cross-section, strips, discrete particles — powders, shorts, granules, shot, chips, etc.), as well as liquid filler.

The most promising are discrete fillers. Filler particles, while melting in the slag pool and being cleaned in it from impurities, come in surface-molten and molten state into metal pool, which is then solidified into deposited metal. At correct selection of particle size and mass velocity of their feeding into the slag pool, formation of a large number of solidification centers in the liquid metal can be ensured. These centers allow modifying the deposited metal, which results in equiaxed and fine-grained structure. Such a changed structure promotes improvement of mechanical and special (wear resistance, thermal fatigue resistance) properties of metal.

As shown by our investigations on physical and mathematical simulation of the process of discrete filler transfer and melting in the form of granules of wear-resistant high-chromium cast iron (16–30 wt.% Cr), granules of up to 4 mm size can be used for circular and end face surfacing. For further increase of process efficiency (increase of mass velocity of filler feed) fractional composition in the range of 0.8–2.5 mm is recommended. As shown by practical experience of circular surfacing of working surfaces (bodies) of mill 2000 forming rolls (roll body diameter of approximately 1 m), efficiency can reach 400–500 kg/h without preservation of unmolten particles of the filler [2].

Shot. The most wide-spread kind of discrete surfacing material is filler in the form of steel or cast iron shot. In view of the fact that in most of the cases we deal with hardfacing, shot from high-chromium and chromium-nickel cast iron («Nickhard» type metal) most often is used as filler.

At present, there exit the following main technologies of metal melt dispersion [3]: mechanical fragmentation of liquid metal jet, dispersion with application of centrifugal forces, and dispersion by energy carrier flows.

Mechanical fragmentation of the jet is achieved as a result of molten metal hitting a solid surface, most often a drum, partially immersed in and rotating in its cooling liquid, and

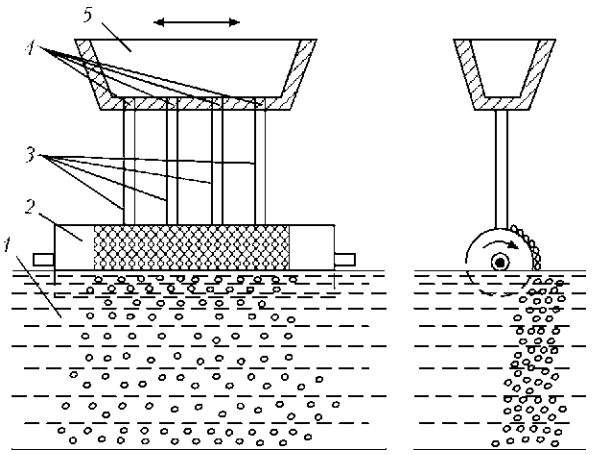

Figure 1. Schematic of producing shot by mechanical fragmentation of liquid metal jet: *1* — cooling water; *2* — atomizing drum; *3* — melt jet; *4* — gate channels for melt outflow; *5* — intermediate ladle

further cooling of formed pellets in the cooling tank (Figure 1). This method is hardly suitable for manufacturing cast shot from steel or other materials with high melting temperature. At high temperature of liquid metal melt sticking to the work tool occurs, erosion or partial destruction of its working surface develops and shot quality is impaired.

Metal melt dispersion by centrifugal forces is performed as follows. Liquid metal jet stabilized as to velocity and consumption, comes to the rotating cup, and becoming accelerated under the impact of centrifugal forces, it is dispersed and thrown over the edge in the form of drops, which form granules (pellets) in flight, and then fall into the cooling tank, where they are finally cooled and solidified (Figure 2). A perforated sleeve can be used instead of the rotating cup. Dispersion by centrifugal forces yields shot of more uniform granulometric composition than in casting on a drum; yield of fine and coarse shot is reduced. The disadvantage of this technology, however, is the low resistance of the work tool.

Dispersion with application of energy carriers is the most wide-spread and promising method of producing steel and cast iron shot, as well as alloys with a high melting temperature. Used as

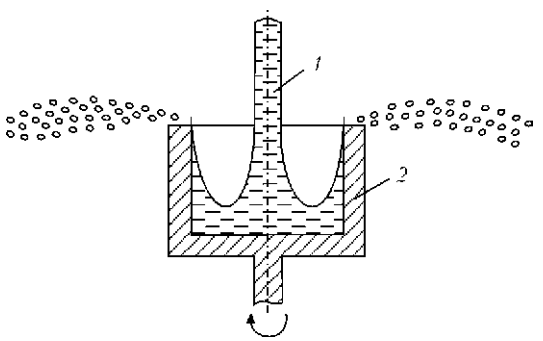

Figure 2. Schematic of producing shot by centrifugal forces: *1* — melt jet; *2* — refractory material cup

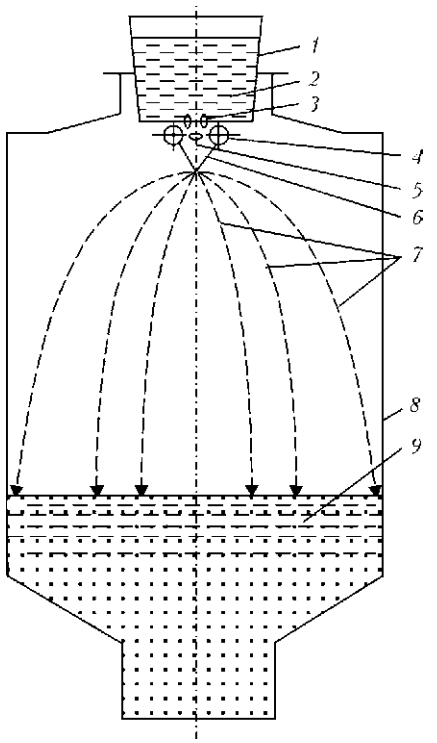

Figure 3. Schematic of producing shot using energy carriers (gas): *1* — intermediate ladle; *2* — liquid metal; *3* — pouring sleeve; *4* — collector; *5* — melt jet; *6* — energy carrier flows; *7* — granule falling trajectory; *8* — dispersion chamber; *9* — cooling water

dispersion agent are various energy carriers: air, water, inert gases, steam, etc. Liquid metal jet breaking up occurs due to kinetic energy of energy carrier (Figure 3).

Some kinds of shot produced by mechanical fragmentation of liquid metal jet (shot from unalloyed cast iron), air atomization (shot from alloyed cast irons and steel), as well as other discrete filler, applied for surfacing, are shown in Figure 4. Microstructure of 2 mm granules (pellets) from unalloyed chromium-nickel and high-chromium cast irons is shown in Figure 5.

Passage of liquid metal jet through the air medium and further cooling in the cooling tank leads to granule oxidation and their certain saturation with hydrogen and nitrogen. Results of chemical analysis of chromium cast iron shot produced by liquid metal air atomization are shown in Table 1.

Presence of oxide films on pellet surface was examined by optical microscopy around the perimeter of microsection cross-section (Table 2). As is seen from this Table, thickness of oxide films depends on shot material, its dimensions and manufacturing method. In all the cases, the oxide film is intermittent, and does not completely cover the entire pellet surface.

Considering that no increased quantity of oxide inclusions has been found in the deposited

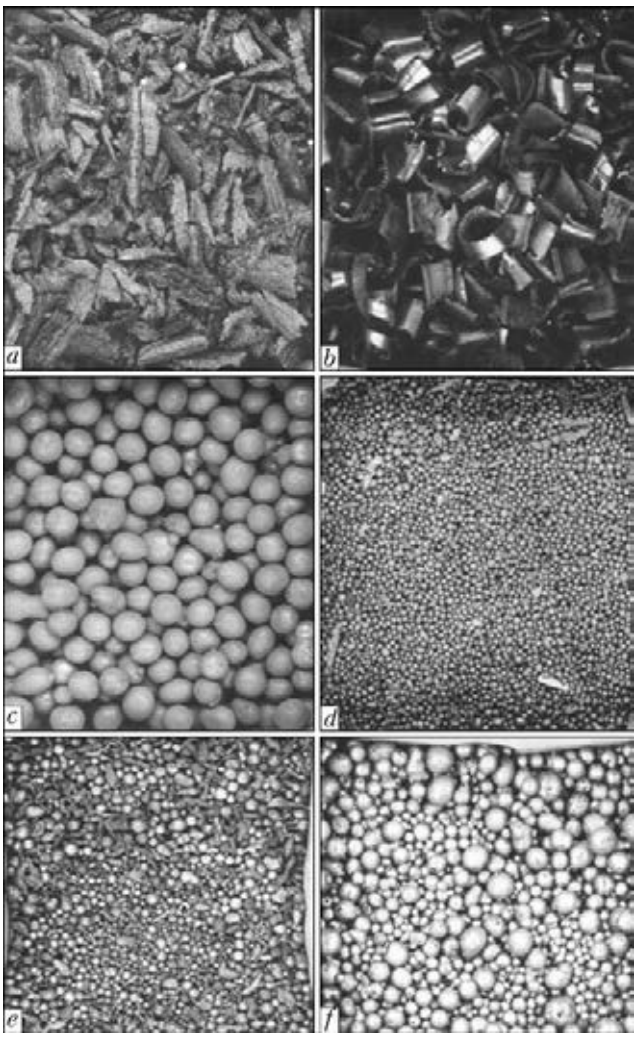

Figure 4. Some kinds of discrete filler applied in ESS in current-conducting mould: *a* — gray cast iron chips; *b* — R6M5 steel chips; *c* — unalloyed cast iron shot; *d* — R6M5K5 steel powder; *e* — chromium cast iron shot (16 % Cr); *f* — Cr–Ni cast iron shot

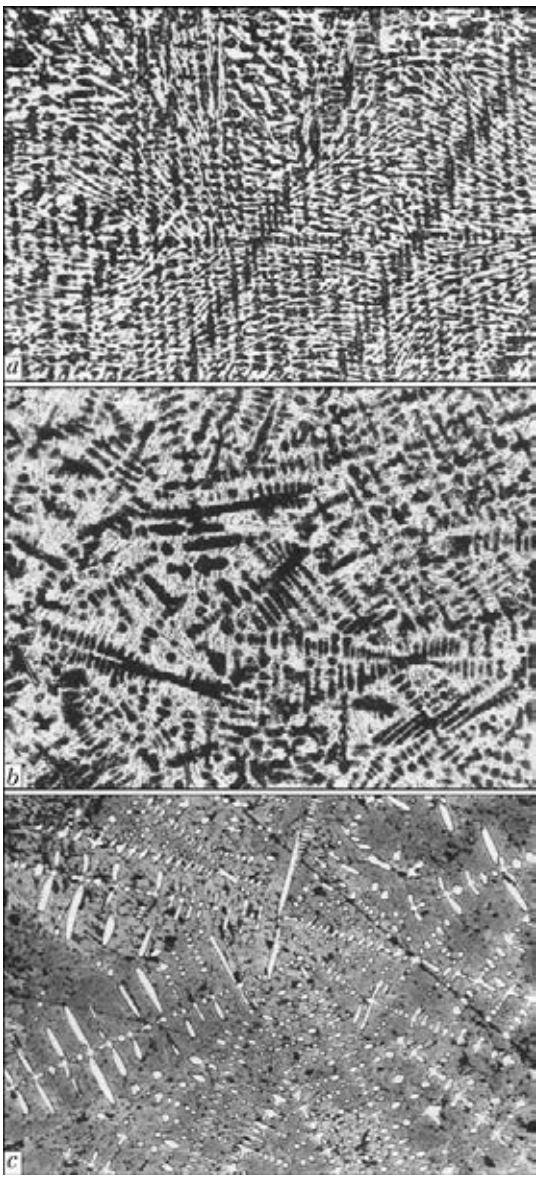

Figure 5. Microstructure (×500) of 2 mm granules (pellets): *a* — unalloyed cast iron; *b* — Cr–Ni cast iron; *c* — high-chromium cast iron

metal, it can be assumed that oxide films present on the pellet surface are assimilated by slag at filler passage through the slag layer.

Filler feed on slag pool surface is performed by dosing units. Two types of dosing units have been tried out so far: with drum-type dosing device (OB-1960) making swinging movements during circular surfacing, and vibrodosimeters (Figure 6). The first type of dosing units has drawbacks associated with ensuring its stable operation, because of the possible jamming of filler, rotating drum and case, in which it rotates; certain difficulties arise at swinging displacement of current-carrying cables of dosing unit motor. The second dosing unit type is the most often used. In the absence of stringent requirements to mass velocity of filler feed, it has proved itself both in end face and in circular ESS. Figure 7 shows surfacing of mill 2000 roll with application of 4 vibrodosimeters with grit hoppers of 500 kg each.

Tablets. At liquid metal spraying by energy carrier flows a wide range of filler fractions is obtained. So, at air atomization of high-chromium cast iron in units of «Grad» model designed by Physical-Technological Institute of Metals and Alloye of NASU the following granulometric composition is produced:

Granule size, mm	<0.5	0.5–1	1–3	3–5	>5
Granule quantity, %	10.1	5.8	51.6	21.5	11.0

Table 1. N_2 and H_2 content in chromium cast iron shot, produced by liquid metal air atomization, and in deposited metal, wt.%

Chemical elements	Shot fraction, mm		Deposited metal
	0.5–1	1–3	
N_2	0.033	0.05	0.043
H_2	0.00501	0.00201	0.00062

Table 2. Dimensions of oxide films on the surface of cast iron and 100KhNM steel pellets, μm*

Shot material	Method to produce shot	Shot fractions, mm					
		1		2		3	
		Thickness	Length	Thickness	Length	Thickness	Length
Unalloyed cast iron	Mechanical fragmentation	–	–	10–25	20	45	50
Chromium-nickel cast iron	Air atomization	5	10	10	15	N/D	N/D
High-chromium cast iron	Same	N/D	N/D	N/D	N/D	N/D	N/D
100KhNM steel	»	10–15	500	10	50	35	500

*Metallographic investigations were performed by I.L. Bogajchuk, Eng.

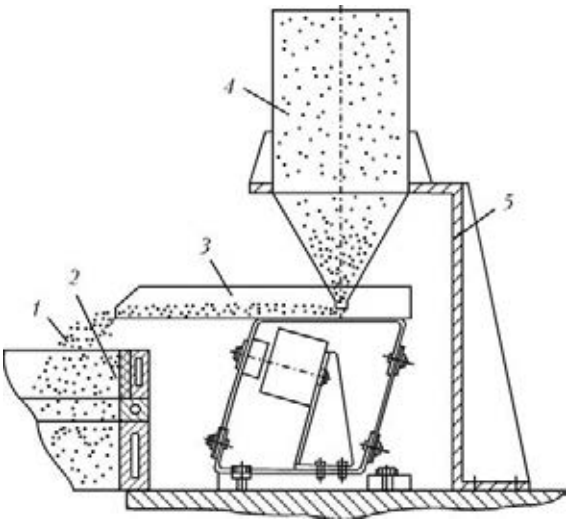

Figure 6. Schematic of vibrodosimeter applied at ESS in current-conducting mould: *1* — discrete filler; *2* — mould; *3* — feeder (working can); *4* — hopper with discrete filler; *5* — bracket

Fraction ratio can change, depending on material composition and dispersion parameters.

As is seen from these data, less than 50 % of produced shot can be used for surfacing. Shot fractions, outside TU specification (0.8–2.5 mm), are used as charge for subsequent melts. Here, chemical element loss increases, melting process becomes more complicated, and shot cost becomes higher. To eliminate these drawbacks of shot production, powder metallurgy methods can be applied. Tablets from granules of high-chromium cast iron of less than 0.8 mm size were pressed at Brovary State Plant of Powder Metallurgy (Ukraine). To produce relatively strong tablets, plasticizer (bakelite lacquer) was added to the mixture during its preparation. Surfacing by the produced tablets was performed in the regular mode (compared to shot surfacing). Gas evolution at tablet melting is regulated by selection of the appropriate plasticizer. Shot of more than 2.5 mm size can also be involved into the single-step process of producing filler surfacing material. Here, it should first be moved to the category of crushed shot with subsequent pressing of fine particles into tablets; larger fragments can be also used as surfacing filler, similar to regular shot, in the case if their dimensions are not larger than those specified by TU norms.

Figure 8 shows end face surfacing of high-chromium cast iron with tablet feeding from vibrodosimeter.

Figure 7. Surfacing mill 2000 roll with application of 4 vibrodosimeters with shot hoppers, each of 500 kg weight

Figure 8. End face surfacing of high-chromium cast iron with tablet feeding from vibrodosimeter

Table 3. Composition and hardness of metal deposited with chips of 15Kh11MF steel at different methods of its cleaning

Treatment of chips with LC before surfacing	Deposited metal composition, wt.%				
	C	Si	Mn	Cr	Mo
15Kh11MF steel to GOST 5632–72	0.12–0.19	≤0.50	≤0.70	10.0–11.5	0.60–0.80
1. Untreated	3.86	0.32	0.41	10.81	0.06
2. Washing in hot water with soda ash + baking at 600 °C for 0.5 h	0.44	0.22	0.36	11.20	0.10
3. 5 times boiling with soda ash and powdered detergent	0.28	0.22	0.27	10.30	0.66
4. Washing in car wash unit	0.17	0.29	0.25	10.34	0.67

Table 3 (cont.)

Treatment of chips with LC before surfacing	Deposited metal composition, wt.%					Hardness, *HB*/*HRC*
	V	Ni	Cu	S	P	
15Kh11MF steel to GOST 5632–72	0.25–0.40	≤0.60	≤0.30	≤0.025	≤0.03	≤285/ND
1. Untreated	0.04	0.19	0.11	0.012	0.03	ND/54
2. Washing in hot water with soda ash + baking at 600 °C for 0.5 h	0.04	0.18	0.30	0.004	0.035	ND/43
3. 5 times boiling with soda ash and powdered detergent	0.30	0.40	0.15	0.004	0.027	–
4. Washing in car wash unit	0.29	0.34	0.15	0.003	0.013	–

Chips. Application of chips from alloyed steels and various types of cast irons in surfacing allows considerable reduction of surfacing operation cost. This is associated with the fact that the cost of surfacing consumables is the main component in surfacing cost.

Non-spiral chips of small size (< 0.5 × 5 × × 5 mm) produced in milling and planing of metal are used for surfacing. For a number of materials (mostly hard and brittle) chips of required size can be produced at lathing and drilling (see Figure 4).

Application of this kind of surfacing consumable is difficult for two reasons. This is presence of lubricoolant (LC) in it and complexity of organizing collection of chips by dimensions and composition. As regards chips collection, at present this problem was begun to be solved in a simpler manner, in connection with a smaller range of applied tool steels (in particular, high-speed) and smaller volume of machining of parts.

Presence of LC in the chips disturbs surfacing process stability, is detrimental to environment in connection with increased gas evolution, changes deposited metal composition (mainly, by carbon), and can affect metal quality (chiefly, because of pore formation).

Usually, chemical methods of chip treatment as well as thermal methods or their combination are used to remove LC. Table 3 gives the results of chemical analysis of metal deposited with chips from 15Kh11MF steel at different methods of its cleaning.

For cast iron chips it is recommended to perform heat treatment at 800–1000 °C [4]. Such

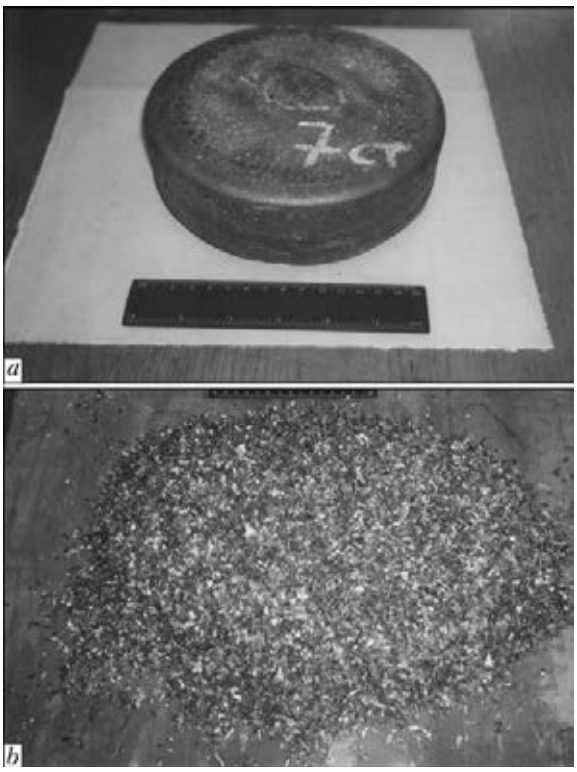

Figure 9. Appearance of molten blank (*a*) and discrete surfacing filler — chips of 15Kh11MF steel (*b*) (experiment 4 acc., Table 3)

treatment ensures lowering of LC content in cast iron chips to 0.3 wt.%.

Appearance of a billet, surfaced with chips from 15Kh11MF steel, is shown in Figure 9.

In addition to the above-given main kinds of filler materials, other materials can be also used for surfacing, the application of which allows speaking about resources-saving surfacing technologies. In particular, these are slurry wastes generated at dressing of alloyed steel ingots, tool treatment, etc. Technology of surfacing with these materials is more complicated, and it is difficult to ensure a high quality of deposited metal. Application of two technological schematics is possible. The first is thorough cleaning (for instance, by magnetic separation) of filler to remove extraneous (most often non-metallic) components, and then application of the cleaned part in surfacing. In this case difficulties arise both during addition of obtained fine particles to the slag pool, and in terms of ensuring the uniformity and stability of their immersion into slag. This kind of problems is related to particle coagulation on slag pool surface and impact of slag surface tension forces. It is difficult to predict deposit quality at application of such filler. The second schematic is a two-stage one. It also envisages initial treatment (less thorough than in the first case), then remelting of cleaned filler, producing an alloyed ingot, its crushing and use of crushed filler similar to the case of crushed shot. Owing to primary slag treatment of filler, the produced ingot metal (furtheron of filler used for surfacing) has improved characteristics, both in terms of structure, and composition.

Conclusions

1. Best quality of metal, surfaced in current-conducting mould, can be achieved with application of discrete filler. The most promising kind of filler is cast shot, produced by the method of liquid metal jet dispersion by energy carrier, in particular, air.

2. To improve ESS economics, filler in the form of tablets or chips can be used in current-conducting mould. With optimization of the technology of producing such filler and methods of its preparation for surfacing, production of sound bimetal items can be guaranteed.

3. Other kinds of fillers, in particular, wastes of various productions containing alloyed metal part, lead to complication of ESS technology, but are preferable, due to being the main cost items of resources-saving processes. Without ensuring a stable high quality of the deposited metal, they, nonetheless, can be used at reconditioning of parts, the main requirement to which is cost-effectiveness.

1. Kuskov, Yu.M. (2006) Resources-saving technology of repair and manufacturing of parts by electroslag surfacing method. *Tekhnologiya Mashinostroeniya*, **6**, 40–42.
2. Kuskov, Yu.M., Ryabtsev, I.A., Sarychev, I.S. (2004) Recovery of cast iron rollers of mill 2000 in current-carrying mould. *Svarshchik*, **1**, 12–13.
3. Zatulovsky, S.S., Mudruk, L.A. (1988) *Manufacturing and application of metallic shot*. Moscow: Metallurgiya.
4. Potapov, V.V., Tsymbalov, S.D., Korostelev, A.B. et al. (2009) Heat treatment of cast-iron chips contaminated by lubricoolant. *Litejn. Proizvodstvo*, **11**, 19–20.

Received 23.03.2014

MANUFACRURING DEFECTS IN WELDING CONSUMABLES INFLUENCING THE QUALITY OF WELDED JOINTS

E.V. TURYK
Institute of Welding
16–18 Bl. Czeslawa Str., 44–100, Gliwice, Poland. E-mail: eugeniusz.turyk@is.gliwice.pl

The characteristic defects of welding wire and steel studs for arc welding-on, influencing the quality of welded joints, were analyzed. The inadmissible defects of the wire are predetermined by increased total content of nitrogen, hydrogen and oxygen in them, high rigidity, low quality winding on the reels, and the defects of studs are caused by incompliance of chemical composition and mechanical properties with the requirements. 6 Ref., 1 Table.

Keywords: *arc welding, welding consumables, steel wire and studs, inadmissible defects of materials, quality of welded joints*

Though a great attention is paid to the quality of welding consumables [1–4], this problem still remains urgent. The analysis performed recently in a number of branches of industry showed that low quality of welding consumables causes the 35 % rejection of welded structures per year [5]. The industrial experience also shows that the properties of welding consumables, produced by different companies according to the same standard, are different, and their defects have a negative influence on the quality of welded structures. Due to this reason, it is recommended to apply the consumables of increased quality for critical structures instead of standard welding consumables, for example, the Thyssen K52 T electrode wire of type G3Si1 is recommended for welding using TIME method [6].

The purpose of this work is the determination of critical (inadmissible) defects of some welding consumables, which should serve as a reason for refuse from their application in industry. As the object of investigations the copper-plated solid wire of grade G3Si1 according to ISO 14341A (analogue of Sv-08G2S-0) was selected applied for MAG welding, and welding-on studs SD1 which are used in bridge construction.

Characteristics of defects of copper-plate electrode wire G3Si1. Determination of critical defects of wire was carried out basing on the results of comparative tests of quality of more than fifty 1.2 mm diameter welding wires of grade G3Si1 according to ISO 14341A of Polish and foreign production, with the Acceptance Certificate 3.1 or Act of plant tests 2.2 according to EN 10204.

Evaluation of quality of welded joints. The strength properties of joints of steel S355J2 + N (analogue of 17GS), made using wires G3Si1 by MAG method in shielding gas M21 (Ar + + 18 % CO_2) applying the standard modes, and by highly-efficient TIME method in gas mixture TIME-Gas (65 % Ar, 26.5 % He, 8 % CO_2 and 0.5 % O_2), correspond to the requirements of ISO 15614-1. However, the impact toughness of a number of welds is characterized by the significant scattering of test results caused by the presence of pores in weld metal in the plane of notch of specimens. Radiographic control of butt joints of type Y of 12 mm thickness showed that the level of porosity corresponds to the requirements of items B, C, D according to ISO 5817, but does not meet the requirements of item D.

According to the results of check analysis the chemical composition of all the wires as to content of carbon, silicon, manganese, phosphorus and sulphur met the requirements of standards EN 440 and EN ISO 14341. Using method of high-temperature extraction the content of nitrogen, oxygen and hydrogen in the as-delivered wires and after removal of surface copper-plated layer (rated wire diameter is 1.2 mm, and diameter without surface layer is 1–1.05 mm) was determined. The characteristic results of analysis of gases in the wires are given in the Table.

After removal of copper layer the total content of gases in wires decreased, difference ΔR amounts from 13.1 to 93.3 ppm. The decrease in content of hydrogen and oxygen after removal of surface layer proves that wire in the layer of copper and/or under this layer contains organic contaminations (technological lubricant). It can

Content of gases in welding wires of G3Si1 grade by ISO 14341A, ppm

Number of wire	Wire state	N_2	O_2	H_2	S	ΔR	K
3	+Cu	58	84	3.2	145.2	13.1	−4.8
	0	57	73	2.1	132.1		
5	+Cu	53	136	9.4	198.4	29.8	48.4
	0	53	110	5.6	168.6		
16	+Cu	28	67	5.2	100.2	27.9	−49.8
	0	25	45	2.3	72.3		
18	+Cu	65	145	6.1	216.1	55.9	66.1
	0	64	94	2.2	160.2		
22	+Cu	157	137	3.0	297.0	14.7	147
	0	157	123	2.3	282.3		
49	+Cu	30	28	3.7	61.7	22.3	−88.3
	0	25	12	2.4	39.4		
53	+Cu	67	163	4.1	234.1	93.3	84.1
	0	65	74	1.8	140.8		

Note. +Cu — zinc-plated wire; 0 — without surface layer; S — total content of nitrogen, oxygen and hydrogen in wire; $\Delta R = S_1 - S_2$, where S_1, S_2 — total content of gases, respectively, in zinc-plated wire and in wire without surface layer; $K = \Delta R + S_2 - 150$.

be assumed that the value ΔR is the criterion of evaluation of level of purity of the surface layer of wire before copper plating. During evaluation of the wire quality the total content of gases in it is also important. The carried out tests showed the intensified porosity of welds, produced using wires with $K > 50$ ppm (they include wires 18, 22 and 53 according to the Table). The $K \le 0$ requirement is fulfilled by wires 3, 16 and 49. In case when the K value of welding wire exceeds 50 ppm, non-destructive testing on the presence of porosity of welds, made by this wire, can be recommended depending on the requirements specified to welded joints.

Basing on the obtained results it can be considered that inadmissible defect of the investigated copper-plated wires is the total content of nitrogen, hydrogen and oxygen in them, exceeding 200 ppm, i.e. in case if the criterion $K > 50$ ppm. For critical structures it is recommended to apply wires with total content of these gases of not more than 150 ppm.

Evaluation of quality of wire winding. Standard ISO 544 requires that winding of wire on the reels should provide the uniform feeding of wire in mechanized welding methods. The most part of investigated wires were winded on the reels or wire frame cassettes with in-line winding-up according to the scheme «turn to turn» by the plants-manufacturers, and only two of them were winded without keeping of this requirement. However, even using some reels with wires, winded in-line, their non-uniform feeding in mechanized welding was observed. The reason was in incorrectly selected width of a reel, not taking into account the tolerance for the rated wire diameter, which resulted in violation of winding linearity. Disturbances and stop of electrode wire feed were observed also in case of welding using two wires without in-line winding. Non-quality winding of wire on the reels by the plant-manufacturer or consumer does not meet the requirements of standard ISO 544, item 5.2, and is an inadmissible defect.

Evaluation of rising (rigidity) of wire turns. The evaluation of rising of turns (planarity of a turn on horizontal surface of a plate) was carried out according to the results of hand unwinding of wire from the reel. Most of the wires meet the requirement of standard ISO 544, according to which the rising of turn should not exceed 50 mm for the reels with outer diameter of not more than 200 mm. In some wires the difference in rising of upper turns of cassette of 300 mm diameter and after consumption of almost half of the wire from the cassette was observed. Turns of the wire from the upper layer met the requirements of standard ISO 544, and turns of the middle layer of the same cassette did not met these requirements, that evidences of non-uniform rigidity of wire in the length, within the limits of one cassette. Extremely high rigidity of welding wire causes oscillations of end of electrode, which can be a cause of lacks of fusion, lacks of penetration of weld root, etc. Due to

this reason the non-uniform rigidity of wire is the inadmissible defect.

Evaluation of stability of wire diameter. The diameter of wire was evaluated by the requirement of standard ISO 544, according to which the admissible deviations of wire diameter of 1.2 mm amount from +0.01 to −0.04 mm. Only 5.7 % of wires (upper maximum deviation of diameter of wires amounted to +0.02 mm) did not meet the requirements of standard. The increased diameter of wire results in wear of channel of copper nozzle and can cause the need in its premature replacement. However, deviation of wire diameter from its rated size does not have a noticeable influence on quality of welded joints, and this disadvantage of wire is accepted as admissible.

Evaluation of roughness of wire surface. Roughness of the wire surface can result in increased wear of channel of current-carrying nozzle in welding. In the investigated wires the roughness of surface is within the limit from class 8 (parameter Ra = 0.63 μm) up to 10 (Ra = = 0.16 μm). Roughness of wire surface determines the service life of copper nozzles and flexible channels of electrode wire feed of hose holders of semi-automatic machines, but it does not significantly influence the stability of process and quality of welded joints. In this connection the increased roughness of wire surface is accepted as an admissible defect.

Other characteristics of copper coating. The quality of adhesion of copper layer with the steel wire and quality of wire surface are not regulated by the standards, but have an influence on evaluation of wire by welder, for example, according to uniformity of color of wire surface, amount of delaminated copper in the feeding mechanism and need in frequent cleaning of channel for electrode wire feeding. During tests the significant differences of these characteristics were noted in the investigated wires. In particular, on some wires during winding on core of diameter equal to wire diameter, the separation of copper coating was not observed, while on the other ones the cracks, tears and coating separation were rather intensive. However, the defects, connected with these characteristics, have no significant influence on the quality of welded joints and are not regulated by the standards, therefore, the decision about purchase of this wire is taken by the customer.

Welding-technological properties of wire. In practice, the evaluation of welding-technological properties is carried out on the basis of intensity of spattering and stability of the process. Coefficient ψ_s of losses for spattering was determined depending on welding mode (100–340 A current) in all the investigated wires. Measurements showed that for 56.6 % of wires being investigated ψ_s = 2.3–8.7 % (conditional estimate of wire is good), for 37.7 % — ψ_s = 5.9–12.3 % (satisfactory) and for 5.7 % — ψ_s = 7.0–15.5 % (not satisfactory). From the estimates of consumers (welders) the process of welding by wires of ψ_s = 7.0–15.5 % group was unstable, and these wires were subjected to reclamation. Excessively high spattering is inadmissible defect of the wire. In case of welding with 1.2 mm diameter wire of grade G3Si1 according to ISO 14341A in shielding gas M21 the inadmissible wire defect is the spattering with ψ_s > 12.3 %.

Characteristic of defects of steel studs for arc welding-on. Determination of inadmissible defects of steel studs for arc welding-on, manufactured by standard ISO 13918:2008, was carried out on the basis of results of comparative tests of quality of seven types of studs-rests SD1 of foreign and Polish production, of standard sizes of 10 × 100, 19 × 150, 22 × 150 and 25 × × 175 mm. These studs are used in critical structures, for example, in bridge construction. According to documents concerning the quality, the studs are manufactured of steel S235J2G3 + C450 (analogue to St3sp (killed)) by EN 10025:2002.

Visual inspection of studs. All the studs-rests being investigated meet the requirements of standard ISO 13918, item 5.3.6.1, and they have no manufacturing defects.

Checking of stud sizes. All the studs being investigated meet the requirements to shape and sizes of standard ISO 13918, item 5.3.6.1. The noted small deviations in length of studs or their diameter can be classified as a low-important defect if they correspond to inner diameter of ceramic rings UF for welding-on of studs of SD type.

Testing of mechanical properties of stud materials. Tensile tests showed that the yield strength and ultimate strength test of material of all the studs meet the requirements for steel S235J2G3 + C450 ($\sigma_y \geq 225$ MPa, $\sigma_t \geq 450$ MPa) and studs SD1 ($\sigma_y \geq 350$ MPa, $\sigma_t \geq 450$ MPa). Requirements to elongation ($A_5 \geq 24$ % by EN 10025:2002, Table 5, and $A_5 \geq 15$ % by ISO 13918:2008, Table 2) were not met by studs SD1 of 19 × 150 mm of production of company 1 conditionally, and SD1 of 22 × 150 mm of production of company 4 conditionally. Material of these studs did not meet also the requirements for value of energy of impact toughness of 27 J minimum (Charpy V-notch test) at −20 °C (for studs 1 — 8.8 and 6.0 J, for studs 4 — 5.5 and 5.0 J), and

all the rest studs met this requirement. Non-conformity of material of studs to requirements for mechanical properties is an inadmissible defect.

Control of chemical composition. Chemical composition showed that the material of studs being investigated (steel S235J2G3) corresponds to the requirements of standard EN 10025, except the above-mentioned studs 1 and 4. Content of silicon (lower than 0.07 %) and aluminium (lower than 0.02 %) in material of these studs does not correspond to content required for killed steel. Non-conformity to requirements for chemical composition of stud material is an inadmissible defect.

Conclusions

1. Inadmissible defects of copper-plated welding wire of G3Si1 grade by ISO 14341A are as follows:

- total content of nitrogen, hydrogen and oxygen in wires, exceeding 200 ppm (in welding in gas mixture M21);
- excessively high rigidity of wire, i.e. rising of wire turn on horizontal plane is more than 50 mm;
- non-quality winding of wire on reel or cassette;
- excessively high spattering (in welding with 1.2 mm diameter wire in mixture M21 the coefficient of losses for spattering $\psi_s > 12.3$ %).

2. Inadmissible defects of metal studs SD1 for arc welding-in are as follows:

- non-conformity to requirements for mechanical properties of material of studs, in particular by impact toughness;
- non-conformity to requirements for chemical composition of studs.

1. Pokhodnya, I.K. (2003) Welding consumables: State-of-the-art and tendencies of development. *The Paton Welding J.*, **3**, 2–13.
2. Voropaj, N.M., Brinyuk, M.V. (2002) Technological properties of copper-plated welding wire. *Svarshchik*, **4**, 16–20.
3. Voropaj, N.M., Degtyaryov, V.G., Ignatchenko, P.V. et al. (1976) Improvement of welding-technological properties of wire Sv-08G2S. *Avtomatich. Svarka*, **8**, 61–65.
4. Voropaj, N.M. (1977) Influence of state of electrode wire surface on metal transfer in shielded-gas welding. *Ibid.*, **3**, 68–69.
5. Denisov, L.S. (2012) *Welding and quality*. Minsk: Pravo i Ekonomika.
6. Pomranke, I., Zwinkert, G. (1998) Peculiarities of shielded arc welding with spray-rotation transfer of electrode metal. *Avtomatich. Svarka*, **11**, 40–47.

Received 30.04.2014

RESTORATION AND STRENGTHENING SURFACING OF PARTS OF DIE EQUIPMENT

E.A. SOLOMKA[1], **A.I. LOBANOV**[1], **L.N. ORLOV**[2], **A.A. GOLYAKEVICH**[2] and **A.V. KHILKO**[2]
[1]Company «Energomashspetsstal»
15 Sovkhoznaya Str., 84306, Kramatorsk, Donetsk oblast, Ukraine
[2]TM.VELTEK Ltd.
15 Bozhenko Str., 03690, Kiev, Ukraine. E-mail: office@veltec.ua

The results of works on increase of life of fixture of forging-press equipment by application of electric arc surfacing using electrodes and flux-cored wires are given. It is preferably to create and apply the specialized flux-cored wires, providing high life of deposited metal by optimization of its alloying. It is shown that application of restoration surfacing considerably increases the cycle between the repairs during operation of press strikers and provides economic effect of equipment service. 8 Ref., 5 Figures.

Keywords: *arc surfacing, parts of die equipment, restoration and strengthening, flux-cored wire, extension of life*

In forging-press workshop of the Company «Energomashspetsstal» the repair and manufacture of fixture for different types of forging-press operations including strikers are constantly carried out. To increase the life and minimize the terms of repair of tools, the analysis of application of existing surfacing materials in surfacing of strikers was carried out basing on the condition of providing combination of price and tool life [1–7].

The repair of tools of forging-press equipment using surfacing is efficient due to a lower price as compared to the purchase of a new part. Dies and strikers for hot stamping and forging, pressmould and die casting undergo thermal shocks, high specific pressures, abrasion wear, which result in formation of cracks, burrs and hairlines, loss of geometry of working surfaces of parts.

During selection of surfacing material as applied to the repair of dies of hammer heads and high-speed presses, the metal should have a complex of properties depending on the conditions of contact with hot metal. Under the conditions of quick deformation the ductility, resistance to flame erosion and plastic deformation are determining. Under the conditions of slow deformation the increased requirements to heat and oxidation resistance are additionally specified [8].

In the present work the peculiarities of technology of repair surfacing of plane striker and plane insert of steel 5KhNM are studied (Figure 1).

This type of fixture is quite intensively used in the press of 31.5 MN force for manufacture of the frequently varied nomenclature of products, which results in its quick local wear. After wear of working surface and formation of overlaps of metal, strikers and inserts are subjected to regrinding of working part of about 70 mm thickness on average.

For repair of tools the application of three variants of surfacing using electrodes of different type of alloying (KhN65MV; Stelloy C-O, Stelloy Ni520-G and OZSh-1, OZSh-6) was considered.

After preliminary study of characteristics and peculiarities of application of these consumables the preference was given to the electrodes OZSh-1 and OZSh-6, as far as they do not require application of special equipment and their cost is

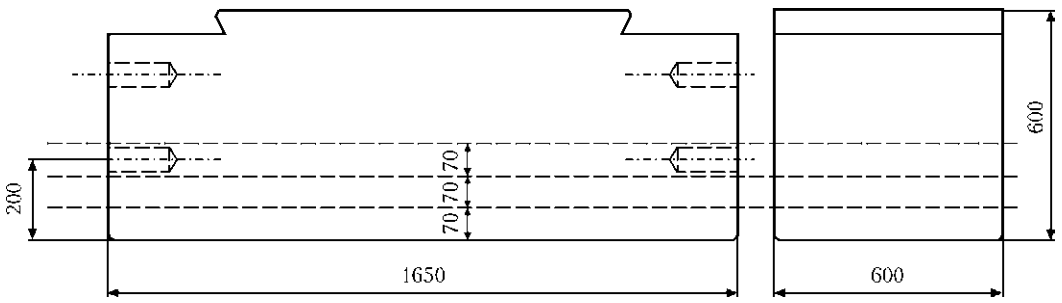

Figure 1. Press striker of 31.5 MN force

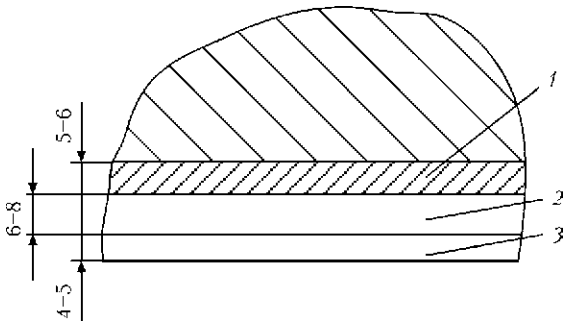

Figure 2. Scheme of location of deposited layers: *1* — sublayer; *2* — interlayer; *3* — working layer

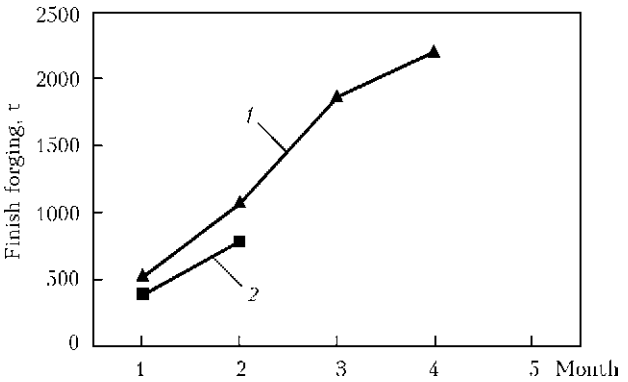

Figure 3. Life of deposited (*1*) and non-deposited (*2*) press striker

lower. The surfacing was performed with preheating of strikers to 300–400 °C simultaneously by two gas-air torches. Surfacing of striker and insert was performed in three layers (Figure 2): sublayer — using wire Sv-08G2S; interlayer — electrodes OZSh-1; working layer — electrodes OZSh-6.

After each pass the peening of deposited layer was carried out. After completion of surfacing the strikers were put to the furnace for tempering at 580 °C. The temperature of preheated furnace was 400 °C, time of soaking was 3 h, rate of furnace heating and cooling was 50 °C/h.

The deposited striker and insert passed verification in the press of 31.5 MN force in the forging press workshop. The comparison of life of non-deposited tool and deposited one showed the following:

- non-deposited striker was used in work since 23.11.2011 till 25.01.2012 and allowed forging of 781.7 t with the norm of consumption of 5.7 kg/t, and the working area of a striker required regrinding;
- deposited striker was used since 25.01.2012 till 07.05.2012 and allowed forging of 2201.13 t with the norm of consumption of 2.1 kg/t, which allowed 2.8 times increasing of the tool life (Figure 3).

In both cases in the working zone of the striker a wear appeared (Figure 4), which was eliminated by surfacing of this area and further treatment of a striker.

The economic effect at 21,000 t/year average finish forging in the press of 31.5 MN force amounted to 98,700 UAH.

For restoration and strengthening surfacing of both the worn out parts of dies (punches, moulds manufactured of tool steels 5KhGM, 5KhNV, 5KhNM, 7Kh3, U10A, etc.) as well as the new ones manufactured of tool and structural grades of steels (45, St5, etc.), the enterprise TM.VELTEK Ltd developed flux-cored wires VELTEK-N460.01, VELTEK-N460.04, VELTEK-N460.05 instead of electrodes TsSh-1 (30V8Kh3), Sh-1, Sh-16, TsN-4 (35G6), TsN-5, NZh-2, NZh-3 (GOST 10051–62).

The system of alloying of flux-cored wires is based on the optimization of deposited metal alloying with carbon, silicon, manganese, nickel, chromium, molybdenum, vanadium, tungsten and titanium, due to which the obtaining of low-carbon martensite matrix, strengthened with disperse carbides and intermetallics, in deposited metal is provided.

The metal deposited by flux-cored wires VELTEK-N460.01 (*HRC* 38–45) and VELTEK-N460.05 (*HRC* 48–54), is characterized by a high wear resistance under the conditions of operation of dies for cold and hot deformation of metals and satisfactory resists to high pressure and shocks. For surfacing of spots in the grooves of a die, requiring high hardness and wear resistance of strikers of forging-press equipment, it is recommended to use the wire VELTEK-N460.05.

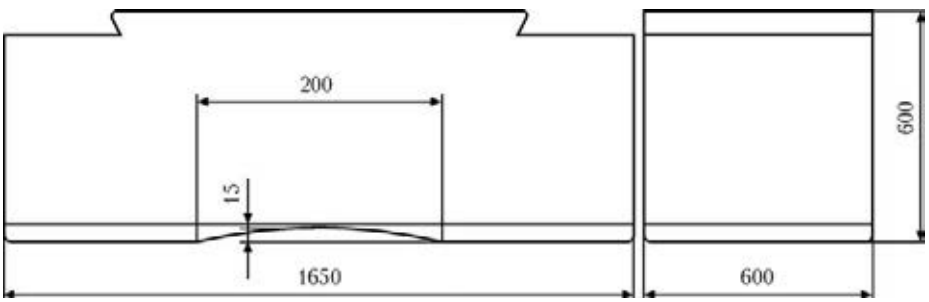

Figure 4. Wear of working surface of press striker

As applied to strengthening and repair of parts of dies of steels 5KhNM, 5KhNV, 38KhN3M-BA for pressing the billets of copper, brass L63, alloys ShV15-1, it is preferable to apply the wire VELTEK-N460.04 (*HRC* 48–54). The deposited metal has an increased resistance to «sticking» of billet with the die working surface. The surfacing is performed at direct current of reverse polarity with shielding in mixture of gases Ar + + 18 % CO_2.

The wire VELTEK-N460.01 was also successfully applied for repair of dies of production of crankshafts and connecting rods of engines of the automobiles «KamAZ» (Naberezhnye Chelny, RF) (Figure 5).

The dies, subjected to surfacing, were exposed to annealing, defective spots were cleaned, cracks were eliminated using milling and chamfers in the grooves were removed for surfacing. The defective spots were milled, and in some cases were simply cleaned using abrasive tool, but without sharp transitions. All the chamfers and grooves after treatment using any method had roundings with radius of not less than 3 mm. The angle of groove removal of cracks is not less than 40°, and width of the bottom was not less than 9 mm.

During repair of spots with cracks, after preparation of crack for surfacing the groove bottom was filled using wire VELTEK-N252-M with the next surfacing by wires VELTEK-N460.01 or VELTEK-N460.05. The dies prepared for surfacing were preheated to 350–400 °C to prevent initiation of cracks during surfacing. The craters were melted by short arc with minimum penetration and sharp interruption of arc. The dies, requiring treatment of working surfaces by cutting tool, immediately after surfacing were subjected to annealing (900 °C during 2 h, furnace cooling). The annealing after slow cooling of parts is admitted. After annealing the mechanical treatment of dies and their next hardening and tempering were carried out.

The experience of application of flux-cored wires VELTEK-N460.01 and VELTEK-N460.05 showed that increase in efficiency of striker, inserts and dies is achieved by increase in efficiency of surfacing process, decrease of costs for additional time and especially by decrease in consumption of surfacing material. Consumption of electrodes per 1 kg of deposited metal amounts to 1.8 kg and that for flux-cored wire is 1.17 kg, at almost equal price of surfacing material.

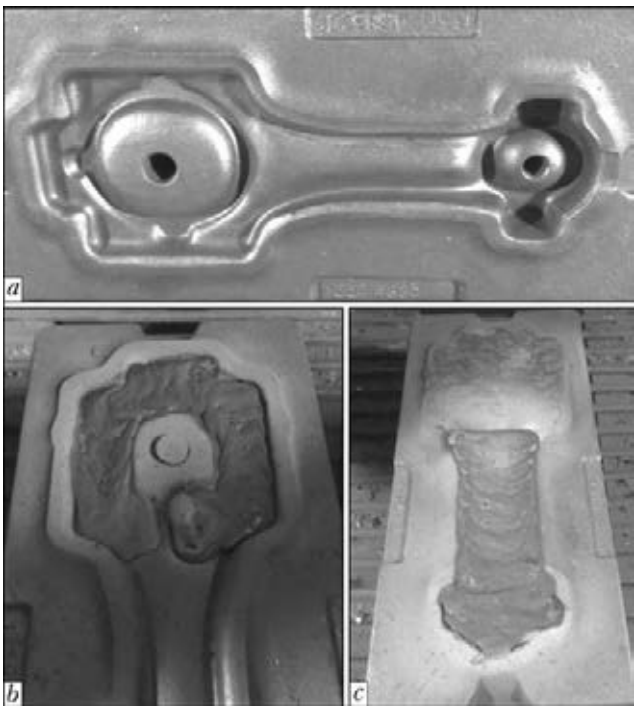

Figure 5. Repair of die part (connecting rod): *a* — condition of worn-out working surface of die; *b* — bead surfacing without oscillations; *c* — surfacing with oscillations

Conclusion

1. The application of semi-automatic electric arc surfacing reduces man-hours during repair of fixture for forging-press equipment and increases the duration of cycle between repairs.

2. The application of flux-cored wire allows increasing the efficiency of surfacing works more than 1.5 times.

1. Atroshenko, A.P. (1971) *Increase in service life of hot pressing dies*. Leningrad: Metallurgiya.
2. Velsky, E.I. (1973) Wear of die and means of increase in its life. *Kuzn.-Shtamp. Proizvodstvo*, **3**, 1–3.
3. *GOST 10543–98*: Steel surfacing wire. Technical requirements. Introd. 01.01.2001.
4. *GOST 10051–75*: Metal coated electrodes for manual arc deposition of surface layers with special properties. Types. Introd. 01.01.1977
5. (1979) *Surfacing materials of CIS countries*: Catalogue. Kiev-Moscow: MTsMTI.
6. Ryabtsev, I.A., Zhudra, A.P., Kirilyuk, G.A. et al. (2007) Surfacing flux-cored wires developed in PWI. *Svarshchik*, **1**, 30–32.
7. Kondratiev, I.A., Ryabtsev, I.A. (2009) Surfacing of stamping tool for hot deformation of metal by maraging steel layer. *Ibid*., **4**, 6–7.
8. Geller, Yu.A. (1983) *Tool steels*. Moscow: Metallurgiya.

Received 21.03.2014

SELECTION OF SHIELDING GAS FOR MECHANIZED ARC WELDING OF DISSIMILAR STEELS

V.P. ELAGIN
E.O. Paton Electric Welding Institute, NASU
11 Bozhenko Str., 03680, Kiev, Ukraine. E-mail: office@paton.kiev.ua

Mechanized multilayer MIG/MAG welding by high-alloy wires is associated with the feasibility of formation of lacks of fusion and slag pieces in weld metal. Therefore, the improvement of technology, in particular the selection of shielding gas composition, is urgent. Feasibility of application of mixtures CO_2 + 3 % N_2 and CO_2 + 3 % N_2 + 0.5 % O_2 as a shielding gas in mechanized arc welding of dissimilar steels is shown. It is shown that the metal oxidation occurs mainly in the inter-dendrite regions, intensity of which is increased with increase in amount of nickel in the welding wire. Weld metal alloying with nitrogen does not change the intensity of metal oxidation process and almost has no influence on slag crust removal from the deposited metal surface. 17 Ref., 2 Tables, 3 Figures.

Keywords: *mechanized arc welding, shielding gas, CO_2, nitrogen, gas mixtures, high-alloy weld metal, slag crust, spinels, alloying with nitrogen*

Mechanized shielded-gas arc welding by high-alloy wire is peculiar by high metal susceptibility to oxidation in welding zone and formation of lacks of fusion and slag pieces in weld [1]. In argon welding this is caused by a low stability of welding arc, leading to violation of welding process and gas shielding, and in mixture of argon with CO_2 or oxygen it is caused by metal oxidation by the shielding gas proper. The nitrogen-containing gas, namely nitrogen [2], argon mixtures or CO_2 with nitrogen [3] or with air [4, 5] is also used, but here the risk of pore formation in weld is occurred [4, 6]. Large selection of different compositions of shielding gases for almost similar technological variants proves that the development of gas mixtures, and also the developing of theory of gas-shielded welding process and still continued, that is confirmed by numerous publications on this subject [7, 8].

Beside the shielding gas composition the electrode wire composition has also a great influence on the weld quality. Its selection, as a rule, is defined by conditions of the welded joint service. For welding of dissimilar steels the welding wires of 08Kh20N25M3G2, 08Kh25N40M8G2 and 08Kh25N60M10G2 types have been developed [9]. The increased content of chromium and molybdenum in them is designed for prevention of hot cracks formation in the weld, and nickel is used for decreasing the martensite interlayer in the zone of fusion with a pearlite steel and delaying the development of structural heterogeneity in this zone during service heating [1]. However, chromium and molybdenum form the spinels of MeR_2O_4 type during oxidation, where Fe, Mn, Mg elements are as Me, and Al, Cr, V, Mo are as R [10], being in solid solution of wire metal. The assumption was given that in this case the transition layer is formed between the slag and weld surface, which contributes to their strong binding [11]. Welding high-alloy wire of 08Kh20N9G7T is known, which was developed for CO_2 welding of high-strength steels [12]. It found the successful application for welding of dissimilar steels [13]. The peculiar feature of its composition is the decreased content of nickel and spinel-forming elements, as well as the presence of active elements-deoxidizers such as silicon, titanium, manganese, that allows producing the weld metal without defects due to self-removal of slag crust from deposited metal surface during cooling. The insufficient content of austenizing elements in this wire limits its application for welding of dissimilar steels because of formation and development of structural heterogeneity in the zone of fusion with a pearlite steel [1].

It was found at the E.O. Paton Electric Welding Institute [14] that the secondary alloying of austenitic weld metal with nitrogen in welding of dissimilar steels allows, the same as alloying with nickel, decreasing the development of structural heterogeneity in the zone of fusion with a pearlite steel. This is explained both by austenizing capability of nitrogen and also by its effect on decrease of carbon diffusion. Moreover, the nitrogen protects the high-alloy metal from oxi-

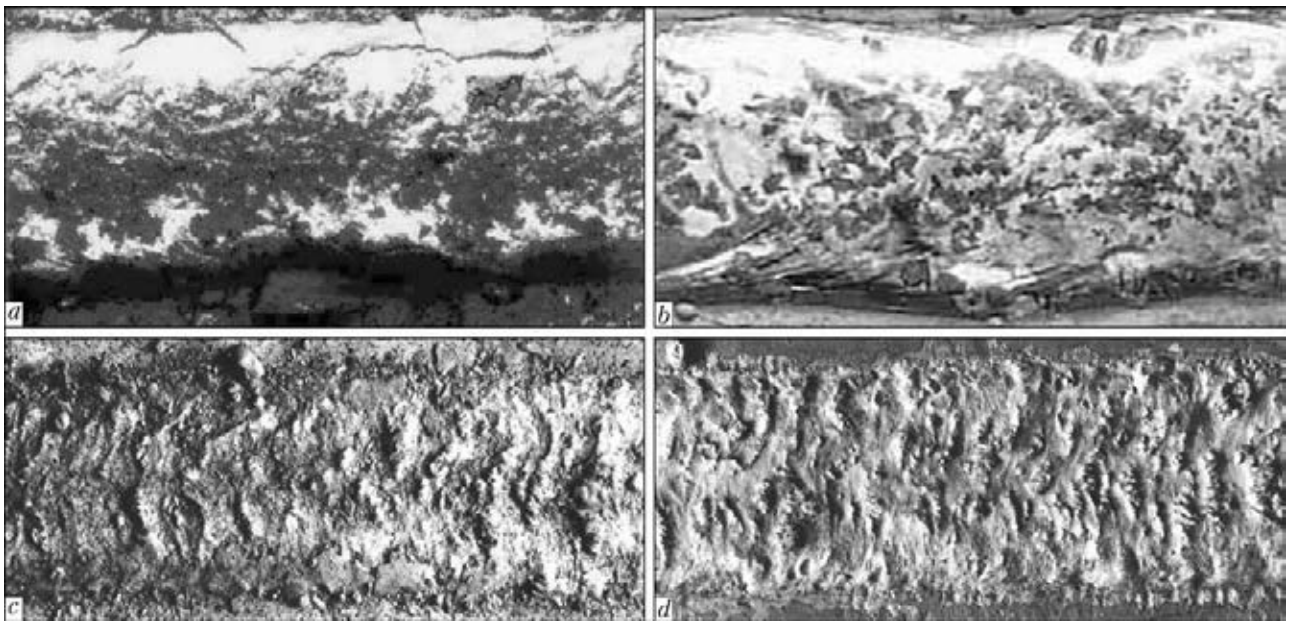

Figure 1. Appearance (×2) of surface of deposits made by arc welding in CO_2 + 3 % N_2 using wires 08Kh20N9G7T (*a*, *b*) and 08Kh25N40M6G2 (*c*, *d*) before (*a*, *c*) and (*b*, *d*) cleaning

dation and provides high stability of the welding process, that prevents the formation of a slag crust on the weld surface and lacks of fusion and slag pieces in weld metal [2]. However, in the zone of fusion with a pearlite steel the pores can form [15–17], which cannot be prevented with decrease of nitrogen amount even to 0.5 % in its mixture with argon. It is possible to prevent the pore formation by adding nitrogen or air to CO_2 up to 14 % with weld metal alloying with nitrogen in the amount of up to 0.4 % [17]. The obtained results were used in the technology of arc welding of heat-resistant steels of petroleum-refining equipment using electrode wire 08Kh20N9G7T [13]. It was interesting to study the effect of nitrogen in the composition of gas mixture of CO_2 and O_2 on oxidation of high-alloy weld metal and slag crust removal in welding by electrode wires of 08Kh20N25M3G2 and 08Kh25N40M6G2 types, recommended for welding of dissimilar steels.

For this purpose, the single-layer deposits by above-mentioned wires of 2.0 mm diameter on plates arranged under different angles to horizon, as well as multilayer welding of 22 mm thick plates of 12Kh5M steel in CO_2 and its mixtures with nitrogen and oxygen were made. For comparison, deposits by wire of 08Kh20N9G7T type, forming a slag crust in CO_2 welding possessing a good removal, were also made.

Deposits and multilayer welds were made by automatic welding machine ADG-502 at welding arc supply by direct current of reverse polarity from rectifier VDU-504. Welding current was 220–320 A, arc voltage — 24–28 V and welding speed — 14–20 m/h, shielding gas consumption — 12 l/min.

Effect of compositions of shielding gas and welding wire on metal oxidation and slag crust removal were evaluated by ratio of total amount of slag, which was collected after careful mechanical cleaning of deposit surface, to the amount of slag, self-removed from the surface of deposited metal during cooling. Results are given in Table 1, and the appearance of surface of deposits before and after cleaning is shown in Figure 1.

As is seen from this Figure, the surfaces of deposits before and after cleaning and also a slag crust, available on it, are significantly different. Surfaces of deposits, made by welding wire 08Kh20N9G7T, have smaller roughness, but they are covered with a thicker layer of a glassy-like slag, which is self-removed from the metal surface during cooling (Figure 1, *a*). After mechanical cleaning from remnants of slag the light surface of deposit is uncovered (Figure 1, *b*). However, on the surface of deposits, made by welding wire 08Kh20N25M6G7, the slag crust possesses a partial removal during cooling and hardly removed in mechanical cleaning, and with use of wire of 08Kh25N40M6G2 type it is not almost removed itself. After mechanical cleaning the deposited surface remains dark and has significant roughness due to metal hills (Figure 1, *c*, *d*). The largest amount of slag is formed on the surface of deposits made by wire 08Kh20N9G7T, and it is decreased with increase in level of welding wires alloying. Adding of nitrogen into shielding

Table 1. Composition of slag crust formed at the weld metal surface

Welding wire	Composition of shielding gas	FeO	SiO_2	MnO	TiO_2	MoO_3	NiO	Cr_2O_3	Amount of slag·10^{-3}*, g/mm^2
08Kh20N9G7T	CO_2	0.7	12.3	38.5	19.4	–	–	12.8	12.9 (11.5) / 1.12
	CO_2 + 3 % N_2	0.6	8.3	32.2	11.3	–	–	6.4	10.5 (9.3) / 1.13
	CO_2 + 3 % N_2 + 0.5 % O_2	0.7	11.4	36.8	17.4	–	–	11.4	12.7 (10.8) / 1.17
08Kh20N25M6G7	CO_2	16.5	5.6	38.5	16.5	1.6	3.25	26.5	10.1 (5.11) / 1.97
	CO_2 + 3 % N_2	15.4	4.4	33.2	12.5	0.8	3.1	22.4	7.8 (4.11) / 1.89
	CO_2 + 3 % N_2 + 0.5 % O_2	17.3	6.7	39.1	17.6	1.4	2.2	21.5	8.5 (3.6) / 2.36
08Kh25N40M6G2	CO_2	22	3.8	10.4	5.06	3.2	5.12	46.5	8.41 (0.2) / 42.1
	CO_2 + 3 % N_2	19.3	2.8	9.7	3.3	2.3	4.2	38.3	5.2 (0) / –
	CO_2 + 3 % N_2 + 0.5 % O_2	21	3.2	6.4	4.4	3.1	4.8	44.3	7.3 (0) / –

*Numerator gives the total and self-removed (in brackets) amount of slag, denominator — their ratio.

gas composition reduces the amount of slag, while oxygen addition increases the amount of slag, but it has not great influence on its removal (see Table 1).

Change in element composition of slag was determined by X-ray spectral fluorescence method in quantometer KRF-18. Slag, possessing a good or partial removal, has much more oxides of silicon, manganese and titanium and lower amount of iron and chromium. Attention is attracted by the fact that with increase of nickel content in the composition of wires

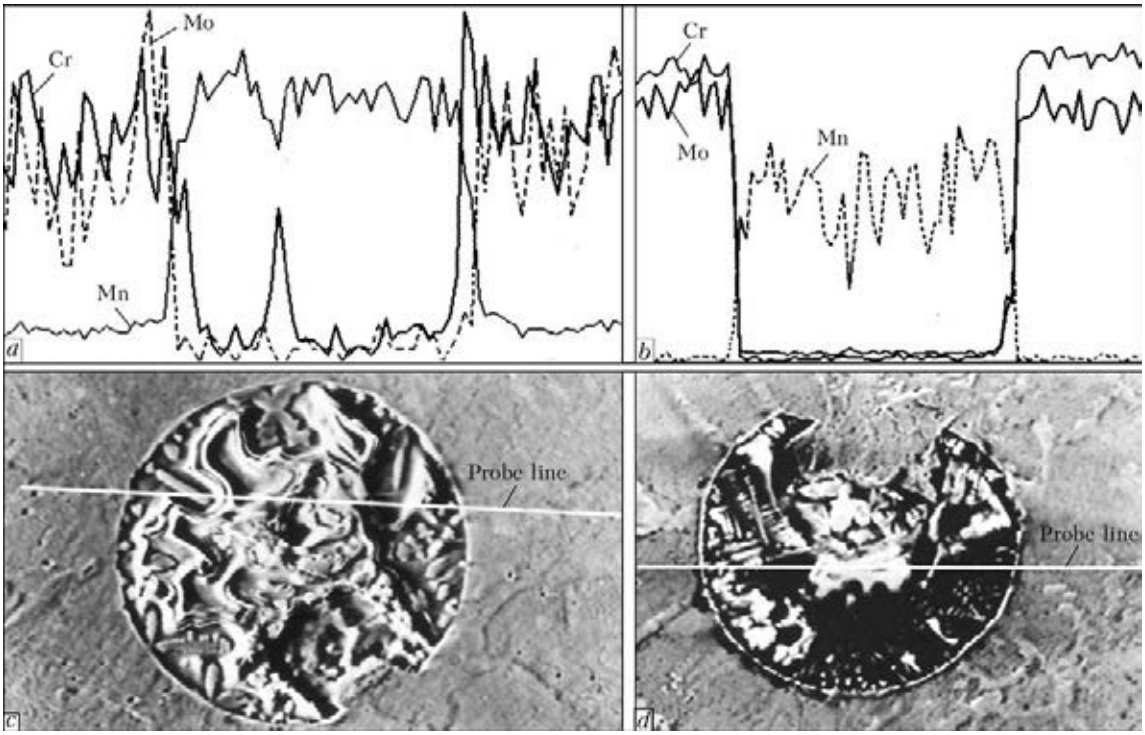

Figure 2. Distribution of chemical elements across a non-metallic inclusion located in subsurface region (*a*, *c*) and lower part of deposit (*b*, *d* — ×1000)

08Kh20N25M6G7 and 08Kh25N40M6G2 the amount of oxides of iron and nickel in the slag composition is growing. Probably, this occurs due to proceeding of silicon-manganese reduction processes on the metal surface, which can be described by the equations [10]

$$(SiO_2)_{sl} + 2Fe_{me} = 2(FeO)_{sl} + [Si]; \quad (1)$$

$$(MnO)_{sl} + Fe_{me} = (FeO)_{sl} + [Mn]; \quad (2)$$

$$(SiO_2)_{sl} + 2Ni_{me} = 2(NiO)_{sl} + [Si]; \quad (3)$$

$$(MnO)_{sl} + Ni_{me} = (NiO)_{sl} + [Mn]. \quad (4)$$

So, it can be assumed that with increase in content of nickel in metal the intensity of proceeding of processes of metal surface oxidation with formation of a thin oxide film is increased. Oxides of chromium and molybdenum in slag come into interaction with it, forming the chrome- and molybdenum spinels, strongly bound with metal surface.

To confirm this, the distribution of chemical elements between the metal and non-metallic inclusion was investigated by X-ray spectral microanalysis using scanning microscope-microanalyzer CAMEBAX SX-50. Investigations were carried out on a subsurface region, located at the 0.2 mm distance from the surface with a slag, and on the region, located in the lower section of bead, deposited by wire 08Kh25N40M6G2 in CO_2 (for results of investigations see Figure 2, *a*, *b*). Table 2 shows microchemical heterogeneity and change in degree of liquation of elements in

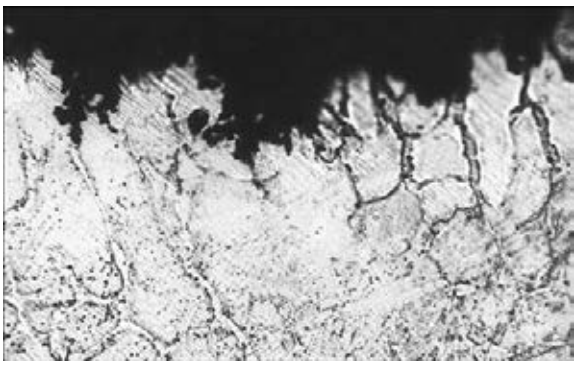

Figure 3. Microstructure (×400) of subsurface region of metal deposited by wire 08Kh25N40M6G2 in mixture CO_2 + 3 % N_2

subsurface region at 0.1–0.2 mm distance from surface and in the lower part of the deposit.

Non-metallic inclusion, located in the subsurface region, has no gap with metal around its entire perimeter (see Figure 2, *a*). Moreover, there are peaks in curves of chromium and molybdenum distribution at the regions of transition from metal to inclusion, proving the increased content of these elements. Such local increase in their amount at the region of transition from metal to non-metallic inclusion, located in the deposit lower part, is not observed and, moreover, it has a gap with metal at the largest part of perimeter (see Figure 2, *b*).

The increased amount of chromium and molybdenum at the regions of transition from metal to inclusion in subsurface zone proves long duration of high-temperature heating of metal of this zone, during which the transfer of these ele-

Table 2. Microchemical heterogeneity of regions of metal deposited by wire of 08Kh25N40M6G2 type in CO_2 and in mixture CO_2 + + 3 % N_2

Object of investigation			Elements, wt.%						
			C	Si	Mo	Cr	Mn	Ni	Fe
Deposition in CO_2	Subsurface part of bead	Inter-dendrite region (C_{tr})	0.283	0.216	5.65	10.28	3.12	14.1	67.6
		Dendrite (C_b)	0.075	0.13	3.086	9.09	2.23	13.69	73.13
		Degree of liquation (C_{tr}/C_b)	3.77	1.66	1.83	1.13	1.4	1.03	0.92
	Lower part of bead	Inter-dendrite region (C_{tr})	0.501	0.257	3.78	11.02	4.23	13.78	68.35
		Dendrite (C_b)	0.19	0.185	2.79	10.31	3.4	13.1	72.53
		Degree of liquation (C_{tr}/C_b)	2.62	1.39	1.41	1.07	1.24	1.05	0.94
Deposition in mixture CO_2 + 3 % N_2	Subsurface part of bead	Inter-dendrite region (C_{tr})	0.203	0.156	5.35	9.05	3.08	13.5	63.6
		Dendrite (C_b)	0.065	0.11	3.186	8.03	2.36	12.91	70.63
		Degree of liquation (C_{tr}/C_b)	3.53	1.41	1.68	1.127	1.3	1.046	0.9
	Lower part of bead	Inter-dendrite region (C_{tr})	0.491	0.223	4.73	11.02	3.93	13.55	69.88
		Dendrite (C_b)	0.187	0.175	2.51	10.11	3.1	12.9	71.54
		Degree of liquation (C_{tr}/C_b)	2.62	1.27	1.48	1.09	1.26	1.05	0.97

ments is occurred to the regions of proceeding of intensive oxygen-reduction processes. This is also confirmed by the results of investigation of chemical microheterogeneity (see Table 2).

Metal of the subsurface region as compared to the lower region is depleted in carbon, silicon, manganese and chromium, but enriched in molybdenum and nickel, here the degree of liquation of almost all the elements in metal near the surface is higher due to their higher amount in inter-dendrite regions than in the dendrite body. This is also proved by microstructure of the subsurface region (Figure 3). In metal layer of up to 0.5 mm thickness the enlargement of inter-dendrite regions and formation of oxidation regions in it are observed. This is correlated with the results of investigations of microchemical heterogeneity (see Table 2). Metal alloying with nitrogen did not almost influence the microchemical heterogeneity of regions being investigated.

Thus, it can be stated that oxygen-reduction processes are proceeding mainly in the inter-dendrite regions of austenitic weld metal in the subsurface region. Increase in amount of nickel in metal increases their intensity with the formation of oxides of chromium and molybdenum of the spinel type, that deteriorates the slag crust removal. Alloying of metal with nitrogen has no significant effect on these processes and, therefore, does not deteriorate the slag crust removal.

Conclusions

1. Feasibility of application of mixtures CO_2 + + 3 % N_2 and CO_2 + 3 % N_2 + 0.5 % O_2 as a shielding gas in mechanized welding of dissimilar steels is shown.

2. In welding by electrode wire of 08Kh20N9G7T type in gas mixtures CO_2 + + 3 % N_2 and CO_2 + 3 % N_2 + 0.5 % O_2 the formed slag crust is self-removed from the weld surface and weld is produced without lacks of fusion and slag pieces.

3. The higher content of nickel in welding wires, as well as the presence of molybdenum, deteriorate the slag crust removal due to increase in intensity of oxygen-reduction processes mainly in the inter-dendrite regions of the austenitic weld metal and formation of oxides of chromium and molybdenum of a spinel type. The defect-free weld is possible in this case only at the careful mechanical layer-by-layer cleaning of the weld surface.

4. Metal alloying with nitrogen has no great influence on the proceeding of oxygen-reduction processes on the austenitic weld metal surface and, therefore, does not deteriorate the slag crust removal.

1. Gotalsky, Yu.N. (1992) *Welding of pearlitic steels by austenitic materials*. Ed. by K.A. Yushchenko. Kiev: Naukova Dumka.
2. Dyatlov, V.I., Korinets, I.F. (1968) Automatic nitrogen-shielded welding of austenitic chrome-nickel steels and alloys. *Avtomatich. Svarka*, **9**, 25.
3. Kakhovsky, N.I. (1975) *Welding of high-alloy steels*. Kiev: Tekhnika.
4. Nechaev, V.A., Timofeev, M.M., Rubennik, Yu.I. (1974) Influence of welding parameters on absorption of nitrogen by metal in non-shielded arc welding with high-alloy austenitic wire. *Svarochn. Proizvodstvo*, **4**, 24–26.
5. Lopukhov, Yu.I., Ivnitsky, B.P., Sorokin, G.A. (1989) Gas-arc surfacing of fittings in nitrogenous shielding atmosphere. *Energomashinostroenie*, **9**, 33–35.
6. Kotvitsky, A.D. (1974) *Shielded-gas welding*. Moscow: Vysshaya Shkola.
7. Lettle, K., Stapon, G. (2005) How to simplify the choice of shielding gas. *Practical Welding Today*, 9(**1**), 22–25.
8. Herold, H. et al. (2005) The use of nitrogen gas at welding of heat-resistant nickel alloys. *Austral. Welding J.*, Vol. 50 (2nd quart.), 40–47.
9. Gotalsky, Yu.N., Snisar, V.V. (1970) Wires for welding of dissimilar steels. *Svarochn. Proizvodstvo*, **2**, 42–44.
10. Potapov, N.N. (1985) *Oxidation of metals in fusion welding*. Moscow: Mashinostroenie.
11. Gotalsky, Yu.N., Stretovich, A.D. (1976) About mechanism of slag crust adhesion with weld metal. *Svarochn. Proizvodstvo*, **11**, 54–56.
12. Musiyachenko, V.F., Mikhoduj, L.I. (1987) *Arc welding of high-strength low-alloy steels*. Moscow: Mashinostroenie.
13. Elagin, V.P., Snisar, V.V., Lipodaev, V.N. (1995) Mechanized welding of steel 15Kh5M without heating and heat treatment. *Avtomatich. Svarka,* **8**, 19–24.
14. Snisar, V.V., Lipodaev, V.N., Elagin, V.P. et al. (1991) Effect of nitrogen alloying of austenitic weld on development of structural heterogeneity in fusion zone with pearlitic steel. *Ibid*., **2**, 10–14.
15. Pidgaetsky, V.V. (1970) *Pores, inclusions and cracks in welds*. Kyiv: Tekhnika.
16. Grishchenko, L.V., Kiselyov, Ya.N., Petrykin, V.M. (1987) Decrease of susceptibility to pore formation in weld metal during welding with austenitic electrodes on chrome-nickel base. *Voprosy Sudostroeniya*, Series Welding, Issue 26, 20–24.
17. Elagin, V.P., Snisar, V.V., Lipodaev, V.N. (1993) Specifics of nitrogenous shielded gas arc welding with austenitic wires of dissimilar and pearlitic steels. *Avtomatich. Svarka*, **7**, 12–16.

Received 14.05.2014

INFLUENCE OF ACTIVE GAS CONTENT AND DISPERSE FILLER CONTINUITY ON THE PROCESS OF BEAD FORMATION IN MICROPLASMA POWDER SURFACING OF NICKEL SUPERALLOYS

K.A. YUSHCHENKO and **A.V. YAROVITSYN**
E.O. Paton Electric Welding Institute, NASU
11 Bozhenko Str., 03680, Kiev, Ukraine. E-mail: office@paton.kiev.ua

Features of deposited metal formation in microplasma powder surfacing of nickel superalloys, depending on presence of active gases in the filler powder, are considered. Conditions of sound formation of deposited metal and requirements to filler powders were established, proceeding from oxygen and nitrogen content. An interrelation between presence of micropores in deposited metal and their presence inside disperse powder particles is shown. A probable mechanism of microporosity formation, influence of technological parameters of the process on micropore quantity and size in deposited metal is described. 25 Ref., 2 Tables, 10 Figures.

Keywords: *microplasma powder surfacing, nickel superalloys, deposited metal, filler powder, oxygen and nitrogen, microporosity of powder and deposited metal*

It is known that presence of defects in welded joints, in particular, deviations from the specified shape and continuity of deposited metal, leads to considerable lowering of item service properties [1].

The main γ′-forming elements of high-temperature nickel alloys — aluminium and titanium, chromium, as well as other refractory alloying elements — because of their high affinity to oxygen are the cause for formation of refractory oxides in fusion welding [2–5], in particular, inclusions in deposited metal and lacks-of-fusion. Their presence in the weld pool necessitates an essential increase of welding current, in order to ensure an acceptable spreadability of metal being deposited [4, 5]. In view of limited solubility of nickel alloys with γ′-phase content of more than 45 vol.%, increase of specific heat input increases the probability of hot cracking in welding and of crack initiation during subsequent heat treatment [2, 5, 6]. Therefore, ensuring sound formation of deposited metal for such materials is closely related to technological strength of welded joint and, alongside the optimum structure, it is a most important component of welded joint quality and operating reliability.

Process of microplasma powder surfacing is applied in repair of sealing, antivibration elements of aircraft gas turbine engine blades [7, 8]. For this process filler disperse powders of nickel alloys with different content of γ′-phase are batch produced. Penetration of relatively small quantities of active gases into deposited metal of nickel superalloys [9] can cause deviations from its sound formation. Proceeding from experience of surfacing and operation of reconditioned blades, quality of disperse filler is important, which, in particular, is determined by oxygen and nitrogen content.

Negative influence of micropores in disperse particles on item performance is known in powder metallurgy. Mechanism of their formation during melt dispersion by inert gas is described in [2, 10, 11]. It runs in four stages: introduction of portions of energy carrier gas into the melt jet flowing out of the atomizer; decomposition of gas portions into bubbles in molten metal jet; jet decomposition into fragments, part of which carries gas bubbles; cooling and solidification of metal drops with gas bubbles or without them. Owing to limited heat input into the item and time of weld pool metal staying in the molten state, continuity of filler powder particles can also affect the process of deposited bead formation in microplasma surfacing.

The objective of this work is more precise definition of ranges of oxygen and nitrogen content in disperse filler material, as well as studying the causes and regularities of microporosity formation in deposited metal of nickel superalloys.

Objects of research were deposited metal and filler powders of nickel superalloys with γ′-phase content of more than 45 vol.%. Vacuum extrac-

tion method was used for quantitative evaluation of active gases in the metal [9, 12, 13]. Active gas content in the cast, deposited metal and filler powder was determined in the LECO systems RO316 (oxygen) and TN114 (nitrogen).

Filler powders of nickel and cobalt alloys with particles size of 63–160 μm were used in surfacing. The following parameters were varied for metallographic investigation of the deposited metal:

- welding current of 10–65 A;
- diameter of plasmatron focusing nozzle d_f = = 5.5 and 3.0 mm, which determined 4.8–20 cm^{-2} concentration of powder feeding into the weld pool by the procedure of [14];
- kind of powder feed (continuous in the quantity G = 5 g/min or portioned feed with microportion weight M_0 = 0.02–0.14 g, and their feeding periodicity t_p = 0.5–2.5 s).

Blanks of deposited metal sample sections and filler powder samples were pressed into plastic holders of 30 mm diameter in the Struers Labo-Press-3. Metallographic analysis of longitudinal section of deposited metal bead (sample length of 15 to 22 mm) was performed in optical microscope Neophot 32. Analysis of quantitative content of micropores in filler powders was conducted by photos taken in Jenavert optical microscope with digital camera Micam TCA-5.0. This allowed detection of micropores greater than 5 μm in the deposited metal and filler powders, and evaluation of their size with the accuracy of ±2.5 μm. At calculation of micropore area it was assumed that its cross-sectional shape is a circumference.

In case of micropore detection their following quantitative characteristics were determined: for deposited metal — total micropore area F_{PD} over an area of 50 mm^2; relative micropore area Π_{PD} = = $0.02F_{PD}$; for photos with cross-section of filler powder particles — total particle number N; number of particles with micropores N_{MPP}; relative number of particles with micropores Π_{MPP} = = N_{MPP}/N; total micropore area F_{MPP}; conditional micropore area per one powder particles F_{MPP}/N. Analysis of disperse filler particles was conducted in six nonintersecting fields of vision for each, stage size was approximately 2 mm^2; total particle quantity was equal to about 1500 pcs. Microstructure of filler powders and individual particles was examined further in electron microscope in back-scattered electrons.

Evaluation of picnometric density of powder and its porosity was performed by the procedure of [15]. Weight of powder sample was 15 ± ± 0.03 g. Before pouring into the densimeter, the powder was dried in air at 150 °C for 0.5 h. Ethyl alcohol was used as picnometric liquid. Densimeter mass at successive weighing was determined

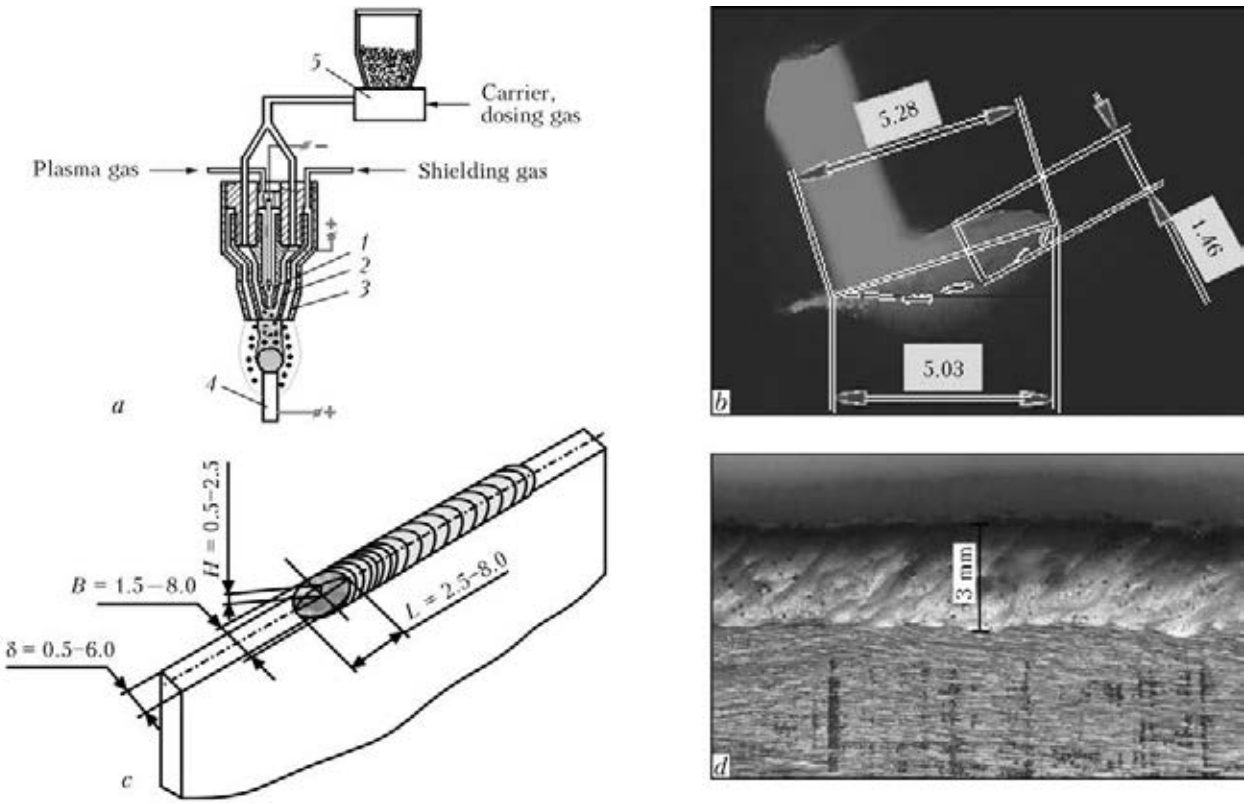

Figure 1. Schematic of the process of microplasma powder surfacing (*a*: *1* — plasma nozzle; *2* — focusing orifice; *3* — protective cone; *4* — item; *5* — powder feeder), weld pool appearance (*b*), its typical dimensions (*c*), and deposited bead appearance (*d*)

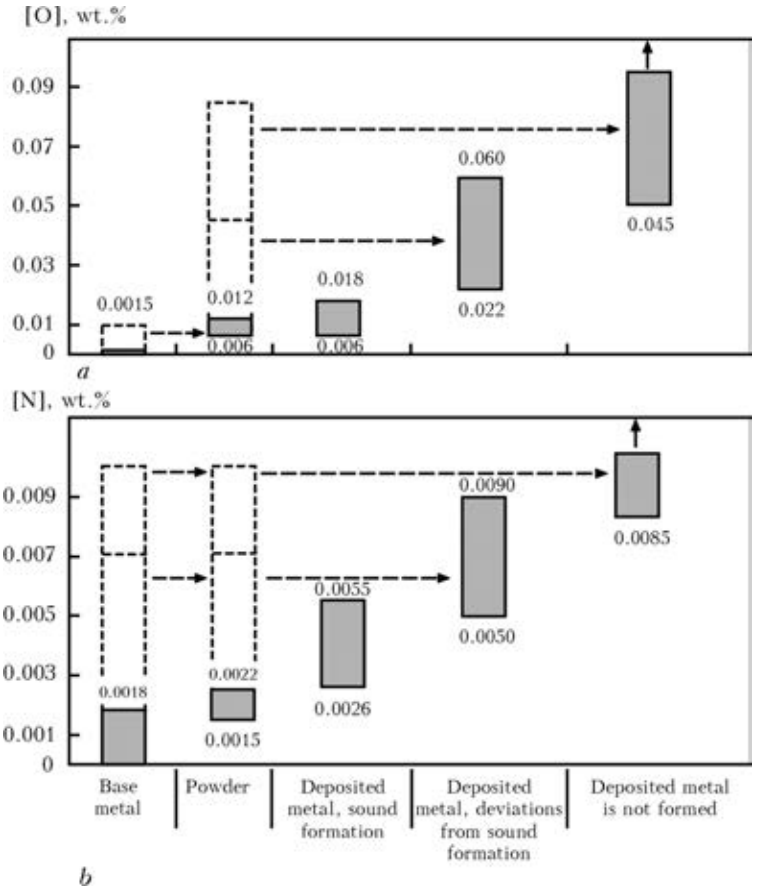

Figure 2. Content of oxygen (*a*) and nitrogen (*b*) after superalloy going through cast billet–disperse powder–deposited metal technological stages (*dashed line* — possible deviations from recommended ranges of active gas content in the metal)

in analytical scales VLP-200 of the 2nd accuracy class to GOST 19491–74. Measurements were performed by direct weighing with the accuracy of ±2.5 mg. Porosity, determined by the procedure of hydrostatic weighing, was calculated as

$$\Pi_{wt} = 100(1 - \rho_p/\rho)\ (\%),$$

where ρ_p is the pictometric density of powder; ρ is the alloy density.

Results of metallographic analysis and hydrostatic weighing after statistical treatment were correlated with process parameters and features of microplasma powder surfacing.

Schematic and features of the process of microplasma powder surfacing are given in Figure 1. As a rule, as current of up to 35 A the weld pool has the shape of an ellipsoid. Depending on the value of specific heat input, the volume of its liquid metal is from 2 up to 125 mm^3. Duration of it staying in the molten state is from 2 to 20 s.

Change of oxygen and nitrogen content in the nickel alloy with γ′-phase quantity greater than 45 vol.% has been analyzed after the following metallurgical processing stages: cast billet–dispersed powder–deposited metal allowing for the features of its formation (Figures 2 and 3). Earlier published in our work [9] data were complemented, generalized and are presented in Figure 2 in the form of a range of these gases content. It is shown that sound formation of deposited metal is achieved at its content of oxygen of not more that 0.018 % and of nitrogen of not more than 0.0055 wt.%. Visual observations showed that the deposited metal readily spreads and wets the base metal; oxide film on weld pool surface is absent.

Deposited metal formation is impaired, if the content of oxygen and nitrogen in the deposited metal rises above 0.022 and 0.005 wt.%, respectively (see Figures 2 and 3). Then, the following features are observed in surfacing:

- dense oxide film forms on greater part of weld pool surface, which can remain on bead surface after deposition;
- pool width is much greater than that of narrow substrate* (more than 1.5–2.0 mm to one side), that makes subsequent bead machining more complicated;

*Surface, the width of which is not greater than that of weld pool [16].

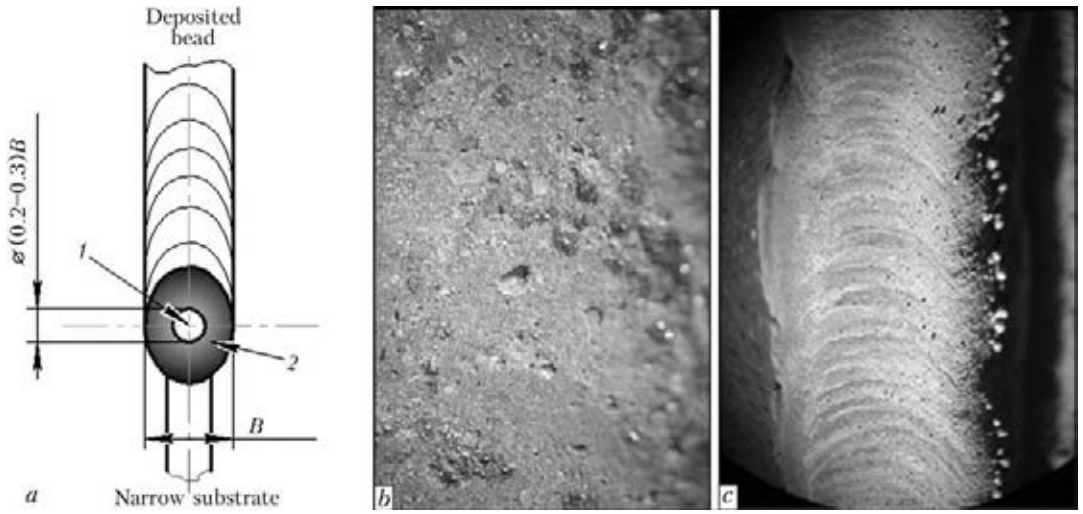

Figure 3. Features of formation of deposited nickel superalloy with more than 45 vol.% of γ′-phase at increased content of oxygen and nitrogen in it: *a* — weld pool (*1* — free section of weld pool surface; *2* — weld pool surface periphery covered by oxide film); *b* — oxide film after bead solidification (×25); *c* — bead appearance

• lacks-of-fusion, oxide inclusions and undercuts periodically form in the deposited metal and on its interface with base metal.

If oxygen and nitrogen content in the deposited metal is more than 0.045–0.060 and 0.0085–0.0090 wt.%, respectively, then continuous formation of deposited metal is disturbed because of presence of dense oxide films (see Figure 2).

The above-described deviations from sound formation of deposited nickel superalloys are also manifested to varying degrees, if oxygen and nitrogen content in the disperse filler exceeds 0.0120 and 0.0022 wt.%, respectively (see Figures 2 and 3). In its turn, quantity of active gases in the powder depends on their content in the initial cast billet [17–20]; method to produce powder [16]; level of humidity of powdered materials [9, 16]; repetition factor of powder use [9, 16].

It is known that oxygen and nitrogen, alongside other elements, are impurities in cast nickel superalloys. Their content in modern alloys after vacuum-induction melting is limited to 0.0015 wt.% [17, 18]. Increase of the content of oxygen to 0.0017–0.0032 and of nitrogen to 0.0015–0.01 wt.% in initial castings can be due to addition of casting production wastes to charge materials [17–20]. Powder remains after reuse [9, 14, 21], wastes from powder manufacture [10, 11] (disperse material outside 40 to 250 μm fraction) can, probably, also be used in the initial billet for powder dispersion and can essentially increase oxygen content in it (tentatively up to 0.012 wt.%). In this case, increased content of active gases in disperse powder can in itself cause unsound formation of deposited bead.

Powder dispersion method can have an essential influence on oxygen and nitrogen content in the disperse filler. Surfacing powders with different dispersion of liquid metal jet, namely by water, air or nitrogen, argon under pressure, and with centrifugal dispersion are batch produced. Oxygen and nitrogen content in them is determined by the medium dispersing the melt, and can be quite high: 0.06–0.12 and 0.061–0.141 wt.%, respectively [16]. For instance, evaluation of the content of active gases in filler powders of nickel alloy IN625 of a number of manufacturers showed that in some cases it may reach 0.04–0.05 wt.% O and 0.007–0.009 wt.% N.

In view of the high affinity to oxygen of the main alloying elements in superalloys, the technology of disperse filler manufacturing should provide guaranteed protection from the impact of active gases on the melt. Method of ingot dispersion by argon with powder cooling in inert medium the most completely meets these requirements [10, 11]. At gas content limited to 0.002 wt.% in the initial billet, it allows producing filler powder from nickel superalloys with oxygen content of up to 0.012 and nitrogen content of up to 0.0025 wt.%.

In microplasma powder surfacing, part of the filler moves around the microplasma arc periphery, does not penetrate into the weld pool, and can be reused [9, 14, 21]. During investigation of such powder morphology by optical microscopy methods (Figure 4, *a*) it is established that at its multiple application it accumulates particles with oxidized surface (up to 50–60 % of the total quantity). Electron microscopy analysis of these particles showed presence of an oxide film of 3 to 4 μm thickness on their surface (Figure 4, *c*–*d*). Application of such powder only slightly increases oxygen and nitrogen content in the deposited metal — not more than 0.003–

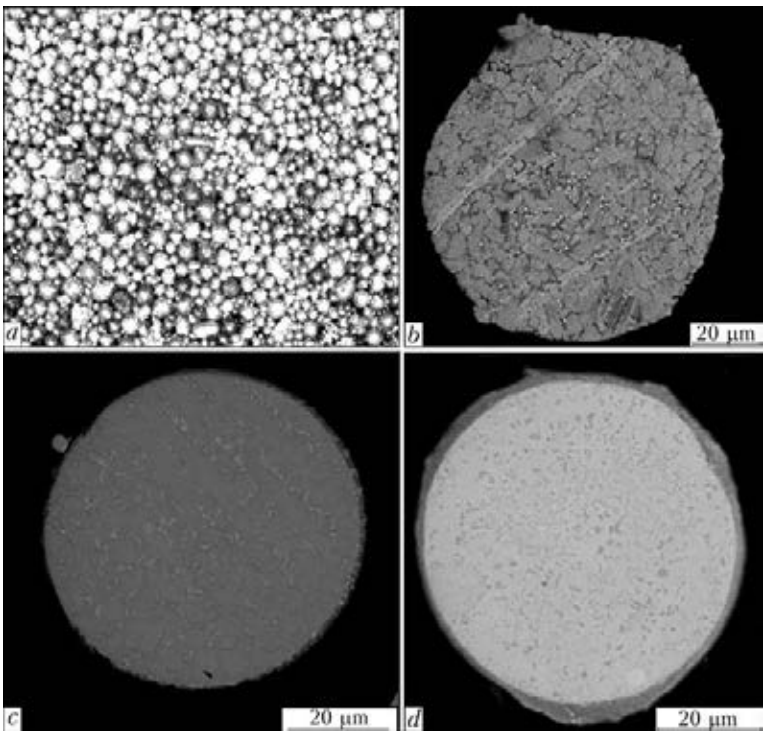

Figure 4. Morphology and microstructure of transverse section of particles of nickel superalloy powder: *a* — powder remains after reusing it several times (darker surface colour — particles oxidized in microplasma arc) (×50); *b* — particle of new powder from JS6U-VI alloy (×650); *c* — particle of JS32-VI alloy powder oxidized in microplasma arc (×1000); *d* — particle of JS32-VI alloy powder oxidized and remelted in microplasma arc (×1000)

0.0015 wt.%, respectively [9], that is admissible at ensuring sound bead formation, oxygen and nitrogen content in the deposited metal not exceeding 0.018 and 0.0055 wt.%, respectively.

At metallographic analysis micropores of 5–75 μm size (predominantly 20–40 μm) in the quantity of 20–30 pcs over an area of approximately 4 mm^2 are periodically revealed in the metal of nickel alloys with γ′-phase content of 15 to 62 vol.% produced by microplasma powder surfacing. Both their uniform distribution and local elongated clusters of micropores, irrespective of the distance from the fusion line, are observed in the deposited metal (Figure 5).

Micropore presence in the deposited metal is not influenced by the kind of shielding gas (argon, argon-hydrogen mixture [7]) or parameters of the mode of powder pre-drying at 300 °C. Investigations of longitudinal sections of beads, deposited predominantly at effective heating power of 200–500 W, showed that over deposited metal area of 50 mm^2 total area of micropores F_{PD} is in the range of 1000–70,000 μm^2, and their relative area Π_{PD} is equal to 0.002–0.140 vol.%.

Appearance of micropores of 5–75 μm size in the deposited metal is associated with presence of predominantly closed micropores of similar size in the filler powder (Figure 6). Electron microscopy analysis of cross-sections of powder particles with inner discontinuities demonstrated absence of oxide films on micropore outer boundary (Figure 6, *c–f*). This is indicative of sufficiently high level of protection from the air medium in melt dispersion and is not contradictory

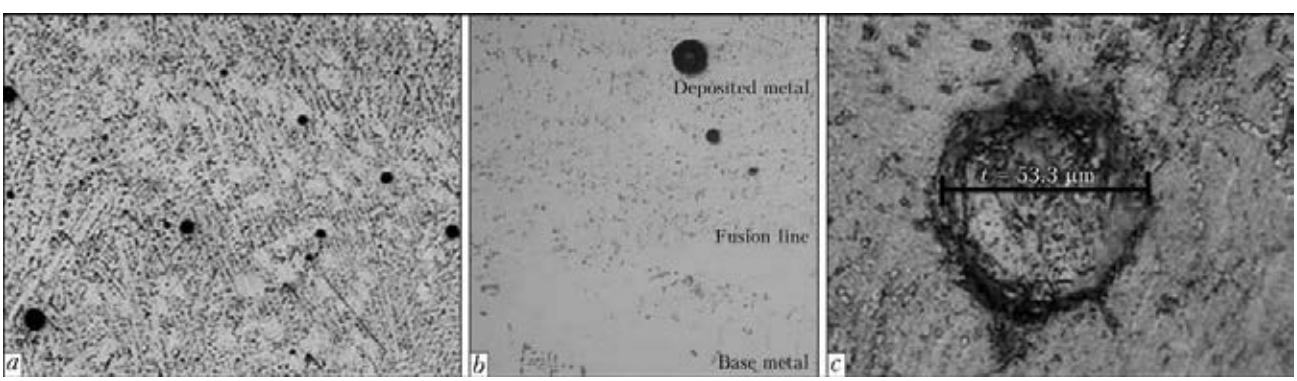

Figure 5. Microstructure of deposited metal with micropores (*a* — ×50; *b* — ×100), and isolated micropore (*c*) in deposited metal of JS32 alloy (*a*, *c* — chemical; *b* — ion etching)

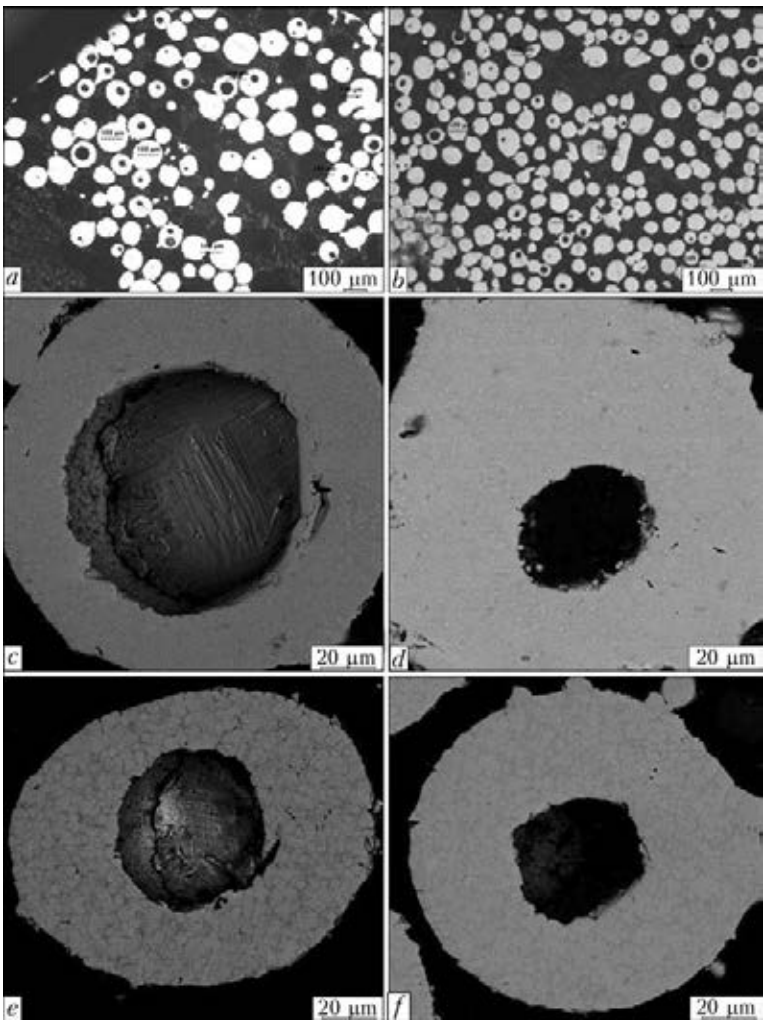

Figure 6. Microstructure of particles of nickel superalloy powder with micropores: *a–d* — powder from JS32-VI alloy; optical (*a*, *b*) and electron microscopy (*c*, *d*) data; *e* — powder from JS26-VI alloy; *f* — powder from JS6U-VI alloy

to described in [2, 10, 11] mechanism of micropore formation.

Metallographic analysis of samples taken from ten batches of filler powder from nickel and cobalt alloys, confirmed the fact of presence of micropores in them, irrespective of alloy grade or powder manufacturer. It is established that the content of inner micropores in the disperse filler rises significantly with increase of quantity of γ′-phase above 45–50 vol.% in the nickel alloy, and specific fraction of particles of more than 100–125 μm size in granulometric composition of used powder fraction. Quantitative characteristics of microporosity for batches of filler powder from JS32-VI alloy are given in Table 1.

Figures 7–9 show the change of quantitative characteristics of microporosity in the deposited metal depending on surfacing process technological parameters and quantitative characteristics of filler powder microporosity. It is established that in microplasma surfacing with I = const and powder feed G = 5 g/min, they depend on:

- quantitative content and size of micropores in the initial filler, decreasing to Π_{PD} = 0.01–0.026 vol.% at their lowering (Π_{MPP} = 2.13–4.51 % and F_{MPP}/N = 2.13–6.56 μm^2/pcs);
- welding current value, decreasing to Π_{PD} = = 0.03–0.06 vol.% at 45–65 A;
- concentration of powder feeding, weight of added powder microportions M_0 = 0.02–0.13 g, their feeding periodicity t_p = 0.5–2.5 s.

Minimum content of micropores in the deposited JS32 metal (Π_{PD} = 0.02–0.03 vol.%) is observed at reduction of weight of filler powder microportion to 0.02 g (see Figure 9).

To limit the quantity and size of micropores in the deposited metal at application of disperse filler containing a considerable quantity of micropores (for instance, Π_{PD} = 13.46 % and F_{MPP}/N = 48.02 μm^2/pcs), powder should be fed in small microportions ($M_0 \approx$ 0.02 g) with not more than 2.5 s periodicity. In this case containing the weld pool on a narrow substrate requires more precise metering of heat input into the item, in order to reduce base metal penetra-

Table 1. Microporosity characteristics of filler powder from JS32-VI alloy (by metallographic analysis data)

Fraction, μm (GOST 6613–86) Powder microporosity parameters	I batch	II batch		III batch	
	Π_{MPPf}, %	N_f/N, %	Π_{MPPf}, %	N_f/N, %	Π_{MPPf}, %
–63	0.19	31.66	0.73	29.74	0.65
63–80	–	19.92	3.71	32.09	10.66
80–100	–	19.73	5.02	28.94	16.07
100–125	–	19.19	8.44	8.02	37.03
125–160	–	8.51	52.17	1.96	30.10
Π_{MPP}, %	0.19	–	8.68	–	13.46
F_{MPP}/N, μm^2/pcs	7.57	–	36.37	–	48.02

Note. N_f/N — relative quantity of powder particles in the fraction; Π_{MPPf} — relative quantity of particles with micropores in the fraction.

tion depth. Such a principle of mode selection is essentially different from plasma-powder surfacing [16] or welding with additional disperse filler [22], where base metal penetration is limited by addition of considerable amounts of disperse filler to the weld pool.

Experimental data (see Figures 7–9) allow assuming that micropore formation in the deposited metal differs from the generally known mechanism of porosity formation in welds [1]. The most probable is the following mechanism of their formation. In microplasma arc column at currents below 35 A, heating of the majority of particles of 63 to 160 μm size to melting temperature T_{melt} is improbable [16]. Powder, including that with inner micropores, penetrates into weld pool in solid aggregate state ($T_{pore} < T_{melt}$). Further heating and melting of disperse particles in the weld pool requires considerable additional losses of thermal energy that causes violation of boundary condition of the third kind*. Energy store that can be spent for powder heating and melting is characterized by the magnitude of thermal energy of pool molten metal overheating and time of its staying in the liquid aggregate state. Disperse filler feeding lowers weld pool average temperature, and its maximum admissible quantity is limited [16, 22]. Powder particle inside the molten metal volume can be regarded as «thermally thin body»**. Time of its heating up to T_{melt} is directly proportional to its diameter and temperature difference $T_{melt} - T_{pore}$, and is inversely proportional to specific thermal energy falling to its surface [23].

Powder distribution at its addition to the weld pool follows a normal law [14], and time of pool metal existence in the molten state is limited [1]. Depending on the quantity of energy, obtained by each particle from overheated metal, five cases

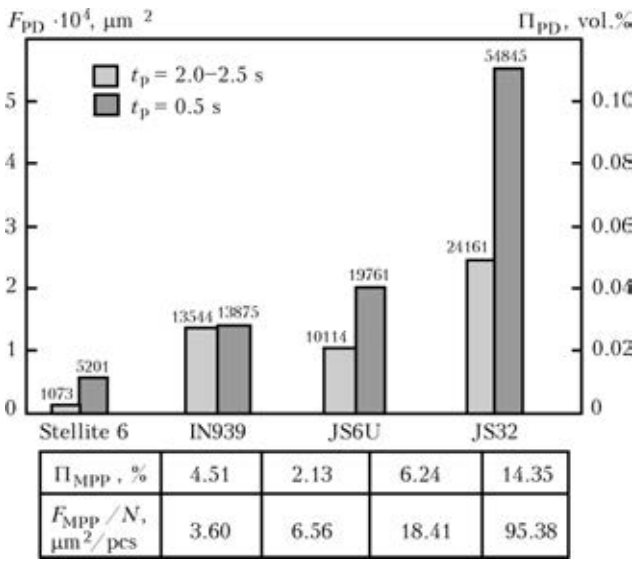

Figure 7. Influence of filler powder microporosity values on deposited metal microporosity characteristics for various alloys at I = 10–15 A

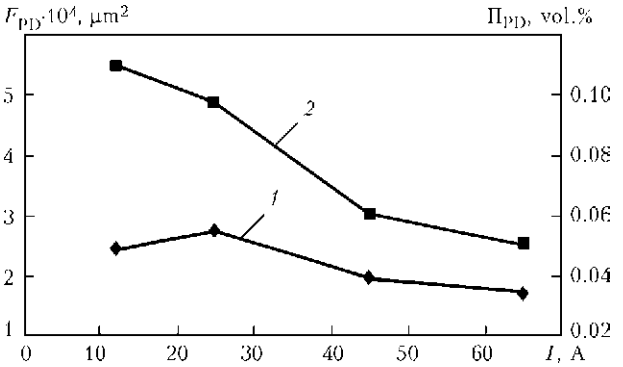

Figure 8. Influence of welding current on microporosity characteristics of JS32 deposited metal at different time periods between addition of powder microportions of weight M_0 = 0.12–0.14 g to weld pool: *1* — t_p = 2.0–2.5 s; *2* — 0.5 s (powder of JS32-VI alloy corresponds to III batch acc. to Table 1)

*Amount of thermal energy, arriving to its surface as a result of convective and radiation heat extcpange, equal to the amount of energy removed through heat conductivity [23].
**Bodies, in which temperature gradient arising in their section is negligibly small [23].

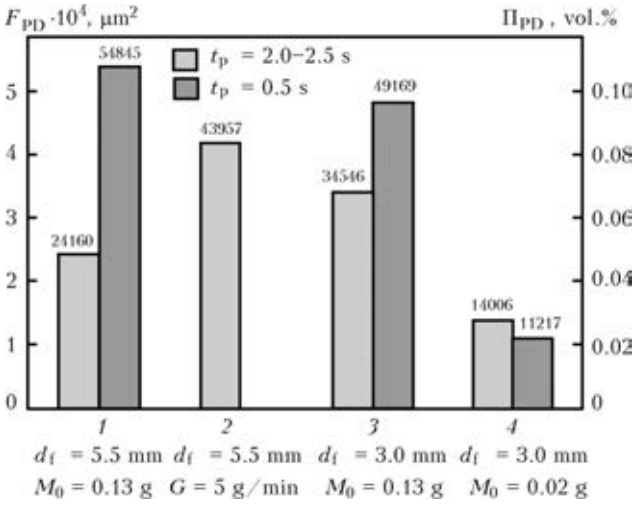

Figure 9. Influence of process parameters and kind of filler feed (*1*, *3*, *4* — portioned; *2* — continuous) on microporosity characteristics of JS32 deposited metal at I = 10–15 A (powder from JS32-VI alloy corresponds to III batch acc. to Table 1)

are possible at the moment of weld pool solidification (Figure 10). The last three of them lead to discontinuities in the deposited metal and then are visually observed at metallographic analysis (see Figure 5). At present it is not known, which process predominates at micropore formation in the deposited metal at the moment of its solidification in the weld pool:

• particle with inner micropore does not have enough time to heat up to T_{melt} and to melt;

• gas bubble released from inner discontinuity of filler particle does not have enough time to float to the surface and forms a micropore.

Porosity formation by the mechanism, different from the generally known one [1], is also observed in laser welding of austenitic stainless steels [24].

Proceeding from the established interrelation between microporosity in filler powder and in deposited metal, the following goals are urgent:

• development of simple and reliable methods of quantitative control of inner discontinuities in filler powders for microplasma powder surfacing;

• optimization of melt dispersion technology in production of nickel alloy powders with more than 45 vol.% of γ′-phase.

The following procedures can be promising for disperse filler control: metallographic analysis of powder particle cross-sections determining the area, quantity and parameters of statistical distribution of micropores depending on particle size, and evaluation of picnometric density and porosity of powder by hydrostatic weighing.

Preliminary evaluation of picnometric density of JS32-VI alloy powder showed that for disperse filler with a smaller quantity of porous particles its average value differs by not more than 4.6 % from alloy material density (Table 2).

Proceeding from the known features of nickel superalloy metallurgy in vacuum-induction melting [17, 19], increased content of oxygen and nitrogen in the initial billet or charge can have an additional influence of susceptibility to micropore formation in manufacture of the respective powders. First, during molten metal dispersion running of the reaction of interaction of oxygen with carbon (up to 0.15–0.18 wt.% content) with precipitation of gaseous oxide or dioxide is probable [17]. Secondly, at increased nitrogen content of 0.0024–0.0050 wt.% susceptibility of

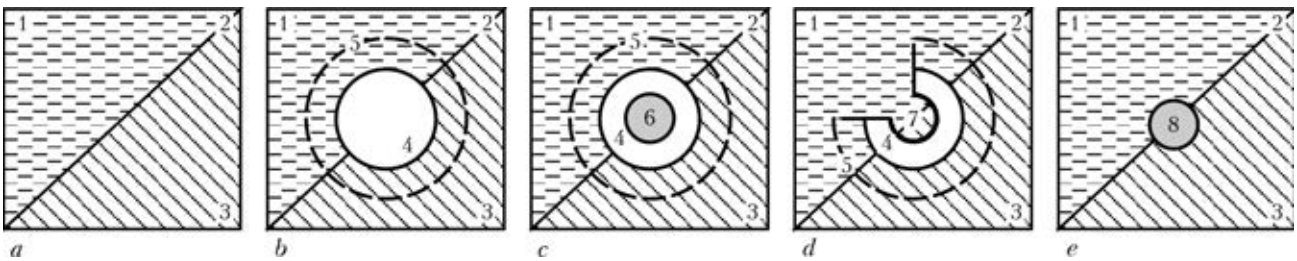

Figure 10. Schematics of possible states of powder particles at the moment of weld pool solidification: *a*, *e* — totally melted; *b* — unmolten particle without micropore; *c*, *d* — unmolten particle with micropore; 1 — molten metal; 2 — solidification front; 3 — solidified metal; 4 — powder particle; 5 — possible area of molten metal local overcooling and further local solidification from particle surface; 6 — closed micropore in particle; 7 — open micropore in particle; 8 — gas bubble released from molten particle with closed micropore

Table 2. Microporosity characteristics of filler powder from JS32-VI alloy (by hydrostatic weighing data)

Parameter	I batch	II batch	III batch
Powder picnometric density ρ_p, g/cm³	$8.489^{+0.1435}_{-0.1629}$	$8.3381^{+0.1285}_{-0.1394}$	$8.1547^{+0.4645}_{-0.3162}$
Porosity ρ, %	$3.097^{-1.3974}_{+2.0037}$	$4.5881^{-1.5910}_{+1.4677}$	$6.9098^{-5.3025}_{+3.6097}$
Alloy density Π_{wt} acc. to [25], ρ, g/cm³	8.76		
Alloy density ρ, g/cm³ (weighing of 75 × 45 × 3.5 mm ground plate)	8.79		

cast nickel alloys with single-crystal structure to microporosity formation is manifested [19].

Conclusions

1. Sound formation of deposited metal in microplasma powder surfacing on narrow substrate from nickel superalloys is ensured by limiting oxygen to less than 0.018 and of nitrogen to 0.0055 wt.% in it.

2. It is shown that active gas content in nickel superalloy gradually increases, as it goes through the cast billet or charge–disperse powder–deposited metal technological stages. It is necessary to control and limit their content after the first two processing stages so that the quantity of oxygen and nitrogen in the deposited metal did not exceed 0.018 and 0.0055 wt.%, respectively.

3. In filler powders for microplasma powder surfacing it is rational to have not more than 0.012 wt.% O and not more than 0.0025 wt.% N. At up to 0.002 wt.% gas content in the initial billet or charge, this is achieved by ingot dispersion by argon.

4. Formation of micropores of 5 to 75 μm size in the deposited metal is associated with presence of inner micropores of similar size in filler powder. It is established that microporosity in deposited metal depends on micropore content in initial powder, welding current, filler microportion weight, concentration and frequency of its addition to the weld pool. Minimum level of microporosity in deposited metal JS32 (0.02–0.03 vol.% in bead longitudinal section) is observed at lowering of fed filler powder microportion weight to 0.02 g.

5. The most probable is micropore transfer with disperse filler into weld pool through microplasma arc. In the pool at the moment of its metal solidification the particle with micropore either does not have enough time to melt, or after its melting the gas bubble does not have enough time to float to pool surface.

6. In-coming inspection of batches of nickel superalloy powders for micropore content in their particles is required. Promising control procedures are evaluation of picnometric density of disperse material and statistic metallographic analysis. It is established that the average picnometric density of filler powders with smaller micropore content deviates from alloy material density by not more than 4.6 %.

1. (1974) *Technology of electric fusion welding of metals and alloys*. Ed. by B.E. Paton. Moscow: Mashinostroenie.
2. Sims, C., Stolloff, N., Hagel, W. (1995) *Superalloys II: Heat-resistant materials for aerospace and industrial power plants*. Ed. by R.E. Shalin. Moscow: Metallurgiya.
3. Zinke, M., Neubert, G., Herold, H. (1999) Properties of welded joints of heat-resistant nickel-base alloys. *Avtomatich. Svarka*, **4**, 35–38.
4. Sorokin, L.I. (2004) Welding-up of cracks with oxidized surface on heat-resistant nickel alloys. *Svarochn. Proizvodstvo*, **12**, 30–31.
5. Sorokin, L.I., Lukin, V.I., Bagdasarov, Yu.S. (1997) Weldability of cast heat-resistant alloys of JS6 type. *Ibid*., **6**, 12–17.
6. Sorokin, L.I. (1999) Strains and cracks in welding and heat treatment of heat-resistant nickel alloys. *Ibid*., **12**, 11–17.
7. Yushchenko, K.A., Savchenko, V.S., Yarovitsyn, A.V. et al. (2010) Development of the technology for repair by microplasma powder cladding of flange platform faces of aircraft engine D18T high-pressure turbine blades. *The Paton Welding J*., **8**, 21–24.
8. (2010) Deloro Stellite technological seminar in Zaporozhie. *Ibid*., **1**, 59–62.
9. Yushchenko, K.A., Yarovitsyn, A.V., Zvyagintseva, A.V. (2008) Properties of microplasma powder welded joints on heat-resistant nickel alloys. *Ibid*., **9**, 2–5.
10. Ternovoj, Yu.F., Kudievsky, S.S., Pashetneva, N.N. (2005) *Engineering calculations of melted metal spraying processes*. Zaporozhie: Zaporozh. GIA.
11. Ternovoj, Yu.F., Baglyuk, S.A., Kudievsky, S.S. (2008) *Theoretical principles of metallic melt spraying*. Zaporozhie: Zaporozh. GIA.
12. Fedorenko, G.A., Shvedikov, V.M., Grishchenko, L.V. (1986) About reliability of methods for examination of jet shielding. *Svarochn. Proizvodstvo*, **6**, 35–37.
13. *GOST 17745–90*: Steels and alloys. Methods for determination of gases. Introd. 01.07.1991.
14. Yushchenko, K.A., Yarovitsyn, A.V., Yakovchuk, D.B. et al. (2013) Some techniques for reducing filler powder losses in microplasma cladding. *The Paton Welding J*., **9**, 30–36.
15. Bulanov, V.Ya., Kvater, L.I., Dolgal, T.V. et al. (1983) *Diagnostics of metallic powders*. Moscow: Nauka.
16. Gladky, P.V., Pereplyotchikov, E.F., Ryabtsev, I.A. (2007) *Plasma surfacing*. Kiev: Ekotekhnologiya.
17. Kablov, E.N. (2001) *Cast blades of gas turbine engines (alloys, technology, coatings)*. Moscow: MISIS.
18. Stroganov, G.B., Chepkin, V.M. (2000) *Cast heat-resistant alloys for gas turbines*. Moscow: ONTI MATI.
19. Kablov, D.E., Sidorov, V.V. (2012) Nitrogen in monocrystalline heat-resistant alloys. *Nauka i Obrazovanie*, **2**, 77-30569/339556 (electron. ed.).
20. Lysenko, N.A., Pedash, A.A., Kolomojtsev, A.G. et al. (2005) Improvement of structure and properties of nickel heat-resistant alloy ZMI3U-VI. *Visnyk Zaporizh. DTU*, **2**, 34–39.
21. Yarovitsyn, A.V.,Yushchenko, K.A., Nakonechny, A.A. et al. (2009) Peculiarities of low-amperage argon-arc and microplasma powder cladding on narrow substrate. *The Paton Welding J*., **6**, 31–35.
22. Ivochkin, I.I., Malyshev, B.D. (1981) *Submerged-arc welding with additional filler metal*. Moscow: Strojizdat.
23. Lykov, A.V. (1967) *Theory of heat conductivity*. Moscow: Vysshaya Shkola.
24. Katayama, S. (2001) Mechanism of formation of different defects in laser welding and methods of their prevention. *J. JWS*, 19(**1**), 213–218.
25. Sharova, N.A., Tikhomirova, E.A., Barabash, A.L. et al. (2009) To problem of choice of new heat-resistant nickel alloys for prospective aircraft gas-turbine engines. *Vestnik Samara GAU*, **3**, 249–255.

Received 30.04.2014

APPLICATION OF PULSE ATOMIZING JET IN ELECTRIC ARC METALLIZING

V.A. ROYANOV[1] and **V.I. BOBIKOV**[2]
[1]Priasovsky State Technical University
7 Universitetskaya Str., 87500, Mariupol, Donetsk region, Ukraine. E-mail: royanov@pstu.ed
[2]Company «Azovobshchemash»
1 Mashinostroitelej Str., 87535, Mariupol, Donetsk region, Ukraine. E-mail: voffka-008@mail.ru

The paper presents the results of investigation of pulse atomizing air jet application in electric arc metallizing. To ensure the pulsed mode, the respective device was developed allowing control of outflowing of a jet with frequency within 0–130 Hz. Oscillograms of variation of dynamic pressure are given. Dependence of pulse atomizing air jet on frequency of closing the spray gun nozzle channel is shown. Coating microstructures are given. Influence of pulsation frequency on composition of coatings spray-deposited with PP-MM-2 wire is shown. 15 Ref., 6 Figures.

Keywords: *arc metallizing, pulsed mode, atomizing air jet, spray gun nozzle channel, coating microstructure, outflow, stationary discontinuity, jet dynamic pressure*

Electric arc metallizing is one of the methods of deposition of thermal spray coatings and features high efficiency, and quite cost-effective and readily realized process of coating spray-deposition. It is known that during metallizing process liquid metal of molten electrode tips is directed by the atomizing air jet onto the item [1, 2]. Quality of produced coatings depends on the quantity of oxygen, dissolved in particle metal. Data given in [3–8] show that during metallizing an intensive chemical interaction of atomizing air jet with the material being sprayed takes place, leading to a considerable burning out of alloying elements. Oxidation intensity increases with increase of parameters, such as compressed air pressure and distance from apparatus nozzle to item being coated, that has a negative influence on coating mechanical properties. Degree of oxidizing reaction depends on spray material oxidation resistance, particle dispersity, component affinity to oxygen. Quantitative evaluation of the degree of oxidation of the components of spray electrode material is given in [5–7].

In order to lower the oxidizing action of atomizing jet on liquid metal of consumable electrode tips, it is proposed to apply a pulse atomizing air jet. To solve the defined task, it was necessary to develop an appropriate device.

Earlier publications [9–12] gave examples of improvement of arc spray gun design by application of inserts and devices to provide pulsation of atomizing air jet. They, however, turned out to be unacceptable in view of their complicated design and inertia in operation.

The Chair of Welding Production Equipment and Technology of Priazovsky State Technical University developed the method of electric arc metallizing with application of pulse atomizing air jet. Investigations were conducted with stationary arc spray gun EM-17 with a device providing pulsed mode of atomizing jet outflow.

In terms of design, the pulse device (further on referred to as pulser) is a cylindrical case with input and output nipples for compressed air input and output, inside which a shaft with an opening

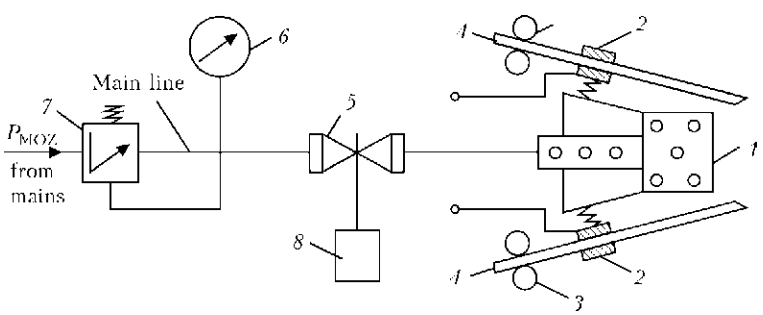

Figure 1. Schematic of head for pulse atomization: *1* — atomizing nozzle; *2* — current conduits; *3* — rollers; *4* — electrode material; *5* — pulser; *6* — pressure gage; *7* — pressure reducer; *8* — electric motor

and rotation capability is mounted. The device is mounted coaxially with spray gun nozzle channel before the spray nozzle. Rotation of the shaft with an opening leads to periodical closure of compressed air feeding along the channel of spray gun nozzle to spray nozzle, thus providing the pulsed mode of outflow. Pulser provided pulsed mode of spray jet outflow in the range of 0–130 Hz. Schematic of the developed pulse spray head is shown in Figure 1.

During development of the device, effectiveness of jet dynamic pressure and pulse shape depending on spray gun channel flow section was studied. Experimental measurements of pulse shape and dynamic pressure, depending on frequency, were performed by the method of atomizing jet impact on a metal plate, on which the strain gauge was mounted (Figure 2). Signals from the strain gauge were recorded by an oscillograph.

The given oscillograms show that the atomizing jet is of a pulsed nature with time intervals. As shown by investigations, application of different flow sections of nozzle channel allows changing also the nature of rise of the pulse proper. So, at application of a round section the pulse has a smoothly rising shape (Figure 2, *a*, *b*). A common feature of the sinusoidal and rectangular shape of closure (Figure 2, *c*, *d*) is presence of a pause in atomizing, required for liquid metal formation at electrode tip. Furtheron, investigations with rectangular pulse shape were performed.

Investigation of dependence of the nature of pulse atomizing air jet on nozzle flow channel was performed by the shadow method. Gas spectrograph of the gas jet without pulsing (Figure 3, *a*) is characterized by a nonstationary spatially non-uniform gas formation [13]. All the jet areas are in oscillatory motion relative to the geometrical axis of the nozzle, from which it flows. A

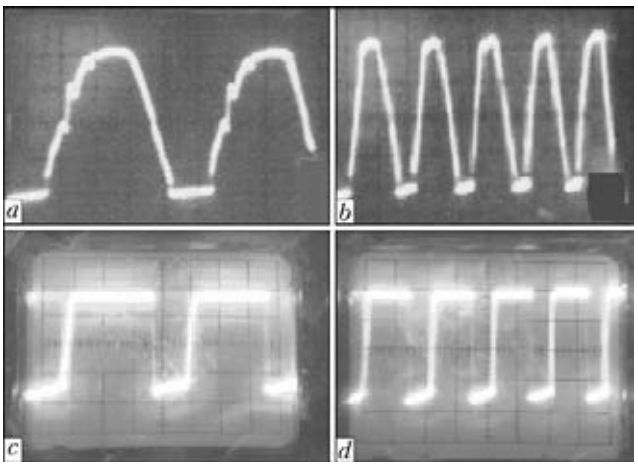

Figure 2. Change of jet dynamic pressure depending on applied flow section of the nozzle with pulsation frequency of 30 (*a*), 65 (*b*), 40 (*c*) and 75 (*d*) Hz

barrel-shaped wave structure of the initial and transition areas is observed with saw-like pressure distribution along the jet axis. Rarefaction flow in the form of a concentrated wave forms at the nozzle edge.

Atomizing jet with air flow pulsation (Figure 3, *b*–*d*) also is a non-uniform gas formation, having a different form, however.

So, at pulse frequency of 25 Hz (see Figure 3, *b*) the gas jet, when leaving the nozzle, forms a centered cone-shaped zone limited by rarefaction waves. At frequencies of 56 and 85 Hz (Figure 3, *c*, *d*) all the jet areas make oscillatory motions. Rarefaction waves, which are accompanied by shock waves, barrel-shaped wave structure of the initial and transition areas with saw-like pressure distribution along the jet axis, are observed. An area of stationary discontinuity of the gas jet is found between the waves. At the frequency of 85 Hz increase of the number of stationary discontinuity areas with pressure gradients is observed.

Coating properties were studied on samples made by electric arc metallizing at different fre-

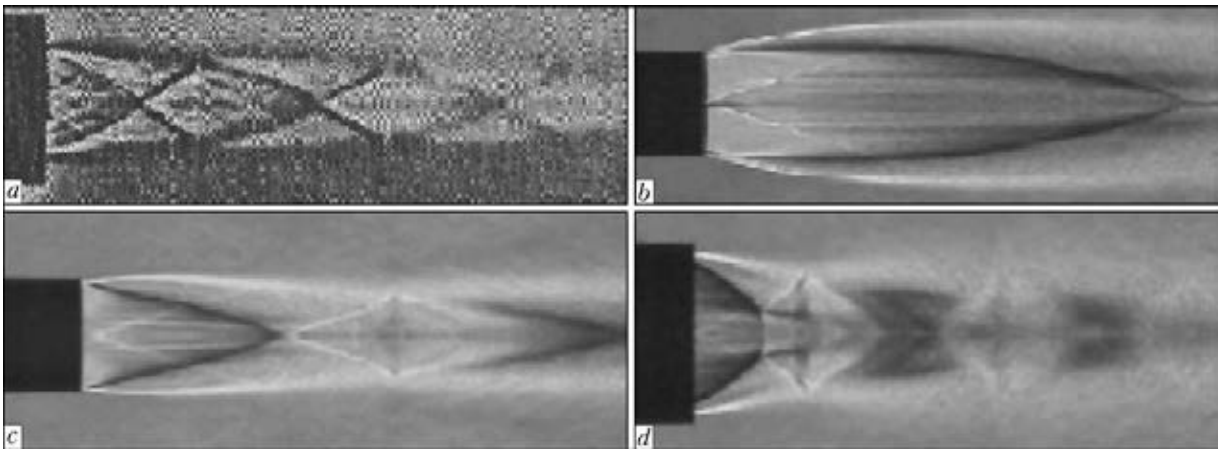

Figure 3. Gas spectrographs of gas jets without pulsation (*a*) and with pulsation frequency of 25 (*b*), 56 (*c*) and 85 (*d*) Hz

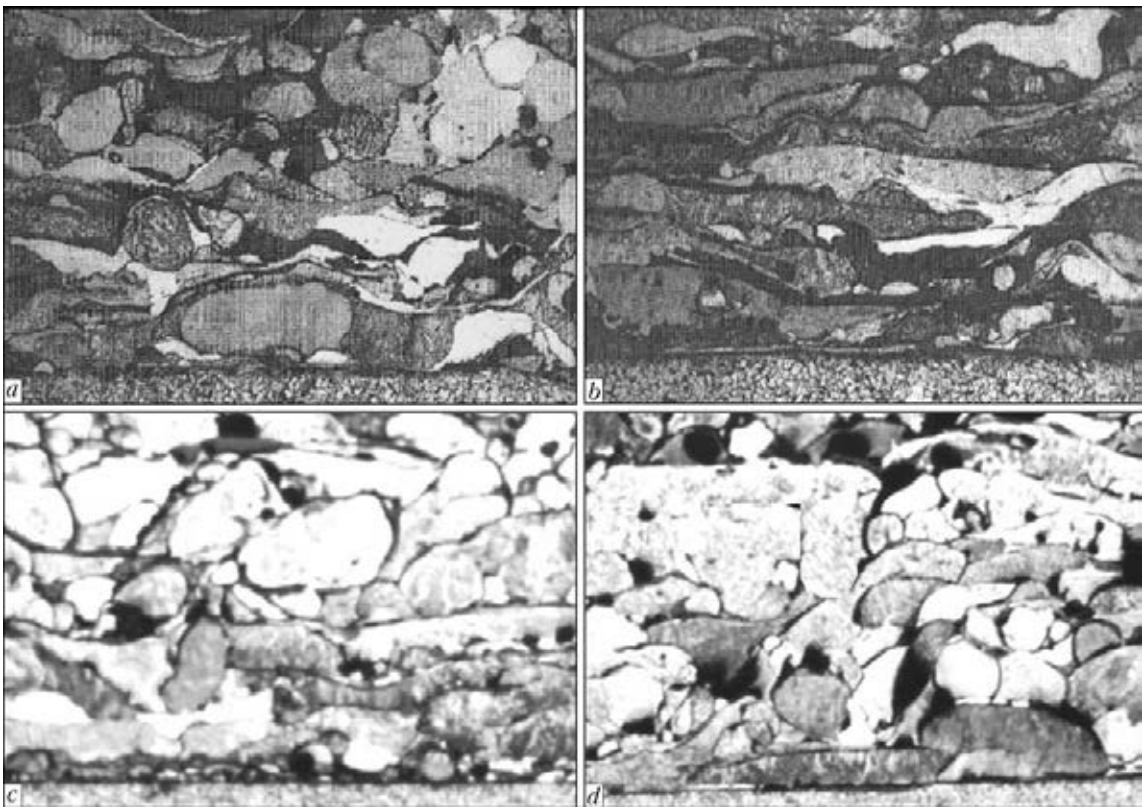

Figure 4. Microstructure (×75) of coatings produced without pulsation (*a*) and with jet pulsation frequency of 43 (*b*), 65 (*c*) and 105 (*d*) Hz

quencies of atomizing air jet. 09G2S steel in the form of plates of 75 × 35 × 5 mm size was used as base material. Before metallizing the samples were degreased with benzene and subjected to sandblasting by corundum with subsequent cleaning by compressed air (to remove dust). Metallizing was conducted using arc spray gun EM-17 with the developed device in the following modes: at pressure P = 0.55 MPa, current I = 210–230 A, voltage U = 30–32 V, and wire feed rate v = 4.8–5.4 m/min. Nozzle of diameter $d = 7 \cdot 10^{-3}$ m^2 was used for atomizing. Distance to sprayed sample was 120 mm. Power was supplied to the arc from VDU-506 source.

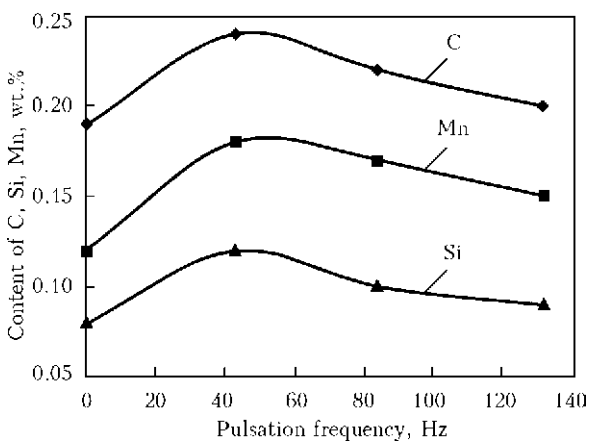

Figure 5. Influence of pulse frequency on C, Mn and Si content in the coating at metallizing with PP-MM-2 wire

Microstructure of coatings, produced at different frequency of pulse atomizing air jet using flux-cored wire PP-MM-2 [14] is shown in Figure 4.

Microstructure, thickness and porosity of coatings were studied in electron optical microscope Zeiss-200M. Structure of produced coatings corresponds to the data given in [5, 7, 8, 15], where the coating consists of individual deformed particles located in layers. Boundaries from oxide films are observed between the particles and layers, and there is a boundary layer between the base and coating.

Without pulsation coating structure is nonuniform, with a large quantity of particles of different shape (see Figure 4, *a*). Particles of spherical shape, not broken up by air pressure into finer ones, are noted. Most of the particles have an elongated deformed shape. Presence of oxide films is noted. At application of a pulse jet the coatings have a more uniform microstructure. Quantity of particles of different size decreases. At pulsation frequency of 43 Hz, coating structure is uniform across the entire thickness that is indicative of process stability. All the particles are subjected to considerable plastic deformation (see Figure 4, *b*). The transition zone has oxide films, but to a smaller degree, compared to structure of coating made without pulsation. Average particle size is within 100–450 μm.

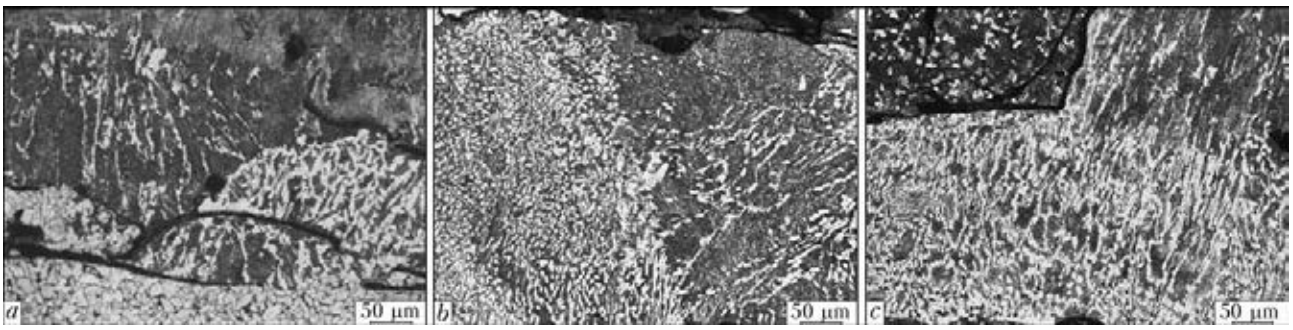

Figure 6. Microstructure of particles, in which oxide film breaking up occurred on the boundary of particles with base (*a*, *c*) and between particles (*b*)

At 65 Hz frequency, an increase of the number of small-sized particles is noted alongside coarse ones (see Figure 4, *c*). Average particle size varies within 50–350 μm. This is attributable to the fact that the interval in repetition of atomizing jet pulses is shorter, compared to particles produced at the frequency of 43 Hz. The rate of electrode melting and formation of liquid metal at the tip has longer time than the time interval in repetition of atomizing air jet pulses at this frequency, that increases the force of liquid metal throwing off electrode tips by the atomizing flow force. At 105 Hz frequency no significant change in particle sizes was noted. Presence of an interval in atomizing jet pulse repetition is of little importance, compared to the time required for liquid metal formation at consumable electrode tips. The force of impact of atomizing flow on liquid metal becomes practically constant.

During research performance variable data on composition of coatings sprayed on samples with application of various frequencies of atomizing pulses were obtained (Figure 5). Difference in chemical element content is attributable to different degrees of oxidizing medium impact on the material being sprayed.

Microstructures of particles, in which oxide film breaking up on the boundaries took place, are an illustration of lowering of oxidizing impact on atomized material (Figure 6).

A test sample was developed of a head for metallizing in the pulsed mode, mounted on a lathe, in order to restore the seats of metallurgical equipment parts in mechanical shop of «Azovstal» Works.

Conclusions

1. A device was developed providing pulsed atomizing mode with rectangular pulses in frequency range of 0–132 Hz.

2. Application of pulse atomization allows stabilizing coating composition.

3. At metallizing with PP-MM-2 wire optimum pulse frequency is equal to 35–60 Hz.

1. Korobov, Yu.S. (2004) Estimation of forces affecting spray metal in electric arc metallizing. *The Paton Welding J.*, **7**, 21–25.
2. Royanov, V.A. (1990) Melting of electrodes in electric arc metallizing. *Svarochn. Proizvodstvo*, **2**, 35–37.
3. Borisov, Yu.S., Vigilanskaya, N.V., Demianov, I.A. et al. (2013) Investigation of dispersion of dissimilar wire materials during electric arc metallizing. *The Paton Welding J.*, **2**, 24–30.
4. Korobov, Yu.S., Boronenkov, V.N. (2003) Kinetics of interaction of sprayed metal with oxygen in electric arc metallizing. *Svarochn. Proizvodstvo*, **7**, 30–36.
5. Hasui, A. (1975) *Technique of metallizing*. Moscow: Mashinostroenie.
6. Konstantinov, V.M., Gubanov, A.S. (2007) Effect of alloying elements of steel wire on structure and properties of coatings in electric arc metallizing. *Svarochn. Proizvodstvo*, **5**, 13–18.
7. Boronenkov, V.N., Korobov, Yu.S. (2012) *Principles of electric arc metallizing. Physical-chemical principles*. Ekaterinburg: UralSU.
8. Katz, N.V. (1966) *Spray coating*. Moscow: Mashinostroenie.
9. Ter-Danielian, B.I., Krasnichenko, L.V. (1983) New spray head of arc spray gun. *Svarochn. Proizvodstvo*, **12**, 30–32.
10. Buryakin, A.V. (2000) Stationary arc spray gun EM-19. *Ibid.*, **9**, 35–36.
11. Royanov, V.A., Mosienko, G.A., Semyonov, V.P. et al. *Atomizing spray head*. USSR author's cert. 1787049. Int. Cl. B 05 B 7/22. Fil. 22.11.89. Publ. 07.01.93.
12. Borisov, Yu.S., Ilienko, A.G., Astakhov, E.A. et al. *Device for arc metallizing*. USSR author's cert. 1727923. Int. Cl. B 05 B 7/22. Fil. 26.06.89. Publ. 23.04.92.
13. Ginzburg, A.P. (1968) *Aerogasdynamics*. Moscow: Vysshaya Shkola.
14. Royanov, V.A., Tsygankov, S.A., Bogoslovsky, A.S. (1990) Flux-cored wire for deposition of wear-resistant coatings by arc spaying. In: *Transact. of TsNIIT-MASh*, 25–26.
15. Kudinov, V.V., Bobrov, G.V. (1992) *Metallizing of coatings. Theory, technology and equipment*: Manual for inst. of higher education. Moscow: Metallurgiya.

Received 05.05.2014

DEVELOPMENT OF HIGH-VANADIUM ALLOY FOR PLASMA-POWDER SURFACING OF KNIVES FOR CUTTING OF NON-METALLIC MATERIALS

E.F. PEREPLYOTCHIKOV
E.O. Paton Electric Welding Institute, NASU
11 Bozhenko Str., 03680, Kiev, Ukraine. E-mail: office@paton.kiev.ua

The results of investigations of structure, hardness and wear resistance of iron-based alloys containing up to 4.5 % C and 15 % V are given. The dependence of structure and type of carbides on chemical composition of these alloys was studied. The analysis of effect of structure on wear resistance at abrasive wear of deposited metal, close by its composition to the investigated alloys, in initial state and after heat treatment was made. It was established that deposited metal of this type has a high wear resistance due to formation of martensite structure with small amount of residual austenite and with disperse, uniformly distributed carbides of vanadium and carbides of $Me_{23}C_6$ type. 6 Ref., 1 Table, 3 Figures.

Keywords: *plasma-powder surfacing, wear resistance, dilatometric analysis, powders for surfacing, high-vanadium alloys*

At the present time for saving of expensive tool steels in manufacture of different tools, including knives for cold and hot cutting of different materials, surfacing is very widely applied. In this case the body of a tool is manufactured of relatively chip structural steel and its working edges or working surfaces are manufactured of a tool steel.

The basic alloying elements for tool steels and alloys are tungsten, molybdenum and chromium, which form comparatively coarse (up to 50 μm) carbides during surfacing, thus leading to crumbling of working edges of knives. Due to this reason thin-blade tool is manufactured either of highly-deformed steels, carbide net of which was fractured in the process of forging and rolling, or of powder tool steels, the technology of production of which excludes the possibility of formation of coarse-grain structures and carbide heterogeneity. In this connection, when selecting the system for deposited metal alloying, the preference is given to vanadium, which forms very tiny and solid carbides [1–3]. The obstacle for application of vanadium as an alloying element in electrode and filler materials for arc surfacing is its capability to form spinels, which complicates the removal of slag crust. Due to this reason the mass fraction of vanadium in flux-cored wires for arc surfacing of tool steels is restricted to 0.5 % [2]. The wider capabilities for alloying the deposited metal with vanadium are opened in using plasma-powder surfacing (PPS) in inert shielding gases.

To create the principally new class of surfacing materials for knives of cold cutting of non-metallic materials the alloys based on iron in the form of powders with calculated mass fracture of vanadium of up to 20 % and carbon up to 4.5 % were investigated. The powders for surfacing were manufactured by spraying of liquid melt using nitrogen.

It is very important for tool steels to select the optimal ratio of concentrations of carbon and carbide-forming elements. Depending on the stoichiometric composition of the forming carbides for each percent of vanadium in steel 0.175 (V_4C_3), 0.196 (V_6C_5) or 0.236 % C (VC) is required. To provide the best combination of properties of alloy it is desirable that the ratio of vanadium to carbon in it was within the limits of 3.5–4.0 [4]. At the presence of other carbide-forming elements in steel the content of carbon should be sufficient to form the appropriate carbides and strengthening of matrix. Taking this into consideration the alloys were selected for investigations, the chemical composition of which is given in the Table.

Except of participation in carbides formation the chromium and molybdenum impart the tendency of alloys to hardening and provide obtaining of martensite base. Chromium at the content of about 15 % should also provide anticorrosion properties of alloys.

Alloys 4 and 5 were alloyed using nickel. It was expected that it would result in formation of austenite in their structure. Moreover, alloy 5 was alloyed using niobium, thus providing the possibility to carry out evaluation of properties of alloy in use of one more strong carbide-former.

Chemical composition, hardness and wear of investigated iron-based high-carbon high-vanadium alloys

Number of alloy	Mass fraction of elements, %							Hardness *HRC*	Loss of mass, mg
	C	Mn	Si	Cr	V	Mo	Ni		
1	3.95	0.91	1.07	16.76	14.15	2.03	–	45–48	12.30
2	4.25	1.76	1.43	16.72	15.18	1.97	–	50–54	5.05
3	4.38	1.11	1.05	16.65	14.62	2.01	–	60–62	4.40
4	4.45	1.01	0.64	16.03	14.66	2.00	1.08	60–62	4.60
5*	4.68	1.00	0.80	14.15	14.91	2.10	1.30	55–59	5.42

*Content of niobium amounts to 1.05 %.

Considering the fact that pilot alloys were supposed to be used for manufacture of bimetallic knives of different purpose, the hardness, wear resistance and structure of deposited metal with chemical composition, corresponding to the pilot alloys, were investigated.

Initially the investigation of welding and technological properties of high-carbon high-vanadium alloys was carried out. The surfacing was carried out using plasma-powder method, as the base metal the plates of steel St3 were used. Edge preparation for surfacing was made in them, the sizes of which corresponded to the sizes on the real tool for cutting of non-metallic materials. The most important parameters of PPS are the arc current I_a, speed of surfacing v_s and rate of powder feed [5]. In the experiments I_a = 140–280 A and v_s = 2.0–5.3 m/h were used. In the investigated range of condition parameters fraction of base metal in the deposited metal is varied from 0 to 25 %. In the region of low values of current the increase by 10 A results in increase of fraction of base metal in the deposited metal by 2–5 %.

In general the composition of deposited metal is differed from the composition of filler (electrode) metal due to its stirring with the base metal and also oxidation or selective evaporation of alloying elements [6]. In PPS according to the optimal modes the fraction of base metal in the deposited layer does not exceed 5–8 %, weld pool is reliably protected from oxidation by argon, and there are no easily-evaporating elements in the composition of investigated alloys. In connection with that the composition of deposited metal almost corresponds to the composition of powder [5].

The optimal I_a values at different deposition rates provide a good formation and constant width and height of beads. Though PPS using high-carbon high-vanadium alloys was carried out without preheating, there was not noticed a single case of crack and pore formation in the deposited metal.

For evaluation of wear resistance of high-vanadium alloys the methods of tests for wear using fixed abrasive were selected. As an abrasive the corundum skin with grain size of 180 μm was used, the area of friction amounted to 1 cm^2, pressure was 30 N, test time was 20 s. Evaluation of wear resistance was carried out according to the loss of mass of tested specimens.

The specimens for metallographic tests were cut out of deposited metal and subjected to etching in the Murakami reagent.

The specimens of the size 3 × 3 × 25 mm for dilatometric investigations were manufactured of metal deposited by powders of selected alloys using plasma method. In the Shevenar dilatometer the specimens were heated at the rate of 2.5 °C/min to 430, 630 and 1045 °C, subjected to holding for 2 h at these temperatures and then cooled at the rate of 40 °C/ min. In quick-response dilatometer during simulation of thermal cycle of surfacing the specimens were heated to 1150 °C at the rate of 130 °C/s and cooled at the rate of 7.5 °C/s without the holding.

In the Table the results of tests on wear resistance of alloys deposited at the optimal modes are also presented. It should be noted for comparison that in the widely known tool steel R6M5F2 tested under the same conditions, the loss of mass amounted to 19.2 and in the solid alloy of the VK8 type — 1.6 mg. As is seen from the given data, high-carbon high-vanadium alloys occupy as to the wear resistance an intermediate position between tool steels and solid alloys but they are considerably cheaper than the latter ones.

It was found, that alloys 1 and 2 have the lowest hardness (*HRC* 45–54). In the process of tempering at 600 °C during 1 h it is increased to *HRC* 59, obviously, due to precipitation of carbides and decay of residual austenite with formation of martensite. Alloys 3 and 4 have the maximum hardness after surfacing (*HRC* 60–62). After tempering at up to 550 °C the hardness of these alloys is almost retained at the initial

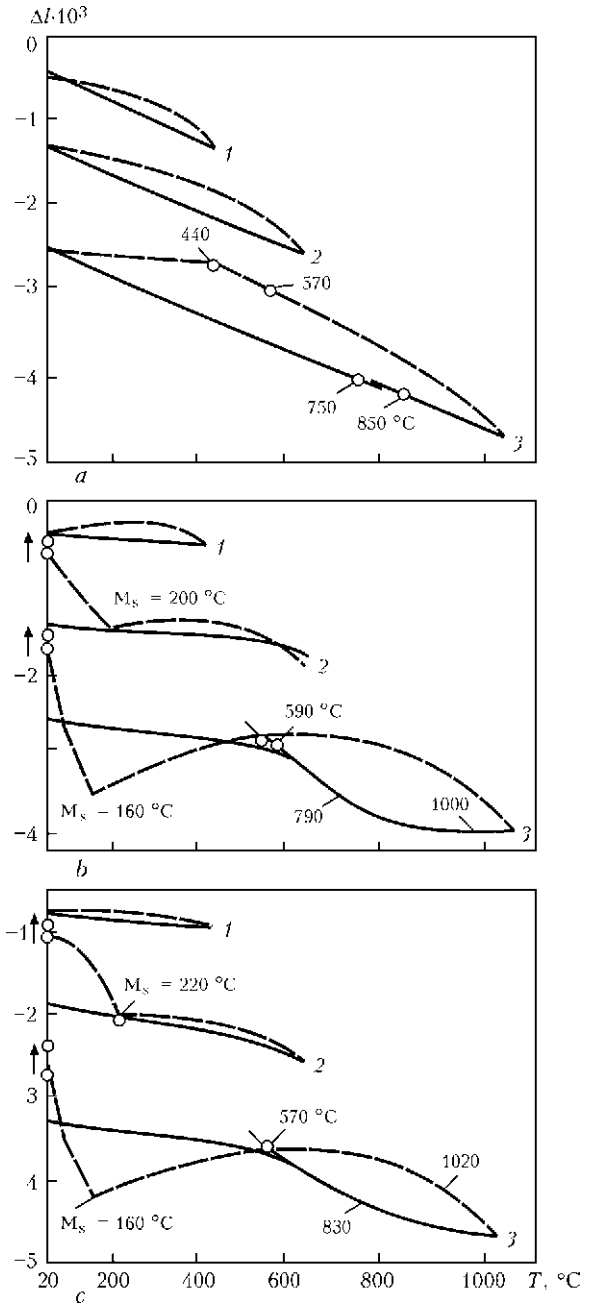

Figure 1. Curves of heating to different temperatures with 2 h holding (*solid lines*) and subsequent cooling (*dash*) of alloys 1 (*a*), 3 (*b*) and 5 (*c*) in Shevenar dilatometer: *1* — temperature of heating 430; *2* — 630; *3* — 1045 °C; Δl — change in length

level. At higher temperature of tempering it starts decreasing.

As is seen from Figure 1, *a*, it is characteristic for alloy 1 to preserve the structure stability at heating up to 1045 °C and subsequent cooling. It should be noted that in the range of 750–850 °C the possible dissolution of carbide particles in matrix α-phase is occurred, and in cooling (570–440 °C) obviously bainite transformation is observed.

Dilatometric curves of alloys 3 and 5 had the other character (Figures 1, *b*, *c*). The curves of heating to 430 °C of both alloys are slightly in-

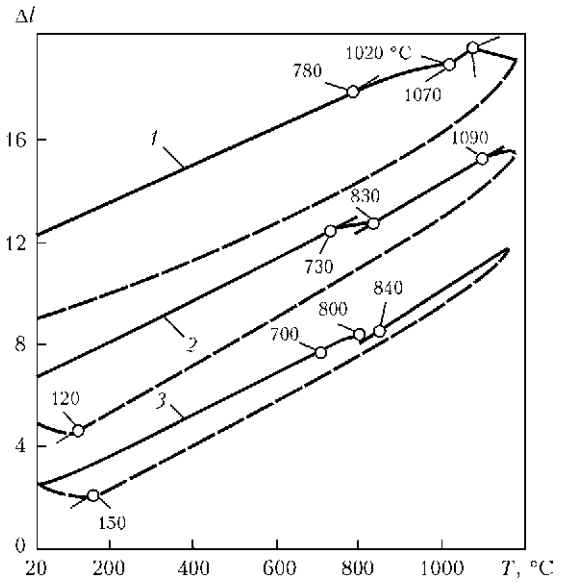

Figure 2. Curves of heating (*solid lines*) and cooling (*dash*) of alloys 1, 3, 5 (*1–3*) in quick-response dilatometer

clined downwards and fully convertible. The increase in temperature of tempering to 630 °C results in a small decrease in length of specimen in the process of 2-hour holding, which is connected with precipitation of carbides. During cooling the residual austenite is transformed into martensite (M_s = 200–220 °C). Martensite transformation is continued in both alloys during holding at room temperature (see arrows in Figure 1, *b*, *c*). The character of curves of heating to 1045 °C and cooling from this temperature for alloys 3 and 5 is almost the same. In the range of temperatures 790–1000 °C (alloy 3) and 830–1020 °C (alloy 5) the structure of alloys is relatively stable. When temperatures are higher the dissolution of carbides in austenite occurs and this process is running with increase in length. During cooling of specimens from 1045 °C martensite transformation (M_s = 160 °C) occurs in both alloys, which is continued in the process of holding at room temperature, the same as at lower temperatures. The inclination of curves for specimens 3 and 5 corresponds to the mixed α + + γ-structure. In these alloys the nature of α-phase is martensite, the structure of matrix is composed of mixture of martensite and residual austenite.

Figure 2 shows dilatometric curves of heating and cooling of alloys 1, 3 and 5 obtained in quick-response dilatometer at simulation of thermal cycle of surfacing. In specimen 1 during heating in the range of 670–880 °C small increase in length occurs, possibly, connected with dissolution of carbides. In cooling the monotonous decrease in length without any transformations takes place. At the curve of heating of specimen 3 the inflection at 730–830 °C was noted connected with α + γ-transformation. In the process of cooling

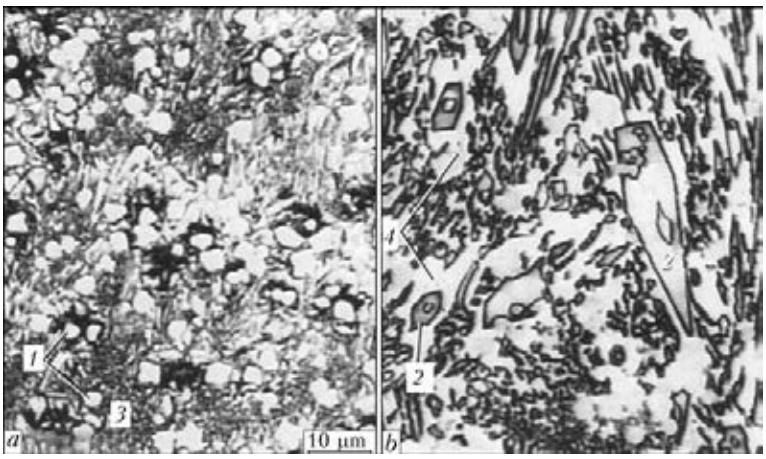

Figure 3. Microstructure (×1000) of high-carbon high-vanadium alloys 2 (*a*) and 3 (*b*): *1* — vanadium carbide; *2* — Me_7C_3 carbide; *3* — martensite-austenite structure with domination of martensite; *4* — martensite-austenite structure with domination of austenite

the martensite transformation (M_s = 120 °C) is observed. The curve of alloy 5 has the similar character: α + γ-transformation occurs at 700–840 °C, M_s = 150 °C. Obviously, the process of carbides precipitation influences the α + γ-transformation in both cases. The M_s points obtained in two types of dilatometers are somewhat differed from each other, which is possibly connected with deviations in chemical composition of specimens of the deposited metal and also peculiarities of methods of investigations in these dilatometers.

Investigations in quick-response dilatometer show that at thermal cycle of plasma surfacing without additional heat treatment of high-vanadium high-carbon alloys can acquire the most favorable martensite-carbide structure with a small amount of residual austenite, from the point of view of wear resistance. The direct investigations of microstructure proved the conclusions of dilatometric investigations that the matrix of alloy 3 has martensite structure with some amount of residual austenite. Carbides of vanadium of the MeC type and chromium carbides of the $Me_{23}C_6$ type are uniformly distributed in the structure of alloy and their size does not exceed 10 μm (Figure 3, *a*). Alloy 5 has also martensite-austenite structure but, as a result of increased carbon content in it, large acicular chromium carbides of the type Me_7C_3 are formed, except of carbides of vanadium and niobium of the type MeC (Figure 3, *b*). Measurements of microhardness ($HV0.05$) of structure components of the investigated alloys showed that hardness of carbides of the type MeC amounts to 2900–3000, carbides of the type Me_7C_3 — 900–1300, martensite — 800–900, austenite — 600–700, and ferrite has hardness of $HV0.05$ = 550–600.

Alloys 3 and 5 showed almost the same wear resistance at abrasive wear, however in alloy 5 chromium carbides have considerable sizes, therefore, alloy 3 will be more preferable for surfacing of knives.

Conclusions

1. It was established that depending on chemical composition the matrix of high-carbon high-vanadium alloys can be composed of combination of different structure components: martensite, austenite or alloyed ferrite. Besides, in the structure of alloys the considerable amount of carbides of basic alloying elements, such as vanadium and chromium, is contained. The highest wear resistance at abrasive wear is provided by martensite-carbide structure with small amount of residual austenite.

2. Thermal cycle of plasma surfacing without additional heat treatment provides obtaining the most favorable martensite-carbide structure with small amount of residual austenite in high-vanadium high-carbon deposited metal, from the point of view of wear resistance.

1. Goudremont, E. (1966) *Special steels*. Vol. 2. Moscow: Metallurgiya.
2. Efimov, Yu.V., Baron, V.V., Savitsky, E.M. (1969) *Vanadium and its alloys*. Moscow: Nauka.
3. Livshits, L.S., Grinberg, N.A., Kurkumelli, E.G. (1969) *Principles of alloying of deposited metal*. Moscow: Mashinostroenie.
4. Meskin, V.S. (1964) *Principles of alloying of steel*. Moscow: Metallurgiya.
5. Gladky, P.V., Pereplyotchikov, E.F., Ryabtsev, I.A. (2007) *Plasma surfacing*. Kiev: Ekotekhnologiya.
6. Ryabtsev, I.A., Kondratiev, I.A. (1999) *Mechanized electric arc surfacing of metallurgical equipment parts*. Kiev: Ekotekhnologiya.

Received 26.03.2014

MATERIALS FOR STRENGTHENING OF GAS TURBINE BLADES

A.M. KOSTIN[1], **A.Yu. BUTENKO**[1] and **V.V. KVASNITSKY**[2]
[1]Adm. S.O. Makarov National Shipbuilding University
9 Geroev Stalingrada Ave., 54025, Nikolaev, Ukraine. E-mail: kostin.weld@gmail.com
[2]NTTU «Kiev Polytechnic Institute»
6/2 Dashavskaya Str., 03056, Kiev, Ukraine

The advantages and disadvantages of existing technologies for strengthening the contact surfaces of working blades of gas turbines applying cast rods of stellite, nickel alloy KBNKhL-2 and plates of alloy KhTN-61 were studied. The necessity of development of new wear-resistant material for strengthening the shroud platforms of working blades was grounded. Two pilot alloys on the cobalt base of Co–Si–B and Co–Si–B–Cr_3C_2 systems were investigated. The high temperature wear resistance of materials was evaluated. 3 Tables, 1 Figure.

Keywords: *surfacing, blades of gas turbines, strengthening technology, stellite, nickel alloy, cobalt-based alloy, high temperature wear resistance*

At the present day the main problem in production of working blades of modern gas turbine engines (GTE) is providing their high wear and heat resistance, which would provide the required characteristics of contact surfaces of the working blades in the whole temperature range of their operation.

In the work the working blades are considered, manufactured of cast nickel alloys of the type ChS88U-VI, the operation characteristics of which are not high, therefore, there is necessity in strengthening the contact surfaces (shroud platforms) of working blades using materials corresponding to the criteria of engines operation.

At the enterprises manufacturing GTE, to provide the contact surfaces of working blades with the necessary properties, in particular, hot hardness and wear resistance, different compositions and methods of strengthening are applied. For example, the method of manual argon arc surfacing using cast rods of Co-based stellite of grade Pr-V3K-r of 2–3 mm diameter is well-known. This stellite is characterized by high hardness, wear and corrosion resistance. However the considered technology has a number of significant disadvantages:

• alloys ChS88U-VI, ChS70U-VI and ChS104-VI have a poor weldability, and in this connection in electric arc surfacing the cracks are formed transferred to base metal. Stellite Pr-V3K-r and the given nickel alloys have different coefficients of linear thermal expansion, that results in appearance of the complex fields of natural stresses during cooling of a deposited part;

• surfacing of parts is performed in two passes to provide the required hardness, as far as in argon arc surfacing the intensive stirring of stellite with the base metal occurs, as a result of which the hardness of the first layer does not exceed *HRC* 32–35. The surfacing in two passes results in excessive consumption of expensive stellite and increase in labor intensiveness of the manufacture.

It is possible to perform strengthening of shroud platforms of GTE working blades using oxy-acetylene surfacing by nickel alloy KBNKhL-2. In this case a high quality of deposited metal without any outer and inner defects with the stable hardness *HRC* 60 over the whole area of end or shroud platform of working blade is provided.

The significant disadvantage of application of alloy KBNKhL-2 is the fact that during overheat temperature of engine operation the fusion of contact surfaces frequently occurs, that further results in coming of engine out of order in general.

The problem of heat and wear resistance of shroud platforms can be solved, for example, by application of brazing-on of plates of Co-based alloy KhTN-61, the operation of which is possible at the temperatures of up to 1100 °C. However, brazing is not an acceptable method for strengthening blades of intricate configuration.

Therefore, the analysis of properties, efficient working temperatures of operation and possible methods of deposition of wear-resistant materials shows that none of the existing industrial wear-resistant materials meets the technical requirements as to the technological process of strength-

ening of contact surfaces of GTE parts considered in this work. Therefore, the development of new heat- and wear-resistant material for strengthening of shroud platforms is required, which could provide the preset conditions of their operation.

To the main criteria of development of new wear-resistant material for strengthening of contact surfaces of blades the following can be referred: high heat resistance, hardness of not less than *HRC* 40 at increased operation temperatures, and high temperature wear resistance.

Besides, the main technological criterion in development of new strengthening material is its melting temperature, which should not exceed 1220 ± 10 °C. Otherwise it will be impossible to avoid softening of base metal and formation of cracks in the transition zone.

To conduct investigations the authors offered two pilot compositions on the base of cobalt of Co–Si–B (No.1) and Co–Si–B–Cr_3C_2 (No.2) systems. Microstructure of surfacing by oxy-acetylen flame using pilot compositions is shown in the Figure.

One of the important characteristics of strengthening material is the hardness of deposited layer. The authors determined hardness of strengthening compositions after heat treatment and thermal cycling. The mode of heat treatment of the specimens is given in Table 1. The mode of thermal cycling of pilot specimens was as follows: starting and end temperature is 20 and 1100 °C, respectively, and number of cycles is 15–20. The measurement results of hardness are given in Table 2. The analysis of results shows that the hardness of pilot materials meets the operation requirements.

Determination of wear resistance was carried out in the installation providing operation conditions of GTE blades maximum close to the real ones. In the process of tests the specimens were under the conditions of dynamic collisions at increased temperatures of operating environment. At the same time pilot specimens of base metal

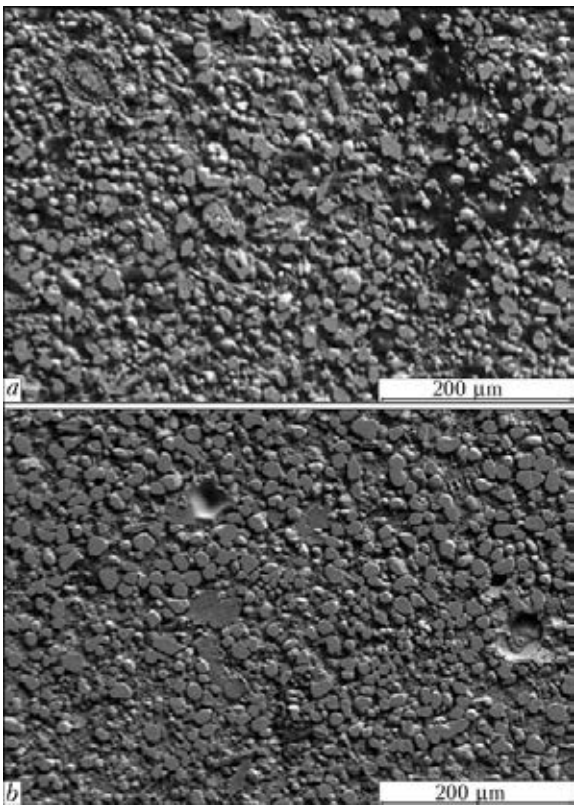

Microstructure of deposited layer of strengthening composition 1 (*a*) and 2 (*b*)

ChS88U-VI and specimens deposited using stellite Kh30N50Yu5T2, which nowadays is the maximum efficient for strengthening of working blades, were tested.

The conditions for tests were as follows: temperature of about 1150 °C, initial load of 50 MPa, amplitude of mutual displacement of 0.169 mm, test period of 2 h. The influence of temperature on wear resistance of specimens was evaluated according to the test results in the environment of combustion products of aircraft fuel of the «kerosene» type. To carry out tests the aircraft kerosene of grade TS-1 was applied.

To eliminate the possible influence of test temperature on physical and mechanical properties of the investigated materials and the next results of evaluation of wear resistance, the tests of specimens were carried out at the contact of only one investigated side.

The wear resistance of pilot materials was evaluated according to the wear intensity

Table 1. Mode of heat treatment of pilot specimens

Succession of performance	Temperature, °C	Exposure time, h
Annealing	1020	2
Cobalting	970±10	6
Aluminizing	970±10	6
Diffusion annealing in vacuum	1030±10	2
Recrystallization annealing	1030±10	2
Vacuum annealing	1030±10	2
Ageing	850±10	16–17

Table 2. Results of measurements of hardness of strengthening compositions

Alloy	Hardness after heat treatment *HV*10	Hardness after thermal cycling *HV*10
No.1	752	572
No.2	606–690	525

Table 3. Results of measurements of wear intensity of pilot alloys

Alloy	Test time, min	Average intensity of wear $J_V \cdot 10^{-6}$, $mm^3/cycle$
ChS88U-VI	120	2.379
Kh30N50Yu5T2	60	10.126
No.1	120	2.761
No.2	120	2.372

$$J_V = V/N,$$

where J_V is the volumetric wear intensity, $mm^3/cycle$; V is the volume of worn-out material (determined according to the profilogram of worn-out specimens), mm^3; N is the number of load cycles (corresponds to the frequency of oscillations of specimens).

The test results of high temperature wear resistance are given in Table 3.

The analysis of test results showed that alloy Kh30N50Yu5T2 can not resist the given dynamic and temperature loads. At the contact surface a great number of scale, spallings, cracks, tears and overlaps are observed, that evidence of fracture of strengthening deposition layer. ChS88U-VI alloy and pilot alloys 1 and 2 show almost the same resistance to high temperature wear.

Thus, in general, the analysis of test results showed that at $T_{test} \approx 1150$ °C, which is close to the temperature of γ′-phase dissolution, the volumetric content and morphology of strengthening disperse phase does not play a decisive role in providing high wear resistance of strengthening compositions. In this case the properties of solid solution base of alloy are of particular importance.

Under the real operation conditions of GTE the particular importance is given not only to serviceability of wear-resistant materials at extra-limiting temperature loads, which make up the minimum percent from the total time of engine operation, but also to wear resistance of alloys during the start (≈ 20 °C) and especially at operation temperatures (≈ 900 °C). Besides, it is known that cobalt alloys demonstrate considerable decrease in wear resistance at the temperatures of about 500 °C, that requires the detailed investigations in the whole operation temperature range from 20 to 1150 °C.

Received 25.04.2014

INVESTIGATION OF COMPOSITION AND STRUCTURE OF WELD METAL OF Kh20N9G2B TYPE MADE IN WET UNDERWATER WELDING

K.A. YUSHCHENKO, A.V. BULAT, N.Yu. KAKHOVSKY, V.I. SAMOJLENKO, S.Yu. MAKSIMOV and **S.G. GRIGORENKO**
E.O. Paton Electric Welding Institute, NASU
11 Bozhenko Str., 03680, Kiev, Ukraine. E-mail: office@paton.kiev.ua

The paper gives the results of investigations of variation of weld metal composition and structure in coated-electrode wet underwater arc welding of 12Kh18N10T steel. It is shown that unlike welding in air, in underwater welding the content of oxygen and hydrogen increases in the weld metal with simultaneous lowering of the quantity of ferritizers. Weld metal structure is characterized by presence of predominantly columnar crystallites, decreased fraction of grain-boundary δ-ferrite and increased volume fraction of oxide non-metallic inclusions, the quantity of which with 0.10 to 1.25 μm dispersion rises 1.5 to 2 times. 14 Ref., 4 Tables, 2 Figures.

Keywords: *wet underwater welding, 12Kh18N10T steel, coated electrodes, weld metal, composition, structure, non-metallic inclusions*

Coated-electrode underwater arc welding has been applied for almost 80 years in repair-reconditioning operations on various-purpose vessels and hydraulic facilities from low-carbon and low-alloyed steels [1–4]. Its features have been quite comprehensively studied [5–9] that allowed development of efficient technologies and specialized welding consumables [10–13].

Over the recent years the task of improvement of the technology of repair of damage of 12Kh18N10T steel lining of concrete pools for storage of NPP spent fuel elements became urgent. In order to solve this problem, it is intended to eliminate the operations of water pumping down and pool deactivation, and to perform repair by the method of coated-electrode wet underwater arc welding (furtheron referred to as underwater welding). However, the features of underwater welding of 12Kh18N10T steel have not been studied well enough; moreover, special-purpose electrodes have not yet been developed.

At the preliminary stage of such electrode development, the influence of welding conditions on weld composition and structure had to be studied. 3 mm test electrodes of E-08Kh20N9G2B type were manufactured for this purpose, the characteristics of which are given in Table 1. It

Table 1. Test electrode characteristics and welding modes

Electrode designation	Test electrode characteristics*			Welding conditions and mode			Sample (section) number
	Total content of CaF_2 and TiO_2 in the coating**, %	CaF_2 and TiO_2 ratio in the coating	Electrode diameter, mm	Medium	I_w^{av}, A	U_a^{av}, V	
K-1	56	1:2	1.6	Air	118.8	24.3	1
				Water	115.7	26.3	4
K-2	56	3:1	1.6	Air	119.3	24.2	2
				Water	111.3	27.4	5
K-3	56	3:1	1.8	Air	113.4	25.5	3
				Water	108.5	28.5	6

*3 mm welding wire from Sv-04Kh19N9 (ER304) steel was used as electrode rods.
**Content of other components of coating of all test electrodes was the same.

Table 2. Composition of weld metal

Sample number	Content, wt.%						
	Cr	Ni	Mn	Nb	Si	O	H
1	21.3	10.8	2.0	1.0	1.2	0.059	0.0027
4	20.0	10.8	1.5	0.9	0.9	0.071	0.0047
2	21.2	10.6	2.5	1.0	1.2	0.044	0.0019
5	21.0	10.9	2.0	0.7	0.8	0.061	0.0040
3	21.2	9.7	2.4	1.0	1.3	0.049	0.0014
6	21.4	10.4	2.3	0.9	1.0	0.066	0.0029

Table 3. Characteristics of structure of weld metal and HAZ

Sample number	Weld metal				HAZ metal	
	Average diameter of γ-cells, μm	Dendrite parameter, μm	Fraction of δ-ferrite, %	NMI volume fraction*, %	Grain size number	Fraction of δ-ferrite, %
1	10	10–12	5.2–8.0	0.22	5	1.5–2.0
4	10	15–25	5–6	0.42	6	1.0–1.5
2	5–7	7–10	9.0–10.5	0.13	6	1.0–1.5
5	5–7	20–25	8–9	0.29	6	1.0–2.0
3	5–7	10–12	9–12	0.19	5	1.0–1.5
6	5–7	15–20	8–11	0.33	6	1.5–2.0

*NMI volume fraction and dispersion were determined by taking their photos with ImigePro computer software.

should be further noted that in order to limit the oxidizing impact of carbon dioxide gas, as well as weld metal hydrogenation, marble content in the coatings was limited to 16 %. Moreover, to evaluate the possibility of screening of electrode metal drops from direct oxidizing and hydrogenating effect of water, K-3 electrodes were made, which differ from K-2 electrodes just by coating diameter.

K-1–K-3 electrodes at DCRP supplied from Kemppi PS-500 inverter at unchanged welding mode settings were used to make rigid butt joints of plates from 12Kh18N10T steel (321) in air and under the water at about 0.5 m depth. Single-layer deposits on plates of the same steel were made in a similar fashion. Welding process analyzer ASP-19 was used to determine electric characteristics of arcing — mean-root-square values of I_w^{av} and U_a^{av}. Samples 1–6 (sections) were cut out of the respective welded joints and deposits. Alloying element content in welds (in their middle part) was determined by the method of emission spectrum analysis with application of the LOMO spectrometer DFS-36, and that of oxygen and hydrogen was determined by the method of restorative melting in carrier gas flow of cylindrical samples (cut out of weld central part) in the LECO units RO-316 and RH-3. Derived results are given in Table 2.

Table 4. Hardness of weld metal, HAZ and base metal

Sample number	*HV*0.1, MPa	*HRA*	*HRA*	
	Weld metal		HAZ	Base metal
1	2100–2130 / 2110	53.0–55.0 / 54.1	52.5–54.5 / 53.5	50.5–54.5 / 52.6
4	2130–2180 / 2146	52.5–55.0 / 53.8	53.0–54.0 / 53.5	49.0–53.0 / 50.3
2	2190–2210 / 2203	52.0–54.0 / 53.2	53.0–53.5 / 53.2	49.0–53.0 / 50.6
5	2190–2360 / 2253	53.5–54.0 / 53.8	54.0–56.0 / 54.8	51.0–52.5 / 51.5
3	2100–2210 / 2136	55.0–55.5 / 55.1	53.0–55.0 / 54.0	51.0–54.0 / 52.6
6	2180–2300 / 2253	54.0–56.0 / 54.8	53.0–55.5 / 54.5	51.0–53.0 / 52.0

Microscope Neophot-32 fitted with digital camera Olympus was used to study the structure of welds and HAZ, as well as take photos of non-metallic inclusions (NMI). Ferrite phase fraction was determined by Ferritgehaltmesser 1.053 ferritometer. Weld metal and HAZ microstructure was revealed by electrolytic etching in 20 % water solution of ammonium sulphide. Results of investigation of weld structure are generalized in Table 3.

Vickers hardness (100 g load) of weld metal was measured using the LECO hardness meter

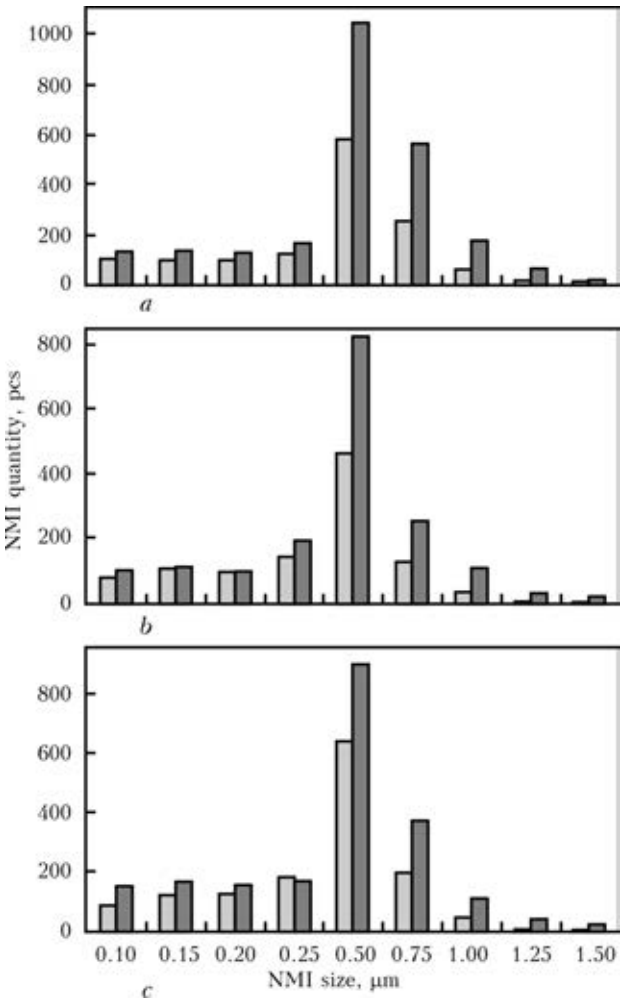

Figure 1. Influence of conditions of welding in air (*light-coloured bars*) and in water (*dark-coloured*) on the quantity of NMI in welds made with electrodes K1 (*a*), K-2 (*b*) and K-3 (*c*)

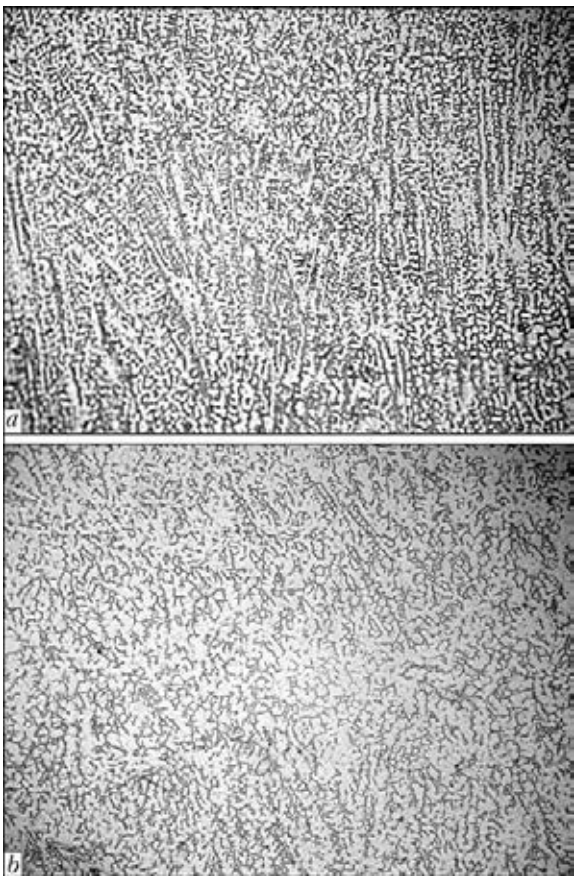

Figure 2. Microstructure (×200) of weld metal made under the water (*a*) and in air (*b*)

M-400, and Rockwell hardness (60 g load) of weld metal, HAZ and base metal was determined by hardness meter TK-2M. Obtained results are given in Table 4.

According to obtained data (see Table 1) increase of CaF_2/TiO_2 ratio in electrode coating, both in welding under the water and in air, leads to lowering of oxygen and hydrogen content in weld metal, that is due to increase of partial pressure of fluorides in the arc atmosphere, lowering of oxygen amount and hydrogen binding into hydrogen fluoride. At other conditions being equal, increase of electrode coating diameter (K-2 and K-3 electrodes) causes increase of oxygen and lowering of hydrogen content in weld metal. Such a situation is attributable to the fact that electrode coating and the formed slag in any case have an oxidizing impact on weld metal. Therefore, increase of the amount of remelted coating (slag) at unchanged amount of metal being melted leads to increase of its oxygen content [14]. Moreover, under the conditions of underwater welding increase of electrode coating diameter improves molten metal protection from water penetration: at the drop stage — due to increase of the depth of the crate from surface-melted coating at electrode tip (screening), and at the pool stage — due to increasing amount of slag. As a result of summary action of these factors, hydrogen content in the metal decreases.

Molten metal saturation with oxygen in underwater welding and its interaction with deoxidizing elements leads to increase of NMI volume fraction in weld metal (see Table 3). Here, quantity of NMI of 0.50 to 1.24 μm size increases (Figure 1). Quantity of NMI of more than 1.25 μm size in all the studied samples practically did not change and was equal to 8 to 10 % of their total quantity, and volume fraction of NMI of 4.7–10 μm size remained within 53–67 % of NMI total volume.

Results of structural investigations (see Table 3) showed that in welds made under the water (sections 4–6), compared to those made in air (1–3), fraction of grain boundary δ-ferrite becomes smaller. In our opinion, this is due to oxidation of ferritizers (silicon, niobium and chromium), having a higher affinity to oxygen than nickel and iron. A characteristic feature of welds, made under the water, is predomination of co-

lumnar crystallites in their structure (Figure 2, *a*), whereas for welds made in air, this is prevalence of cellular crystallites (Figure 2, *b*). In the case of underwater welding, dendrite parameter rises almost 1.5–2 times (see Table 3) at unchanged size of austenite cells, that is indicative of development of dendritic axes of second order and expansion of temperature interval of weld metal solidification. At application of all the test electrodes fraction of δ-ferrite and austenite grain size number remained constant, irrespective of welding conditions (see Table 3).

According to the results of measurement of weld metal Vickers hardness (see Table 4), in samples welded under the water (4–6) hardness is somewhat higher than in those welded in air (1–3). However, Rockwell hardness measurements did not confirm such changes and showed that in all the studied samples *HRA* is minimum in base metal and is higher in HAZ and weld metal; here hardness values in the HAZ and weld metal practically do not differ. Such an increase of hardness, compared to base metal, is, most probably, due to plastic deformation localizing in these zones during welding.

Conclusions

1. At all other conditions being equal, the characteristic features of welds made under the water, compared to those made in air, are their higher content of oxygen (by 1.2 to 1.4 times) and hydrogen (by 1.7 to 2.1 times); lower content of ferritizers (silicon, niobium, chromium); 1.7 to 2.2 times increased volume fraction and quantity of oxide NMI; prevalence of columnar crystallites in their structure at a smaller fraction of grain boundary δ-ferrite.

2. Increase of CaF_2 and TiO_2 ratio in electrode coating, as well as electrode diameter under the conditions of underweater welding, allows lowering by approximately 1.5 times hydrogen content in weld metal, that is attributable to increase of partial pressure of fluorides in the arc atmosphere and molten metal screening from water impact by a crate from electrode coating with increased content of forming slag.

3. Both in welding under the water and in air, increase of electrode coating diameter increases oxygen concentration in weld metal, that is due to increase of oxidizing action of electrode coating and slag on weld metal.

1. Khrenov, K.K., Yarkho, V.I. (1940) *Technology of arc electric welding*. Moscow; Leningrad: Mashinostroenie.
2. Khrenov, K.K. (1946) *Underwater electric welding and cutting of metals*. Moscow: Min. VS SSSR.
3. Avilov, T.I. (1958) Investigation of underwater arc welding process. *Svarochn. Proizvodstvo*, **5**, 12–14.
4. Savich, I.M., Smolyarko, V.B., Kamyshev, M.A. (1976) Technology and equipment for semiautomatic underwater welding of metal structures. *Nefteprom. Stroitelstvo*, **1**, 10–11.
5. Madatov, N.M. (1965) About properties of vapor-gas bubble around arc in underwater welding. *Avtomatich. Svarka*, **12**, 25–29.
6. Kononenko, V.Ya. (2006) *Technologies of underwater welding and cutting*. Kiev: PWI.
7. Reynolds, T.J. (2010) Service history of wet welded repairs and modifications. In: *Proc. of Int. Workshop on State-of-the-Art Science and Reliability of Underwater Welding and Inspection Technology* (Houston, USA, Nov. 17–19, 2010), 31–64.
8. Logunov, K.V. (2003) *Underwater welding and cutting of metals*. St.-Petersburg: Kosta.
9. Kononenko, V.Ya. (2011) *Underwater welding and cutting*. Kiev: Ekotekhnologiya.
10. Savich, I.M. (1969) Underwater flux-cored wire welding. *Avtomatich. Svarka*, **10**, 70–71.
11. Maksimov, S.Yu. (1998) New electrodes for underwater wet welding in all positions. In: *Proc. of 1st Int. Conf. of CIS Countries on State-of-the-Art and Prospects of Development of Welding Consumables in CIS Countries*, 125–128.
12. Murzin, V.V., Murzin, V.T., Russo, V.L. et al. *Composition of electrode coating for manual arc welding*. USSR author's cert. 1540992. Int. Cl. B 23 K35/365. Publ. 1990.
13. Murzin, V.V., Russo, V.L., Evseev, V.R. et al. *Electrode for manual arc welding*. USSR author's cert. 15497706. Int. Cl. B 23 K35/365. Publ. 1989.
14. Pokhodnya, I.K. (1972) *Gases in welds*. Moscow: Mashinostroenie.

Received 24.03.2014

ELECTRODES FOR WELDING OF DISSIMILAR CHROMIUM MARTENSITIC AND CHROMIUM-NICKEL AUSTENITIC STEELS

L.S. ZAKHAROV, A.R. GAVRIK and **V.N. LIPODAEV**
E.O. Paton Electric Welding Institute, NASU
11 Bozhenko Str., 03680, Kiev, Ukraine. E-mail: office@paton.kiev.ua

Carried are the investigations on development of low-carbon chromium electrodes of 05Kh6MF type. Effect of coating composition on carbon content in deposited metal of Kh6M type was investigated. It is determined that joint introduction of chromium and zirconium oxides in 5–10 wt.% amount at simultaneous removal of marble from the coating is the most efficient for carbon reduction. Slag system of fluoride-magnesium oxide type coating was developed, providing reduction of carbon content in the deposited metal to 0.04–0.06 wt.% at sufficiently low content of diffusible hydrogen. Electrodes of ANL-10 grade for welding of dissimilar joints of chromium martensitic steels of 10Kh9NMFB type and chromium-nickel austenitic steels of 10Kh18N10T type were developed on its basis. The electrodes provide for stable arcing, insignificant spattering, good weld formation in all spatial positions and easy separation of slag crust. 12 Ref., 3 Tables, 2 Figures.

Keywords: *arc welding, dissimilar steels, coated electrodes, deposited metal, carbon reduction, diffusible hydrogen, welding-technological properties*

Martensitic steels of 10Kh9NMFB type are currently used in power-generating units with supercritical vapor parameters (operating temperature 600 °C). They have higher long-term strength and larger corrosion resistance due to complex system of alloying and high-content of chromium than traditional low-alloy pearlitic and bainitic steels [1]. Such steels are included in the joints of pipe systems having operating temperature more than 610 °C and manufactured from austenitic steels of 10Kh18N10T type during construction of new power units and repair of old pipe systems.

It is well-known fact that filler materials, providing high-nickel austenitic deposited metal, are usually used in welding of dissimilar joints, operating at temperature above 500 °C. However, our investigations showed that formation of chains of grains of structurally free ferrite is observed in HAZ of P91 steel in welding of martensitic steel 10Kh9NMFB (P91) to austenitic steel 10Kh18N10T, even at nickel content in the weld metal more than 50 wt.% (Figure 1, *a*). This can promote significant reduction of serviceability of welded structures [2]. Therefore, necessity in change of technology of welding of such joints has emerged.

The investigations performed showed that prevention of formation of ferrite interlayer and providing of necessary strength characteristics of fusion zone require preliminary cladding of 10Kh9NMFB steel edge by special filler material (Figure 1, *b*), containing 5–7 wt.% Cr and 0.8–1.0 wt.% Mo. Content of carbon in the deposited metal should lie in 0.04–0.06 wt.% limits. In this case, materials of 10Kh16N25 type can be used for filling of main section of the weld. Since the

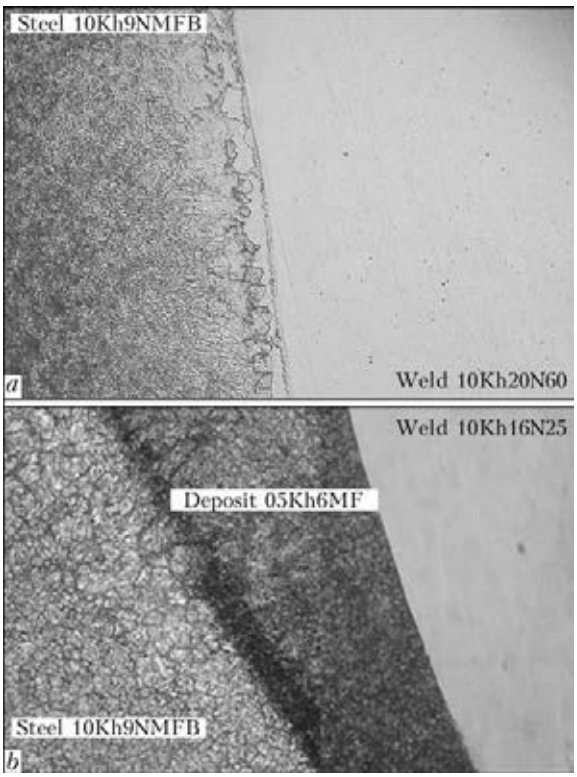

Figure 1. Microstructure (×300) of fusion zone of steel 10Kh9NMFB with austenitic weld

Table 1. Chemical composition of deposited metal, wt.%, in use of standard electrodes with 8–12 wt.% Cr

Electrode grade	C	Si	Mn	Cr	Ni	Mo	S	P
TsL-32	0.12–0.16	<0.50	0.3–0.7	10–12	0.8–1.1	0.90–1.25	<0.03	<0.035
TsL-41	<0.10	<0.75	0.2–0.6	11–14	1.0–1.5	–	<0.03	<0.035
TsL-51	<0.04	<0.35	0.15–0.60	12–15	1.8–2.5	–	<0.025	<0.030
TsL-57	0.06–0.14	<0.60	0.3–0.8	8.5–10.5	–	0.9–1.2	<0.025	<0.030

electrodes providing such alloying and reduced content of carbon in the deposited metal were not used earlier, the investigations on their development were carried out.

Electrodes of two types, namely carbonate-fluorite (TsL-32, TsL-41) and rutile-fluorite-carbonate (TsL-51, TsL-57), are usually used for welding of steel with 8–12 wt.% Cr. At that, fluorite to marble proportion changes in large ranges (from 3.5:5.0 to 5.3:3.5). Table 1 shows that only TsL-51 electrodes provide for reduced content of carbon in the deposited metal. They are produced using low-carbon wire of Sv-01Kh12N2-VI grade with 12–15 wt.% Cr and 2–3 wt.% Ni. Such a wire can provide for the necessary content of alloying elements, therefore, the investigations were carried out on development of low-carbon chromium electrodes of 05Kh6MF type based on wire of Sv-08A grade with alloying through coating. Since carbon content in it can achieve 0.10 wt.%, it was necessary to select coating composition, providing its reduction to 0.04–0.06 wt.%.

Burning-out of carbon in welding depends on number of factors, i.e. method and mode of welding, composition and amount of shielding medium, initial content of carbon in filler material etc. [3–7].

Transfer of carbon in the deposited metal during manual welding using coated electrodes is effected by coating composition, its thickness (coating mass factor) as well as mode of welding. Welding with electrodes having quartz and hematite-based coating shows the largest burning-out of carbon and the lowest one is observed applying fluorspar [3].

Increase of carbon content in the weld metal during manual welding using electrodes with lime fluorspar coating takes place mainly due to carbon oxide, which is formed as a result of decomposition of marble as well as carbon of ferroalloys, being introduced into the coating. In this connection, quantity of marble in the coating of electrodes for welding of high-alloy low-carbon steels is reduced to the minimum or completely removed [6].

Carbon reduction from the coating takes place due to deoxidizing agents, which are included in it or in the electrode core. Thus, rise of carbon content as a result of interaction with carbon dioxide, which is formed at $CaCO_3$ dissociation, is observed during heating of ferromanganese in mixture with marble up to 600–900 °C. Rise of content of carbon in chromium from 0.08 to 0.7–1.5 wt.% [3] is noted in coatings from marble mixture with metallic chromium after specimen heating in the furnace.

It should be noted that transfer of carbon in the deposited metal depends not only on coating composition, but also on carbon content in electrode core metal. Its burning is observed in rise of marble/fluorite proportion at high content of carbon in wire (Sv-18GSA). It is explained by increase of oxidizing potential of the coating. On the contrary, its content increases in the deposited metal at low carbon content in wire (Sv-06Kh19N9T) [5].

Reduction of marble content and introduction of iron oxides (hematite, magnetite or iron dross) in electrode coating can prevent increase of carbon content in the deposited metal as well as somewhat decrease it [7]. Using of more thermally resistant oxides Cr_2O_3 and ZrO_2 is more efficient in welding by electrodes with rutile-lime fluorspar coating, which contains up to 10 wt.% of marble [8]. This is explained by the fact that they have more than 2000 °C melting temperature and react with carbon at higher temperature, at which it becomes more active deoxidizing agent. Besides, carbon oxidation is possible at drop stage, since dissociation of Cr_2O_3, on data of [9], takes place at temperature below the temperature of its melting. In addition, chromium oxides are volatile at melting temperature (~2400 °C) [8, 10] and, thus, they can be present in gaseous phase of arc gap.

According to work [7], the higher the oxide melting temperate and the lower the chemical affinity of given oxide with oxygen, characterizing by thermodynamic potential of oxide formation ΔZ^0, the more intensive is oxidizing of carbon, manganese or chromium. Due to high chemical affinity of zirconium with oxygen in

Table 2. Content of components in dry charge, wt.%

Charge component	Number of variant								
	1	2	3	4	5	6	7	8	9
Marble	53	10	10	0	0	0	0	0	0
Flourite	10	10	10	10	10	10	10	15	20
Fired magnesite	0	30	30	30	30	30	30	30	30
Chromium oxide	–	–	–	2	5	8	12	12	12
Zirconium concentrate	–	–	–	–	–	–	–	5	10
Ferrotitanium	15	15	10	10	10	10	10	10	10

Note. Chromium, molybdenum, ferrosilicon and manganese were introduced in composition of all variants of electrodes.

comparison with chromium, oxide of the first provides for smaller oxidizing of the elements than oxide of the second. The oxides of iron and nickel with melting temperature below 2000 °C provide for insignificant oxidizing of carbon and sufficiently intensive oxidizing of manganese and, in particular, of silicon.

Probably, chromium oxide should get advantage in application during development of low-carbon chromium electrodes, since, in this case, chromium reduction takes place simultaneously with electrode burning-out.

Treatment of raw materials, namely high-temperature baking of mineral slag-forming components of charge, can be additional mean for limitation of quantity of carbon in the weld metal except for effect of coating slag system. Soaking of fluorite concentrate, rutile, hematite etc. at 800 °C during 2 h allows reducing content of carbon in the deposited metal per 0.01–0.03 wt.% [11].

Modes of welding also influence transfer of carbon in the deposited metal. Thus, increase of arc voltage (arc length) in welding using UONI-13/55 electrodes promotes decrease of carbon content almost 2 times. It can be explained by rise of period of droplet existence and more overall reaction. At the same time, change of welding current has virtually no effect on this process [12].

Analysis of reference data allows determining the following directions of performance of the experiments on development of low-carbon high-chromium electrodes, namely reduction of content or complete removal of carbonates from coating composition, additional introduction of active oxides, rise of coating mass factor, preliminary baking of charge components.

Pilot batches of electrodes were manufactured for selection of optimum coating composition. Influence of type of coating on transfer of alloying components, content of gases in the deposited metal and welding-technological properties of the electrodes were studied.

In the first series of experiments fired (metallurgical) magnesite was introduced in the coating of UONI-13/45 type electrodes instead of marble. It was experimentally stated that reduction of carbon in the deposited metal is observed only at simultaneous decrease of ferrotitanium content in the coating. Otherwise, carbon reduction can be even observed.

Chromium and zirconium oxides (Table 2, variants 4–9) were additionally introduced in the coating composition for more efficient reduction

Table 3. Chemical composition of deposited metal, wt.%, in use of pilot electrodes

Number of variant (acc. to Table 2)	C	Si	Mn	Cr	Mo	V
1	0.079	0.27	0.37	5.1	0.71	0.24
2	0.091	0.57	0.53	5.8	0.77	0.31
3	0.067	0.63	0.38	6.6	0.75	0.38
4	0.075	0.37	0.51	7.2	0.84	0.35
5	0.063	0.30	0.49	7.8	0.76	0.22
6	0.052	0.41	0.38	8.2	0.72	0.25
7	0.055	0.32	0.42	7.3	0.77	0.28
8	0.044	0.22	0.37	6.3	0.81	0.21
9	0.045	0.20	0.28	6.0	0.84	0.22

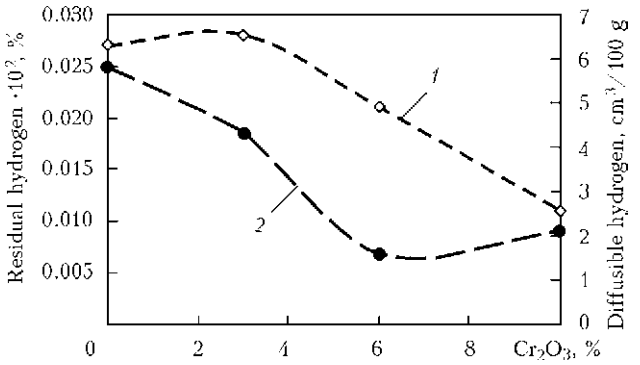

Figure 2. Effect of chromium oxide on content of residual (*1*) and diffusible (*2*) hydrogen in deposited metal 05Kh6MF

of carbon content in the deposited metal. This allows decreasing carbon content in the deposited metal to 0.04 wt.% (Table 3).

Experiments on adjustment of coating composition were carried out for providing of optimum welding-technological properties. At that, effect of proportion of its components on quality of weld formation in different spatial positions, stability of arcing, easiness of slag crust separation and resistance of weld metal to pore formation were investigated. Evaluation of indices specified above was carried out on five-point grading system. Content of magnesite, fluorite and chromium oxide was changed in the ranges, wt.%: 10–45 MgO, 10–45 CaF_2, 1–15 Cr_2O_3 and 1–15 ZrO_2. The experiments performed showed that proportion of magnesite and flourite has virtually no effect of arcing stability, but content of flourite above 35 wt.% or chromium oxide more than 10 wt.% promotes deterioration of weld formation in vertical position. Separability of slag crust becomes worse at reduction of chromium oxide less than 5 wt.% and increase of magnesite more than 20 wt.%. Optimum content of zirconium dioxide makes 2–6 wt.%.

Effect of coating composition on content of hydrogen in the deposited metal was also investigated. The experiments performed showed that introduction of chromium oxide is the most efficient for reduction of content of diffusible hydrogen at fired magnesite to flourite proportion 1.0:2.5. As can be seen from Figure 2, it is reduction of not only content of diffusible hydrogen, but content of residual one as well, that can be explained by bonding of hydrogen atoms into hydroxyl insoluble in liquid metal.

Thus, new flour-spar-magnesium-oxide slag system was proposed, providing carbon content in the deposited metal at the level of 0.04–0.06 wt.% and diffusible hydrogen at the level of 1.0 $cm^3/100$ g. Optimum content of coating was determined, and pilot batch of electrodes was manufactured. Test also showed significant improvement of welding-technological indices. Typical chemical composition of the deposited metal makes, wt.%: 0.041 C; 0.23 Si; 0.47 Mn; 0.83 Mo; 0.25 V; 0.017 S; 0.026 P. Mechanical properties of the deposited metal in as-heat-treated condition (760 °C, 2 h) at 20 °C characterized by such indices, namely $\sigma_{0.2}$ = 290 MPa; σ_t = 515 MPa; δ = 30 %; ψ = 65 %; *KCU* = = 62 J/cm^2.

Developed electrodes were marked as grade ANL-10 and specification on their production was prepared.

1. Skulsky, V.Yu., Tsaryuk, A.K. (2004) New heat-resistant steels for manufacture of weldments in heat power units (Review). *The Paton Welding J.*, **4**, 32–37.
2. Skulsky, V.Yu. (2005) Metal structure in the fusion zone and HAZ of welded joints on high-chromium heat-resistant steels. *Ibid.*, **5**, 10–18.
3. Erokhin, A.A. (1964) *Kinetics of metallurgical processes of arc welding*. Moscow: Mashinostroenie.
4. Erokhin, A.A., Kuznetsov, O.M. (1959) Electrodes with nonoxidation coating. *Svarochn. Proizvodstvo*, **12**, 1–4.
5. Erokhin, A.A., Kuznetsov, O.M. (1961) Decrease in carbon content in weld metal during welding of stainless steels. *Avtomatich. Svarka*, **11**, 1–4.
6. Sokolov, E.V., Sidlin, Z.A., Vagapov, I.M. (1968) Development of electrodes providing low carbon content in deposited metal of austenite class. In: *Welding of structures from high-alloy steels*. Leningrad: LDNTP.
7. Kakhovsky, N.I., Lipodaev, V.N. (1968) Electrodes for welding of chrome-nickel stainless steel of 18-10 type with low carbon content. *Avtomatich. Svarka*, **12**, 8–10.
8. Kakhovsky, N.I., Lipodaev, V.N., Kakhovsky, Yu.N. (1970) Decrease in carbon content in weld metal during manual arc welding of stainless steels. *Ibid.*, **6**, 8–10.
9. Knunyants, I.L. (1967) *Concise chemical encyclopedia*. Moscow: Sov. Entsycl.
10. Rode, T.V. (1962) *Oxygen chromium compounds and chromium catalyzers*. Moscow: AN SSSR.
11. Kakhovsky, N.I., Lipodaev, V.N., Zakharov, L.S. (1977) Decrease of carbon content in weld metal by high-temperature baking of electrode coating components. *Avtomatich. Svarka*, **2**, 8–10.
12. Potapov, N.I. (1985) *Oxidation of metals in fusion welding*. Moscow: Mashinostroenie.

Received 04.04.2014

INVESTIGATION OF TRANSITION ZONE OF LOW-CARBON STEEL JOINT WITH HIGH-ALLOYED Cr–Ni DEPOSITED METAL

K.A. YUSHCHENKO, Yu.N. KAKHOVSKY, A.V. BULAT, R.I. MOROZOVA, A.V. ZVYAGINTSEVA, V.I. SAMOJLENKO and **Yu.V. OLEJNIK**
E.O. Paton Electric Welding Institute, NASU
11 Bozhenko Str., 03680, Kiev, Ukraine. E-mail: office@paton.kiev.ua

Causes for fracture of repair layer deposited with electrodes of E-08Kh20N9G2B type on the surface of St3sp (killed) steel lining of water wheel chamber of HPS hydraulic unit are analyzed. It is established that its failures (cracking, delamination) arise as a result of lower chromium content (less than 12 %) and formation of martensite phase in the transition zone between steel St3sp and high-alloyed deposited metal. State of transition zone between St3sp and deposited metal of E-10Kh25N13G2, E-11Kh15N25M6AG2 and 10Kh28N14G2 type at welding current variation in the range of 80–140 A has been studied. It is shown that sufficient content of chromium (less than 12 %) and absence of martensite in the transition zone can be ensured in the case of application of electrodes of 10Kh28N14G2 type for repair surfacing at limitation of I_w to not more than 90 A. 6 Ref., 5 Figures, 1 Table.

Keywords: *coated-electrode manual arc welding, low-carbon steel, high-alloyed deposited metal, transition zone, structural and chemical inhomogeneity, martensite, microhardness, cracks, corrosion*

Dissimilar steel welded joints are widely applied in chemical engineering. Their performance is largely determined by the state of transition zone (its structure and chemical inhomogeneity), which undergoes degradation in structure service as a result of the effect of higher temperatures and pressure, cyclic mechanical loads, thermal cycling and aggressive media, and initiates metal delamination. The main regularities, determining the inhomogeneity of chemical composition and structure in the fusion zone of dissimilar metals, are associated with appearance of interlayers conditionally named «solidification» ones [1–4].

In enterprises of petrochemical industry and power generation repair operations with application of different kinds of arc welding are performed. So, in hydro-power engineering, in order to maintain generating capacity of units, repair of damage of lining of water wheel chambers (WWC) from St3sp (killed) steel is periodically performed by restoration of its design dimensions and subsequent deposition of high-alloyed cavitation- and corrosion-resistant metal layer on the working surface. Deposition of the latter is most often performed with TsL-11 electrodes of E-08Kh20N9G2B type.

During investigations of fragments of damaged metal of WWC lining in one of the hydraulic units, the authors found that failure of the layer deposited with TsL-11 electrodes occurs through cracking, delamination and corrosion (Figure 1), that is due to formation of martensite phase with microhardness of 3100–3850 MPa and lower content of chromium (up to 9 %) and nickel (up to 4 %) in the transition zone between St3sp steel and high-alloyed metal. According to [5], minimum content of chromium, ensuring corrosion resistance in humid atmosphere and various low-aggressive solutions, should be not less than 12 %.

Thus, requirements of high enough corrosion resistance, limited content of δ-ferrite (its excess can lead to ductility lowering), as well as minimum formation or elimination of martensite phase, should be made of transition zone metal.

This work is devoted to investigation of the possibilities of minimizing structural inhomogeneity in the fusion zone due to variation of deposited metal composition and welding cur-

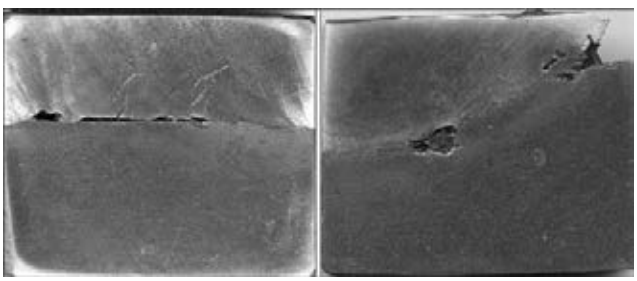

Figure 1. Typical patterns of transition zone failures between steel St3sp and deposited metal of TsL-11 electrodes

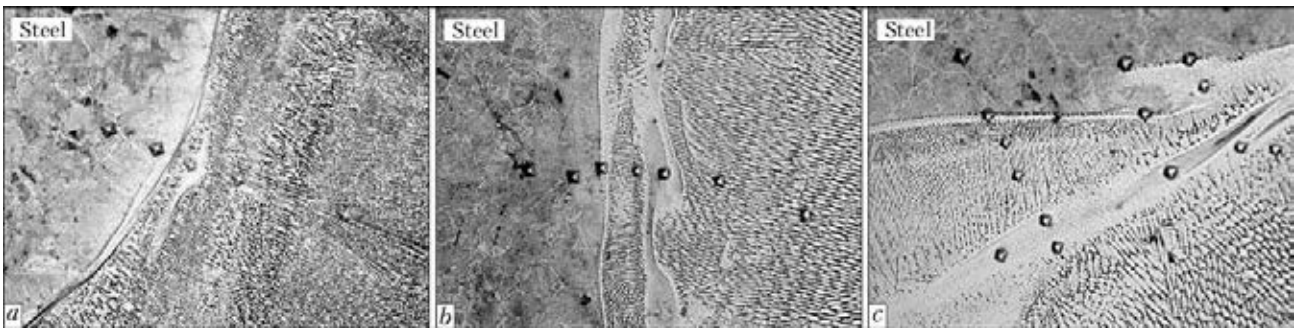

Figure 2. Microstructure (×200) of transition zone between St3sp steel and deposited metal of E-10Kh25N13G2 type at I_w = 80–90 (*a*), 100–110 (*b*) and 130–140 (*c*) A

rent. For this purpose, single-layer deposits were made on St3sp steel plates by electrodes of E-10Kh25N13G2, E-11Kh15N25M6AG2 and 10Kh28N14G2 type with varying degrees of austenicity at welding current variation in the range of 80 to 140 A. Metallographic investigations were performed on the respective microsections.

Microhardness of structural components was determined with metallographic microscope PMT-3 at 100 g load on the indentor, quantity of magnetic phase — with Ferritgehaltmesser 1.053 ferritometer, and microstructure of transition zone metal — with Neophot-32 microscope. Data on composition of transition zone metal were obtained using energy-dispersive X-ray microanalyzer of Camscan microscope. Transition zone profile was detected by combined chemical and electrolytic etching.

At the first stage of the work it was established that in all the studied samples the transition zone has a wavy profile, and its width varies within 2 to 135 μm, that is in good agreement with the results of [6].

Microstructure of deposited metal of electrodes of E-10Kh25N13G2 type at I_w = 80–90 A consists of austenite + 5 % of ferrite and martensite (Figure 2, *a*; the Table), and martensite microhardness in the transition zone is equal to 3250 MPa.

At increase of welding current to 100 and 140 A, respectively (Figure 2, *b*, *c*; the Table) quantity of ferrite and martensite in the deposited metal rises, that is due to greater penetration of low-carbon steel and lowering of chromium and nickel content to 9.7 and 5.5 %, respectively. Microhardness of martensite in the transition zone (see the Table) at I_w = 100 A reaches 3250–3940 MPa, and at I_w = 140 A it is 3310–4140 MPa.

Data on the influence of welding current on the structure and microhardness of deposited metal and transition zone at application of E-11Kh15N25M6AG2 type electrodes is given in the Table and in Figure 3. It follows from the given data that despite increased nickel content in the transition zone, martensite phase with microhardness of 3720–3840 MPa formed at $I_w \geq$ 100 A. Its X-ray microprobe analysis showed that its chromium content is equal to 4.5–8.0 % and that of nickel is 7.4–11.3 %. Such a low content of chromium in it in the transition zone regions can initiate corrosion attack on metal in service.

Thus, to ensure sufficient corrosion resistance of the transition zone, it is necessary to increase chromium content here. To check the validity of

Influence of welding current on structure and properties of deposited metal and transition zone

Deposited metal type	I_w, A	Microhardness, MPa			Deposited metal microstructure
		Transition zone	Deposit middle	Deposit top	
E-10Kh25N13G2	80–90	2180–3250	1980–2080	2250–3110	A + F
	100–110	3250–3940	2320–3120	2480–3720	A + F
	130–140	3310–4140	2780–3310	2860–3720	A + F
E-11Kh15N25M6AG2	80–90	2120–3140	2160–2480	2180–2530	A
	100–110	2020–3720	1800–2160	1760–2530	A
	130–140	2160–3840	2120–2780	1975–2080	A
10Kh28N14G2	80–90	1595–2580	1688–1780	1875–1940	A + F
	100–110	1942–3600	1900–2120	1900–2200	A + F
	130–140	2380–3840	1971–2080	1800–2080	A + F

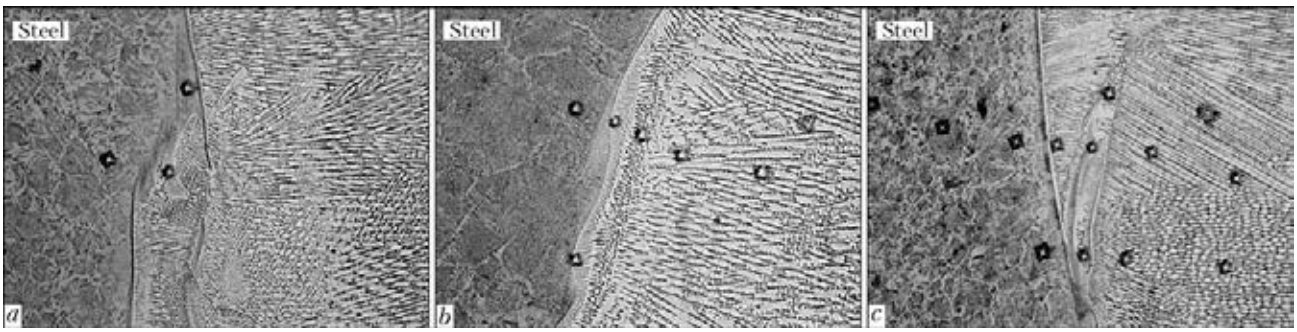

Figure 3. Microstructure (×200) of transition zone between St3sp steel and deposited metal of E-11Kh15N25M6AG2 type at I_w = 80–90 (*a*), 100–110 (*b*) and 130–140 (*c*) A

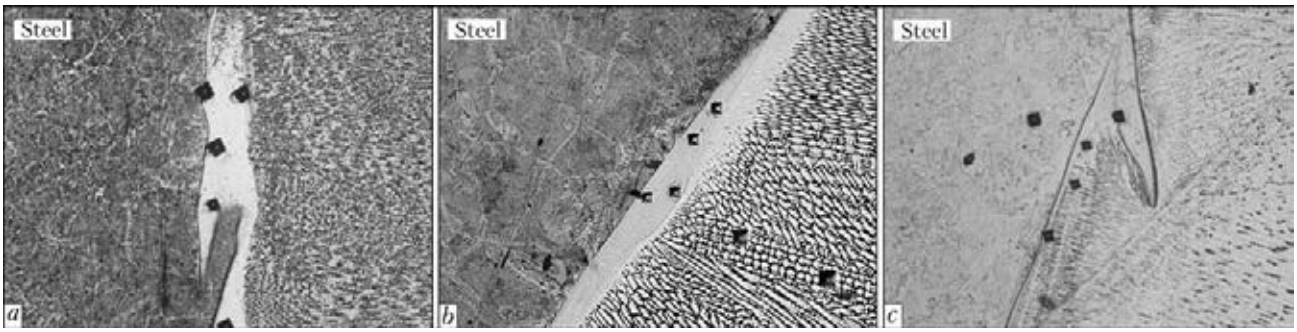

Figure 4. Microstructure (×200) of transition zone between St3sp steel and deposited metal of 10Kh28N14G2 type at I_w = 80–90 (*a*), 100–110 (*b*) and 130–140 (*c*) A

this statement, the transition zone of test electrodes of 10Kh28N14G2 type was studied. Microstructure and microhardness of deposited metal of these electrodes, depending on welding current, are given in Figure 4 and in the Table. As is seen from the Table, at I_w = 80–90 A microhardness of all the transition zone regions was equal to 1595–2580 MPa, except for one of ~40 μm length, where it reached 3050 MPa. In this section energy dispersion analyzer was used to determine chromium and nickel content. Nickel content in it was equal to 7.85 %, and that of chromium was 15.16 %, i.e. microstructure of the transition zone in this case consists of austenite + 3.5 % of ferrite, and chromium content is quite sufficient to ensure the corrosion resistance. At I_w increase to 100–140 A, microhardness in the transition zone rises (3600–3840 MPa), and alloying element content decreases significantly (8.2–12.3 % Cr, 4.8–6.8 % Ni), i.e. a phase with martensite component formed here alongside austenite.

Thus, for electrodes of 10Kh28N14G2 type welding current increase above 90 A increases the structural and chemical inhomogeneity of transition zone metal, that may lead to lowering of its ductility and corrosion resistance. Generalized pattern of the influence of deposited metal type and welding current on the quantity of martensite in the transition zone is given in Figure 5.

Comparative analysis of the results of metallographic, durometric and X-ray microprobe analyses shows that in surfacing St3sp steel with E-10Kh25N13G2 type electrodes a martensite structure forms in the transition zone metal and chromium content drops below 12 %, that is insufficient to ensure the corrosion resistance. An optimum variant is application of electrodes of 10Kh28N14G2 or E-11Kh15N25M6AG2 type, which at I_w = 80–90 A provide the highest quality of transition zone metal. On the other hand, it should be noted that electrodes of 10Kh28N14G2 type are more cost-effective (1.5 times less expensive).

At testing of samples of metal deposited by test electrodes of 10Kh28N14G2 type and TsL-11

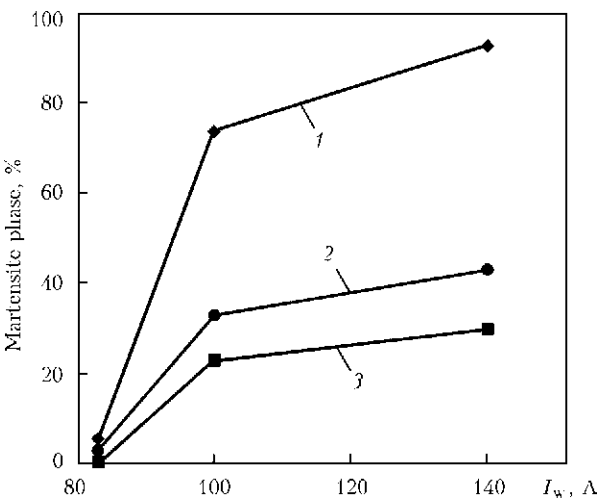

Figure 5. Quantity of martensite phase in transition zone between St3sp steel and deposited metal of E-10Kh25N13G2 (*1*), E-11Kh15N25M6AG2 (*2*) and 10Kh28N14G2 (*3*) type

electrodes of E-08Kh20N9G2B type conducted in the test facilities of the Laboratory of Hydrogas Systems of National Aviation University it is established that in the first case cavitation wear resistance is 2 times higher, and hydroabrasive wear resistance is higher by 10–15 %.

Conclusions

1. Failure of metal, deposited with TsL-11 electrodes of E-08Kh20N9G2B type on working surface of lining of hydrounit WWC from steel St3sp, is due to martensite phase formation in the transition zone and lower chromium content, that initiates cracking and delamination of the deposited high-alloyed layer.

2. Methods of metallography, durometry and X-ray spectrum microprobe analysis were used to study the state of transition zone between steel St3sp and deposited metal of E-10Kh25N13G2, E-11Kh15N25M6AG2 and 10Kh28N14G2 type at welding current variation in the range of 80 to 140 A. It is established that sufficient corrosion resistance of transition zone metal can be ensured and martensite phase formation here can be avoided at surfacing with electrodes of 10Kh28N14G2 type and welding current limitation to not more than 90 A.

3. It is proposed to apply new welding electrodes of 10Kh28N14G2 type for deposition of cavitation-resistant metal layer on the working surface of hydrounit WWC lining, which ensure the high quality and cost-effectiveness of repair-welding operations.

1. Gotalsky, Yu.N. (1981) *Welding of dissimilar steels*. Kiev: Tekhnika.
2. Zemzin, V.N. (1966) *Welded joints of dissimilar steels*. Moscow: Mashinostroenie.
3. Lebedev, V.K., Kuchuk-Yatsenko, S.I., Chvertko, A.I. et al. (2006) *Machine-building*: Encyclopedia. Vol. III-4: Technology of welding, brazing and cutting. Moscow: Mashinostroenie.
4. Elagin, V.P., Gordan, G.N. (2013) To mechanism of lowering of chemical and structural heterogeneity in fusion zone of austenitic weld with carbon steel. In: *Abstr. of Int. Conf. on Welding and Related Technologies — Present and Future* (Kiev, 2013), 70.
5. Babakov, A.A., Pridantsev, M.V. (1971) *Corrosion-resistant steels and alloys*. Moscow: Metallurgiya.
6. Pavlov, I.V., Antonets, D.P., Gotalsky, Yu.N. (1980) To problem of mechanism of transition layer formation in fusion zone of dissimilar steels. *Avtomatich. Svarka*, **7**, 5–7.

Received 24.03.2014

HEATING AND MELTING OF ELECTRODES WITH EXOTHERMIC MIXTURE IN COATING

A.F. VLASOV, N.A. MAKARENKO and **A.M. KUSHCHY**
Donbas State Machine Building Academy
72 Shkadinov Str., 84313, Kramatorsk, Donetsk region, Ukraine. E-mail: dgma@dgma.donetsk.ua

It is a well known fact that introduction of exothermic mixtures in electrode coating composition can increase efficiency of manual arc welding. At that, distribution of heat between electrode and workpiece is not enough studied. This work studies thermal characteristics of heating and melting of the electrodes with different content of exothermic mixture in the coating. It is shown that introduction of the mixture in amount to 53.4 wt.% results in rise of coefficient of core melting from 8.7 to 11.6 g/(A·h), weld deposition coefficient from 8.1 to 13 g/(A·h) as well as growth of efficiency of base metal heating. 10 Ref., 2 Tables. 1 Figure.

Keywords: *arc welding, coated electrodes, exothermic mixture, heating and melting of electrode, thermal characteristics*

One of the main tasks for developers is increase of process efficiency and finding of new types of raw materials for manufacture of welding and surfacing consumables. One of the direction for solving of this problem can be utilization of effect of exothermic reactions at introduction of exothermic mixtures in form of corresponding oxidizers (dross, hematite, manganese ore) and deoxidizers (ferrotitanium, ferrosilicon, aluminum powder) in composition of the used materials [1–4]. Their heating provides for exothermic process resulting in melting of the electrode core. If quantity of iron oxides and element-deoxidizers is not enough in electrode coating, then the exothermic process takes place in a stage of droplet formation and transfer. Investigations performed [5] showed that change of content of exothermic mixture from 35 to 64 % in the electrode coatings, consisting of dross and aluminum powder, promotes for increment of the temperature that makes 1280 °C and being enough for complete melting of the coating. However, distribution of heat between electrode and workpiece, emitted during exothermic reaction, is not sufficiently studied.

Aim of the present work is study of effect of quantity of exothermic mixture in the electrode coating on thermal characteristics of their melting.

The electrodes containing marble, fluorspar, rutile concentrate, ferromanganese, ferrotitanium, iron brass and aluminum powder in the coating were manufactured for the investigations. A coating mass factor was constant at core diameter 5 mm and different content of exothermic mixture in the coating. Bead-on-plate welding using direct current of reversed polarity was carried out by these electrodes on plates of 10 × × 80 × 120 mm size with strip, preliminary installed over a heat-insulated rack. Welding converter PS-500 with ballast rheostats of RB-300 type was used as a power source. Deposition of each specimen was carried out during 20 s. Time of electrode melting was determined using stopwatch, average value of welding current and arc voltage were defined according to recorders, and temperature of water heating was measured by

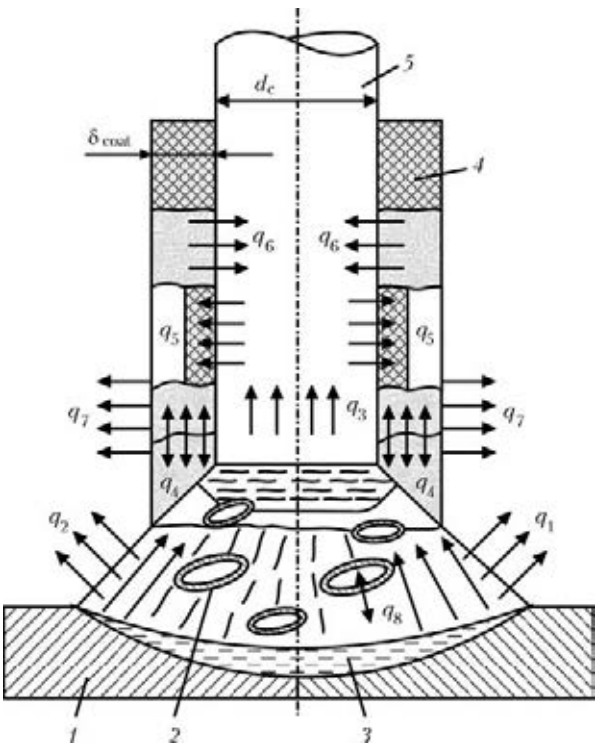

Model of heating and melting of electrode with exothermic mixture in coating: *1* — base metal; *2* — droplet of electrode metal; *3* — weld pool; *4* — coating; *5* — core (for designations see the text)

thermometer with up to 0.05 °C accuracy. 3–5 measurements were carried out for each electrode composition.

The Figure shows that heat, emitted in metallic core of d_c diameter during electrode current heating, is consumed for rise of temperature of core (q_3) and coating layer (q_5) and transferred (q_7) into ambient atmosphere through side surface. Heat flow of arc q_1, irradiation heat and heat of convective transfer q_2 have effect on the electrode tip. Temperature of 1000 °C (at content of more than 35 % of exothermic mixture in the electrode coating) provides for the exothermic reaction with emission of heat q_4, one part of which is consumed for heating and melting of the coating (q_5) and another is transferred to the electrode core (q_6). Heat from convective heat transfer through electrode side surface to ambient atmosphere (q_7) and heat, lost by drops of motel metal (q_8), are important in this process.

Instantaneous heat balance

$$Q = q_1 + q_2 + q_3 + q_4 + q_5 + q_6 + q_7 + q_8$$

or

$$Q = q_1 + q_2 + q_3 + q_4 = q_5 + q_6 + q_7 + q_8.$$

Three sources heat the electrode. Firstly, it is a lumped source — welding arc, heat of which is introduced through heating spot at the electrode working tip (q_1). Secondly, it is heat of irradiation and convective heat transfer (q_2) and distributed on volume source — heat, emitted by electric current according to Joule–Lenz law along the whole length of electrode core from current-carrying contact to arc (q_3). Thirdly, it is heat, emitted during exothermic reaction (q_4).

Distribution of temperatures $T(x)$ in the electrode core was investigated during heating by power source at the tip depending on quantity of exothermic mixture in the electrode coating. Power source at the electrode tip can be considered as movable and traveling at electrode melting rate. Distribution of temperatures $T(x)$ in the electrode core during heating by source at the tip can be received using equation of limiting state of process of heat distribution from movable plane source in the core in area before source (at initial coefficient of thermal efficiency for core $b = 0$). The following equation is generated by inserting set values in known equation [6] at $x \geq 0$ and $t \to \infty$:

$$T - T_c = (T_d - T_c)e_{wx/a},$$

where T_c is the temperature of current heating of electrode core, °C; x is the distance from tip of consumable electrode, temperature of tip of which equals average temperature of drops T_d, cm; w is the rate of electrode melting, cm/s.

Temperature of drops, detaching from the consumable electrode, was determined on known formulae [7] considering data of work [8] according to average value of droplet enthalpy (ΔH = = 1850 J/g) in melting of Sv-08A wire and I_w = = 290 A (reversed polarity):

$$T_{d.av} = 1798 + (\Delta H - 1330)/0.92 = 1798 + + 520/0.92 = 565 + 1798 = 2326 \text{ K} = 2090 \text{ °C}.$$

Table 1 gives the data characterizing effect of quantity of exothermic mixture in the electrode coating on temperature of section x heated by arc at T_d = 2100 °C; T_c = 20 °C; w = 0.475–0.645 cm/s; a = 0.08 cm^2/s. Temperature of 1000 °C, which promotes active exothermic reaction, is achieved at 1 mm distance from the electrode tip.

Temperature of heating [9] of coated electrode ET-2 of 5 mm diameter was determined in 60 s after beginning of arc burning at direct current 290 A. Initial electrode temperature T_0 = 20 °C. Calculation was carried out considering scientific recommendations [6] in the following way:

current density in the electrode

$$j = \frac{4I}{\pi d^2} = \frac{4 \cdot 290}{\pi \cdot 0.5^2} = 14.8 \text{ A/mm}^2,$$

Table 1. Temperature of section x of electrode heated by arc, and quantity of exothermic mixture in coating at different rate of electrode melting

Length of section x, cm	Quantity of exothermic mixture (%) at T (°C) and w (cm/s)								
	0	10.0	17.5	26.2	35.2	42.5	44.4	47.5	53.4
	0.475	0.505	0.525	0.55	0.575	0.6	0.615	0.63	0.645
0.09	1230	1190	1164	1131	1099	1069	1051	1034	1017
0.1	1159	1117	1090	1056	1023	992	973	955	938
0.2	640	595	565	531	499	469	451	435	419
0.5	108	89.5	79	67.5	57.7	49.4	44.1	41	37.3
1.0	5.6	3.8	2.97	2.3	1.6	1.2	0.96	0.8	0.7

Table 2. Experimental and calculation values of characteristics of melting of electrodes with exothermic mixture in coating at I_w = = 290 A

Index	Quantity of exothermic mixture, %								
	0	10.5	17.5	26.2	35.2	42.5	44.4	47.5	53.4
$\alpha_{c.m}$, g/(A·h)	8.7	9.4	9.7	10.2	10.4	10.9	11.2	11.4	11.6
α_d, g/(A·h)	8.1	9.1	9.7	10	10.9	11.4	12	12.2	13
U_a, V	25	25.7	26	26.5	27	27.3	27.5	27.7	28
Q_a, J/s	7250	7453	7540	7685	7830	7917	7975	8033	8120
Q_{chem}, J/s	0	45.2	138.7	274.6	442.5	619.5	701.6	777.3	926.5
w, cm/s	0.475	0.52	0.525	0.55	0.58	0.6	0.615	0.63	0.645
$v_{coat.m}$, g/s	0.40	0.42	0.44	0.47	0.50	0.54	0.56	0.58	0.59
Q_h, J/s	5220	5610	5716	6046	6405	6700	6886	7090	7373
m_{sl}, g	7.5	7.43	7.37	7.3	6.7	6.4	6.2	6.3	6.3
m_c, g	14	15	15.8	16.7	17.1	18.5	19.2	19.6	20
$m_{d.m}$, g	10.5	12.1	13.5	15	17.5	18.5	19.5	20	20.8
η_e	0.28	0.3	0.315	0.34	0.365	0.385	0.392	0.405	0.415
$\eta_{b.m}$	0.715	0.735	0.745	0.76	0.773	0.79	0.795	0.805	0.815
Q_e, J/s	2030	2236	2375	2613	2858	3048	3126	3253	3370

where I is the welding current, A; d is the core diameter, cm;

coefficients

$$w_0 = 2.4\cdot10^{-2}I^2 = 2.4\cdot10^{-2}\cdot14.8^2 = 5.26 \text{ deg/s};$$

$$b_0 = \frac{0.96\cdot10^{-2}}{d} = \frac{0.96\cdot10^{-2}}{5} = 0.192\cdot10^{-2} \text{ 1/deg};$$

$$nt = [5\cdot10^{-3}\cdot5.26 + 0.192\cdot10^{-2}(1 + 5\cdot10^{-3}\cdot20)]\cdot60 = 1.68;$$

$$\beta(\omega_0/b_0 + T_0) = 5\cdot10^{-3}(5.26/0.192\cdot10^{-2}) + 20) = 13.8.$$

According to known nomogram [6] coefficient $\beta T = 3.5$ and coefficient $\beta = 5\cdot10^{-3}$ 1/deg. In that case maximum temperature of heating of studied electrodes using optimum current makes $T = 3.5/5\cdot10^{-3} = 700$ °C.

Thermal effect of the exothermic reaction due to interaction of element-deoxidizers with iron oxide was determined on known equation [10]

$$Q_{chem} = \sum_{i=1}^{i=k} \frac{G_{m.c}}{t} K_m \frac{Q_{i\ ex.m}}{100} q_{i\ ex.m},$$

where $G_{m.c}$ is the quantity of molten core, g; K_m is the coating mass factor; $Q_{i\ ex.m}$ is the quantity of exothermic mixture in electrode coating at interaction of i-th element-deoxidizer (Al, Ti, Si, Mn) with iron oxide, %; $q_{i\ ex.m}$ is thermal effect of exothermic mixture at interaction of 1 % of ferrous oxide with element-deoxidizers, J/s.

Table 2 gives the indices of effect of quantity of exothermic mixture in the electrode coating on characteristics of their melting.

The results received showed that introduction of exothermic mixture in the electrode coating rises quantity of molten core in the ranges of 14–20 g and coating from 8 to 11.8 g at constant coating mass factor. It takes place mainly due to heat emitted during exothermic reaction, and reduction of heat consumed for coating melting due to corresponding reduction of gas-slag-forming section of the coating and rise of metallic constituent. Introduction of up to 53.4 % of exothermic mixture in the coating composition varies electrode heating coefficient from 0.280 to 0.415, at that, variation has directly proportional nature. Increase of quantity of deposited metal in the ranges of 10.5–20.8 g at almost similar quantity of slag on the plate shows that additional heating of the plate takes place mainly due to increase of quantity of electrode metal being transferred in the same time. The electrode with exothermic mixture in the coating can be used with maximum efficiency in welding and surfacing works, performance of which requires preliminary and concurrent heating and delayed cooling.

Conclusions

1. Introduction of up to 53.4 % of exothermic mixture in the electrode coating rises coefficient of core melting ($\alpha_{c.m}$ = 8.7–11.6 g/(A·h)) and deposition (α_d = 8.1–13.0 g/(A·h)), effective

efficiency of heating of base metal ($\eta_{b.m}$ = 0.715–0.815) and electrode (η_e = 0.280–0.415).

2. Introduction of exothermic mixture in the electrode coating increases rate of electrode melting due to rise of thermal power of arc; heat emitted during exothermic reaction; reduction of heat consumption for melting of gas-slag-forming section of the coating; improvement of technological properties of arc.

3. It is determined that maximum temperature of heating of the studied electrodes by passing optimum current makes 700 °C.

4. Temperature of 1000 °C, which makes exothermic reaction efficient, was received at around 1 mm distance from the electrode tip.

1. Karpenko, V.M., Vlasov, A.F., Bilyk, G.B. (1980) Factors of welding electrode melting with exothermic mixture in coating. *Svarochn. Proizvodstvo*, **9**, 23–25.
2. Ioffe, I.S. (1980) Effect of titanium thermal mixture in electrode coating on increase of welding efficiency. *Ibid*., **3**, 26–28.
3. Zarechensky, A.V. (1985) Peculiarities of melting of flux-cored strips with thermit mixtures. *Ibid*., **8**, 39–41.
4. Chigarev, V.V., Zarechensky, D.A., Belik, A.G. (2007) Peculiarities of melting of flux-cored strips with exothermic mixtures contained in their filler. *The Paton Welding J*., **2**, 46–48.
5. Vlasov, A.F., Karpenko, V.M., Leshchenko, A.I. (2006) Experimental definition of exothermic process proceeding in heating and melting of electrodes. *Visnyk DDMA*, 4(**2**), 65–68.
6. (1970) *Theoretical principles of welding*. Ed. by V.V. Frolov. Moscow: Vysshaya Shkola.
7. Ando, K., Nishiguchi, K. Mechanism of formation of pencil point-like wire tip in MIG welding. *IIW Doc. 212-156-68–69*.
8. Erokhin, A.A. (1973) *Principles of fusion welding*. Moscow: Mashinostroenie.
9. Vlasov, A.F., Oparin, Yu.N., Belaya, V.M. et al. *Composition of electrode coating*. USSR author's cert. 737175. Int. Cl. B 23K, 35/36. Fil. 10.11.77. Publ. 30.05.80.
10. Vlasov, A.F., Kushchy, A.M. (2011) Technological characteristics of electrodes with exothermic mixture in coating for surfacing of tool steels. *Svarochn. Proizvodstvo*, **4**, 10–15.

Received 16.04.2014

ULTRAVIOLET RADIATION IN MANUAL ARC WELDING USING COVERED ELECTRODES

O.G. LEVCHENKO[1], **A.T. MALAKHOV**[1] and **A.Yu. ARLAMOV**[2]
[1]E.O. Paton Electric Welding Institute, NASU
11 Bozhenko Str., 03680, Kiev, Ukraine. E-mail: office@paton.kiev.ua
[2]NTTU «Kiev Polytechnic Institute»
37 Pobedy Ave., 03056, Kiev, Ukraine

Welding arc is the source of intensive flow of optic radiation in infrared, visible and ultraviolet (UV) ranges, among which the most severe UV-C radiation with a strong harmful effect on the human organs of vision and skin covering should be distinguished. The aim of this work consisted in complex investigation of integral characteristics of UV radiation covered-electrode in manual arc welding (MAW), with covered electrodes of different grades (MR-3, UONI-13/55, ANO-12, ANO-36) and types of coatings (rutile, basic, rutile-cellulose), designed for welding of carbon and low-alloyed steels. The intensity of UV-C and UV-A radiation was measured using dosimeter of optic radiation DAU-81 at the distances of 0.55–1.50 m from the spot of welding. It was established during analysis and statistic processing of measurement results that at this distance at, which usually welder and support personnel are staying during MAW, the integral intensity of UV-C radiation amounts to 0.7–5 W/m^2, which 700–5000 times exceeds the standard value of 0.001 W/m^2 specified by the acting sanitary standards SN 4557–88 for workers with non-protected skin surfaces. Here the minimum distance, at which staying of the mentioned category of workers at direct visibility of welding place is admissible, amounts from 25 to 65 m (depending on the grade of electrode and value of welding current). Intensity of UV-C radiation depends, in the first turn, on the grade of applied electrodes but not on the type of their coating. It was shown that the intensity of UV radiation is inversely proportional to the square of distance from welding arc and greatly depends on welding current. The results of this work can be used in sanitary-hygienic certification of working stations of welders. 6 Ref., 4 Tables.

Keywords: *ultraviolet radiation, integral characteristics, safe distance, manual arc welding, covered electrodes*

Welding arc is the source of not only the intensive light flow in visible range and infrared radiation, but also of invisible ultraviolet radiation (UVR) at the wave length of 200–400 nm. According to the wave length UVR is subdivided into three ranges: UV-A (315–400 nm), UV-B (280–315 nm) and UV-C (200–280 nm). The most severe is UV-C radiation possessing an intensive harmful effect on the human organs of vision and skin covering. It should be noted that UV-C rays are almost absent in the spectrum of solar radiation at the earth surface, being intensively absorbed mainly in the upper ozone layer of atmosphere.

In spite of the importance of investigations of UVR in welding to provide safety of the personnel, the publications on this subject in the CIS countries are almost absent. The publications in the countries of the EU, the USA and Japan are of a specific nature characterized by a sanitary-hygiene orientation in evaluation of radiation in welding in compliance with the national standards different from those valid in Ukraine and the CIS countries.

Therefore, the aim of this work consisted in the complex investigation of integral characteristics of UVR in manual arc welding (MAW) using covered electrodes of different grades and types of coatings designed for welding of carbon and low-alloyed steels.

Methods of investigations. The investigations were carried out in MAW with electrodes of 4 mm diameter in flat position of a weld, indoor at the air temperature of 15–20 °C and average relative humidity of the air with exhaust ventilation over the place of welding. The welding source was welding rectifier VDU-506. Welding current was fixed at the values of 150, 175 and 200 A, corresponding to the range of recommended modes for electrodes ANO-4, ANO-12, ANO-36, MR-3, UONI-13/55. The sensor of UV-C and UV-A radiation of a single-channel automatic dosimeter of optic radiation (DAU-81) was located at the fixed distances of 0.55 (outstretched arm distance), 1.0 and 1.5 m from welding spot in the direction under the angle of 27–30° to the horizontal welding surface. The sensors were directed to the spot of welding arc under

the conditions of its direct visibility. The value of radiation dose (J/m^2) was fixed within 30–60 s. The value of average intensity of radiation E (W/m^2) was obtained by dividing the dose to the time of measurement. For monitoring this value was checked up with the values of arrow measurer of radiation intensity of the dosimeter DAU-81. To improve the reliability of results of experiments the measurements were repeated 2–3 times under the same conditions.

Investigations results. Processing of measurement data was carried out on PC using method of the least squares. It was established in the course of measurements that the intensity of radiation depends greatly on the distance d (m) to the radiation source (welding arc) and on welding current I (A). Preliminary the hypothesis was offered that at the given distances the intensity of radiation is governed by the law of inverse squares ($E \sim 1/d^2$). During processing of results of measurements this dependence was proved with a high accuracy. It should be noted that the same dependence was obtained in the work in CO_2 welding [1]. From the physical point of view, this corresponds to the conditions of free spreading of optic radiation from the spot source and means that the welding arc at the investigated interval of distances (0.55–1.50 m) can be considered as a spot source, from which the processes of absorption, diffusion dissipation and reflection of light flow do not considerably influence the spreading of radiation flow. This phenomenon is quite expected under the given conditions of welding and measurements. Then we shall write the dependence $E(d, I)$ as

$$E = \frac{a + bI}{d^2}. \quad (1)$$

The coefficients a and b were calculated using method of the least squares in the matrix form [2]. Such approach allowed including the results of measurements at different distances to the processing, which increased the validity of calculated coefficients due to growth in number of measurement spots. The obtained values of the coefficients are given in Table 1. The values of correlation coefficients R^2 in the Table indicate a quite high accuracy of relation between the factorial (current strength) and resulting (radiation intensity) characteristics.

Let us note that the similar (1) dependence of efficient intensity of radiation on welding current at a fixed distance from the place of welding was obtained in work [3]. The wider range of changes in welding current (45–250 A) was obtained by integration of measurements results in MAW using electrodes of different diameter.

For comparative evaluation of influence of electrode grade and coating on the intensity of radiation, Table 2 was compiled, where values of radiation intensity, calculated according to

Table 1. Coefficients of dependence (1) obtained as a result of processing of measurement data

Grade of electrode	Type of coating	UV-C			UV-A		
		a, W	b, W/A	R^2	a, W	b, W/A	R^2
UONI-13/55	Basic	–7.7275	0.0562	0.9736	–5.4838	0.0439	0.9645
ANO-12	Same	–10.14	0.0719	0.9901	–7.4335	0.0530	0.9562
MR-4	Rutile	–6.0125	0.0459	0.9942	–9.1275	0.0682	0.9310
MR-3	Same	–8.485	0.0629	0.9683	–9.4144	0.0706	0.9322
ANO-36	Rutile-cellulose	–8.8575	0.0627	0.9686	–9.5375	0.0730	0.9627

Note. R^2 — statistic correlation coefficient.

Table 2. Calculated values of UVR intensity (d = 1 m)

Grade of electrode	Type of coating	UV-C, W/m^2			UV-A, W/m^2		
		I, A			I, A		
		150	175	200	150	175	200
ANO-4	Rutile	0.87	2.0	3.2	1.1	2.8	4.5
UONI-13/55	Basic	0.70	2.1	3.5	1.1	2.2	3.3
ANO-36	Rutile-cellulose	0.55	2.1	3.7	1.4	3.2	5.1
ANO-12	Basic	0.65	2.4	4.2	0.5	1.8	3.2
MR-3	Rutile	0.95	2.5	4.1	1.2	2.9	4.7

formula (1) at different values of current at the distance of 1 m, are given.

In this Table the values of intensities of UV-C radiation are ranged in the growing order at the average value of welding current of 175 A. As is seen, approximately the same ranging is preserved also for 200 A current. At the lower boundary of the investigated range at the current of 150 A the ranging is considerably different. Obviously, it is connected with instability of arcing process at these modes of welding using electrodes of 4 mm diameter.

The analysis of Table 2 shows that emission of UV-C radiation in welding is determined by the grade of electrode but not by the type of its coating. The emission of UV-C rays in even greater extent depends on the strength of welding current. The significant current dependence allows assuming that intensity of optic radiation mainly depends on power generating in the zone of welding arc, and in the less extent on spectral peculiarities of radiation predetermined by the grade and type of electrode coating.

In compliance with the sanitary standards SN 4557–88 [4] in the industrial facilities the following admissible UVR intensities were established:

- admissible intensity of radiation of personnel at the presence of non-protected areas of skin surface of not more than 0.2 m^2 and radiation period of up to 5 min, at duration of pauses between them of not less than 30 min and total duration of effect per shift of up to 60 min, should not exceed, W/m^2: 50 for UV-A, 0.05 for UV-B, and 0.001 for UF-C radiation;
- admissible intensity of UVR of personnel with unprotected areas of skin surface is not more than 0.2 m^2 (face, neck, hands, etc.) at total duration of effect of radiation of 50 % of working shift and duration of one-time radiation of more than 5 min and more, should not exceed, W/m^2: 10 for UV-A and 0.01 for UV-B rays; radiation in the UV-C range at the mentioned duration is not admitted.

Considering these standards, let us define the safe distances d_s for workers with non-protected areas of skin surface, staying in the direction of direct visibility of welding place. Let us assume free spreading of UV rays with inverse-proportional dependence of intensity on square of distance $E \sim 1/d^2$. In this case the d_s value can be calculated according to formula

$$d_s = \sqrt{\frac{a + bI}{E_s}} \text{ (m)}, \qquad (2)$$

where a, b are the coefficients, the values of which are given in Table 1; E_s is the boundary admissible value of radiation intensity corresponding to the safety standards.

In Table 3 the calculated values of d_s at E_s = = 0.001 W/m^2 for UV-C and E_s = 50 W/m^2 for UV-A range are given.

As we see, minimum distances, at which the support personnel in MAW can stay in the direction of direct visibility of welding place, are very long in case of effect of UV-C rays. For UV-A radiation these distances are considerably smaller, therefore, the spectrum area determining the safety is the UV-C radiation. In case of necessity of staying of support personnel in a quite wide area of dangerous effect it is necessary to take measures for protection of skin covering and eyes from the mentioned radiation.

In Table 3 the safe distances are given for temporary characteristics of effect according to sanitary standards SN 4557–88 valid in Ukraine. In particular, during the working shift the summed time of effect of UV-C radiation should not exceed 60 min. In the EU countries the conditions of safety are determined by Directive 2006/25/EC [5]. In particular, the limited efficient dose of UVR effect during the working shift (8 h) is restricted by the value H_{es} = = 30 J/m^2. Knowing the value of intensity of UV-C radiation under the specified conditions the admissible time of effect t_s can be calculated by dividing H_{es}/E. In Table 4 the calculated values of safe distances at the certain time of effect of UV-C radiation are given. For the preset time of effect t_s the admissible value $E_s = H_{es}/t_s$ was found, and then the d_s value was calculated according to formula (2).

It should be noted that calculated values of safe distances obtained using the analogue method [6], are not considerably differ from the values given in Table 4.

Comparison of values in Tables 3 and 4 show that at the same intensity of radiation the sanitary

Table 3. Calculated values of safe distances (d_s, m) at the UVR effect on support personnel in MAW

Grade of electrode	UV-C			UV-A		
	I, A			I, A		
	150	175	200	150	175	200
ANO-4	30	45	57	0.15	0.24	0.30
UONI-13/55	27	46	60	0.15	0.21	0.26
ANO-36	24	46	61	0.17	0.25	0.32
ANO-12	26	49	65	0.10	0.19	0.25
MR-3	31	50	64	0.16	0.24	0.31

Table 4. Calculated values of safe distances (d_s, m) at the UV-C radiation effect on support personnel in MAW depending on time of effect (I = 200 A)

Grade of electrode	t_s, min						
	1	10	30	60	120	240	480
	E_s, W/m^2						
	0.5	0.05	0.017	0.008	0.004	0.002	0.001
ANO-4	2.6	8.2	14	20	29	40	57
UONI-13/55	2.7	8.7	15	21	30	42	60
ANO-36	2.8	8.8	15	22	31	43	61
ANO-12	3.0	9.4	16	23	33	46	65
MR-3	2.9	9.2	16	23	32	45	64

standards SN 4557–88, unlike the EU standards specify the more severe restrictions for the admissible time of effect. Besides, the EU standards admit the effect of UV-C radiation with intensity of more than 0.001 W/m^2, which is prohibited by SN 4557–88. In this sense the EU standards are developed in the greater details, flexible and grounded from the physical point of view.

Conclusions

1. It was established that at the distances from 0.5 to 1.5 m, at which welder and support personnel are usually staying in MAW using covered electrodes, the integral intensity of UV-C radiation amounts from 0.7 to 5 W/m^2, which 700–5000 times exceeds the standard value of 0.001 W/m^2 specified by the efficient sanitary standards SN 4557–88 for working personnel with non-protected areas of skin surface. Here, the minimum distances, at which staying of the mentioned category of workers at direct visibility of welding place is admissible, amounts from 25 to 65 m (depending on grade of electrode and strength of welding current).

2. It was established that the intensity of UV-C radiation depends, in the first turn, on the grade of applied electrodes but not on the type of their coating (rutile, basic, rutile-cellulose). It was shown that intensity of UVR is inversely proportional to the distance from welding arc.

1. Okuno, T, Ojima, J., Saito, H. (2001) Ultraviolet radiation emitted by CO_2 arc welding. *Annals Occup. Hygience*, 45(**7**), 597–601.
2. Magnus, Ya.R., Katyshev, P.K., Peresetsky, A.A. (1998) *Econometrics: Basic training*. Moscow: Delo.
3. Schwass, D., Witllich, M., Shmitz, M. et al. (2011) Emission of UV radiation during arc welding. *www.dguv.de/ifa. 1–12*
4. *SN 4557–88*: Sanitary norms of ultraviolet radiation in production premises. Introd. 23.02.1988. Moscow: Minzdrav SSSR.
5. *Directive 2006/25/EC* of the European Parliament and of the Council of 5 April 2006 on the minimum health and safety requirements regarding the exposure on workers to risks arising from physical agents (artificial optical radiation).
6. Terry, L. Lyon. (2002) Knowing the dangers of actinic ultraviolet emissions. *Welding J.*, Dec., 28–30.

Received 09.04.2014

TOWARDS THE PROBLEM OF DISPERSITY AND MORPHOLOGY OF PARTICLES IN WELDING AEROSOLS

I.P. GUBENYA[1], **I.R. YAVDOSHCHIN**[1], **S.N. STEPANYUK**[1] and **A.V. DEMETSKAYA**[2]
[1]E.O. Paton Electric Welding Institute, NASU
11 Bozhenko Str., 03680, Kiev, Ukraine. E-mail: office@paton.kiev.ua
[2]Institute of Occupational Health, AMSU
75 Saksagansky Str., 03680, Kiev, Ukraine. E-mail: torovchik@mail.ru

The hard component of welding aerosol is one of the main hazards, which are encountered by those working with welding and related technologies. The investigations on this subject have been carried out for more than half a century. The size and dispersity of the particles are of particular interest among the properties and peculiarities of structure of hard component of welding aerosol, as these parameters define the ways of penetrating into a living organism. The present study examines dispersity of particles of hard component of welding aerosol by means of several types of equipment, involving different analysis principles. It was shown that the technique of preparation of a sample for analysis and peculiarities of equipment greatly influence the results. The morphology of particles was also examined. 20 Ref., 5 Figures.

Keywords: *welding aerosol, hard component, dispersity, morphology, nanoparticle, agglomerate, laser granulometry, diffusion spectrometer*

For more than half a century, welding aerosol has been one of the main objects of investigation of negative factors affecting human organism in the process of welding. Nowadays these investigations are of extreme importance in view of new data in medicine and toxicology.

Welding aerosol is a by-product of welding process and consists of hard and gassy components, predetermined by its formation processes. Under high-temperature heating during welding, the components of coating undergo thermal destruction, and some part of base and electrode materials evaporates. As a result of blowing out of the formed gas-vapor mixture into relatively low-temperature environment, condensation of vapor phase occurs and the small hard particles are formed [1]. The primary object of investigation is the hard component of welding aerosol (HCWA), as it contains main hazardous constituents.

The HCWA influence on a living organism (toxicity) is a complex characteristic and depends on many factors, namely size and morphology of single particles or their agglomerates, total quantitative distribution by sizes (dispersity), chemical composition, content of highly-toxic compounds, solubility. Each of these factors should be analyzed separately and in combination with others.

The size of particles is an important factor, which to a great extent determines the HCWA toxicity: solid particles with a diameter of less than 20 μm may remain suspended in air flow [2]. Size of single particles and their agglomerates varies from several dozens of nanometers to dozens of micrometers [3–5]. About 70–80 % of particles with a diameter of 0.1–2.0 μm, which penetrate into organism through respiratory organs, may be removed in breathing out. The particles of coarser size may be removed from the organism by spitting [6, 7]. The most hazardous are nanosized and submicron particles, which due to their small size may penetrate through skin [8], as well as directly to brain via nerve endings [9–12].

The particles of HCWA are of regular and irregular spherical shape. The majority of particles has heterogeneous structure (particles consist of core and shell) [1, 13, 14], which is predetermined by selectivity of the process of evaporation and condensation (various constituents of high-temperature vapor are condensed at different temperature). First, the condensation of the elements with lower vapor pressure and higher melting temperature (manganese, iron) occurs, and then the elements with higher vapor pressure and lower melting temperature (sodium, potassium, silicon and others) condense. Thickness of shell depends on temperature and oxidation potential of arc atmosphere [1]. Figure 1 shows the appearance of particles and agglomerates of HCWA.

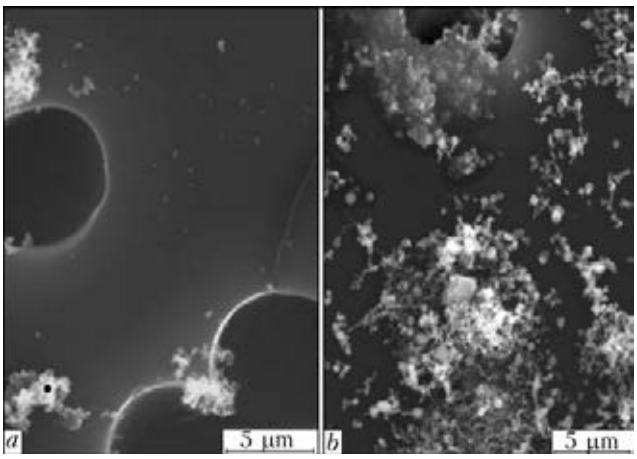

Figure 1. Typical size and morphology of HCWA particles [15]: *a* — coarse particle with deposition of nanosized particles; *b* — agglomerates of nanosized particles

Dispersity is analyzed by using several types of equipment, operating on different principles. The aerodynamic separation (Berner and Anderson impactors) [2–5, 15, 16] is the most widely applied method. The method of measurement of charged particles mobility in electric field (SMPS scanning analyzers) [2, 16, 17] is applied more rarely. Laser granulometry (laser analyzers with flow-through and fixed cells) [18] is relatively new and scarcely applied method.

It is difficult to define the characteristics of single particles in common with their total quantitative distribution by sizes due to the wide range of particle sizes. The substantial drawback of applying aerodynamic separation method is destruction of clusters as a result of collision in their passing through separate levels of the impactor. The drawback of the HCWA analysis, carried out by the method of laser granulometry, is the specifics of technique of preparation and carrying out of analysis, namely mechanical effect on the mass of deposited aerosol in its separating from the filter, use of dispersion medium (usually it is distilled water with or without surface active agent), and ultrasonic oscillations. The most promising method is the HCWA investigation using equipment, which analyzes the particles directly in air flow, namely diffusion, laser and electrical analyzers.

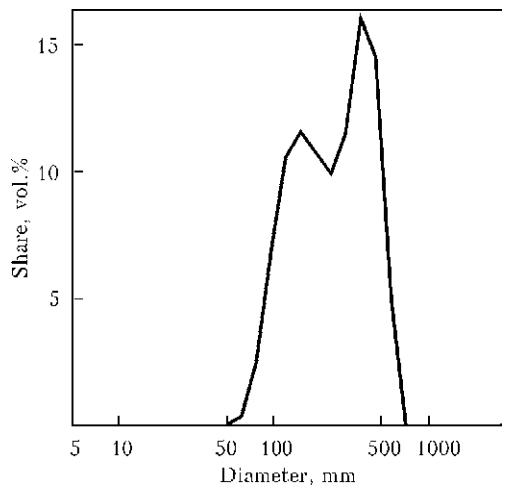

Figure 2. Dispersity of HCWA particles obtained by means of Zetasizer 1000 HS instrument

To examine the morphology of single particles, the electron microscopy is applied (SEM, TEM, EPMA electron probe) [3, 5, 7, 16, 19, 20]. In this case, HCWA is deposited on metal substrates.

To examine the dispersity, the Malvern Zetasizer 1000 HS (Great Britain, measurement range of 0.002–3 μm, fixed cell), HORIBA LA-300 (Japan, measurement range of 0.1–600 μm, flow-through cell), and AeroNanoTech diffusion aerosol spectrometer DAS 2702 (Russia, measurement range of 3–200 μm, analysis in air flow) were used.

It should be mentioned that the equipment for dispersity analysis has limited measurement range, which makes it difficult to get comprehensive and real description of HCWA characteristics.

The first two analyzers are working on the principle of laser granulometry method, while the third one is working on the method of transmission of the air flow with particles through diffusion batteries and determination of deposition (or slippage) coefficient of aerosol particles during passing. In each case, the object of investigation was HCWA, obtained in welding with rutile-type electrodes.

The technique of standard sampling of HCWA (mechanical separation of the aerosol deposited on filter) leads to the formation of «briquette» accumulation, and mechanical disintegration does not allow obtaining the qualitative object for analysis. Thus, the ultrasonic treatment was applied to destroy briquettes.

To carry out the investigation by means of Zetasizer 1000 HS, the HCWA, removed from the filter, was crushed mechanically and put into the container, filled with distilled water and surface active agent (1 % solution of sodium hexametaphosphate). The suspension was stirred for 10 min in the UZDN-A ultrasonic disperser, then put in the cuvette, filled with dispersion medium for the two-thirds, and then the analysis was carried out (Figure 2).

The obtained data prove that the HCWA has a bimodal distribution of particles by sizes. The average particle diameter for each spike is 156 and 370 nm.

To analyze by means of HORIBA LA-300, the HCWA sample, obtained by removing the deposited aerosol from filter, was put into the analyzer

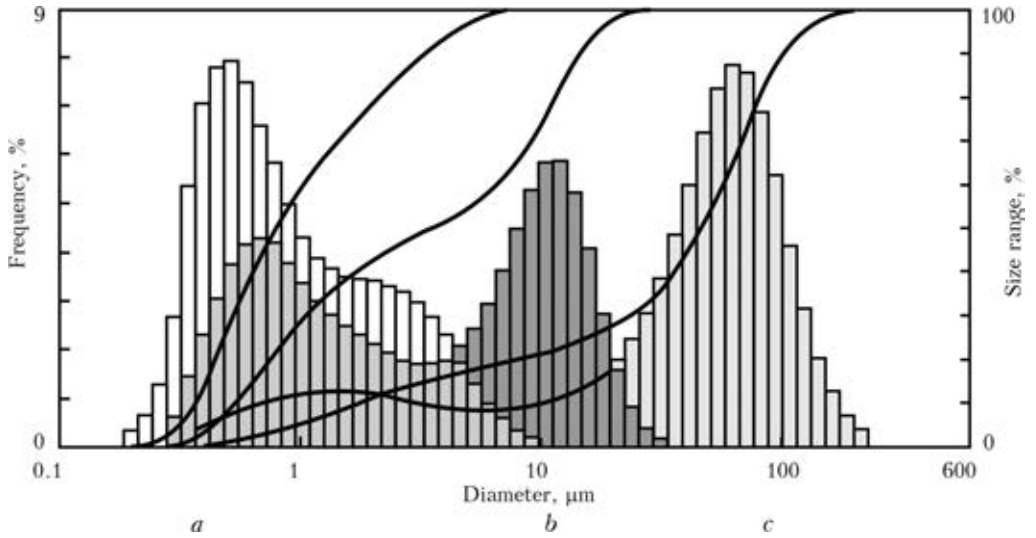

Figure 3. Range of HCWA distribution by sizes after 30 s ultrasonic treatment (*a*), at medium speed of purge pump without ultrasonic treatment (*b*) and at minimum speed of purge pump without ultrasonic treatment (*c*)

cuvette, filled with the distilled water. The analysis of each sample was made in three stages: immediately after sample putting at the minimum speed of the purge pump without ultrasonic treatment; repeatedly at the medium speed of the purge pump without ultrasonic treatment, and at the medium speed of the purge pump after ultrasonic treatment for 30 s.

HCWA sample, after its putting into distilled water, represented rather coarse agglomerates of 50–80 μm average size (Figure 3, spike *c*). However, when the speed of the purge pump was increased, the agglomerates were refined to the average size of 10 μm (spike *b*) and considerable amount of constituents of less than 1 μm size appeared. The application of ultrasonic treatment causes their further destruction. As a result, the average size of the fine-dispersed fraction makes up about 0.5–0.6 μm (spike *a*). In all three cases, the HCWA has a bimodal distribution.

Thus, the samples, obtained by mechanical removing of HCWA from the filter, are hardly suitable for analysis without additional ultrasonic treatment, which duration changes significantly the results of analysis. The further treatment can, probably, provoke the destruction of agglomerates, formed in the air flow, and represent the natural shape of HCWA, that does not make it possible to judge about real sizes of particles and agglomerates.

To investigate the HCWA by means of DAS 2702, the air intake was realized at the distance of 70–80 cm from the arc burning zone. The process of analysis started since the moment of arc ignition and continued after completion of arcing till the beginning of substantial total reduction

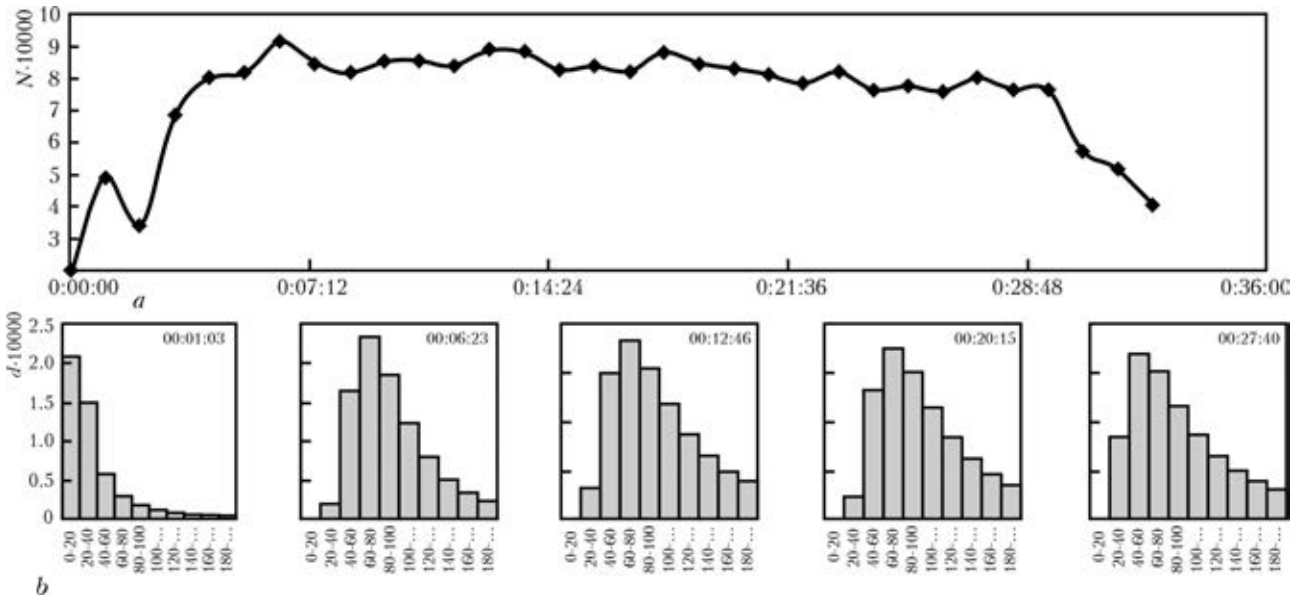

Figure 4. Change in amount of particles *N* (*a*) and their size distribution *d* within time of analysis (*b*) using DAS 2702 spectrometer

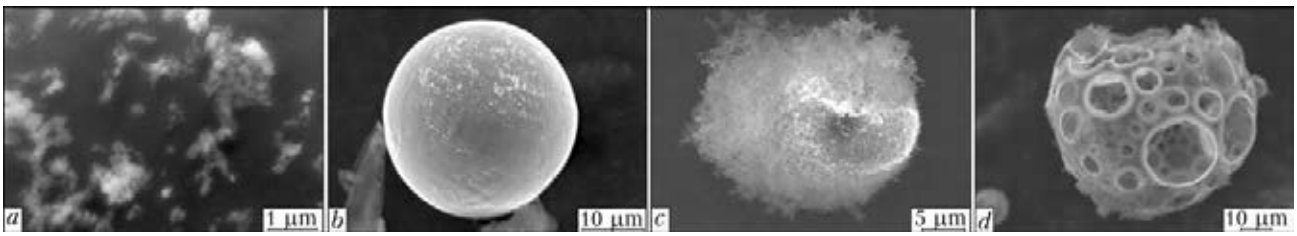

Figure 5. Results of examination of morphology of agglomerates (*a*) and particles (*b–d*) of HCWA

of the amount of particles. Before the analysis started, the background amount of particles was determined.

The obtained results (Figure 4) prove that there is a great amount of primary particles of about 20 nm size in the HCWA immediately upon the start of welding process. As a result of fast agglomerating, their amount increases rapidly, and they are missing in the air flow already after several minutes upon completion of welding. However, the amount of nanosized particles remains high and the spike occurs at the size range of 60–80 nm.

Sampling for investigation of morphology of the HCWA particles was realized by deposition of the latter on the adhesive carbon film, located at the wall of chamber for sampling the HCWA bulk samples at the height of 70 cm from the welding arc zone. Such an approach allows us not only to obtain the sample with the monolayer of particles, but also to examine their morphology (Figure 5). The examination was carried out in JEOL scanning electron microscopes JSM-35CF and JSM 6490-LA.

The morphology of particles, formed during welding, is heterogeneous. The nanosized particles form agglomerates (Figure 5, *a*), which may consist both of several particles, and also of several thousands. There are also coarse round particles, having the size from several micrometers to several tens of micrometers (Figure 5, *b*). Sometimes they have cavity inside (Figure 5, *d*), which explains their ability to reach considerable height (70 cm) in the flow of welding aerosol. Most often, these particles are formed due to metal spattering. Moreover, they are ofteny covered with the layer of nanosized particles (Figure 5, *c*).

Thus, the results, obtained in course of the HCWA analysis by using different types of equipment and different techniques of preparation of samples and their analysis itself, may diverge considerably. The results, obtained by using the «no-contact» analysis in DAS 2702 spectrometer, may be considered as the most valid ones.

1. Pokhodnya, I.K., Gorpenyuk, V.N., Milichenko, S.S. et al. (1990) *Metallurgy of arc welding. Processes in arc and melting of electrodes*. Ed. by I.K. Pokhodnya. Kiev: Naukova Dumka.
2. (2001) *Aerosol measurement: Principles, techniques and applications*. 2nd ed. Wiley-Interscience Publ.
3. Sowards, J.W., Lippold, J.C., Dickinson, D.W. et al. (2008) Characterization procedure for the analysis of arc welding fume. *Welding J.*, **87**, 76–83.
4. Sowards, J.W., Lippold, J.C., Dickinson, D.W. et al. (2008) Characterization of welding fume from SMAW electrodes. Pt 1. *Ibid.*, **87**, 106–112.
5. Sowards, J.W., Lippold, J.C., Dickinson, D.W. et al. (2010) Characterization of welding fume from SMAW electrodes. Pt 2. *Ibid.*, **89**, 82–89.
6. Hewett, P. (1995) The particle size distribution, density and specific area of welding fumes from SMAW and GMAW mild and stainless steel consumables. *Amer. Ind. Hygiene Assoc. J.*, **56**, 128–135.
7. Sterjovski, Z., Norrish, J., Monaghan, B.J. The effect of voltage and metal-transfer mode on particulate-fume size during the GMAW of plain-carbon steel. *IIW Doc. VIII-2092–08*.
8. Hoet, P.H.M., Brueske-Hohlfeld, I., Salata, O.V. (2004) Nanoparticles known and unknown health risks. *J. Nanobiotechnol.*, 12(**2**).
9. Raloff, J. (2010) Destination brain. *Sci. News*, 177(**11**), 16–20.
10. Glushkova, A.V., Radilov, A.S., Rembovsky, V.R. (2007) Nanotechnologies and nanotoxicology: Opinion on the problem. *Toksikolog. Vestnik*, **6**, 4–8.
11. Elder, A., Gelein, R., Silva, V. (2006) Translocation of inhaled ultrafine manganese oxide particles to the central nervous system. *Environ. Health Perspect.*, 114(**8**), 1172–1178.
12. Simko, M., Fiedeler, U., Gazso, A. et al. (2010) Can nanoparticles end up in the brain. *NanoTrust-Dossier*, **14**.
13. Voitkevich, V. (1995) *Welding fumes: Formation, properties and biological effects*. Cambridge: Abington Publ.
14. Terjovski, J., Drossier, J., de Thoisy, E. et al. (2006) An investigation of particulate weld fume generated from GMAW of plain carbon steel. *Austral. Welding J.*, **51**(1st quart.), 21–40.
15. Worobiec, A., Stefaniak, E.A., Kiro, S. et al. (2007) Comprehensive microanalytical study of welding aerosols with X-ray and Raman based methods. *X-Ray Spectrometry*, **36**, 328–335.
16. Berlinger, B., Benker, N. et al. (2011) Physicochemical characterization of different welding aerosols. *Analyt. Bioanalyt. Chemistry*, **10**, 1773–1780.
17. Zimmer, A.E., Biswas, P. (2001) Characterization of the aerosols resulting from arc welding processes. *Aerosol Sci.*, **32**, 993–1008.
18. Kippax, P. (2005) Measuring particle size using modern laser diffraction techniques. *Paint & Coatings Industry*, **21**, Issue 8, 42.
19. Carpenter, K.R., Monaghan, B.J., Norrish, J. (2009) Analysis of fume formation rate and fume particle composition for gas metal arc welding (GMAW) of plain carbon steel using different shielding gas compositions. *ISIJ Int.*, 49(**3**), 416–420.
20. Jenkins, N.T., Eager, T.W. (2005) Chemical analysis of welding fume particle. *Welding J.*, **6**, 87–93.

Received 24.04.2014

STATUS OF NORMATIVE BASE, CERTIFICATION AND ATTESTATION OF WELDING CONSUMABLES IN UKRAINE

N.A. PROTSENKO
E.O. Paton Electric Welding Institute, NASU
11 Bozhenko Str., 03680, Kiev, Ukraine. E-mail: office@paton.kiev.ua

Membership in the World Trade Organization and preparation for signing of agreement with the European Union oblige Ukraine to carry out harmonization of National standards with International and European ones. Technical Committee «Welding and allied processes», created on basis of the E.O. Paton Electric Welding Institute of the NAS of Ukraine, carries out the works on harmonization of standards, determining the requirements to welding production. These requirements refer to production, testing and classification of welding consumables. A list of indicated standards is shown below.

Today Ukraine has the National Certification System (UkrSEPRO), which includes mandatory certification of products, indicated in the List of Products being subjected to mandatory certification in Ukraine, and facultative certification, determining conformity of characteristics of the products to requirements of the normative documents, which are specified by customer. Welding consumables refer to facultative UkrSEPRO System of Product Certification. A result of certification of welding consumables is a Certificate of Conformity, recognized in the countries, with which Ukraine has a bilateral agreement on mutual recognition of certification results.

1. Covered electrodes for manual arc welding

EN ISO 2401	Covered electrodes. Determination of the efficiency, metal recovery and deposition coefficient
EN ISO 2560	Welding consumables. Covered electrodes for manual metal arc welding of non-alloy and fine grain steels. Classification
EN ISO 18275	Welding consumables. Covered electrodes for manual metal arc welding of high-strength steels. Classification
EN ISO 636	Welding consumables. Rods, wires and deposits for tungsten inert gas welding of non-alloy and fine-grain steels. Classification
EN ISO 1071	Welding consumables. Covered electrodes, wires, rods and tubular cored electrodes for fusion welding of cast iron. Classification
EN ISO 14172	Welding consumables. Covered electrodes for manual metal arc welding of nickel and nickel alloys. Classification
EN ISO 3580	Welding consumables. Covered electrodes for manual metal arc welding of creep-resisting steels. Classification
EN ISO 3581	Welding consumables. Covered electrodes for manual metal arc welding of stainless and heat-resisting steels. Classification
EN ISO 6848	Arc welding and cutting. Non-consumable tungsten electrodes. Classification

2. Solid welding wires, solid strips and rods

EN ISO 14341	Welding consumables. Wire electrodes and weld deposits for gas shielded metal arc welding of non-alloy and fine-grain steels. Classification
EN ISO 14343	Welding consumables. Wire electrodes, strip electrodes, wires and rods for arc welding of stainless and heat resisting steels. Classification
EN ISO 16834	Welding consumables. Wire electrodes, wires, rods and deposits for gas-shielded arc welding of high strength steels. Classification

EN ISO 18273	Welding consumables. Wire electrodes, wires and rods for welding of aluminium and aluminium alloys. Classification
EN ISO 18274	Welding consumables. Wire and strip electrodes, wires and rods for fusion welding of nickel and nickel alloys. Classification
ISO/CD 19288	Welding consumables. Solid wire electrodes, solid wires and rods for fusion welding of magnesium and magnesium alloys. Classification
EN ISO 21952	Welding consumables. Wire electrodes, wires, rods and deposits for gas shielded arc welding of creep-resisting steels. Classification
EN ISO 24034	Welding consumables. Solid wire electrodes, solid wires and rods for fusion welding of titanium and titanium alloys. Classification
EN ISO 24373	Welding consumables. Solid wires and rods for fusion welding of copper and copper alloys. Classification
EN ISO 24598	Welding consumables. Solid wire electrodes, tubular cored electrodes and electrode-flux combinations for submerged arc welding of creep-resisting steels. Classification
EN ISO 26304	Welding consumables. Solid wire electrodes, tubular cored electrodes and electrode-flux combinations for submerged arc welding of high strength steels. Classification
EN ISO 6848	Arc welding and cutting. Non-consumable tungsten electrodes. Classification

3. Tubular cored electrodes

EN ISO 17632	Welding consumables. Tubular cored electrodes for gas shielded and non-gas shielded metal arc welding of non alloy and fine grain steels. Classification
EN ISO 17633	Welding consumables. Tubular cored electrodes and rods for gas shielded and non-gas shielded metal arc welding of stainless and heat-resisting steels. Classification
EN ISO 17634	Welding consumables. Tubular cored electrodes for gas shielded metal arc welding of creep-resisting steels. Classification
EN ISO 18276	Welding consumables. Tubular cored electrodes for gas-shielded and non-gas-shielded metal arc welding of high-strength steels. Classification
EN ISO 12153	Welding consumables. Tubular cored electrodes for gas shielded and non-gas shielded metal arc welding of nickel and nickel alloys. Classification

4. Welding consumables for hardfacing

EN 14700	Welding consumables. Welding consumables for hard-facing

Welding fluxes

EN ISO 14171	Welding consumables. Solid wire electrodes, tubular cored electrodes and electrode/flux combinations for submerged arc welding of non-alloy and fine grain-steels. Classification
EN ISO 14174	Welding consumables. Fluxes for submerged arc welding and electroslag welding. Classification

5. Shielding gases

EN ISO 14175	Welding consumables. Gases and gas mixtures for fusion welding and allied processes

6. Testing of welding consumables

EN ISO 3690	Welding and allied processes. Determination of hydrogen content in arc weld metal
EN ISO 6847	Welding consumables. Deposition of a weld metal pad for chemical analysis
ISO 8249	Welding. Determination of Ferrite Number (FN) in austenitic and duplex ferritic-austenitic Cr–Ni stainless steel weld metal
ISO/TR 13393	Welding consumables. Hardfacing classification. Microstructures
EN ISO 14372	Welding consumables. Determination of moisture resistance of manual metal arc welding electrodes by measurement of diffusible hydrogen
EN ISO 4136	Destructive tests on welds in metallic materials. Transverse tensile test
EN ISO 5173	Destructive tests on welds in metallic materials. Bend tests

EN ISO 17639	Destructive tests on welds in metallic materials. Macroscopic and microscopic examination of welds
EN ISO 9015-1	Destructive tests on welds in metallic materials. Hardness testing. Part 1: Hardness test on arc welded joints
EN ISO 9015-2	Destructive tests on welds in metallic materials. Hardness testing. Part 2: Microhardness testing of welded joints
EN ISO 15610	Pecification and qualification of welding procedures for metallic materials. Qualification based on tested welding consumables
EN ISO 15792-1	Welding consumables. Test methods. Part 1: Test methods for all-weld metal test specimens in steel, nickel and nickel alloys
EN ISO 15792-2	Welding consumables. Test methods. Part 2: Preparation of single-run and two-run technique test specimens in steel
EN ISO 15792-3	Welding consumables. Test methods. Part 3: Classification testing of positional capacity and root penetration of welding consumables in a fillet weld
EN ISO 14532-1	Welding consumables. Test methods and quality requirements. Part 1: Primary methods and conformity assessment of consumables for steel, nickel and nickel alloys
EN ISO 14532-2	Welding consumables. Test methods and quality requirements. Part 2: Supplementary methods and conformity assessment of consumables for steel, nickel and nickel alloys
EN ISO 14532-3	Welding consumables. Test methods and quality requirements. Part 3: Conformity assessment of wire electrodes, wires and rods for welding of aluminium alloys

7. Requirements to quality and delivery of welding consumables

EN ISO 544	Welding consumables. Technical delivery conditions for welding filler materials and fluxes. Type of product, dimensions, tolerances and markings
EN 10204	Metallic materials. Types of inspection documents
EN 13479	Welding consumables. General product standard for filler metals and fluxes for fusion welding of metallic materials
EN ISO 14344	Welding and allied processes. Flux and gas shielded electrical welding processes. Procurement guidelines for consumables

According to Ukrainian course for European integration, a transfer from product certification in UkrSEPRO system to verification of its conformity with technical regulations, determining the requirements for products in respect of safety and activity of human and environment as well as methods of its assessment based on these requirements, takes place at present time. The approval of conformity of products, which come under Technical regulations, is mandatory based on Ukrainian laws «On Approval of Conformity» and «On Standards, Technical Regulations and Conformity Assessment Procedures». In accordance with the Conformity Assessment Procedure, Technical regulations provide for the Conformity Assessment Modules:

Module A	Internal production control	
Module B Type examination	Module C	Internal production control
	Module D	Quality assurance of the production process
	Module E	Product quality assurance
	Module F	Product verification
Module G	Each unit verification	
Module H	Full quality assurance acc. to ISO 9001	

A module for performance of Conformity Assessment Procedure is chosen depending on type of product, its description and functional peculiarities, present or potential risks, necessity of participation of the third independent party in conformity assessment.

Certification procedure, based on European Directives and Technical regulations, is divided on modules (schemes of certification):

- A — internal production control, Conformity declaration;
- A1 — internal production control plus supervised product testing;
- A2 — internal production control plus supervised product checks at random intervals;
- B — type examination;
- C — conformity to type based on internal production control «Type conformity declaration»;
- C1 — conformity to type based on internal production control plus supervised product testing;
- C2 — conformity to type based on internal production control plus supervised product checks at random intervals;

• D — conformity to type based on quality assurance of the production process;

• D1 — quality assurance of the production process;

• E — conformity to type based on product quality assurance;

• E1 — quality assurance of final product inspection and testing;

• F — conformity to type based on product verification;

• F1 — conformity based on product verification (Conformity certificate CE);

• G — conformity based on unit verification;

• H — conformity based on full quality assurance;

• H1 — conformity based on full quality assurance plus design examination.

Manufacturers of welding consumables in order to expand product markets and satisfy the consumers should fulfill the requirements of legislative and normative base of probable market.

In accordance with EN 13479 the manufacturer of welding consumables should develop, verify by documents and continuously maintain own system of plant production control (PPC) in order to guaranty that the products, proposed in the market, confirm the indicated characteristics. PPC system should consist of procedures, regular checks and tests and/or assessments and application of the results in control of raw, component materials, production process and products. Development of PPC system should be based on requirements of EN ISO 9001 and EN 12074.

It is also necessary to develop a program and carry out primary tests of indices of welding properties and characteristics based on classification of welding consumables in accordance with requirements of the standards, indicated in sections 1–5 of given above List of welding consumables. Types of tests and frequency of their performance should correspond to guidelines, given in EN ISO 544, ISO 15792-1, ISO 15792-2, ISO 15792-3, and EN 14532-1. The requirements for testing of welding consumables as well as allowable values and deviations should correspond to section 6 of EN 13479.

It is reasonable from economic point of view to carry out primary tests of welding consumables, considering the requirements of EN ISO 15610, and invite the third party for simultaneous receiving of Welding Procedure Qualification Record according to the requirements of series of standards EN ISO 15614 «Specification and qualification of welding procedures for metallic materials». At that, full complex of tests is carried out using classified grade of welding consumables and control welded joints by means of visual testing, radiographic or ultrasonic, magnetic particle or die-penetrant flaw detection, transverse tensile tests, transverse bend, impact toughness, hardness, macroscopic examination and, if necessary other tests, for examples, intercrystalline corrosion.

The results of tests listed above can be used for verification of conformity to the requirements of Technical regulations and European Directives, if welded structures were made using classified welding consumables, which are subjected to mandatory marking by National Conformity Mark or CE Conformity Mark.

The conformity marks indicate that these products were manufactured in accordance with acting Technical regulations and European Directives, and fulfill the critical requirements regarding safety of its operation and have no negative effect on environment.

Manufacturer or its authorized representative are responsible for applying of Conformity mark on welding consumable or, if it is possible, it can be marked on assembly label, package or accompanying documents for corresponding products.

Below is given the information which should be indicated on label, package and/or accompanying documents for corresponding products:

CE	Marking of CE conformity which consists of CE symbol, given in Directive 93/68/EEC
1234	Identification number of authorized body (if necessary)
AnyCo Ltd, PO Box 21 B-1050 14	Name or trade mark Address of manufacturer Last to figures of the year, when the making was made
1234-CPD-00234	Number of certificate (if necessary)
EN 13479+EN ISO 2560	Numbers of European standards
Coated electrode EN ISO 2560 — E46 3 1Ni B 54 H5 Hazardous substance «x» < «n»·10^{-6} (ppm)	Characteristics of welding consumable

If production of welding consumables is declared, the manufacturer completes the declaration, example of which is shown in new version of standard EN 13479.

Received 05.05.2014

EFFECT OF CHARGE GRAIN COMPOSITION ON RHEOLOGICAL CHARACTERISTICS AND STRUCTURE OF PRESSURE FLOW OF COMPOUNDS FOR LOW-HYDROGEN ELECTRODES

A.E. MARCHENKO
E.O. Paton Electric Welding Institute, NASU
11 Bozhenko Str., 03680, Kiev, Ukraine. E-mail: office@paton.kiev.ua

It is determined in course of investigation of compound of low-hydrogen electrodes UONI-13/55, carried out with the help of capillary viscosimeter, that their rheological indices and structure under flow pressure condition significantly depend on grain composition of coating materials. Charge should contain 50 % of fine fraction from point of view of minimizing of energy consumption, necessary for extrusion application of compounds on rods. Deviation of its portion in one or another side from indicated optimum significantly rises energy consumption on electrode extrusion. The compounds with fine- or coarse-grain filler are not similar to each other on structure. It confirms nature of change of level of compound dissipative heating, value of natural convergence angle in entrance zone (to capillary) as well as shape of deformation (extrusion) curves at increase of flow velocity. Profile of flow of compounds with coarse-grain filler expands at rise of pressure jet rate. It remains virtually of the same narrow shape as at creep flow velocities for flow of compounds with fine-grain filler. The results of analysis of form of extrusion curves $P = f(t)$ indicate that pressure flow of compound with coarse-grain filler is realized on viscosity mechanism. The compounds with excessive content of fine-grain filler are more structured, since liquid glass binder in these cases in addition to filling of intergrain voids should cover significantly more developed grain surface. Rise is observed in their molecular interaction and strength of structure formed by them, which is fractured in deformation and accompanied by specific phenomena of unsteady flow. 8 Ref., 2 Tables, 8 Figures.

Keywords: *low-hydrogen welding electrodes, coating thickness difference, rheology of compounds, viscosity and elasticity indices of compounds*

Grain composition of coating materials significantly effects consistency and technological properties of electrode compounds. It is confirmed by results of investigation of viscosity of UONI-13/55 compound, published in [1, 2]. It was evaluated as pressure loss in pumping of compound from feed cylinder of viscosimeter in round nozzle of 5 mm diameter and 50 mm length at constant consumption $Q = 5$ cm^3·s^{-1} (average gradient of shear rate 100 s^{-1}). Powders for dry charge were composed of preliminary screened fractions of materials in order to receive continuous packing of particles with two earlier selected indices of dispersion and polydispersity for each of them. Afterwards, prepared in such a way powders were taken in proportions, specified in mathematic plan of experiment so that grain composition of charge was changed in the limits, which can be found in practice of electrode production, i.e. volume fraction of particles finer than 0.063 mm in the charge was varied in the limits from 5 to 95 vol.%, at that its specific surface varied from 3000 to 12,000 cm^{-1}.

As a results, grain compositions of one part of charge specimens was continuous, and another one has random particle package. It was a reason for detection of number of grain compositions, providing minimum for given series of experiment pressure loss, value of which is changed at transfer from one series of compositions to another. At the same time, even small deviation of grain composition of the mixture in one or another side from each of the optimum grain compositions is accompanied by rapid, as a rule, almost symmetric increase of compound viscosity. And only series, relating to the field of coarse- and fine-grain compositions, have deviation of grain composition from the optimum accompanied by asymmetric rise of compound viscosity. In other words, identical rise of portion of fine-grain fraction in the charge in comparison with the optimum is accompanied by significantly smaller rise of compound viscosity in the first case than in the second [2]. The reason of this effect is not determined.

Study [3] investigated liquid glass compositions of marble powder with similar on width range of grain compositions (pass through mesh

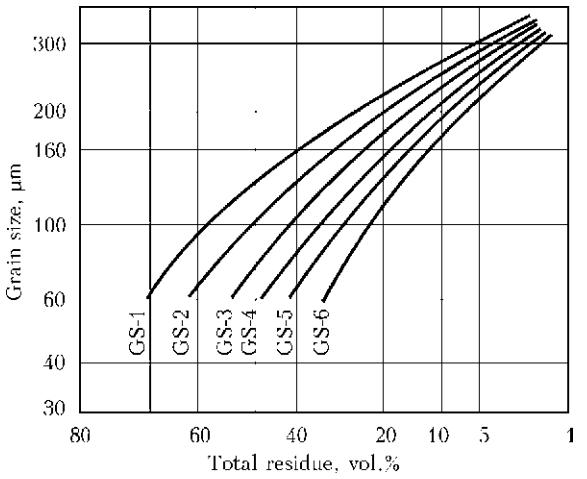

Figure 1. Grain compositions of dry charge mixtures used for production of electrode compounds GS-1–GS-6

0063 was changed in the range from 0 to 94 wt.%, and specific surface varied from 1500 to 11,500 cm^{-1}). In this series of experiments grain compositions of powders were characterized by three levels of course and width of distribution of particles by sizes, and packings of all particles, were continuous. Compositions on consistency correspond to real compounds at content of 30 % of liquid glass with M 3.2 modulus and viscosity 670 mPa·s. Round nozzles of diameter/length 4/20 mm at Q = 1 $cm^3 \cdot s^{-1}$ or 8/60 mm at Q = = 5 $cm^3 \cdot s^{-1}$ (average gradient of shear rate 40 and 25 s^{-1}, respectively) were used as measuring instrument.

This series of experiments showed one relatively wide minimum of viscosity, which falls on 30–60 % of fine fraction in the charge. Position of minimum is constant in studied range of flow velocities. However, flow velocity significantly effects viscosity of extreme (the most coarse- and fine-grain) specimens of marble. At that, the same decrease of shear rate from 40 to 25 s^{-1} is accompanied by rise of viscosity of suspension with coarse-grain filler and its reduction in suspension with fine-grain filler. It can be assumed that such suspensions, characterized approximately by similar fractional void space (free intergranular space) of filler, have at the same time different structure.

Table 1. Characteristics of charge and compound

Designation of compound	Portion of fine fraction, %	Specific surface of charge, cm^{-1}	Maximum allowable concentration F_m	Plastic strength P_m, MPa
GS-1	26	2250	0.720	0.13
GS-2	36	3900	0.800	0.10
GS-3	43	4900	0.815	0.12
GS-4	47	5850	0.815	0.13
GS-5	56	8100	0.750	0.22
GS-6	65	9250	0.705	0.28

In general, the results obtained in the works indicated above can be well explained from point of view of hydrodynamic theory of viscosity based on matching of real density of packing of particles of filler F with their maximum allowable concentration F_m reaching, which the suspension loses flow capability. Significant part of binder becomes kinetically free liquid as a result of reduction of fractional void space, typical for monodisperse filler due to filling of the voids by finer particles. It simplifies shear movement of grains relatively each other, i.e. suspension viscosity is reduced.

Aim of the present work is an investigation of effect of charge grain composition on rheological characteristics and structure of pressure flow of compounds for low-hydrogen electrodes at flow velocities, corresponding to real conditions of electrode extrusion (application of compound) using extrusion presses.

Procedure of investigation. Rheological characteristics of pilot compound having the following component characteristics of dry charge, wt.%: 51 marble, 18 fluor-spar concentrate, 5 quartz sand, 3 synthetic mica, 2 ferromanganese, 13 (15 % Si) granulated ferrosilicon and 8 ferrotitanium, were investigated. Grain composition of charge was regulated by means of changing of proportion of weight fractions of preliminary screened powder fractions of marble, fluorspar and quartz sand. Powders of ferro-alloys and synthetic mica ANS-1 were used with constant grain composition. General proportion of fine fraction in the charge was varied in the limits from 25 to 65 wt.%, at that proportion of fractions was changed in such a way as shown in Figure 1. Grain composition of mixture with the most compact packing of grains, corresponding to Furnas rule, lies in the range between curves GS-4 and GS-5. Real indices of specific charge surface and density of their random packing as well as plastic strength of the compounds are given in Table 1.

Compounds were prepared in intensive counter-flow mixer. Na–K liquid glass having M 2.9, 1495 kg/m^3 density and 1000 mPa·s viscosity was used. Weight fraction of liquid glass in the compound makes 25 %.

Investigations were carried out using capillary viscosimeter of OB-1435 model, representing itself plunger extruder [2, 4] with electro-mechanical drive and diameter of operating cylinder 30 mm. Using stepwise change of march rate of piston, per second consumption of compounds was regulated in the range Q = 1–25 $cm^3 \cdot s^{-1}$.

Using of round nozzles («capillary») with flat outlet and diameter d_c = 1–6 mm at such consumptions allowed regulating average gradient of shear rate on smooth wall of channel in the ranges from 10 to 65,000 s^{-1}.

Shear stress on channel wall τ was calculated on formula $Pd_c/4L$, where $L = 10d_c$ is the length of channel; $P = (P_c - P_0)$ is the drop of pressure at this length; P_0 is the pressure loss at inlet to the nozzle (determined by means of passing of the compound through round hole of d_c diameter in the center of steel disk of 1 mm thickness); P_c is the general loss of pressure before inlet to the nozzle and over its length.

Similar level of thixotropic fracture (reconstruction) of coagulation structure of compounds for all nozzle diameter was maintained by L/d_c constant relationship. Duration of compound extrusion was varied depending on flow velocity in 5–15 s range, and P_c and P_0 values were registered at the moment of piston stop. The capillaries are not temperature-controlled. Thermalcouple, calked in the body of capillary of 4 mm diameter and 56 mm length, was used for sampling testing of temperature of jet surface at Q = = 1 $cm^3 \cdot s^{-1}$. Thermoelectromotive force was registered using potentiometer KSP-4. The experiments were carried out by Dr. Gnatenko M.F. and Eng. Voroshilo V.S.

Efficient shear viscosity of the compound in pressure flow state was calculated on formula $\eta = \tau/\dot{\gamma}$ and longitudinal viscosity λ was received using the following formula from works [5, 6]:

$$\lambda = \frac{9(n_0 + 1)^2}{32\eta}\left(\frac{P_0}{\dot{\gamma}}\right)^2, \quad (1)$$

where $n_0 = d(\lg P_0)/d(\lg \dot{\gamma})$ is the index of compound flow in convergent zone, which was determined by angle of inclination of rheograms $P_0 = f(\dot{\gamma})$ to axis of shear rate gradients, represented in logarithmical coordinates. Similar on meaning index of shear flow of compound through cylinder channel $n_c = d(\lg \tau)/d(\lg \dot{\gamma})$ was also used. Both indices characterize relationship of energy of activation of material viscous flow at $\dot{\gamma}$ = const and τ = const, respectively $n_c < n_0$ as a rule.

Structure of compound flow was estimated on value of angle of natural convergence α_0, which corresponds to equality of shear and extension components of force, overcoming resistance of indicated zone [6].

Angle α_0 reduces with rise of flow velocity for those materials, where longitudinal viscosity decreases intensively than shear one. Convergent zone of such materials acquires watering-can shape [1, 2, 4, 5].

The following formula was used for determination of average compound extension stress:

$$(\sigma_E)_{av} = \frac{3}{8}(n_0 + 1)P_0, \quad (2)$$

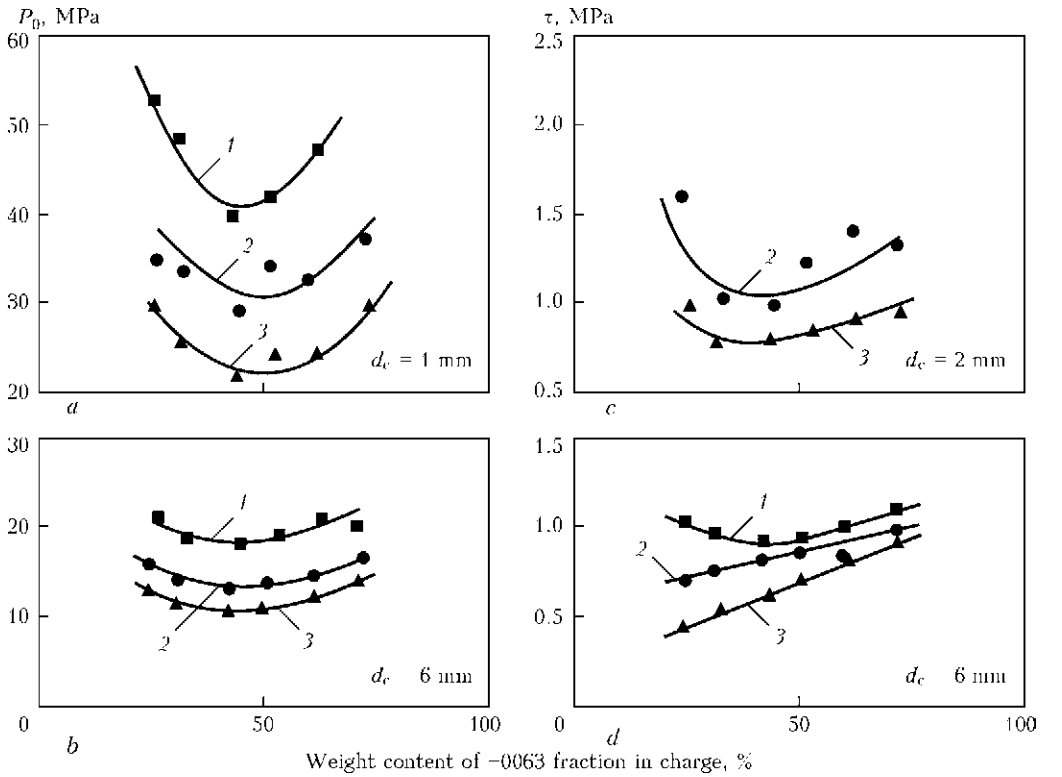

Figure 2. Effect of fine fraction in charge on pressure loss at inlet (*a*, *b*) and shear stress on capillary wall (*c*, *d*): *1* — Q = 25.5 $cm^3 \cdot s^{-1}$; *2* — 5.3; *3* — 1.0

and gradient of extension rate was calculated on formula

$$\dot{\varepsilon} = \frac{(\sigma_E)_{av}}{\lambda}. \quad (3)$$

Angle of natural convergence at the inlet of compound in shaping cylinder nozzle was estimated on formula

$$\text{tg}\,\alpha_0 = \left(\frac{2\eta}{\lambda}\right)^{1/2}. \quad (4)$$

Results of investigation and their discussion. Figures 2 and 3 show determined in course of experiments dependencies of input resistances P_0 and shear stress on wall of cylinder nozzle τ, received using the nozzles with extreme sections of channels, on portion of fine fraction in the charge, as well as their dependence on shear rate gradient on channel wall. It can be seen that charge grain composition, changing even in the range of such narrow limits, significantly effects rheological characteristics of the compounds. Particularly, if we are taking on compound flow resistance in convergent zone. As it is was predicted, P_0 value is varied on extreme law in dependence of portion of fine fraction in the charge

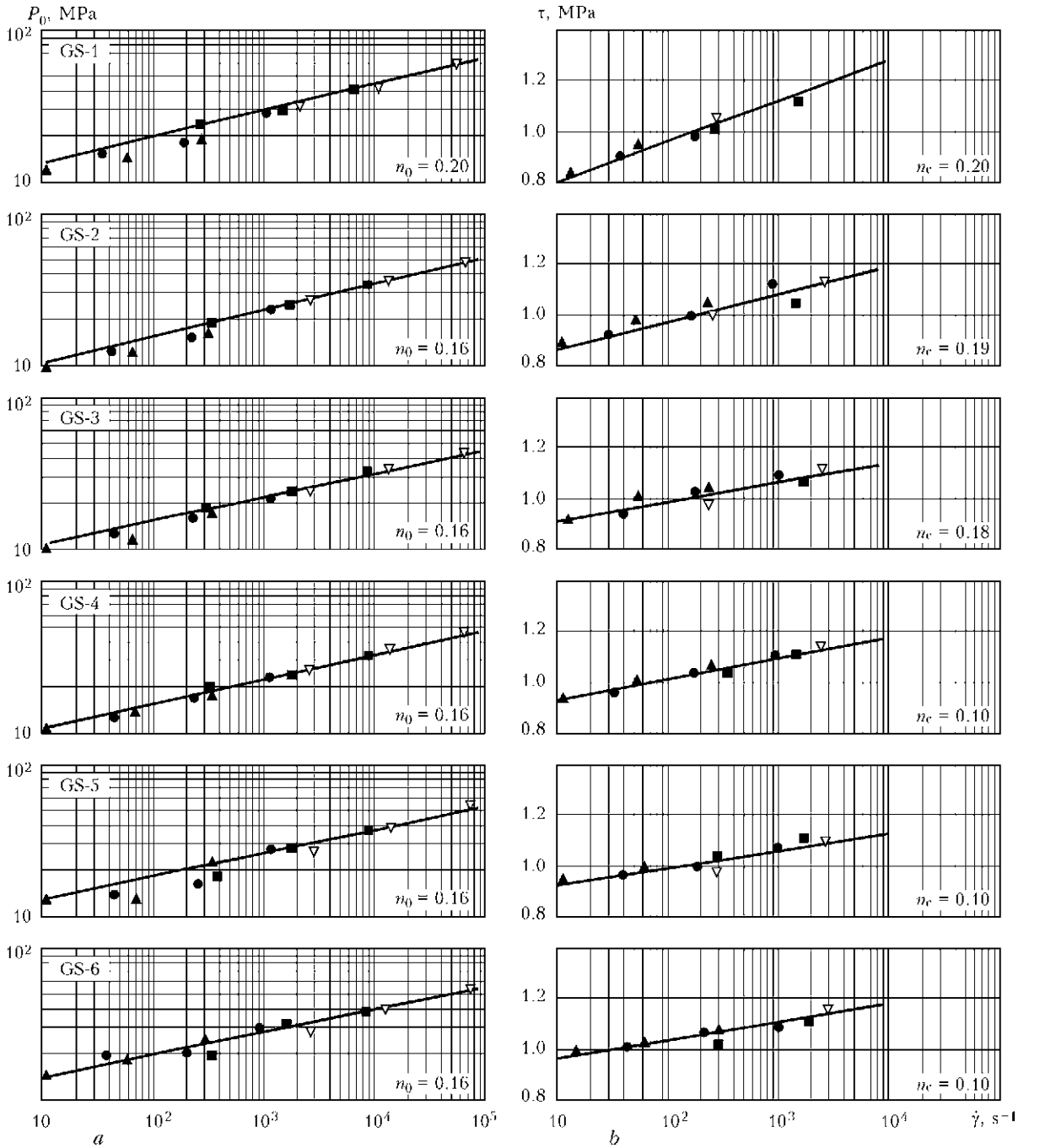

Figure 3. Dependence of gradient of shear rate on inlet resistance (*a*) and shear stress on capillary wall (*b*) on portion of fine fraction in compound: ▲ — d_c = 6 mm; ● — 4; ■ — 2; ∇ — 1

and significantly rises with its deviation in one or another side from 50 % being the optimum value. The smaller the section of outlet hole and the lager the volume consumption of the electrode compound, the greater is the reaction of compound on change of charge grain composition, when overcoming input resistance in shaping cylinder channel. Nevertheless, only the most fine-grained among them (65 % of fine fraction in charge) do not pass through diaphragm of 1 mm diameter at Q = 25.5 $cm^3 \cdot s^{-1}$. The rest of compounds passed through this and other diaphragms at all volume flow velocity.

Behavior of compounds in cylinder nozzles is more complex. First of all, any of compounds overcame resistance of nozzles with channels of 1 and 2 mm diameters at Q = 25.5 $cm^3 \cdot s^{-1}$. Part of compounds passed through the nozzles of 2 mm diameter, if consumption did not exceed 5.1 $cm^3 \cdot s^{-1}$. Nozzle with channel diameter 6 mm passed through all the compounds at all consumptions and charge grain compositions. Secondly, extreme variation of shear stress on nozzle wall depending on portion of fine fraction in the charge is less expressed than in inlet resistances. Extreme τ dependence on portion of fine fraction in the charge degenerates into monitonically rising at flow modes with 1 and 1.5 $cm^3 \cdot s^{-1}$ consumption, when using nozzles with channel diameter 4 and 6 mm. These peculiarities cannot be explained considering provisions of only hydrodynamic viscosity theory.

It is important to be noted that all compounds behave themselves as materials with pronounced non-Newtonian properties. It is indicated by values of flow indices, which are significantly smaller than one, namely in convergent zone n_0 = = 0.16 independent on charge grain composition; in capillary n_c monotonically reduces from 0.2 to 0.1 with increase of portion of fine fraction in the charge. Therefore, non-Newtonian nature of compounds is more pronounced.

Change of charge grain composition influences the structure of flow in the entrance zone as well as cylinder nozzle. The results given below show that increase of portion of fine fraction in the charge provides for change of values of longitudinal and shear viscosity and together with them variation of convergence angle in the entrance zone, which, as follows from (4), is determined by their relationship. At that, tendency to slug nature of compound flow (index of flow is reduced) in the nozzle should intensify due to what shear is more and more concentrated in near-wall layer.

Figure 4 gives the results of calculation of shear and longitudinal viscosity of studied compounds depending on shear rate gradient and extension, respectively. It can be observed that η and λ reduce with rise of deformation rate. This confirms good structure of electrode compounds and thixotropic fracture of their coagulation structure in rise of $\dot{\gamma}$ and $\dot{\varepsilon}$. It also can be seen that experimental points in logarithmic metamorphosis can be well matched with straight lines, generalizing interesting for us dependencies. The $\eta = f(\dot{\gamma})$ and $\lambda = f(\dot{\varepsilon})$ straight lines itself are almost mutually parallel and only being shifted relatively to each other on scales of gradients of shear and extension, respectively. It is assumed that charge grain composition has small effect on relationship of values of shear and longitudinal viscosities (and so, on profile of compound flow in the entrance zone).

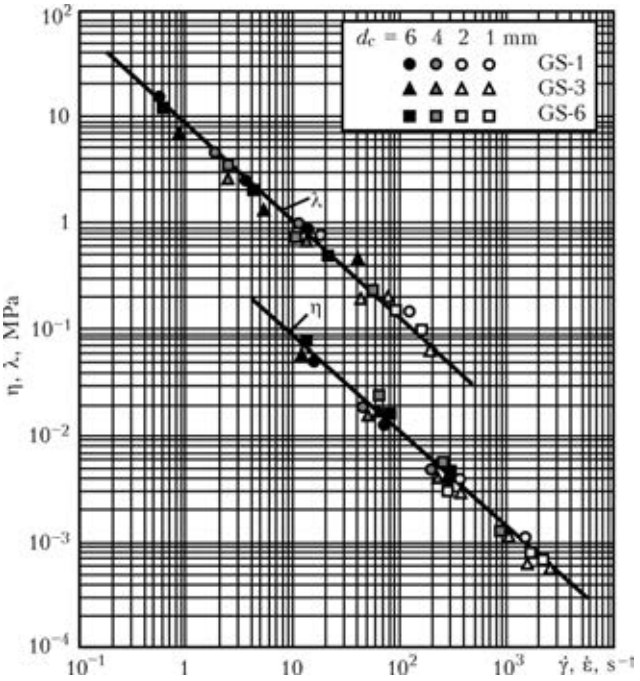

Figure 4. Dependence of shear η and longitudinal λ viscosity of electrode compounds with different charge grain composition on average gradient of shear rate $\dot{\gamma}$ and extension $\dot{\varepsilon}$

In fact, close to parallel behavior of rheograms $\eta = f(\dot{\gamma})$ and $\lambda = f(\dot{\varepsilon})$ in logarithmic coordinates does not indicate at all a consistency of λ/η viscosity relationship. It was determined in the following way. Firstly, relationship of shear and longitudinal viscosities of compounds was determined for each mixture grain composition. Examples of such dependencies for three grain compositions with extreme and average portion of fine fraction in the charge are shown in Figure 5. Afterwards, inclination of straight lines lg λ/lg η to abscissa axis was evaluated. It firstly decreases with increase of portion of −0063 fraction in the charge, and it rises after reaching the minimum value (Figure 6). In this connec-

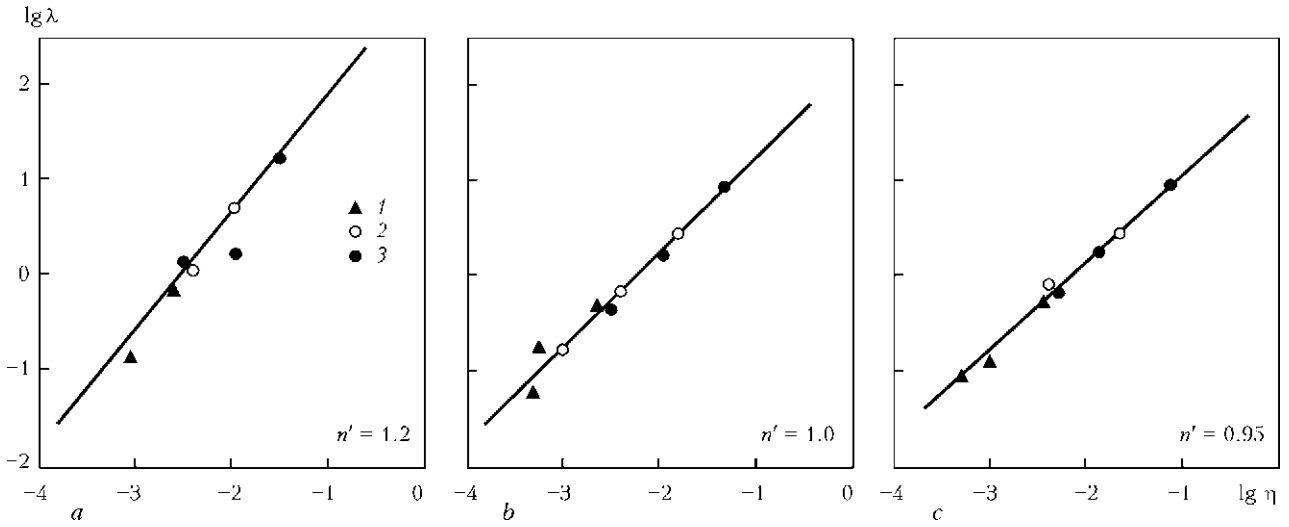

Figure 5. Relationship of longitudinal (λ, MPa·s) and shear (η, MPa·s) viscosity of electrode compounds GS-1 (*a*), GS-4 (*b*), GS-5 (*c*) with different charge grain composition: *1* — d_c = 6 mm; *2* — 4; *3* — 2

tion, the value of convergence angle α_0 shows ambiguous reaction on change of charge grain composition and compound flow modes. It follows form Figure 7 that low and average gradients of shear rate also promote change of convergence angle depending on portion of fine fraction in the charge based on extreme law (it nature is in P_0 inverse relation on portion of fine fractions in the charge, and maximum falls at 50 % of fine fraction).

In this case, fine- and coarse-grain filler promotes narrow profiles of compound flow, that can result in formation of leading outflow of its internal layers in comparison with external layers. Usually, the narrow flow profiles provide for pulsing and twisting of the jet, i.e. position of such flow in principle can not be stably oriented in space. Using of charges with intermediate grain having, as a rule, the widest grain size distribution, promotes formation of more distributed and, it can be assumed, more stably oriented in space flow at low velocities.

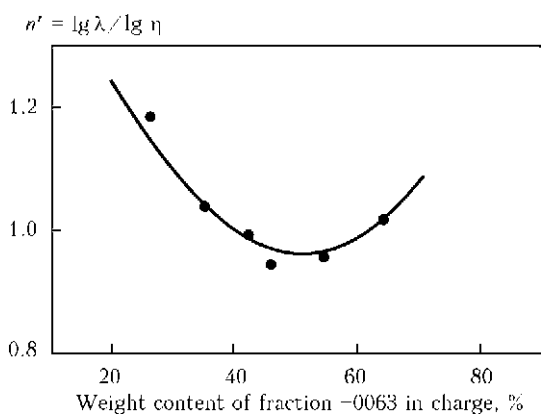

Figure 6. Effect of charge grain composition on relationship of longitudinal and shear viscosities of electrode compounds of GS series

Rise of shear rate gradient provides for gradual evening of curve maximums, and indicated dependencies become monotonic at $(1–2)\cdot10^3$ s^{-1} gradients, which are predicted for compound flow velocities under real conditions of electrode extrusion. At that, the compounds with coarse-grain filler, in which portion of fine fraction makes 20–25 wt.%, form wider flow profiles. The flow with such profile should have more stable orientation in space. Advancing flow of material in core and, respectively, appearance of periphery dead zones are less probable in it.

Compounds with average- and, in particular, fine-grain filler (in which portion of −0063 fraction makes 40 and 60–65 wt.%, respectively) almost preserve initial profile of flow velocities in these modes. The reasons of such changes can be related with non-isothermal flow conditions as well as different structure of compared compounds.

Table 2 shows that their dissipative heating in creep flow mode (Q = 1 $cm^3\cdot s^{-1}$) is insignificant (to 34–37 °C) and the same for all. It rarely can effect viscosity characteristics of the compounds and does not allow determining their structural peculiarities. Increase of shear rate gradient promotes for heating of the compounds to higher temperatures, compound GS-4 is the most intensive. Since portion of kinetically free liquid glass

Table 2. Results of estimation of temperature condition in compound flow zone at 4 mm nozzle diameter

Compound consumption, $cm^3\cdot s^{-1}$	Gradient of shear rate, s^{-1}	Temperature of jet, °C		
		GS-1	GS-4	GS-6
1.0	11.8	34	37	37
5.1	203	58	54	53
25.5	1015	76	91	77

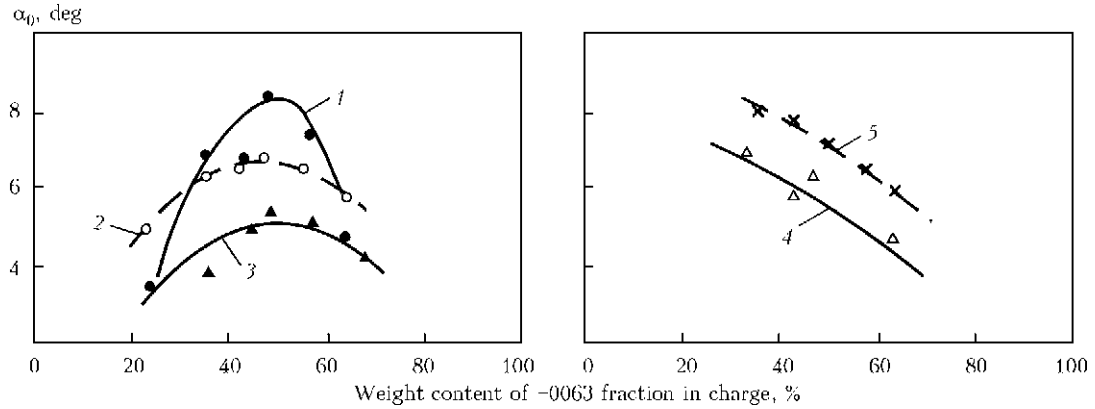

Figure 7. Effect of charge grain composition and flow velocity of compound on value of natural convergence angle of its pressure flow in pre-capillary zone: *1* — $\dot{\gamma}$ = 118 s^{-1}; *2* — 203; *3* — 318; *4* — 1015; *5* — 2550

in intergrain space of this compound is the largest, it less structural than GS-1 and GS-6 compounds. Energy consumptions for structure fracture do not mask its dissipative heating, and this is a reason of so rapid rise of temperature. GS-1 with coarse-grain filler is the next compound on level of structuring. It is heated to 76 °C, but at little bit higher intermediate rate in comparison with compound GS-4. Compound GS-6 reaches the same level of temperature with the lowest intermediate rate. Respectively, it should have the highest level of structuring.

It is shown above that change of $\alpha_0 = f(-0063)$ function of the same compounds also demonstrates ambiguous reaction on increase of shear rate. It supports an assumption made earlier that we are dealing with the materials having different rheological structures.

This is also confirmed by comparison of form of extrusion (deformation) curves $P = f(t)$, given in Figure 8, and received during study of different compounds. Indicated curves describe the changes of pressure from moment of viscosimeter start, including reaching the maximum, consequent drop, promoted by compound flow, fracture of its structure and relaxation of accumulated stresses, up to setting of pressure corresponding to steady compound flow.

It should be considered in this case that rate of compound deformation in course of extrusion at constant consumption per second rises with decrease of capillary diameter. Shape of specified curves indicates that matched compounds should differ between themselves by relationship of viscosity and elasticity, accumulated in process of extrusion [7].

It follows from Figure 8, *b* that compound GS-4 is characterized by constant rate of pressure rise in time independent on deformation rate. It is only one of three compounds capable to overcome resistance of capillary of 1 mm diameter at Q = 25.5 $cm^3 \cdot s^{-1}$. According to provisions of viscoelasticity theory, it indicates low capability of material for accumulation of elastic stresses in course of pre-stationary stage of pressure flow.

The higher the extrusion rate, the more is the rate of pressure rise after deformation beginning in compounds GS-1 and GS-6 with excessive content of coarse- and fine-grain filler. Therefore, they more intensively accumulate elastic stresses and reduce portion of net energy, which is consumed for compound extrusion, at rise of extrusion rate.

Compound flow is accompanied by stress relaxation. The higher the set rate of deformation, the lager is the level of pressure rise, outrunning

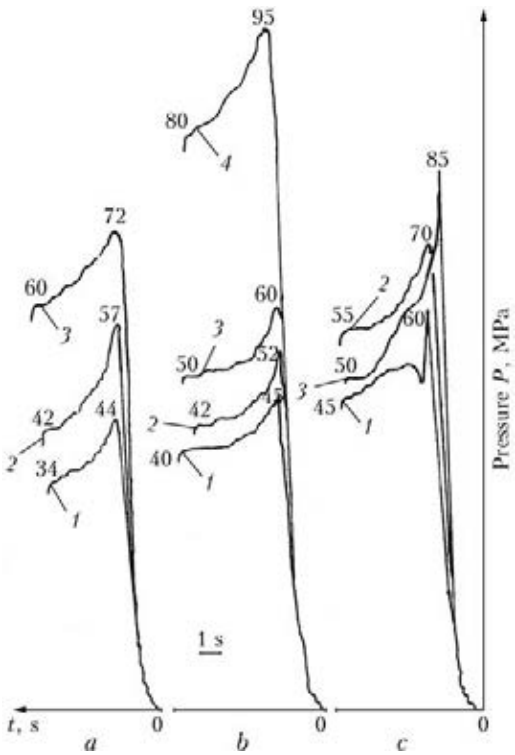

Figure 8. Curves of extrusion of compounds GS-1 (*a*), GS-4 (*b*) and GS-6 (*c*) with different quantity of fine fraction in charge passing through capillaries of 6 (*1*), 4 (*2*), 2 (*3*) and 1 (*4*) mm diameter at Q = 1 $cm^3 \cdot s^{-1}$

the rate of stress relaxation, after deformation beginning. This in particular intensifies accumulation of the elastic deformations. This process is more pronounced in compound GS-6 with fine-grain filler. It is shown by almost linear rate of pressure rise, on the one hand, and sharp peak of pressure in maximum, on the other hand. Compound GS-1 is less structured, therefore, rising branch of extrusion curve coming to peak significantly deviates from the straight line, that is caused by overlaying of viscosity flow to elastic deformation.

Relaxation of the accumulated stresses in compared compounds takes place in different way after passing the maximum. The relaxation of momentary elastic stresses in compound GS-6 extruded at low rates (Figure 8, *c*, curve *1*) provokes short, but rapid pressure drop. After drop it is partially recovered and then continues smooth reduction to receiving of steady flow. Pressure in maximum is smoothed and structural branch is reduced without intermediary drop at average rate of extrusion (Figure 8, *c*, curve *2*). Level of pressure under condition of steady flow is more than at previous curve. Structural branch of the curve at the highest flow velocity (Figure 8, *c*, curve *3*) after sharp maximum shows so intensive reduction that it falls below than in the similar curve, registered at intermediate extrusion rate. Namely, this anomaly of deformation curves is usually related with high structuring of coagulation dispersions. Compounds GS-1 and GS-4 have no such anomaly.

The lager level of structuring of GS-6 compound in comparison with GS-1 compound is explained in the following way. Increase of portion of fine fraction above the optimum values in the charge provides for rise of not only portion of intergrain voids (and, respectively, reduction of quantity of kinetically free binder from liquid glass), but also specific surface of the particles, which should be covered by binder. Thus, the system as though is transferred in the condition with lager space filling, i.e. higher concentration of solid particles contacting with each other. Considering indicated factors, thickness of intergrain film is reduced and molecular interaction of the filler particles, being the most intensive in the points of their interaction, is significantly risen. It is verified by increase of strength of coagulation structure P_m (see Table 1).

Results of our experiments match well with calculations carried out in work [8]. The latter show that position of viscosity minimum of suspension with multimodal filler deviates to larger extent in the side of lower concentration of coarse fractions in the filler in comparison with that, which is provided by the densest particle packing for given grain composition.

The similar effect can be achieved, if viscosity liquid glass is replaced by low-viscosity one, reducing at that its portion in compound within the due limits. In this case, elastic relaxation of GS-6 compound is not compensated by damping capability of the low-viscosity liquid glass and can promote pulsing of its flow in creep flow mode or different type irregular effects under flow modes, exceeding creep deformation on rate. The first and the second can, in particular, be the reason of coating thickness difference.

There is no pulsing of flows of GS-1 and GS-4 compounds, filler of which contains less fine fractions.

Conclusions

1. Rheological characteristics of electrode compounds were investigated depending on charge grain composition. Portion of fine fraction in the charge was varied in the limits close to that given in specification (40–60 % of particles finer than 0.063 mm). It was found that charge should contain 50 % of fine fraction for minimizing of consumption of energy necessary for extrusion application of compounds over the rods. Deviation of its content in one or another side from the indicated optimum, even in such narrow limits, significantly rises consumption of energy for electrode extrusion, in particular, at rates which are used under real conditions of their manufacture.

2. Such dependence from point of view of hydrodynamic theory is explained by increase of compound viscosity, caused by rise of void free space between filler grains, which should be filled by liquid glass with certain excess, before the compound will gain a capacity to pressure flow. Filling of the voids between the filler coarse grain by fine particles promotes displace of liquid glass from them, transforming it in kinetically free liquid. This results in reduction of compound viscosity.

3. The compound containing excessive quantity of coarse or fine fractions in comparison with the specified optimum are not similar to each other. It is indicated by nature of change of compound temperature, value of convergence angle, which is formed in the entrance zone as well as shape of extrusion curves at rise of deformation rate. Flow profile of compounds with coarse grain filler expands with rise of pressure jet rate, and this promotes its stabilizing in space and time. Flow of the compound with fine-grain filler is almost the same narrow as at creep flow veloci-

ties, that is unfavorable moment from technological point of view.

4. The results of analysis of shape of extrusion curves $P = f(t)$ indicate that pressure flow of the compound with equal portions of coarse- and fine-grain filler takes place on viscosity mechanism with the lowest energy consumption. Flow of the compound with excessive content of coarse-grain filler is also performed on viscosity mechanism, but with larger viscosity, since glass is often used for void filling. Their viscosity is higher than in compounds with equal portions of coarse- and fine-grain filler, since part of liquid glass is consumed for filling of intergrain voids of the filler, volume of which in this case is larger, as necessary quantity of fine particles for their filling is absent. The compounds with excessive content of fine-grain filler are more structured, since liquid glass binder in addition to filling of intergrain voids should cover significantly more developed surface of fine grains. The rise is observed in molecular interaction of filler grains and strength of structure formed by them, which can be easily fractured in shear deformation, accompanied by specific effect of unsteady flow.

5. Consideration of peculiarities of electrode compound pressure flows with high deformation rates should take into account the peculiarities of coagulation structures formed by them and their reaction on change of deformation rate in addition to provisions of hydrodynamic theory of viscosity of highly concentrated dispersion systems.

1. Marchenko, A.E., Pokhodnya, I.K., Skorina, N.V. et al. (1994) Development of technology for manufacture of low-carbon electrodes. *Svarochn. Proizvodstvo*, **5**, 14–18.
2. Marchenko, A.E. (1978) *On rheological methods of evaluation of technological properties of electrode compounds*: SMEA Inform. Doc., Issue 1, 121–128. Kiev: Naukova Dumka.
3. Marchenko, A.E. (2013) Examination of concentrated suspensions of marble in liquid glass as a rheological model of electrode compounds. In: *Proc. of 7th Int. Sci.-Techn. Conf. on Welding Consumables. Arc Welding. Materials and Quality* (Krasnodar, vil. Agoj, 17–21 June 2013), 98–115.
4. Marchenko. A.E., Gnatenko, M.F. (1980) *Peculiarities of flow of electrode compounds detected by capillary plastometer*: SMEA Inform. Doc., 106–117. Kiev: Naukova Dumka.
5. Marchenko, A.E. (2011) About rheological properties of electrode compounds in convergent zone during electrode extrusion. In: *Proc. of 6th Int. Conf. on Welding Consumables. Development. Technology. Manufacture. Quality. Competitiveness* (Krasnodar, 6–9 June 2011), 223–232.
6. Cogswell, F.N. (1972) Converging flow of polymer melts in extrusion dies. *Polymer Eng. and Sci.*, 12(**2**), 64–70.
7. Belkin, I.M., Vinogradov, G.V., Leonov, A.I. (1967) *Rotary devices. Measurement of viscosity and physico-mechanical characteristics of materials*. Moscow: Mashinostroenie.
8. Moshev, V.V. (1977) Viscosity principles of highly filled polymers. In: *Rheology (polymers and petroleum)*: Transact. of All-Union school on rheology, 53–64. Novosibirsk: ITF.

Received 15.04.2014

IMPROVEMENT OF ADAPTABILITY TO FABRICATION AND WELDING PROPERTIES OF ELECTRODES FOR TIN BRONZE WELDING AND SURFACING

T.B. MAJDANCHUK and **N.V. SKORINA**
E.O. Paton Electric Welding Institute, NASU
11 Bozhenko Str., 03680, Kiev, Ukraine. E-mail: office@paton.kiev.ua

The paper gives the results of investigation of the influence of various kinds of alkali-silicate binder on adaptability to fabrication and welding properties of coated electrodes for tin bronze welding and surfacing. Both standard (sodium, potassium and mixed) and test lithium-containing liquid glasses were used during investigations. A procedure developed at PWI was used to determine plastic properties of electrode coating mixture and to assess the strength and hygroscopicity of electrode coatings. Studies of welding-technological and sanitary-hygienic properties of test electrodes were also performed. This resulted in selection of optimum kind of liquid glass, the most suitable for manufacture of coated electrodes for tin bronze welding and surfacing. 8 Ref., 4 Tables, 5 Figures.

Keywords: *tin bronze, surfacing, coated electrodes, liquid glass, adaptability to fabrication*

At present tin bronzes are becoming widely applied in components and friction mechanisms subjected to increased wear in different operation conditions, that is greatly promoted by a favourable combination of their physical and technological properties. Various welding processes are used in order to save this expensive non-ferrous metal. The simplest and least expensive method is manual arc welding (surfacing) by coated electrodes. Ukraine has no production of coated electrodes for welding and surfacing, and for repairing casting defects of tin bronzes, and the cost of foreign electrodes is high, that is why PWI developed electrodes of ANBO grade [1, 2].

The coating has specific composition, associated with presence of chemically active towards the binder (liquid glass) components of sodium salts (hexafluorosilicate, hexafluoraluminate and fluroride) in it, as well as non-traditional metal components (tin, copper-phosphorus powders). In this connection, it is necessary to perform research and selection of optimum kind of alkali-silicate binder, the properties of which largely determine the technology of manufacturing, quality and service properties of electrodes.

Standard (sodium, potassium and mixed sodium and potassium) and test lithium-containing liquid glasses were prepared for investigations, which give unique properties to some electrode types [3]. Their physico-chemical characteristics are given in Table 1.

Testing included determination of plastic properties of electrode coating mixtures, assessment of strength and hygroscopicity of electrode coatings; checking welding-technological properties and determination of sanitary-hygienic properties of electrodes.

Coating mixture plasticity. Plasticity properties of coating mixtures were evaluated using procedures and instruments developed at PWI [4–6]. Coating mixture fluidity was determined with capillary viscosimeter OB-1435 by its extrusion through a die of 4 mm diameter and 40 mm length at minimum (1 cm^3/s) and maximum (10 cm^3/s) volume flows. Here, pressure and

Table 1. Physico-chemical parameters of liquid glasses used at testing

Glass type	Density ρ, g/cm^3	Viscocity η, MPa·s, at 20 °C	Composition, wt.%				Module
			SiO_2	Li_2O	Na_2O	K_2O	
Na	1.430	392	29.03	–	8.83	2.15	2.93
Na–K	1.435	606	28.80	–	6.94	4.56	2.99
K–Na	1.428	304	27.85	–	4.00	8.79	2.94
K	1.415	260	26.92	–	0.03	13.78	3.05
Na–Li	1.396	526	30.19	2.69	0.99	5.17	2.73
K–Li	1.421	554	27.93	1.42	0.94	10.67	2.65
Li	1.258	287	25.08	3.19	–	–	3.91

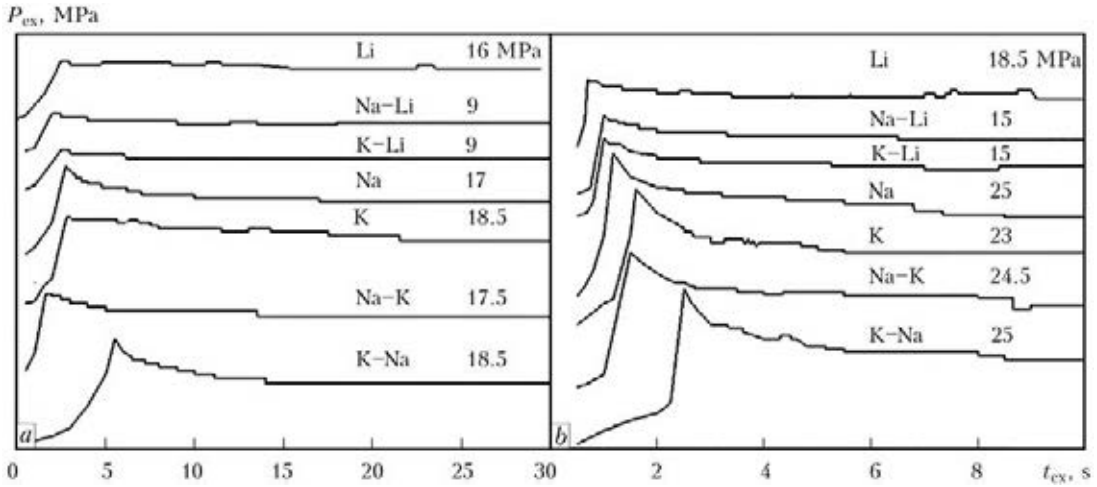

Figure 1. Curves of extrusion of ANBO electrode coating mixture prepared with different kinds of binders: *a* — Q = = 1; *b* — 10 cm^3/s

nature of coating mixture extrusion were recorded. Strength (hardness) of raw coating mixture were assessed by the value of plastic strength measured on conical autoplastometer OB-2059. The coating mixture, which at the same fluidity has higher values of plastic strength or at equivalent plastic strength, is characterized by lower extrusion pressures is believed to be more ductile.

Moreover, preservation of plastic state of coating mixture in time (up to 3 h) required for its processing was checked by the nature and magnitude of extrusion pressure.

Results of evaluation of plasticity of coating mixtures, made with application of various binders, are shown in Table 2 and Figure 1.

As follows from these data, the binders influence the plasticity of electrode coating mixtures. Coating mixtures, prepared with four standard Na–K liquid glasses, are characterized by smooth and stable extrusion both at minimum and at maximum flow at practically the same extrusion pressures (17–18.5 MPa at Q = 1 cm^2/s and 23–25 MPa at Q = 10 cm^3/s). An essential difference in strength properties of coating mixtures is found, however. The highest plastic strength of coating mixture is reached at application of K and K–Na liquid glasses; the lowest value of plastic strength is found in coating mixtures made from Na and Na–K binders. A similar phenomenon is observed in electrode coating mixtures designed for welding steels, and is attributable to differences in size and degree of hydration of potassium and sodium cations.

Compared to Na–K binders, purely lithium liquid glass provides the most favourable combination of strength and extrusion properties of coating mixtures (plastic strength reaches $63 \cdot 10^5$ Pa at lower extrusion pressures).

Mixtures of Li–Na and Li–K liquid glasses at their equivalent dose form less consistent coating mixtures (lower plastic strength and extrusion pressure) that is, probably, related to smaller modulus of the above-mentioned silicates.

Coating mixtures, made of the studied Na–K binders, do not harden with time (Figure 2). Extrusion pressure practically does not change during 2 h. Li-containing liquid glasses unambiguously change the consistency of coating mixtures at storage. So, in coating mixture, made

Table 2. Plastic properties of coating mixtures

Glass type	Glass dose, %	Plastic strength $P_m \cdot 10^{-5}$, Pa	Extrusion pressure P_{ex}, MPa, at consumption Q, cm^3/s	
			1	10
Na	28	5.8	17	25
Na–K	28	3.45	17.5	24.5
K–Na	28.2	16.7	17	25
K	28	18.0	18.5	23
Na–Li	28	~0.4	9	16
K–Li	28	~0.4	9	15
Li	29	63.2	13.5	18.5

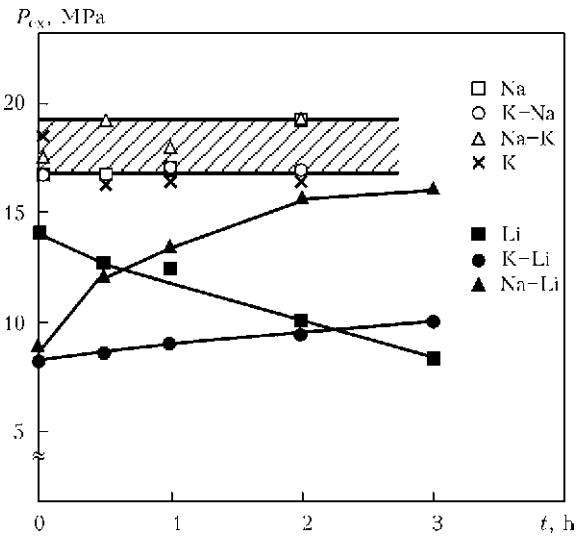

Figure 2. Change of extrusion pressure of ANBO electrode coating mixture made with different binders with time at Q = 1 cm^3/s and 4.0/40 die

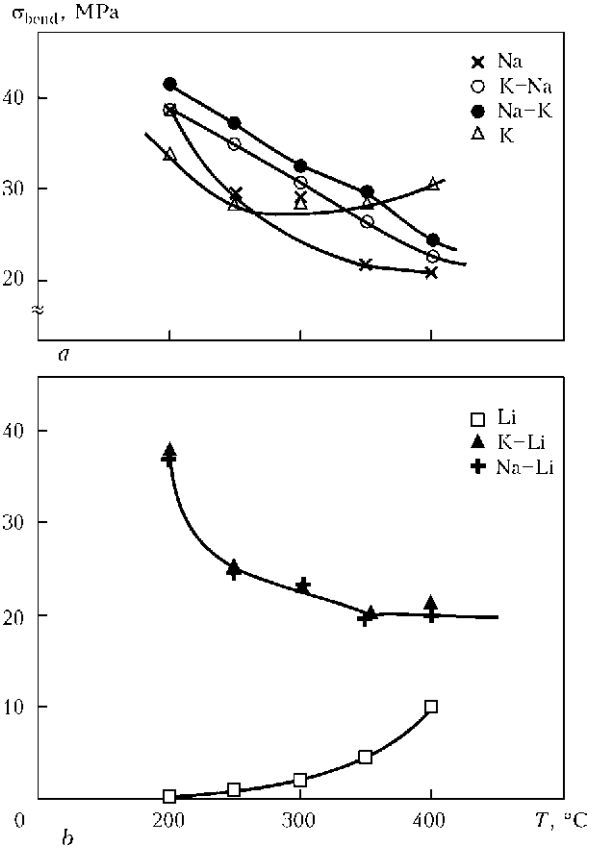

Figure 3. Dependencies of bending strength on baking temperature of ANBO electrodes coating mixture made with different binder types

with purely lithium binder, a noticeable «thinning» in time is observed as a result of interaction with fluorides contained in the coating mixture: extrusion pressure drops by 40 % after 3 h of storage. At application of K–Li liquid glass the coating mixture only slightly changes its consistency during the controlled time. At the same time, application of Na–Li liquid glass causes hardening of coating mixture. Here, extrusion pressure rises by 50 % within 3 h, that is indicative of chemical reaction running in the coating mixture.

Coating mixture strength. Coating mechanical strength was evaluated by bending strength of 4 mm cylindrical samples of coating mixture baked at different temperatures, which were obtained by extrusion in capillary viscosimeter OB-1453. Strength was determined by three-point bending method in a special attachment, developed at PWI, for conical autoplastometer. Test results are given in Figure 3.

It follows from the obtained data that strength of coating mixtures of electrodes for welding tin bronzes depends on binder kind and sample baking temperature. Similar to the case of coating mixture fluidity, bending strengths of coating mixtures made from Na–K liquid glasses, on the whole, differ only slightly from each other in the entire range of studied baking temperatures. Here, strength decreases with increase of baking temperature. A certain difference is observed only at application of potassium binder: coating mixture strength is somewhat lower at the lowest baking temperature (200 °C) and is the highest at maximum temperature (400 °C). In the temperature range of 300–350 °C characteristic for heat treatment of electrodes for welding bronzes, coating mixture strength is practically equivalent for all Na–K binders.

Na–Li and K–Li binders provide the same level of coating mixture strength, somewhat lower compared to Na–K liquid glass (Figure 3, *b*).

Lithium binder behaves differently from other studied binders. Coating mixture with this binder is characterized by a quite low level of strength with increase of baking temperature, that does not occur at application of other binders.

Electrode coating hygroscopicity. Atmospheric moisture absorption by electrode coatings has an adverse impact on quality of electrodes and welds. The main cause for coating hygroscopicity is the dry residue of binder in the coating: alkali silicate, determined by its composition and characteristics. Hygroscopicity was assessed by kinetics of moisture sorption by coating of electrodes baked in the chamber furnace at 300 °C in a hydrostat with 84 % relative humidity at room temperature. Two test cycles were performed: with short- (8 h) and long-term (2 weeks) exposure. The results are given in Figure 4.

It is seen that the kind of binding has an essential influence on hygrosorption resistance of coatings of electrodes for bronze welding. Regularities of moisture absorption by coatings, made with Na–K binders, are similar to those of electrodes for steel welding. The highest hygrosorption resistance is found in coatings with Na and Na–K binders, and the lowest — with K and K–Na binder. Level of moisture absorption by the coating is quite high: during 8 h the coatings absorb 0.6–0.8 % of moisture at application of Na and Na–K binders and about 1.1 % for K and K–Na binders; during 14 days moisture absorption reaches from 1.8 up to 3.3 % for all the binders (Figure 4, *a*, *b*).

Li-containing binders in coatings of electrodes for bronze welding manifest an effect opposite to that in coatings of electrodes for steel welding. Increase of coating hygroscopicity to the level close to coatings with potassium and potassium-sodium silicates is observed (Figure 4, *c*, *d*). Coating with pure lithium silicate is characterized by the highest level of moisture sorption. Such an influence is, probably, related to interaction of Li-containing binders with sodium fluoride compounds present in the charge, during coating mixture preparation. As a result, lithium cation from liquid glass is bound into practically insoluble lithium fluoride and lithium is substituted by sodium in the silicate.

Welding technological properties of electrodes. Welding-technological properties of elec-

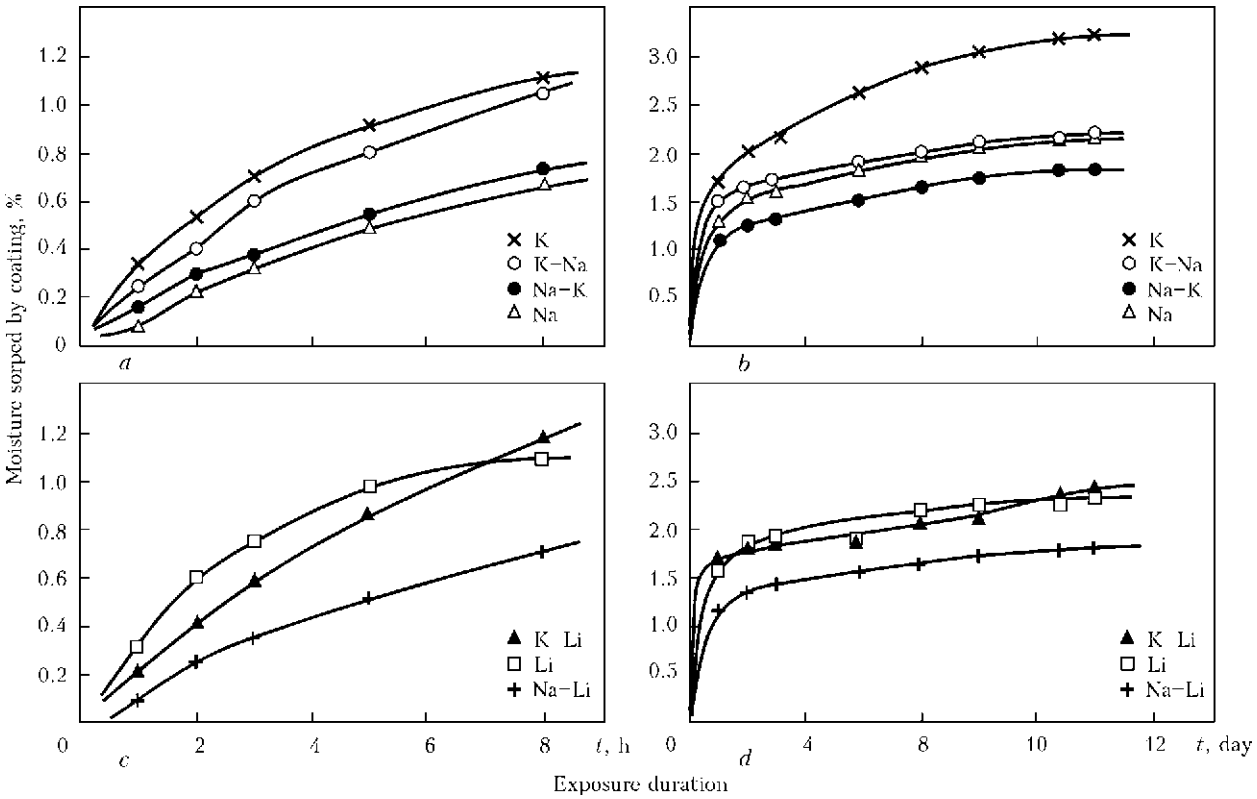

Figure 4. Kinetics of moisture sorption by coating of 4 mm ANBO electrodes manufactured with application of different binder types: Na–K (*a*, *b*) and Li-containing (*c*, *d*) at short- (*a*, *b*) and long-term (*c*, *d*) exposure at relative humidity of 84 % and 20–23 °C

trodes were assessed by the procedure of point ranging [7, 8] of welding process and weld formation. Some changes were made, because of specific requirements to application of ANBO electrodes. For comparison, OZB-2M electrodes, manufactured by Company «Spetselektrod», and UTP-32 German electrodes were used as reference ones.

Arcing stability was evaluated with application of an automated system for diagnostics and monitoring of welding process parameters with subsequent program processing of investigation results. Investigation results are given in Table 3.

Analysis of welding-technological properties showed good arc excitation in surfacing with the studied electrodes, except for OZB-2M. Here, one can see that arc elasticity characteristics are the highest in UTP-32 electrodes that is, possibly, associated with higher coefficient of coating mixture, compared to OZB-2M and ANBO electrodes, made with application of different kinds of glass. Uniform distribution of peak values of voltage and current when studying all the electrodes is indicative of high arcing stability. Despite the fact that UTP-32 electrodes provide the best coverage, high spatter is observed here, and bead surface is coarse-rippled, particularly at deposition of the first layer on steel (Figure 5). At visual inspection of beads and transverse macrosections, pores were revealed at application of OZB-2M grade electrodes made with K and K–Na liquid glasses. Proceeding from that, UTP-

Table 3. Welding-technological properties of coated electrodes

Electrode type	Arc excitation	Weld formation quality	Arcing stability	Arc elasticity	Slag coverability	Slag detachability	Nature of coating melting	Weld metal spattering	Defects in deposited metal	Total points
OZB-2M	3	2	4	3	2	2	1	4	3	24
Na	5	4	4	4	3	3	4	4	5	36
K	5	4	4	3	3	3	5	5	2	34
K–Na	5	4	5	4	3	3	4	5	5	38
Na–K	4	5	5	4	3	3	4	5	5	38
K–Li	5	4	5	3	3	3	3	5	3	34
Na–Li	5	4	5	3	3	3	4	5	5	37
Li	5	4	5	4	3	3	4	5	5	38
UTP-32	5	3	5	5	5	4	5	3	5	40

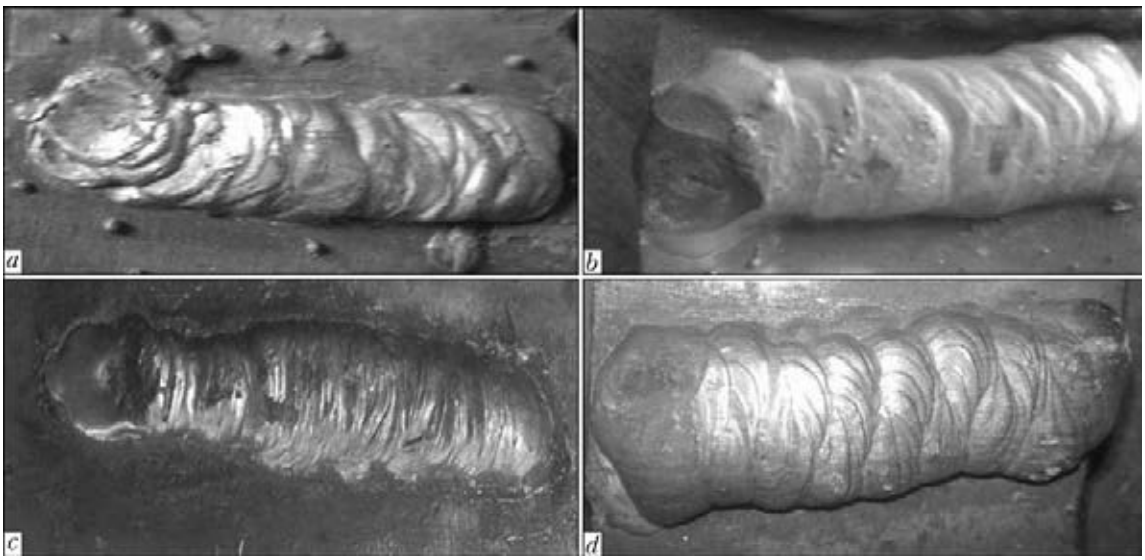

Figure 5. Appearance of deposited metal: *a* — UTP-32 electrode, single-layer deposit; *b* — UTP-32 electrode, three-layer deposit; *c* — electrode based on Na–K glass, single-layer deposit; *d* — electrode based on Na–K glass, three-layer deposit

Table 4. Sanitary-hygienic characteristics of electrodes for bronze welding (4 mm diameter, I_w = 120–130 A, U_a = 23–25 V)

Binder	V_{SCWA}, g/min	G_{SCWA}, g/kg
Na	0.461	10.20
Na–K	0.404	9.13
K–Na	0.435	10
K	0.493	11.29
Na–Li	0.393	8.71
K–Li	0.484	11.35
Li	0.414	9.23

32 electrodes, as well as electrodes made with Li, Na–K and K–Na liquid glasses are the best in terms of welding-technological properties.

Sanitary-hygienic characteristics of electrodes. Sanitary-hygienic characteristics of electrodes were assessed by intensity of formation V_{SCWA} and specific evolution G_{SCWA} of the solid component of welding aerosol (SCWA). Determination of intensity of formation and specific evolution of SCWA was conducted by gravimetric method. Obtained results are presented in Table 4.

It is seen that the lowest levels of SCWA evolution are achieved in welding with electrodes made with application of Na–Li glasses (V_{SCWA} = = 0.393 g/min, G_{SCWA} = 8.71 g/kg). Electrodes based on Na–K and Li binders are close to them as to SCWA evolution. The most favourable in terms of sanitary-hygienic characteristics are electrodes with K and K–Li binders. So, for instance, the intensity of formation and specific evolutions in electrodes, made with K binder, are by 22.0 and 23.6 % higher, respectively, than those in electrodes with Na–K glass. Electrodes made with K–Na and Na binders, in terms of their sanitary-hygienic properties take an intermediate position between the two extreme electrode groups.

Conclusion

Procedure developed by PWI was used to study standard sodium, potassium and mixed sodium-potassium and test lithium-containing liquid glasses, used in manufacture of electrodes for tin bronze welding and surfacing. As shown by comprehensive investigations of test electrode properties, the best results on adaptability to fabrication and welding-technological properties are ensured by sodium-potassium liquid binder.

1. Ilyushenko, V.M., Anoshin, V.A., Skorina, V.N. et al. (2013) Choice of slag-forming base of electrode coating for arc welding and surfacing of cast tin bronzes. In: *Proc. of 7th Sci.-Techn. Conf. of Junior Scientists and Specialists* (Kiev, 22–24 May 2013).
2. Ilyushenko, V.M., Anoshin, V.A., Bondarenko, A.N. et al. (2013) Development of electrode materials for welding and surfacing of complex-alloyed bronzes. In: *Abstr. of Int. Conf. on Welding and Related Technologies: Present and Future* (Kiev, 25–26 Nov. 2013), 72–73.
3. Skorina, N.V., Kisilyov, M.O., Paltsevich, A.P. et al. (2011) Properties of lithium-containing liquid glasses for manufacture of welding electrodes. In: *Proc. of 4th Int. Conf. on Welding Consumables of CIS Countries* (Krasnodar, 2011), 75–82.
4. Marchenko, A.E., Gnatenko, M.F., Chalykov, A.I. et al. (1983) *Comparative evaluation of technological properties of electrode coating mixtures Rouen, Vitosha and YONI/13 made with capillary and conic plastometers*: SMEA Inform. Doc., Issue 1/23, 69–74. Kiev: Naukova Dumka.
5. Sokolov, V.A., Sotchenko, V.P., Marchenko, A.E. et al. (1981) *Autoplastometer*. Kiev: PWI.
6. Marchenko, A.E., Shkurko, S.A. (1975) Examination of electrode mixtures by capillary plastometer method. *Svarochn. Proizvodstvo*, **5**, 11–13.
7. *RD 03-613–03*: Procedure for application of welding consumables in manufacture, mounting, repair and reconstruction of technical devices for hazardous industrial facilities. Introd. 19.06.2003.
8. Ershov, A.V., Ershov, A.A. (2013) Welding-technological properties of electrodes used for welding of building metal structures. *Svarka i Diagnostika*, **3**, 56–60.

Received 15.04.2014

THICKNESS DIFFERENCE OF ELECTRODE COATINGS CAUSED BY ELASTIC TURBULENCE OF ELECTRODE COMPOUNDS UNDER CONDITION OF NONISOTHERMAL PRESSURE FLOW

A.E. MARCHENKO
E.O. Paton Electric Welding Institute, NASU
11 Bozhenko Str., 03680, Kiev, Ukraine. E-mail: office@paton.kiev.ua

Generalized and analyzed are the results of investigations carried at the E.O. Paton Electric Welding Institute on technological properties of electrode compounds, promoting thickness difference of electrode coatings. The investigations were carried out using capillary viscosimeter of fixed flow — rheometer with electric drive, which can be used for simulation of the conditions of compound extrusion application over the electrode rods, typical for commercial electric extrusion presses. Thus, specific pressure on compound under condition of stationary flow achieves 60–75 MPa, average gradient of shear rate is gradually regulated in the ranges from 1 to $5 \cdot 10^3$ s^{-1}, and it makes to $65 \cdot 10^3$ s^{-1} for separate types of compound. The compounds for rutile, low-hydrogen and cellulose electrodes, differing by wide range of consistency indices, were investigated. In addition to shear and longitudinal viscosity, the investigations were carried out on a range of change of their modulus of shear elasticity, period of relaxation, criterion of Reynolds elastic turbulence, elastic potential and reversible (elastic) deformation. The results received were analyzed from point of view of existing phenomenological theory of elastic turbulence of polymer materials, combining viscosity and elasticity properties. It is successfully used in the course of many years in rheology of melts and solutions of high-molecular compounds for solving of technological problems of their extrusion processing. Variants of elastic turbulence, detected in capillary and pre-capillary zones, were analyzed. Quality relation of this phenomenon to appearance and nature of coating thickness difference in course of real extrusion application of compound over the electrode rods was shown. 24 Ref., 4 Tables, 9 Figures.

Keywords: *arc welding, coated electrodes, coating thickness difference, electrode compounds, viscosity, elasticity modulus, elastic turbulence*

Alignment of coating casing and rod [1, 2] is one of the most important among number of indices of GOST 9466–75, which are used by customer for assessment of quality of the electrode production. Thickness difference prevents normal welding process as well as results in deterioration of quality and mechanical properties of the welds. Thickness difference of the coating, which is maximum allowable by standard, i.e. not exceeding 5 % of the rod diameter, and, moreover, one which is above the norm, promotes formation one-side «peak» at the end of consumable electrode that disrupts air protecting gas and slag coverage of molten metal during welding, as well as formation of weld metal. This results in unfavorable changes of chemical composition, deterioration of mechanical properties, formation of pores and other weld defects [3–5].

It is believed that number of factors result in appearance of thickness difference of the coating (type, portion and grain composition of constituents, technological characteristics of compounds, quality of rods, condition of equipment, qualification and level of discipline of staff, engaged in manufacture of electrodes [6]), and they prevent finding the real reasons and regularities of its appearance in course of many years. This limited the capabilities of accurate prediction of quality of the electrodes on this index.

Compound is applied over steel rods by means of extrusion. This process should be termed in such a way, since change of shape in order to transform the compound in concentric circular casing around the rod is preceded by its all-round compression in a head of extrusion press. It is the key operation in technology of production of welding electrodes, which, in particular, results in coating thickness difference.

Experience, gained in other technological processes, using extrusion method for processing of paste, including filled materials, similar on consistency to the electrode compounds, shows that interruption of their stable and uniform flowing from the shaping instrument is determined by the following main reasons [7]:

- slipping of flow near the walls of shaping instrument;

• breaking of elastic liquids under effect of huge stresses;

• elastic hydrodynamic instability, accompanied by increasing disturbances (it is called elastic turbulence);

• structural instability, caused by viscosity abnormity (appearing, in particular, in form of its reduction under effect of increase of rate gradient and temperature).

Studies of rheological properties of the electrode compounds, carried by the E.O. Paton Electric Welding Institute in course of many years, showed that elastic turbulence is considered as the main reason of appearance of coating thickness difference. The rest can intensify it, whereas flow interruptions under effect of huge stress can be observed extremely rare.

Elastic hydrodynamic instability takes place in the electrode compounds, combining viscous and elastic properties, relationship between which is changed during their extrusion treatment. Excess of elasticity can promote regular (oscillatory) or irregular disturbances in the flow. Viscosity can be a damping constituent of the rheological system, i.e. suppress elastic constituent. If viscosity and elasticity modulus are equal, then loss of electrode compound stable flow takes place. Point, where it happens, can be the surface of gage sleeve and other sections of the shaping instrument. Time, when it happens, depends on the fact when compound viscosity is reduced due to temperature and/or structural breaking of the coagulation structure to such extent that capability to suppress flow pulses, promoted by elastic stresses, is lost. The higher elasticity in comparison with viscosity, the more is the difference of irregular disturbances from the regular form. In particular, if the system has more than one center of such disturbances. Aim of the present work is to show dependence between plastic turbulence of the electrode compound and thickness difference of electrode coating.

Rheological model of visco-elastic materials and mathematical formulae of their description. The simplest one-dimension rheological model, which can be used during investigation of properties of the electrode compounds, was proposed by Maxwell [8]. It is represented in form of spring (Hooke elastic body) connected in sequence with hydraulic damper (viscous Newtonian fluid). The model shows the reason of appearance and allows explaining the process of stress relaxation in visco-elastic material under constant deformation or stress. Visco-elastic liquid on Maxwell model, being subjected to the deformation promoted by constant force applied to it, should deform step-like by value of compression (extension) of the elastic element, and further deform with constant rate, corresponding to the applied force. If the same model is quickly deformed using the set value γ, and the force (or stress) change, proportional to the set deformation, is examined after fixing γ on this level, then they will gladually reduce (relax) in time due to shear of damper piston. Mathematic law, describing rheological behavior of such model is the fowling:

$$\dot{\gamma} = \frac{\tau}{\eta}\frac{1}{G}\dot{\tau}, \qquad (1)$$

and process of stress relaxation under constant deformation

$$\tau = \tau_0 e^{(G/\eta)t}. \qquad (2)$$

Since, $\lim_{t\to\infty} \tau = \lim_{t\to\infty} e^{(G/\eta)t} = 0$, then the stress τ under constant deformation in time will exponentially go to zero (here and below for designations see Table 1).

Relationship of dynamic viscosity η to elasticity modulus G has time dimension and is termed as a period of relaxation, $\tau_1 = \theta$. Taking this into account

$$t_1 = \frac{\eta}{G}; \quad \frac{\tau_1}{\tau_0} = e^{(G/\eta)t} = e^{-1} = 0.37, \qquad (3)$$

and $\tau_1 = 0.37\tau_0$.

Therefore, initial stress reduces by 63 % per time θ.

Combining the relaxation period θ and duration t_h of the external influence on material can help to evaluate its behavior in change of deformation rate.

τ and η are determined, first of all, in order to evaluate rheological behavior of the compound at its forced flow [9]. Then, such indices as G, θ and elastic potential W are calculated using formulae, proposed and tested in the technology of extrusion processing of polymer materials. They together provide for complete and objective characteristic of visco-elastic indices of the compounds.

There are three methods for calculation of pressure drop on capillary length, ΔP, necessary for calculation of τ and η from general resistance of measuring cell as a constituent of capillary and pre-capillary (entrance) zone. These are methods of Couette, Bagley and lock disk.

Couette method, assuming that resistance of capillary to flow rises in proportion to its length, for calculation of shear stress on capillary wall applies a pressure difference, registered in use of

long and short capillaries of the same diameter ($\Delta P = P_{long} - P_{short}$).

In Bagley method [10] the dependence of pressure difference on specific length of channel, L/R, at fixed shear rate was also assumed linear, and ΔP_0 value is calculated by means of extrapolation of $\Delta P = f(L/R)$ dependence to L/R zero value. The extrapolation of the same dependence for zero pressure value gives the value of dummy channel extension, n_B, equivalent to input pressure loss on resistance. It is called Bagley correction.

Couettee and Bagley methods cannot always be used in rheological testing of the electrode compounds, since pressure loss in their flowing through capillaries is not always proportional to their given length, L/d_c.

On the one hand, it is caused by accumulation of elastic stresses in initial sections of the short capillaries; on the other one, it is promoted by excessive dissipative heating of the compound jet in near-wall layer in use of capillaries of excessive length. The first and the second do not allow determining the slope of line $\Delta P = f(L/d_c)$ with accuracy necessary for τ calculation. Therefore, lock disk was used for determination of P_0 and ΔP was calculated as $(P_L - P_0)$ difference at $L = 10d_c = 20R$. In our case such a procedure provides for the highest accuracy of the test results.

At the same time, by example of the other authors, Bagley approach was used for reveal of rheological principle of correction n_B, as well as for separation from it of the elastic constituent, necessary for G calculation.

Rheological essence of Bagley correction can be determined using the following mathematical developments.

Shear stress on the capillary wall according to Couettee method, considering taken by us designations (see note to Table 1), is calculated on formulae

$$\tau = \frac{PR}{2L} = \frac{P}{2(L/R)} = \frac{P}{2n_C}. \qquad (4)$$

Taking into account Bagley correction the expression for calculation of τ from (4) is transformed into

$$\tau = \frac{P}{2(n_C + n_B)}; \quad 2\tau(n_C + n_B) = P; \quad n_B = \frac{P - 2\tau n_C}{2\tau} = \frac{P}{2\tau} - n_C. \qquad (5)$$

When $L = 0$ (as in the case when input resistance is found by lock disk method), $n_C = 0$, $P = P_0$, $n_B = P_0/2\tau$. Therefore, Bagley correction represent itself a value of input resistances, rated on shear stress on the capillary wall.

In such a form Bagley correction was used as a basis for evaluation of value of natural convergence angle, which is formed in pre-capillary zone at extrusion processing of visco-elastic materials [11–13].

It can be shown that in this meaning n_B correction is equivalent to criterion of Reynolds elastic turbulence, Re_e, or, as it was called earlier by Rainer, Deborah number (name of ancient pythoness) [14, 15].

In general, this is a reversible elastic deformation of the visco-elastic material, γ, subjected to it under the effect of deformation stress. It was mention above that it is estimated as a relationship of period of relaxation to typical time, θ/t_h. For capillary viscometer t_h equals the value inverse to gradient of shear rate [14, 15] and, respectively, $Re_e = \theta\dot{\gamma}$.

Reynolds criteria is transformed in the same form in the following way:

$$Re_e = \frac{\theta R}{UT^2} = \frac{\theta}{UT^2/R} = \frac{\theta}{\dot{\gamma}T^2} = \theta\dot{\gamma}. \qquad (6)$$

On the other hand, considering that $\theta = \eta/G$ and $G = \tau^2/P_0$, equation (6) can be equated to expression P_0/τ approving, in such a way, that Bagley input correction represents itself criterion of Reynolds elastic turbulence.

Assuming, as it proposed in work [16], that n_B in formula (5) together with Couettee correction includes elastic deformation S_R as well, which is part of formula of Hooke's law $\tau = GS_R$, then $n_B = n_C + (S_R/2) = n_C + (1/2G)\tau$. It follows that τ and P_0 value, determined by means of capillary measurements, can help to calculate modulus of shear elasticity G of the electrode compounds.

In fact, at $n_C = 0$

$$G = \tau/2(n_B) = \tau^2/P_0. \qquad (7)$$

Elastic potential W is calculated on input resistances. It is elastic energy referred to consumption per second, accumulated by the compound during flow through capillary: $W = P_0/12$. It is revealed at the output from capillary in form of free elastic recovery of jet, which is accompanied by deformation — β times increase of its diameter and β^2 times of length. A balance of revealed and accumulated energy is described by relationship [8]

$$W = \frac{G}{2}(\beta^4 + 2\beta^{-2} - 3), \qquad (8)$$

Table 1. Summary table of formulae used for calculation of rheological indices of compounds under condition of pressure flow through capillary of viscosimeter

Index of viscoelastic material	Formula
Shear viscosity, MPa·s	$\eta = \tau/\dot{\gamma}$
Longitudinal viscosity, MPa·s	$\lambda = \frac{9(n_0+1)^2}{32\eta}\left(\frac{P_0}{\dot{\gamma}}\right)^2$
Modulus of shear elasticity, MPa	$G = \eta/\theta = \tau^2/P_0$
Angle of natural convergence, deg	$\mathrm{tg}\ \alpha_0 = \sqrt{2\eta/\lambda}$
Characteristic Maxwell relationship. Dimensionless time of relaxation	$n_B = \theta/t_h = \theta\dot{\gamma} = P_0/2\tau = \mathrm{Re}_e$
Elastic potential, MPa	$W = \tau^2/6G = P_0/12$
Reversible (elastic) deformation	$\gamma = \tau/G = \sqrt{3(\beta^4 + 2\beta^{-2} - 3)}$

Here, τ — stress on capillary wall, MPa; $\dot{\gamma}$ — average gradient of shear rate, s^{-1}; n_0 — flow index equal $\lg \tau/\lg \dot{\gamma}$; P_0 — losses of flow in entrance zone, MPa; G — modulus of shear elasticity, MPa; θ — period of relaxation, s; α_0 — angle of natural convergence, deg; γ — reversible elastic deformation of jet; t_h — characteristic time of monitoring, in capillary viscosimetry, $t_h = 1/\dot{\gamma}$; W — elastic potential, specific elastic energy, accumulated by compound in flowing through capillary, in calculation per unit of its volume (consumption per second Q); β, β^2 — level of expansion of compound jet at the output from capillary on diameter and length, respectively, rel. un.

and value of deformation, promoted by jet swelling — by relationship

$$\gamma = \sqrt{3(\beta^4 + 2\beta^{-2} - 3)}. \quad (9)$$

In order to make it simple in use, received formulas are given in Table 1.

Electrode compounds as pasty compositions having visco-elastic properties. There is sufficient number of publications, indicating that electrode compounds together with viscosity should actually have elasticity properties.

Thus, author of work [17] characterizes plasticity of compounds by such rheological coefficients as shear elasticity and viscosity, and curve of its flowing is represented in «pressure P–consumption per second Q» variables. At low consumption it is differ from classical Bingham rheogram, describing plastically-viscous body, termed as a consequence by his name, by power splash of pressure, which at $Q_{cr} \approx 1$ $cm^3 \cdot s^{-1}$ smoothly transfers into line, slightly inclined to consumption axis. The reasons of maximum appearance had no explanations. We assumed that it is a result of relaxation of accumulated elastic stresses.

Thesis in [18] describes a procedure for determination of mentioned above indices of elasticity and viscosity of the electrode compounds. For this, the compound was slowly pressed by plunger through capillary sectioned on length. Flow pressure and volume of compound, escaping from the capillary under effect of elastic forces, were registered two times (during plunger stop and after switching off at stationary plunger in capillary end section). Indices of shear elasticity and viscosity, calculated using obtained data, are given in Table 2.

Our investigations of ANO-4 compound, pressed between two corrugated plates, also carried out in modes of shear creep flow, showed that it, the same as other types of concentrated dispersions of particles with crystalline structure, is significantly strengthened under the effect of shear stresses of around 0.01 MPa value. Initial deformation capacity of the compound in repeated loading is reproduced only after 4 hours

Table 2. Technological properties of compounds TsM-7 and UONI-13/55 in mode of creep pressure flow [18]

Liquid glass			Portion of Na_2CO_3, %	P, MPa	G, MPa	$\eta \cdot 10^{-6}$, mPa·s
Modulus	Density, kg/m^3	Portion, wt.%				
Compound of electrodes TsM-7						
$Na_2O_2 \cdot 8SiO_2$	1450	23	–	88	0.30	6.1
			2	50	0.225	3.1
Compound of electrodes UONI-13/55						
$Na_2O_2 \cdot 8SiO_2$	1430	23	–	40	0.08	–
			2	34	0.03	5.0

of «rest», when stresses accumulated as a result of specimen strengthening are relaxed [19].

Results of testing of the same on consistency compounds using conical plastometer showed that accumulated by it elastic stresses reduce (following the stop of cone introduction in them) with period of relaxation equal 100–150 s [20]. Complete relaxation of the elastic stresses requires the time significantly exceeding test duration.

Thus, it can be considered that obtained compound indices, even ones being tested in free state, contain significant portion of elastic constituent.

The compounds in course of testing of rheological properties in press chamber of capillary plastometer OB-1435 [9] stay in the conditions of all-round compression, the same on value as in press chamber of industrial electric extrusion unit. Extrusion curves from Figure 1 reflect changes of pressure during pressing-out of the compound from plastometer chamber through lock disk *1* or capillary *2*. It can be seen that there are several stages in course of capillary testing:

- stage of development of compound to all-round compression in course from beginning of piston movement to moment, when pressure reaches the maximum (P_{max});
- pre-stationary (structural) stage, accompanied by pressure drop (from P_{max} to P_c);
- setting of pressure of stationary (conditionally equilibrium) capillary flow P_c, the value of which is usually used for calculation of τ and θ;
- pressure drop in the moment of inertia-free stoppage of the piston, caused by free elastic recovery of jet, accompanied by sufficiently quick relaxation of accumulated elastic stresses ($\Delta P_c = P_c - P_{ck}$).

Initial structure of the material is deformed during the first stage, and its elements are oriented and compacted to such extent that so-called structure with limited volume is formed as a result [21]. Considering that this takes place under conditions of virtually zero deformation rates, then huge energy is consumed for such structure formation. Its significant part is accumulated in form of elastic constituent. The material under conditions of all-round compression becomes the elastic body independent of the fact it was solid body or liquid before [14].

The reasons of pressure drop after the maximum lie in growing mechanical and temperature fracture of compound structure, formed in course of previous stage. The center of structure fracture appears in front of enter into the capillary under the effect of pressure gradient and provoked by

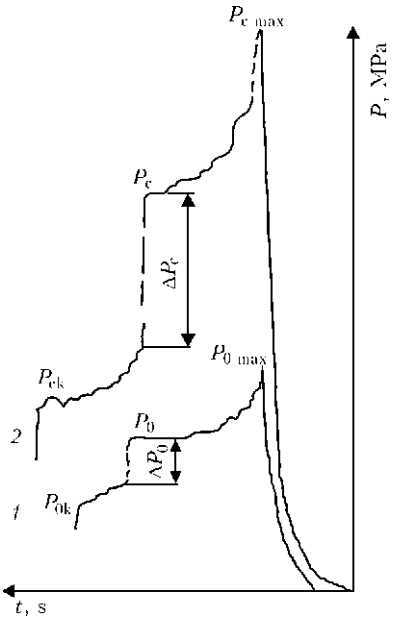

Figure 1. Types of extrusion curves $P = f(t)$ of ANO-4 compound received in its testing by capillary plastometer OB-1435 at $Q = 5$ cm^3·s^{-1}, diameter of capillary 0.4 cm, length 0 (*1*) and 4 (*2*) cm (for designations see the text)

it asymmetry of potential of molecular interaction between filling agent grains. It facilitates movement of filling agent grains on shear mechanism [21]. The deformation processes, responsible for fracture of the structure, are accumulated in specific moment mainly in the limits of forming natural convergent flow zone. The elastic potential, accumulated in course of the first (growing) branch of pre-stationary process, is a trigger of such energy rearrangement of the structure and transfer of compounds in pressure flow. Fracture of the structure is accompanied by change of relaxation properties of the compound (θ reduction).

Rates of fracture and recovery of the structure during equilibrium capillary flow became even on value. However, the system preserves in it significantly larger margin of elastic potential than in studied above tests of open specimens, and it is «relaxed» only after piston stop. Immediate pressure drop is as a rule accompanied by emission of some amount of the compound from shaping head.

Since extrusion takes place under non-isothermal conditions (isothermal ones can not be developed in principle in real rate of compound flowing), then the value of pressure drop, together with compound consistency, should, obviously, be effected by viscous heating, to which the compound is subjected begining from its structural phase. It should also be considered, that liquid glass is a piezo-sensitive liquid [22]. Reduction of its viscosity, caused by excessive pressure, influences the compound structure in the same way as viscous heating. Their properties

at very high level of compression can change in opposite directions under effect of temperature and pressure. Therefore, the final result is difficult to be predicted.

Results of experimental estimation of visco-elastic characteristics of the compounds under condition of pressure flow. Value of accumulated elastic energy can be estimated on ΔP_0 value, if lock disk is used, as in the case of determination of input resistances, or ΔP_c, if capillary is applied. The results of estimations are matched on absolute scale ΔP_0 and ΔP_c as well as on relationships $\Delta P_0/P_0$ and $\Delta P_c/P_c$, $P_0 - \Delta P_0/P_0$ or $P_c - \Delta P_c/P_c$.

Results of testing of the compounds of rutile, low-hydrogen and cellulose types, which were carried out using capillary plastometer OB-1435 at the E.O. Paton Electric Welding Institute in different time, were used for evaluation of visco-elastic indices. Table 3 shows compound characteristic. Compound consistency was regulated by means of change of filling agent composition, its grain composition as well as characteristics of liquid glass. Plastic strength of compounds at that was changed in the ranges from 0.13 (very weak consistency) to 1.40 MPa (structured composition).

Preliminary evaluation of value of pressure drop ΔP_0 and ΔP_c at the moment of piston stop found that the compounds are significantly differ from each other by elastic properties. Portion of elastic constituent in the results of their testing, depending on flow rate and method of its regulation (Q = const or d_c = const), was changed in proportion to P_0 and P_c value in the ranges from 0 to 60 %. It was effected by number of accompanying factors.

For example, notable dissipative heating of the jet was specifically observed in testing of ANO-4 compounds having low heat-conductivity, and UONI-13/55 compounds (ST) manufactured based on liquid glass, which were significantly «fluidized» even under effect of moderate viscous heating. In both cases, effect of dissipative factor dominated at flow mode Q = = const and portion of revealed elastic energy was overstated due to this. In contrast, results of viscous heating in UONI-13/55 (NT) compounds, manufactured based on low-viscosity liquid glasses, were masked by heat consumption used for fracture of their coagulation structure. In this case, the results of tests were understated.

In general, interesting information was received on number of properties of compared compounds, however, they do not allow making single opinion on elastic characteristics.

Table 4 generalizes the results of evaluation of viscous and elastic properties, produced using calculation formula given in Table 1.

Value of rate gradients and, respectively, shear stress, which were used in course of investigations, are limited by ranges, in which studied compounds can be extruded through the nozzles of used sections (consumption per seconds was changed in the ranges from 1 to 2.25 cm^3, and d_c = 1–6 mm). Some compounds lock the channels of particularly small diameters, when specific shear rate is exceeded. Shear (as well as longitudinal viscosity) reduces with increase of deformation rate, and this confirms thixotropic fracture of the compounds, forced by their viscous heating to the extent in which they susceptible to it. Longitudinal viscosity 2 times higher than shear one, and relationship λ/η between them

Table 3. Characteristic of charge, liquid glasses and compounds used

Compound	Index	S_{sp}, cm^{-1}	Indices and portion of liquid glass				P_m, MPa
			Modulus	ρ, kg/m^3	η, mPa·s	Portion, %	
ANO-4	A2	8300	2.9	1465	800	29.6	0.30
	A1					29.8	0.75
	A4					29.8	1.30
UONI-13/55 (ST)	GS-1	2250	2.9	1495	1000	25.0	0.15
	GS-4	3900					0.13
	GS-6	4900					0.28
UONI-13/55 (NT)	GS-1	2250	3.2	1334	50	22.0	0.45
	GS-4	3900					0.30
	GS-6	4900					0.80
VSTs-4	Ts	–	2.9*	1407	100	51.5	–

*Soda glass, other glasses — soda-potash.

Table 4. Indices of viscous elasticity of electrode compounds (capillary zone)

Compound	Indices	γ, s^{-1}	Value of indices of viscous elasticity						
			τ, MPa	η, MPa·s	G, MPa	θ, s	W, MPa/cm^3	$\theta\dot{\gamma}$	P_0, MPa
ANO-4	A2	11.8 1445	0.43 0.70	0.000470 0.039090	0.018 0.035	0.014 2.110	0.83 1.92	19.4 33.3	10.0 23.0
	A1	11.8 1211	0.61 1.10	0.008900 0.055890	0.022 0.034	0.026 2.320	1.23 2.83	22.3 32.6	15.5 34.0
	A4	11.8 1211	0.78 1.19	0.000860 0.025785	0.020 0.045	0.040 2.830	1.96 4.10	11.7 48.5	23.5 49.0
UONI-13/55 (ST)	GS-1	11.8 1650	0.50 1.55	0.000950 0.041113	0.017 0.085	0.010 2.450	1.15 2.75	11.8 31.7	14.0 33.0
	GS-4	11.8 1650	0.70 1.40	0.000550 0.060170	0.038 0.065	0.018 1.255	1.15 2.55	14.8 21.3	10.5 42.0
	GS-6	11.8 1650	0.80 1.25	0.000080 0.069500	0.028 0.075	0.008 1.425	1.15 2.50	16.8 38.5	13.8 90.2
UONI-13/55 (NT)	GS-1	11.8 8120	0.31 0.75	0.000090 0.026270	0.005 0.019	0.005 4.370	1.25 2.50	34.8 61.8	15.3 30.0
	GS-4	11.8 64970	0.25 0.75	0.000010 0.033900	0.003 0.023	0.001 3.390	1.28 2.50	25.0 86.0	15.9 37.2
	GS-6	11.8 64970	0.40 0.95	0.000015 0.037290	0.007 0.027	0.001 3.720	1.35 2.25	26.0 65.0	19.8 33.0
VSTs-4	Ts	150.0 64970	0.38 0.60	0.000005 0.003490	0.005 0.025	0.001 0.140	0.90 3.10	20.9 65.0	11.0 37.0

Notes. 1. Minimum values are given in numerator, and maximum — in denominator. 2. Viscosity (ST) and low-viscosity (NT) glass were used.

rises with increase of shear rate, that promotes decrease of angle of natural convergence, or reduction, but at that rise of α_0. Small α_0 value indirectly indicate that compound jet in pre-capillary zone overcomes resistance of the material with high elasticity. Modulus of elasticity under these conditions also shows ambiguous change.

Its value in all ANO-4 compounds does not depend on their consistency and shear rate.

Modulus of elasticity for compounds UONI-13/55 (ST) significantly increases with rise of shear rate. It is initially the lowers one on value for GS-1 variant with the coarsest filling agent. The finer filling agent grains, the higher is the modulus of elasticity for this type of compounds at low shear rates, and it is lower at high shear rates. The weakest reaction on deformation rate was observed in compound GS-6 with the most pronounced structure. Grain composition of the filling agent has the similar effect on modulus of elasticity of UONI-13/55 (NT) compound with low-viscosity liquid glass. However, value of their modulus of elasticity, is initially smaller on value than in CT compounds and has weaker response to deformation rate. The compound with average grain-size of the filling agent showed significant scatter of results. The reason of this is unknown.

Modulus of elasticity in VSTs-4 compound reduces with rise of shear rate gradient.

Generally, it should be noted that average value of elasticity modulus of compound changed in sufficiently narrow limits regardless the wide range of change of consistency of compared compounds.

There was no information in mastering of procedure of evaluation of compound elasticity on actual value of their modulus of elasticity, except for data of V.I. Klementov, received in mode of creep flow. In this connection, predicted order of value of this index was calculated in the following way.

It is well know fact that one of the effects, accompanying free recovery of jet of visco-elastic compositions, is its swelling at output from the capillary (Barrus-effect). Technologies of polymer processing, characterized by pronounced non-Newtonian properties, can have relationship of jet diameter and extrusion nozzle achieving 4-fold value. Introduction of filling agents in the polymers together with reduction of price of products provide for suppression of this undesirable effect. Electrode compounds are also filled compositions with liquid-glass matrix, having weak non-Newtonian properties. There should be

no swelling of jet in such compositions by this reason. It is indicated by good matching of coating diameters (jet, when it is a question of compound extrusion at capillary testing) and extrusion nozzle (capillary).

In fact, insignificant swelling of the compound jet still takes place. It is determined that rearrangement of rate profile in the jet takes place at the output from capillary in hydraulic and rheology, as a result of what, its diameter should decrease at least by 13 % based on law of momentum conservation.

In other words, elastic swelling of the compound jet as though stays in $\beta = 0.13$ limits, compensating its constriction, promoted by rearrangement of rate profile.

If $\beta = 0.13$ in equitation (9) is substituted, then swelling-caused deformation will make $\gamma = 18.5$ %. On the other hand, it was taken into account that γ and G are related with each other by $\gamma = \tau G$ relationship [8].

As a rule, shear stress on the capillary wall in compounds varies in the ranges from 0.5 to 1.5 MPa. It should be expected based on this that value of elasticity modulus of the electrode compounds lies in the ranges from 0.025 to 0.075 MPa. According to order of value it agrees with our results, given in Table 4, and results of V.I. Klimentov (see Table 2).

Change of elastic potential and input resistances are symbate to each other in rise of shear rate. This verifies that elastic state of the compounds takes place in the convergent zone. Its relaxation manly appears out of its limits.

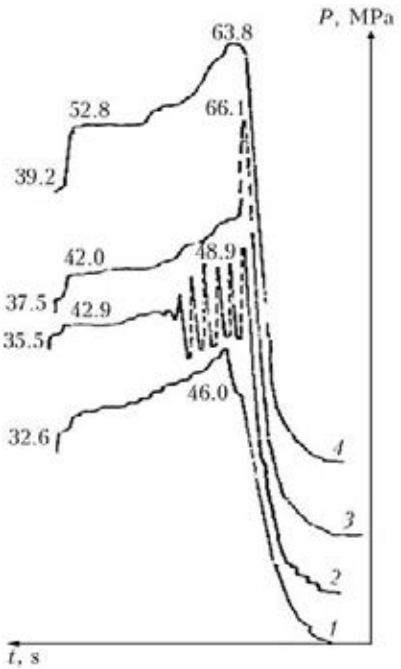

Figure 2. Extrusion curves of compounds GS-6 (NT) at $Q = 1$ cm^3·s^{-1} and capillary diameter of 6 (*1*), 4 (*2*), 2 (*3*) and 1 (*4*) mm

Period of relaxation of studied compounds at capillary stage in logarithmic interpretation linearly reduces with rise of deformation rate. This indicates dispersal of the elastic energy, accumulated in the pre-capillary zone, due to mechanical and temperature fracture of the compound structure. Level of viscosity exceeds the elasticity modulus at small shear rates, and becomes smaller than at high ones. Zero transition point is easy to determine, assuming that viscosity and modulus of elasticity become equal in value at $\theta = 1$. In this moment any accidental influence on the system can promote different nature oscillations of the compound flow rate under the effect of stress elastic constituent, since viscosity of the extruded material can not already suppress them. Most often pulsations appear in the stage of incident (structural) branch of the extrusion diagram. Figure 2 as example shows pulsation curve registered in extrusion of GS-6 (NT) compound through 4 mm diameter capillary at $\dot{\gamma} = 40$ s^{-1} rate. Nature of pulsation allows assuming that detachments of the jet take place on the capillary wall. Other variants of compounds of GS series tested in parallel show no pulsation.

Two reasons can explain this. The first is related with step-like nature of change of mode of compound extrusion in plastometer OB-1435. As a result, only experiment with compound GS-6 (NT) provides the extrusion conditions suitable for critical period of relaxation $\theta = 1$, at which pulsation of pressure flow can take place. Measurements of the rest experiments were out of such critical point. The second reason is connected with the fact that flow pulsation in the capillary zone takes place on channel surface. Decrease of capillary diameter promotes rise of flow rate, reduction of material viscosity and, seemingly, conditions for pulsing improve at relatively stable value of elasticity modulus. In reality, reduction of channel diameter results in simultaneous rise of specific surface of nozzle (in calculation per unit of volume) and its suppressive action on the jet. It is known from theory of near-wall slipping that it mostly appears in using of wide channels and being suppressed in their replacing by small diameter capillary.

Figure 3 shows the diagrams of extrusion of the same compounds GS-1, GS-4 and GS-6, made based on low-viscosity glasses, through capillary of 4 mm diameter with movable insert («vane») in front of capillary input. It was designed for provoking of non-stationary flow. It was found

that flows of the compounds with coarse- (SG-1) and average-grain (GS-4) filling agents showed no reaction on flexible insert before input into the shaping channel. Indicated insert in the case of GS-6 compound with fine-grain filling agent provoked sufficiently continuous gradually attenuating pulsation of the flow. This experience proves that tendency to non-stationary flow modes is, first of all, a compound property and only then being a condition of its pressure flow. Pulsation modes of compound flow can be developed not only on the capillary wall, but in the convergent zone as well. And conditions for their appearance in the convergent zone are more favorable than on the capillary wall.

It is confirmed by results of investigation of pilot variants of UONI-13/55 compound, marked by T-9 index. The compound is made on three-module liquid glass with 850 mPa·s viscosity. Share of liquid glass in it makes 26 %. Characteristic feature of the filling agent is its grain composition. It in accordance with the experiment purposes has the following share proportion of fractions, i.e. total residual on meshes of 250, 160, 100 and 63 μm made respectively 6, 8, 13 and 37 vol.%. Specific surface of charge S_{sp} = = 10,000 cm^{-1}, level of volume filling by particles makes F_m = 0.67. Consistency of compound is sufficiently tight, thus P_m = 0.58 MPa (0.85 MPa after hour holding). Results of experiments are given in Figure 4.

It was determined in process of extrusion tests that pressure of compound flow through lock disks with hole diameters 6, 4 and 2 mm made 50, 55 and 57 MPa. The figures themselves are not very high. The compound passed through 6 mm diameter hole with sufficiently small pulsations. Flowing through 4 and 2 mm diameter holes was accompanied by significant rate pulsations. The first of them reflects the flow at 40 s^{-1} shear rate gradient, the same as in experiment with GS-6 compound in capillary of the same diameter. Therefore, the first experiment with T-9 compound also reproduced the critical conditions (η and G), under which pulsations of flow rate take place, in this case in the entrance zone. Extrusion of T-9 compound through 2 mm diameter hole in disk takes place at 318 s^{-1} rate, i.e. 8 times higher than in previous case. At that shear viscosity of the compound should significantly reduce, and modulus has to rise. The conditions for flow pulsation have become more favorable, and shape of extrusion curve verifies this. In fact, flow pulsation, caused by excess of the compound elasticity, is already suppressed no by viscosity, neither by capillary limiting surface, since compound flow in the convergent zone takes place over shear layers. Shape of peaks is smoother in contrast to sharp peaks in the case of GS-6 compound, which slipped over capillary surface.

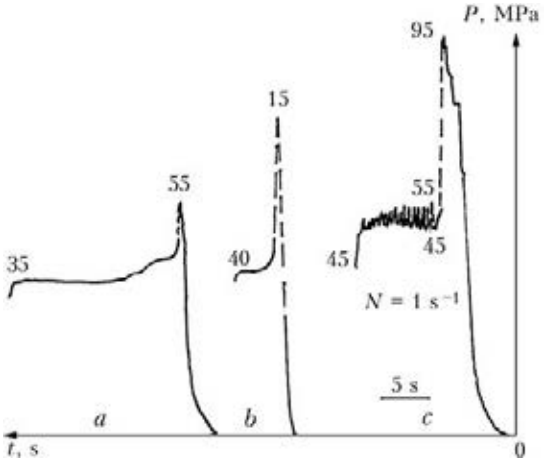

Figure 3. Diagrams of extrusion of UONI-13/55 compound manufactured based on high-modulus liquid glass with viscosity 100 mPa·s at Q = 1 $cm^3 \cdot s^{-1}$, conical nozzle (2α = 40°, 4/40 mm diameter) and portion of fine fraction of 20 (*a*), 40 (*b*) and 60 (*c*) %

Immediate relaxation of accumulated elastic stresses in the convergent zone is often observed in form of pulsing outcomes of the compound from shaping channels of extrusion head under real conditions of electrode extrusion. For example, if extrusion head has two-channel guide, compounds with excessive elasticity can by turn select one of the channels for flowing, whereas its flow in parallel channel of the same profile is stopped for this time. Flow pattern in the next phase of the process is changed to the opposite, i.e. compound chooses for passing the channel,

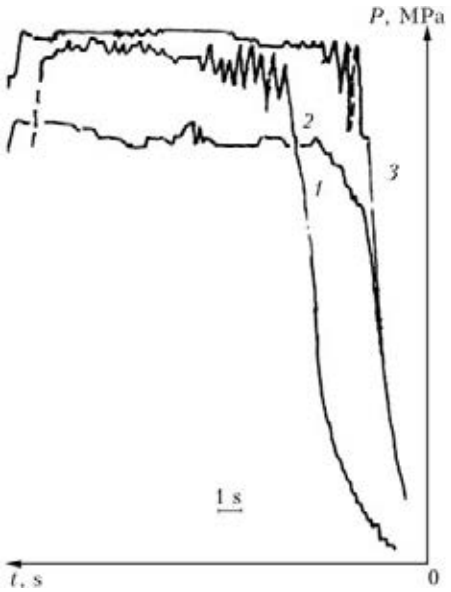

Figure 4. Comparison of extrusion curves $P_0 = f(t)$ of T-9 compound, produced with the help of capillary viscosimeter, at nozzle diameter of 2 (*1*), 6 (*2*) and 4 (*3*) mm

in which it was stationary up to this moment. Compound flow in the parallel channel is stopped for the same period time.

Some results of investigation of regularities of thickness difference appearance under real conditions of electrode extrusion. Thickness difference of the coating appear in bi-component flow coming from coating to rod, as a result of stochastic on its nature energy interaction of the components, one of which (the coating) is characterized by non-linear visco-elastic properties, susceptible to appear in form of pulsating flows, and another (the rod) is elastic element. Relation of viscosity and elasticity in coating material to greater or lesser degree is changed under the effect of dissipative and mode flow factors, and accompanied by breaking of its stability, whereas elastic properties of the rod remain unchanged at that. Role of the effects, related with elastic turbulence, is characterized by $\mathrm{Re}_e = Ut^2/\theta R$ criterion. Effects of interruption of flow stability, appearing in turning of compound flow, in dividers and conical channels before entering into the shaping head, as well as in area of hydrodynamic stabilizing of flow at input of the extrusion nozzle, can be characterized by monochromatism criterion $H_0 = Ut/R$ [15].

Stationary or attenuating, regular or irregular oscillations of the compound rate, accompanying by pulsation of rate and pressure, provoke alternating transverse deviations of the rod from axis of the calibration insert. As a result, significant distortion of uniform on section circular shape of the coating takes place. Combination of transverse oscillations with longitudinal movement of the rod can result in oscillation as well as helical change of position of maximum value of thickness difference along the electrode.

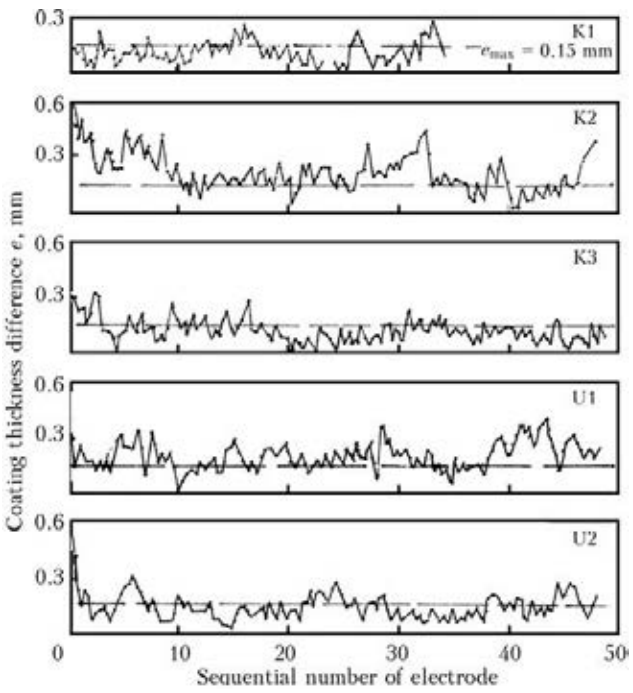

Figure 5. Dynamics of change of coating thickness difference during extrusion of pilot low-hydrogen electrodes of 3 mm diameter with index K1–K3, U1 and U2

Eccentric position of coating cross section relatively to the rod does not change its area in comparison with its concentric shape. However, many liquids experience lower resistance in their flowing through the eccentric channels in comparisons with the channels of concentric shape. Work [23] determined this during investigation of pressure flow of water solutions KMTs, GETs and MTs through the circular channels between coaxial pipes. It was found that pressure falls, necessary for their pressure flow through the eccentric channels at fixed flow rate, reduce with rise of eccentricity. The liquids with more pronounced non-Newtonian properties show slower rate of pressure drop reduction depending on rise of value of eccentricity between external and internal pipe. Such a flow pattern can be used during circular extrusion of rod casing, replacing surface of internal pipe to rod surface, moving synchronously with compound.

Monitoring of dynamics of thickness difference change show that it reflects well the effect on this index of found by us peculiarities of viscoelastic behavior of compounds.

Figure 5 gives the results of testing of five types of compounds for low-hydrogen electrodes different in technological properties. Thickness difference of the coating was measured at the beginning, middle and end of each electrode, came out from head of the press. Extrusion of electrodes with 3 mm diameter rod was carried out on the Oerlikon straight-flow press EP-120. It can be seen that more or less pronounced initial period can be, first of all, outlined in change of thickness difference of the coating during application of each of tested compounds over the rods. In course of this period the compound passes from condition of the most compression into relatively stationary flow mode. At that, larger on value initial thickness difference of the coating reduces and gradually reaches the level, which varies with respect to some average oscillating value. Waves of these oscillations differ on amplitude and frequency, at that drop and rise of low-frequency wave is also accompanied by finer on amplitude, but more often (even in the limits of one electrode) oscillations of thickness difference. It indicates its random nature, reflecting very complex changes in relationship of viscous and elastic characteristics of the compounds un-

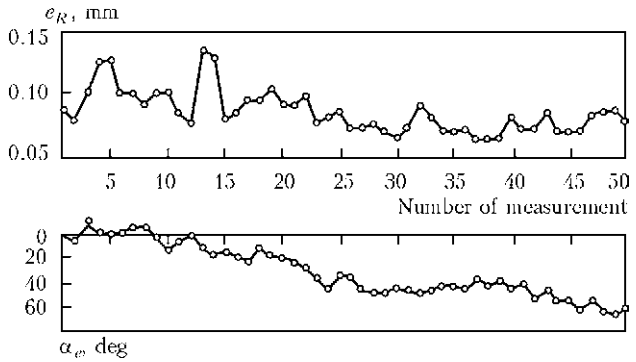

Figure 6. Change of value and angle of orientation of vector of coating thickness difference on oscillography data

der condition of pressure flow with rod. Given examples do not show the cases of thickness difference, reason of which could be explained by entering of some random inclusions in the compound.

Figure 6 gives data on value and angle of orientation (in plane normal to electrode axis) of vector of coating thickness difference. They were obtained by oscillographic measurements of its horizontal and vertical constituents in the course of production of UONI-13/55 electrode with 4 mm diameter rod using the Havelock straight-through press [24].

200 electrodes were produced by head of the press during monitoring, value of thickness difference vector e_R changed from 0.15–0.17 to 0.07–0.10 mm (i.e. almost 2 times) and angle of its orientation with respect to α_e horizont rised from 0 up to 60°. Pulsation of e_R and α_e was observed against a background of their general changes. Vertical constituent of thickness difference shows specific pulsation and it is explained by vertical positioning of two windows of diaphragm-divider, through which the compound is pumped from cylinder to press chamber (gap between tip of rod-guide and calibrating insert). Figure 7 shows relationship of value and angle of orientation of vector of thickness difference. The lager its deviation from horizontal line, the smaller is the amplitude of its oscillations. However, its absolute value at that increases. It seems that there are wave-like asynchronous oscillations of e_R and α_e (the first are faster in time than the second), thus some kind of spatial (spiral) wave is formed. In one direction e_R reduces with α_e rise and in other, normal to the first, it increases with the same increments of e_R and α_e. It is supposed that flow oscillations, caused by its 90° horizontal turning at the output from cylinder in front of the divider, are superimposed over compound pulsation through the divider windows. It can be assumed that in this case internal and external surfaces should move at

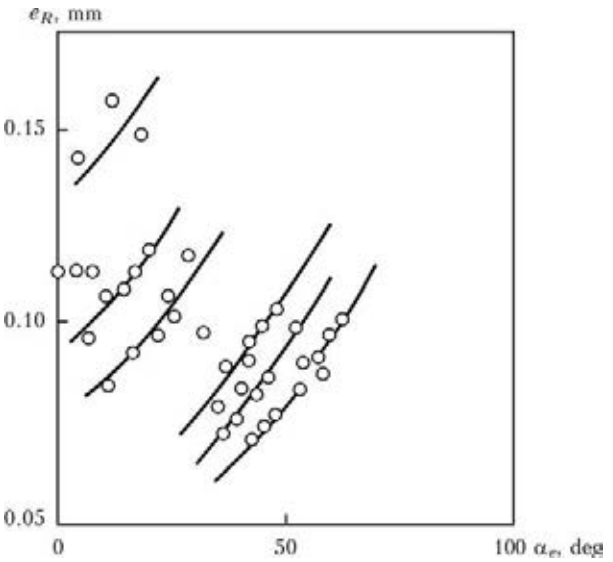

Figure 7. Relationship of value and angle of orientation of vector of coating thickness difference found by oscillography

different rates due to necessity of fulfillment of principle of compound flow homochronicity (continuity). The closer to the horizon the positioning of thickness difference vector, the greater is the effect of this factor on thickness difference.

Boundaries and levels of randomness of deviation of coating thickness difference on its main orientation can be judged on results of measurements, carried out using concentricity meter KRP-12 during extrusion of ANO-4 electrodes with 4 mm diameter rod at angle press MAOE-1.

Vertical press has compound flow turning angle 90°. «Windows» of the divider of compound flow are vertically oriented in head of the press.

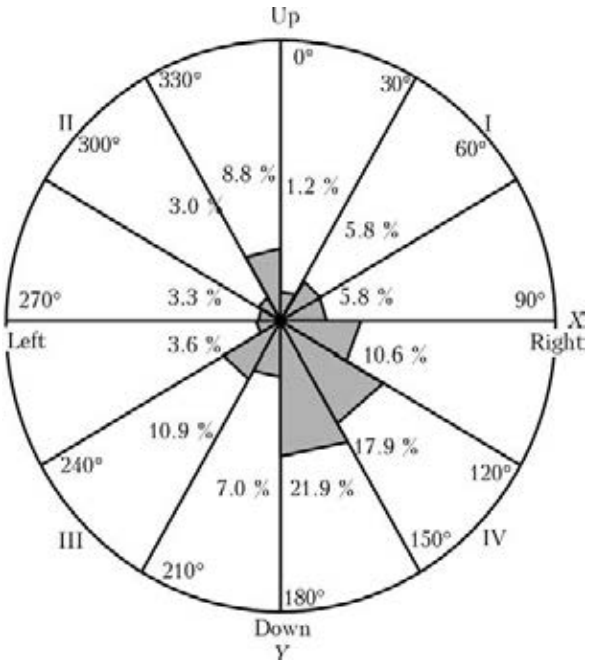

Figure 8. Statistical distribution of angle of orientation of vector of coating thickness difference in plane normal to axis of coming electrodes for 980 electrodes in sampling

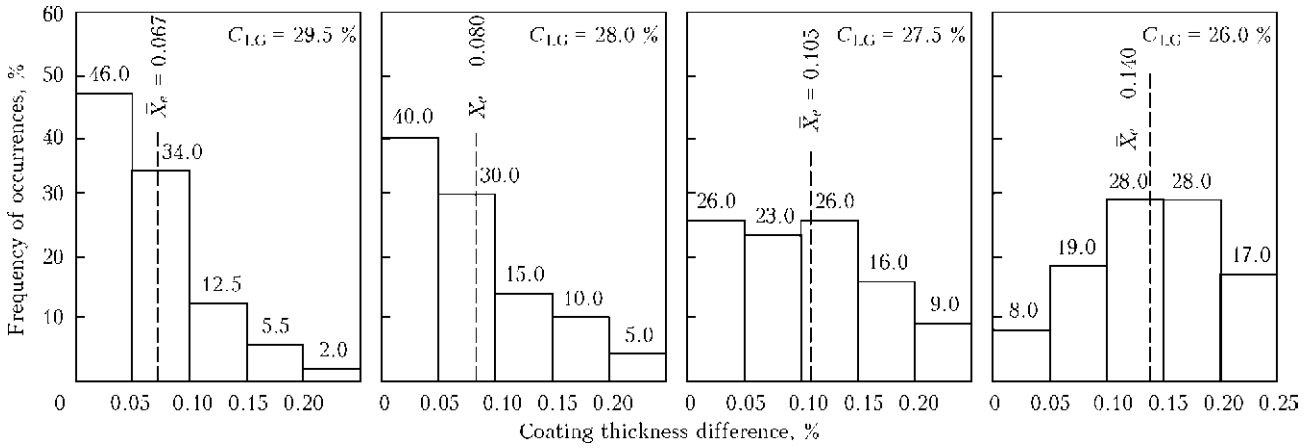

Figure 9. Effect of portion of liquid glass *C* in compound on tendency of ANO-4 electrodes to coating thickness difference

Solid line, plotted as generatrix in zenith position of coating of the electrodes produced by press, was a reference point for angle α_e. During measurement the second reference mark, corresponding to the position of maximum thickness difference, was plotted in each of 11 control sections of the electrode. Angle between these marks in plane normal to the electrode axis was taken as e_R orientation angle. Frequency distribution of measurement results in earlier selected sectors is shown in Figure 8. This shows that the maximum values of coating thickness difference are oriented mainly in the sectors between 120 and 180°. Shifting of the rod, being the reason of coating thickness difference, is manly promoted by external side of compound flow upward and to the left relatively to vertical line.

Figure 9 represents the results of estimation of coating thickness difference of the electrodes, portion of liquid glass in which was changed from 29.5 to 26.0 wt.%.

As far as consistency of the compound became more and more elastic, share of electrodes with excessive coating thickness difference increased from 2 to 17 %. Effect of increased portion of elastic constituent promoted rise of average value of thickness difference from 0.067 to 0.140 mm. Shape and width of static scattering of this index (from one-sided to Gaussian) were changed.

Conclusions

1. Coating thickness difference takes place in bi-component flow, in which casing from compound is characterized by non-linear visco-elstic properties and rod is the component with constant elasticity modulus. Relationship of viscosity and elasticity in the casing material reduces under the effect of structure fracture and dissipative heating, and this, as a result, provokes instability of shear deformation modes, and so, can be the reason of violation of uniform coating application over the rods.

2. It is determined that mathematical apparatus, developed in the polymer rheology, can be used for calculation of such visco-elastic characteristics of the electrode compounds under condition of capillary flow as relaxation period, modulus of elasticity, elastic potential and Reynolds criterion of elastic turbulence.

3. Using of indicated apparatus allows calculation of listed indices of visco-elastic electrode compounds for rutile, low-hydrogen and cellulose electrodes, consistency of which was regulated in sufficiently wide limits by change of grain compositions of charge, characteristics of liquid glass and its portion in electrode compound. On the other hand, changing of modes of capillary testing of indicated compounds allows determining their effect on rheological properties.

4. It is determined that modes of compound pressure flow provide for the largest effect on shear viscosity and period of compound relaxation, whereas their elasticity modulus is significantly less effected. Thus, 4–5 order rise of gradient of shear rate promoted 4 orders reduction of viscosity and relaxation of compounds. It is caused by mechanical and dissipative fracture of compound coagulation structure. Modulus of elasticity under the same conditions of testing is constant for many compounds (all types of rutile and low-hydrogen compounds with fine-grain filling agent), it rises not more than by order (low-hydrogen compounds with coarse-grain filling agent, manufactured based on viscous-liquid glass) or reduces to insignificant level (cellulose compounds).

5. Slope opposition of change of viscosity and period of relaxation, on the one hand, and modulus of elasticity, on the other hand, suggest that viscosity and modulus of elasticity become even

on value at determined rate, and period of relaxation, which is a relationship of viscosity and modulus of elasticity, become equal one. After this, viscosity loses the possibility to damp elastic oscillations of the compounds, which can be caused by any random reasons, and system passes in mode of unsteady flow, expressed with different level of regularity.

6. The work shows two types of unsteady flow, namely in capillary and entrance (pre-capillary) zone. In the first case, it has features of jet blowing out on capillary wall and it can be suppressed by using of smaller section capillaries, that is typical for near-wall slipping effect. In the second case, unsteady flow mode does not disappear at transfer to lock disk with hole of smaller section. Therefore, in this case, unfavorable relationship of viscosity and elasticity is preserved in rise of shear rate. Introduction of soft elements, capable to promote unsteady flow, works only with those compounds, which can pulsate without flexible insert. Thus, tendency to unsteady flow modes, capable to result in coating thickness difference, and external disturbing factors only reveal this capability.

7. Qualitative dependence of elastic turbulence of electrode compounds on nature and character of appearance of coating thickness difference under real extrusion application of coating over rod electrodes is shown.

1. Marchenko, A.E. (2000) Coating thickness difference as a factor of process state and quality of manufacture of welding electrodes. In: *Proc. of Sci.-Techn. Seminar on Electrode Manufacturing on the Threshold of New Millennium* (St.-Petersburg, 22–26 May 2000), 124–125. Cherepovets: Elektrod.
2. Vornovitsky, I.N. (1989) Coating thickness difference as a main factor of quality of electrodes. *Svarochn. Proizvodstvo*, **4**, 7–19.
3. Mayasaka, K., Oshiba, F., Akamatsu, T. (1982) Effect eccentricity of the coating upon the deposition of weld metal. *J. JWS*, **7**, 47–55.
4. Ovchinnikov, V.A., Bazhenov, V.V. (1978) Influence of electrode coating geometry and presence of defects in it on reliability of melted metal shielding from air action. *Svarochn. Proizvodstvo*, **5**, 39–40.
5. Pokhodnya, I.K., Makarenko, V.D., Milichenko, S.S. (1985) Influence of coating eccentricity on welding-technological properties of electrodes and quality of deposited metal. *Avtomatich. Svarka*, **11**, 20–22.
6. Stepanosov, A.R. (1989) Expert judgement of causes of coating thickness difference of welding electrode. *Svarochn. Proizvodstvo*, **4**, 7–9.
7. Belkin, I.M., Vinogradov, G.V., Leonov, A.I. (1967) *Rotary devices. Measurement of viscosity and physico-mechanical characteristics of materials*. Moscow: Mashinostroenie.
8. Vinogradov, G.V., Malkin, A.Ya. (1977) *Rheology of polymers*. Moscow: Khimiya.
9. Marchenko, A.E., Gnatenko, M.F. (1980) *Peculiarities of flow of electrode compounds detected by capillary plastometer*: SMEA Inform. Doc., Issue 1, 106–117. Kiev: Naukova Dumka
10. Bagley, E.B. (1957) End correction in the capillary flow of polyethylene. *J. Appl. Phys.*, 28(**5**), 624–627.
11. Cogswell, F.N. (1972) Converging flow of polymer melts in extrusion dies. *Polymer Eng. and Sci.*, 12(**2**), 64–70.
12. Marchenko, A.E. (2011) About rheological properties of electrode compounds in convergent zone during electrode extrusion. In: *Proc. of 6th Int. Conf. on Welding Consumables. Development. Technology. Manufacture. Quality. Competitiveness* (Krasnodar, 6–9 June 2011), 223–232.
13. Shoff, R.N., Cancio, L.V., Chida, M. (1977) Extrusial flow of polymer melts. *Transact. of Soc. of Rheology*, 21(**3**), 429–434.
14. Khan, Ch.D. (1979) *Rheology in processes of recycling of polymers*. Moscow: Khimiya.
15. Malkin, A.Ya., Leonov, A.I. (1963) On criteria of instability of shear deformation conditions of elastic-viscous polymer systems. *Doklady AN SSSR*, 151(**2**), 380–383.
16. Philippoff, W., Gaskins, F.H. (1958) The capillary experiment in rheology. *Transact. of Soc. of Rheology*, 263–284.
17. Sokolov, E.V. (1950) Electrodes with high quality coating and their production. *Avtogen. Delo*, **11**, 26–29.
18. Klementov, V.I. (1953) *Liquid glass as a material of electrode coatings for electric arc welding*: Syn. of Thesis for Cand. of Techn. Sci. Degree. Moscow.
19. Marchenko, A.E., Skorina, N.V. et al. (1972) State-of-the-art and prospects of improvement of technology and equipment for manufacture of welding electrodes. In: *Proc. of All-Union Conf. on Welding Consumables* (Kiev, 31 Oct.–3 Nov. 1972), Pt 2, 210–250.
20. Marchenko, A.E., Shkurko, S.A. (1973) Control of electrode compounds by conic plastometer. In: *Proc. of Short-Term Seminar on Electrodes and Fluxes for Electric Arc Welding* (Leningrad, 12–14 March 1973), 22–32.
21. Bibik, E.E. (1981) *Rheology of dispersion systems*. Leningrad: LGU.
22. Marchenko, A.E., Skorina, N.V., Sidlin, Z.A. et al. (1992) Investigation of viscosity of liquid glasses under electrode extrusion pressure. In: *New Welding and Surfacing Materials and their Application in Industry*: Proc. of Sci.-Techn. Seminar Dedicated to 100th Anniversary of K.V. Petranya (St.-Petersburg, 19–20 May 1992), 43–49.
23. Mitsubishi, N., Aoyagi, Y. (1973) Non-newtonian fluid flow in an eccentric annulus. *J. Chem. Eng. of Japan*, 6(**5**), 402–408.
24. Marchenko, A.E., Gnatenko, M.F. (1992) Peculiarities of coating thickness difference formation detected by oscillography In: *Abstr. of Sci.-Techn. Conf. on Metallurgy of Welding and Welding Consumables* (St.-Petersburg, 1–2 June 1992), 98–100.

Received 22.04.2014

STATE OF RAW MATERIAL BASE OF ELECTRODE PRODUCTION

E.A. PALIEVSKAYA and **Z.A. SIDLIN**
TECHPROM Ltd.
57 Gilyarovsky Str., 107996, Moscow, Russia. E-mail: techprom-ru@yandex.ru

State of raw material base in Russia regarding the production of covered electrodes was analyzed focusing on the changes occurred in this field in the recent years. Such categories of raw materials as electrode wire, mineral components of coatings, ferroalloys and liquid glasses were studied. The critical positions on production of single components, search for new sources of raw materials as well as changing conjuncture of materials at the market were mentioned. The conclusion was made that the Russian manufacturers of raw materials still dominate at the domestic market. 9 Ref., 1 Table.

Keywords: *arc welding, covered electrodes, raw materials, electrode wire, mineral components, ferroalloys, liquid glasses, market*

Russia is still the leading European manufacturer of welding consumables, though in 2013 the volume of production of electrodes as compared to the previous year somewhat decreased. However in medium-term prospect, considering the estimated rate of growth of rolled metal at the level of 5–6 % per year, respectively the growth of volume of electrodes production is expected. The composition of enterprises-manufacturers is changed: the volume of Russian enterprises is increased belonging to the largest world producers, in the first turn, ESAB (Sweden) and Lincoln Electric (USA). The enterprises aimed only at the growth of quantitative values, loose consumers and even collapse. At the same time young, ambitious enterprises are being developed, the products of which are oriented to the consumer. The requirements of users towards quality of welding consumables are constantly increasing, the determining values for which (at other equal values) relate to the characteristics of raw materials. If the nomenclature of components used for electrode coatings is very conservative in the whole world (according to the data, for example, of patent studies), then the mineralogical origin and technology of processing of raw materials can influence significantly the properties of electrodes.

In the Soviet times the attempts to increase the quality of products (including also welding consumables) were made at governmental level, in particular through certification according to three categories of quality. However, they were bound to fail both due to total deficiency, as well as due to incorrect methodical approach. Thus, for metallurgy industry the raw materials were excluded from certification, which made all the further efforts hopeless. At the present time the attention to quality characteristics of raw materials changed essentially. The problems of raw materials base of production of welding consumables were considered in detail in the previous works of authors [1, 2], but during the last period of time certain changes occurred, elucidation of which is actually the aim of this publication.

Electrode wire. It is generally known that the quality of welding electrodes depends to a great extent on the welding wire being used. In the domestic practice, to manufacture the overwhelmed volume of electrodes the low-carbon wires of grades Sv-08 and Sv-08A according to GOST 2246–70 are used. During many years the complains of electrode manufacturers to the manufacturers of a wire were caused by a low quality of its surface, including the presence of rust, contaminations, increased amount of lubricants, bad coiling and packing, difficulties in producing metal with decreased content of sulfur and phosphorus. Though ovality and tolerances of accuracy of diameter correspond to the standard, they do not provide modern requirements for different thickness of electrode coating. During delivery of wire in reels the need in their additional balancing adjustment during unwinding and cutting constantly arose.

Steel and hardware makers performed immense cost effective works on technical re-equipment and reconstruction of plants, which resulted in considerable improvement of quality of wire. At the present time the purchase of wire Sv-08A does not represent any problems, all wires are delivered in heavy-load bundles with tight winding and binding in the proper packing. In general,

according to the evaluation of specialists, the quality of domestic rolled wire is inferior to the imported one only as to the state of bundles. For example, after carried out reconstruction the Nizhneserginsky Hardware-Metallurgical Plant produces rolled wire of two-stage cooling of welding wire of grades Sv-08 and Sv-08A of diameter from 5.5 mm with the content of ≤0.01 % Al, 0.05–0.08 % C, σ_t ≤420 MPa, with the further manufacture of wire at the Ural plant of precision alloys. The rebreeding of the latter in the NLMK-Metiz was carried out in 2013 according to its corporative appertaining and production profile.

At the end of 2013 at the Beloretsk Metal Works the capital repair of rolling mill 150 was finished, where rolled wire is produced of 5.5–14 mm diameter of carbon, alloyed and high-alloyed steels. Only the problems of providing quality of wire surface, mostly determined by geometry of drawing dies, on the optimal shape of which the presence of tears, defects of surface layers, superhardening depend, were not completely solved [3].

On the surface of a wire, as well as on any other product of drawing production, there is always a certain amount of contaminations of different kind, formed in the process of its manufacture or during storage, transportation, etc. Though GOST 2246–70 admits only the presence of traces of soap lubricant without graphite and sulfur (for high-alloyed wire even they are not admissible) on the surface of low-carbon and alloyed wire, contaminations almost of three groups are found: organic (oils, remnants of technological lubricant, preservation coatings), oxide (rust of all kinds), foreign (mud, dust, occasional substances). For most of the grades of electrodes the use of such wire not only deteriorates their welding and technological characteristics, but also is fraught with defectiveness of welds. At the same time the efficient technologies of cleaning of wire surface during its processing at the electrode enterprises [4] are seldom used.

In the existing GOST 2246–70 the standards to welding-technological properties of wires and their rigidity are absent. But GOST 2246–70 (item 11) contained the standard: «Wire in bundles should be supplied in the state admitting its cutting and straightening»! At the present time in the post-Soviet regions only the national standard of Ukraine on steel welding wire, harmonized with the International standards, envisages the requirements to rigidity and welding-technological properties of the wire. And already in 1997 Krodeks Ltd. and the E.O. Paton Electric Welding Institute developed and implemented the technical conditions for welding wire for mechanized types of welding, nominating the values of its welding-technological properties required by the user [5].

The situation with wires for manufacture of high-alloyed electrodes is much worse. From the most skillful manufacturer of the widest assortment of high-alloyed welding wires: Moscow metallurgical plant «Serp i Molot» with more than 130 years of history, only the territory of 87 ha remained now, intended for multifunctional complex building.

For the plants of special metallurgy the constant difficulties are encountered even to provide the requirements of standards as to the norms of mechanical properties and uniformity of their values within the range of bundle, tolerances for ovality, frequently even in chemical composition. At the domestic market cheap not-welding foreign wires of metal with increased content of harmful impurities, nitrogen, with considerable plus tolerances as to diameters and often with «faked» certificates are already available. High-quality wire of qualified manufacturers at competitive prices is also delivered. The latter passes all the required certificate procedures and is admitted for use by domestic organizations. The successful experience of its use for manufacture of electrodes was gained, that requires, however, extremely high technical level of production. It must be stated that this market for domestic producer was lost to a large extent. Whereas world production of high-alloyed steels is growing continuously by 4–5 % each year, requiring, respectively, welding consumables.

Components of electrode coatings. In electrode coatings the following materials are used in the largest volumes: of non-metallic minerals — marble and fluorspar concentrate (for the coatings of basic type), and of concentrates — rutile and ilmenite (for the coatings of appropriate type). Until recently Russia, having in its disposal the considerable reserves of raw materials, has no industrially developed deposits of rutile and ilmenite. The works in this direction are in the process. Thus, in Murmansk region the projecting of an enterprise on production of prospective enriched perovskite concentrate of African deposit of perovskite titanium magnetite ores (joint project of the company «Arkmineral» and Kolsky Research Center of the RAS) is planned. The increased natural radioactivity of material is supposed to be decreased to acceptable level using methods of chemical processing.

At the end of 2013 the successful results of geological prospecting works at the large Pizhem-

sky deposit of friable titanium in Komi republic were obtained, which alongside with the famous Yargensky deposit make this region very prospective. The corporation VSMPO-A-Visma (the largest world producer of titanium alloys) acquired license on development of large rutile-zirconium deposit Tsentralnoe in Tambov region. Kuranakhsky titanium-magnetite deposit in Amursky region is explored. All these works should be evaluated considering the falling volumes of deliveries of rutile and ilmenite concentrates from the Volnogorsky Mining and Smelting Works (Ukraine), the main supplier of these materials. Unfortunately, all the last years Russian and Ukrainian enterprises were bearing constant and growing difficulties with purchase of these materials. The appeal of Association «Elektrod» to the government of Ukraine on this issue did not have a success. In this connection rutile-zirconium concentrate of Sierra Leone, SAR, Vietnam, Australia find ever wider practical application, ilmenite concentrates of India, Sri-Lanka, Mozambique have passed the positive testing. But the concentrate of the Volnogorsky MSW according to its technical characteristics and stability of properties completely meets the requirements of all the producers of electrodes, including European ones and at a reasonable policy of the supplier there would be no need in its change.

The demand on cheap electrodes with ilmenite coating, welding technological properties of which are inferior to the characteristics of rutile electrodes, decreased considerably, respectively the need in ilmenite concentrate also decreased.

Achromous titanium dioxide of rutile modification used in coatings of high-alloyed electrodes, is produced by the STC «Pigment Ltd.» (Chelyabinsk, Russia) since 2012.

Main producers of ferroalloys of Russia [7]

Holding (group)	Enterprise	Produced ferroalloys
ChEMK	Chelyabinsk electro-metallurgical works	FeSi
	Kuznetsk ferroalloys	FeCr, FeSi
	Yurga plant of ferroalloys	FeSiMn
ENRC (Kazakhstan)	Serovsky plant of ferroalloys	FeSi, FeCr
	Satka cast iron melting plant	FeMn
Mechel	Bratsk plant of ferroalloys	FeSi
	Yuzhuralnikel	FeNi
	Tikhvin plant of ferroalloys	FeCr
Rosspetssplav	Russky khrom	FeCr
	Klyuchevsky plant of ferroalloys	FeTi
Evraz	Vanady-Tula	FeV
OMK	Chusovsky metallurgical plant	FeV

The situation with marble, the second material by volumes of its application and the first one by its importance, was improved. Within several last years fractioned micro marble of electrode conditions is supplied by CJSC «Koelgamramor». The supplier reached stability in granulometric composition and humidity of material during deliveries in big-bags with a polyethylene insert.

The critical situation was over fluorspar (fluorite concentrate) [6]. The largest Russian producer of fluorite concentrate «Yaroslavsky Mining Ltd.» (Primorsk region) is capable to produce only concentrate with the content of $CaF_2 \leq$ $\leq$ 92 %, its cost is approximately by 30 % higher than that of foreign analogues. Due to these reasons stoppage of the enterprise was planned to carry out its complete modernization. One of the main suppliers of fluorite concentrate for electrode manufacturers is the Haydarkansky Quicksilver (mercury) Works (Kirgizia). At the present time it carries out works on draining of mine «Zapadnaya» to resume the deliveries. The main supplier, the Kalanguysky Ore-Dressing Works (Transbaikal region) stopped his works because of environmental characteristics, the deliveries of natural pure lumpy fluorspar of mining company «Suran» (Bashkiriya) make no progress. However, from the middle of 2011 the mine Usugli (Uluntuysky deposit, Chita region) started its work and Garsonuysky Ore-Dressing Works started delivery of welding fluorite concentrate. Besides, the deliveries from Mexico and Iran at average market prices were started. The situation with deliveries was improved, however, it can not be accepted as stable.

Electrode plants still have to manufacture solutions of binders (silicate liquid glasses) for their needs on their own. The situation with deliveries of silicate lump was improved. Company «Zaporozhstekloflyus», producing sodium lump, is working stably. Besides the CJSC «Stroitelny Kompleks», being a part of Magnitogorsk Metal Works, the Magnitogorsk plant for manufacture and processing of glass «MagniZa Ltd.» increased its production. Such competition, undoubtedly, has a benefit for the consumer. The lump is supplied in big-bags.

Certain changes occur at the market of ferroalloys [7, 8]. In the production of ferroalloys China is leading (51 % of the world volume), the next is SAR (12 %), Kazakhstan (5.7 %), Ukraine (4.5 %), Russia (3.7 %). Among the materials produced in Russia: 48 % — silicon

alloys, 30 % — chromium alloys, 16 % — manganese alloys; their main producers are presented in the Table.

The problems of Russia with providing ferromanganese were supposed to be solved by building of the Yenisei Ferroalloy Plant on the base of Usinsky deposit at 11 km from Krasnoyarsk. However, the final decision about building of this enterprise, considering the environmental factors, was not yet taken (mass protests of people, the movement «Krasnoyarsk against»).

The Urals-Siberian Mining-Metallurgical Company carries out integrated works connected with exploration of Selezensky deposit of manganese ores in Tashtagol region of Kemerovo province. Melting of manganese ferroalloys, in the first turn ferrosilicon manganese, will be carried out at the «Kuznetsk Ferroalloys Ltd.», where plasma furnaces were put into operation.

The increase of volume of ferrosilicon manganese in production of welding consumables, which is characterized, for example, by a low content of phosphorus in the most widespread grade MnS17A, is challenging. The Russian producer of FeSiMn, the group of ChEMK, is working with imported raw materials (up to 70 %). The plants of Ukraine (ferroalloys plants of Nikopol, Zaporozhie and Stakhanov) have immense output capacities, however, due to a high cost of electric power, the volume of which in the cost of products exceeds 45 %, two latter plants were stopped in December 2012 as those being unprofitable. The capacities of only one Nikopol Plant are seemed to be enough (more than 1 mln t of FeSiMn and 250,000 t of FeMn), but its production does not exceed 25 t of FeSiMn per month. Import of ferroalloys from Bulgaria to Russia sharply increased, but it is supposed to be the products of Indian and Georgian producers. In 2011 FSUE «Prometey» together with «Butkinsky Titan Ltd.» developed and agreed technical conditions on challenging titanium alloys with manganese and ferrotitanium with a number of leading enterprises, which unfortunately did not find industrial application till now. At the same time the problems with quality ferrotitanium were successfully solved with increase of output volumes of the Kluchevsky Plant of Ferroalloys, which has a required experience.

Such is the situation with basic ferroalloys consumed by the electrode manufacturers. It is pleasant also to mention about the stable work of «Meldis-Ferro Ltd.» with increase of volumes of production at accepted prices of the supplier of powders of ferroalloys and metals ready to application in electrode coatings [9].

In spite of the abovementioned problems with raw materials, the Russian producers dominate at the domestic market, but further intensive work is required to keep the positions.

1. Palievskaya, E.A., Sidlin, Z.A. (2009) Problems of raw materials sources for manufacturing of welding consumables. *Svarochn. Proizvodstvo*, **9**, 25–31.
2. Palievskaya, E.A., Sidlin, Z.A. (2010) Problems of raw materials sources for manufacturing of electrodes. Electrode wire. *Ibid*., **11**, 38–40.
3. Zheltkov, A. (2013) Current technologies for manufacturing of hard-alloy drawing dies. *MSiS*, **10**, 22–28.
4. Zhirnova, T.I., Lebedev, N.M. (2002) Ultrasonic technologies and equipment for steel rolling and welding production. In: *Proc. of Sci.-Pract. Seminar on Metal Electrodes for Welding and Surfacing* (20–22 May, 2002, Sudislavl), 41–44.
5. Brinyuk, M.V., Semenov, S.E. (2001) Improvement of consumer characteristics of welding wire. *Svarshchik*, **6**, 14–15.
6. Marchenko, A.A., Kiselyova, S.P. (2011) About state-of-the-art in production of fluorite designed for welding. In: *Proc. of 4th Int. Conf. on Welding Consumables* (Krasnodar, 2011), 130–133.
7. Leontiev, L., Sheshukov, O., Kataev, V. (2013) Ferroalloys at the junction of science and production. *Metally Evrazii*, **5**, 24–27.
8. (2013) Ferroalloys. Ambiguous year. *Metallurg. Bull*., **1/2**.
9. Davydov, A.V. (2005) Experience of manufacture of fine powders of different type ferroalloys. In: *Arc welding. Materials and quality*, 231–233. Magnitogorsk.

Received 29.04.2014

DIRECTIONS OF IMPROVEMENT OF EQUIPMENT AND TECHNOLOGY FOR ELECTRODE MANUFACTURE

M.F. GNATENKO, V.S. VOROSHILO and **A.D. SUCHOK**
WELMA Ltd.
3 Kaunasskaya Str., 02160, Kiev, Ukraine. E-mail: welma@welma.kiev.ua

The paper gives recommendations on improvement of coated electrode manufacture through the entire sequence of technological process, including direct grinding of coating components, preparation of liquid glasses and electrode rods, coating mixture preparation, electrode extrusion and heat treatment.

Keywords: *coated electrodes, manufacturing quality, engineering and technology solutions, component grinding, liquid glass, rods, coating mixture, extrusion, heat treatment*

At the current stage the volumes of consumption and manufacture of coated welding electrodes are reduced all over the world. This also leads to a significant lowering of attention and of investments into development of new engineering and technology solutions in this industry.

However, electrode productions that intend to stay in the electrode market, urgently need to work on the following: improvement of equipment and technology; development and introduction of new electrodes with highly effective welding-technological properties (specialists-electrode developers are working in this direction).

In the first area the objective in known: it is an essential improvement of stability and quality of electrode manufacturing at lowering of cost/productivity ratio. This can be achieved by applying a number of engineering and technology solutions.

1. Stage of preparation of welding electrode coating components — grinding:

a) at grinding it is necessary to stabilize the grain composition of each component by optimizing the respective mill operating modes (rotations, balls and their loading, time, size of ground component particles and its charging weight);

b) ensure production and utilization of powders of various materials with different required grain composition:

- fine (not less than 80 % of < 0.063 mm fraction), using special mills or batch-operation mills;
- coarse (within 80 % of > 0.160–< 0.355 mm fraction) with application of mills with continuous sieving.

Combining such grain compositions of different components at charge preparation allows, on the one hand, an essential improvement of technological (also plastic) properties of coating mixtures and, on the other, improvement of welding-technological properties of electrodes. This is achieved due to:

- minimizing the content of medium fraction of grain composition (> 0.063–< 0.160 mm) in the charge;
- presence of coarse fraction of grain composition in the charge in the amount of up to 30 vol.% (reinforcing component); the rest is fine fraction.

Reduction of production expenses will be not less than 10 %.

2. Liquid glass preparation:

a) soft-boiling of the lump and achieving stable parameters of liquid glass (with modulus of ≈ 3±0.05 and small viscosity of 100–500 cP, depending on electrode grade) due to application of no-autoclave method of lump soft-boiling without subsequent correction of viscosity (density);

b) stabilizing liquid glass properties after no-autoclave method of its manufacture proceeds very quickly — within about one day in settling tanks with simultaneous cooling and precipitation of a small residue.

This is followed by just liquid glass stabilizing by temperature (with mixing).

After silicate lump soft-boiling, when its impurities (contamination) and the rest have already had their effect on liquid glass properties (its characteristics) it is not rational to perform its filtering (i.e. expenses without effect).

Thus, liquid glass parameters will be stable, that, in its turn, stabilizes the technological properties of coating mixtures and process of electrode manufacture as a whole. Moreover, cost reduction in its manufacture will be equal to approximately 20 %.

3. Manufacture of sound rods with application of:

a) machine tools of simple design, easily readjusted and maintained with smooth cutting speed regulation;

b) efficient unwinding devices:

• for large bundles (1–1.5 t) — inertialess (without jerking and without stub-rods, respectively; smooth starting and stopping of bundle without braking);

• for small bundles (special wire) — rotating self-braking (with lubricator);

c) «octagon-shaped» knife to ensure the cut quality (without dents or burrs);

d) feed rollers with knurling and disc spring for their pressing up — stability of rod length and low wear of rollers;

e) funnel-shaped blocks from two sides.

It results in high quality of rods, minimum rejects, cost reduction and guarantee of their stable extrusion.

4. Preparation of coating mixtures and ensuring their high uniformity and plasticity by:

a) application of intensive counterflow mixers, that, in addition, eliminates the need for dry charge mixer:

• design of mixer, including actuators, should eliminate formation of dead areas and premature formation of mixture lumps with increased content of the liquid phase and hydrophylic components; in order to eliminate them, it is important that the velocity of impact of high-speed actuator was sufficient for breaking up such lumps along the entire height of coating mixture layer in the mixer;

b) rational method of plasticization, depending on charge composition, in particular grain composition, type and characteristics of liquid glass. This should result in good wettability of particles by liquid glass and medium rigidity of the structure of liquid glass gel in the film between charge particles. This is achieved by taking the charge–liquid glass–plasticizer system to medium activity, and to medium rigidity of liquid glass in the film.

Eventually, we get high plasticity and stability of coating extrusion process, particularly, in terms of non-uniform thickness; and higher efficiency.

5. Electrode extrusion.

Quality and stability are achieved at:

a) stable feeding of rods;

• high quality of manufactured and applied rods;

• stable axis of rod feed: vertical descent (including agitator), grip, first guide, feed rollers, second guide;

• smooth regulation of nip roller speed (depending on rod steel grade, amount and type of lubricant on the rods, rod surface condition, etc.);

• regulation of the distance between the gripping cage (nip roller axis) and feeding cage (feed roller axis) — $x = L_r - (10 \div 20)$ mm, where L_r is the rod length

• regulation of the distance between feed roller axis and outlet of extrusion head stalk tip — $y = L_r n$, where n is the rod number, i.e. extrusion ratio;

b) high plasticity of the mixture (considered above);

c) high angle of entrance zone (up to 160–180°) and minimum value of discard (10–15 mm thick);

d) efficient design of extrusion head:

• extrusion chamber of minimum volume between the tip and forming bushing (die);

• local expansions of mixture flow, also in the extrusion chamber in the course of flow formation from sleeve diameter up to die entrance, are not allowed;

• rod in extrusion chamber should constantly be slightly pressed-up by the mixture in one transverse direction;

• mixture flow in the extrusion head should be organized in the channel lined with wear-resistant replaceable elements;

• regulation of difference in thickness of electrode coatings during extrusion should be simple and reliable, due to minimizing the cross-sectional area of the composite cone in front of the die holder;

e) proper maintenance of the press (including briquetting press):

• elimination of formation of coating mixture blocks and their penetration into extrusion area (cleaning of briquetting press, hermetic storage of briquettes, cleaning of piston rod seal of extrusion cylinder to remove coating mixture remains, including discard, particularly at extrusion of electrodes of calcium fluoride type);

• timely replacement of worn working elements, including piston rod seals;

f) as regards dressing of electrode tips sound working elements and thorough adjustment of dressing machine.

All these measures will improve the quality of electrode extrusion at increase of efficiency by 10–15 %.

6. Electrode heat treatment.

This is the most labour-consuming and delicate stage of electrode manufacturing process. A rather tangible effect in heat treatment of electrode coating can be achieved:

a) due to improvement of technological, in particular, drying properties of coating mixtures associated with optimization of charge granulometric composition; application of low-viscosity liquid glasses; application of certain plasticizers (special additives);

b) due to application of the most effective heat treatment method (heating method), namely, induction, when the rod is heated by an induced field of high-frequency currents (8000 Hz). Here the heat and moisture flows in the coating are oriented in the same direction, that markedly accelerates the process of moisture removal. Moreover, heat losses during heat treatment are markedly lowered. Unfortunately, however, it is very costly to realize this method in the currently available productions: it is too expensive and takes a long time;

c) at convective heating method due to improvement of the carrying frame design, eliminating electrode coating damage, with minimizing of frame weight, and by organizing the optimum flows of heat carrier in the furnace working space so that the electrodes were blown along their axis. This provides uniform heat application over the entire coating surface and effective moisture removal at low blowing speeds, respectively. Under such conditions it is possible to heat treat, for instance, UONI-13/55 electrodes of 4 mm diameter, without preliminary curing, to moisture content of 0.2 % in 110–120 min.

At this stage 20 % reduction of power consumption for the process at simultaneous improvement of coating heat treatment quality can be achieved.

It is believed to be rational to strongly recommend application of operative simple instrument for non-destructive testing of difference in coating thickness of electrodes of any typesize.

Quite important also is sound piece-by-piece marking of electrodes with application of readily adjustable and maintainable device.

In conclusion it should be noted that in all the considered areas we have concrete design and technological solutions, verified and implemented in equipment and in productions.

Optimizing the other components of electrode production should be performed by production managers on the modern level (staff, training and certification, raw materials, all kinds of control and accounting, certification testing, packing, sale, etc.).

Received 16.04.2014